3rd International Symposium on Gully Erosion

Identifying PROBLEMS . . .

Finding SOLUTIONS . . .

The University of Mississippi
Oxford, Mississippi, U.S.A.
April 28 - May 1, 2004

Hosted by:

- USDA ARS National Sedimentation Laboratory
- The University of Mississippi

To Table of Contents

United States Department of Agriculture

Research, Education and Economics
Agricultural Research Service

August 18, 2004

Dear III GEGC Participants:

Enclosed is the long-awaited CD of the Proceedings of the Third International Symposium on Gully Erosion under Global Change that was held in Oxford, Mississippi, from April 28 through May 1, 2004. The CD contains the program, a list of the attendants, a list of authorship, full papers and abstracts, some of the Power Point presentations if approval was given, and a summary of the Panel discussions. Also, we received one manuscript from a participant, who at the last moment, was not able to attend the conference. This article was added to the proceedings. Also several submitted abstracts were included on the CD although the presenters were not able to attend for various reasons. Because there are many different computer systems, it is possible that the Power Point presentations might not work on certain computers. At the time the CDs were made, all presentations were working using Microsoft Power Point 2002.

We very much appreciate your participation in and contribution to the success of this Symposium. We regret the delay in getting this CD to you, but we opted to wait in order to include all of the completed manuscripts that were promised.

With this mailing, our work is not yet completed. We are still pursuing the possibility of having the contributions published as a special publication or as a batch of articles in a refereed outlet. We are in contact with the Soil and Water Conservation Society (SWCS) and the American Geophysical Union (AGU) to explore the best option. The selection will be based on cost, expected circulation, and the type of paper that these societies are likely to accept for publication. We will keep you posted about developments.

It was a pleasure having the opportunity to host this Conference in Oxford, Mississippi.

For the Organizing Committee,

M.J.M. RÖMKENS, Co-chair
Laboratory Director

Enclosure

National Sedimentation Laboratory
598 McElroy Drive
P.O. Box 1157, Oxford, Mississippi 38655
Voice: 662 232-2940 ● FAX: 662 232-2915 ● E-mail:mromkens@msa-oxford.ars.usda.gov

Acknowledgments

The Organizing Committee of the 3rd International Symposium on Gully Erosion would like to thank the following entities for their contributions and financial support. Their assistance has helped assure the success of this Conference.

United States Army Corps of Engineers
USDA National Sedimentation Laboratory
The University of Mississippi Department of Civil Engineering
The University of Mississippi Department of Information Technology

We would like to pay a special tribute to Dr. Rusty Cooper and his Staff at the University of Mississippi Department of Outreach and Continuing Education. Their expertise in conference organization has been invaluable, and their contributions and hard work have made this conference possible.

Committees

Advisory Committee
Mr. J. Bernard, U. S. Dept. of Agriculture, Natural Resource Conservation Service
G. D. Glysson, United States Geological Survey
J. R. Gray, United States Geological Survey
Mr. T. Hengst, U. S. Army Corps of Engineers
Dr. Y. Li, Chinese Academy of Agricultural Sciences (CAAS), Beijing, P.R. China
Prof. Dr. J. Poesen, Katholieke Universiteit, Leuven, Belgium
Prof. Dr. S.S.Y. Wang, NCCHE, University of Mississippi
Dr. M. A. Weltz, U. S. Dept. of Agriculture, Agricultural Research Service
Dr. T. Yang, U. S. Dept. of the Interior, Bureau of Reclamation

Sponsorship/Endorsement
U.S. Army Corps of Engineers
Agricultural Research Service
U.S. Geological Survey
Natural Resource Conservation Service
The University of Mississippi
U.S. Dept. of the Interior Bureau of Reclamation

Local Organizing Committee
Dr. M.J.M. Römkens, USDA-ARS, co-chair
Dr. S.N. Prasad, University of Mississippi, co-chair
Dr. Alex Cheng, University of Mississippi, Department of Civil Engineering
Dr. Sean Bennett, USDA-ARS
Dr. Carlos Alonso, USDA-ARS
Mr. Rusty Cooper, University of Mississippi
Ms. Lucienne Savell, USDA-ARS
Ms. Myra Shaw, USDA-ARS

Scope and Objectives

Gully erosion is the most visible but least attended to form of soil erosion. Gullys affect land use, land accessibility, soil productivity, farming, roads, the stream system, etc. It produces more sediment than any other erosion mode. Gully erosion has received comparatively less attention than rainfall or overland flow induced erosion due to the complicated nature and scale of the processes involved.

Gullys are the pathways sediment to move from upland areas to channels and lakes of the drainage system. Given the import and dominant nature of gully erosion on many landscapes in many parts of the world, a series of International Symposia on Gully Erosion were organized in recent years to bring together erosion research scientists and specialists from many parts of the world to discuss this problem area. The first Symposium was held in April, 2000, in Louvain, Belgium, the second one in May, 2002, in Chengdu China. This Symposium, planned for April 2004, very much continues the topics and themes of the previous conferences and has as general objectives: 1 to improve the understanding of fundamental processes and mechanisms of gully erosion, 2 to improve gully erosion prediction, and 3 to develop techniques, technologies and strategies to control/prevent gully erosion.

Specific themes of interests related to this gully erosion symposium are:

Experimental investigations on gully erosion
Characterization of gully erosion processes and topology
Gully erosion thresholds, mechanics, and evolution
Hydrodynamic, hydrologic, and subsurface flow effects on gully erosion
Effects of agricultural practices and anthropogenic activities on gully erosion
Soil properties, land form, landscape, and watershed effects on gully erosion and their interaction
Effect of temporal and spatial scales on gully erosion
On-site and off-site impacts of gully erosion
Gully erosion and global change
Modeling gully erosion processes
Gully erosion prevention, control and restoration

To Table of Contents

3rd International Symposium on Gully Erosion
April 28-May 1, 2004
Participant List

Mr. Kwame Andy Agble
AG Andy Enterprise
Box AN 10123
Accra North, AC 23321

Mr. Jack Alderson
USDA
14150 Hereford Dr.
Chico, CA 95973

Dr. Carlos Alonso
USDA
P.O. Box 1157
Oxford, MS 38655
USA

Mr. Richard Asamoah
Council for Scientific Research
P.O. Box M32
Accra, ACCRA

Mr. Mark Asante
Council for Scientific Research
P.O. Box M32
Accra, ACCRA

Mr. Nate Bartholomew
University of Minnesota
7920 Hearthside Ave. #219
Cottage Grove, MN 55016
USA

Mr. V.R. Belyaev
The Laboratory of Soil Erosion
Faculty of Geography, Moscow State University
GSP2, Vorob'evy Gory, Moscow 119992
RUSSIA

Dr. Sean Bennett
University of Buffalo
Dept. of Geography
Buffalo, NY 1426-0055, USA

Mr. Jerry Bernard
USDA
PO Box 2890
Washington, DC 30013, USA

Mr. Ron Bingner
USDA
PO Box 1157
Oxford, MS 38655
USA

Mr. Chaudhary Binod
Liberty Research Forum Pvt. Ltd.
DILLIBAZAR, GPO. Box 8974, EPC: 5572
Kathmandu, Bagmati 977, NEPAL

Mr. William T. Brown
26 Laurie Circle
Jackson, TN 38305
USA

Dr. Rorke Bryan
University of Toronto
33 Willcocke St.
Toronto, Ontario M5S3B3
CANADA

Dr. Javier Casali
Public University of Navarre
Dept of Projects
Pamplona, NA 31006
SPAIN

Dr. Robert Cullum
USDA
PO Box 1157
Oxford, MS 38655
USA

Dr. Seth Dabney
USDA
PO Box 1157
Oxford, MS 38655
USA

Mrs. Luisa De Santisteban
Public University of Navarre
Camino de Altxutxate 3
Olaz, NA 31620
SPAIN

Mr. Joaquin Del Valle
Public University of Navarre
Carretera el Sadar s/n Edificio El Sario
Pamplona, NA 31006-000
SPAIN

Dr. David DiCarlo
USDA
P.O. Box 1157
Oxford, MS 38655
USA

Dr. Markus Dotterweich
University of Koblenz-Laudau
University of Koblenz-Landau, Fortstrasse 7
Landau, Germany 76829
GERMANY

Dr. George Foster
USDA ARS (Retired)
5688 Broach Rd.
Bryan, TX 77808
USA

Mr. Lee Gordon
University of New York-Buffalo
68 Raintree Island #10
Tonawanda, NY 14150
USA

Dr. Antonio Guerra
Federal Univresity of Rio de Janeiro
Avenida Canal De Marapendi, 1100 APTO, 608
Barra Da Tijuca, Rio De Janeiro, RI 22631
BRAZIL

Ms. Ananda Das Gupta
Indian Inst. of Technology Kanpur
303B WLE, Dept. of Civil Engineering
ITT Kanpur, Kanpur, Uttar Pradesh 208016
INDIA

Dr. Satish Gupta
University of Minnesota
360 Bear Ave. St.
St. Paul, MN 55127
USA

Mr. William Hansen
USDA Forest Service
4931 Broad River Road
Columbia, SC 29212
USA

Dr. Greg Hanson
USDA
1301 N. Western Rd.
Stillwater, OK 74075
USA

Mr. Derek Holland
Calibre Systems Inc.
4471 Shellfield Rd.
Enterprise, AL 36330
USA

Dr. Chihua Huang
USDA
275 South Russell St.
West Lafayette, IN 47907
USA

Dr. Yafei Jia
University of Mississippi
School of Engineering
University, MS 38677
USA

Dr. David Kinner
US Geological Survey
Box 25046 DFC Mail Stop 966
Denver, CO 80225
USA

Ms. Anke Knapen
Laboratory for Geomorphology
Redingenstraat 16
Leuven, BE 3000
BELGIUM

Mr. Roger Kuhnle
USDA
PO Box 1157
Oxford, MS 38655
USA

Ms. Yong Lai
Sedimentation & River Hydramatics
Bureau of Reclamation
Denver, CO 80225
USA

Mr. Joe Larkin
University of Georgia
UGA
Athens, GA 30602
USA

Mr. Dennis Law
USDA Forest Service
4931 Broad River Rd.
Columbia, SC 29212
USA

Mr. Joel Leonard
INRA
INRA rue Fernand Christ
Laon, France F02007
FRANCE

Mr. Donald McCool
USDA
215 Johnson Hall, WSU
Pullman, WA 99164-6420
USA

Mr. John Moody
U.S. Geological Survey
3515 Marine St. Ste E-127
Boulder, CO 80303-1066
USA

Mr. Olaleye Olurin
Saint Augustine's College the Gambia
PO Box 410 Banjul the Gambia
Banjul, Banjul 00220
BANJUL

Mr. Eniola Omosanya
Inst. of Agric. Res. & Training
PO Box 1554
Sapon, Abeokuta OG
11000

Dr. Jean Poesen
Catholic University of Leuven
K.U. Leuven, Redingenstraat 16
B-3000, Leuven Vlaams Brabant
BELGIUM

Dr. S.N. Prasad
University of Mississippi
Civil Engineering
University, MS 38677
USA

Dr. Fred Rhoton
USDA
PO Box 1157
Oxford, MS 38655
USA

Dr. M.J.M. Römkens
USDA
PO Box 1157
Oxford, MS 38655
USA

Dr. Li Rui
Institute of Soil and Water Conservation
Chinese Academy of Sciences
NWSUAF, Yangling, Shaanxi 712100
P.R. China

Mr. Scot Serafin
Fort Knox
6034 Pickett Rd.
Fort Knox, KY 40121
USA

Dr. Doug Shields
USDA
PO Box 1157
Oxford, MS 38655
USA

Mr. Andrew Simon
USDA ARS NSL
PO Box 1157
Oxford, MS 38655
USA

Dr. Dungan Smith
U.S. Geological Survey
3215 Marine St.
Boulder, CO 80302
USA

Mr. Jovan Stefanovic
University of Toronto
33 Willcocks St.
Toronto, Ontario M5S3B3
CANADA

Mr. Fred Theurer
USDA, NRCS, NWCC
7413 Cinnabar Ter.
Gaithersburg, MD 20789
USA

Mr. David Thoma
USDA
2000 E Allen Rd.
Tucson, AZ 85719
USA

Mrs. Nataliya Vasyliv
Inst. of Agroecology & Biotechnology
40/1 Shestakova St.
Khmelnytskyy, UK 29000
UKRAINE

Ms. Ana Claudia Viero
Rue Vicente Feilace n 252
Porto Alegre
RS, Cep 90-900-270
BRAZIL

Mr. Kirk Vincent
US Geological Survey
3215 Marine St.-Mail Room E127
Boulder, CO 80303
USA

Dr. Sam Wang
NCCHE-The University of Mississippi
Carrier Hall Room 102A
University, MS 38677, USA

Mr. Mark Weltz
USDA
5601 Sunnyside Ave.
Beltsville, MD 20705-5140
USA

Dr. Glenn Wilson
USDA
PO Box 1157
Oxford, MS 38655
USA

Dr. Weiming Wu
The University of Mississippi
School of Engineering
University, MS 38677
USA

Dr. Ted Chih Yang
Colorado State University
Colorado State University
Fort Collins, CO 80523-1320
USA

Mrs. Saveta Yerychuk
Inst. of Agroecology and Biotechnology
40/1 Shestakova St.
Khmelnytskyy, UK 29000
UKRAINE

Mrs. Yongping Yuan
USDA
PO Box 1157
Oxford, MS 38655
USA

Ms. Fenli Zheng
Institute of Soil and Water Conservation
CAS/MOWR
PR. CHINA

Dr. Claudio Zucca
Via Enrico De Niola 9
Sassari, ITALY 1-07100
ITALY

3rd International Symposium on Gully Erosion Papers Table of Contents

The papers and abstracts have been placed on the CD in the order that they were originally scheduled to be presented and not in the order that they were presented.

Gully Erosion – Geographic Occurrences and Characteristics

Gully Erosion in Europe (Abstract only)
Poesen, J., T. Van Walleghem, G. Gyssels, G., J. de Vente, (Keynote)
G. Verstraeten, G., A. Knapen, A., J. Nachtergaele, and L. Vandekerckhove 1

Late Holocene Stages of Gully Development in the Central Part of the Russian Plain
Belyaev, V.R., E.A. Eremenko, A.V. Panin, Yu.R. Belyaev 2

Cutting and Refilling of a Gully System during the Last 1300 Years in Northern Bavaria, Germany (Abstract only)
Dotterweich, M. and H.-R. Bork 16

Gully Erosion and Environmental Degradation in the Southern Gangetic Plains, India (Abstract only)
Das Gupta, Ananda S., and R. Sinha 17

Natural and Anthropogenic Factors Controlling Gully Erosion in the Basaltic Upland of Rio Grande Do Sul, Brazil
Viero, Ana Cláudai, Nilza Maria dos Reis Castro, and Joel Avruch Goldenfum.....19

Morphological Characteristics and Development of Gully Head in Arid Environment, China (Abstract only)
Wang, Xiaodan, Xianghao Zhong, Shuzhen Liu, Jianrong Fan, and Jianhui Zhang 42

*Investigations of the Contrasting Distribution of River-bank Gullies in the Northern and Southern Gangetic Plains Using an Integrated Approach Including Remote Sensing, Geophysical Data and Field Investigation***.** (Abstract only)
Das Gupta, Ananda S. 44

Gully Erosion – Sediment Sources, Properties, Measurements, Routing and Spatial Variability

A Unified Approach in Erosion and Sedimentation Studies (Abstract only)
Yang, Chih Ted (Keynote) 46

Flow Near a Model Spur Dike with a Fixed Scoured Bed
Kuhnle, Roger A. , Yafei Jia, and Carlos V. Alonso.....47

Sediment Source Identification using Soil Geomorphological Characteristics in a Semi-Arid Watershed (No abstract nor paper available at time of printing)
Rhoton, F.E., W.E. Emmerich, and D.C. Goodrich .....N/A

Gully Erosion after Wildfire
Moody, J.A. and D.A. Kinner.....58

Routing of Flow and Sediment in a Gully Network (Abstract only)
Smith, J. Dungan and J. W. Kean 69

An Experimental Study on Gully Detachment and Transport on the Loess Plateau (Abstract only)
Zheng, Fenli, Peiqing Xiao, Yuanyuan Jia, Min Wu, and Yubin Zhang.....70

Accuracy of Methods for Field Assessment of Ephemeral Gully Erosion
Casalí, J., J. Loizu, M.A. Campo, L.M. De Santisteban.....71

Ephemeral Gullies: a Persistent Source of Sediment from Agricultural-related Lands (Abstract only)
Bernard, Jerry M., Jon G. Werner, and Fred D. Theurer.....85

Evaluation of Topographic Indices for Ephemeral Gully Assessment
Casalí, J., L.M. De Santisteban, J.J. López, J.V. Giráldez, J. Poesen, and J. Nachtergaele.....86

Airborne Laser Scanning for Riverbank Erosion Assessment
Thoma, D.P., S.C. Gupta, M.E. Bauer, and C. Kirchoff.....95

Alternating Pattern of Narrow Shooting Flow and Wide Tranquil Flow in Gullies (Abstract only)
Vincent, Kirk R., and J. Dungan Smith.....107

Spatial Distribution and Morphological Features of Gullies in an Agropastoral Area in Sardinia (Italy) (Abstract only)
Zucca, Claudio, Annalisa Canu, and Raniero Della Peruta.....108

A Simple Device to Monitor Sediment Yield from Gully Erosion
Guerra, Antonio Jose Teixeira and Figueiredo, Marcos 109

Gully Erosion – Models and Processes

Modeling Ephemeral Gully Erosion for Conservation Planning
Foster, George R. (Keynote).....118

The next Generation of Watershed-scale Erosion Models: Towards a Dynamic, Spatially Adaptive Representation of Rills and Gullies (Abstract only)
Favis-Mortlock, David and Paul Van Dijk 150

Numerical Simulation of Migration of Head-cut with A Two-layered Bed
Jia, Yafei, Kitamura Tadanori, and Sam, S. Y. Wang 151

Modeling Headcut Development and Migration in Upland Concentrated Flows
Bennett, Sean J. and Carlos V. Alonso 166

Empirical-numerical Analysis of Headcut Migration
Wu, Weiming and S.S.Y. Wang 188

Computer Modeling of Erosion and Sediment Delivery (Abstract only)
Lai, Yong G. and C. Ted Yang 206

AnnAGNPS & Ephemeral Gullies (Abstract only)
Theurer, F.D., R.L. Bingner, J. Stafford, and W. Merkel 207

Evaluation of Rill and Ephemeral Gully Erosion in Cultivated Areas of Navarre (Spain)
De Santisteban, L.M., J. Casalí, J.J. López 208

Experimental Study of Conditions for Rill Bank Collapse (Abstract only)
Stefanovic, Jovan R. and Rorke B. Bryan.....225

Modeling of Erosion Processes and Estimation of Interrill Erodibility Soil Parameters in Forest-Steppe Zone of Ukraine (Abstract only)
Vasyliv, Nataliya 226

Macropore Flow and Mass Wasting of Gullies in the Loess Plateau, China
Wilson, G.V., Xu Mingxiang, Chen Yun Ming, and Liu Guobin.....228

Hydraulic Characteristics of Knickpoints in Rill Confluence Zones (Abstract only)
Brunton, D.A. and R.B. Bryan 244

Hydrologically Driven Mechanisms of Head-Cut Development
Römkens, M.J.M. and S.N. Prasad 245

Overview of Dam Gully Erosion Research
Hanson, G. J., D. M. Temple, K. M. Robinson, K. R. Cook.....259

Freeze/Thaw Effects on Rill and Gully Erosion in the Northwestern Wheat and Range Region
McCool, D. and J.D. Williams 278

Resistance of Topsoils to Concentrated Flow Erosion: a Review of the Available Experimental Data
Knapen, Anke and J. Poesen 296

Grass Hedge Effects on Gully Hydraulics and Erosion
Dabney, S.M. , F.D. Shields, Jr., E.J. Langendoen, and D.M. Temple 298

Gully Erosion Land Use and Reclamation

Regional Ecosystem Rehabilitation on the Loess Plateau (Abstract only)
Rui, Li, Oinke Yang, Guobin Liu (Keynote) 319

Soil Structural State and Erosion by Concentrated Flow: in Situ Experiments on Three Different Cropping Systems (Abstract only)
Léonard, J., H. Boizard, J. Duval, and G. Richard.....320

Sediment from a Small Ephemeral Gully in South Carolina
Hansen, William F. and Dennis L. Law.....321

Native Plants and Fertilization Help to Improve Sites and Stabilize Gullies on the Sumter National Forest
Law, Dennis L. and William F. Hansen 344

Response of Gully Development to Land Use Change in West China (Abstract only)
Li, Yong, Lingyu Bai, Xingchang Zhang, Fuhong He, and Dignhui Liu 376

Agroecological Estimation of Grey Forest-steppe Soil of South Bug's Basin and its Erosion Reduction Methods (Abstract only)
Yerychuk, Saveta 377

Gully Erosion Prediction and Warning in Black Soil Region of Northeastern China (Abstract only)
Wu, Yongqiu, Gang Hu, and Baoyuan Liu.....378

Gullies in China: Form, Process and Control: a Comprehensive Literature Review (Abstract only)
Li, Y.Q......379

Comprehensive Gully Reclamation in the Loess Plateau, Northwest China: from Warping Dams to Gully Gardens (Abstract only)
Liu, Rengkui and Y.Q. Li 380

3rd International Symposium on Gully Erosion Panel Discussions

Panel Discussions.....382

To Table of Contents

Gully Erosion – Geographic Occurrences and Characteristics

Gully Erosion in Europe (Abstract only)
Poesen, J., T. Van Walleghem, G. Gyssels, G., J. de Vente, (Keynote)
G. Verstraeten, G., A. Knapen, A., J. Nachtergaele, and L. Vandekerckhove

Late Holocene Stages of Gully Development in the Central Part of the Russian Plain
Belyaev, V.R., E.A. Eremenko, A.V. Panin, Yu.R. Belyaev

Cutting and Refilling of a Gully System during the Last 1300 Years in Northern Bavaria, Germany (Abstract only)
Dotterweich, M. and H.-R. Bork

Gully Erosion and Environmental Degradation in the Southern Gangetic Plains, India (Abstract only)
Das Gupta, Ananda S., and R. Sinha

Natural and Anthropogenic Factors Controlling Gully Erosion in the Basaltic Upland of Rio Grande Do Sul, Brazil
Viero, Ana Cláudai, Nilza Maria dos Reis Castro, and Joel Avruch Goldenfum

Morphological Characteristics and Development of Gully Head in Arid Environment, China (Abstract only)
Wang, Xiaodan, Xianghao Zhong, Shuzhen Liu, Jianrong Fan, and Jianhui Zhang

*Investigations of the Contrasting Distribution of River-bank Gullies in the Northern and Southern Gangetic Plains Using an Integrated Approach Including Remote Sensing, Geophysical Data and Field Investigation***.** (Abstract only)
Das Gupta, Ananda S.

Keynote

Gully Erosion in Europe

J. Poesen[*], Professor of Geomorphology
T. Van Walleghem
G. Gyssels
J. de Vente
G. Verstraeten
G., A. Knapen
A., J. Nachtergaele
L. Vandekerckhove
Laboratory for Experimental Geomorphology
Katholieke Universiteit Leuven
Redingenstraat 16
Leuven, Vlaams Brabant 3000; Belgium

Abstract

In Europe gully erosion has received significant less research attention compared to sheet and rill erosion although interest in gully erosion processes is increasing. This study reviews recent research findings related to gully erosion by addressing the following questions. Where does gully erosion occur in Europe and why? What is the contribution of present-day gully erosion to overall sediment production by water erosion processes? What are the major consequences of gully erosion ? What are the major factors triggering and controlling past and recent gully erosion and infilling phases ? Do we have good gully erosion models ? How is gully erosion controlled? In general, these research results contribute a)to a better understanding of spatial and temporal patterns of gully erosion rates and factors and b) to improving gully erosion control measures. This presentation will conclude by addressing a selection of research issues/questions which need to be solved in order to better predict the impacts of environmental change on gully erosion rates and to improve gully erosion control techniques.

Keywords: connectivity, sediment yield, environmental change, erosion control

[*]Correspondence author

Late Holocene Stages of Gully Development in the Central Part of the Russian Plain

V.R. Belyaev* (E-Mail: river@river.geogr.msu.su)
The Laboratory of Soil Erosion and Fluvial Processes
Faculty of Geography, Moscow State University
GSP-2, Vorob'evy Gory, Moscow, 119992, Russia.

E.A. Eremenko
A.V. Panin
Yu.R. Belyaev
Department of Geomorphology and Palaeogeography
Faculty of Geography, Moscow State University
GSP-2, Vorob'evy Gory, Moscow, 119992, Russia.

Abstract

Two gullies located in the Protva River basin (central part of the European Russia, 100 km southwest from Moscow) have been studied in details to investigate history of their development during the Late Holocene. The case study included detailed topographic and geomorphologic survey, geological sections and subsequent radiocarbon dating of organic matter in gully sediments. For one of the studied gullies, two pollen diagrams were constructed for sediment sections from bottom infill of its upper part and its mouth. For both gullies studied, incision has been the main tendency of the long profile evolution for most of Holocene. It is proved by limited occurrence of the infill sediment. First datable interruption of incision is dated between ~3.6 and ~3.2 ka BP and observed in the Chugunkin gully only. It resulted in the fan surface stabilization and soil formation. The following intensive deposition burying that soil horizon took place in the gully lower part and on its fan only. It is dated to ~2.8 ka BP and was very intensive. No traces of that are found in its upper part. We conclude that sedimentation in the lower part of the system resulted from a few high magnitude regressive erosion events in its upper part. These stabilization and erosion-accumulation stages were most likely caused by climatic signal of regional importance, as proved by intensified aggradation and burying of soil horizon on the Protva River floodplain during that period. Beginning of the next infill period is dated as 1.5-1.8 ka BP in both of the gullies. This was most likely triggered by severe forest fire affecting large area. The following aggradation was gradual. In the Chugunkin gully fragments of that infill (terraces) are observed along its entire length except the deepest middle part. It continued until the beginning of intensive human impact, as well as in the Uzkiy gully upper part. However, in middle and lower parts of the latter, another episode of erosion and deposition took place at ~1.0-0.9 ka BP. It was also associated with forest fire, but that affected the Yazvitsy valley catchment only. The last period of active agricultural development of the study territory (~500 years) resulted in accelerated incision, followed by deposition of catchment-derived material. The latter was limited to the upper parts of the gullies, while incision has continued in the middle and lower parts until present, expanding regressively up the gullies. Similarities and differences in discovered sequences of erosion and accumulation stages for the two gullies point out the importance of distinguishing between local and regional controls.

*Corresponding author

Evidence of role of internal system behavior and self-development in gully long-term evolution is clear from asynchronous response of different parts of gullies. The contribution of human impact into evolution of the studied gullies has been very limited. This suggests that within the forest zone of the Russian Plain many gullies earlier attributed to anthropogenic impact can in fact represent essentially natural phenomena.

Keywords: gully erosion, incision and infill, environmental change, Late Holocene, human impact, Russian Plain.

1. Introduction

Studies of evolution of fluvial landforms are very important for better understanding mechanisms and processes of their development, external and internal controls (Poesen *et al.*, 2003). With a long-term reconstructions, there is also an opportunity to validate the existing information on past environmental conditions, obtained by other palaeogeographical methods. In order to confidently predict gully network behavior under changing environmental conditions in the future, we need to discover, analyze and establish causal links for similar changes in the past. However, dealing with development of small fluvial landforms such as gullies, there is always a problem of distinguishing general regional trends driven by large scale climatic changes or other major environmental variables from those of local origin and importance, characteristic for certain catchments only. Of particular interest is a problem of determining relative contribution of natural and anthropogenic factors into gully evolution. It is often arbitrarily assumed that most of the gullies on the Russian Plain have been formed as a result of human environmental impact (Zorina *et al.*, 1975; Kosov, 1978). However, detailed investigations of individual fluvial landforms point out that this is not always the case, as we aim to show in this paper.

Most of detailed reconstructions of small fluvial landform history for the Russian Plain dealt with steppe and forest-steppe zones (Panin *et al.*, 1998; Sycheva *et al.*, 1998), whereas forest zone has been paid much less attention (Panin *et al.*, 1999). It is suggested that gully network of the latter may have substantially different history of development to that of forest-steppe and steppe zones. The main reasons for that are specific geologic and geomorphic settings, different environmental change history and pattern of human impact during the last few hundred years. This study aims to compare Late Holocene evolution of two gullies chosen in the south of the Russian Plain forest zone.

2. Area Description, Methods and Material Studied

The case study area is situated in the centre of the Russian Plain, about 110 km to the south-west from the Moscow (Fig. 1). Modern landscape conditions and relief morphology both make the study area typical for the humid temperate centre of the Russian Plain. It is a southern terminal area of the Middle Pleistocene (Moscow, Riss, Illinois age) glaciation. During the Late Pleistocene, the territory has been subject to severe periglacial climate resulted in serious relief transformation. Major intensification of erosion processes took place during the transition from the most severe Late Pleistocene conditions (20-15 ka BP) to mild Early Holocene climate. During this period, permafrost thawing led to surface instability and increased runoff, whereas vegetation was not developed enough to protect soil surface from erosion processes. It is believed that many of gullies and small valleys of central European Russia have been formed or undergone significant transformation during that period.

Both studied gullies are located on slopes of water divide between the Protva River and its left tributary – the Isma River (Fig. 1), but drain opposite sides of that interfluve. The Chugunkin gully (Fig. 1, 2) drains the southern aspect convex slope of the Protva River valley. Its length is ~400 m, height range between its head and base of its fan ~32 m. Base of the gully fan is on the surface of the Protva River high-level floodplain (about 3 m above the mean river level). The Uzkiy gully (Fig. 1, 3) is located on the northwestern aspect convex slope of the Yazvitsy small valley, right tributary of the Isma River. Its length is ~250 m, height range between its head and mouth ~22 m. The gully has no depositional fan, only limited sedimentation is observed in its lower part.

Gully morphology was studied in the field and using 1:5000 topographic maps. Detailed investigations of geological structure of both gullies were carried out at locations where gully sediments from earlier stages of its evolution were expected to be observed. Additional information on geological structure of gully slopes was acquired from descriptions of deep coring program carried out earlier for general geological survey purposes (unpublished sources). A number of radiocarbon dates of gully infill and fan sediment were obtained by analyzing fossil organic matter and buried soils (Table 1). Samples were analyzed in radiocarbon laboratory of the State Centre of Environmental Radiogeochemistry National Academy of Science of Ukraine (Kiev) by Dr. N.N. Kovalyukh. All dates in the text below are in non-calibrated radiocarbon timescale. Pollen analysis and interpretation of results for two sediment sections from the Uzkiy gully was carried out by Dr. I.A. Karevskaya (Department of Geomorphology and Palaeogeography, Faculty of geography, Moscow State University).

3. Results and Analyses

Morphology and geology of the studied gullies

The Chugunkin gully

Long profile and geological structure of the Chugunkin gully is schematically presented on the Figure 2. The general long profile shape is slightly concave (average gradient ~0.08), with convexity in the upper part resulted from the Late Holocene aggradation. Cross profile is box-shaped in the upper ~100 m and lower ~100 m, with V-shaped in the middle. Three prominent nickpoints (about 100, 130 and 220 m below the main gully head) observed in the modern gully thalweg reflect its continuing modern incision.

The gully has large depositional fan overlying alluvial sediment of the first terrace and floodplain of the Protva River. Fragments of depositional surface cut by modern incision (terraces) are also observed within the gully, except its deepest middle part. The upper part (about 100 m from the main gully head) has flat depositional bottom not yet reached by the last erosion cycle. According to radiocarbon dating of sediment exposed in the section Ch-3 (Fig 2) it was formed during the last pre-anthropogenic aggradation stage (~1.5-1.8 ka BP). Upward decrease of sediment coarseness in that section suggests a shift from gully-derived to catchment-derived material. The boundary at a depth of 16 cm dated as no younger than 550±110 BP (Fig. 2) is believed to represent base of anthropogenic sediment layer.

In the deepest middle part of the gully no sediment is found, the gully is cut into interbedded Middle Pleistocene glaciofluvial and limnoglacial material. In the lower part, terraces formed by sediment similar to that observed in the section Ch-3 are observed. However, only upper layer of that sediment, represented by loamy material, can be correlated to that from the section Ch-3, as suggested by date from the section 1 (1810±50 BP). The lower sediment layer characterized by coarser texture was deposited earlier. It is observed throughout the gully

lower part and fan, where it is underlain by buried soil horizon dated between ~3.2 and 3.6 ka BP. Deposition of that layer was relatively rapid on the fan and much slower up the gully, as evident from comparison of dates from its top in the section 6 (2825±60 BP) and its base and middle part in the section 2 (2880±70 and 2230±60 BP) (Fig. 2). Oldest material found in the gully fan underlies the buried soil horizon. Lowest part of this sandy loam sediment layer of complex alluvial and colluvial origin contained no datable material. Nevertheless, from stratigraphic consideration it can be suggested that it represents initial stage of gully development relatively dated between ages of the Protva River first terrace and floodplain.

The Uzkiy gully

The most profound difference of the Uzkiy gully from the Chugunkin gully is in the absence of depositional fan and very limited occurrence of remnants of bottom infill (terraces), which are found only in its upper part and mouth (Fig. 3). The general long profile shape is also slightly concave (average gradient 0.09), but the concavity is less developed. This results from more resistant material (Middle Pleistocene boulder clays) cut by the gully in its middle and lower parts. The gully cross profile is box-shaped for upper ~30 m and lower ~60 m, the rest is V-shaped. Numerous actively eroding nickpoints, of which only a few could have been adequately shown in a scale of Figure 3, show that the Uzkiy gully is at present incising along its entire length.

Absence of the Uzkiy gully fan in the Yazvitsy valley bottom suggests that the sediment delivered from the gully during its first and most active stage of incision was relatively quickly removed by the recipient stream. Depositional surface in the gully lower part cut by the modern incision extends only about 60 m up the gully. Further up the gully it has been destroyed by the following erosion stage. Composition of that sediment is essentially simple, as can be seen from sections TE-4 and TE-5 (Fig. 3). It consists of lower coarse basal layer, resulted from erosional reworking of underlying glacial boulder clay, and aggradational layer composed of loamy material with some coarse particles, sandy and gravely lenses. Base of the latter was dated in section TE-4 as 1040±70 BP. Pollen analysis showed no evidence of cultural vegetation during deposition of that layer.

Middle part of the gully is completely erosional, almost no traces of sedimentation are observed. Important morphological features of that part are numerous small tributary gullies (not shown on Fig. 1 because of generalization) with hanging mouths at some 0.8-1.0 m above the modern thalweg. Only one of those contained a small remnant of fan sediment in its lower part. Base of the fan sediment was dated as 960±70 BP.

The oldest gully sediment observed in the Uzkiy gully upper part infill (Fig. 3, section TE-1) was dated as 1760±100 BP. Underlying older material in that section represent the Late Pleistocene infill of initial slope depression, formed by intensive solifluction during the domination of periglacial conditions. Solifluctional origin of that material is evident from specific sedimentary structures observed (Fig. 3, section TE-1). This depression bottom was subsequently cut by the developing gully.

The overlying lowest layer of the gully infill sediment (Fig. 3, section TE-1) can be subdivided into two sublayers. Lower lens of loamy sand material with some coarse material at the base, from which the above date was obtained, is believed to represent initial regressive erosion into the periglacial slope depression bottom, the following lateral migration and limited sedimentation in the gully bottom. Upper sublayer (up to depth 1.2 m in the eastern part of section TE-1, Fig 3) composed of thinner laminated sandy and silty loam reflects the phase of slow and continuous infill. Pollen analysis shown no traces of cultural vegetation in that layer.

Relatively weakly developed humic horizon formed along the upper boundary of that layer shows the position of former gully bottom during short phase of stabilization. Dates from the top of the humic horizon (220±100 BP) and from charcoal lens inside it (430±100 BP) shows that its burying was probably associated with beginning of intensive agricultural development of the area.

This conclusion is further supported by evidences from the upper sediment layer in the section TE-1 (Fig. 3). Its thin silty loam composition, visible lamination and brownish-gray color suggests that this sediment was originated from intensive topsoil erosion from cultivated parts of the gully catchment. This is also proved by abundance of cultural vegetation pollen grains in that layer. Analysis of sediment stratigraphy in the section TE-1 (Fig. 3) brings us to conclusion that gully infill represented by the upper sediment layer was preceded by fast phase of regressive erosion and channel lateral migration (probably, just few events) when part of the buried humic horizon and lower sediment layers was destroyed and western gully bank was downcut (central and western part of section TE-1, Fig. 3).

The Late Holocene evolution of the studied gullies

The Chugunkin gully

Incision was most likely the main tendency of the both studied gullies evolution until the Late Holocene, as proved by the long profile morphology and lack of the infill sediment. Therefore, precise information on the earlier stages of their evolution is unavailable. It can only be suggested that the Chugunkin gully was most likely formed during the transitional period from the Late Glacial to Early Holocene. Some indirect support is provided by analyses of geology of the Chugunkin gully fan. Beginning of its deposition can be relatively dated between the Late Valday alluvial sediment of the Protva River first terrace below it (index aQ_{III}^{os} on Fig. 2, dated as deposited between ~25 and ~10 ka BP – Antonov *et al.*, 1989) and palaeochannel infill near its distal part (index $a_{st}Q_{IV}$ on Fig. 3, beginning of infill dated as 7830±190 BP). Some limited episodes of aggradation might have taken place afterwards. But, as all possible traces of those are destroyed by later erosion, cumulative effect for long-term gully evolution may be considered as negligible.

First datable stage of the Chugunkin gully development was associated with increased precipitation and runoff reconstructed for the study area and other areas of Central Russian Plain at about 3.0 ka BP (Fig. 2, 4a,c). This resulted in accelerated incision in the most of the gully length and substantial sedimentation in its lower part and on its fan. Dating of this sedimentation is available from sections 2, 5 and 6 (Fig. 2). Palaeosol horizon buried during that stage of active erosion-accumulation is observed within both gully fan and the Protva river floodplain, suggesting that the preceding stabilization phase in fluvial landform development also was of regional importance (Fig. 2).

In the upper part of the Chugunkin gully incision was interrupted between 1.8 and 1.5 ka BP (Fig. 4b). The aggradation was most likely triggered by large forest fire, traces of which are also observed in other sedimentary records from small fluvial landforms of the study area (sections Ch-3 and 1, Fig. 2). Subsequent sedimentation was gradual and continuous. Its traces are also observed in the gully lower part, but corresponding sediment thickness there is lower.

In the gully upper part aggradation has not been interrupted by the beginning of intensive cultivation in the area at ~0.5 ka BP (Fig. 4b). Anthropogenic sedimentation is believed to have been limited to the upper part of the gully, in section Ch-3 only ~0.20 m of sediment was accumulated (section Ch-3, Fig. 2). By contrast, lower and middle parts of the Chugunkin gully

experienced accelerated incision. This was caused by anthropogenic increase of runoff that was not balanced by increased sediment load as most of catchment-derived sediment was intercepted by the gully upper part (Fig. 2, 4b). Recently the upper gully part was reached by the upper nickpoint retreat. As a result, depositional surface was partly cut by modern reincision channel and terraces were formed.

The modern incision cycle in the Chugunkin gully is obviously tended to reestablish its older buried long profile. At present, not much sediment is delivered to the system from catchment as cultivated area has recently substantially shrunk. Within-gully sediment delivery is close to 100%. There are no visible traces of within-gully sediment redeposition. All eroded material is delivered to the gully fan, where it is partly accumulated mainly on the segment to the east from sections 4, 5 and 6 locations (Fig. 1, 2), partly moved further to the Protva River floodplain (thinner particles mainly).

The Uzkiy gully

For the Uzkiy gully, all fan sediment was remobilized by the recipient Yazvitsy valley stream. From the absence of the fan we conclude that that most of the gully volume was formed no later than the time of a high runoff period in the Yazvitsy stream, dated back to the Atlantic – Subboreal transition (5.0-4.5 ka BP). Otherwise it would not be possible for the Yazvitsy stream to completely rework such a large volume of sediment (approximate estimation of the gully volume gives about 16200 m^3 equivalent to about 24300 t), because during the Late Holocene its discharges were lower and relative stability or aggradation prevailed in the valley (Panin *et al.*, 1999).

Similarly to the Chugunkin gully, there is no evidence of interruption in general incision trend during most of the Uzkiy gully evolution in its morphology and geological structure. First evidences of aggradation are available for the upper gully part at about 1.7 ka BP. It can be argued that slow but continuous aggradation occurred there for about 1 ka (Fig. 4a). It was most possibly associated with internal system controls realized by long profile self-development. But the environmental trigger for beginning of aggradation could be large forest fire, which traces are found also in sedimentary records of the Chugunkin gully and some other small fluvial landforms nearby. The aggradation was followed by relatively short period of stability associated by humic horizon formation. Its notable gradient towards the modern thalweg suggests that the infill phase presiding stabilization was not complete and gully upper part shape remained prominent (section TE-1, Fig. 3).

Another aggradational phase traced by the gully lower part terraces and hanging mouths of tributary gullies along most of the main gully length was more intensive and prominent (Fig. 4a). Its traces are seen in the section TE-2, but it did not reach section TE-1a and TE-1 (Fig. 3). From available evidences and data from the recipient Yazvitsy stream, where that deposition was also dated previously (Panin *et al.*, 1999) it can be concluded that its deposition ceased before ~500 BP when intensive cultivation in the area is known to begin. Sediment texture and structure also suggest relatively fast aggradation. Date from the base of the tributary gully fan proves its formation during the same depositional cycle, as the main gully fan. Relative height of tributary gully hanging mouths above the main gully modern thalweg shows that those had former depositional surface produced by that aggradation in the main gully bottom as an erosion baselevel.

We conclude that aggradation was associated with forest fire affecting mainly the Yazvitsy valley catchment. This conclusion has support from the Yazvitsy valley sedimentary record (Panin *et al.*, 1999). It triggered tributary gully development and soil erosion on steeper

catchment slopes during a few years following destruction of vegetation. The main gully was overloaded with sediment, but its influx was soon ceased after vegetation regrowth and tributary gullies stabilization. The aggradational bottom formed was not in equilibrium with normal gully runoff and quickly became subject to erosion.

The following period of incision was prolonged (Fig. 4a). It destroyed most of the infill sediment and resulted in hanging of the tributary gully mouths. Incision was accelerated by coincidence of the general trend of the gully evolution with shorter-term reaction of its long profile on preceding aggradation resulted in increased thalweg gradients. Its beginning was most possibly triggered by the anthropogenic influence – increased runoff from the cultivated part of catchment. This regressive incision occupied almost the entire gully length.

In the lower part of the gully incision was limited by the position of the baselevel associated with the recipient Yazvitsy stream. In the upper part initial incision was fast but very short. The following infill of the Uzkiy gully upper part by the catchment-derived anthropogenic sediment was complete, but did not expand far down the gully as seen from limited extent of the upper part depositional surface (Fig. 3). In the middle part incision and regressive nickpoint erosion has continued until present. Recently it reached upper part of the gully and resulted in the cutting of the anthropogenic gully infill sediment, almost down to the initial pre-anthropogenic thalweg. Morphological evidences show that the Uzkiy gully at present experiences strong tendency of incision and regressive growth, probably except its lower part controlled by the relative stability of erosion basis – the Yazvitsy valley bottom.

4. Discussion and Conclusions

Comparison of geological structure and reconstructions of the Late Holocene evolution of the studied gullies shows that general similarity is observed. Both gullies are characterized by general domination of incision tendency during longer-term evolution. However, during the Late Holocene it was interrupted by limited aggradation episodes. Main similarity is associated with reconstruction of the last stages of infill and incision reflected in sediment records from the upper part of both gullies. Major events of the both gullies evolution during the Late Holocene are summarized in Figure 4, together with suggested environmental controls.

First important stage of development during the Late Holocene is intensification of erosion and sediment delivery from gullies associated with increased precipitation and (hypothesized) runoff at about 3.0 ka BP (Fig. 4). Traces of that phase are found in the Chugunkin gully only. But from generally widespread occurrence of that in fluvial sedimentary records all over the region (burying of soil horizon in the Protva River floodplain, Fig 2) (Panin & Karevskaya, 2000), that can also be inferred for the Uzkiy gully. Domination of erosion and absence of the depositional fan for the latter does not allow to find any direct evidences of that phase in the latter.

The next stage associated with relatively slow continuous aggradation started at about 1.5-1.8 ka BP was associated with more localized event – severe forest fire (Fig 4). However, it relatively equally influenced both studied catchments, as well as a few catchments nearby. Therefore it can be treated as general feature for evolution of fluvial landforms of the studied locality.

Another fire-induced erosion-accumulation event was traced for the Uzkiy gully catchment only. More general investigation of the recipient Yazvitsy stream valley carried out earlier suggests that this forest fire was important event in the entire Yazvitsy catchment (Panin

et al., 1999). From the present data, however, it can be seen that it did not affect even the nearby catchments, so should be considered as a catchment scale event.

To determine exact cause of the both forest fires remains problematic. It is known that pre-Slavonic and Slavonic tribes populated the area for more than 2 ka. They knew and applied "cut-and-burn" cultivation practice, so one or both fires might be anthropogenic. It is rather likely for the later one, although its area also seems too large (the entire Yazvitsy catchment has an area of ~6 km^2). Unfortunately no direct evidence of that has been found. Ceramic pottery piece found at the base of gully infill in the section TE 2 (Fig. 3) proves that area was visited by men, but this evidence does not seem to be enough for any precise conclusion.

Limited contribution of human impact into evolution of the studied gullies suggests that profound differences in the gully network development exist between forest zone on one side and forest-steppe and steppe zones on the other. This can most likely be related to differences in geology and vegetation. Forest zone on the Russian Plain approximately coincides with the Middle Pleistocene (Moscow) glaciation zone. In forest zone, a presence of resistant glacial boulder clays predetermines the general trend of incision, and rapid vegetation succession limits erosion and mass wasting processes on gully banks and infill by colluviation for most of the gully development period. Under such conditions, the complete cycle of gully evolution from initiation to infill and stabilization can last for hundreds and thousands years. By contrast, in forest-steppe and steppe zones, thick cover of easily erodible Late Pleistocene loessy loams and weaker vegetation favor rapid changes from intensive incision to infill mainly by bank-derived material. The complete cycle of gully thus shrinks to few tens of years. Therefore, for large gullies in forest zone, period of intensive cultivation affects only small part of evolution cycle, whereas in forest-steppe and, especially, steppe zones it can include more than one complete cycle of gully incision and infill. Within the forest zone of the Russian Plain many gullies earlier attributed to anthropogenic impact can in fact represent essentially natural phenomena.

Observed differences in tendencies of development between different parts of individual gully show an importance of internal controls, thresholds, relaxation periods and complex response in gully systems evolution. Those must be always taken into consideration when predicting gully reaction on future environmental change. Of the most importance seem to be the observed for both studied gullies superimposition of longer-term development tendencies onto shorter-term fluctuations and individual erosion-accumulation events.

Acknowledgement

This work has been made possible by financial support of the Russian Fund for Basic Research (RFBR) grant No. 03-05-64021. Authors are grateful to all those involved in the fieldwork activity which was necessary to collect the data discussed in this paper.

References

Kosov, B.F. (1978). Rel'efoobrazuyuchaya rol' antropogennoy ovrazhnoy erozii (Role of anthropogenic gully erosion in relief formation) (in Russian with English summary). *Vestnik MGU. Series 5, Geography*. 5, 19-26.

Panin, A.V., & Karevskaya, I.A. (2000) Istoriya formirovaniya poimy reki Protvy v predelah Satinskogo poligona MGU. (History of the Protva river floodplain near the Satino key site) (in Russian with English summary). *Vestnik MGU. Series 5, Geography.* 4, 52-62.

Panin, A.V., Karevskaya, I.A., & Markelov, M.V. (1999). Evoluciya doliny ruchiya Yazvitsy (bassein sredney Protvy) vo vtoroy polovine Golocena. (Evolution of Yazvitsy stream

valley (middle Protva basin) in the second half of the Holocene) (in Russian with English summary). *Vestnik MGU. Series 5, Geography.* 2, 63-72.

Panin, A.V., Malayeva, E.M., Golosov, V.N., Ivanova, N.N., & Markelov, M.V. (1998) Geologo-geomorphologicheskoe stroenie i Holocenovaya istoriya razvitiya Berestovoy balki (Rostovskaya oblast). (Geologic-geomorphologic structure and development of berestovaya ravine (Rostov region) during Holocene) (in Russian with English summary). *Geomorphology*. 4, 70-85.

Poesen, J., Nachtergaele J., Verstraeten, G., & Valentin, C. 2003. Gully erosion and environmental change: importance and research needs. *Catena*. 50, 91-133.

Sycheva, S.A., Chichagova, O.A., Dayneko, E.K., Sulerzhitskiy, L.D., & Uzyanov, A.A. (1998). Etapy razvitiya erosii na Srednerusskoy vozvyshennosty v Golocene. (Erosional stages on the Middle-Russian upland in Holocene) (in Russian with English summary). *Geomorphologiya*. 4, 12-21.

Zorina, E.F., Kosov, B.F., & Prokhorova, S.D. (1975). Opyt ucheta roli antropogennogo factora v razvitii ovrazhnoy seti v stepnoy i lesostepnoy zonah Evropeiskoy territorii SSSR (Contribution of anthropogenic factor into gully network development in steppe and forest-steppe zones of the European USSR) (in Russian with English summary). *Vestnik MGU. Series 5, Geography.* 6, 63-72.

List of Figures

Figure 1. The case study site location and general schemes of the Chugunkin gully and the Uzkiy gully catchments.

Figure 2. Long profile and geology of the Chugunkin gully.

Figure 3. Long profile and geology of the Uzkiy gully (for legend see Fig. 2)

Figure 4. Schematic reconstruction of main tendencies of the Uzkiy gully (a) and the Chugunkin gully (b) evolution during the Late Holocene and suggested environmental controls (c).

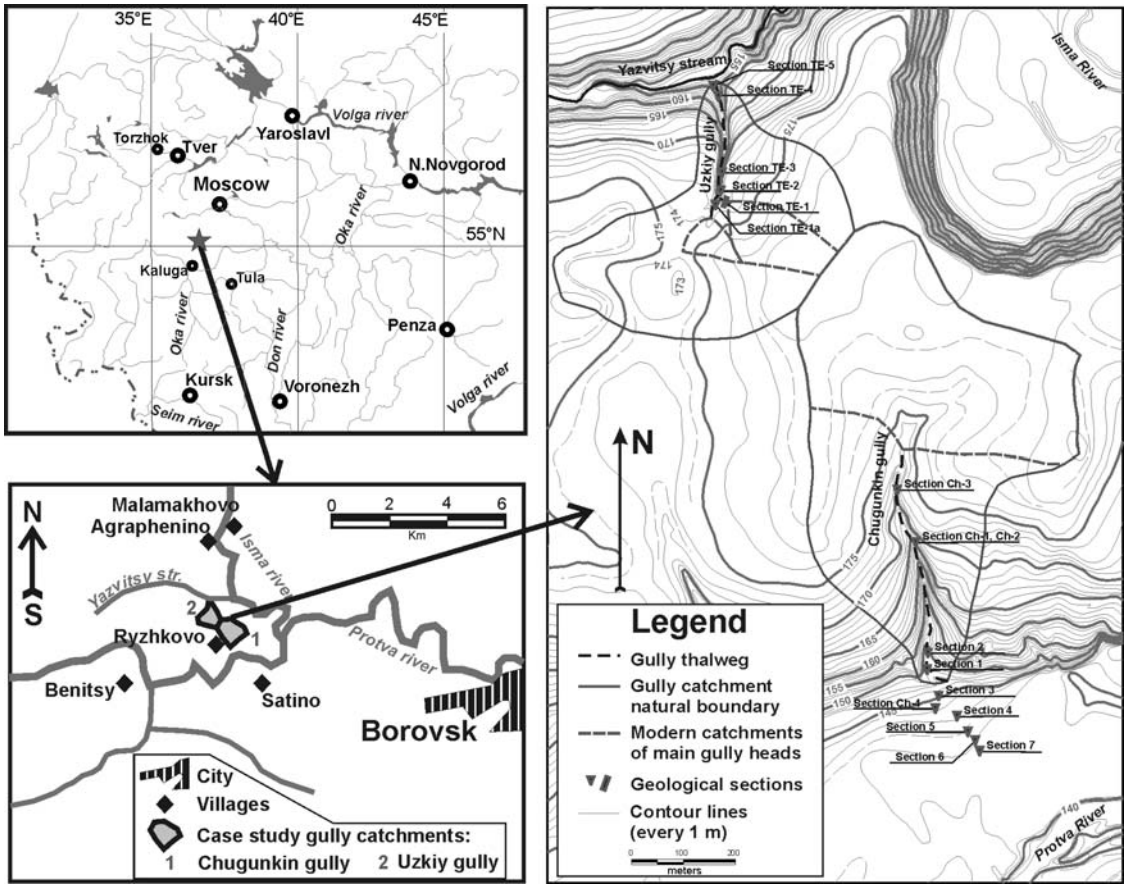

Figure 1. The case study site location and general schemes of the Chugunkin gully and the Uzkiy gully catchments.

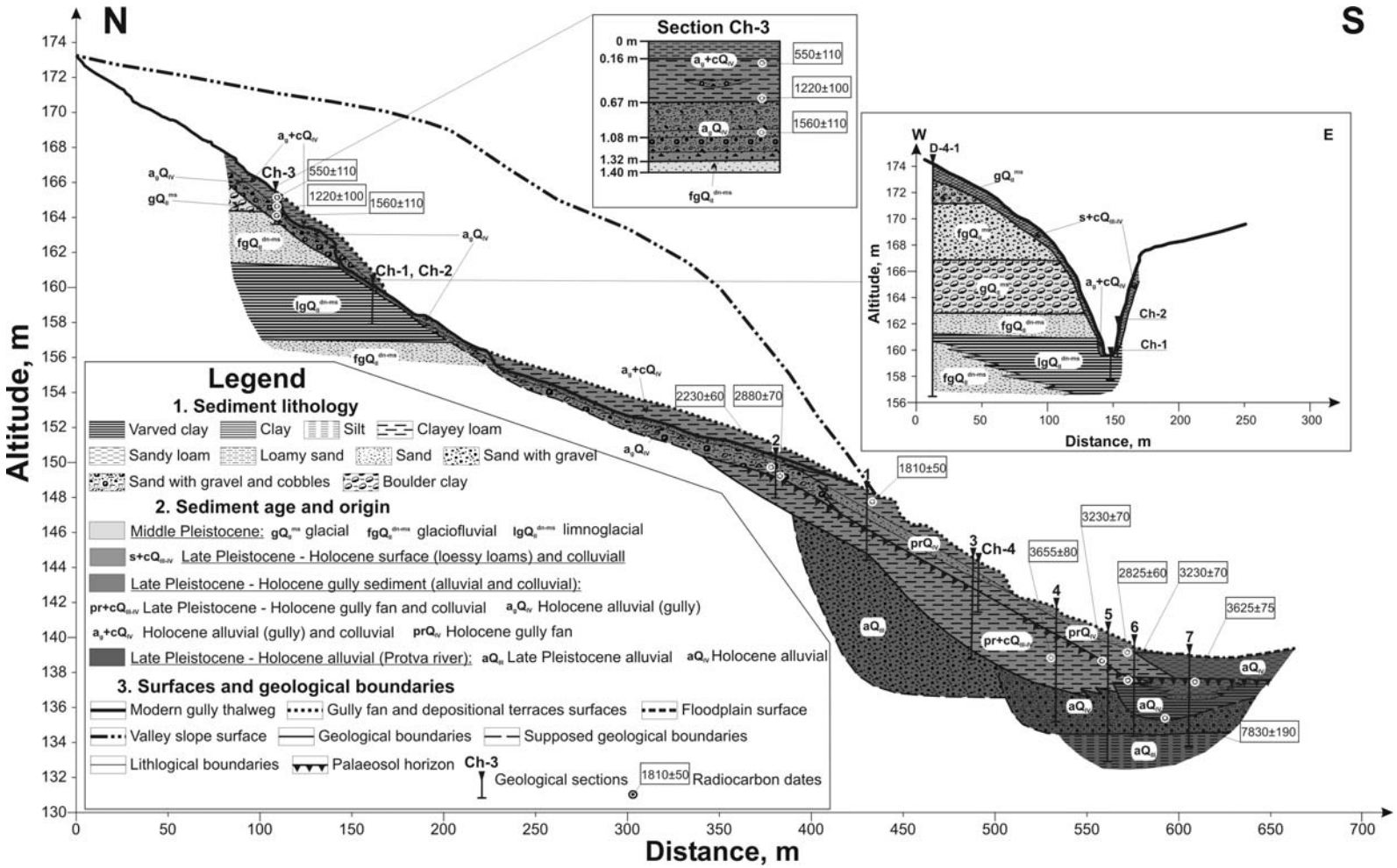

Figure 2. Long profile and geology of the Chugunkin gully.

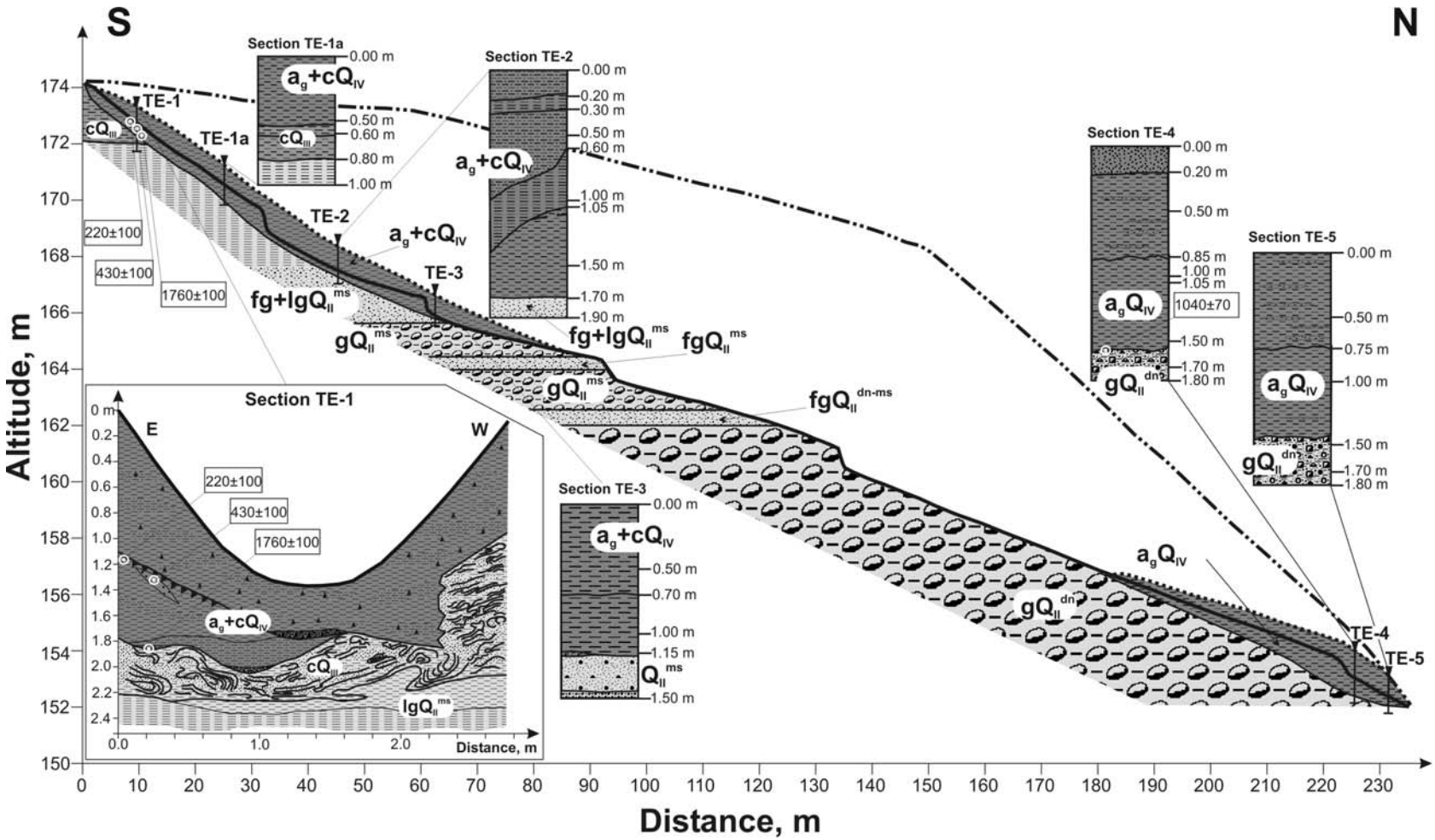

Figure 3. Long profile and geology of the Uzkiy gully (for legend see Fig. 2)

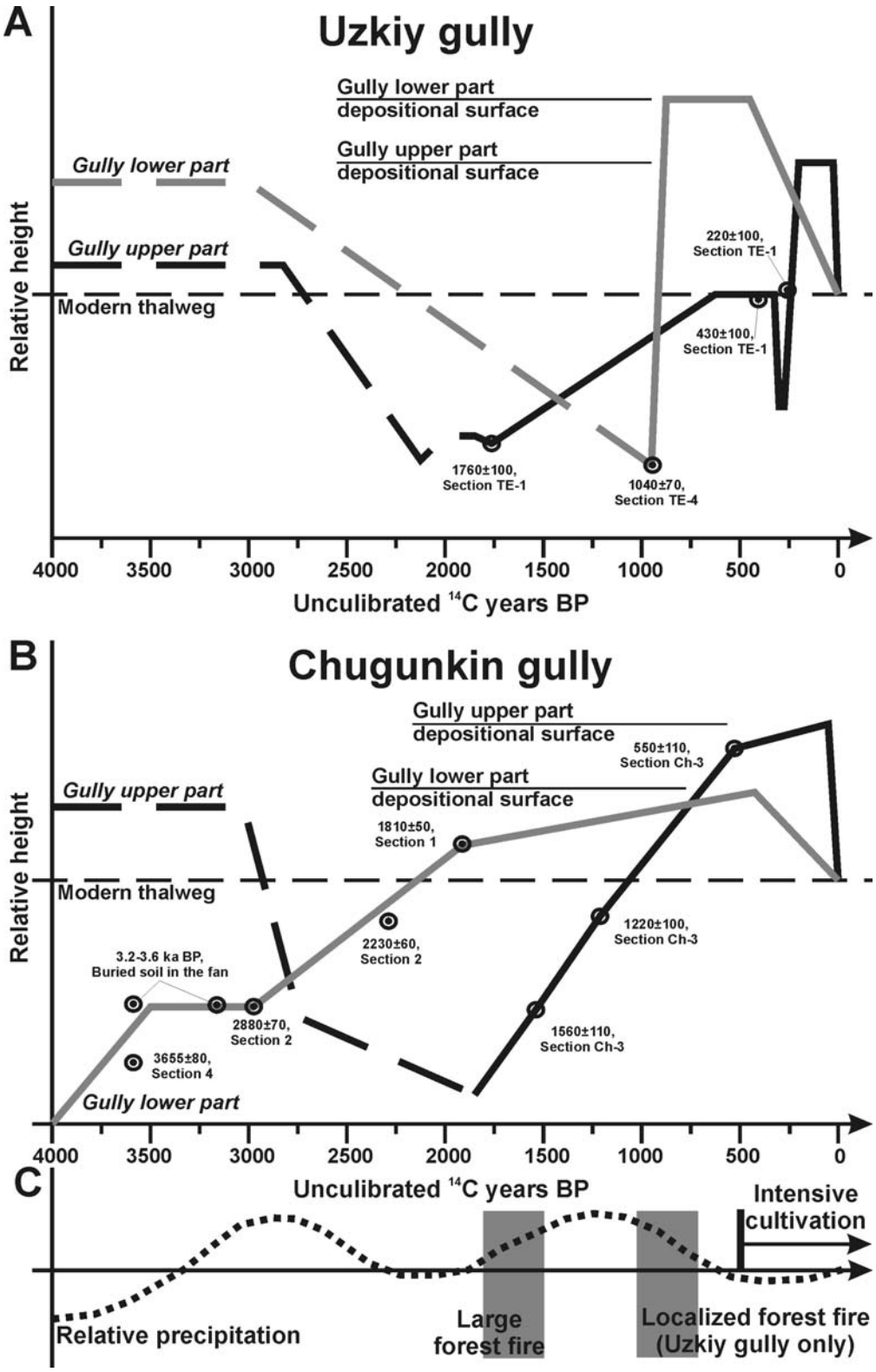

Figure 4. Schematic reconstruction of main tendencies of the Uzkiy gully (a) and the Chugunkin gully (b) evolution during the Late Holocene and suggested environmental controls (c).

Cutting and Refilling of a Gully System during the Last 1300 Years in Northern Bavaria, Germany

Marcus Dotterweich
Institute of Environmental Science, University of Koblenz-Landau, Fortstrasse 7,
76829 Landau, Germany
Phone: ++49 (0) 6341 280 328, Fax: ++49 (0) 6341 280 367,
E-mail: mail@marku0s-dotterweich.de

Abstract

The onset of agricultural practices around 5,000 years BC changed the European landscape significantly. Woodland clearance and subsequent farming facilitated soil erosion. Runoff caused by heavy rainfall events eroded the bare surfaces of arable land.

The accumulation sequences of these soil erosion events can be found as colluvial fans and terraces of gullies or in small sedimentary basins. In Central Europe peaks of soil erosion due to human impact have been reconstructed for the Bronze Age, the Iron Age, late Middle Ages and modern times.

At the location Hainbach in northern Bavaria, more than 150 colluvial layers found in a gully-system revealed the detailed history of gully development during the last 1,300 years.

First gullying took place in early Middle Ages during several heavy rainfall events. In high Middle Ages the gully head grew upslope while the sediments filled the lower parts of the gully.

In late Middle Ages land use changed the runoff pattern. Farming terraces and field borders enlarged the catchment area by 50%. Subsequently overflowing field furrows led to the development of two gullies in late medieval and early modern times. Up to 6 m deep, these gullies cut into the clayey-sandy material.

The following time was dominated by sheet erosion in the catchment area visible as clay layers in the sediment sequence.

From the middle of the 19th century until today only little soil erosion has taken place. Most of the catchment area has turned into grassland or forest.

During the 1,050 years from 800 AD to 1850 AD a soil volume of about 6,430 m³ was eroded by gullying. It destroyed 15% of the arable land.

Keywords: historical gully erosion, erosion events, quantifying soil loss, modelling long term gullying, Northern Bavaria

Gully Erosion and Environmental Degradation in the Southern Gangetic Plains, India

Ananda S. Das Gupta*
R. Sinha
Indian Institute of Technology Kanpur
India, 303B, WLE, Department of Civil Engineering
IIT Kanpur, Kanpur
Uttar Pradesh 208016, India

Abstract

The Gangetic Plains of northern India constitute one of the world's most extensive alluvial tracts in the Himalayan foreland basin. The southern fringe of these plains is marked by an extensive network of gullies and ravines ('badlands') unlike the rest of the plains which are devoid of any such gullies. The gullies are characteristically river-bank gullies, with their depths varying from 20m to nearly 80m. A study of the regional distribution of these gullies through satellite imagery and digital elevation models generated from topographic sheets has been carried out. Of the two major rivers draining the Gangetic plains, viz Ganga (in the north) and Yamuna (in the south), the Yamuna banks are extensively gullied whereas gullying is absent along the banks of Ganga and all other smaller rivers north of Yamuna. Further observations reveal that the gullying in the Yamuna river starts downstream of the near-easterly bend near Agra, just upstream of its confluence with two major peninsular rivers, Chambal and Betwa. Both Chambal and Betwa river banks are strongly gullied and both of them flow northerly from the cratonic area (Bundelkhand Granite Massif) lying to the south of the Gangetic plains. It would seem therefore that these tributaries from south influence the hydrological budget of the Yamuna river leading to incision and floodplain dissection. The standard FCC prepared from the multispectral data reveals distinctly different spectral characteristics of the regions north and south of Yamuna. On the Normalised Difference Vegetation Index map of the area, we pick out a distinct class in the region south of Yamuna characterized by very low moisture content and thin soil cover with scanty vegetation. The DEM of the region shows a distinct variation in the overall topography north and south of Yamuna, thus emphasizing the role of surface topography on gully formation and distribution. A map of the basement configuration based on regional geophysical data shows that the cratonic basement underneath the plains are shaped in a convex bulge. Further, the course of Yamuna after its easterly bend (mentioned earlier) nearly follows one of the subsurface contours. A comparison of the DEM and basement contour map shows that the thickness of alluvium reduces drastically to the south of Yamuna due to the effect of the basement topography. It seems that the formation of gullies in the southern Gangetic plains are controlled by a variety of factors such as hydrological budget, soil characteristics and basement topography. Further work is continuing to collect additional field data and also to establish anthropogenic effects, if any.

*Correspondence author

Keywords: hydrological budget, basement topography, DEM, satellite imagery

Natural and Anthropogenic Factors Controlling Gully Erosion in the Basaltic Upland of Rio Grande Do Sul, Brazil

Ana Cláudai Viero* (E-mail: anaclaudia@pa.cprm.gov.br)
Nilza Maria dos Reis Castro (E-mail: nilza@iph.ufrgs.br)
Joel Avruch Goldenfum (E-mail: joel@iph.ufrgs.br)
Alfonso Risso (E-mail: risso@iph.ufrgs.br)
CPRM-Geological Survey of Brazil
Rua Banco da Provincia 105
Morrow Santa Teresa
Porto Alegre, RS 90.840-030, Brazil

Abstract

This paper describes an analysis of natural and anthropogenic factors controlling the evolution of gullies in a rural basin in the basaltic upland in the State of Rio Grande do Sul, Southern Brazil. In this region of deep ferrallitic soils with more than 60% clay, runoff and the consequent erosion are of increasing concern. A change in land use, from conventional tillage using disc plough to no-tillage on residues without terracing, began in the 1990s and spread rapidly, with crops of soya taken in summer and wheat in winter.

In the Taboão drainage basin (100 km^2), factors affecting gully erosion were studied by field survey and measurements of rills and gullies. Eighty-four gullies were identified and mapped, with average length 136 m, width 10 m, depth 3 m deep and volume 15.458 m^3; the volume of the largest was 819000 m^3. Each gully was characterised in terms of factors that included slope, geological structure, presence of piping, drainage, soil use, and the presence of surface and subsurface flow. The evolution of gully structure was also monitored from 1991 to 2003. On average, the main channels of gullies show falls from 2 m to 7 m, and their evolution in the vertical plane increases until bed-rock basalt is reached, after which gullies increase in width and length. Subsurface flow appears to be the principal agent controlling their evolution. Results show that both natural (slope, surface curvature, geological structure and rainfall) and anthropogenic (soil use, road construction) factors are important factors in gully evolution. The change in cultural practice throughout the drainage basin from conventional to direct sowing has led to increased subsurface flow, and this was shown to be more important than surface runoff for increasing erosion. However, the higher rainfall during ENSO events and the consequently higher subsurface flow were the dominant factors in the process. From 1991 to 2003 a total land loss of 1013 m^3 was observed in one gully, with 236 m^3 lost during the 1992 ENSO and 702 m^3 during the 1997 ENSO; 95% of the total volume lost occurred during ENSO periods.

Keywords: gully, drainage basin, basaltic upland, geological structure, subsurface flow, no-tillage

*Corresponding author

1. Introduction

Throughout history, erosion has inflicted damage on human society. The main effects and damage caused by erosion and sediment transport are in terms of the following: agricultural soil degradation; losses of agricultural yield, due to deposition of sediments; flooding of agricultural areas, due to obstruction of natural drainage; maintenance costs of drainage and irrigation systems; need for water treatment for industrial and domestic use; maintenance costs of roads, railroads and oil networks; cost of sediment removal from flooded areas.

Gully erosion is identified as the most complex and complete of all erosion processes, with great local destructive power (São Paulo, 1990). This characteristic is the result of the many processes that occur in gullies, including surface erosion, internal erosion caused by piping, landslides and collapse of lateral walls.

The design of erosion control projects and the adoption of adequate land use and occupation practices is only possible when the characteristics of the natural and anthropogenic factors that control the formation and evolution of erosive processes are known (Guerra 1998, Guerra 1999).

This paper describes a study in the drainage area of the Taboão creek (approximate area: 100 km^2) which is part of the Potiribu River basin (approximate area: 563 km^2), considered by Bordas and Borges (1990) as representative of the South American Basaltic Plateau (230,000km^2 including Rio Grande do Sul, Santa Catarina and Paraná states, in Brazil) because of its physical and climatic characteristics and erosive potential. Most of the catchment is used for intensive agriculture, which has led to severe erosion in rills and gullies

The purpose of the present work is to identify natural and anthropogenic factors influencing gully development in this 100 km^2 catchment through the use of geoprocessing techniques combined with field work. The natural factors analysed in this work consist of some variables related to geology, geomorphology and soils, more specifically: lithology and geological structures, terrain slope, flow acumulation area, plan and profile curvature, and soil type. The anthropogenic factors analysed are land use and runoff concentration promoted by some anthropic building. The evolution of a gully during a tem-years period is described and discussed.

2. Area Description, Methods and Material Studied

2.1. Area description

The Taboão catchment lies in the northwestern part of the State of Rio Grande do Sul (Figure 1) with an area close to 100 km^2. The Taboão creek is a tributary of the Potiribu River, which in turn joins the Ijuí River. The Ijuí is a tributary of the Uruguai River, draining part of the la Plata basin.

Geology – The area under study shares the geological context of the Paraná Basin, which occupies a surface of 1,200,000 km^2 in Brazil, Uruguay, Paraguay and Argentina. The Paraná Basin is an intracratonic sedimentary basin, aligned roughly northeast-southwest, paralleling to structural trends of the underlying basement. The earliest, Paleozoic, sediments are largely marine siliciclastics, but the Mesozoic sequences are exclusively continental sediments that culminate in the aeolian sandstones of the Jurassic Botucatu Formation. The Early Cretaceous lavas were erupted subaerially directly onto the Botucatu sandstones all over the basin, giving rise to the volcanic rocks of the Serra

Geral Formation. The aeolian sandstones persist as intercalations within the lava sequences indicating arid and desert-like climatic conditions throughout the period of lava eruption (Peate, 1997). In the intermediate and superior levels of the lava sequences intercalations of thin layers of volcanogenic sediments occur that are not related to the desertic system of the Botucatu sandstones (Wildner *et al.*, 2003).

In the Taboão catchment, the rock outcrops are related to Serra Geral basalts and to sediments inserted into the basic volcanic sequence.

The evenly distributed orientation of the structures present in the area under study indicates that it was uniformily subjected to the influence of the structural patterns of the basement beneath Paraná Basin. Small multidirectional lineaments predominate, with high-density distribution and bigger concentration sectors in the NE and NW orientations.

Geomorphology – The regional relief is characterised by a homogeneous dissection with gently-rounded hills, regionally known as "*coxilhas*" (Fundação, 1986). The drainage density is low and the depth of river valleys ranges from 22 to 28 m. River channels generally have sub-vertical, regular walls, showing that the drainage network is controlled by geological structures. The relief varies between 330 and 495 m, with mean a catchment slope of 8%, although gradients from 10 to 20% can be found in the valleys.

Soils - Carvalho *et al*. (1990) identified the following soil classes in the Taboão catchment: *Latossolo Vermelho distroférrico* (Oxisols1), *Latossolo Vermelho distrófico* (Oxisols), *Nitossolo* (Alfisols) , *Gleissolo* (Inceptisols) , *Neossolo Flúvico* (Entisols) e *Neossolo Litólico* (Entisols). The predominant soils are the *Latossolos Vermelhos* and the *Nitossolos*. The *Latossolos Vermelhos* are present as gently-undulating relief with slopes from 0 to 13% and present good resistance to erosion when in their natural state, due to their high clay flocculation level, high porosity, good permeability and also because they appear in areas of gentle relief. However, when badly managed, they tend to develop a compacted layer, which favors water runoff and consequent erosion. The *Nitossolos* occupy the lower areas, with slopes generally from 8 to 15%, close to the watercourses draining the region. They are very likely to exhibit both laminar and concentrated erosion when badly managed because they appear where slopes are steeper.

Vegetation – The vegetation consists of the remaining intermediate tropical/subtropical forests, with woody species, bushes and creepers. The original forest has been felled over time and replaced by crops (Carvalho *et al.,* 1990). Small remnants of the original forest can be found close to roads and property boundaries. Gallery woodland is preserved where watercourses are enclosed and are absent where streams become wider and where over-bank flooding occurs.

Climate - Nimer (1989) describes the region's climate as humid-temperate, without a dry season, and characterised by evenly-distributed rainfall throughout the year. Mean annual rainfall is around 1700mm, with monthly rainfall during the 1945-85 period varying between 120 and 160mm (Chevallier e Castro, 1991). However this apparently regular distribution can be interrupted by marked variations, both in annual and monthly total. One such event occurred in 1992 when 396 mm of rain were recorded in two days, May 26-27, while in 1997, 840 mm of rain fell in the months October-November,

---

1 correlation to first categorical level in the Soil Taxonomy is indicated between parenthesis.

associated with an El Niño event (Castro *et al*., 1993). Regarding temperature, the July and January monthly means are 14°C and 24°C respectively.

Land use – The LANDSAT TM classification of the Taboão catchment (Risso, 1993) showed 61.1 km² of cultivated land, 32.5 km² pasture, 10.3 km² forest and only 1.4 km² urban area. Soya and corn (maize) are the principal summer crops, with oats and barley grown in winter. The introduction of no-tillage practices has greatly reduced the use of machinery relative to previous methods of cultivation. With no-tillage, machines go on the land to harvest and then sow, and between sowing and harvest for herbicide application.

Erosion – As intensive agriculture has developed on fertile but structurally-fragile soils, a number of erosion problems have arisen in the area, as shown by the formation of gullies where surface runoff becomes concentrated and by soil compaction which reduces infiltration capacity (Castro *et al.*, 1993). As a result, sediment load in rivers is significantly increased, together with sediment deposition in reservoirs, more severe flooding and lower flows. Measures adopted by farmers to avoid these problems consisted of terrace construction in places where the slope exceeded 5%, reduction of the number of operations needed in soil preparation, and in the use of appropriate machinery (Castro *et al.*, 1993). From the 90s onwards, the initiatives of some farmers encouraged by the Brazilian Federation for No-tillage on Crop Residues started to bring about direct seeding without the use of terracing (Castro *et al*., 1999). Castro *et al*. (1999) evaluated the effects of this cultivation change and found that the new practice resulted in a relative reduction in surface runoff from hill-slopes and an increase in subsurface flow, as well as a significant reduction in both laminar and linear erosion and soil loss, at both plot and basin scale.

2.2. Methods

The relations between the gullies and the variables that describe some natural factors in the Taboão catchment were identified through managing the data in a Geographic Information System (GIS). Some of these variables were generated and others were simply manipulated to be used in GIS.

The procedures adopted to identify some natural factors important to the emergence and development of gully systems, include data acquisition, combination of data layers and data analysis.

The anthropogenic factors influencing the development of gully systems in this area were registered during the fieldwork of gully mapping carried out among the data acquisition procedures.

The role of the climatic factors in the development of the gullies in the area under study is also analysed based on the evolution through a ten-year period of a gully located at the Donato sub-basin.

Data acquisition – The gully erosion were identified and represented in a 1:25,000 scale map. Identification of gullies was made by stereoscopic analysis of 1:60,000 aerial photographs taken in 1996; results from this preliminary analysis of aerial photographs were checked by field observation and in sites indicated by farmers and other community members.

In the field work, observations were recorded on field-sheets describing gullies in terms of: grid reference; dimensions; cross-section of the erosive facies and of the drainage channel; slope measurements along the longitudinal axis and lateral slopes;

concentration of surface runoff; position relative to the drainage network; vegetation cover; present and past land use; existence and position of soil piping.

The map of the gullies was constructed by digitizing polygons interpreted on aerial photographs or obtained by field measurement. When constructing raster files, a 20 m resolution was used.

The Digital Elevation Model (DEM) was generated from a 1:25,000 topographic map, with 10 m equidistant contour lines. The lines with elevation information found in the map were digitized as vectors and converted into the compatible structure. The modeling of the elevation data was based on a triangular irregular network, using the Delaunay triangulation process. Finally, a grid with 20 m resolution was generated from the triangular network.

The terrain slope, the plan curvature and profile curvature were derived from the DEM using algorithms adapted by Collischonn *et al*. (1998), based on Zevenbergen and Thorne (1987). Five curvature radii were tested to estimate plan and profile curvature: 3000 m, 1500 m, 1000 m, 800 m and 600 m. For each curvature radius, grids were generated and exported to the GIS. The differences observed as function of the distinct curvature radii were greater in plan curvature than in profile curvature. In both cases, as the curvature radius increases there is an increase of concave and convex elements of plan and profile curvatures. As a consequence, the number of straight elements decreases. The comparison of the images with field observations showed that the curvatures generated with the 1000 m curvature radius were nearest to reality.

The flow acumulation area was estimated from the depressionless DEM by using algorithms adapted by Collischonn *et al*. (1998).

The lithology variable represents the sandstone layers that exist between the lava flows and that were identified in few rock outcrops found in the Taboão catchment during the fieldwork. The three elevation levels where the sandstones outcrops were represented in a binary raster file through buffers zone of 40 m width.

The lineaments were extracted from 1:60.000 and 1:110.000 aerial photographs. As the drainage network in the area presents a strong structural control, the lineaments were traced based on the drainage paths. The lineaments were digitized as vectors on screen as an overlay of the aerial photographs images. The lineament orientations were analysed in the rose diagrams created from the vectors by the program Rockworks 99 ®. Directional filtering of the vector data created distinct datasets according to the different orientation patterns. In the GIS, all the datasets were represented together in a raster file as distinct classes. Buffer zones with 40 m width were created from each lineament.

The soil was represented as a variable considering the soil units mapped by Carvalho *et al*. (1990). The data available did not allow the use of others important variables in the erosive process such as organic matter, soil texture and soil thickness.

The soil units were digitized as polygons in a computer aided drawing (CAD) program and exported to the GIS program. The vector data were transformed into a raster image.

Data integration by geoprocessing methods – Relationships between gullies and variables describing geology, geomorphology and soils were determined by combining the 7 layers for these variables with the layer representing the gullies. As this layer is binary, the images resulting from the overlays show the values related to the classes of each variable inside the gully polygons and zero value elsewhere. The relationships

between the gullies and the variables were identified in the histograms of each image resulted from the overlaying procedures

Evolution of a gully in the Donato Basin – A gully lying within the drainage basin of the Donato creek (area approximately 1 km^2), a sub-basin of the Taboão, has been monitored quantitatively since 1991 by means of topographic measurement, and qualitatively by field observation and photographs. Topographic measurements of the active part of the gully have been made since July 1991 using equipment such as a theodolite with millimeter precision from 1991 to 1997, giving latitude, longitude and altitude at each point. The points are referenced with respect to three known points. Thus it is possible to compare measurements over different years. Subsequently, data are analysed in the laboratory and the gully volume is calculated. Differences between the calculated volumes show how gully volume evolves over time.

3. Results and Analyses

3.1. Gully erosion mapping

Eighty-three gullies resulting from the action of linear erosion in the Taboão catchment were identified, 45 of which are active, 28 stable, and 10 have already been reclaimed. The gullies are homogeneously distributed throughout the catchment (Figure 2) and are of different sizes, as can be seen in Table 1.

The dimensions of the gullies present a positive correlation with the contribution area. Figures 3 and 4 show that the depth and area of the gullies tend to increase as their contribution area increases.

Considering the situation of the gullies as to the drainage network, it is observed that 18% of the gullies are connected to drainage channels and, therefore to the drainage network, 78% of the gullies are located in thalwegs, but unconnected to the drainage network, and 4% of the gullies do not have any relationship with the drainage network.

No pipings were identified in 55% of the gullies. Among the gullies where there is piping, 24% of the total, these features in the vast majority of cases are in the C horizon of the soils. The mean slope of the terrain at the sites of gullies formed with the contribution from subsurface flow, shown by the presence of pipings, is 7.5%. This value is little higher than the 5% value presented by Mendiondo *et al* (1998) as a maximum limit for the concentration of subsurface flow in the sub-basin of Turcato. New pipings that appeared in areas with steeper slopes, as a result of increased infiltration due to the dissemination of no-tillage cultivation practices may account for this.

It was found that 39% of the cases present a concentration of surface runoff only due to the fact that the gullies are located in thalwegs. The concentration of surface runoff in these cases is natural, and occurs due to the converging forms of the slope on the plane. In 54% of the cases, besides the concentration of surface runoff that occurs because the gullies are located in thalwegs, there is concentration of the laminar flow due to the existence of roads and/or fences upstream from the gullies. In 7% of the gullies, the concentration of surface runoff is promoted by the existence of fences in the headwaters.

As to land use, in 67.5% of the cases the soil is cultivated by no-tillage methods; 23% of the cases occur in areas where the land is used for cattle, and in 9.5% of the cases the gullies develop in grassy areas. The areas described as grassy are related to larger gullies in the catchment and are not being used, with a view to stabilizing the gullies.

Considering that no-tillage is a relatively recent farming practice in the region, it was sought to identify the previous land use in the areas where there are gullies, by getting information from the farmers.

In 83% of the cases the land was tilled in terraces; in 14.5% of the cases the land was used for cattle, and in only 2% of the cases did the gullies develop in grassy areas.

The diminished percentage of areas used for cultivation and the increased percentage of areas used for cattle observed when comparing the land use data in the past and the present, indicate that areas that were previously cultivated began to be used for cattle. This may indicate an attempt to control gully development by identifying the form of land use responsable for triggering them.

As to vegetation, 36.5% of the gullies are in cultivated areas or covered with straw generated by farming, 34% of the gullies present grass-type plants, 21.5% bush-type plants and grasses and 8% present bushes, grasses and woods.

3.2. Relationships between gullies and geology, geomorphology and soils

Geology – The analysis of the hypothesis of that geology controls gully development was performed considering the presence of sediment deposits between and over the lava flows and the evidence of structural control in the development of the drainage network in the study area. Both the more porous lithologies and the contacts beween different rocks, such as the lineaments, may represent discontinuities and more pervious zones that favor the infiltration of surface and subsurface waters and potentiate the linear erosion process.

The few rock outcrops found in the study area, located in old quarries and at the substrate of some gullies, indicate the existence of more than one lava flow and sandy levels between these flows. The information obtained in the outcrops suggests the existence of at least 3 levels of sandstones in the basin, at the altimetric intervals of 350 to 600 m, 410 to 420 m and 465 to 475 m. Correlations between outcrops indicate that the two lower levels correspond to sandstones deposited between the lava flows. The information available is not sufficient to characterize the upper sandy level as such and even as cover sediment. At least the intermediate level of sandstone was deposited under volcanogenic conditions as indicated in petrographic analysis by the presence of volcanic fragments.

Although no appropriate control is available concerning the occurrence of sandstones in the area, and there is an accepted possibility that lateral discontinuities may occur, considering the relevance of the analysis of these levels in the study, the hypothesis presented is that they are sub-horizontal.

The integration of the layers with the gullies and the altimetric intervals related to the sandstone occurrences indicates that 54% of the gullies develop over these intervals or immediately downstream from them.

The lineaments are linear features visible from aerial images that can be the result of faulting and fracturing (Erdélyi and Gálfi, 1988). They represent zones of increasing porosity and permeability in massive rocks, where groundwater is stored and flows. In the present work they were considered a geological element that could possibly control linear erosion development, since in the area under study a strong structural control is observed in the development of the drainage network, in relation to which 96% of the gullies develop.

Considering the low porosity of the rocks in the area, geological structures may represent preferential zones for water circulation and enable the removal of soil particles at the sites where these waters rise to the surface.

This particle transport mechanism was observed in the gully located in the Donato sub-basin. A period with heavy rainfalls allowed the soil to become saturated and the fractures to be recharged. After a few days, it was found that the soil had become less wet, and therefore a small volume of water could spring in C horizon of the soil profile and the groundwater could surge in the fractures occurring in the gully floor, where altered volcanic rock outcrops (Figure 5).

The lineaments present many different orientations in the study area, although a relative predominance of lineaments in the NW quadrant is observed, and a relatively greater frequency of lineaments in the N30-45E, N80-90E and N20-40W directions. Although there was an apparently homogeneous distribution in the lineament orientations, four classes were defined in the generation of the lineament map, based on their directions and the possibility of structure intersection: NE lineaments, NW lineaments, EW lineaments and lineament intersection.

The overlay of the layers representing the gullies and the lineaments indicate that 61% of the gullies develop on lineaments. Of these, 51% of the gullies occur over lineaments in the NW direction, 23.5% over NE lineaments, 21.5% over intersection of at least two structures, and 4% over lineaments in the EW direction.

Geomorphology – The characteristics of the variables that represent the geomorphology were analyzed in the areas of the gullies and their catchments, the latter estimated based on DEM.

The gullies develop within a broad interval of slope values, although the mean value is 9%. The same occurs in the gully catchments, where the mean is 8.3%. Considering the mean slope of the basin equal to 8%, it was found that 61% of the gullies occur in areas with a declivity greater than the basin mean.

The flow acumulation area in the gullies, which indicates the size of the catchment upstream, has a mean value of 61,683 m². In the catchments, the mean is 4,490 m², the lower value indicating the proximity of the watersheds.

The relationship between slope forms and the occurrence of gullies is shown in Table 2.

Although only 5% of the basin consists of concave-concave slopes, 32.4% of the gullies develop at these sites. In 58.3% of the cases, considering the plan curvature, the gullies occur in concave slopes, 31.2% present on straight slopes and 10.5% in convex slopes. As to the profile curvature, it is found that 45% of the gully surfaces are concave, 45% are straight and 10% are convex.

The relationships found among the plan and profile curvatures, and the occurrence of gullies are consistent with what was observed by Oliveira and Méis (1985) on studying the gully conditioning factors and erosion mechanisms in the region of the middle Paraíba do Sul river valley. The authors found that the gullies concentrate in the contour environment with a concave profile, although these environments occur in 1/3 of the study area.

On the other hand, in the relationship between gullies and the mean slope of the basin, the result found by authors is practically the opposite of what was observed in the Taboão catchment. In the catchment, 61% of the gullies are located in an area with a

slope that is greater than the basin mean, while in the Paraíba do Sul river valley, only 25% of the cases occur in environments with a greater slope than the average. This result is justifiable if we consider that, in the region, different from the Taboão catchment, gullies develop over colluvial ramps, which consist of slightly inclined surfaces, with erosive discontinuities separating the different strata that constitute them, which may be determining factors in the erosion mechanisms.

The total area of the gully catchments tends to vary inversely according to its mean slope, as shown in Figure 6.

In other words, the steeper the slope upstream from a given point, the smaller is the contribution area needed to trigger the gully erosion phenomenon.

Soils – The gullies develop mainly over *Latossolo Vermelho distrofico* and *Nitosolo* soils, although they are not the most frequent in the area. In 36.1% of the cases, they occur scarving *Latossolos Vermelhos distróficos*, in 35.4% of the cases they occur over *Nitosolos*, and in 26.8% of the cases over *Latossolos Vermelhos distroférrico*.

Practically half the gullies catchments have *Latossolo Vermelho distroférrico*, agreeing with the fact that these soils occur in 40% of the Taboão catchment. The *Latossolo Vermelho distrófico* also takes up a significant surface of the basins and the *Nitosolos* are less significant. Both in the gullies and in the contribution basins, the other soil classes occupy negligible areas.

3.3 Gully evolution in the Donato Basin

Table 3 presents the results of topographical measurements of the gully over time. Figure 7 illustrates gully evolution between 1991 and 2003. Figure 8 shows the active part of the gully in December 1994.

The gully evolved a total of 1013 m^3 from 1991 to 2003, and remained relatively stable in normal periods, with an eroded volume of 236 m^3. But 95% of its volume (702 m^3) was eroded during the El Niño periods in 1992 and 1997. The El Niño Southern Oscilation (ENSO) phenomenon is a complex climatic anomaly that occurs periodically at intensities and volumes that are very variable from one year to the next. El Niño appears at Christmas-time (hence the name El Niño, the Christ Child) with the heating of ocean currents, normally cold on the west coast of South America at the level of Peru. This heating influences the climate regime in Brazil, causing heavy rainfalls in the South and drought in the Northeast (Chevallier and Dhein, 1992).

This greater gully evolution during the El Niño period is observed both in 1992 and in 1997. During these periods, the total precipitation volume was much higher than the mean precipitation in the basin. In 1992, the raingauge located in the Potiribu basin, recorded a total rainfall of 396.5 mm in 26 hours, on May 26 and 27, with maximum intensities of 104 mm/h in 10 minutes, 72 mm in 30 minutes, 62 mm/h in 1 hour and with interruptions of not more than 3 hours in the rainfall (Chevallier and Dhein, 1992). The authors estimated the return period of the total accumulated rainfall during these two days as several centuries, but the maximum intensities had return periods of 2 to 3 years. These results indicate that, despite the large volume in this period, the intensities observed are no higher than those in normal events.

On the other hand for the El Niño period in 1997 the phenomenon presented as distributed over several months, between September 1997 and April 1998, with a total rainfall of 2282 mm in these 8 months, while the annual mean is 170 mm. This rainfall volume was distributed as follows: 160 mm in September, 534 mm in October, 313 in

November, 252 mm in December, 206 mm in January 1998, 394 mm in February, 133 mm in March and 291 mm in April, while the monthly mean in this basin is from 120 to 160 mm.

4. Discussion and Conclusions

This work identified natural and anthropogenic factors influencing gully development in the Taboão catchment. The natural factors analysed were: lithology and lineaments, terrain slope, contribution area, plan and profile curvatures, and soil type. The anthropogenic factors were land use and artificial runoff concentration. The role of the climatic factors in the development of one gully were analysed based on its evolution through a ten-years period.

Gully mapping allowed the definition of a portrait of gully erosion problems in the Taboão catchment and were also fundamental to define the spatial limits for recognition of the variables that represent the natural factors.

The dimensions of the gullies measured during the mapping present a positive linear correlation with their contribution areas.

Through mapping it was observed that the subsurface flow acts in the majority of the gullies. It was indicated by the presence of pipings in 45% of the gullies and by the presence of a wet layer at the bottom of the soil profile inside the gullies. The gullies where the pipings were observed are situated in terrains with 7.5% average slope.

The runoff concentration in 54% of the gullies is natural as the gullies are located in thalwegs, and anthropogenic due to the existence of roads and/or fences upstream from the gullies. In 7% of the gullies, runoff concentration is anthropogenic, promoted by the existence of fences in the headwaters.

As to land use, in 67.5% of the cases the soil is cultivated by no-tillage methods; 23% of the cases occur in areas where the land is used for cattle, and in 9.5% of the cases the gullies develop in grassy areas.

The integration of the gullies map and the layers representing lithological variations, lineaments, terrain slope, flow acumulation area, plan and profile curvatures, and soil types, provided elements to evaluate the relationship between these variables and the gullies at the Taboão catchment.

The integration of the layers with the gullies and the altimetric intervals related to the sandstone occurrences indicates that 54% of the gullies develop over these intervals or immediately downstream from them.

The overlay of the layers representing the gullies and the lineaments indicates that 61% of the gullies develop on lineaments. Of these, 51% of the gullies occur over NW lineaments, 23.5% over NE lineaments, 21.5% over the intersection of at least two lineaments, and 4% over EW lineaments.

The results of the integration of the layers with the variables related to geology, which represent discontinuities and more pervious zones that favor the infiltration of surface and subsurface waters and potentiate the linear erosion, support the hypothesis of a strong control of the subsurface flow in the development of the gullies in the Taboão catchment.

It was found that 61% of the gullies occur in areas with a declivity greater than the basin mean equal to 8%.

Although only 5% of the basin consists of concave-concave slopes, 32.4% of the gullies develop at these sites. More than half of the gullies occur in concave slopes in plan while, as to the profile curvature, it is found that 45% of the gully surfaces are concave, 45% are straight and 10% are convex. As the plan curvature is related to the runoff and subsurface flow accumulation, the role of the subsurface flow in the development of the gullies in the Taboão catchment is even clearer.

The control of soil type on gully development is made clear by the fact that the gullies develop mainly over *Latossolo Vermelho* and *Nitosolos* soils, although they are not the most frequent in the area.

The monitored gully presented 95% of the total eroded volume (1013 m^3) during the El Niño periods of 1992 e 1997 (702 m^3) and only 236 m^3 during other periods, from 1991 to 2003. The increase of subsurface flow as a consequence of no-tillage practices can be the main factor for gully evolution during El Niño years.

Besides land use, public works also contribute to accelerate the erosive processes, as the majority of the gullies is located close to roads or fences that help to concentrate runoff from other catchments, directioning it to the drainage network where the erosion take place.

The introduction of new agricultural practices and attempts to recover degraded soils show that the farmers are concerned with solving the erosion problem in the region. However, the gullies persist, despite all these efforts.

More detailed studies are necessary to identify the characteristics of the physical environment that can cause water flow concentration, as well as studies to evaluate the subsurface flow patterns close to the gullies. A more detailed study of rainfall volumes and intensities during yeras with and without El Niño variations would also be very useful to help analyse gully evolution in this region.

Acknowledgements

The authors would also like to acknowledge:
CNPq/FINEP for the financial support of the research;
CPRM - Geological Survey of Brazil for the financial support and interest in the research;
CNPq for post-doctoral scholarship to Joel Avruch Goldenfum at INSA-LYON, France;
The technicians Cesar Gonçalves Dias de Castro and José Carlos Nunes for the topographical survey an for the data processing of Donato's gully during 10 years;
The technician Dalton Leão for support during gully identification and mapping;
Mr Abilio Cadore, owner of the area where the Donato Gully is located and other landowners in the Taboão basin, that allowed our activities on their lands;
Professor Robin Thomas Clarke for the help in the translation and correction of the English-language version of the paper, and
Librarian Jussara Silva (IPH/UFRGS) for preparing the references.

References

Bordas, M.P., Borges, A. L. O., 1990. Escolha de bacias representativas e experimentais para estudo da erosão e do seu controle. 8. Congresso Brasileiro e Encontro Nacional de Pesquisa sobre Conservação do Solo. Sociedade Brasileira de Ciência do Solo, Londrina, Brazil, pp.1-9.

Carvalho, A.P., Abrao, P.U.R., Fasolo, P. J., Potter, R. J., 1990. Levantamento semidetalhado dos solos da bacia do arroio Taboao (Pejuçara/ Ijuí-RS). Multigr., + mapa 1:25.000.

Castro, N. M. dos R., Auzet, A. V., Chevallier, P., Leprun, J. C., 1999. Land use change effects on runoff and erosion from plot to catchment scale on the basaltic plateau of southern Brazil. Hydrological Processes, 13:1621-1628.

Castro, N. M. dos R., Chevallier, P., Silveira, A. L.L. da, 1993. Agriculture on the Brazilian basaltic plateau. Cultivations practices and soil conservation: first results of the Potiribu project. In: Wicherek, S. (Ed.), Farm land erosion: In temperate plains environment and hills. Elsevier, Amsterdam, pp. 403-414.

Chevallier, P., Castro, N. M. R., 1991. As precipitações na região de Cruz Alta e Ijuí (RS-Brasil). 5.Simpósio Brasileiro de Recursos Hídricos. ABRH/APRH, Rio de Janeiro, Brazil, pp.183-192.

Chevallier P., Dhein R. A., 1993. Les précipitations exceptionnelles des 26 et 27 mai 1992 dans la région d'Ijuí (Rio Grande do Sul, Brésil). Sécheresse, 4:159-164.

Collischonn, W., Mediondo, E.M., Mendes, C.A.B., 1998. Modelos numéricos do terreno e suas aplicações a bacias hidrográficas 1 : princípios gerais. 17. Congreso Nacional del Agua. Facultad de Ingenieria y Ciencias Hídricas de la Universidad Nacional del Litoral, Santa Fe, pp.82-90.

Fundação Instituto Brasileiro de Geografia e Estatística, 1986. Folha SH.22 Porto Alegre parte das folhas SH.21 Uruguaiana e SI.22 Lagoa Mirim. IBGE, Rio de Janeiro, Brazil.

Guerra, A.J.T., 1998. Processos erosivos nas encostas.In:Guerra, A.J. T., Cunha, S.B.da(Eds.),Geomorfologia: uma atualização de bases e conceitos. Bertrand Brasil, Rio de Janeiro, pp. 149-209.

Guerra, A.J.T., 1999. O início do processo erosivo. In:Guerra, A.J.T. , Silva, A. S. da, Botelho, R. G. M. (Eds.), Erosão e conservação de solos: conceitos, temas e aplicações.Bertrand Brasil, Rio de Janeiro, pp. 17-50.

Mendiondo, E. M., Castro, N. M. dos R., Auzet,A.V., Chevallier, P., 1998. Surface flow pathways in subtropical agricultural headwaters: a case study from southern Brazil. 4. International Conference on Headwater Control. IAHC/WASWC, Merano, pp.285-292.

Nimer, E., 1989. Climatologia do Brasil. IBGE, Rio de Janeiro, Brazil.

Oliveira, M.A.T., Coelho Neto, A.L., Avelar, A. de S.., 1994. Morfometria das encostas e desenvolvimento de boçorocas no médio vale do rio Paraíba do Sul. Geociências, 13: 9-23.

Peat, D.W., 1997. The Parana-Etendeka basin. In: Mahoney, J. J., Coffin, M. F. (Eds.), Large igneous provinces: continental, oceanic and planetary flood volcanism. American Geophysical Union, Washington, pp.217-245.

Risso, A., 1993. Obtenção e manipulação dos parâmetros da equação universal de perda de solos através de técnicas de geoprocessamento. Dissertação (Mestrado) – Instituto de Pesquisas Hidráulicas, UFRGS, Porto Alegre, Brazil.

São Paulo. Secretaria de Energia e Saneamento. Departamento de Águas e Energia Elétrica., 1990. Controle de erosão. Instituto de Pesquisas Tecnológicas, São Paulo, Brazil.

Wildner, W., Lopes, R.da C., Romanini, S., Camozzato, E., 2003. Contribuição à estratigrafia do magmatismo Serra Geral na Bacia do Paraná. 1. Encontro de Estratigrafia do Rio Grande do Sul: Escudos e Bacias. UFRGS, Porto Alegre, Brazil, pp. 204-210.

Zevenbergen, L.W., Thorne, C.R., 1987. Quantitative analysis of land surface topography. Earth Surface Processes and Landforms, 12: 47-56.

Table 1. Dimensions of the gullies in Taboão catchment

Value	Length (m)	Width (m)	Depth (m)	Area (m^2)
Minimum	6.00	2.00	1.00	19.80
Maximum	910.00	60.00	15.00	54,600.00
Average	136.66	10.77	3.59	2,051.75

Table 2. Relationship between slope forms and gullies

Profile Curvature – Plan Curvature	Gullies (%)
Concave-concave	32.4
Straight- concave	20.3
Convex- concave	5.6
Concave - straight	10.7
Straight - straight	18.6
Convex - straight	1.9
Concave - convex	1.9
Straight - convex	6.1
Convex - convex	2.5

Table 3. Gully evolution over 10 years

Date	Volume (m^3)	Volume Variation	Natural or Anthropogenic Phenomena
07/17/1991	299.8		26, 27/05/2002 El Niño 1992
07/13/1992	567.51	268 m^3 in 2 days	
11/18/1993	594.82	27 m^3 in 1 year and 4 months	
12/19/1994	558.76	Gully stable with sedimentation	
03/05/1997	546.06		
10/13/1997	693.97	148 m^3	09/1997 to 04/1998 El Niño 1997
10/15/1997	703.76	10 m^3 in 2 days	
11/18/1997	1121.9	418 m^3 in 33 days	
10/20/1998	1248.95	127 m^3 in 11 months	
08/03/1999	1199.34	sedimentation	
09/27/2001	1249.21	50 m^3 in 2 years	Upper channel section was filled
01/28/2003	1312,38	63 m^3 in 1 year and 4 months	Gully upstream

List of Figures

Figure 1. Situation map of Taboão catchment

Figure 2. Map of gullies in Taboão catchment

Figure 3. Relationship between contribution area and gully depth

Figure 4. Relationship between contribution area and gully area

Figure 5. Groundwater surgence in joint with N 50 E orientation

Figure 6. Relationship between average slope and gully catchment area

Figure 7. Evolution of Donato gully

Figure 8. Active part of Donato gully – December 1994

Figure 1. Situation map of Taboão catchment

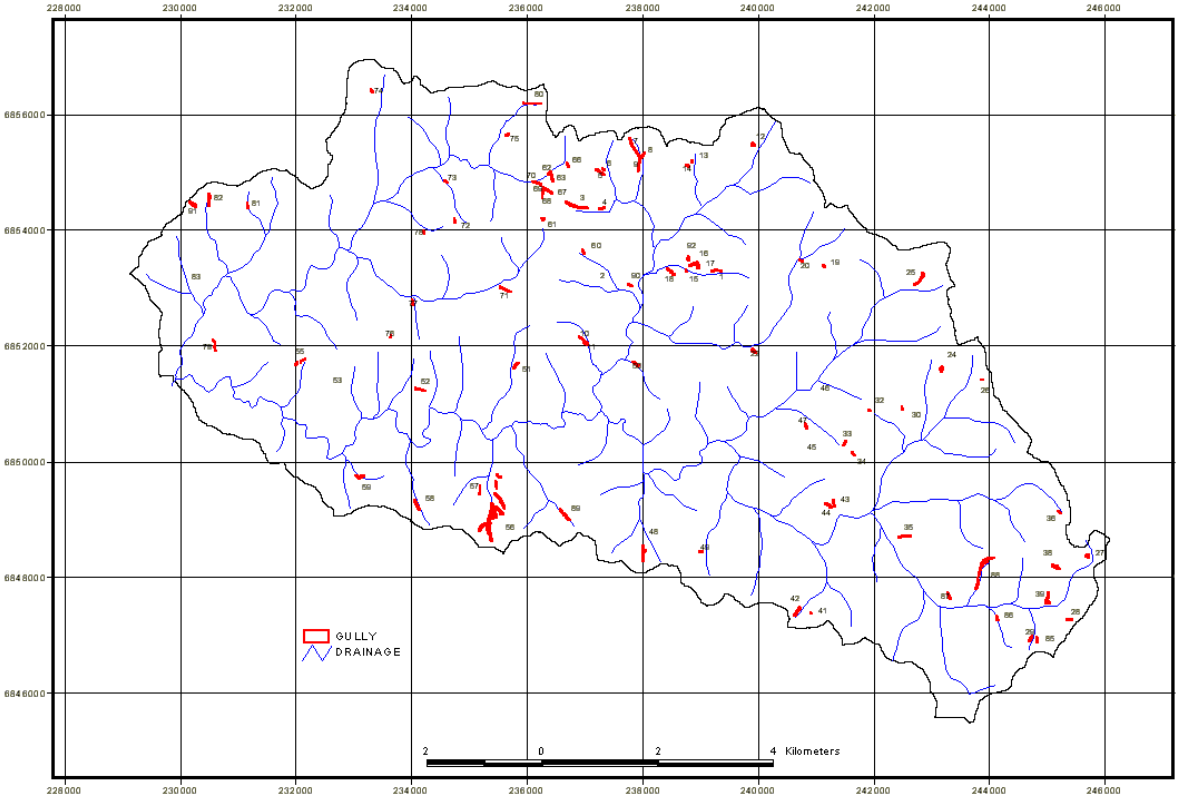

Figure 2. Map of gullies in Taboão catchment

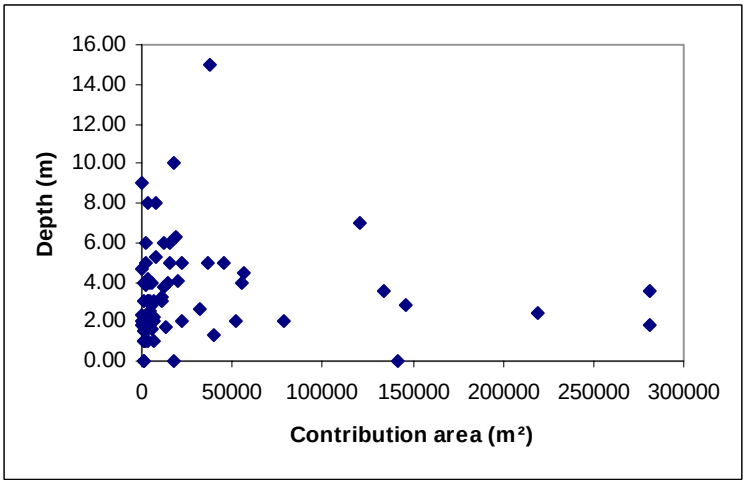

Figure 3. Relationship between contribution area and gully depth

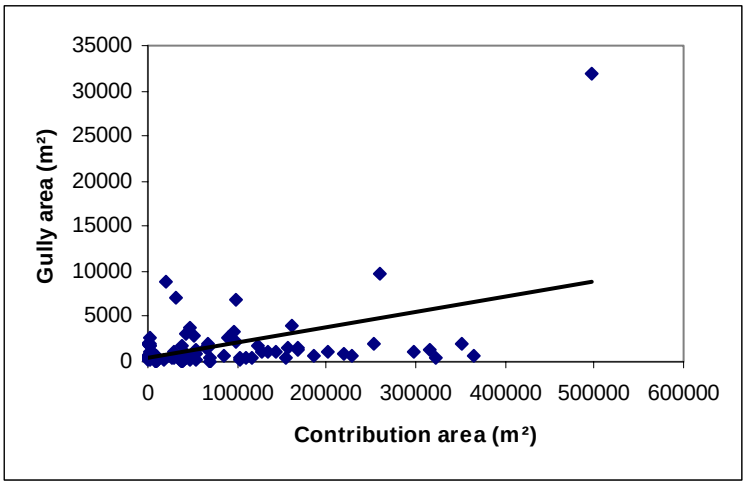

Figure 4. Relationship between contribution area and gully area

Figure 5. Groundwater surgence in joint with N 50 E orientation

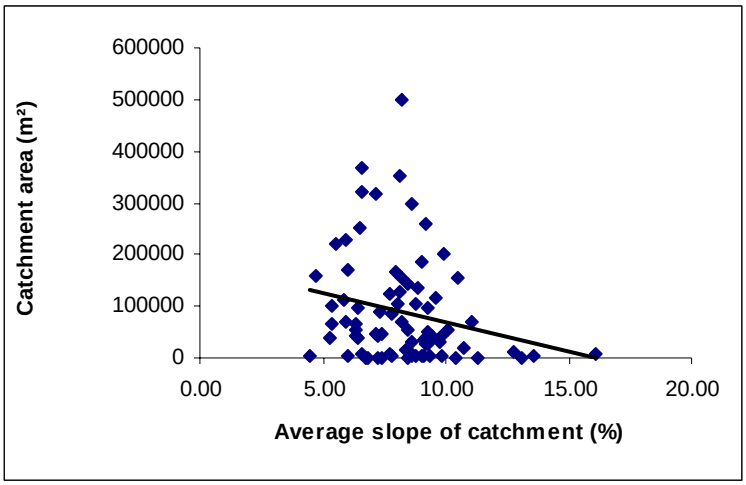

Figure 6. Relationship between average slope and gully catchment area

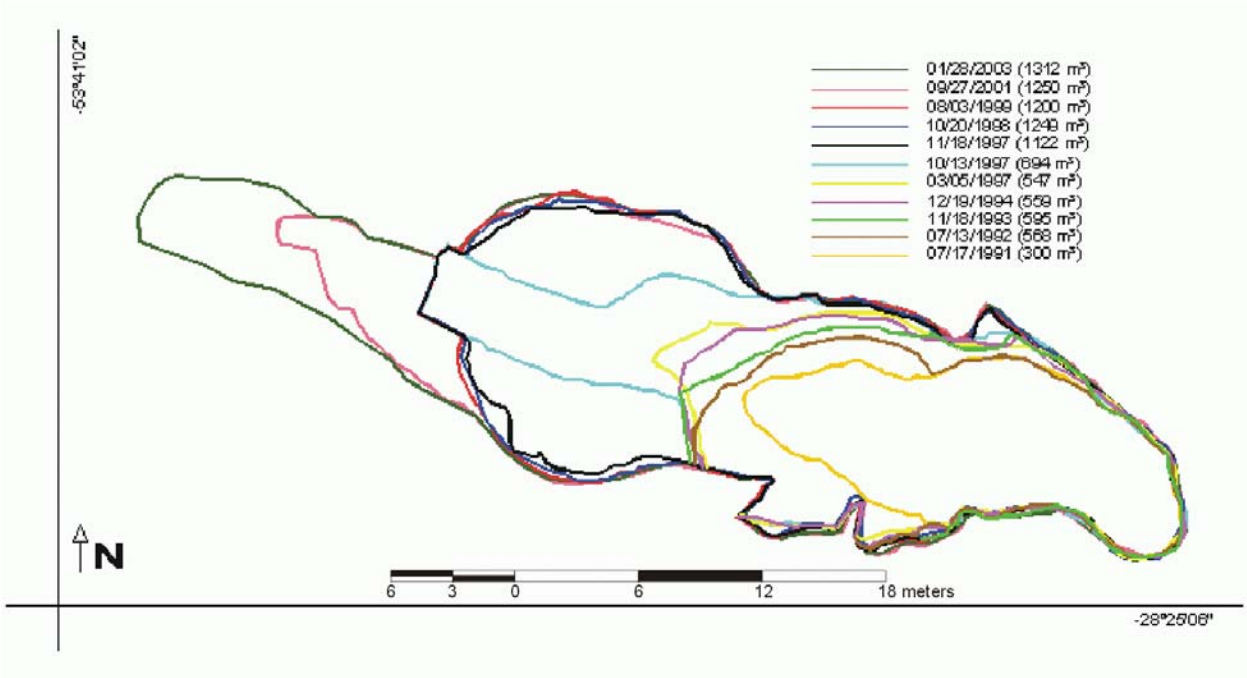

Figure 7. Evolution of Donato gully

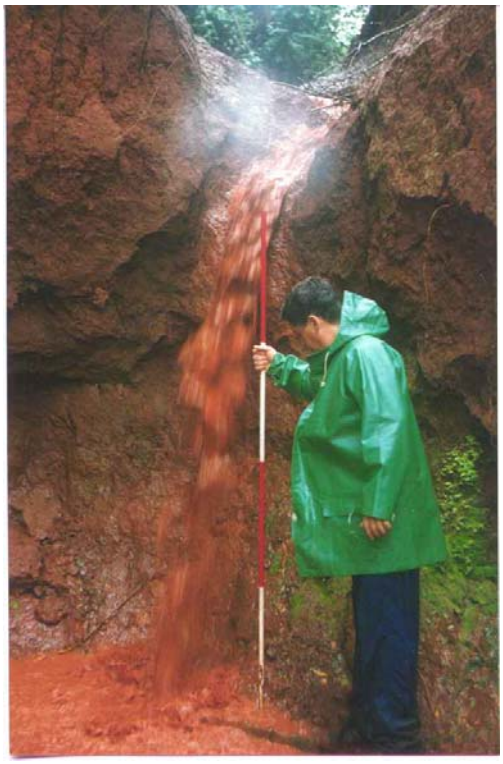

Figure 8. Active part of Donato gully – December 1994

Morphological Characteristics and Development of Gully Head in Arid Environment, China

Xiaodan Wang* (E-Mail: wxd@imde.ac.cn)
Xianghao Zhong
Shuzhen Liu
Jianrong Fan
Jianhui Zhang
Institute of Mountain Hazards and Environment
Chinese Academy of Science and Ministry of Water Conservancy
Rd, No.9, section 4 of Renming South
Chengdu 610041, China
This paper was supported by the Seed Foundation from Institute of Mountain Hazards and Environment, Chinese Academy of Science.
Tel/Fax:+86-28-85229891

Abstract

Gully erosion is the main cause that make heavy sediment into a river due to arid climate and special soil type in the dry-hot valley of Jinsha River, which locates Yuanmou County of southwest China. This study aims (i) to analyze morphological characteristics of gully heads whose other controlling factors are similar except land-use method, and, (ii), to find the relationships among gully growth, land-use pattern and gully-head morphology which mainly focus on the fractal dimension and curvature of gully head. The ultimate goal is to identify the effect of land-use pattern on gully-head morphology and development, and to assess the correlation between growth speed of gully and fractal characteristic. In study area, there are mainly five land-use methods distributing in the direction of gully-head development including (i) forest and grass, (ii) orchard and crop (interplanted), (iii) farm (only crop), (iv) forest, shrub and grass, (v) bare soil. A number of gullies with different land-use patterns have been investigated in 1998, whose other controlling factors have no obvious discrepancy such as topographical parameters, material properties and climate. Therefore, the study considers their influence uniform for each gully so that which has been ignored in study course. As a result it is easy and clear to show the effect of land-use change on gully head.

As a tool probing into irregular structures and forms, fractal geometry starts with non-linear characteristics to directly discover the internal rules without simplifying or abstracting research subjects , thus providing a new tool for studying gully morphology, and offering new ways to investigate soil erosion. In the study, non-linear parameters as fractal dimension (D value) and curvature (P_τ) are applied to estimate geometrical morphology of gully head. The development results of investigated gully heads have been compared after four years. At last, conclusions of the study are (i) that the rate of gully development is remarkably relative with land-use method of gully head, (ii),that fractal curvature (P_τ) of gully head is a useful parameter to indicates the rate of gully

*Correspondence author

development in the future, namely the greater P_{τ} value is, the faster the gully head develops.

Keywords: gully head; morphology; land use; fractal curvature; development

Investigations of the Contrasting Distribution of River-bank Gullies in the Northern and Southern Gangetic Plains Using an Integrated Approach Including Remote Sensing, Geophysical Data and Field Investigation.

Ananda S. Das Gupta*
Indian Institute of Technology Kanpur
India, 303B, WLE, Department of Civil Engineering
IIT Kanpur, Kanpur
Uttar Pradesh 208016, India

Abstract

The focus of the study is on the Yamuna-Chambal gullies in southern Gangetic plains of India, on the banks of Yamuna and Betwa rivers. IRS Satellite imagery reveals that there is a marked contrast in the northern and southern Gangetic plains with respect to the distribution of gullies. The rivers from Yamuna and to the south of it characteristically have banks which are highly gullied. In contrast, gullies are totally absent in the region north of Yamuna. All rivers (minor and major, including Ganga) north of Yamuna lack any sort of gullying on their banks, whereas even small rivers such as Sengar near Yamuna have extensive gullies. Further, there is a distinct contrast in the tone of surface soil, as evident in the False Colour Composite of the area. The areas south of Yamuna show a distinct bluish tone in the FCC image, unlike the areas north of it. The multispectral data has been further used to generate NDVI image which has been sliced into classes of fine intervals. The sliced NDVI image enables to figure out a distinct soil type that is characteristically present in the region south of Yamuna and absent north of it. The distribution of this particular soil class matches with that of the bluish-toned area in the FCC image. Further, detailed elevation data including point heights , contour heights and relative heights of gullied areas have been used to generate a Digital Elevation Model of the area. The DEM shows a distinct variation in the overall topography of the regions north and south of Yamuna, thus emphasizing the role of surface topography on gully distribution. Apart from surface topography, the subsurface topography of the basement in the area has been reproduced using subsurface geophysical data. Interestingly, the subsurface topography is also found to be different in the regions south and north of Yamuna. The basement rocks in the region are shaped in a convex bulge (this may be related to the bulge formed in relation to the compressional tectonics in the Himalayas). The basement rocks are exposed just to the south of river Betwa, and their slope increases gradually towards the north-east of Yamuna. The subsurface contours run nearly parallel to the course of river Yamuna and thus seems to play a vital role in characterising the regions north and south of Yamuna. The subsurface and surface data has been correlated in order to understand the topographic controls on the generation and distribution of the gullies in the area. The difference in the surface soil characteristics evident from the NDVI image also appear to be correlated to the subsurface and surface

*Correspondence author

topography since the later control the soil moisture contents. The soil moisture contents in the two regions have been estimated by testing soil samples collected from the field in different locations north and south of Yamuna and the results are found to be at par with the conclusions drawn from the remote-sensing studies. Finally the relative contribution of natural and anthropogenic factors in the formation and distribution of the gullies has also been investigated suggesting a greater influence of the natural factors in the area of study.

Keywords: gangetic plains' river bank gullies, remote sensing, NDVI, DEM, basement topography

To Table of Contents

Gully Erosion – Sediment Sources, Properties, Measurements, Routing and Spatial Variability

A Unified Approach in Erosion and Sedimentation Studies (Abstract only)
Yang, Chih Ted (Keynote)

Flow Near a Model Spur Dike with a Fixed Scoured Bed
Kuhnle, Roger A. , Yafei Jia, and Carlos V. Alonso

Sediment Source Identification using Soil Geomorphological Characteristics in a Semi-Arid Watershed (not available at time of printing)
Rhoton, F.E., W.E. Emmerich, and D.C. Goodrich

Gully Erosion after Wildfire
Moody, J.A. and D.A. Kinner

Routing of Flow and Sediment in a Gully Network (Abstract only)
Smith, J. Dungan and J. W. Kean

An Experimental Study on Gully Detachment and Transport on the Loess Plateau (Abstract only)
Zheng, Fenli, Peiqing Xiao, Yuanyuan Jia, Min Wu, and Yubin Zhang

Accuracy of Methods for Field Assessment of Ephemeral Gully Erosion
Casalí, J., J. Loizu, M.A. Campo, L.M. De Santisteban

Ephemeral Gullies: a Persistent Source of Sediment from Agricultural-related Lands (Abstract only)
Bernard, Jerry M., Jon G. Werner, and Fred D. Theurer

Evaluation of Topographic Indices for Ephemeral Gully Assessment
Casalí, J., L.M. De Santisteban, J.J. López, J.V. Giráldez, J. Poesen, and J. Nachtergaele

Airborne Laser Scanning for Riverbank Erosion Assessment
Thoma, D.P., S.C. Gupta, M.E. Bauer, and C. Kirchoff

Alternating Pattern of Narrow Shooting Flow and Wide Tranquil Flow in Gullies (Abstract only)
Vincent, Kirk R., and J. Dungan Smith

Spatial Distribution and Morphological Features of Gullies in an Agropastoral Area in Sardinia (Italy) (Abstract only)
Zucca, Claudio, Annalisa Canu, and Raniero Della Peruta

A Simple Device to Monitor Sediment Yield from Gully Erosion
Guerra, Antonio Jose Teixeira and Figueiredo, Marcos

Keynote

A Unified Approach in Erosion and Sedimentation Studies

Chih Ted Yang*
Borland Professor of Water Resources and
Director of Hydroscience and Training Center
Colorado State University
Fort Collins, CO 80523, USA

Abstract

Different theoretical and empirical approaches have been applied to our erosion and sedimentation studies. Most theoretical approaches are based on simplified and idealized assumptions which may not be applicable to field conditions. Results from empirical approaches are site specific and should not be transferred to conditions other than those from where the data were collected. The fundamental problem we have in the study of erosion and sedimentation is that there are more unknowns than independent equations available to solve them.

Erosion and sedimentation studies in a river basin consist of not only surface, rill and gully erosion, but also the sediment transport, scour and deposition processes in rivers, lakes, and reservoirs. There is a need to develop a unified approach based on sound theories applicable to field conditions. Due to the complexity of the river and reservoir systems in a watershed, a physically based computer model is also needed to simulate and predict the processes of surface, rill, and gully erosion and sediment transport, scour and deposition.

The Theory of Minimum Energy Dissipation Rate (TMEDR) can be derived from basic laws in thermodynamics as well as from mathematics. The Theory of Minimum Stream Power (TMSP) and Theory of Minimum Unit Stream Power (TMUSP) are special and simplified versions of TMEDR applicable to alluvial systems. The use of TMEDR, or its simplified versions, can provide us the additional equation needed to solve fluvial hydraulic and river morphology problems. TMEDR and the Theory of Unit Stream Power (TUSP) stem from the study of river morphology. The river system observed today is the cumulative result of surface, rill, and gully erosion, followed by sediment transport, scour and deposition. A unified approach based on TMEDR and TUSP should enable us to explain and predict the erosion and sedimentation processes in a river basin. Bureau of Reclamation's Generalized Sediment Transport model for Alluvial River Simulation (GSTARS) computer model series is based on TMEDR and TUSP.

This paper will briefly summarize the theoretical basis and development of TMEDR, TMSP, TMUSP, and TUSP. Laboratory and field data will be used to illustrate how the GSTARS computer models can be applied to simulate and predict a wide range of erosion and sedimentation processes with accuracy.

*Correspondence author

Flow Near a Model Spur Dike with a Fixed Scoured Bed

Roger A. Kuhnle* (E-Mail: rkuhnle@msa-oxford.ars.usda.gov)
National Sedimentation Laboratory
USDA-Agricultural Research Service
Oxford, MS 38677

Yafei Jia (E-Mail: jia@ncche.olemiss.edu)
National Center for Computational Hydroscience and Engineering
University of Mississippi
University, MS 38677

Carlos V. Alonso (E-Mail: calonso@msa-oxford.ars.usda.gov)
National Sedimentation Laboratory
USDA-Agricultural Research Service
Oxford, MS

Abstract

Three-dimensional flow velocities were measured using an acoustic Doppler velocimeter at a closely spaced grid over a fixed scoured bed with a submerged spur dike. Three-dimensional flow velocities were measured at 3484 positions around the trapezoidal shaped submerged model spur dike over a fixed scoured bed. General velocity distributions and detailed near field flow structures were revealed by the measurement. Clear differences were revealed between flow over fixed flat and scoured beds. Strong lateral flows were the dominant cause of the observed local scour.

Keywords: submerged spur dike, 3-dimensional flow, velocity measurements, free surface flow, hydraulic structure

1. Introduction

A spur dike may be defined as a structure extending outward from the bank of a stream for the purpose of deflecting the current away from the bank to protect it from erosion. Where the bank material is erodible, streams and rivers often erode the banks and move laterally, resulting in land loss, channel change, excessive sediment yield and degradation of the water quality. The use of a series of spur dikes is one of the most effective means of stabilizing or realigning channel banks. For economic reasons, spur dikes are often constructed of riprap and are commonly designed to be submerged during high flows. The pools formed from the local scour associated with spur dikes have been used successfully to enhance aquatic habitat in unstable streams (Shields et al., 1995). Despite the widespread use of spur dikes, many aspects of their design are based on prior experience and are only applicable to streams of a similar nature (e. g. Copeland, 1983). An improved understanding of the complicated 3-D flow in the vicinity of spur dikes and its interaction with the entrainment and transport of sediment is needed.

*Corresponding author

There have been few previous studies of the flow in the vicinity of spur dikes. Rajaratnam and Nwachukwu (1983) studied the flow in a laboratory flume near groin-like structures represented by an aluminum plate which projected above the water surface. A pitot-static tube was used to measure the flow in regions of undisturbed flow and a three-tube yaw probe was used in regions of skewed flow. They found that the bed shear stresses at the upstream corner of the plate were up to five times the bed shear stresses in the approach flow section. The initiation of local scour is associated with the increase in shear stress caused by the accelerating flow around the obstruction. For cylindrical bridge piers, scour has been observed to be dominated by a strong downflow on the upstream side of the pier and a horseshoe vortex which surrounds the upstream and lateral sides of the pier (e.g. Mellville and Raudkivi, 1977; Graf and Yulistiyanto, 1998; Istiyato and Graf, 2001). For bridge abutments, which are in many ways similar to spur dikes, flow features resembling those observed around one-half of a cylindrical bridge pier have been measured, including the primary vortex (essentially one half of the horse-shoe vortex), which forms around the structure and contributes to the development of scour (Kwan and Melville, 1994). These investigators have determined that the flow structures around a model wingwall abutment are dominated by the large primary vortex and an associated downflow.

Detailed velocity measurements around a submerged spur dike with a trapezoidal shape are rare. Flow around this structure would be expected to vary from that of flat plates and abutments due to the over-topping flow and three-dimensional shape of the structure. The over-topping flow and trapezoidal shape would be expected to affect the characteristics of the primary vortex and make the recirculation zone behind the spur dike more three-dimensional. Because the flow is the key to understanding the performance of a submerged spur dike, the velocity field around the spur dike was measured in a laboratory flume at the National Sedimentation Laboratory.

2. Physical model and Velocity Data

All of the flow measurements were collected in a recirculating flume with a test channel 30 m long, 1.2 m wide, and 0.6 m deep located at the National Sedimentation Laboratory. Flow rate in the flume was measured using a pressure transducer connected to a Venturi meter in the return pipe. Flow depth was controlled by the amount of water in the flume and measured by taking the difference in elevation between 12-m long bed and water surface transects in the approach flow section. The bed of the approach flow section was covered with sediment (D_{50} = 0.8 mm, $[D_{84}/D_{16}]^{1/2}$ =1.35). The bed sediment was allowed to scour for 30 hours under steady flow conditions. The bed was then immobilized with a thin layer of cement from 21.9 m downstream of the channel inlet to the tail box to prevent the bed from changing. The zero location of the X (streamwise) coordinate was located 22.6 m downstream of the channel inlet and the center of the spur dike model was located 1.19 m downstream from the zero coordinate. The spur dike model (Fig. 1) was located on the left wall of the channel facing downstream. A topographic map of the scoured fixed bed is shown in Figure 2. Flow conditions were very similar to those used in one experiment from Kuhnle, et al. (1999) and are summarized in Table 1. The ratio of the flow shear velocity to the critical shear velocity of the bed material sediment obtained from the Shields (1936) curve was 0.7 in the approach flow section.

The velocity data was collected using a commercially available Acoustic Doppler Velocimeter (ADV). The measurement head of the ADV is mounted on a stainless steel mast 0.60 m long and 0.01 m in diameter. The measurement head has three sensors mounted at a

spacing of 120° around a circle approximately 70 mm in diameter. The sampling volume of the ADV is a cylinder 6 mm in height and 6 mm in diameter (170 mm^3) located 50 mm away from the head of the ADV. Flow velocity data at each point was collected at 50 Hz for 5 minutes. The 5 minute sample duration was determined empirically as the optimum length of time to capture the mean and fluctuations of the velocity at the sampling location within a reasonable time frame.

Flow velocities were measured at 288 locations on the X-Y plane as shown in Figure 3. At each location the flow was measured at vertical positions: 0.0100, 0.0225, 0.0350, 0.0475, 0.0600, 0.1000, 0.1400, 0.1800, and 0.2200 m above the pre-scoured bed elevation. At locations where the bed had been scoured, flow measurements were also made at 0.25 cm below the pre-scoured bed elevation and at 1.25 cm intervals for as many measurements as possible to the bed. This resulted in from 9 to 19 measurements in the vertical for each position. The vertical measurement positions were adjusted accordingly at the locations above the spur dike to arrive at nine measurement positions. A total of 3484 velocity vectors were measured over the fixed scoured bed. All velocity records were processed using the public domain program, WinADV. Measurements were filtered using WinADV to reject points with a correlation coefficient less than 0.7. In most files 90% or more of the data was above 0.7.

3. Velocity Data

The velocity data is presented as vector plots in the X-Z and Y-Z planes (Figs 4 and 5, respectively). The blank spaces at the bottom of the plots, below the pre-scour bed level (0.0), represents areas of the bed that were not scoured and thus no data could be collected. The blank zone at the top of the plots represents the top 8 cm of the flow that could not be measured because of the design of the ADV probe. It is clear from Figure 4 that the flow converges over the top of the structure and a large separation cell occurs downstream (Figure 4C). There is also evidence for a small separation cell near the bed just upstream of the structure (x = 0.8). Evidence for a cell upstream of the structure near the bed was not present in flow measurements taken over a fixed flat bed with the same flow and structure (Kuhnle et al., 2002). Based on the flow measurements over the flat bed, it was not expected that the local scour would reach the magnitude that was observed upstream of the structure (Fig. 2).

The plots in Figure 5 illustrate the change in the flow vectors as the flow converges and then diverges around the structure. The vectors in Figure 5A show the convergence of the flow around the structure and the lateral flow into the scour hole. In Figure 5B there is evidence for a vortex forming as the flow moves around the spur dike. The vortex is shown to be fully formed at the downstream end of the structure (Fig. 5C). Downstream of the spur dike the flow diverges and the vortex is dissipated (Fig. 5D). Zones of maximum local scour are seen to correlate to regions of large lateral flow velocities (Fig. 2, Figs. 5A and 5D).

4. Discussion

These results differ from those that were collected on an unerodible flat bed with the same flow and spur dike model (Kuhnle, et al., 2002). In the flat bed case there was no evidence of the primary vortex described in previous studies (e.g. Copeland, 1983; Kwan and Melville, 1994). In this study the primary vortex was clearly in evidence (Fig. 5B and 5C). However, the major zones of local scour were associated with large lateral flows rather than in a region of down flow as observed by Rajaratnam and Nwachukwu (1983) and Kwan and Melville (1994). This difference stems from the fact that the structure used in these experiments was trapezoidal

in shape and submerged. This three-dimensional submerged shape generates a flow pattern that tends to not "pile up" on the upstream edge of the structure, and to facilitate the formation of strong lateral flows upstream and downstream of the structure.

The secondary flows around the spur dike include a small vortex in the front edge and a larger recirculation cell behind the spur dike. Unlike the flow around two dimensional obstructions, the flow around the submerged trapezoidal spur dike has a fully three-dimensional recirculation cell. For structures with a vertical front, the blockage to the oncoming flow creates a strong down-flow and a primary or horseshoe vortex forms. This has been observed in studies of cylindrical piers and bridge abutments (Melville and Raudkivi, 1977; Kwan and Melville, 1994; Graf and Yulistiyanto, 1998). Some down-flow in front of the spur dike is present, however, it is relatively weak and the lateral flow component is dominant in the scour hole formation. This leads to a more complicated flow and local scour pattern (Fig. 2.). A vortex was measured in this study (Fig. 5B and 5C), however, it was not the key flow structure to cause the observed pattern of local scour.

5. Conclusions

Three dimensional flow measurements around a model spur dike on a stationary scoured bed showed flow patterns that differed from a previous study of flow over a stationary flat bed with the same upstream flow and model structure. In this study, strong lateral flows upstream and downstream of the spur dike were found to be the dominant cause of the local scour. Down flow and vortex structures were present but were found not to be the principal flow structures forming the local scour. The differences in flow features and resulting scour observed are believed to be the result of the three-dimensional shape of the model spur dike and the over-topping flow used in this study.

6. Acknowledgements

The flow data used in this study was collected by John Cox and Emery Sayre. John Cox carried out the initial processing of the flow data.

References

Copeland, R. R., 1983, "Bank protection techniques using spur dikes." Miscellaneous Paper HL-83-1, U. S. Army Waterways Experiment Station, Vicksburg, Mississippi, 32 pp.

Graf, W.H., and Yulistiyanto, B., 1998, "Experiments on flow around a cylinder; the velocity and vorticity fields", Journal of Hydraulic Research, IAHR, 36(4), 637-653.

Istiyato, I., Graf, W.H., 2001, "Experiments on flow around a cylinder in a scoured channel bed", International Journal of Sediment Research, 16(4), 431-444.

Kuhnle, R., Alonso, C.V., and Shields, F.D., 1999,"Geometry of scour holes associated with 90° spur dikes", Journal of Hydraulic Engineering, ASCE, 125(9), 972-978.

Kuhnle, R., Jia, Y., Alonso, C., 2002, "3-Dimensional measured and simulated flow for scour near spur dikes", First International Conference on Scour of Foundations, ICSF-1, Texas A&M University, College Station, Texas, p. 349-363.

Kwan, T.F., and Melville, B.W., 1994, "Local scour and flow measurements at bridge abutments", Journal of Hydraulic Research, IAHR, 32(5), 661-673.

Melville, B.M., and Raudkivi, A., 1977, "Flow characteristics in local scour at bridge piers", Journal of Hydraulic Research, IAHR, 15(4), 373-380.

Rajaratnam, N., and Nwachukwu, B. A. 1983. "Flow near groin-like structures." Journal of Hydraulic Engineering, ASCE, 109(3), 463-480.

Richardson, J.E., and Punchang, V.G., 1998, "Three dimensional simulation of scour-induced flow at bridge piers", Journal of Hydraulic Engineering, ASCE, 124(5), 530-540.

Shields, A., 1936, Anwendung der Aenlichkeitsmechanik und der Turbulenzforschung auf die Geschiebebewegung, Mitteilungen der Preussischen Versuchsanstalt fur Wasserbau und Schiffbau, Berlin, Germany, translated to English for W.P. Ott and J.C. van Uchelen, California Institute of Technology, Pasadena, CA.

Shields, F. D., Jr., Cooper, C. M., Knight, S. S., 1995, "Experiment in stream restoration." Journal of Hydraulic Engineering, ASCE, 121(6), 494-502.

Table 1. Flow condition of the flume experiments.

Exp. Run	Flow rate (m^3/s)	Flow depth (m)	Mean Flow velocity (m/s)	Froude Number
Flat fixed bed	0.129	0.3048	0.347	0.201

List of Figures

Figure 1. Definition sketch of experimental setup. The shaded block represents the model spur dike. All dimensions are in meters.

Figure 2. Topographic map of fixed scoured surface with contour interval of 0.02 m. Original bed surface was at 0.48 m above bottom of well.

Figure 3. Plan view of experimental flume with measurement locations indicated by diamond symbols. Outline of spur dike is also shown.

Figure 4. Flow vectors in X-Z plane. (A) Y = 0.73 m, (B) Y = 0.85 m, (C) Y = 1.10 m.

Figure 5. Flow vectors in Y-Z plane, view upstream. (A) X = 0.77 m, (B) X = 1.19 m, (C) X = 1.42 m, (D) X = 1.79 m.

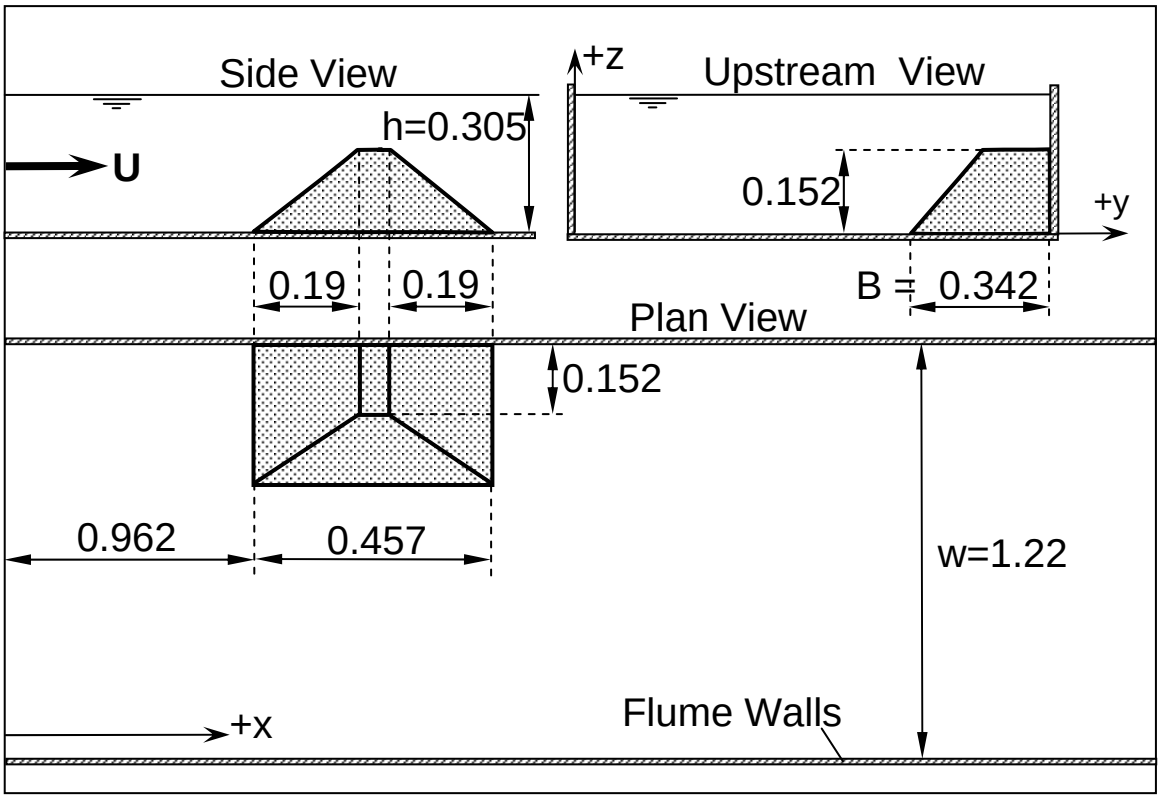

Figure 1. Definition sketch of experimental setup. The shaded block represents the model spur dike. All dimensions are in meters.

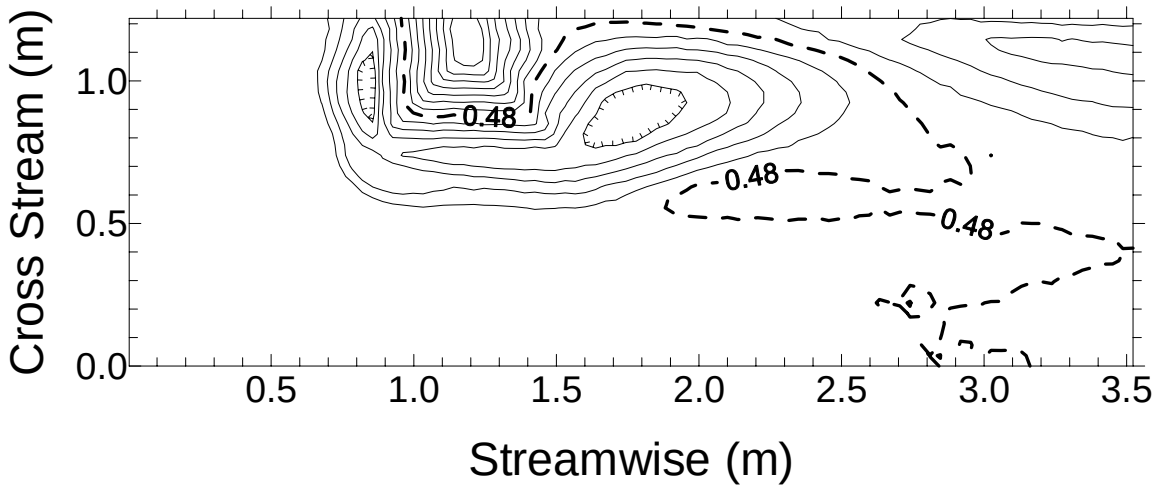

Figure 2. Topographic map of fixed scoured surface with contour interval of 0.02 m. Original bed surface was at 0.48 m above bottom of well.

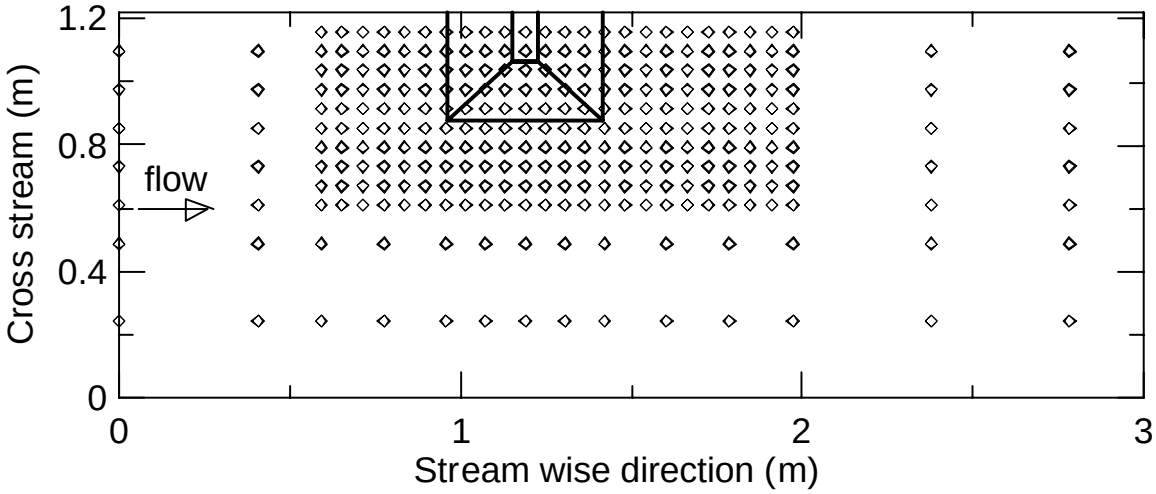

.

Figure 3. Plan view of experimental flume with measurement locations indicated by diamond symbols. Outline of spur dike is also shown.

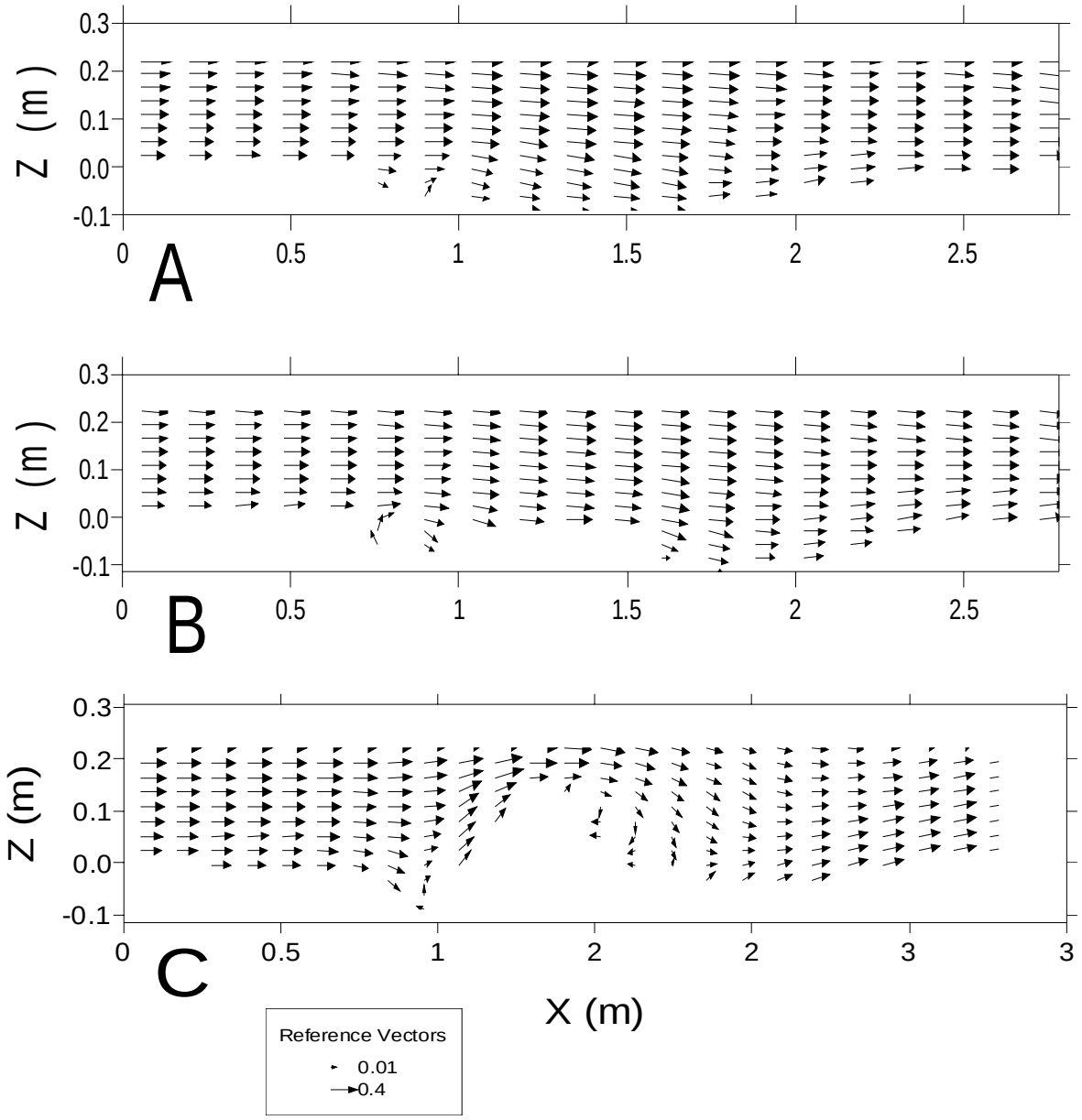

Figure 4. Flow vectors in X-Z plane. (A) Y = 0.73 m, (B) Y = 0.85 m, (C) Y = 1.10 m.

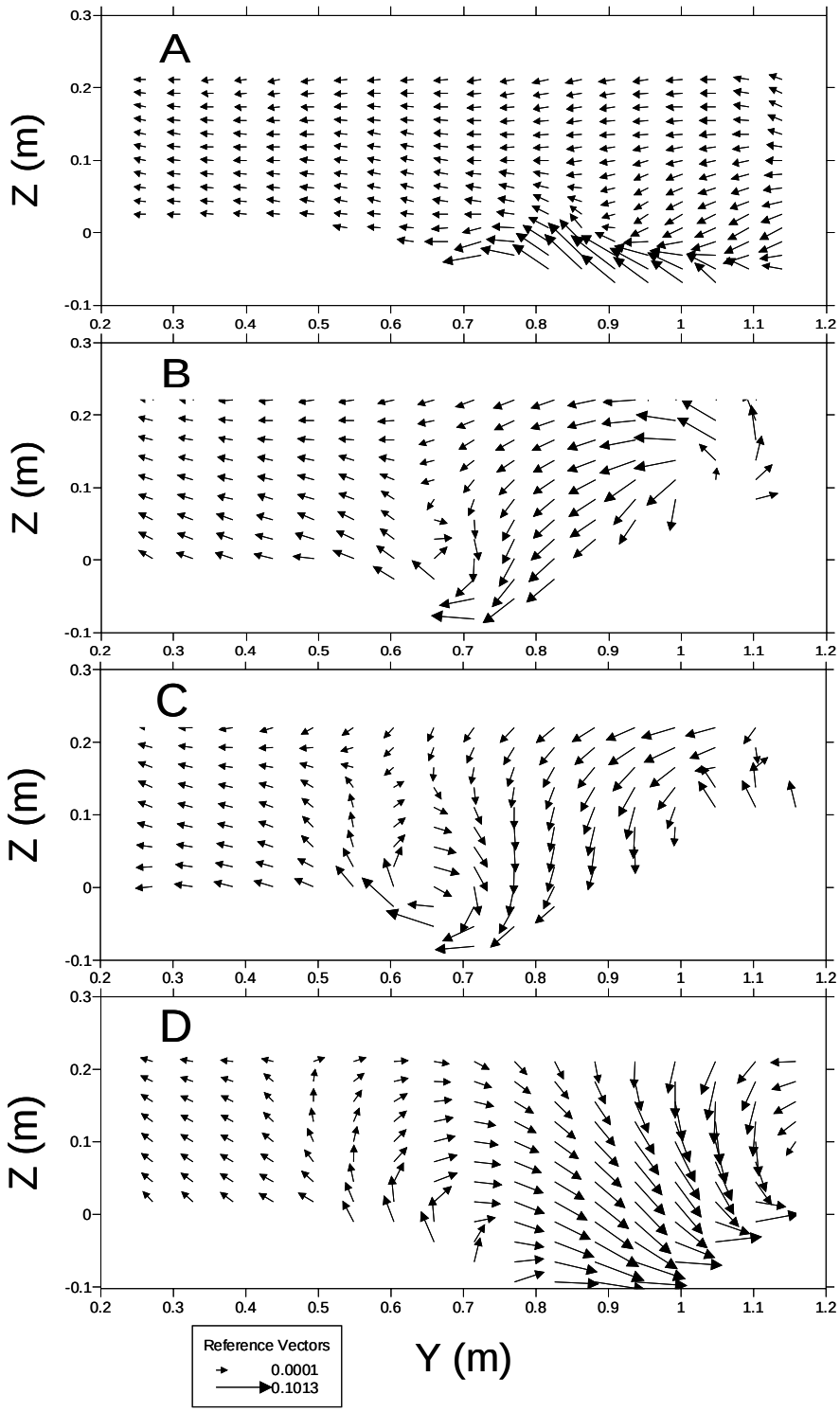

Figure 5. Flow vectors in Y-Z plane, view upstream. (A) X = 0.77 m, (B) X = 1.19 m, (C) X = 1.42 m, (D) X = 1.79 m.

Gully Erosion after Wildfire

J.A. Moody* (E-mail: jamoody@usgs.gov)
D.A. Kinner
U.S. Geological Survey
3215 Marine Street
Suite E-127
Boulder CO 80303
Phone 303-541-3011; FAX 303-447-2505 (fax)

Abstract

Predicting runoff and erosion from watersheds burned by wildfires requires an understanding of the spatial structure of both hillslope and channel drainage networks. We investigate the small-scale and large-scale structures of drainage networks using field studies and computer analysis of 30-m digital elevation model. Topologic variables were derived from a composite 30-m DEM, which included 14 order 6 watersheds within the same geological terrain (Pikes Peak batholith). Both topologic and hydraulic variables were measured in the field in two burned watersheds (3.7 and 7.0 hectares) located within one of the order 6 watersheds burned by the 1996 Buffalo Creek Fire.

Horton ratios of topologic variables (stream number, drainage area, stream length, and stream slope) for small-scale and large-scale watersheds are shown to scale geometrically with stream order (i.e., to be scale invariant). Hydraulic variables (width, depth, cross-sectional area, and bed roughness) for small-scale watersheds also were found to be scale invariant across 3 to 4 stream orders. Bed roughness and width-to-depth ratio were constant across all scales. Fewer order 1 and order 2 streams were observed in the field than predicted by theory. The different hillslope drainage network pattern, composed of multiple parallel rills or multiple converging rills, may replace some order 1 streams. This reduction in the number of order 1 and 2 streams appears to be a consequence of hillslope processes.

Keywords: channel network, hillslope network, wildfire, gullies, scaling

1. Introduction

Wildfires are landscape disturbances that change the hydrologic response of watersheds. When substantial rainfall follows a wildfire, the subsequent runoff and erosion can extend the existing pre-fire channel network farther up the hillslope. With an increase in wildfire throughout wildland-urban interface areas in the western United States and elsewhere, a need exists to model burned hillslope and channel systems in order to predict floods and subsequent erosion from burned watersheds. One fundamental question related to this erosion is how the channel network structure of this newly incised terrain is similar to or different from the network as a whole. If the channels follow previously defined, but unchannelized drainages, then it is possible that the larger drainage pattern is preserved during the new period of erosion and incision. However, it is also possible that new hillslope rills and gullies may define a new drainage network with a

*Corresponding author

different structure particularly at the hillslope-channel interface. Full-scale 3-D numerical models of entire watersheds are impractical to implement because they require extensive site-specific topographic input and are limited to a single-thread reach of a channel rather than channel networks with numerous confluences. They are inappropriate because these models are designed to resolve small-scale (0.01-1m) detailed flow and sediment erosional and depositional features within the channel reach and this scale of resolution is unnecessary for predictions of runoff and erosion at the watershed scale. Therefore similarities and scaling properties are needed to simplify runoff and erosion modeling of both hillslope and channel networks.

Initially, the theoretical random model (Shreve, 1966, 1969) suggested that channel networks in a particular lithology or similar geological terrain developed as a random structure with a bifurcation ratio of 4.0. Later theoretical models of channel networks were based on such physical principles of effective connectivity, an empirical power law that relates slope to discharge, and the minimum energy expenditure and dissipation (Howard, 1990; Sun et al., 1994a; Rodriguez-Iturbe and Rinaldo, 1997). These theoretical networks often have a fractal dimension near 2, which indicates the networks are "space filling" and drain a watershed efficiently or with minimum energy expenditure. Sun et al. (1994b) investigated the effect of including a hillslope process threshold to determine theoretical channel networks and later Tucker and Bras (1998) expanded the idea by investigating several different hillslope thresholds. Theoretical models are limited by the resolution of the large-scale digital elevation models (DEMs) and do not resolve small-scale structures at the hillslope-channel interface. A summary by Abrahams (1984) of field studies and an analysis by Peckham (1995) of large river basins suggest that channel networks diverge from a random structure and these investigations have begun to explain channel network structure based on physical principles.

Our purpose in this short paper is to characterize spatially (for modeling applications) the drainage networks of hillslopes and channels in a watershed disturbed by wildfire. We rely on both field studies and computer analysis to 1) examine the small scale (0.01-1.0 km^2) structures of the post-fire hillslope and channel networks, 2) compare them to the structure of channel networks in unburned watersheds derived from computer analysis of large scale (1-1000 km^2) digital elevation models, and 3) explore how the channel network interfaces with the hillslope network.

2. Background

In May 1996, the Buffalo Creek Fire burned approximately 50 km^2 in the Pike National Forest southwest of Denver, Colorado. The fire burned two adjacent watersheds, Buffalo Creek and Spring Creek (Figure 1). A larger proportion of the Spring Creek watershed burned, 79% (21.2 km^2), compared with the Buffalo Creek watershed, 21% (25.7 km^2). These watersheds are underlain by the Pikes Peak granite batholith and have soil profiles that include emerging corestones and thick zones of decomposed granite called grüs. Two months after the wildfire, runoff from a short-duration, high-intensity rainstorm changed the topography of the watersheds. The storm lasted about one hour and the maximum rainfall intensity was ~90 mm h^{-1} (Moody and Martin, 2001a). It removed most of the ash from the hillslopes, rilled the hillslope surfaces, channelized drainages, led to a head-ward extension of the channel network into previously unincised terrain, and deposited sediment on alluvial fans at the mouths of tributaries and in the main channel of Spring Creek (Moody, 2001).

Two subwatersheds, W960 and W1165 (the number equals the distance in meters from the mouth of Spring Creek) were investigated to determine the amount of erosion and the

structure of the hillslope and channel drainage networks in this newly incised terrain (Figure 1). Subwatershed W960 (7.01 ha) is a south-facing watershed with an average hillslope length (1/2 x drainage density, Horton, 1945) of 24 m and W1165 (3.71 ha) is a north-facing watershed with an average hillslope length of 10 m.

3. Methods

3.1. Small-Scale Measurements

Field measurements of hydraulic variables were made in 1999 at 5-m intervals in all gullies and channels incised into the existing drainage network in watershed W960 and W1165 as well as in some rills. Assuming that the post-flood surface adjacent to the rills, gullies, and channels was the same as the pre-flood surface, the volume of material removed from the recently incised drainages was calculated by extending this post-flood surface across the channel, measuring the depth down from this imaginary surface to the bottom of the incised channel, and multiplying by the average of the top width and bottom width. Identification of the location of the pre-flood surface above the incision was aided in many places by using tree roots left exposed after the floods. These roots and rootlets, typically, were unbroken and in some cases spanned the entire gully or channel. Some topologic variables were measured from digital and photogrametric products. Statistical measures (means, coefficient of variation, skewness, and kurtosis) of the distribution of each topologic and hydraulic variables were computed separately for W960 and W1165 (Table 1).

A Horton ratio is a descriptor of the change in spatial structure of stream variables across scales (stream orders). The Horton ratio of stream variable X, R_X (Table 1 and 2), can be redefined for mathematical convenience as $R_X = \frac{c}{|c|}e^{|c|}$ and then c is the slope of a log-linear plot of the following equation

$$X = ae^{ck} \tag{1}$$

where a is a constant and k is the scale factor or stream order.

3.2. Large-Scale Measurements

A regional topologic analysis of stream networks was completed using data from 36, 7.5-minute quadrangles joined to create a single composite 30-m DEM that encompassed the topography of much of the Pikes Peak granite batholith. The extent of the batholith was determined from the digital geologic map of Green (1992) projected to match the projection of the composite DEM. The individual DEMs were joined to create the composite 30-m DEM by using the program RiverTools (Peckham, 1998; Rivix Limited Liability Company, 2001), which was also used to analyze the channel network. We used the D-8 flow direction algorithm (O'Callahan and Mark, 1984) and iterative-linking flat resolution (Jenson and Domingue, 1988) in order to determine flow directions on the DEM. Streams were differentiated from surrounding hillslopes by using a threshold contributing area of 0.01 km^2 (1 ha). This area is consistent with an average contributing area shown by Montgomery and Dietrich (1994, Figure 11.9) for a channel slope equal to the average channel slope for W960 and W1165 and is on the order of the size of the study watersheds. Field evidence indicates that little, if any, channel incision existed within the study watersheds before the flooding events.

After delineating the stream network for the composite 30-m DEM, large-scale measurements of topologic variables (bifurcation, drainage area, length, and slope) were derived

from the DEM only for those watersheds that were within the batholith. Spring Creek was an order 6 watershed, so large-scale measurements were derived for 14 order 6 watersheds within the batholith for comparison with the small-scale data.

4. Results

Numerous hydraulic measurements were made for each stream order in the small-scale W960 and W1165 subwatersheds, which provide information on the probability distribution of each topologic and hydraulic variable. All of the distributions are positively skewed except for the drainage area for the order 2 streams in W1165. Similarly, the negative kurtosis (flatness of the distribution) is relatively small (<-2.6), while the positive kurtosis (peakedness of the distribution) has a wide range from 0.01 to greater than 20 for cross-sectional area and width-to-depth ratio for some stream orders. Mean width-to-depth ratios at individual cross sections ranged from 5-9 for order 1, 2, and 3 streams, values typical of rills and gullies. This ratio for individual cross sections changed abruptly to about 20 for the order 4 stream in W1165, a value typical of channels.

4.1. Channel Network

The Horton ratios for bifurcation, drainage area, and stream length (R_B, R_A, and R_L) were computed for 14 watersheds in the 30-m DEM (Table 2). The coefficient of determinations (r^2) for fitting equation (1) were equal to 1.00. These ratios are close to those ratios published by Peckham (1995) for the "humid" order 8 Kentucky River watershed and for the "semi-arid" order 8 Powder River watershed (Table 2). At the small scale, the coefficient of determinations ranged from 0.96 to 1.00 for the Horton ratios derived from field data (with one exception, W1165-length, r^2= 0.86). The Horton ratios for slope, bed roughness, and width-to-depth ratio at both large and small scales were nearly equal to 1.

4.2. Hillslope Drainage Network

The number, length, and width of rills (order 0 streams) were measured but the actual drainage area for each rill was not (Table 1). Many order 1 streams began where more than two rills joined. An average of 6.3 rills produced an order 1 stream in W960 and 3.6 rills produced an order 1 stream in W1165. The average rill spacing (total rills/(2 x total stream length)) along all stream orders was 11.5 m in W960 and 10.6 m in W1165.

5. Discussion

5.1. Channel Network

Horton ratios computed from the large- and small-scale data were definitely scale invariant and thus, scaled geometrically with stream order. The Horton ratios derived for the small-scale measurements are generally less than those derived from the large scale 30-m DEM. This is expected as the ratios tend to approach an asymptotic value as the scale of the watershed increases (Peckham, 1995). Slopes, bed roughnesses, and width-to-depth ratios are scale invariant in the gullies, but rather than scaling geometrically, these variables are approximately constant (i.e. varying slowly) across all scales. Based on the similarity of the Horton ratios of the topologic variables from both large and small scales, we hypothesize that these hydraulic variables may be scale invariant over larger scales provided larger watersheds are still within similar geological terrain.

5.2. Hillslope Drainage Network

Rills appear to be ephemeral on a decadal time scale in the Spring Creek watershed (Pine, 2002) and were observed to have two different spatial patterns within each watershed.

One pattern was nearly parallel rills with a long and narrow drainage shape on small-scale segments of hillslopes that approximate a planar surface with a constant hillslope inclination. The other pattern was a group of rills that converge together to form an order l channel head at the lower end of the obovate-shaped critical drainage area. If this hillslope surface is divided into triangular segments equal to the number of converging rills (6.3 rills in W960 and 3.6 rills in W1165), then each rill can be approximated to flow on a small planar surface.

Planar surfaces appear to be fundamental units composing hillslopes and will by definition have a constant slope. On planar surfaces, flow in rills is straight and parallel. We propose (based on field measurements that indicate nearly constant cross-sectional area with down-slope distance; Moody and Martin, 2001b, Fig. 4.7) that discharge does not accumulate significantly in rills in the downstream direction. This is in contrast to channels networks where discharge can increase abruptly at channel confluences. Sun et al. (1994b) explicitly differentiated hillslopes from channels by assuming hillslopes were those areas with constant slope and with a drainage area less than the critical area for channel initiation (Montgomery and Dietrich, 1994).

Sun et al. (1994b) have shown that the number of order 1 and 2 streams is dependent on inclusion of hillslope processes in theoretical, optimal channel networks. A *hillslope effect ratio* can be defined to be equal to the number of streams in the watershed without hillslope processes divided by the number of streams in the watershed with hillslope processes. The theoretical ratios derived from Sun et al. (1994b, Figure 6) for a watersheds with a hillslope inclination of 30° were 1.8, 1.1, and 1.0 for order 1, 2, and 3 streams. A similar ratio can be calculated from field data presented in this paper to verify this prediction. The ratio is the number of streams predicted by using the Horton ratio (derived from the large-scale 30-m DEM) divided by the measured number of streams. The *hillslope effect ratios* for W960 are then 1.4, 1.0, and 1.0, values which are very similar to the theoretical *hillslope effect ratio*. For W1165 the *hillslope effect ratios* (4.2, 3.6, and 2.0) are larger suggesting that hillslopes in this subwatershed may have a more dominant role in determining channel networks. These order 1, 2, and some order 3 channels are gullies (width-to-depth ratio <10), which have developed after the wildfire disturbance, as incised features in an interface region between the hillslope and channel network. They are transient and with time will refill with colluvium and revert back to drainages (swales or hollows) on a millennium time scale (Welter, 1995; Moody and Martin, 2001a).

The pattern of the gully and channel network is dependent on the threshold criteria used to define a hillslope. Tucker and Bras (1998) have created channel networks using several hillslope criteria and found differing slope-area and slope-drainage density relations. The simple definition of a hillslope used by Sun et al. (1994b) results in numerous long, parallel channels beginning wherever the area exceeds the critical area on a constant slope. This is not observed in the field and this definition does not account for the concave, obovate surfaces at the head of order 1 channels. Therefore, additional parameters are needed to define the hillslope such as slope or curvature. Slope and critical area have been proposed by Montgomery and Dietrich (1994) and the nature of the concave, obovate surfaces suggests that curvature should be included in the definition of a hillslope.

6. Conclusion

The scale invariant property of Horton ratios of topologic variables derived from large scale DEMs (1-1000 km^2) can be used to approximate and simplify channel (width-to-depth > 10) networks at small scales (0.01-1km^2) for modeling purposes. Large-scale DEMs probably do

not resolve gullies (width-to-depth < 10) and rills, which are part of the hillslope drainage network. Channel slope, bed roughness, and channel width-to-depth variables have Horton ratios near 1 and thus are constant across scale. Horton ratios of hydraulic variables derived from field measurements at the small scale also are scale invariant and may be extrapolated to the larger scale provided higher order watersheds are within the same geological terrain.

Evidence in this paper supports the theoretical prediction that the watershed drainage network depends on the interaction between hillslope and channel processes in an interface region. The number of gullies (low order streams) in the interface region, required to efficiently drain water from the watershed, were less than the number of channels predicted by using the Horton ratios for the large scale composite 30-m DEM, which did not include hillslope processes. Three regions with differing drainage network characteristics have been identified after erosion following a wildfire: 1) a hillslope region characterized by rills with a decadal time scale, a width-to-depth ratio less than 10, and two spatial patterns; 2) an interface region characterized by gullies with a millennial time scale and a width-to-depth ratio less than 10; and 3) a channel region with a geological time scale and a width-to-depth ratio greater than 10.

Acknowledgments

Field measurements at this detail can never be done alone. Tanya Ariowitsch, Lisa Pine and Deborah Martin contributed patience, time, and suggestions that made the data collection successful. Lengthy discussions with Deborah Martin, Scott Peckham, and Jim Smith clarified many concepts. This work was in part supported by a Mendenhall Post-Doctoral Fellowship awarded to David Kinner. The use of trade, product, or firm names in this paper is for descriptive purposes only and does not constitute endorsement by the U.S. Geological Survey.

References

Abrahams, A., 1984. Channel networks—a geomorphological perspective. Water Resources Research, 20(2): 161-188.

Green, G., 1992. The digital geologic map of Colorado in ARC/INFO Format. U. S. Geological Survey Open-File Report, OF-92-0507.

Howard, A.D., 1990. Theoretical model of optimal drainage networks. Water Resources Research, 26(9): 2107-2117.

Horton, R.E., 1945. Erosional development of streams and their drainage basins; Hydrophysical approach to quantitative morphology. Bulletin of the Geological Society of America, 56, 275-370.

Jenson, S.K., Domingue, J.O., 1988. Extracting topographic structure from digital elevation data for geographic-information system analysis. Photogrammetric Engineering and Remote Sensing, 54(11), 1593-1600.

Montgomery, D.R., Dietrich, W.E., 1994. Landscape dissection and drainage area-slope thresholds. In: Kirkby, M.J. (Ed). Process Models and Theoretical Geomorphology, John Wiley & Sons Ltd., 221-246.

Moody, J.A., 2001. Sediment transport regimes after a wildfire in steep mountainous terrain. In Proceedings of the Seventh Federal Interagency Sedimentation Conference, March 25 to 29, 2001, Reno Nevada, X-41 to X-48.

Moody, J.A., Martin, D.A., 2001a. Initial hydrologic and geomorphic response following a wildfire in the Colorado Front Range. Earth Surface Processes and Landforms, 26, 1049-1070.

Moody, J.A., Martin, D.A., 2001b. Hydrologic and sedimentologic response of two burned watersheds in Colorado. U.S. Geological Survey Water-Resources Investigation Report 01-4122, 142 p.

O'Callahan, J. Mark, D., 1984. The extraction of drainage networks from digital elevation data. Comput. Vision and Graph. and Image Processes, 28, 328-344.

Peckham, S.D., 1995. New results for self-similar trees with applications to river networks. Water Resources Research. 31(4), 1023-1029.

Peckham, S.D., 1998. Efficient extraction of river networks and hydrologic measurements from digital elevation data, In: Barndorff-Nielsen et al., (Eds.), Stochastic Methods in Hydrology: Rain, Landforms and Floods. Singapore, World Scientific, 173-203.

Pine, E.J., 2002. Short-term rill evolution following the Buffalo Creek Fire, Buffalo Creek, Colorado. Masters Thesis, Department of Natural Science, Mathematics, and Engineering, University of Denver, Denver.

Rodriguez-Iturbe I, Rinaldo A. 1997. Fractal River Basins Chance and Self-Organization. Cambridge University Press, New York.

Rivix Limited Liability Company, 2001. RiverTools User's Guide release 2001.

Boulder, Colorado, Research Systems, Inc., 202 p.

Shreve, R.L., 1966. Statistical law of stream numbers. Journal of Geology, 74, 17-37.

Shreve, RL., 1969. Stream lengths and basin areas in topologically random channel networks. Journal of Geology, 77: 397-414.

Sun, T., Meakin, P., Jøssang, T., 1994a. The topography of optimal drainage basins. Water Resources Research, 30(9), 2599-2610.

Sun, T., Meakin, P., Jøssang, T., 1994b. A minimum energy dissipation model for drainage basins that explicitly differentiates between channel networks and hillslopes. Physica A, 210, 24-47.

Tucker, G.E., Bras, R.L., 1998. Hillslope processes, drainage density, and landscape morphology. Water Resources Research, 34(10), 2751-2764.

Welter, S. P., 1995. Topographic influences on erosion and soil development in hollows of the Rampart Range, Colorado. PhD Dissertation, Department of Geography, University of Colorado, Boulder, Colorado.

Table 1. Topologic and hydraulic stream variables of subwatersheds W960 and W1165 [--, no data]

		Number of measurements		Mean		Coefficient of variation		Skewness		Kurtosis	
	Order	W960	W1165	W960	W1165	W960	W1165	W960	W1165	W960	W1165
Number of streams	0	--	--	365	378	--	--	--	--	--	--
	1	--	--	13	19	--	--	--	--	--	--
	2	--	--	4	5	--	--	--	--	--	--
	3	--	--	1	2	--	--	--	--	--	--
	4	--	--	--	1	--	--	--	--	--	--
Drainage area (ha)	1	11[a]	18	0.20	0.06	1.20	0.85	2.8	1.6	8.4	2.4
	2	4	4[a]	0.95	0.27	0.69	0.56	--	-1.7	--	2.7
	3	1	2	7.02	0.94	--	0.35	--	--	--	--
	4	--	1	--	3.72	--	--	--	--	--	--
Length (m)	0	36[a]	38[a]	27	29	0.70	0.48	0.3	0.6	-0.1	-1.0
	1	13	18	49	55	0.69	0.56	0.9	0.9	0.1	-0.4
	2	4	5	137	50	0.40	0.57	1.2	0.7	1.9	-2.6
	3	1	2	292	113	--	0.16	--	--	--	--
	4	--	1	--	223	--	--	--	--	--	--
Slope	1	120	172	0.41	0.40	0.24	0.29	0.50	0.20	1.4	-0.4
	2	106	42	0.34	0.35	0.35	0.43	0.78	0.7	1.0	0.8
	3	57	47	0.22	0.30	0.18	0.53	0.16	0.9	-0.8	-0.1
	4	--	41	--	0.22	--	0.64	--	2.7	--	7.4
Width (m)	0	109[b]	--	0.30	--	0.43	--	1.3	--	1.4	--
	1	120	172	0.98	0.55	0.62	0.49	1.6	1.4	3.2	2.5
	2	106	42	1.93	1.06	0.59	0.55	1.6	1.4	3.4	2.8
	3	57	47	5.03	1.44	0.35	0.42	1.1	0.7	2.3	0.2
	4	--	41	--	4.02	--	0.30	--	0.5	--	0.0
Depth (m)	1	120	172	0.20	0.12	0.86	0.64	1.7	1.4	2.7	1.9
	2	106	42	0.42	0.33	0.79	0.80	1.3	1.2	1.5	0.7
	3	57	47	0.86	0.39	0.40	0.64	1.1	1.3	1.5	2.2
	4	--	41	--	0.38	--	0.75	--	0.7	--	-0.8
Cross-sectional area (m^2)	1	120	172	0.19	0.049	1.63	0.92	4.6	3.7	25.8	23.2
	2	106	42	0.69	0.29	1.06	1.00	1.9	0.6	3.9	-0.3
	3	57	46	4.35	0.43	0.79	0.79	3.3	1.5	13.6	2.6
	4	--	41	--	1.33	--	0.72	--	0.8	--	-0.1
Bed z_0=k/10, (mm)	1	120	163	5.5	5.2	0.61	0.69	0.9	1.1	-0.3	1.0
	2	106	36	10.4	11.8	0.64	0.62	1.1	0.6	0.5	-0.3
	3	57	27	4.8	15.9	0.50	1.02	2.4	1.3	7.1	0.6
	4	--	39	--	4.7	--	1.04	--	1.5	--	1.7
Width-to-depth ratio	1	120	172	8.6	7.3	1.20	1.28	2.7	3.8	7.8	16.1
	2	106	42	8.9	5.4	0.52	1.04	5.4	2.5	31.9	6.9
	3	57	47	6.5	5.7	0.40	1.14	0.7	4.0	0.8	20.4
	4	--	41	--	22.2	--	1.09	--	2.8	--	10.1

[a] areas for 1 or 2 streams were unavailable

[b] subsample of all the rills

Table 2. Horton ratios for different spatial scales
[na, not available; negative sign indicates variable decreases as stream orders increases]

Variable	Kentucky River order 8	Powder River order 8	Pikes Peak batholith 14 watersheds order 6	W960 order 3	W1165 order 4
			Topologic variables		
Bifurcation	4.6	4.7	4.3	3.6	2.6
Drainage area	4.7	5.0	4.8	5.9	3.8
Length	2.5	2.4	2.2	2.5	1.6
Slope	na	na	-1.4	-1.4	-1.2
			Hydraulic variables		
Width	na	na	na	2.3	1.9
Depth	na	na	na	2.1	1.4
Cross-sectional area	na	na	na	5.0	2.7
Bed roughness	na	na	na	-1.1	-1.0
Width-to-depth ratio	na	na	na	-1.2	1.4
Percent total net erosion	na	na	na	3.2	1.8

List of Figures

Figure 1. Location of the two burned subwatersheds W960 and W1165 in the Pikes Peak granite batholith and within the Spring Creek watershed.

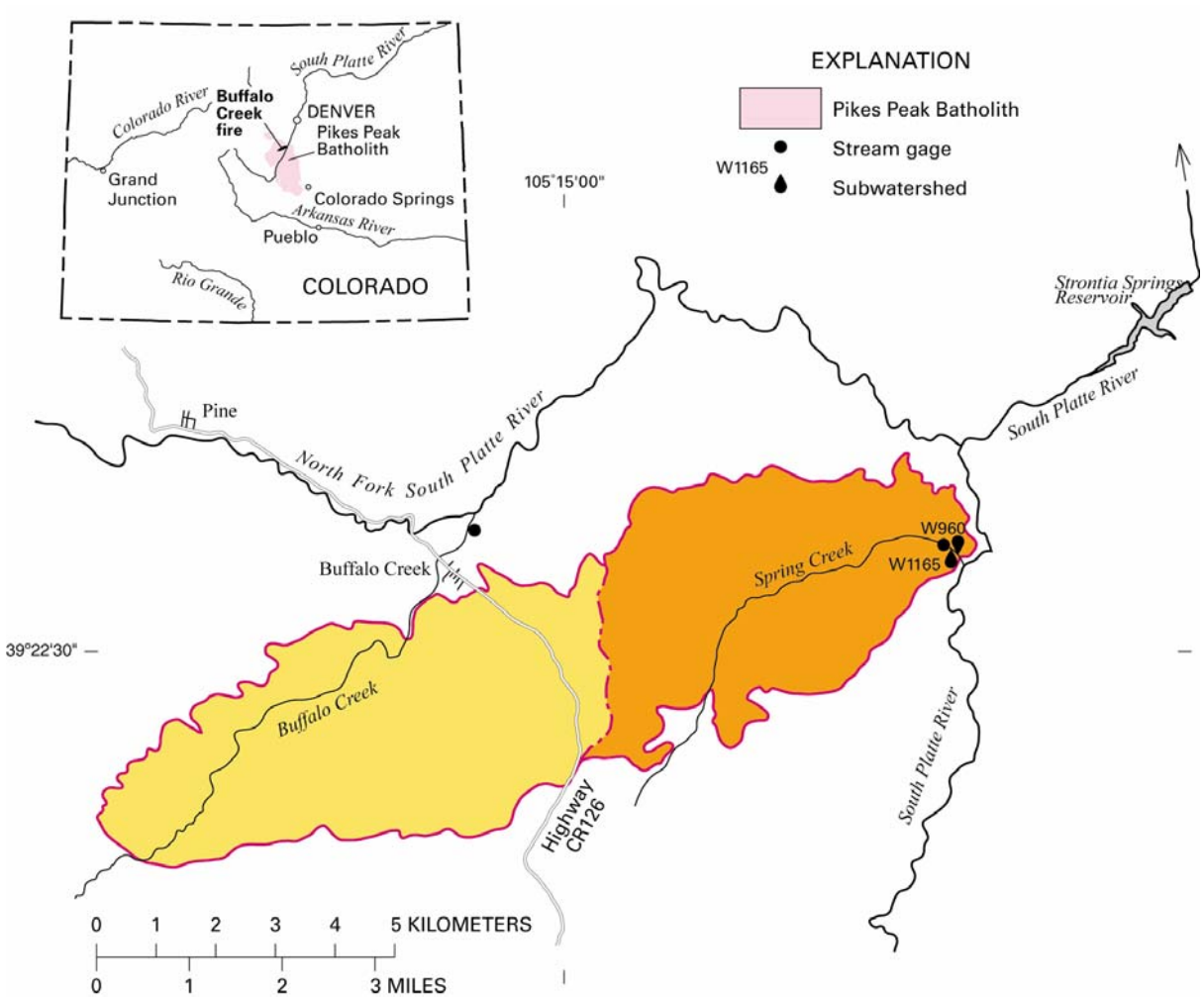

Figure 1. Location of the two burned subwatersheds W960 and W1165 in the Pikes Peak granite batholith and within the Spring Creek watershed.

Routing of Flow and Sediment in a Gully Network

J. Dungan Smith*
J. W. Kean
U.S. Geological Survey
3215 Marine Street, Suite E-127
Boulder, CO 80303, USA

Abstract

Wildfires leave hillslopes vulnerable to rill and gully erosion during subsequent heavy rains. Consequently, the ability to route water and sediment through gully networks during post-fire storms is critical to predicting sediment loading in streams, rivers, lakes, and reservoirs downstream of large, severely burned areas. Development of simple yet effective procedures for predicting incision of gully networks and for calculating flow and sediment transport in them is a fundamental problem in hillslope geomorphology. Owing to the small area involved, discharge at the downstream end of each link in the network can be approximately partitioned by upstream drainage area. Flow depth, not discharge, is the critical hydraulic variable on which boundary shear stress on the channel perimeter, perimeter-averaged sediment transport, and gully-bed erosion all depend. Unfortunately, flow depth at peak discharge throughout the gully network is not the depth of the gully below the pre-erosion surface and it has to be computed with a model that includes sidewall, as well as bed friction. Moody and Kinner comprehensively measured two gully networks that were incised during a single storm after the Buffalo Creek wildfire in Colorado. Using their data on network geometry, gully cross-section, and local waning-stage deposition, we have constructed a reach-averaged flow model for one of the networks. This model permits computation of maximum flow depth and boundary shear stress on the wetted perimeter of each link for the period of maximum flow. We also have computed cross-sectionally averaged sediment transport rates and erosion rates for each link and successfully compared the pattern of erosion rates with those measured by Moody and Kinner. Using cross-sectionally averaged velocities computed with the model, the peak flow then is routed through the network assuming spatially uniform rainfall. Partitioning of discharge by drainage area is shown to be an adequate initial hypothesis upon which some improvement in local peak discharge and peak-flow depths can be made iteratively.

Keywords: networks, erosion, routing

*Correspondence author

An Experimental Study on Gully Detachment and Transport on the Loess Plateau

Fenli Zheng*
Peiqing Xiao
Yuanyuan Jia
Institute of Soil and Water Conservation
CAS/MOWR, China

Min Wu
Northwestern Sci-tech University of Agriculture and Forestry

Yubin Zhang
Institute of Soil and Water Conservation

Abstract

A dual-box system, consisting of a test-box with 6-m long by 2-m wide and a feeder-box with 2-m long by 2-m wide feeder box was used to quantify gully detachment- transport. The results showed that gully formation and development were dominated by rainfall intensity, slope gradient, especially upslope runoff rate. Gully detachment-transport was higher 2-3 times than rill. 1-liter upslope-runoff caused 0.15 to 0.25 kg m-1 min-1 gully detachment rate. These results demonstrated that understanding gully erosion process is greatly important for erosion control and erosions modeling.

Keywords: gully, detachment, loess plateau

*Correspondence author

Accuracy of Methods for Field Assessment of Ephemeral Gully Erosion

J. Casalí* (E-mail: jcs@unavarra.es)
J. Loizu
M.A. Campo
L.M. De Santisteban (E-mail: luisa.satinsteban@unavarra.es)
Public University of Navarre
Department of Projects and Rural Engineering
Campus de Arrosadia s/n
31006 Pamplona, Spain
FAX: 34 948 169148

Abstract

In order to assess soil erosion, it is necessary to determine precisely the volume of ephemeral gullies in the field by using direct measurement procedures, in spite of this few information is available on the accuracy of the different methods. The procedure analysed in this paper consists on determining the cross sectional area of several cross sections along the gully, calculating the average cross sectional area of the sub-reaches considered and, after measuring the length of the sub-reaches, computing the total gully volume. The main purpose of this paper is to explore the measurement errors associated to some of the methods used for field measurement of ephemeral gully cross sectional areas, and to assess the effect of cross section measurement density, i. e., the number of cross sections per unit gully length. Three methods were considered to determine the gully cross sectional areas: micro-topographic profile meter (1); detailed measurement with a tape of section characteristic lengths (bottom and top width, heights, etc.) (2); measurement with a tape of cross section width and depth (3). Five ephemeral gullies of different morphology were selected. In each one of them, a homogeneous reach of 14 or 30 m was chosen. On each reach, the cross sectional areas were measured using the three above mentioned methods, with a separation (*s*) between cross sections of 1 m. Then, the corresponding total erosion volumes where computed. Finally, the effect on the resulting eroded volume of decreasing the cross section measurement density, by gradually increasing *s* (2-10 m) was explored. Even for *s* values as small as 1 m, large measurement errors occurred. Often, errors showed a high level of randomness and dispersion. The selection of the more suitable method for a certain gully shape and size seemed to be much more important than the distance between cross sections *s*, at least when $s < 10$ m. The smallest probability of large errors always occurred with method 1. For this method, *s* did not have much influence on the errors. Results with method 2 were similar to the ones from method 1, except for small but wide and shallow cross sections (group I), where were not acceptable. For those big, deep and narrow gullies (group II) where method 1 cannot be used, method 2 was leading to more accurate results than method 3. For group I gullies, method 3 should be used when a profiler was not available. Method 3 was similar to method 1 for group I gullies, but it was not valid for group II gullies. In summary: it was very important to select the most suitable method for each gully form; method 1 should be always the first option; method 2 could only be used with group II gullies or similar;

* Corresponding author

method 3 could only be used with group I gullies or similar. The repeatability of the results and thus its consistency should be checked in future field works.

Keywords: Ephemeral gully erosion; field assessment; assessment methods; accuracy of methods

1. Introduction

Ephemeral gullies are small channels caused by concentrated surface runoff flowing on erodible agricultural soils during rain events. Since the scoured soil volume is not very large they may be easily refilled by the farmers, often reappearing after some time in the same locations. While rills are restricted to planar elements of watersheds, ephemeral gullies appear on valley bottoms or within swales. Shape, size and growth pattern of ephemeral gullies are affected by soil factors like erodibility, occurrence of fragipans within the profile or moisture content (Moore et al., 1988), by topographic factors such as the size of the contributing watershed (Poesen and Govers, 1990), bed and slope steepness (Foster, 1986; Poesen and Govers, 1990; Poesen, 1993), and by agronomic practices. Ephemeral gullies can cause large soil losses (table 1, Poesen et al., 2003) contributing to the nonpoint pollution, and can alter farm operations and accelerate rill and interrill erosion increasing local slope after several voiding-filling cycles. Ephemeral gullies facilitate coarse particle transport, including soil aggregates, in a more efficient way than rills (Foster, 1986).

Considering the importance of this erosion type, measurement methods to precisely determine the volume of the ephemeral gullies are required. On table 2, a summary of some of the different methods used for assessing gully erosion, paying especial attention to ephemeral guliies, is shown. Very frequently, the authors do not provide information on probable errors that can be associated to each method.

The main purpose of this paper is to explore the measurement errors associated to: a) three of the methods used for field assessment of ephemeral gully cross sectional areas; b) to cross section density, i. e., the number of cross sections used per unit gully length and; c) to the gully form (Imeson and Kwaad, 1980). The three methods considered to determine the gully cross secional areas were: micro-topographic profile meter (1); detailed measurement, with a tape, of section characteristic lengths (bottom width, top width, heights, bank lengths and slopes, etc.), trying to take into account the complex cross section geometry (2); measurement with a tape of cross section width and depth (3).

These methods were selected because the direct assessment is often essential: it can be very precise, simple and low-cost compared with many indirect methods, which in turn require direct assessment for validation purposes.

2. Area Descriptions, Methods and Material Studied

Five ephemeral gully reaches 14 or 30 m long of different types were selected for this study, trying to cover a wide range of channel forms (table 3). The study sites were located in the town councils of San Martín de Unx and Beire, in Central Navarre (Spain) (De Santisteban et al., 2004).

After selecting the gully reach, the cross sections were marked with plastic sticks spaced 1 m apart (figure 1). On each reach, such cross sectional areas were measured using the three above mentioned methods, with a separation (*s*) between cross sections of 1 m. Then, the corresponding total erosion volumes where computed. Finally, the effect on the resulting eroded

volume of decreasing the cross section measurement density, by gradually increasing *s* (2-10 m), i. e., increasingly neglecting cross sections for calculations, was also explored on each gully.

The three methods used for cross section characterizazion and the procedure to calculate the volume of eroded soil are described below (see also figure 2).

Micro-topographic profiler (1). Cross-section morphologies were characterized using a gully profiler that consisted of 50 stainless steel pins spaced 20 mm apart (figure 3), placed perpendicularly to the gully axis. The pin configuration and hence channel geometry was photographed, and pin heights were digitized directly from these pictures, finally obtaining the cross sectional area.

Detailed characterization of cross sections with a tape and rule (2). Each cross section was assimilated to a simple geometric form, like a rectangle, a triangle or a trapezium, or a combination of some of those forms. Usually, a tape was used for directly measuring in the field horizontal distances, and the rule was used for measuring the vertical distances (depths). As many points as required for an accurate cross section characterization were determined. For upper cross section width definition, only points with evidence of recent water erosion were considered.

Approximated characterization of cross sections with a tape (3). This method consists in assuming that a rectangle is a good representation of all cross sections. One of its advantages is that a high number of cross sections can be characterized very quickly. Also in this case, only points with evidence of recent water erosion were considered for cross section width definition. For characterizing the cross section representative depth, an average value was considered when required. It was also the case when the cross sections were complex and more than one gully bed could be identified.

The volume of eroded soil was calculated for each sub-reach *i*, from its corresponding cross sectional areas A_{i-1} and A_i, spaced *s* meter apart. Thus, the volume of eroded soil in each complete gully reach is:

$$V = \sum_{i=1}^{n} V_i = \sum_{i=1}^{n} \frac{A_{i-1} + A_i}{2} \cdot s \qquad (1)$$

where:
V: Volume of eroded soil in the reach
n: Number of sub-reaches considered
V_i: Volume of eroded soil within the sub-reach *i*
A_{i-1}: Downstream cross sectional area of the sub-reach
A_i: Up stream cross sectional area of the sub-reach
s: Distance between adjacent cross sections

The volume calculated with micro-topographic profile meter (1) and with *s*= 1 m, was considered as the most precise, and it was took as the reference method. Elliot et al. (1997) also considered this method as the reference one, because of its high accuracy for estimating the hydraulic radius, an important variable for many water erosion models. For each gully, and for each one of the possible combinations previously described, the relative and absolute measurement error defined with respect to the reference method was calculated (equations 2 and 3):

$$E_{sm}^{r} = \frac{V_{sm} - V_{11}}{V_{11}} \cdot 100 \qquad (2)$$

where:
E^r_{sm} (%): Relative measurement error associated to *s* and to the cross section characterization method *m*
V_{sm}: Volume of eroded soil computed for a separation *s* and for the cross section characterization method *m*
V_{11}: Volume of eroded soil computed for the reference method, i. e, *s*= 1 and for the cross section characterization method 1 (micro-topographic profiler)

$$E^a_{sm} = \left| \frac{V_{sm} - V_{11}}{V_{11}} \right| \cdot 100 \qquad (3)$$

where:
E^a_{sm} (%): absolute measurement error associated to *s* and to the cross section characterization method *m*

3. Results and Analyses

On figure 2, examples of representative cross sections for each of the studied gullies, obtained by the three methods used for cross section characterization, are shown. As well, the different gully forms can be observed. The channel was characterized according to the gully average cross sectional area, the average width-depth ratio and the average cross section upper width (table 3).

Figure 4 shows the main results. First, an individualized gully by gully analysis of E^a_{sm} and E^r_{sm} was made (figure 4a-e, 4i-m). Then, values for E^a_{sm} were grouped in sets that were homogenous with respect to the width-depth ratio (*WDR*) and the cross sectional area (*A*). It can be assumed that these two variables comprise a substantial part of the gully properties, as *WDR* is related to the gully shape and *A* is related tol the gully size. The gullies were classified into two groups: gullies with *WDR*> 5 and *A*< 0.06 m^2 (I); gullies with *WDR*< 5 and *A*> 0.06 m^2 (II) (table 3). At Lakar 2 gully, *A*< 0.06 m^2, but it was included in group II, because *A* is not far from 0.06 m^2, it is only one gully, and *WDR* is clearly less than 5. It can be accepted that, in summary, group I correspond to small but wide and shallow gullies, and group II to large but narrow and deep gullies. Finally, the average E^a_{sm} for I and II groups and for all gullies were calculated (figure 4f, g, h).

Let's start the discussion about the average the average absolute measurement error (E^a_{sm}) for all gullies (figure 4h). Although the maximum *s* value was only 5 m, the smallest errors, on average, clearly occurred with method 1, ranging from 4.0% (*s*= 2 m) to 8.5% (*s*= 4 m). For method 2, average errors ranged between 9.0% (*s*= 3 m) and 15.0% (*s*= 5 m). As expected, method 3 was the less precise, with errors ranging from 8.0 to 17% (*s*= 3 m and *s*= 5 m, respectively). The slope of the straight lines corresponding to the linear regression between E^a_{sm} and *s* (figure 4h), despite the fitting was not statistically significant, indicated that, when method 1 was used, the dependence of E^a_{sm} on *s* was the smallest, and that when method 3 was used, such dependence was the largest.

For group I gullies (figure 4f), method 2 was leading the largest errors on both average and maximim errors. Curiously, methods 1 and 3 yielded almost the same results. On the other hand, any trend was found between E^a_{sm} and *s*. Method 1 was the most precise and its errors were on average 10.1%. Average errors for methods 2 and 3 were 10.3 and 18.8% respectively.

Maximum errors ranged between 22% for method 1 and 30% for method 2, meaning that, for that kind of gullies, large errors can occur with any measurement method. Besides, a great variability and dispersion of E^a_{sm} was observed, mainly in Navafría 2 gully (figure 4b), with sudden and often in alternation changes in its values. This variability may be bound to the high value of the cross section area variation coefficient A_{cv} (table 3) of that gully, meaning that, for irregular gullies (i. e., those with high A_c values) a small value of s is necessary to ensure small measurement errors. The dispersion of E^a_{sm}, tended to increase with s: when s increases, the probability that the surface area of few representative cross sections plays an important role in the final value of the computed volume, and thus in the error. Explanations for some of these results can come from the analysis of the characteristics of the gullies, mainly Navafría 1 (figure 4a), the smallest and the one with the largest *WDR*. In small, shallow and relatively wide gullies like these, the assessment of the characteristic lengths required for method 2 can be especially difficult. Even the uncomfortable posture of who is measuring can have an influence on the results, because small lengths have to be accurately assessed with a tape and ruler for quite a long time, also assimilating a few clean gully form. It seems to be that a more simple assessment of gully width and depth can result in higher accuracies than a more complex, uncomfortable and time-consuming assessment of characteristic lengths. This can explain the better results obtained with method 3 compared with those with method 2 for Navafría 1 gully. On the other hand, is in Navafría 1 gully where the highest errors were found, reaching up to 50% with method 2 (s= 6 m), and 30% with method 3 (s= 6 m).

Thus, for assessing volumes of irregular ($A_{cv}\approx$ 40% or higher), small (A_A< 0.03 m^2) and wide with WDR_A> 5 gullies, it seems to be necessary to use s values of 1-3 m with methods 1 and 3 to guarantee that errors remain below 10%.

For group II gullies (figure 4c), measurements with method 1 were also the most precise, with E^a_{sm} values always below 10%, and frequently smaller (figure 4c, d, e). Errors were almost non-dependent on s, and without sudden changes in its values. Errors greatly increased for method 3, mainly in the case of Beire gully, which is the largest and the one with smallest *WDR*. The good results with method 2 could be explained now from the big size of Beire gully, what allows for a good definition, visually and manually with the tape or rule, of the cross section characteristic lengths. Errors for method 3 were similar to the values found for group I gullies, and around 20%.

4. Conclusions

This paper intended to offer some first guidance for selecting the most suitable procedure when assessing ephemeral gully erosion in the field by direct measurement methods. The analysis of data showed that the issue addressed is not as simple as suspected, although the repeatability of the results and thus its consistency should be checked in future field works. Even for small s values, probably much smaller than the ones used in the majority of field surveys, large measurement errors occurred. In many cases, errors to be expected show a high level of randomness and dispersion. The selection of the more suitable method for a certain gully shape and size, defined by A, *WDR* an A_{cv}, seemed to be much more important than the distance between cross sections s, at least when s< 10 m. For the same gully, errors when applying one method or another method can differ in up to 6 times (figure 4e). The highest difficulties seemed to be for small but wide gullies (group I) because, even using method 1, were leading to large errors. On the contrary, with group II gullies (large but narrow) quite accurate assessments could be made with methods 1 and 2. The smallest probability of large errors always occurred with

method 1. For this method, *s* did not have influence on the errors so, *s* can be as high as 5 m without errors greater that 10%. When the gullies were homogeneous (i. e., for example, for A_{cv}< 40%), *s* could be even greater. The importance of the errors found even with method 1, suggests that the assessment of eroded volumes in this class of gullies (I) should be made with a profiler with more and thinner pins spaced few millimetres apart. Results with method 2 were similar to the ones from method 1, except for small and wide cross sections, where were not acceptable. For big gullies where method 1 cannot be used, method 2 should be always selected instead of 3. The use of profiler (method 1) is also recommended compared to method 2: supposedly, the main possible supposed advantage was rapidity but, in fact, a lot of time was required for a suitable assessment of characteristic lengths in many cross sections. For group I gullies, method 3 should be used when a profiler was not available, since it was giving similar measurements for this gully type, but it was not valid for group II gullies. In summary: it is very important to select the most suitable method for each gully form; method 1 should always be the first option; method 2 could only be used with group II gullies or similar; method 3 could only be used with group I gullies or similar. For further studies, several points of interest can be explored: a) estimate the errors after choosing representative cross sections instead of using cross sections fixed by a constant distance between sections (*s*); b) increase the data set with information from other gully forms, with A_A, WDR_A and A_{cv}, etc. values different from the ones used in this paper; c) increase the data set with information from rills, and verify if they could be assimilated to one of the gully groups; d) consider longer reaches and assess the impact of *s* values higher than 10 m.

Acknowledgements

This work was possible by the financial support of: a) the Department of Education and Culture of the Government of Navarre, with a graduate and postdoctoral fellowship awarded to the fourth author; b) by the financial support of the Department of Education and Culture of the Government of Navarre, through the Research Project *Characterization of soil erosion in cultivated areas of Navarra*; c) by the financial support of the Spanish Ministry of Science and Technology, through the Research Project REN2003-03028/HID. This material is based upon work supported by the U. S. Department of Agriculture, under Agreement No. 58-6408-0-F137. Any opinions, findings, conclusion, or recommendations expressed in this publication are those of the authors and do not necessarily reflect the view of the U. S. Department of Agriculture.

References

Auzet, A.V., Boiffin, J., Papy, F., Ludwig, B., Maucorps, J., 1993. Rill erosion as a function of the characteristics of cultivated catchments in the North of France. Catena. 20, 41-62.

Betts, H.D., DeRose, R.C., 1999. Digital elevation models as a tool for monitoring and measuring gully erosion. JAG (ITC) Journal. 1(2), 91-101.

Bocco, G., Palacio, J.L., Valenzuela, C.R., 1993. Gully erosion modelling using geographic information systems and geomorphological knowledge. In: Ripple, W. (ed.), The GIS Applications Book. American Society for Photogrammetry and Remote Sensing.

Carvajal, F., 2000. Estudio de la influencia del microrelieve del suelo sobre el flujo de escorrentía superficial mediante fotogrametría digital. Ph.D. Thesis, School of Agricultural Engineers, University of Almería. Almería, Spain.

Casalí, J., López, J., Giráldez, J.V., 1999a. Ephemeral gully erosion in Southern Navarra (Spain): description and measurement. Catena. 36, 65-84.

Casalí, J., Laburu, A., López, J.J., García, R., 1999b. Digital terrain modelling of drainage channnel erosion. Journal of Agricultural Engineering Research. 74, 421-426.

Crouch, R.J., 1990. Erosion processes and rates for gullies in granitic soils bathurst, New South Wales, Australia. Earth Surface Processes and Landforms. 15, 169-173.

DeRose, R.C., Gomez, B., Marden, M., Trustrum, N.A., 1998. Gully erosion in Mangatu Forest, New Zealand, Estimated from digital elevation models. Earth Surface Processes and Landforms. 23, 1045-1053.

De Alba, S., Benito, G., 2001. Effects of soil surface management on erosion during extreme rainfall events in semiarid agricultural lands (Central Spain). Final Proc. Int. Symposium: The significance of soil surface characteristics in soil erosion. Strasburg, France.

De Santisteban, L.M., 2003. Análisis de factores topográficos para predecir la erosión por cárcavas efímeras. Ph.D. Thesis, School of Agricultural Engineers, Department of Projects and Rural Engineering, Public University of Navarre. Pamplona, Spain.

De Santisteban, L.M., Casalí, J, López, J.J., 2004. Evaluation of rill and ephemeral gully erosion in cultivated areas of Navarre (Spain). Final Proc. 3rd Int. Symposium on Gully Erosion. Oxford (MS), USA

Elliot, W.J., Laflen, J.M., Thomas, A.W., Kohl, K.D., 1997. Photogrammetric and rillmeter techniques for hydraulic measurement in soil erosion studies. Transactions of the ASAE. 40(1), 157-165.

Foster, G. R., 1986. Understanding ephemeral gully erosion. In: Soil Conservation. Assesing the National Resources Inventory, 2. Comittee on Conservation Needs and Opportunities. Board on Agriculture. National Research Council. National Academy Press. Washington, pp. 90-125.

Grissinger, E.H., Murphey, J.B., 1989. Ephemeral gully erosion in the loess uplands, Goodwin Creek watershed, Northern Mississippi, U.S.A. Proc. Int. Conf. River Sedimentation. Beijing, China, pp. 51-58.

Harvey, A.M., 1987. Seasonality of processes on eroding gullies: A twelve-year record of erosion rates. Processus et mesure de l'érosion, Éd. Du CNRS, pp. 439-454.

Hidalgo, R.E., Giráldez, J.V., Moral, F.J., Gutiérrez de Ravé, E., Laguna, A., 1998. Levantamiento topográfico y estimación de la pérdida de suelo de una cárcava. Final Proc. Inter. Conf. on Graphic Engineering. Málaga, Spain, pp. 241-249.

Imeson, A.C., and Kwaad, F.J.P.M, 1980. Gully types and gully prediction. K.N.A.G. Geografisch Tijdschrift XIV. 5, 430-441.

Jackson, T.J., Ritchie, J.C., White, J., LeSchack, L., 1988. Airborne laser profile data for measuring aphemeral gully erosion. Photogrammetric Engineering and remote sensing. 54.8, 1181-1185.

Laflen, J. M., 1985. Effect of tillage systems on concentrated flow erosion. Final Proc. Int. Conf. Soil Conservation. Maracay, Venezuela, pp. 798-809.

Lentz, R.D., Dowdy, R.H., Rust, R.H., 1993. Soil property patterns and topographic measures associated with ephemeral gully erosion. J. Soil Water Conserv. 48, 355-361.

Martínez-Casasnovas, J.A., 2003. A spatial information technology approach for the mapping and quantification of gully erosion. Catena. 50, 293-308.

Miller, H.A., 1984. Estimating erosion on gullied cropland. In: Thorne, C.R. (Ed.), Extended Bibliography of Ephemeral Gully Erosion in Arable Fields. Colorado State Univ. Fort Collins.

Moore, I.D., Burch, G.J., Mackenzie, D.H., 1988. Topographic effects on the distribution of surface soil water and the location of ephemeral gullies. Transactions of the ASAE. 31(4), 1098-1107.

Osborn, H.B., Simanton, J.R., 1989. Gullies and sediment yield. Rangelands. 11, 51-56.

Poesen, J., Govers, G., 1990. Gully erosion in the Loam Belt of Belgium: Typology and Control Measures. In: Boardman, J., Foster, I. D. L., Dearing, J. A., Eds. Soil Erosion on Agricultural Land. John Wiley & Sons, Londres, pp. 513-530.

Poesen, J., 1993. Gully typology and gully control measures in the European loess belt. In: Wicherek, S. (Ed.), Farm Land Erosion in Temperate Plains Environment and Hills. Elsevier, Amsterdam, pp. 221-239.

Poesen, J., Vandaele, K., Van Wesemael, B., 1996. Contribution of gully erosion to sediment production on cultivated lands and rangelands. In: Walling, D.E., Webb, B.W. (Eds.), Erosion and Sediment Yield: Global and Regional Perspectives, IAHS Publ. no. 236, pp. 251-266.

Poesen, J., Nachtergaele, J., Verstraeten, G., Valentin, C., 2003. Gully erosion and environmental change: importance and research needs. Catena. 50, 91-133.

Ries, J.B., Marzolff, I., 1997. Identification of sediment sources by large-scale aerial photography taken from a monitoring blimp. Phys. Chem. Earth, 22 (3-4), 295-302.

Rowntree, K.M., 1991. Morphological characteristicis of gully networks and their relationship to host materials, Baringo District, Kenya. Geojournal. 23(1), 19-27.

Smith, L.M., 1993. Investigation of Ephemeral Gullies in Loessial Soils in Mississippi. U. S. Army Corps of Engineers. Technical Report GL-93-11. Vicksburg.

Sneddon, J., Williams, B.G., Savage, J.V., Newman, C.T., 1988. Erosion of a gully in duplex oils. Results of a long-term photogrammetric monitoring program. Aust. J. Soil Res. 26, 401-408.

Spomer, R.G., Hjelmfelt, A.T., 1986. Concentrated flow erosion on conventional and conservation tilled watersheds. Transactions of the ASAE. 29, 129-147.

Thomas, A.W., Welch, R., Jordan, T.R., 1986. Quantifying concentrated-flow erosion on cropland with aerial photogrammetry. J. Soil Water Conserv. 41, 249-252.

Thomas, A.W., Welch, R., 1988. Measurement of ephemeral gully erosion. Transactions of the ASAE. 31, 1723-1728.

Valcárcel, M., Taboada, Mª.T., Paz, A., Dafonte, J., 2003. Ephemeral gully erosion in northwestern Spain. Catena. 50, 199-216.

Vandaele, K., 1993. Assessment of factors affecting ephemeral gully erosion in cultivated catchments of the Belgian Loam Belt. In: Wicherek, S. (Ed.), Farm Land Erosion in Temperate Plains Environment and Hills. Elsevier, Amsterdam, pp. 125-136.

Vandaele, K., Poesen, J., 1995. Spatial and temporal patterns of soil erosion rates in an agricultural catchment, central Belgium. Catena. 25, 213-226.

Vandaele, K., Poesen, J., Marques da Silva, J.R., Desmet, P., 1996. Rates and predictability of ephemeral gully erosion in two contrasting environments. Geomorphologie: Relief, Processus, Environnement. 2, 83-96.

Table 1. Main characteristics of watersheds affected by ephemeral gully erosion, measured soil losses and estimated values of AS1 and AS2 topographic indices

Region; *P* (mm); *R* USLE (hJ cm m^{-2} h^{-1} a^{-1}); sources	Watershed; *A* (m^2); *S* (%)	Upper horizon USDA soil texture; USLE *K* (T m^2 h ha^{-1} hJ^{-1} cm^{-1}); soil use and management	Erosion period	Soil loss (m^3); *AS1*(m^2); *AS2* (m^2)
Navarre, Spain; 546; 50; (1), (2)	La Abejera 0; 19,116; 9.0	Loam-silty loam; 0.28-0.49; winter grains, conventional tillage	Oct 1995-Sep 1996; Oct 1998-Sep 1999	5.50, 4.79; 1,636; 1,374
	La Matea 1; 1,000; 11.0	Idem	Idem	1.76, 2.16; 113; 121
	La Matea 2; 3,672; 10.0	Idem	Idem	2.73, 3.90; 364; 364
	Cobaza 1; 7,280; 6.0	Idem	Idem	3.85, 4.25; 443; 331
Mississippi, USA; 1,421; 749; (3)	1; 3,397; 3.0	Silty-loam; 0.64; soybean, conventional tillage	Jun 1982-Apr 1983; May 1983-Apr 1984; May 1984-Apr 1985	6.76, 2.65, 2.16; 102.3; 86.0
	2; 275; 6.0	Idem	Idem	3.01, 1.36, 1.06; 15.1; 14.8
	3; 874; 3.0	Idem	Idem	4.08, 1.60, 1.03; 24.5; 25.4
	4; 450; 5.0	Idem	Idem	2.97, 0.68, 0.64; 21.2; 18.3
Alentejo, Portugal; 550; 95; (4)	1-8; 2,560-25,176; 10.0-22.0	Sandy loam; 0.49; winter grains, conventional tillage	Sep 97-Jun 98	0.8-66.4; 392-1,717; 384-1,909
	9-15; 2,495-25,229; 7.0-18.0	Sandy loam; 0.49; herbaceous mixture I, abandoned	N.a.	0.2-27.1; 408-1,777; 443-1,786
	16-18; 2,604-28,466; 12.0-18.0	Sandy loam; 0.49; herbaceous mixture II, abandoned	N.a.	3.3-48.8; 387-2,386; 396-2,771
	19-22; 3,923-10,796; 10.0-15.0	Sandy loam; 0.49; rangeland	N.a.	2.1-8.0; 554-1,170; 575-1,265
	23-32; 789-15,060; 10.0-16.0	Sandy loam; 0.49; winter grains, conventional tillage	Sep 97-Jun 98	1.0-48.4; 142-1,411; 144-2,015
Murcia, Spain; 225-483; 80; (4)	1-7; 887-4,046; 16.0-40.0	Sandy loam; 0.20; almonds, conventional tillage	N.a.	2.26-22.89; 139-1,236; 144-1,226
	8-10; 2,560-15,443; 7.0-14.0	Sandy loam; 0.20; abandoned, grazed	N.a.	1.09-6.99; 707-3,281; 400-1,236
Flanders, Belgium; 750; 65; (5)	1-5; 3,702-16,987; 4.5-27.0	Silty loam; 0.37; corn, conventional tillage	Mar-Oct 1997	4.99-42.24; 167-1,019*; 249-1,189

**AS1* is approximated by the multiplication of total watershed surface area times watershed slope.
(1) Casalí *et al.* (1999); (2) De Santisteban (2003); (3) Smith (1993), (4) Nachtergaele *et al.* (2000); (5) Nachtergaele *et al.* (2001)
P: annual average rainfall; *A*: watershed surface area; *S*: average watershed slope; N.a: not available

List of Figures

Figure 1. View of Beire ephemeral gully. The selected cross sectional areas spaced 1 m apart are marked with plastic sticks.

Figure 2. Example of representative cross sections for each of the studied gullies, obtained by the three methods used for cross section characterization: (1) micro-topographic profiler (left hand side column); (2) detailed measurement with a tape (central column) and; (3) approximated measurement with a tape (left hand side column).

Figure 3. Micro-topographic profiler measuring one of the gully cross sections.

Figure 4. Absolute (E^a_{sm}) and relative (E^r_{sm}) measurement errors as a function of gully type, distance between adjacent cross sections (*s*) and measurement method: absolute error for each gully (a-e); average absolute errors for *WRD*>5 gullies (f); average absolute errors for *WRD*<5 gullies (g); average absolute errors for all gullies (h), where r^2 is the correlation coefficient for the linear regression; relative error for each gully (i-m); average relative errors for *WRD*>5 gullies (n); average relative errors for *WRD*<5 gullies (o); average absolute errors for all gullies (p).

Figure 1. View of Beire ephemeral gully. The selected cross sectional areas spaced 1 m apart are marked with plastic sticks.

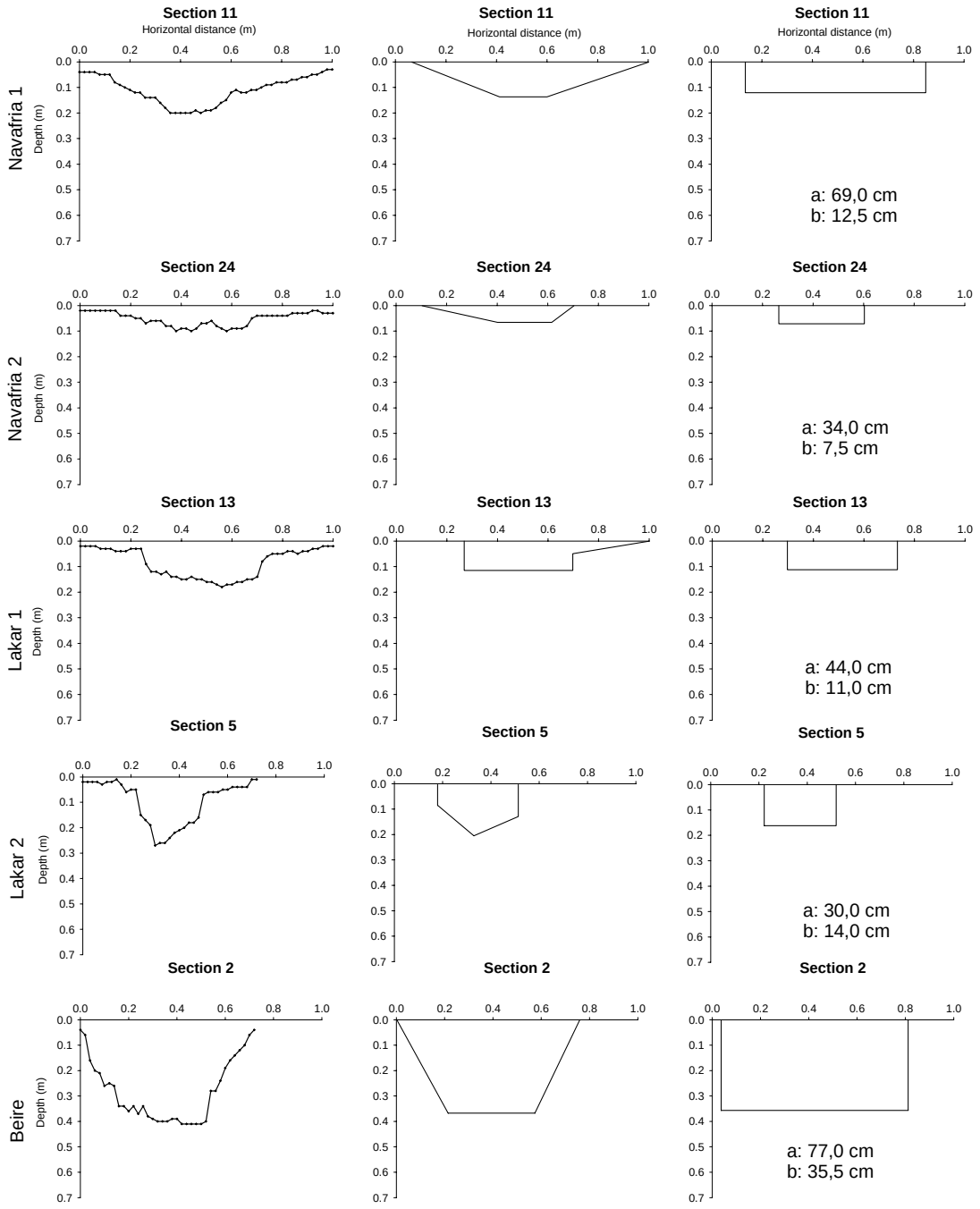

Figure 2. Example of representative cross sections for each of the studied gullies, obtained by the three methods used for cross section characterization: (1) micro-topographic profiler (left hand side column); (2) detailed measurement with a tape (central column) and; (3) approximated measurement with a tape (left hand side column).

Figure 3. Micro-topographic profiler measuring one of the gully cross sections.

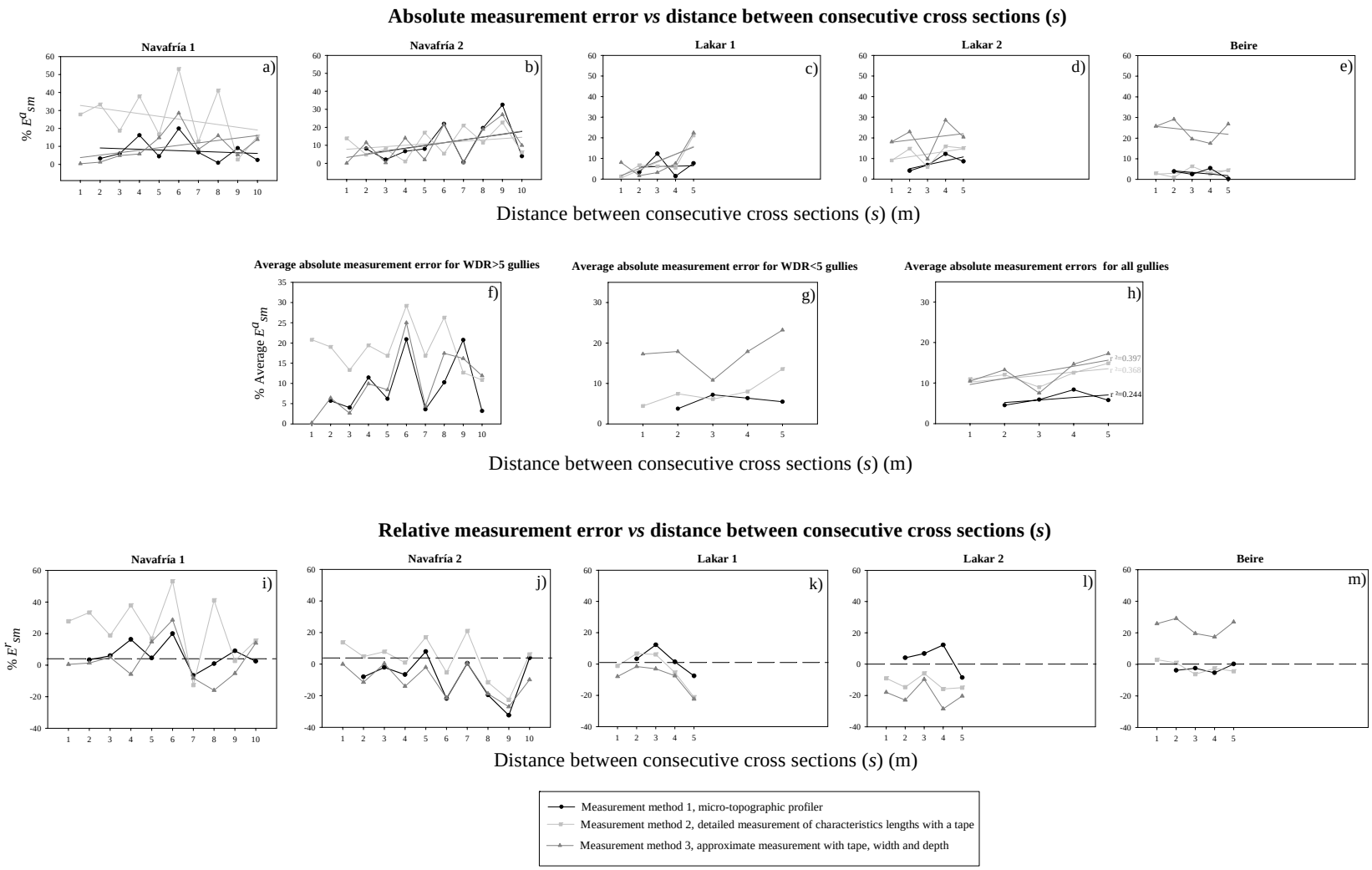

Figure 4. Absolute (E^a_{sm}) and relative (E^r_{sm}) measurement errors as a function of gully type, distance between adjacent cross sections (s) and measurement method: absolute error for each gully (a-e); average absolute errors for WRD>5 gullies (f); average absolute errors for WRD<5 gullies (g); average absolute errors for all gullies (h), where r^2 is the correlation coefficient for the linear regression; relative error for each gully (i-m); average relative errors for WRD>5 gullies (n); average relative errors for WRD<5 gullies (o); average absolute errors for all gullies (p).

Ephemeral Gullies: a Persistent Source of Sediment from Agricultural-related Lands

Jerry M. Bernard*
Jon G. Werner
Fred D. Theurer
USDA NRCS, NWCC; 7413 Cinnabar Terrace;
Gaithersburg, MD 20879-4575

Abstract

Ephemeral gully erosion is a significant source of sediment from agricultural-related erosion. With the installation of best management practices (BMPs) for sheet & rill erosion protection, the magnitude of gully erosion has become a very important issue. Some watershed models, such as AnnAGNPS, may include a state-of-the-art gully feature that accepts regression coefficients that can be generated from output from an event-type, ephemeral gully model. One such gully model is the Ephemeral Gully Erosion Model (EGEM) which was developed and is supported by NRCS. This paper will offer pictorial and heuristic evidence as to the pervasiveness of ephemeral gullies, and their significance as a source of cropland erosion and sediment yield. Evidence from the Upper Auglaize watershed, which is in the Maumee River basin and drains through Toledo, Ohio into Lake Erie, will be presented to show gully erosion. This source of the sediment is important when planning and implementing BMPs to reduce sediment from cropland reaching the stream system. This paper will also attempt to indicate where research is needed to complete the gaps in our current knowledge of ephemeral gully erosion, and what is needed to make the resulting science readily useable for the ordinary professional.

Keywords: ephemeral gully, models, AnnAGNPS, EGEM

*Corresponding author

Evaluation of Topographic Indices for Ephemeral-Gully Erosion Assessment

J. Casalí∗ (E-mail: jcs@unavarra.es)
L. M. De Santisteban (E-mail: luisa.satinsteban@unavarra.es)
J. J. López (E-mail: jjlr@unavarra.es)
Department of Projects and Rural Engineering, Universidad Pública de Navarra
Campus de Arrosadía s/n, 31006 Pamplona (Navarra), Spain
FAX: 34 948 169148

J.V. Giradles (E-mail: ag1gicej@uco.es)
Department of Agronomy, University of Córdoba
Apdo. 3048, 14080 Córdoba, Spain
FAX: 34 957 016043

J. Poesen (E-mail: Jean.Poesen@geo.kuleuven.ac.be)
J. Nachtergaele
K.U. Leuven, Laboratory for Experimental Geomorphology
Redingenstraat 16, B-3000 Leuven, Belgium
FAX: 32 16 326400

Abstract

Erosion caused by concentrated flows in agricultural areas is responsible of important soil losses, and of quick sediment flows through the channel network. The main factors controlling concentrated flow erosion include the erodibility of materials, soil use and management, climate and watershed topography. In this paper, two topographic indices, closely related with mathematical expressions suggested by different authors, are used to characterize the influence of watershed topography on gully erosion. The *AS1* index is defined as the product of the watershed area by the partial area-weighted average slope. The *AS2* index is similar to the *AS1* but using the swale slope as the weighting factor. Formally, *AS2* is the product of the watershed area by the length-weighted average swale slope. From studies made from different ephemeral gully erosion data bases, a high correlation consistently existed between the topographic indices and the volume of eroded soil. The resulting relationships are useful to assess soil losses from gully erosion, to identify the most susceptible watersheds within large areas, and to compare the susceptibility to gully erosion among different catchments. This information can be also important to study the response of natural drainage network systems to different rainfall inputs.

Keywords: concentrated flow erosion; ephemeral gully erosion; erosion prediction; watershed topography

1. Introduction

Erosion caused by ephemeral flows is a frequent phenomenon in nature, which contributes to model the landscape. This type of erosion may cause great soil losses in agricultural areas, that are quickly transferred to the watershed outlets through the rill and gully network (Bennett et al., 2000; Poesen et al., 2003).

∗ Corresponding author

Concentrated flow erosion is conditioned by the erodibility of surface materials, climate, soil use and management, and watershed topography. Several methods were developed to determine and quantify the influence of such factors. Many authors have considered the influence of topography, watershed area and slope, mainly, in the occurrence of concentrated flow erosion (Patton and Schumm, 1975; Moore and Burch, 1986; Thorne et al., 1986; Zevenbergen, 1987; Montgomery and Dietrich, 1988). Basically, most of them demonstrated that, the larger the watershed surface area, the lesser is the slope required to initiate an incision leading to a gully, when the other factors involved remained constant.

From those studies, several methods were developed to locate the position of gully headcuts, to predict the location of the channel and, in some cases, to estimate volumes of eroded soils (Thorne et al., 1986; More et al., 1988; Montgomery and Dietrich, 1992; Vandekerckhove et al., 1998; Desmet et al., 1999). In this paper, a simpler method to determine the effect of topography on the volume eroded by concentrated flows is explored.

The method is based on the topographic indices first outlined by Casalí et al. (1999), which consider watershed area and slope. The possible relationship between the topographic indices and the volumes of eroded soil from watersheds under the same climate, soil class, soil use and soil management, was firstly suggested by Casalí et al. (1999). Nevertheless, these authors did not provide an experimental evidence of the proposed relation between erosion and topographic indices, nor an extended discussion on it. In this paper, the topographic indices defined by Casalí et al. (1999) are applied to the study of ephemeral gullies from Spain, United States, Portugal and Belgium. From it, the meaning, applicability and usefulness of the topographic indices is discussed. Most soil erosion data compared were collected at the same time, and after the same period of time after last gully erasing process by tillage, so rainfall and other metheorologycal variables were the same for most or all of the watersheds compared (table 1). So, although it is probable that there are additional differences (e. g. land use history or soil depth), it is assumed that the observed differences in erosion are due to variations in watershed topography. Ephemeral gullies are channels of variable size formed by the scouring of concentrated surface runoff flowing on erodible soils during rain events (Foster, 1986; Thorne et al., 1986). In many cases the channels are refilled by the farmers, shortly after the rains, but they reappear in the next rainy season. While the presence of rills is restricted to planar elements of watersheds, ephemeral gullies occur on valley bottoms or within swales. Ephemeral gully systems are common in cultivated soils in many areas around the world (Bennett et al., 2000; Poesen et al., 2003). Due to their relatively small size, it is possible to assess precisely the watershed topography and the eroded soil volumes within them.

2. Materials and Methods

Topographic Indices and Gully Data Sets

Casalí et al. (1999) defined two topographic indices. The first index, *AS1*, is based on the area-weighted mean slope,

$$AS1 = \sum_{i=1}^{n} A_i \cdot S_i \qquad (1)$$

where S_i is the slope of each of the n sub-watershed units with uniform slope, and area A_i.

There is another alternative index, *AS2*, based on the length-weighted average slope, that is formulated as,

$$AS2 = \frac{\sum_{j=1}^{m} L_j \cdot I_j}{A^{-1} \sum_{j=1}^{m} Lj} \qquad (2)$$

where I_j is the slope of each of the *m* segments of the watershed swales with uniform slope and length L_j, and *A* as the entire watershed area.

Casalí et al. (1999) showed that the indices are closely related with expressions for the stream power and for cumulative sediment yield per unit width proposed by Moore and Burch (1986); and with expressions to estimate the contribution of the channel to the total energy expenditure function of the watershed, which should be a minimum (Rigon et al. 1993).

The main characteristics of the watersheds studied are shown on table 1. All ephemeral gullies considered in this paper can be classified as classic ephemeral gullies, according to the Casalí et al. (1999) criteria.

Detailed Digital Elevation Models, DEM, were available from field surveys in Navarre or digitalization of paper maps in Mississippi. The topographic indices of these watersheds were estimated with the support of a Geographic Information System, GIS, PC Raster (ftp://pop.frw.ruu.nl/pcraster/version2, e.g. Burrough and McDonnell, 1998, app. 2) in this case. For calculating *AS1* index, the watersheds were divided in units of homogeneous slope (~1 % of variation), ranging from 0.10% to 20.00% in Navarre, and from 0.00% to 13.10% in Mississippi. For *AS2* index, the swale length was divided in reaches of almost completely homogeneous slope (~1 % variation), ranging from 0.60% to 14.50% in Navarre, and from 0.03% to 12.00% in Mississippi.

Information available for the other study areas (Alentejo, Murcia and Flanders) was much more limited, restricted to the area and slope of the entire watershed and that contributing to the head of the gully, respectively, and the slope of several swale reaches. Surface areas were determined by a Global Position System unit, (GPS), and slopes with a clinometer (Nachtergaele et al., 2000; Nachtergaele et al. 2001).

In order to maintain the homogeneity of the analysis, the selected watersheds from Alentejo, Murcia and Flanders were of similar characteristics to those considered in Navarre and Mississippi, within the 0.085-3.0 ha range. Watersheds smaller than 0.085 ha are more related to rill than to gully systems. Consequently they were not considered in this paper, except when there was certainty about their relation with ephemeral gullies. In all cases, the watershed outlet was determined from the deposition area, which in general remains stable from year to year and can be easily identified. In all cases, possible errors in erosion rate assessment caused by not considering some erosion masked by sedimentation and aggradation processes, (Thorne et al. 1986), were neglected. In fact, it is possible that the estimated volume of soil loss was underestimated due to the sedimentation of solid particles in the channels after the gully formation and growth.

Gully cross section areas were measured in Navarre and Mississippi with a profiler (Smith, 1993, Casalí et al., 1999), and with a tape in the other areas. The distance between cross sections was measured with a tape. The eroded soil volume within channel reaches were estimated by the product of the average cross section of every reach and the distance between the successive cross sections.

3. Results and Analyses

The relationships between the two topographic indices and the eroded soil volume within the watersheds are presented on figure 1 and table 2. A straight line was fitted to the data. The rain depths of gully-forming storms in the Navarrese watersheds are shown on figure 1. The rain data of the Mississippi watersheds correspond to all the recorded events. These data are also included on figure 1. Rainfall information for the other study areas is not available. Watersheds of cereal cropping areas in Alentejo (1-8 and 23-32) are grouped in two figures (figures 1*e*,*f* and 1*g*,*h*) because each group is placed in different locations within the Alentejo area.

A clear relationship between topographic indices and eroded soil volumes is found in watersheds having a detailed topographic and erosive information for each of the two or three years considered. Although information concerning the specific rainfall events that caused erosion in Mississippi is not available, it may be assumed that erosion rates may be more related to total annual depth, than to the rain of isolated events. In Navarre, erosion was caused by one only storm during the period considered (Casalí et al., 1999; De Santisteban, 2003). Therefore, it can be stated that it was possible to quantify, in a simple way, the effect of topography on concentrated flow erosion. The quality of the regression (r^2) is lower for Alentejo watersheds. The lower r^2 values might be due to the less accuracy in topographic and erosive surveys. It is also remarkable that *AS1* and *AS2* indices yielded a very similar response. Results for Murcia and Flanders have not been included on figure 1, as the number of available points is not considered representative. Anyway, r^2-P values for watershed in Murcia are around 0.56 and 0.05 respectively, while the corresponding numbers for watershed in Flanders are around 0.55 and 0.15. The use of exponents different than 1 for area and slope in equations 1 and 2, as proposed by Moore and Burch (1986) and Rigon et al. (1993) did not improved the quality of the fits.

For watersheds with highly erodible soils and with high rainfall depths (*i.e.* Mississippian watersheds), the values of the topographic indices required for gully erosion were much lower that in those drier watersheds with less or similarly erodible soils (*i.e.* Navarrese watersheds).

Besides, on those watersheds, once the threshold value is exceeded, erosion volumes are high, whereas in areas like Alentejo, eroded volumes for small values of topographic indices are also very low, increasing gradually. This behavior can be observed, for example, from the analysis of topographic indices threshold values. For Navarrese watersheds, gully erosion was not observed in watersheds with an *AS1* and *AS2* values lower than around 125, whereas for Mississippi, those values were of about only 12, less than one order of magnitude. Those values for Alentejo were of about 140-350, very similar to the ones in Navarre, under relatively similar conditions. The results from this study indicate the presence of a threshold value for erosion initiation, in agreement with others works (*e.g.* Patton and Schumm, 1975; Zevenbergen, 1987; Montgomery and Dietrich, 1988). There is linear response once the threshold value is exceeded (figure 1) similar to the equation for determining the detachment capacity of a flow (Foster and Lane, 1983): $D_c = K_c \cdot (\tau - \tau_c)$, where D_c is the flow detachment capacity $(M\,L^{-2}\,T^{-1})$; K_c is an erodibility factor $(T\,L^{-1})$; τ and τ_c are, respectively, the flow shear stress and its critical value, $(ML^{-2}T^{-2})$. The topographic indices, therefore, would be useful to estimate ephemeral gully erosion in wide areas, with support of GIS and DEM, after collecting a large data set (Goñi, 2003; Goñi et al., 2003). On the other hand, the identification of threshold values for gully formation, previously discussed, allows for a qualitative classification of watersheds as susceptible or not for ephemeral gully erosion. Thus, the proposed methodology can be considered as a promising tool to get information on erosion susceptibility in large areas. The interest of such methodology increases after considering that information about erosion rates is usually restricted to small areas and short periods of time, and that ephemeral gully erosion is

responsible of an important fraction of total erosion (Bennett et al., 2000; Poesen et al., 2003). Finally, it could be explored that natural non-agricultural watersheds exhibit a similar response to the one found for ephemeral gully systems studied here. It would be of considerable interest for determining the influence of topography on the erosion phenomenon in a more general way.

4. Conclusions

It has been shown that, for a wide range of soil, climate, soil use and management conditions, the close relationship between soil erosion due to ephemeral gullies and topography can be easily quantified with two simple indices. From it, a methodology for identifying areas susceptible to soil erosion and for quantifying soil erosion is proposed, which can be strongly enhanced with the support of GIS and DEM. It is possible that more complex natural systems behave in a similar way, what would be of interest in a wider scope, like Geomorphology and related Geosciences.

Acknowledgements

The authors acknowledge the assistance in the field work of Dr. M. Donézar and Mr. J. Del Valle de Lersundi, from the Agricultural Structures Service of the Government of Navarre; of Dr. Sean Bennett and Mr. Kimble White, from the USDA-ARS National Sedimentation Laboratory in Oxford (Mississippi), for his assistance in processing and analyzing data sets from Mississippi; and of Mr. Mikel Goñi, from the Public University of Navarre, for his assistance in using the GIS PCRaster. This work was possible by the financial support of: a) the Department of Education and Culture of the Government of Navarre, with a graduate and postdoctoral fellowship awarded to the first author; b) by the financial support of the Department of Education and Culture of the Government of Navarre, through the Research Project *Caracterización de la erosion de suelo en areas cultivadas de Navarra*; c) by the financial support of the Spanish Ministry of Science and Technology, through the Research Project REN2003-03028/HID. This material is based upon work supported by the U. S. Department of Agriculture, under Agreement No. 58-6408-0-F137. Any opinions, findings, conclusion, or recommendations expressed in this publication are those of the authors and do not necessarily reflect the view of the U. S. Department of Agriculture.

References

Bennett, S.J., Casalí, J., Robinson, K.M., Kadavy, C.K., 2000. Characteristics of actively eroding ephemeral gullies in an experimental channel. Trans. ASAE 43, 641-649.

Burrough, P.A., McDonnell, R.A., 1998. Principles of Geographical Information Systems. Oxford University Press, Oxford.

Casalí, J., López, J.J., Giráldez, J.V., 1999. Ephemeral gully erosion in Southern Navarra (Spain). Catena 36, 65-84.

De Santisteban, L.M., 2003. Análisis de factores topográficos para predecir la erosión por cárcavas efímeras. Ph.D. Thesis, School of Agricultural Engineers, Department of Projects and Rural Engineering, Public University of Navarre. Pamplona, Spain.

Desmet, P.J.J., Poesen, J., Govers, G., Vandaele, K., 1999. Importance of slope gradient and contributing area for optimal prediction of the initiation and trajectory of ephemeral gullies. Catena 37: 377-392.

Flint, J.J., 1974. Stream gradient as a function of order, magnitude and discharge. Water Resources Research 10, 969-973.

Foster, G.R., 1986. Understanding ephemeral gully erosion. In: Committee on Conservation Needs and Opportunities, Board on Agriculture, National Research Council Soil Conservation (Eds.), Assessing the National Resources Inventory, 2. National Academy Press, Washington D. C., pp. 90-125.

Foster, G.R., Lane, L.J., 1983. Erosion by concentrated flow in farm fields. Final Proc. D. B. Simons Symposium on Erosion and Sedimentation. Colorado State University, Ft. Collins, pp. 9.65-9.82.

Goñi, I., 2003. Application of GIS in an erosion study in the Municipality of Pitillas (Navarre), Spain. School of Agricultural Engineers, Department of Projects and Rural Engineering, Public University of Navarre. Pamplona, Spain.

Goñi, I., Meyles, E., Casalí, J., 2003. Influence of DEM resolution on the topographic index erosion calculations. Final Proc. Symposium 25 Years of Assessment of Erosion. Ghent, Belgium.

Montgomery, D.R., Dietrich, W.E., 1988. Where do channels begin? Nature 336, 232-234.

Montgomery, D.R., Dietrich, W.E., 1992. Channel initiation and the problem of landscape scale. Science 255, 826-830.

Moore, I.D., Burch, G.J., 1986. Modelling erosion and deposition: Topographic effects. Trans. ASAE 31, 1624-1630.

Moore, I.D., Burch, G.J., Mackenzie, D.H., 1988. Topographic effects on the distribution of surface soil water and the location of ephemeral gullies. Trans. ASAE 31(4), 1098-1107.

Nachtergaele, J., Poesen, J., Vandekerkove, L., Oostwoud, D., Roxo M., 2000. Testing the ephemeral gully erosion model (EGEM) for two mediterranean environments. Earth Surf. Proc. Landforms 26, 17-30.

Nachtergaele, J., Poesen, J., Steegen, A., Takken, I., Beuselinck, L., Vandekerckove, L., Govers, G., 2001. The value of a physically based model versus an empirical approach in the prediction of ephemeral gully erosion for loess-derived soils. Geomorphology 1007, 1-16.

Patton, P.C., Schumm, S.A., 1975. Gully erosion Northwestern Colorado: A threshold phenomenon. Geology 3, 88-90.

Poesen, J., Nachtergaele, J., Verstraeten, G., Valentin, C., 2003. Gully erosion and environmental change: importance and research needs. Catena 50, 91-133.

Rigon, R., Rinaldo, A., Rodríguez-Iturbe, I., Bras, R.L., Ijjasz-Vasquez, E., 1993. Optimal channel networks: A framework for the study of river basin morphology. Water Resour. Res. 29, 1635-1646.

Smith, L.M., 1993. Investigation of ephemeral gullies in loessial soils in Mississippi. US Army Corps of Engineers, Technical Report GL-93-11. Vicksburg (MS).

Thorne CR,. Zevenbergen LW, Grissinger EH, Murphey JB. 1986. Ephemeral gullies as sources of sediment. Final Proc. Fourth Federal Interagency Sedimentation Conference. Las Vegas, pp. 3-152, 3-161.

Vandekerckhove, L., Poesen, J., Oostwoud, D., De Figueiredo, T., 1998. Topographical thresholds for ephemeral gully initiation in intensively cultivated areas of the Mediterranean. Catena 33, 271-292.

Zevenbergen, L.W., 1987. Modelling erosion using terrain analysis. Ph.D. Thesis, London University, Department of Geography and Earth Science. London.

Table 1. Main characteristics of watersheds affected by ephemeral gully erosion, measured soil losses and estimated values of AS1 and AS2 topographic indices

Region; *P* (mm); *R* USLE (hJ cm m^{-2} h^{-1} a^{-1}); sources	Watershed; *A* (m^2); *S* (%)	Upper horizon USDA soil texture; USLE *K* (T m^2 h ha^{-1} hJ^{-1} cm^{-1}); soil use and management	Erosion period	Soil loss (m^3); *AS1*(m^2); *AS2* (m^2)
Navarre, Spain; 546; 50; (1), (2)	La Abejera 0; 19,116; 9.0	Loam-silty loam; 0.28-0.49; winter grains, conventional tillage	Oct 1995-Sep 1996; Oct 1998-Sep 1999	5.50, 4.79; 1,636; 1,374
	La Matea 1; 1,000; 11.0	Idem	Idem	1.76, 2.16; 113; 121
	La Matea 2; 3,672; 10.0	Idem	Idem	2.73, 3.90; 364; 364
	Cobaza 1; 7,280; 6.0	Idem	Idem	3.85, 4.25; 443; 331
Mississippi, USA; 1,421; 749; (3)	1; 3,397; 3.0	Silty-loam; 0.64; soybean, conventional tillage	Jun 1982-Apr 1983; May 1983-Apr 1984; May 1984-Apr 1985	6.76, 2.65, 2.16; 102.3; 86.0
	2; 275; 6.0	Idem	Idem	3.01, 1.36, 1.06; 15.1; 14.8
	3; 874; 3.0	Idem	Idem	4.08, 1.60, 1.03; 24.5; 25.4
	4; 450; 5.0	Idem	Idem	2.97, 0.68, 0.64; 21.2; 18.3
Alentejo, Portugal; 550; 95; (4)	1-8; 2,560-25,176; 10.0-22.0	Sandy loam; 0.49; winter grains, conventional tillage	Sep 97-Jun 98	0.8-66.4; 392-1,717; 384-1,909
	9-15; 2,495-25,229; 7.0-18.0	Sandy loam; 0.49; herbaceous mixture I, abandoned	N.a.	0.2-27.1; 408-1,777; 443-1,786
	16-18; 2,604-28,466; 12.0-18.0	Sandy loam; 0.49; herbaceous mixture II, abandoned	N.a.	3.3-48.8; 387-2,386; 396-2,771
	19-22; 3,923-10,796; 10.0-15.0	Sandy loam; 0.49; rangeland	N.a.	2.1-8.0; 554-1,170; 575-1,265
	23-32; 789-15,060; 10.0-16.0	Sandy loam; 0.49; winter grains, conventional tillage	Sep 97-Jun 98	1.0-48.4; 142-1,411; 144-2,015
Murcia, Spain; 225-483; 80; (4)	1-7; 887-4,046; 16.0-40.0	Sandy loam; 0.20; almonds, conventional tillage	N.a.	2.26-22.89; 139-1,236; 144-1,226
	8-10; 2,560-15,443; 7.0-14.0	Sandy loam; 0.20; abandoned, grazed	N.a.	1.09-6.99; 707-3,281; 400-1,236
Flanders, Belgium; 750; 65; (5)	1-5; 3,702-16,987; 4.5-27.0	Silty loam; 0.37; corn, conventional tillage	Mar-Oct 1997	4.99-42.24; 167-1,019*; 249-1,189

**AS1* is approximated by the multiplication of total watershed surface area times watershed slope.
(1) Casalí *et al.* (1999); (2) De Santisteban (2003); (3) Smith (1993), (4) Nachtergaele *et al.* (2000); (5) Nachtergaele *et al.* (2001)
P: annual average rainfall; *A*: watershed surface area; *S*: average watershed slope; N.a: not available

List of Figures

Figure 1. Relationships between the two topographic indices and the eroded soil volumes within the watersheds presented on table 1. a,b: data from Navarre; c,d: data from Mississippi; e,f: watersheds 1-8 from Alentejo; g,h: watersheds 23-32 from Alentejo; i,j: watersheds 9-22 from Alentejo. r^2 is de correlation coefficient for the linear regression; P is the probability that the two variables are not correlated; P_e is the rainfall depth of the events that caused erosion in Navarre during the period considered; P_a is the total rainfall depth during the erosion period in Mississippi.

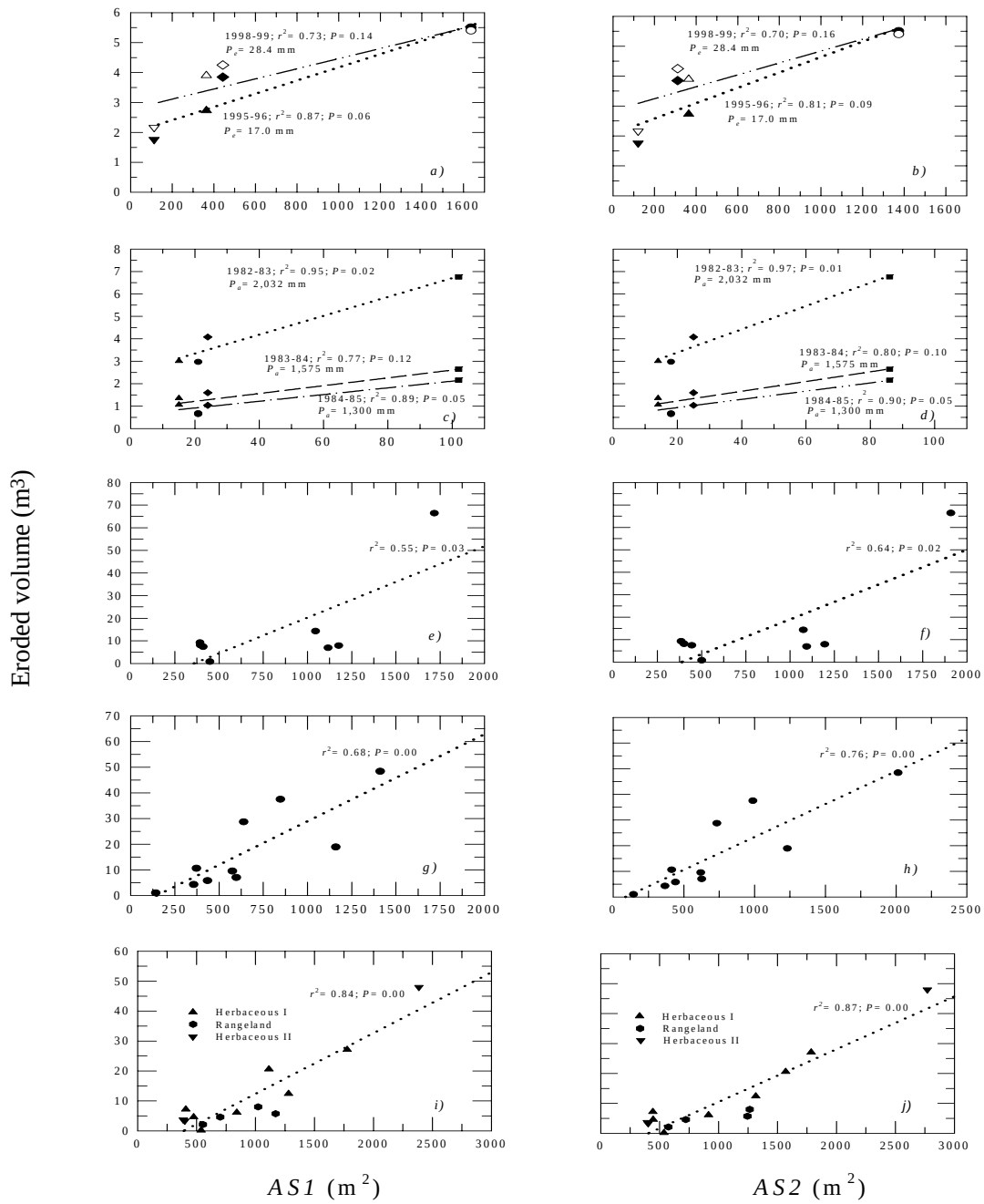

Figure 1. Relationships between the two topographic indices and the eroded soil volumes within the watersheds presented on table 1. a,b: data from Navarre; c,d: data from Mississippi; e,f: watersheds 1-8 from Alentejo; g,h: watersheds 23-32 from Alentejo; i,j: watersheds 9-22 from Alentejo. r^2 is de correlation coefficient for the linear regression; P is the probability that the two variables are not correlated; P_e is the rainfall depth of the events that caused erosion in Navarre during the period considered; P_a is the total rainfall depth during the erosion period in Mississippi.

Airborne Laser Scanning for Riverbank Erosion Assessment

D.P. Thoma[*] (E-mail: dthoma@tucson.ars.ag.gov)
USDA ARS SWRC Tucson
2000 East Allen Road
Tucson, AZ 85719
520-670-6381 x-111

S.C. Gupta (E-mail: gupta002@umn.edu)
University of Minnesota Department of Soil, Water and Climate
1991 Upper Buford Circle, St. Paul, MN 55108
Tel: 612-625-1241 FAX: 612-625-2208

C. Kirchhof (E-mail: E-mail: cal@instrumental.com)
Instrumental, Inc.
2748 East 82nd Street, Bloomington, MN 55425
Tel: 952-345-2825 FAX: 952-345-2837

M.E. Bauer (E-mail: mbauer@umn.edu)
University of Minnesota Department of Forestry
Room 115 Green Hall, 1530 North Cleveland Ave., St. Paul, MN 55108

Abstract

Understanding the proportion of sediment and phosphorus having its source from agricultural fields versus river banks is a difficult yet important question for determining cost effective erosion control practices. This research was designed to characterize the contributions of sediment and phosphorus due to bank erosion along the main stem of the Blue Earth River. Detailed topographic data was collected twice on an annual basis in April 2001 and April 2002 over a 56 km length of the Blue Earth River with a helicopter mounted Topeye laser system. The database includes X, Y, Z coordinates of laser returns from the river valley spaced at 60 to 100 cm intervals. Interpolated one meter grid cell resolution bare earth digital elevation models were made by stripping vegetation laser returns. The two models were differenced to determine volume change over time which was then converted to mass wasting by multiplying volume change and bulk density. Mass wasting rates were converted to sediment load based on percentage of transportable material in the bank strata. The percentage of sediment in the river sourced from bank materials was determined as the proportion of mass wasting to sediment load measured at a downstream gauging station. The percentage of sediment from bank erosion varied from 23 to 56 depending on the range of textural material that was considered transportable once in the river. Based on analysis of riverbank samples, total P contributions were estimated at 201 Mt/yr due to bank erosion and slumping.

Keywords: sediment pollution, laser altimetry, LIDAR, bank erosion

[*]Corresponding author

1. Introduction

The National Water Quality Inventory report (USEPA, 2000) indicates 12% of assessed rivers and streams in the U.S. are impacted negatively by sedimentation. Negative impacts of siltation include suffocation of fish eggs, decreased light penetration for photosynthesis, decreased aesthetic value for recreational uses, and added cost of water treatment. Agriculture is implicated as the major source for sediment pollution in many rivers. However, because of its diffuse nature reductions in sediment are difficult to achieve except through the implementation of best management practices (BMPs). Conservation tillage and grassed waterways as well as buffer strips at field edges can reduce sediment transport to surface waters (Randall et al., 1996; Gupta and Singh, 1996). However, sediment sources in agricultural landscapes include both bare fields as well as riverbanks in dynamic fluvial systems. Therefore, determining the proportion of sediment having its source from either of these locations is a difficult yet important question for cost effective implementation of BMPs.

The Blue Earth River watershed in south central Minnesota is a good example of a landscape where non-point source sediment pollution is prevalent, but difficult to apportion between upland and bank erosion. The Blue Earth River is a major tributary of the Minnesota River and contributes roughly 55% of the sediment load carried by the Minnesota River at Mankato, MN (Payne, 1994). The river flows through a deeply incised landscape with river banks as tall as 30 m. Comparatively, the landscape in the Blue Earth River Basin is relatively flat; 54% of the land area has 0-2% slope, and 82% of the land has 0-6% slope. The flat landscape is however, connected to the river through surface inlets that carry runoff and sediment into tile lines which in turn empty into ditches and thus the river.

The Minnesota Pollution Control Agency (MPCA, 1985) stated that a 40% reduction in sediment load is required to meet federal water quality standards and beneficial use criteria. The agency assumes that a major proportion of these pollutants are from upland areas of the watershed. Therefore, the strategy for controlling these pollutants has focused on agricultural practices that promote delivery of sediments and nutrients to the river (Randall et al., 1996). However, this strategy may not be effective since it is not clear what proportion of the sediment and nutrient pollution in the Minnesota River is from upland erosion or stream bank collapse.

Airborne laser altimetry, or Light Detection and Ranging (LIDAR), has been used in numerous topographic and land use change detection studies (Krabill et al., 1999; Murakami et al., 1999; Huising and Pereira 1998; Irish and Lillycrop, 1999 and Sallenger et al., 1999). Laser altimetry has also been used for gully erosion estimates (Jackson et al., 1988; Ritchie et al., 1994), earthquake fault mapping (Harding and Berghoff, 2000; Hudnut et al., 2002) and to map riverbank elevations for flood management (Pereira and Wicherson, 1999).

As the aircraft moves along a predetermined flight line many thousands of laser pulses per second are directed by a rotating mirror to the ground in a circular pattern centered on the flight line. Up to five echoes from each laser pulse are received by the sensor to compute elevations based on laser travel times. Typically, the first returned pulse is the elevation of the top of vegetation canopy while the last is usually the ground. In situations where the last echo return is not the ground, filtering must be employed to remove these elevation data if interest is purely in the bare earth elevation (Ritchie et al., 1994). The typically high density of data from combinations of multiple passes allows averaging without loss of systematic variation in the landscape surface (Ritchie et al., 1994). Resulting data resolution depends on aircraft elevation and speed as well as laser pulse rate, scan width, scan rate, and vegetation cover. Data collection in the fall or winter during leaf-off conditions optimizes sampling density and accuracy of bare earth models.

The objectives of the study were: 1) to quantify mass wasting and phosphorus inputs along a 56 km length of the Blue Earth River, and 2) to estimate proportion of total annual suspended sediment load due to bank and bluff collapse.

2. Methods

Research focused on the Blue Earth River reach between Amboy, MN and the confluence of the Blue Earth and Wantonwan rivers (~56 km, Figure 1) that contained 10 minor, 30 moderate and 15 severely eroded sites according to Bauer (1998). Severely eroded sites were classified as exposed river banks greater than 3m high. In this stretch of river, there were 5 county highway bridges that were used as ground reference control.

2.1. Scan specifications

Laser scans were conducted annually on April 23-24, 2001 and April 26-28, 2002 with a Saab Topeye helicopter mounted laser range finding system. Laser pulse rate was 7 kHz with foot prints spaced 0.30 m and foot print diameter of 0.16 m. Scan width was 273 m.

2.2. Fieldwork

Twelve soil samples were collected from 6 exposed riverbanks representing typical strata and textures in bank materials. The taller stream banks were primarily composed of glacial till and glacial lake sediments (Bauer, 1998), while shorter banks were composed of river alluvium. On replicates of each sample, bulk densities were determined using the clod method (Blake and Hartge, 1986), and the textural analysis was done using the hydrometer method (Gee and Bauder 1986). Averages of bulk density and textural analysis were used in conjunction with laser determined volume change to derive mass wasting rates, and then mass suspended solids. All samples were analyzed for extractable phosphorus (Kuo, 1986) using 0.01 M $CaCl_2$, and total P via perchloric acid digestion (USEPA, 1981).

Elevation accuracy of both annual scans was determined by comparing scan elevations for bridges crossing the river to bridge elevations determined by rea-time kinematic global positioning system (RTK-GPS) survey. A total of 137 bridge reference points were collected on 5 highway bridges that crossed the scanned portion of the Blue Earth River. Accuracies of scan elevations on the bridge surfaces were determined as the difference between a bridge reference point and the nearest scan point that fell on the surface.

The planimetric accuracy was determined by matching bridge edges in the 2001 scan to edges in the 2002 scan. Edges were determined by linear regression of scan line points that fell closest to, but still on, the bridge surface. The average distance between points on the best fit lines describing the bridge edges served as an estimate of planimetric shift.

2.3. Scan characteristics

Raw scanning laser data were differentially corrected and stripped of vegetation returns using a proprietary smoothing filter. Any last-return point greater than 1.5 m above ground surface was considered a return from vegetation and was removed by the algorithm. Because data points were not uniformly distributed along the flight path due to mirror rotation and aircraft trajectory, they were gridded to a uniform $1m^2$ spacing before being used in volume change calculations. The resulting data product was an ordered set of 24 million and 30 million X,Y,Z coordinates for the 2001 and 2002 scans respectively.

2.4. Mass wasting estimates

All data points below the 2001 high water mark were eliminated from both data sets manually by digitizing and clipping. Vertex matching produced two dry surface files (2001 data and 2002 data) with identical X,Y coordinates that differed only in the Z (elevation) dimension. The differences in Z values were determined for every vertex and summed. The sum was then

multiplied by the spatial extent of the scans to derive an estimate of volume change that occurred due to erosion or deposition between the two scans.

Mass wasting estimates were made by multiplying the volume change determined from the laser scans with the average bulk density. Similarly, phosphorus load was derived by multiplying the concentration of extractable and total phosphorus in sediment samples by the mass wasting estimates.

3. Results

3.1. Properties of bank materials

The bulk density of bank materials ranged from 1.46 to 2.13 Mg/m^3 with an average of 1.83 Mg/m^3. The clay content of bank materials ranged from 6.1 to 29.3% with an average of 20.1%. Silt content ranged from 0.74% to 41.6% with an average of 27.3%, while sand content ranged from 32.8% to 92.4% with an average of 55.7%. The extractable P concentration for bank materials ranged from 0 to 0.25 mg/kg with an average of 0.08 mg/kg, while the total P concentration ranged from 249 to 452 mg/kg with an average of 392 mg/kg. For comparison purposes, a surface soil (0-2 cm) collected from the summit of an eroding bank had an extractable P concentration of 3.1 mg/kg and total P concentration of 622 mg/kg.

3.2. Accuracy

The vertical accuracy of the real RTK-GPS reference points was determined to be between 1.22 cm and 1.83 cm in 2001 and 2002, respectively. The strong correlation coefficient ($r^2 = 0.9998$) between elevations of the bridge reference points and LIDAR scan points (Figure 2) indicated a very close fit over an elevation range of 10's of meters across approximately 16km of horizontal survey distance.

A close inspection of vertical error indicated the average error for the 2001 scan (2.5cm) was less than that for the 2002 scan (8.8cm), but distribution of error terms was somewhat normally distributed in each. Both scans were biased in that they under estimated true elevation relative to bridge reference point elevations.

3.3. Mass wasting and P inputs

A volume change of –281,454m^3 was computed as the difference in elevations between the 2001 and 2002 LIDAR scans without applying a vertical or horizontal bias correction. This was equivalent to 512,247 t of sediment, 201 t total P, and 40 kg extractable P input to the river assuming a bulk density of 1.83 Mg/m^3, average of 392 mg/kg total P, and an average extractable P concentration of 0.08 mg/kg, in the bank materials. More precisely these values represented net input of sediment and extractable and total P from above the 2001 water line.

The mass of sediment transported past the gauging station near the mouth of the Blue Earth River for the period between the two scans was 407,252 t (Heather Offerman, Metropolitan Council Environmental Services, personal comm.). This amount represents the sediment carried by the Blue Earth and the Watonwan Rivers. However, not all of the eroded bank and bluff materials that made it to the river were transported past the gauging station within the year. For this reason a range of bank contributions to the suspended sediment load (23 to 56%) was provided assuming different proportions of the clay plus silt fractions were transportable (Figure 3).

4. Discussion

4.1. Scanner accuracy

The vertical bias in the scans is most likely due to GPS positioning errors resulting from a less than optimal satellite configuration or tropospheric factors that degrade GPS signals (James

Hawkins, Aerotec LLC; Adrain Borsa, Scrips Institute of Oceanography, personal comm.). In spite of the seemingly large error in 2002 relative to 2001, both scan errors are less than the specified noise level of the Topeye system (15cm). The mean elevation error in this study was similar to mean elevation errors reported in the literature (Krabill et al., 1995; Abdalati and Krabill, 1999; Huising and Gomes Pereira, 1998; Favey et al., 1999).

Planimetric accuracy was more difficult to determine than vertical accuracy. An attempt was made to quantify planimetric accuracy by surveying bridge edges, but because scan line points typically didn't fall on bridge edges it was impossible to determine accurately where bridge edges fell in the scan image. Nevertheless, the difference between bridge edges determined from the scaned data and edges surveyed on the ground with RTK-GPS averaged 0.83 m.

4.2. Mass wasting accuracy

No vertical or planimetric correction was applied in the calculation of mass wasting because error budgets were determined only for flat homogenous bridge surfaces that were not representative of steep, rough and variably vegetated riverbanks. Furthermore, the detected errors were predominantly within the noise level of the measurement system, and were somewhat normally distributed. Additional research is needed to determine the cause of vertical and planimetric error before application of correction factors.

While bias changes significantly due to time dependent variables associated with resolving GPS positions, it is less likely that variance, or system noise, will change significantly in future scans. One-way to minimize the impact of variance on mass wasting estimates is to have a longer time period between scans. If erosion continues at a high rate the real topographic change will then be large relative to system noise, which will improve the capability to detect and measure change.

4.3. Vegetation effects on mass wasting estimate

Since laser scans were conducted before the leaves emerged on trees (April 2001 and 2002), the influence of forest canopy on the bare earth digital elevation model was negligible. This was also apparent because the last returned pulse of most laser 'shots' made it to the ground, as evidenced by the small proportion of 'shots' that were obviously reflections from canopy elements (to large change in vertical dimension over short horizontal distance) relative to the much larger number of points that represented reflections from the ground. The influence of low growing vegetation was difficult to determine. However, most of the actively eroding banks were devoid of vegetation that would cause interference, and banks with dense brush and grass cover were likely more stable and hence less likely to be contributing to erosion.

4.4. Effect of gauge accuracy on mass wasting estimate

The accuracy of sediment transport measured by the Metropolitan Council Environmental Services is unclear. The water intake is located near shore in fast current about 0.46m above the river bottom. Error in the sediment transport estimates is due to inaccuracies in measuring flow past the gauge and concentration of sediment carried by that flow. Flow accuracy is dependent on accuracy of rating curves that change over time, and the accuracy and timing of stage measurements. This particular site has had a stable stage / discharge relationship largely due to bedrock control of channel morphology.

Without information on grain size distribution of transported sediment it was difficult to precisely estimate what proportion of the sediment input to the river was transported as suspended load due to variations in particle size distributions of slumped materials and stream power available for transport. Material not transported as suspended load was transported as bed load or settled out in low velocity areas of the stream. For this reason a range of possible

sediment transport values was presented (23 to 56%) based on the assumption that all the clay and some or all of the silt was transported (Figure 3). These estimates assume all material that made its way into the river became dispersed and all clay was transportable. The veracity of this assumption improves over longer time scales as slumped clay blocks disintegrate.

4.5. Interpretation of mass wasting results

In this study, the highest mass wasting estimate ranged up to 56% of the transported load measured by a downstream gauging station. This does not imply that 56% of the load in that year had its source in bank materials, because other sources were not measured. The other sources included sediment contribution from eroding banks upstream or downstream of the section scanned in 2001 and 2002, bed load, and overland erosion, specifically from the surface inlets commonly used to drain fields in the watershed. The contribution of bank materials downstream from the scan limit was assumed minimal as those banks were relatively stable and often composed of bedrock. Contribution from upstream banks was more likely, but will be relatively small as the most actively eroding sections were contained within the scanned reach. Of 18 severely eroding sites along 157 km of the Blue Earth River, Bauer (1998) identified only two that were above or below the section scanned in this study. It is important to note that the river gauging station was located downstream from Rapidan Dam, providing a settling reservoir for coarser particles. If significant settling of fine particles occurred in the reservoir, then the estimate of bank contribution would be proportionately less.

5. Conclusions

This study demonstrated the potential of scanning laser altimetry for partitioning non-point source sediment pollution. Using two scans made one year apart on the Blue Earth River in southern Minnesota estimated bank erosion inputs could represent up to 56% of the transported sediment measured at a river gauging station. For the same period up to 201 t of total P was added to the river via bank erosion. Bank erosion inputs are not directly related to transported sediment measured downstream unless the ratio of bedload to suspended load is consistent over long periods. Erosion or deposition below the waterlines could not be quantified because the laser wavelengths used were strongly absorbed by water. Similarly, bank loads above and below the scanned reach were not accounted in this estimate.

Interpretation of mass wasting estimates derived from scanner data must be made in light of several factors that affect accuracy. There are inherent errors in both laser altimetry measurements and river gauging station measurements that could significantly influence sediment partitioning results.

Bias in scan elevations and planimetric accuracy may be corrected if systematic error can be separated from system noise. However, for the two annual scans used in this study the vertical error was within specifications. While there were sources for error in partitioning sediment using this method, it should be recognized that there are no conventional means of surveying at this level of accuracy for such extensive areas.

This study illustrated how scanning laser altimetry could be used in conjunction with river gauging station data to estimate the contribution of eroding bank materials to total suspended load. Operationally, resource managers at federal, state and local levels would use this technology to determine allocation of resources to projects with the greatest potential for pollution abatement. In addition, isolating stream bank inputs and upland contributions by difference with total sediment load can help determine effectiveness of upland soil erosion control efforts.

References

Abdalati, W. and W.B. Krabill, 1999. Calculation of ice velocities in the Jakobshavn Isbrae area using airborne laser alitmetry. Remote Sens. Environ. 67:194-204

Bauer , D.W., 1998. Stream bank erosion and slumping along the Blue Earth River. M.S. thesis Dept. Soil, Water and Climate. University of Minnesota.

Blake, G.R., and K.H. Hartge, 1986. Bulk density, clod method. In Klute, A. (ed). Methods of soil analysis: Part 1 Physical and mineralogical Methods, Second ed. American Society of Agronomy, Soil Science Society of America, Madison, WI.

Favey, E., A., Geiger, G.H. Gudmundsson, and A. Wher, 1999. Evaluating the potential of an airborne laser-scanning system for measuring volume changes of glaciers. Geogr. Ann., 81 A(4): 555-561.

Gee, G.W., and J.W. Bauder, 1986. Particle size analysis, hydrometer method. In Klute, A. (ed). Methods of soil analysis: Part 1 Physical and mineralogical Methods, Second ed. American Society of Agronomy, Soil Science Society of America, Madison, WI

Gupta, S.C., and U.B. Singh, 1996. A review of non-point source pollution models: Implications for the Minnesota River Basin. Department of Soil, Water, and Climate, College of Agricultural, Food, & Environmental Sciences, University of Minnesota, St. Paul, MN.

Harding, D.J., and G.S. Berghoff, 2000. Fault scarp detection beneath dense vegetation cover: Airborne LIDAR mapping of the Seattle Fault Zone, Bainbridge Island, Washington State. Proceedings of the American Society of Photogrammetry and Remote Sensing Annual Conference, Washington, D.C., May, 2000.

Hudnut, K.W., A. Borsa, C. Glennie, and J.B. Minster, 2002. High-resolution topography along surface rupture of the 16 October 1999 Hector Mine, California, Earthquake (M_w 7.1) from airborne laser swath mapping. Bulletin of the Seismological Society of America (92)4:1570-1576.

Huising, E.J., and L.M. Gomes Pereira, 1998. Errors and accuracy of laser data acquired by various laser scanning systems for topographic applications. ISPRS Journal of Photogrammetry & Remote Sensing 53:245-261.

Irish, J.L., and W.J. Lillycrop, 1999. Scanning laser mapping of the coastal zone: the SHOALS system. ISPRS J. Photogramm. and Rem. Sens. 54:123-129.

Jackson, T.J., J.C. Ritchie, J. White and L. LeSchack 1988. Airborne laser Profile Data for measuring ephemeral gully erosion. Photogramm. Eng. And Rem.Sens., 54(8):1181-1185.

Krabill, W.B., R.H. Thomas, C.F. Martin, R.N. Swift, and E.B. Frederick, 1995. Accuracy of airborne laser altimetry over the Greenland ice sheet. Int. J. Rem. Sens. 16(7):1211-1222.

Krabill, W., E. Frederick, S. Manizade, C. Martin, J. Sonntag, R. Swift, R. Thomas, W. Wright, and J. Yungel, 1999. Rapid thinning of parts of the southern Greenland ice sheet. Science 283:1522-1524.

Kuo, S., 1986. Phosphorus, extraction with water or dilute salt solution. In Klute, A. (ed). Methods of soil analysis: Part 1 Physical and mineralogical Methods, Second ed. American Society of Agronomy, Soil Science Society of America, Madison, WI

Minnesota Pollution Control Agency (MPCA), 1985. Lower Minnesota waste load allocation study, St. Paul, MN, 190 p.

Murakami, H. K. Nakagawa, H. Hasegawa, T. Shibata, and E.Iwanami, 1999. Change detection of buildings using an airborne laser scanner. ISPRS J. Photogramm. and Rem. Sens, 54:148-152.

Payne, G.A., 1994. Sources and transport of sediment, nutrients, and oxygen-demanding substances in the Minnesota River Basin, 1989-1992. In Minnesota River Assessment Project Report, Volume II: Physical and Chemical Assessment. Minnesota Pollution Control Agency, St. Paul, MN.

Pereira, L.M.G. and R.J. Wicherson. 1999. Suitability of laser data for deriving geographical information: A case study in the context of management of fluvial zones. ISPRS J. Photogramm. and Rem. Sens, 54:105-114.

Randall, G.W., S.D. Evans, J.F. Moncrief, and W.E. Lueschen, 1996. Tillage best management practices for continuous corn in the Minnesota River Basin. Minnesota Extension Service publication FO-6672-C.

Ritchie, J.C., E.H. Grissinger, J.B. Murphey, and J.D. Garbrecht, 1994. Measuring channel and gully cross-sections with an airborne laser altimeter. Hydrological Processes, Vol. 8, 237-243.

Sallenger, A.H., W. Krabill, J. Brock, R. Swift, J. Jansen, S. Manizade, B. Righmond, M. Hampton, and D. Eslinger, 1999. Airborne laser study quantifies El Nino-induced coastal change. EOS Transactions, American Geophysical Union 80(8)

Sekely, A.C., D.J. Mulla and D.W. Bauer, 2002. Streambank slumping and its contribution to the phosphorus and suspended sediment load of the Blue Earth River, Minnesota. J. Soil and Water Cons. 57(5):243-250.

United States Environmental Protection Agency (USEPA), 1981. Procedures for handling and chemical analysis of sediment and water samples. U.S. Environmental Laboratory. U.S. Army Engineer Water Ways Exp. Sta., Vicksburg, MS.

United States Environmental Protection Agency (USEPA), 2000. The quality of our nation's waters: Water quality report. http://www.epa.gov/305b/2000report/

List of Figures

Figure 1. The study area location was a 56 km section of the Blue Earth River (thick line in the figure on right) scanned with a laser altimeter in 2001 and 2002. This reach of river is between the confluence of the Blue Earth and Watonwan Rivers and the Highway 30 Bridge near Amboy, MN

Figure 2. Correspondence of bridge surface elevations obtained via RTK-GPS survey on the ground versus elevations for the same surfaces determined by 2001 and 2002 LIDAR.

Figure 3. Range in fraction of transported sediment that had its source in riverbank materials based on particle size of sediments added to the flow. Numbers above bars represent percentage of total load due to bank erosion for the given size fraction

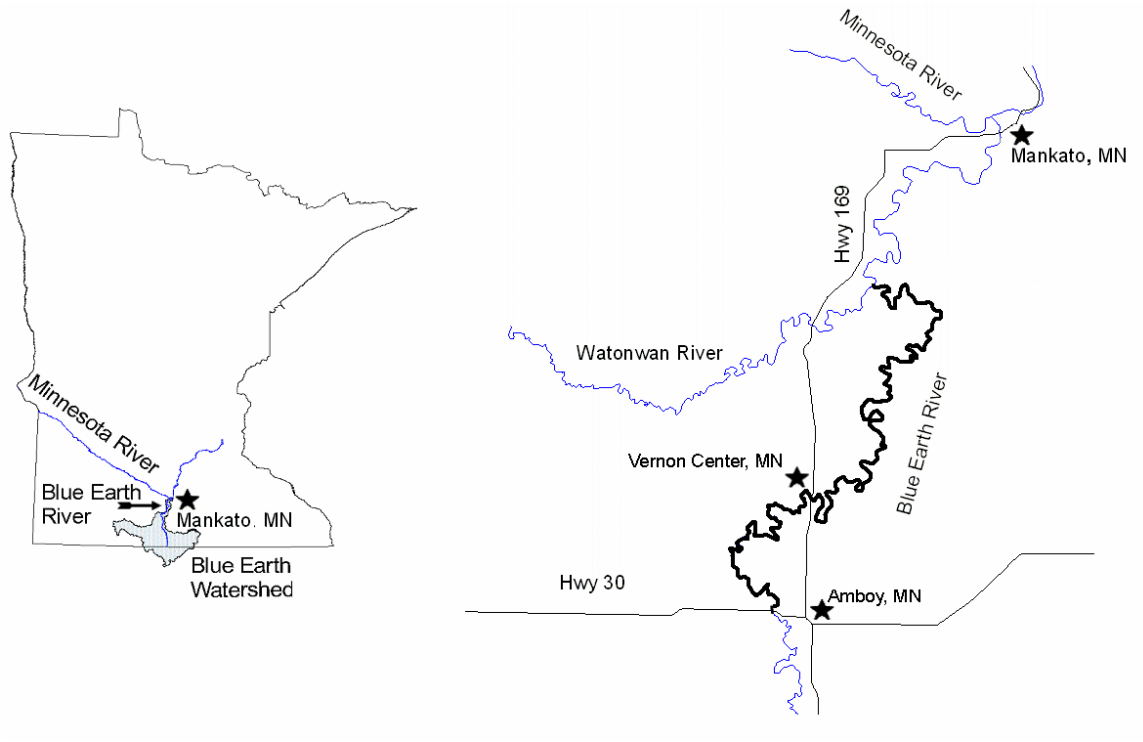

Figure 1. The study area location was a 56 km section of the Blue Earth River (thick line in the figure on right) scanned with a laser altimeter in 2001 and 2002. This reach of river is between the confluence of the Blue Earth and Watonwan Rivers and the Highway 30 Bridge near Amboy, MN

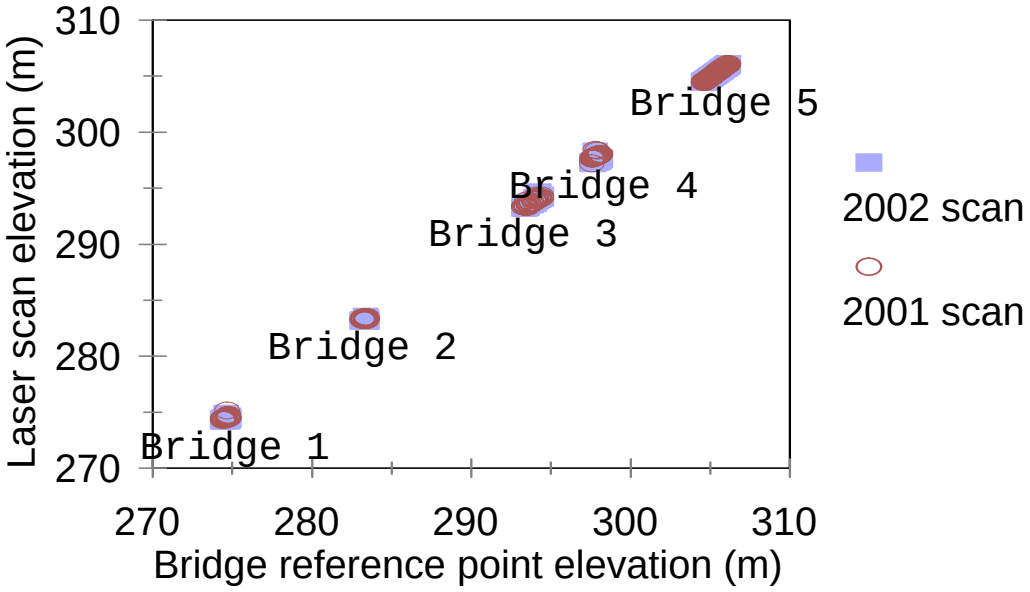

Figure 2. Correspondence of bridge surface elevations obtained via RTK-GPS survey on the ground versus elevations for the same surfaces determined by 2001 and 2002 LIDAR.

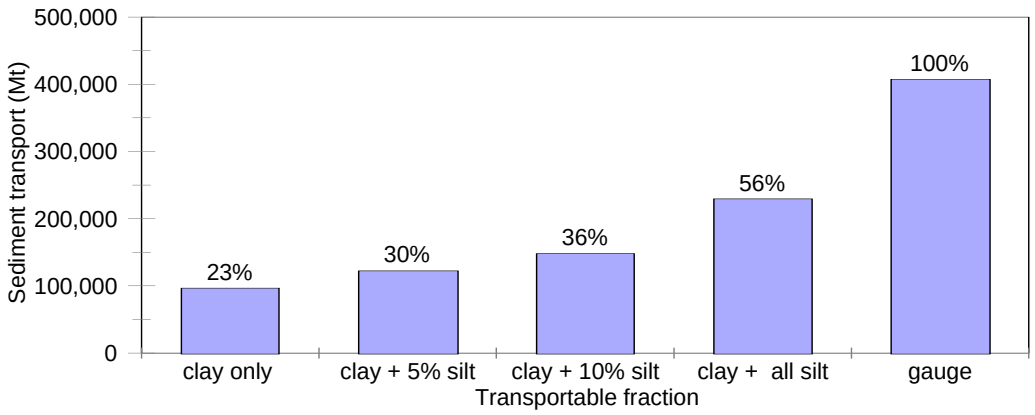

Figure 3. Range in fraction of transported sediment that had its source in riverbank materials based on particle size of sediments added to the flow. Numbers above bars represent percentage of total load due to bank erosion for the given size fraction

Alternating Pattern of Narrow Shooting Flow and Wide Tranquil Flow in Gullies

Kirk R. Vincent*
J. Dungan Smith
US Geological Survey
3215 Marine St.
Mail Room E127
Boulder, CO 80303, USA

Abstract

We discuss a characteristic narrow/wide/narrow channel geometry driven by spatial alternation of 1), as it applies to gullies. We have previously observed and measured this pattern and have detailed its salient hydraulic characteristics for hydraulically steep streams on alluvial fans with sand beds. An instability in the interacting flow and sediment transport fields leads to a stable but propagating pattern composed of shooting flow in steep, narrow reaches (with concave profiles) followed by tranquil flow in wide, shallow and less-steep reaches (with convex profiles). Erosion occurs in the steeper reaches followed by deposition in the broader ones of lower slope. In its simplest manifestation, rapid deposition at the upstream end of the less steep reach causes the thalweg to split, forcing two zones of highest flow to the margins of the expanding area of tranquil flow and, thereby, promoting bank erosion and an expanding width. As the flow nears the downstream end of the broad reach the threads converge and the flow accelerates into the steeper zone of shooting flow, causing incision into the bed of the broad reach and broadening of the entrance of the next narrow reach. As a consequence of the incision at the downstream end of the broad reach, bed erosion in the steep, narrow reach, and lateral erosion at the upstream end of the next broad reach, the whole pattern slowly migrates upstream with a fixed form. We have recently observed this pattern and its process in gullies that have ceased incising into the landscape. Measurements made of the wide-narrow pattern in a local gully are analyzed herein with the assistance of a simple flow model. Despite the confinement of the gully banks, the width ratio (widest/narrowest = 2 to 4) is similar to that for unconfined alluvial fan channels. The relative wavelength (L), the wavelength divided by the widest width, for our gully (L = 4 to 7) is shorter in general than that for alluvial fan channels (L = 6 to 10). Presumably this is because the gradient (S) of the gully (S = 0.1 m/m) is substantially steeper then that for the alluvial fans we have studied (S = 0.01 to 0.03 m/m). Ultimately the existence of this instability in gullies is a primary energy dissipation mechanism and causes the gullies to widen and their hydraulic geometries to change. Our results should be useful to others studying the hydraulics of ephemeral gullies.

*Correspondence author

Spatial Distribution and Morphological Features of Gullies in an Agropastoral Area in Sardinia (Italy)

Claudio Zucca[*] (E-Mail: nrd@uniss.it)
Nucleo Ricerca Desertificazione
Università di Sassari
Tel. 39 0792111016
FAX 39 079217901 nrd@uniss.it

Annalisa Canu (E-Mail: a.canu@ibimet.cnr.it)
Raniero Della Peruta
CNR - IBIMET
Via Funtana di lu colbu 4/A
07100 Sassari

Abstract

According to the United Nations Convention to Combat Desertification (UNCCD) soil erosion is one of the main causes of desertification in the Northern Mediterranean. Recently the role of channelled erosion in sediment delivery has been underlined by different experimental researches. The aim of the present work is to set up a simplified experimental methodology to study the relationships between gully erosion, land types and landuse.

The experimental area (about 720 ha) is located in a hilly region threatened by desertification in Central Eastern Sardinia (Italy), characterised by uneven morphology with steep slopes, where agropastoral activities, particularly tillages with heavy machinery and overgrazing, are causing severe soil erosion and compromising agricultural productivity. Precedent studies carried out in the same area highlighted the need to quantify and monitor soil erosion to be able to give the farmers management guidelines. In this study, carried out in May 2003, an inventory of gullies of the area was made through an integrated use of aerial photographs and field surveys. The degree of activity and morphological features of gullies were assessed in the field by using simple criteria. The approach adopted included the measurement of the position and shape of gullies heads and their width and depth at specific points. Relationships were studied among distribution, frequency, morphological characteristics of gullies and geomorphological features and landuse.

Keywords: gully erosion, landuse, overgrazing, desertification

[*]Correspondence author

A Simple Device to Monitor Sediment Yield From Gully Erosion

Antonio Jose Teixeira Guerra*
Senior Lecturer in Physical Geography
Federal University of Rio de Janeiro
Av. Canal de Marapendi
1100 apto. 608, Bloco 2, Barra da Tijuca-CEP
Rio de Janeiro, Rio de Janeiro 22.631-050, Brazil
(E-mail: antonioguerra@openlink.com.br)

Marcos Figueiredo
Lecturer in Physical Geography
State University of Mato Grosso
(E-mail: marcosunemat@bol.com.br)

Abstract

The focus of this paper is the design and use of a simple device to determine sediment yield from gully erosion. The simplicity and low cost of the design make it particularly appropriate for use when resources are limited. Here, it is used to measure sediment yield at a site called Anão Gully, in a study area in Cáceres municipality (15º 57' S and 57º 31' W, Mato Grosso State, Brazil). This gully is only 28 kilometres from Cáceres town centre, which makes it easy to reach the site immediately during and after storm events and obtain measurements from the device.

Keywords: Gully erosion, sediment yield, gully monitoring, simple device

1. Introduction

Soil erosion has been investigated by several researchers throughout the world, in order to comprehend how the process evolves and also to understand the several sub-processes that take place within the erosion process (Small and Clark, 1982; Morgan, 1986; Hasset and Banwart, 1992; Boardman and Favis-Mortlock, 1993; Selby, 1993; Goudie and Viles, 1997; Guerra and Favis-Mortlock, 1998; Favis-Mortlock and Guerra, 1999, 2000; Figueiredo, 2003; Garcia and Guerra, 2003). Soil properties, rainfall regime, slope characteristics, vegetation cover and land use play an important role on the erosion process. In Mato Grosso State all those factors are significant for the erosion process and therefore one site has been selected to investigate sediment yield, using a simple device.

Land use is a particular significant factor regarding the ocurrence of erosion on the site selected for monitoring. The vegetation on almost all the slopes has been cleared, partly in order to grow crops but mainly for cattle grazing. Also this area (Caceres Municipality – Mato Grosso State) (Figure 1) is crossed by a gas pipeline, which comes from Bolivia and reaches Cuiabá City (capital of Mato Grosso State), in order to supply natural gas to a power plant. The Brazilian pipeline is 267 km long and during the construction process erosion has taken place, due to the digging operations and other earth movement, which are necessary for a gas pipeline instalation. Furthermore, erosion still takes place, due to the bad maintenance of the whole structure of the

*Corresponding author

soils along the pipeline, together with the concentrated rainfall, during the summer and the sandy loam soils in the area (Figueiredo, 2003).

Several gullies have developed in Caceres Municipality due to the environmental conditions and land use, putting at risk the soils and also the gas pipeline, especially where the vegetation has been cleared and cattle grazing takes place, without taking into account soil erodibility and concentrated rainstorms. Some of the gully heads, which are very close to the pipeline (some of them only 15 metres), may retreat in a few years and put at risk the pipeline and, consequently the lives of the people who live nearby.

Therefore, this area has been chosen to monitor the gully head retreat, putting stakes into the soil, and taking measurements from the stakes to the gully border, every month. Also a simple device has been created to monitor the sediment yield from one of the gullies. In this article we outline only the results obtained with this device, which has proved to be very useful for small gullies.

2. Study Area

Annual rainfall in the study area during the last 30 years has ranged between 944 mm and 1872 mm, with a high concentration of storm events in the southern summer between December and April, when almost 80% of the rains fall in this period, reaching up to 300 mm in one month alone. The temperatures range between 24º C and 38º C. The winter is dry in this part of Brazil, when the rains range between 2 mm and 50 mm in one month. The air moisture reaches up to 80%, during the rainy season, whereas during the dry season is only around 50%.

The occurrence of two distinct seasons – one wet and the other dry – plays an important role regarding the natural vegetation cover. This is known as *Cerrado*; a kind of savannah, but most has now been cut down for cattle and agriculture. In fact, where the *Cerrado* still exists, it shows different characteristics, according to soil type, slope angle and characteristics, proximity to rivers, etc.

The geology of the area dates mainly from 500 million to 100 million years old, in a very typical sedimentary environment, where the climate was cold and glacial, and this was an ocean bottom (Vieira, 1965). Those environmental conditions have given rise to mainly fine sandstones and shales, which weather to oxisols with a high sand content (70%), medium silt content (25%), and very low clay content (5%). Some conglomerates can also be found in the study area.

Furthermore, the pH in most soils range between 4.3 and 4.9, which makes them very acidic, with very low organic matter content, ranging in most cases between 0.5% and 0.9%. This makes these soils rather unstable and, consequently, very prone to crusting and erosion.

The average slope length of the agricultural fields is 1500m and the average slope angle is 8 degrees. These characteristics make the area very prone to gully erosion. Together with the lack of soil conservation measures, this has led to serious gully erosion throughout the study area.

3. Methods and Materials

Differing environmental and land use characteristics have resulted in different types of gullies in the area, all with different dimensions. The trial version of the flume, which was made for this investigation, is suited only to rather small gullies. Only one gully in the area was of appropriate dimensions (Figure 2). This gully has an area of 7.12 m2, 6.22 m long, depths ranging from 0.50m to 1.57m and widths ranging from 0.52m (gully outlet) up to 2.65m. The

gully shape allowed us to place the flume exactly on the gully outlet, in order to collect all the soil eroded on each storm event.

A simple raingauge was placed next to the Anão Gully, in order to measure daily rainfall at 7:00 am, during the monitoring period. Budgetary constraints meant that it was not possible to purchase a more sophisticated raingauge, so that rainfall intensity could not be directly monitored. However, we were able to make an estimate of the rainfall intensity, since we recorded the total rainfall, and the approximate duration of the event at Cáceres City, near Anão Gully, was noted. We also collected the total soil eroded inside the flume for each event.

The measuring device resembles a miniature flume 4 cm deep (Figure 3), 52 cm wide x 52 cm long, made in aluminium. It was placed into and level with the soil at the gully outlet, so that total volume of soil eroded during each storm was collected. The small size of this device is applicable only to small gullies, like the one selected for this research work. Although the monitoring period was not very long (from September 2002 to April 2003 – eight months only), it was enough to obtain some very interesting results, because it included the rainy season, which runs from December to April, concentrating more than 70% of the total annual rainfall, within the research area.

4. Results and Discussions

During the whole monitoring period, only three main events have been monitored within eight months of observation (Table 1). All occurred during the summer, which is when the heaviest rainstorms take place. Since the area of the gully is known (7.12 m2), it is possible to estimate the area-averaged soil loss from within the gully for each event and for the period of observation (55 t/ha). This means that while the gully is being eroded, the average rate of erosion is approximately 0.5 t/ha per minute, which is a very high soil erosion rate, even for tropical areas.

While these results are for only one gully, the majority of the soils in this municipality are also sandy loams, so one can conclude that several hundreds of tons of sediment are being exported each year from this municipality as a result of gully erosion. Hundreds of gullies have formed within Cáceres and also in other municipalities in Mato Grosso State; some of them cause river siltation in Paraná River Basin, which flows southwards, where others cause river siltation in Amazonas River Basin, due to the sediments which flow northwards.

5. Conclusions

This investigation has outlined a simple method for estimating soil loss from small gullies on an event basis, which is especially suited to researchers with a limited budget.

This methodology will be used for small gullies in regions of Brazil. The long-term aim of future research is to improve our estimates of rates of soil erosion in different parts of Brazil, and to devise better methods both for recuperating already eroded areas and for preventing soil erosion in other areas.

Acknowledgements

We are most grateful to Dr. David Favis-Mortlock, from Queen´s University Belfast, for reading the first draft of this paper and making very good comments and correcting the English. We are also grateful to the Brazilian Research Council (CNPq – *Conselho Nacional de Desenvolvimento Científico e Tecnológico*) and to the Rio de Janeiro State Research Council

(FAPERJ – *Fundação de Amparo a Pesquisa do Rio de Janeiro*), which provided the funds for this research.

References

Boardman, J. and Favis-Mortlock, D.T. 1993. Climate change and soil erosion in Britain. Geographical Journal, 159, 2, 179-183.

Favis-Mortlock, D.T. and Guerra, A.J.T. 1999. The implications of general circulation model estimates of rainfall for future erosion: a case study from Brazil. Catena, 37, 329-359.

Favis-Mortlock, D.T. and Guerra, A.J.T. 2000. The influence of Global Greenhouse-Gas Emission on Future Rates of Soil Erosion: a Case Study from Brazil Using WEPP – CO2. In: Schmidt, J. (Ed.), Soil Erosion – Application of Physically Based Models. Springer-Verlag, Berlin, pp. 3-31.

Figueiredo, M. 2003. Análise dos Processos Erosivos Associados ao Escoamento Superficial Concentrado na Microbacia do Córrego Jaberão, Área da Seção de Construção do Gasoduto Bolívia-Brasil – Município de Cáceres – MT. PhD Thesis, Department of Geography, Federal University of Rio Janeiro, Brazil.

Garcia, M. and Guerra, A.J.T. 2003. Environmental impacts of HEP: a Brazilian case study. Geography Review, 17, 1, 11-14.

Goudie, A. and Viles, H. 1997. The Earth Transformed – An Introduction to Human Impacts on the Environment. Blackwell Publishers, Oxford.

Guerra, A.J.T. and Favis-Mortlock, D.T. 1998. Land degradation in Brazil. Geography Review, 12, 2, 18-23.

Hasset, J.J. and Banwart, W.L. 1992. Soils and Their Environment. Prentice Hall, New Jersey.

Morgan, R.P.C., 1986. Soil Erosion and Conservation. Longman Group, London.

Selby, M.J. 1993. Hillslope Materials and Processes. Oxford University Press, Oxford.

Small, R.J. and Clark, M.J. 1982. Slopes and Weathering. Cambridge University Press, Cambridge.

Vieira, A.J. 1965. Geologia do Centro-Oeste. CENPES – Petrobrás, Ponta Grossa, Paraná State, Brazil.

Table 1. Results obtained by using the device

Date	Event duration (minutes)	Rainfall during event (mm)	Sediment yield from event (kg)	Area-averaged soil loss from gully (t/ha)
13/2/2003	45	130	15.01	21
24/3/2003	30	105	13.73	19
17/4/2003	45	80	10.46	15
Total	120	315	39.20	55

List of Figures

Figure 1. Location of the study area

Figure 2. Anão Gully

Figure 3. Flume design

Figure 4. Flume filled with eroded soil

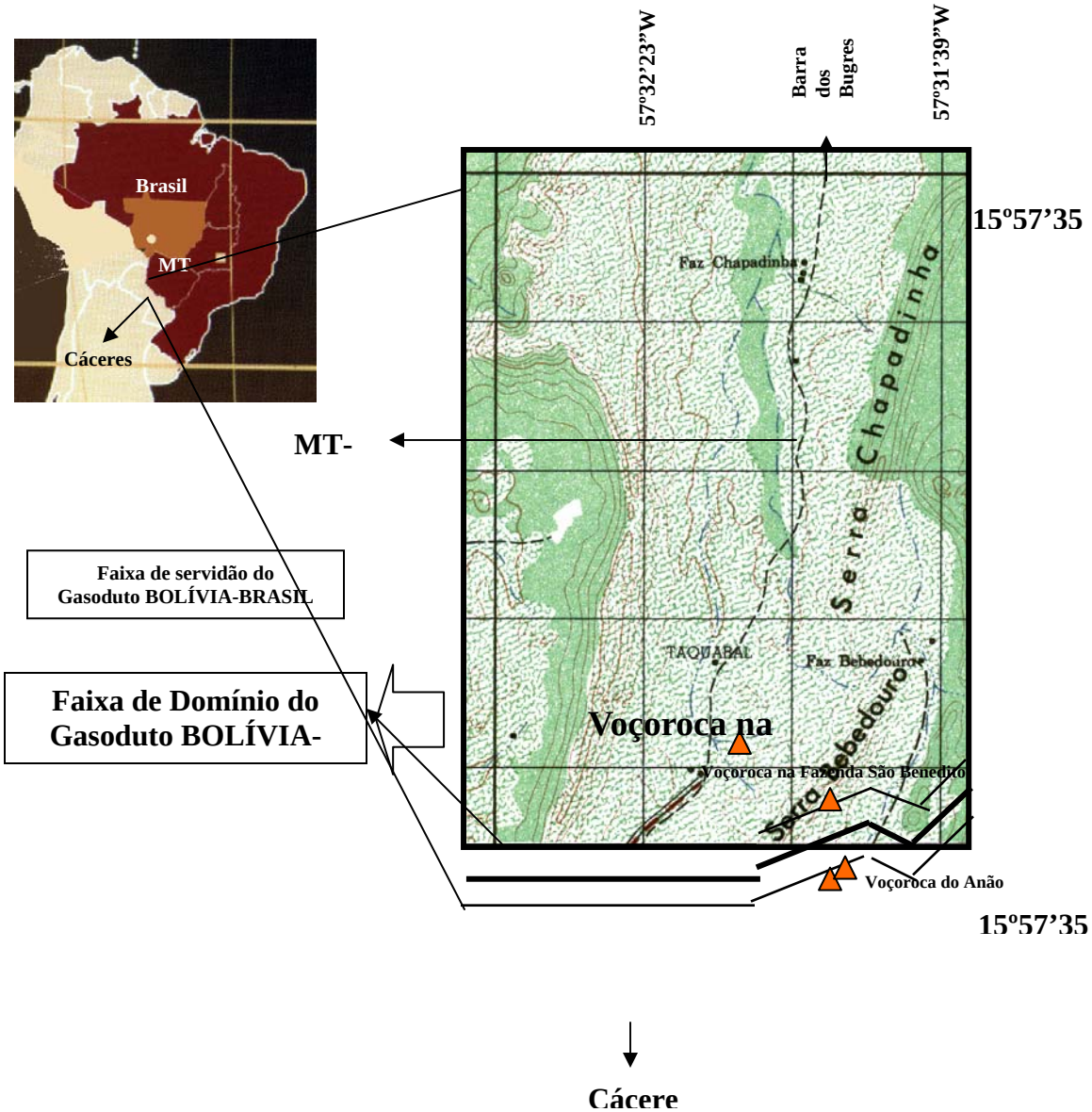

Fonte: DSG Folhas SD.21-Y-D-V e SD.21-Y-D-VI
Escala 1:100.000

Figure 1. Location of the study area.

Figure 2. Anão Gully

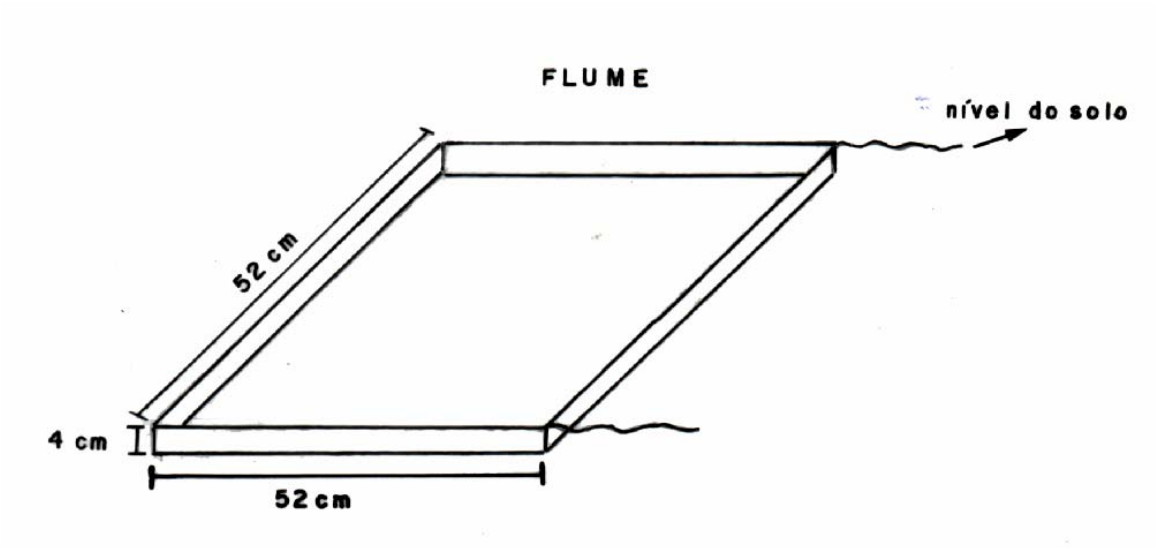

Figure 3. Flume design.

Figure 4. Flume filled with eroded soil.

To Table of Contents

Gully Erosion – Models and Processes

Modeling Ephemeral Gully Erosion for Conservation Planning
Foster, George R. (Keynote)

The next Generation of Watershed-scale Erosion Models: Towards a Dynamic, Spatially Adaptive Representation of Rills and Gullies (Abstract only)
Favis-Mortlock, David and Paul Van Dijk

Numerical Simulation of Migration of Head-cut with A Two-layered Bed
Jia, Yafei, Kitamura Tadanori, and Sam, S. Y. Wang

Modeling Headcut Development and Migration in Upland Concentrated Flows
Bennett, Sean J. and Carlos V. Alonso

Empirical-numerical Analysis of Headcut Migration
Wu, Weiming and S.S.Y. Wang

Computer Modeling of Erosion and Sediment Delivery (Abstract only)
Lai, Yong G. and C. Ted Yang

AnnAGNPS & Ephemeral Gullies (Abstract only)
Theurer, F.D., R.L. Bingner, J. Stafford, and W. Merkel

Evaluation of Rill and Ephemeral Gully Erosion in Cultivated Areas of Navarre (Spain)
De Santisteban, L.M., J. Casalí, J.J. López

Experimental Study of Conditions for Rill Bank Collapse (Abstract only)
Stefanovic, Jovan R. and Rorke B. Bryan

Modeling of Erosion Processes and Estimation of Interrill Erodibility Soil Parameters in Forest-Steppe Zone of Ukraine (Abstract only)
Vasyliv, Nataliya

Macropore Flow and Mass Wasting of Gullies in the Loess Plateau, China
Wilson, G.V., Xu Mingxiang, Chen Yun Ming, and Liu Guobin

Hydraulic Characteristics of Knickpoints in Rill Confluence Zones (Abstract only)
Brunton, D.A. and R.B. Bryan

Gully Erosion – Models and Processes

Hydrologically Driven Mechanisms of Head-Cut Development
Römkens, M.J.M. and S.N. Prasad

Overview of Dam Gully Erosion Research
Hanson, G. J., D. M. Temple, K. M. Robinson, K. R. Cook

Freeze/Thaw Effects on Rill and Gully Erosion in the Northwestern Wheat and Range Region
McCool, D. and J.D. Williams

Resistance of Topsoils to Concentrated Flow Erosion: a Review of the Available Experimental Data
Knapen, Anke and J. Poesen

Grass Hedge Effects on Gully Hydraulics and Erosion
Dabney, S.M. , F.D. Shields, Jr., E.J. Langendoen, and D.M. Temple

Keynote

Modeling Ephemeral Gully Erosion for Conservation Planning

George R. Foster
Research Hydraulic Engineer (retired)
USDA-Agricultural Research Service
National Sedimentation Laboratory
Oxford, Mississippi, USA
Fax: 979-589-1305
Email: gfoster@iolbv.com

Abstract

This paper discusses the overland flow and concentrated flow systems that occur in most farm fields. The paper emphasizes the important role of concentrated flow areas and how these areas are distinct from overland flow areas. The paper also describes how ephemeral gully erosion, which occurs in concentrated flow areas, differs from rill and classical gully erosion. Concentrated flow areas, which are not often considered in watershed hydrologic, soil erosion, and sediment delivery models, are the main conduits that convey runoff and sediment from most farm fields. Concentrated flow areas occupy much of the flow area between the actual end of overland flow areas and defined stream channels. Neglect of concentrated flow areas results in large errors of predicted erosion and sediment yield for farm fields. The paper describes erosion and deposition processes in concentrated flow areas, emphasizing the effect of soil and cover management on these processes. Ephemeral gully erosion is a major source of sediment that is not estimated with rill-interrill erosion prediction methods. Much deposition can also occur in concentrated flow areas resulting in sediment load leaving a farm field being much less than the sediment produced by erosion within the field. Although practices are available that control ephemeral gully erosion, many of these practices have drawbacks. The paper describes cover-management and topographic representation and model structure needed in models used for conservation planning on farm fields. The need for input topographic data on a much finer scale and resolution than is commonly used is discussed.

1. Introduction

Ephemeral gully erosion, which is caused by concentrated flow within cultivated farm fields, is distinct from rill erosion. Ephemeral gully erosion is also distinct from gully erosion in permanent, deep, incised channels, formed by headcuts moving upstream. Ephemeral gully erosion is often overlooked. It is not estimated with rill-interrill erosion prediction technology such as the Revised Universal Soil Loss Equation (Renard et al., 1997), and it is often not measured in field surveys used to inventory erosion. Ephemeral gully erosion degrades the landscape and is a major source of sediment. Concentrated flow areas where ephemeral gully erosion occurs are the main conduits that convey runoff and sediment from most farm fields (Toy et al., 2002). Deposition in the lower reach of concentrated flow areas can greatly reduce sediment yield from farm fields. Improved prediction methods that estimate erosion, deposition,

and sediment delivery from overland flow and concentrated flow areas in farm fields are needed for conservation planning to ensure that appropriate erosion control are being selected to protect both on-site and off-site resources.

2. Ephemeral Gully Erosion Characteristics

A commonly used soil erosion classification defines rills as eroded channels that can be obliterated by routine tillage operations (Toy et al., 2002). Classical gullies are permanent, deep, wide eroded channels that can not be obliterated by common tillage operations or crossed with farm equipment. An alternate classification discussed in this paper defines rills and gullies based on their landscape position and hydrologic function.

Rill-Interrill Areas

Rill areas occur on the overland flow part of the landscape (Foster and Meyer, 1975; Meyer et al., 1975; Toy et al., 2002). Although a common hydrologic assumption is that overland flow occurs as a broad sheet flow, this runoff actually occurs in many small flow concentrations. If runoff erosivity in these flow concentrations is sufficiently high, the flow erodes soil, forming small incised channels that are called rills. These small flow concentrations are referred to as rill areas even if no rill erosion occurs in them.

Interrill areas occupy the space between the rill areas. Surface runoff on the interrill areas occurs as a broad sheet flow. Detachment of soil on interrill areas is by raindrop impact and not surface runoff. Interrill runoff flows laterally to rill areas that collect and convey runoff downslope.

An area where surface runoff detaches soil is by definition a rill area, and the erosion is rill erosion by definition. Erosive surface runoff on the overland flow areas erodes numerous rills, small eroded channels about 100 mm wide and deep, across the slope. Rills tend to be uniformly spaced and sized across slope. Rills are parallel on a smooth soil surface on those portions of the landscape where orthogonals to the contour lines are parallel. Rills converge on those landscape areas where the orthogonals converge such as in landscape hollows. Conversely, rills diverge where the orthogonals diverge such as on landscape noses. Figure 1 illustrates these rilling patterns. Micro-topography left by tillage marks affects rilling pattern. For example, rilling pattern associated with up and downslope tillage differs from the rilling pattern associated with across slope tillage.

Concentrated Flow Areas

In contrast to rill areas that occur in new locations after being obliterated by tillage, concentrated flow areas occur in permanent locations determined by the landscape's macro-topography (Foster, 1985). Similarly concentrated flow areas end overland flow areas just as rill areas end interrill areas. Runoff from overland flow areas is collected in the concentrated flow areas, which are a few well defined channels that convey runoff from farm fields.

Gully Erosion

Both classical and ephemeral gullies occur in concentrated flow areas. Figure 2 shows a classical gully. Classical gullies are primarily formed by advancing headcuts that greatly widen and deepen the concentrated flow area (Toy et al., 2002). Classical gullies also experience localized and periodic slumping of sidewalls. Flow in the gullies

transports away the slumped soil. Classical gullies are sometimes referred to as edge-of-field gullies whereas ephemeral gullies are referred to as within-field gullies.

Ephemeral gully erosion occurs in farmed-across concentrated flow areas as shown in Figure 3. Although tillage partly obliterates an ephemeral gully, ephemeral gullies are reformed in permanent locations on the landscape where previous ephemeral gullies existed. Most ephemeral gullies in cultivated fields are wide and shallow having a width to depth ratio of about 10:1. The typical width to depth ratio of a rill is 1:1. A freshly tilled soil surface layer in seedbed condition can be easily eroded while untilled soil or large soil clods left by primary tillage can be quite resistant to erosion. This difference in susceptibility to erosion between soil layers produces wide, shallow eroded channels. Un-tilled soil and large soil clods act as a non-erodible layer that limits downward erosion (Foster, 1982; Foster and Lane, 1983).

Not all ephemeral gullies are wide and shallow. Ephemeral gullies in no-till cropped, hay, and permanent pasture fields can be incised channels with a small width to depth ratio. Incised channels occur because soil resistance to erosion is relatively uniform with depth.

Neither rills, ephemeral gullies, nor classical gullies create concentrated flow areas. An ephemeral gully is determined not by size but by where it occurs on the landscape and whether periodic farming operations fill the eroded channels. Ephemeral gully erosion occurs in pre-existing concentrated flow areas that may not be obvious without ephemeral gully erosion. Ephemeral gullies do not shorten the overland flow path length.

3. Why Ephemeral Gully Erosion is Important

Rill-interrill erosion prediction procedures do not include ephemeral gully erosion in their estimates. These procedures apply only to overland flow areas, which are terminated by concentrated flow areas where ephemeral gully erosion occurs. The overland flow path length assumed in hydrologic models used to compute watershed runoff and sediment yield are often much longer than actual field overland flow path lengths. For example, actual overland flow path lengths are about 50 m, while overland flow path lengths greater than 300 m are commonly used in hydrologic models. Assuming broad sheet overland flow when the flow is actually channelized distorts values for parameters such as hydraulic roughness from the values used for overland flow alone. Serious errors result when rill-interrill erosion prediction technologies are applied to excessively long overland flow path lengths. The typical plot length used to derive rill-interrill erosion prediction technologies is about 20 m. Extrapolating these empirically derived procedures to overland flow path lengths as long as 300 m is questionable. Furthermore, ephemeral gully erosion did not occur on these plots. Consequently these empirically derived erosion prediction technologies do not measure (estimate) the ephemeral gully erosion that occurs in a typical farm field.

Concentrated flow paths convey runoff and sediment from most farm fields. The profile along many concentrated flow paths is concave where ephemeral gully erosion occurs in the upper channel reach and deposition occurs in the lower channel reach. A low channel grade reduces the concentrated flow's sediment transport capacity to less than the incoming sediment load produced by both rill-interrill and ephemeral gully

erosion, which causes deposition. Also, restricted outlets at the field edge can greatly reduce the flow's sediment transport capacity, causing much deposition. Sediment load leaving a field can be less than eighty percent of the sediment produced by erosion within the field because of deposition in concentrated flow areas (Foster et al., 1980a; Foster et al., 1981).

Ephemeral gully erosion is a significant sediment source within farm fields. Sediment produced by ephemeral gully erosion approximately equals the sediment produced by rill-interrill erosion in conventionally tilled row crop and small grain fields on about six percent steep land (Thomas et al., 1986). That is, rill-interrill erosion prediction procedures underestimate sediment production in these fields by about half. The error is even greater for no-till, hay, and pasture cropping where sediment produced by ephemeral gully erosion can be ninety percent or more of the total sediment produced in the field.

Ephemeral gully erosion degrades landscape quality. Ephemeral gullies hinder harvest and crossing ephemeral gullies can damage farm equipment. Plowing in the gullies before harvest takes time, increases cost, and reduces crop production.

Ephemeral gully erosion also reduces soil productivity. Tillage loosens the soil in the concentrated flow area, which accelerates erosion in the concentrated flow area. Tillage moves soil from adjacent overland flow areas into the concentrated flow area. The area affected by the ephemeral gully erosion expands as shown in Figure 3. The overland area adjacent to the concentrated flow area becomes increasingly convex, which increases rill-interrill erosion as the concentrated flow area becomes incised. Both erosion and translation of soil by tillage reduce soil depth over the affected area, which in turn reduces soil productivity. Reduced income because of decreased crop production and decreased land value are measures of the impact of ephemeral gully erosion. Land dissected with ephemeral gullies is less valuable than similar land without ephemeral gullies.

4. Ephemeral Gully Erosion Control

The typical conservation planning objective is to prevent ephemeral gully erosion rather than control it to an acceptable rate, which is the conservation planning objective for rill-interrill erosion (Toy et al, 2002). The conservation planning procedure is to first visually identify that excessive ephemeral gully erosion is occurring. The practices primarily methods used to prevent ephemeral gully erosion are grassed waterways, contouring and contour strip cropping, parallel tile outlet terraces, and subsurface drainage.

Grassed waterways prevent ephemeral gully erosion by reducing the erosive forces that concentrated flow applies to the soil. Grassed waterways must be properly designed, installed, and maintained. A common failure is that runoff flows along both edges of the grassed waterway without entering the waterway. Ephemeral gully erosion can occur within the waterway if vegetation quality is poor. Wet soil in the waterway and pesticides accidentally sprayed on the grass result in poor vegetation. Grassed waterways inconvenience farming operations, are expensive to install and maintain, and take land out of production.

Contouring, especially when accompanied with strip cropping, can significantly reduce ephemeral gully erosion. Contouring must be almost perfectly on the contour to

be highly effective. Off-contour ridges and furrows left by tillage can increase ephemeral gully erosion as illustrated in Figures 4 and 5. This problem arises when the tillage path is straightened across concentrated flow areas, which increases row-furrow grade. Rather than runoff flowing uniformly over the ridges along their length, runoff flows along the ridges-furrows to concentrated flow areas, which extends concentrated flow upslope and lengthens the ephemeral gully erosion area. Contouring is not effective where very intense rainfall and high runoff rates occur. Contouring and contour strip cropping lines must be carefully laid out with surveying equipment, and these lines must be carefully followed with tillage equipment. Farm operations are inconvenienced. Also, strip cropping involves strips of dense vegetation that are typically hay crops, which may not be desired or profitable crops for some farms.

Parallel tile outlet terraces, illustrated in Figure 6, reduce flow rate and erosivity in concentrated flow areas. Terraces must be spaced sufficiently close together to prevent ephemeral gully erosion. Terrace spacing varies with land steepness, dominant rainfall intensity, and inter-terrace cropping-management conditions. Widely spaced terraces have little effect on ephemeral gully erosion. Parallel tile outlet terraces are expensive to install, require maintenance, take land out of production if the terraces involve grassed backslopes, and are inconvenient to farm. However, these terraces trap and keep a large amount of sediment on the field (Foster et al., 1980a).

Subsurface drainage reduces runoff rate and amount, which reduce ephemeral gully erosion (Skaggs et al., 1982). Subsurface drainage most effectively reduces ephemeral gully erosion on relatively flat lands.

Although these measures effectively control ephemeral gully erosion, conservation planning in many fields is limited to considering rill-interrill erosion. Controlling sediment yield from farm fields is important for protecting downstream water quality and preventing excessive off-site sedimentation. The sediment generated by ephemeral gully erosion and the deposition that occur in concentrated flow areas is often not considered in conservation plans.

A model is needed for conservation planning that considers rill-interrill erosion and deposition on overland flow areas, ephemeral gully erosion and deposition in the concentrated flow areas within a field, and sediment delivery from the field. The model must fill the gap between where overland flow areas actually end and where flow enters recognized, defined stream channels. Concentrated flow areas within fields, where channel flow occurs, occupy a major portion of this gap.

5. Ephemeral Gully Erosion Processes

Principal Processes

Understanding channel erosion processes and the factors that affect them is a requirement for modeling ephemeral gully erosion for conservation planning. The principal ephemeral gully erosion processes are headcut, sidewall, and wetted perimeter erosion. Secondary erosion processes include slumping of soil caused by undercutting at headcuts and sidewalls. The slumped soil is subsequently cleaned out by the channel flow. Piping, which is water flowing through the soil, affects ephemeral gully erosion (Huang and Laflen, 1996). Subsurface flow increases soil moisture and decreases soil resistance to erosion where the water exits the soil in a concentrated flow area. Also, the exiting subsurface flow applies forces to the soil that increase soil susceptibility to

erosion by surface flow. Local erosion begins and a headcut evolves that advances up the concentrated flow area. Piping most often occurs in coarse textured soils and soil having large macro-pores above a shallow impermeable layer along which the subsurface water flows.

Local Erosion

Soil detachment occurs where hydraulic forces applied to soil exceed the soil's resistance to erosion (i.e., critical shear stress). Erosion in concentrated flow areas varies greatly in space and time because hydraulic forces vary spatially and temporally (Foster et al., 1984). Much concentrated flow erosion is highly localized, which produces mobile features such as head cuts and steep chutes. Figure 7 shows uniformly spaced headcuts moving up a channel. Headcuts and steep chutes evolve to a steady shape, advance up the channel at a steady rate, and erode the channel at a steady rate when flow rate is steady. These features must move up the channel to maintain their geometry. Their geometry and the rate that they move upslope are functions of flow rate, channel grade, soil conditions, and the presence of non-erodible materials.

Channel Incisement

Concentrated flow erosion also occurs by channels becoming incised as illustrated in Figure 8 where downward movement of the channel is not restricted by a non-erodible layer (Foster, 1982). During incisement, the channel evolves to an equilibrium shape that moves downward at a steady rate. Hydraulic forces on a channel's wetted perimeter are greatest in the middle of the channel and decrease to zero at the water surface, which produces a particular channel cross-sectional geometry illustrated in Figure 9. The cross section and the rate that a channel moves downward are functions of flow rate, channel grade, soil properties, and the presence of non-erodible material.

Non-erodible Layer

Regularly tilled fields have an easily eroded soil surface layer underlain by an erosion resistant soil layer, which acts as a non-erodible layer. Concentrated flow erosion occurs in two phases as illustrated in Figure 10 for steady flow. The initial phase is downward erosion. After the channel reaches the non-erodible layer, the channel widens and erosion rate decreases. The channel eventually reaches a final width and erosion ceases, which occurs when the hydraulic force at the base of the channel sidewall become equal to the soil's critical shear stress as illustrated in Figure 11 (Foster, 1982). The channel's final width is a function of flow rate, channel grade, soil properties, and presence of non-erodible material.

Erosion rate is a function of previous erosion as well as flow rate, channel grade, soil properties, and presence of non-erodible material. An important effect of the non-erodible layer is that erosion by any single storm and cumulative erosion over several storms depends on storm sequence. A small or even a moderate storm causes little erosion if it occurs after an intense, large storm that greatly widened the channel. However, the same small or moderate storm causes much more erosion if it occurs before the large storm.

Soil Management Effects

Flow erosivity and the hydraulic forces applied to the soil are directly related to flow rate, channel grade, and the presence of non-erodible, stable material, such as crop residue and plant roots on and in the soil. The flow's total hydraulic force is divided between that applied to the soil and that applied to the non-erodible elements (Foster et

al., 1980a; Foster, 1982). The presence of non-erodible material reduces the hydraulic forces applied to the soil. Heavy amounts of these materials can greatly reduce, if not eliminate ephemeral gully erosion (Brown et al., 1989; Van Liew and Saxton, 1983)

Soil management and inherent soil properties affect concentrated flow erosion. The most important inherent soil property is texture, which is the distribution of primary particles (i.e., sand, silt, and clay) in the soil. Increased clay content significantly increases critical shear stress because clay is a bonding agent that increases soil cohesion and soil strength (Smerdon and Beasley, 1959; Foster, 1982). Mechanical soil disturbance (e.g., tillage) is perhaps the most important soil management activity that affects concentrated flow erosion. Typical soils in farm fields are a cohesive mass when the soils have not been recently disturbed. Tillage divides the soil mass into individual soil aggregates that are more easily eroded than soil particles from an undisturbed, cohesive soil mass. After a mechanical soil disturbance, wetting and drying in the presence of clay, organic, and chemical, and other bonding agents reforms a cohesive soil mass. The soil becomes much less susceptible to erosion after tillage over a relatively few months (Foster et al., 1980b, Foster, 1982; Toy et al., 2002).

The degree that tillage affects soil susceptibility to erosion by concentrated flow depends on soil texture. The decrease in critical shear stress caused by tillage is much greater for soils high in clay than for soils high in sand. The difference in critical shear stress immediately after tillage is much less among soil textures than when the soil has not been recently disturbed. Soil organic matter, which is a bonding agent, interacts with soil texture to affect erosion by concentrated flow (Toy et al., 2002). The effect of organic matter is less in high sand soils than in other soils. Soil organic matter is affected by crop type, production level, incorporation of crop residue into the soil, and degree of soil disturbance.

Aggregate size left by a mechanical soil disturbance affects the soil's critical shear stress. Primary tillage implements like moldboard plows, chisel plows, and heavy disks leave an aggregate size mixture that range from small aggregates to relatively large clods. Secondary tillage implements used after primary tillage to create a seedbed leave a relatively uniform mixture of small aggregates. Such finely tilled soils are easily eroded (Foster et al., 1980b; Foster, 1982).

Small aggregates fill the voids between the large aggregates (clods). Even though small aggregates are easily eroded, large aggregates act as grade control structure to control erosion. The susceptibility of tilled soil to erosion depends on the presence of large, erosion resistant clods. The surface soil layer tilled with secondary tillage implements is much more erodible than the underlying soil left by primary tillage that creates large, erosion-resistant aggregates. The top of the primary tilled sub layer illustrated in Figure 12 acts as a non-erodible layer even though the layer includes pockets of easily eroded small aggregates. Consequently, ephemeral gullies tend to be wide and shallow on fields where erosion occurs soon after secondary tillage. Most of the erosion occurs by channel widening rather than by channel incisement.

In contrast, ephemeral gullies tend to be narrow and incised on fields such as those in no-till cropping and pasture where tillage does not often occur. The dominant form of concentrated flow erosion is by headcuts/steep chutes advancing upstream. The lack of a non-erodible layer causes the difference in channel geometry. Other factors

such as local soil weakness and subsurface flow affect headcut/steep chute development and influence ephemeral gully erosion in these fields.

Storm Timing

Concentrated flow erosion depends on storm timing with respect to soil conditions as affected by environmental conditions and cropping-management activities. Erosion is greatly increased when a storm occurs on a thawing or recently thawed soil, which has increased susceptibility to erosion (Van Klaveren and McCool, 1998). Concentrated flow erosion is greatly reduced when a storm occurs after the soil susceptibility to erosion has greatly decreased over time by wetting and drying and other processes (Toy et al., 2002). Differences in plant materials on the soil surface and in the soil during the year affect both flow erosivity and the soil resistance to erosion (Foster, 1982; Brown et al., 1989; Van Liew and Saxton, 1983). Another effect is temporal variation in hydrologic conditions that affect runoff. For example, runoff tends is greater when soil water content tends to be high in winter and early spring than in summer and early fall because of differences in evapo-transpiration.

6. Requirements for Modeling Ephemeral Gully Erosion for Conservation Planning

General Requirements

Conservation planning objectives for farm fields involve protecting the on-site soil resource for crop production, protecting landscape quality for convenience to farming operations and maintenance of land value, and controlling sediment delivery to prevent excessive off-site sedimentation and to protect off-site water quality. A model to guide conservation planning on farm fields must compute estimates for rill-interrill erosion, deposition, and sediment delivery for the overland flow areas and ephemeral gully erosion, deposition, and sediment yield for concentrated flow areas that deliver runoff and sediment from farm fields. Figures 3 and 13 show typical farm field where these processes are occurring.

The resources required to use the model must be consistent with the value gained from use of the model (Toy et al. 2002). The adequacy of a model is judged on the basis of the quality of the conservation planning decisions that result from use of the model. If two models result in the same conservation planning decision, then both models perform equally well and the chosen model is the one that is easiest to use, requires the least resources, or has other user preferred attributes. A well constructed empirical model often out performs a well constructed process-based model (Tiwari et al., 2000). An accomplished model user can often overcome scientific weaknesses in a model, but model misuse usually defeats the best model, including those based on exceptional science. Model science is not always the determining factor in selecting a model for conservation planning.

Significant improvements in models used for conservation planning on farm fields are needed in cover-management and topographic representation and model structure. In particular, concentrated flow areas must be well represented

Representing Cover-Management

Accurately representing cover-management effects is perhaps the major technical requirement for the model. Cover-management is manipulated to reach conservation planning objectives. Of the major factors (climate, soil, topography, and land use) that

affect erosion and sediment yield from farm fields, cover-management as embodied in land use is the factor that can be changed most easily. Accurate representation of cover-management effects is especially important to the farmer because adopting excessive and unnecessary erosion control treatment based on a model's estimates reduces the farmer's profitability. The cover-management practices chosen as a part of conservation planning for a farm field must be consistent with the farmer's requirements. For example, grass prevents erosion, but growing grass is not acceptable unless the farmer makes a profit from the practice. Many variables and complex interactions are involved in cover-management's effects on runoff, erosion, deposition, and sediment delivery. The effects vary with location, soil, and topography in ways that are not well represented in current conservation planning models, especially for concentrated flow.

Model Structure and Topographic Representation

The adequacy of a conservation planning model depends on the combination of model structure and topographic representation. Concentrated flow areas must be represented separately from overland flow areas even though the same processes occur in both rill areas and concentrated flow areas. Although each individual concentrated flow areas can be represented in a typical farm field, the rill areas, which are micro-concentrated flow areas, are far too numerous to represent each rill area individually. A typical rill area can be chosen to represent a set of rill areas. Rill and interrill sub-areas on the overland flow area must be represented separately because of differences in erosion processes. Erosion on interrill areas is primarily by raindrop impact while erosion on rill areas is primarily by surface flow. The rill areas collect runoff and sediment from the interrill areas and convey runoff and sediment from the overland flow areas to the concentrated flow areas, which in turn convey the runoff and sediment to the field outlets.

A comparison of concentrated flow paths along uniform and concave profiles illustrates the combined importance of both model structure and topographic representation. A uniform grade terrace channel is an example of a concentrated flow path along a uniform profile. Deposition occurs everywhere along the channel if the terrace is on a sufficiently flat grade. An example of concentrated flow along a concave profile is where the concentrated flow path begins on a relatively steep grade in the upper part of a field as shown in Figure 13. Grade along the concentrated flow path continuously decreases to a relatively flat grade at the field outlet. Deposition occurs on the lower reach of the concave profile if grade is sufficiently flat.

Figure 14 illustrates erosion and deposition in two cases for concentrated flow on a uniform profile. In case 1, sediment delivery from the overland flow area is low, resulting in concentrated flow erosion beyond the location where the flow's shear stress exceeds the soil's critical shear stress. Deposition does not occur anywhere along the concentrated flow path because the sediment load in the concentrated flow area is less than the flow's sediment transport capacity. In case 2, high erosion on the overland flow area causes sediment delivery to the concentrated flow area to be high. Deposition occurs uniformly along the entire length of the concentrated flow area because the incoming sediment load is greater than transport capacity in the concentrated flow area.

Figure 15 illustrates concentrated flow along a concave profile. In case 1, erosion occurs in the upper reach of the concentrated flow area where the flow's shear stress exceeds the soil's critical shear stress and sediment load is low. Erosion increases and

then decreases along the concentrated flow path, reflecting the combination of an increasing flow rate and a decreasing grade along the channel. Deposition occurs in the lower reach of the channel, beginning where sediment load equals transport capacity. Transport capacity increases and then decreases along the concentrated flow area, also reflecting the combination of an increasing flow rate and a decreasing grade along the channel. Case 2 is like case 1, except that deposition begins at a shorter distance down the concentrated flow path because of the increased sediment load coming into the concentrated flow area. To describe the differences for the concave and uniform profiles, the model structure must represent separately sediment inflow to the concentrated flow area and erosion, deposition, transport capacity, and sediment load along the concentrated flow path. The effects illustrated in Figures 13, 14, and 15 can be described using the fundamental principle that deposition occurs where sediment load exceeds transport capacity, a principle that applies to interrill, rill, and concentrated flow areas (Foster and Meyer, 1975; Foster, 1982; Toy et al., 2002). The model must also represent the spatial variability in steepness along the flow path. A model can have superb process-based deposition equations, but the model will not correctly compute deposition on a concave profile that is represented with a uniform grade channel.

Input Topographic Data

Not only must the model represent topographic variability, the input topographic data to the model must have sufficient detail and resolution. The accuracy with which overland flow and concentrated flow areas can be defined depends on the resolution and scale of the topographic data. Actual field overland flow path lengths are often much shorter than are assumed based on commonly available topographic maps. For example, a typical overland flow path length is about 50 m whereas overland path lengths as long as 1000 m are sometimes used in erosion models. The input topographic data must also accurately represent steepness along flow paths such as the concave profiles represented in Figures 13 and 15. Deposition is greatly affected by steepness over a relatively short distance of no more than 5 m, which is much less than the 30 m resolution of commonly used topographic data. For example, RUSLE2 computes 15.0 Mg/ha for the overland flow profile in Table 1 when three segments are used to represent the last 13.7 m of the profile (Foster, 2004). The computed sediment yield is 26.8 Mg/ha when a single segment is used to represent the last 13.7 m of the profile. This difference illustrates how poor representation of topographic variability causes large errors, even in models that represent erosion and deposition processes in great detail. Similar errors occur when topographic data with insufficient detail and resolutions are used to represent convex shaped profiles. The model should also represent convergence and divergence of overland flow in the plan view.

Spatial and Temporal Variability

A model used for conservation planning can represent spatial variability in soil, topography, and cover-management by "routing" the runoff and sediment through a flow system that represents interrill, rill, and concentrated flow areas. Routing is the numerical solution of the governing equations along the flow path by stepping through the equations, starting at the origin of overland flow. Similarly, the model must step through time to represent temporal changes in storms, soil, and land use conditions. The model must represent temporal conditions through the year and over a crop rotation because both runoff and erosion processes vary greatly as cover-management changes.

Also, the temporal distribution of erosive rains interacts with the temporal distribution of cover-management conditions to greatly affect runoff and erosion processes on overland flow areas. Temporal variations in storms and susceptibility to erosion are especially important for concentrated flow areas. For example, soil is much more susceptible to erosion by concentrated flow immediately after tillage or soon after a late winter thaw than in late fall after several months have elapsed since the last soil disturbance. Also, the influence of a non-erodible layer requires that the model describe a sequence of storms in relation to how previous storms have affected eroded channel width. Representing the presence or absence of a non-erodible layer is a critically important part of the model. A shallow non-erodible soil layer, which is present because of tillage or natural occurrence, greatly influences channel geometry and erosion rate. Widening of the channel by channel sidewall erosion is the principal erosion process when a non-erodible layer is present. Non-erodible layers, which occur most frequently in fields that are routinely tilled, may not be present in fields not regularly tilled such as pasture, hay, and no-till cropped lands. In those fields, the dominant concentrated flow erosion process is erosion by headcuts that move up the concentrated flow areas. Most of the erosion may be from a single headcut or multiple headcuts moving upstream.

Hydrology

Accurately representing the hydrology of farm fields is required to accurately estimate how soil, topography, and land use affect erosion, deposition, and sediment load on both overland and concentrated flow areas. Erosion on overland flow areas can be estimated without explicitly representing runoff, but estimates of runoff amount and rate are needed to compute deposition on overland flow areas and both erosion and deposition on concentrated flow areas. A major hydrologic requirement for the model is that it accurately estimates how inherent soil properties (e.g., texture) and cover-management affect infiltration and surface hydraulic roughness as conditions change through time.

When applied to some fields, the model must represent subsurface flow through the soil, especially when a shallow impermeable layer occurs within about 200 mm of the surface and the surface soil is coarse textured or has many macro-pores. Water flowing through the soil along the surface of the impermeable layer increases soil moisture at low elevations in a field. Increased soil moisture increases rill-interrill erosion and significantly increases the likelihood of ephemeral gully erosion (Huang and Laflen, 1996).

Flow Hydraulics

Flow hydraulics is extremely important for computing deposition where vegetation slows runoff on both overland and concentrated flow areas. Flow erosivity is directly related to flow rate and slope of the energy gradeline (Foster et al., 1980a). Although slope of the energy gradeline is often assumed to equal land steepness or channel grade, the two can greatly differ. For example, the local slope of the energy grade line can be much steeper than the channel grade where flow accelerates as it approaches a sharp drop in the channel bottom. Examples include a locally steep chute, headcut, or a terrace channel discharging into a main collection channel, and a concentrated flow area at a field edge discharging into a deep drainage ditch. Concentrated flow erosion, including a headcut, is likely where the slope of the energy gradeline is steep. Conversely, the slope of the energy gradeline can be much less than the land steepness or channel grade where an obstruction such as a ridge or dense

vegetation retards the flow to create backwater, which often occurs at field edges. Deposition is likely where the slope of the energy gradeline is low and the incoming sediment load is high.

Flow hydraulics in the model must represent how crop residue, rock, other materials on the soil surface and buried in the soil, and live and dead roots in the soil affect the forces applied to the soil by concentrated flow. These materials decrease the forces applied to the soil by flow provided the materials are not moved by the flow. One representation of this effect is to divide the flow's total shear stress into the part acting on these materials on and in the soil (i.e., form roughness) and the part acting on the soil (i.e., grain roughness). The part acting on the soil is assumed to be responsible for erosion and sediment transport (Foster et al., 1980a; Foster, 1982).

In addition to inputs for flow hydraulics, information on sediment characteristics are required to compute sediment transport capacity and deposition. The soils in most farm fields are cohesive, which results in sediment being eroded as a mixture of primary particles and aggregates (Foster et al., 1985). Aggregates are conglomerates of primary particles (i.e., sand, silt, and clay) where the diameters of the aggregates are much larger than the diameter of the primary particles. Conversely, the density of the aggregates is less than the density of the primary particles. Deposition is a highly selective process such that large and dense sediment particles are deposited first leaving the sediment load enriched in fine and less dense particles. The model must compute this enrichment of fines because downstream sedimentation and water quality impacts are directly related to the characteristics of sediment leaving farm fields.

7. Summary

Two distinct flow areas exist in most farm fields. One flow area is the overland flow area where both rill and interrill flow sub areas occur. Rill flow areas are composed of many micro-flow concentrations where the flow is directly downslope. Erosion in rill areas is by flow, which creates small eroded channels that are obliterated by routine tillage. The interrill flow areas lay between the rill flow areas. Flow on these areas is essentially broad sheet flow where erosion is principally by raindrop impact. Runoff on the interrill areas is lateral to the rill areas, which collect runoff and sediment and convey it downslope on the overland flow areas. Micro-topography created by tillage marks determines the pattern of rill flow areas.

Concentrated flow areas end overland flow paths, collect runoff and sediment from the overland flow areas, and convey the flow and sediment to the edge of fields. Macro-topography determines the location of concentrated flow areas. Unlike classical gullies, concentrated flow areas within fields can be crossed with farm equipment and filled by tillage operations. Unlike rills that are reformed in new locations, ephemeral gullies, which occur in concentrated flow areas in farm fields, are reformed each time in the same location. Major amounts of erosion and deposition can occur in the concentrated flow areas, which are not often considered in hydrologic and erosion/sediment delivery models applied to farm fields. Ephemeral gully erosion degrades the landscape by decreasing crop production, inconveniencing farming operations, and reducing land value.

Tillage greatly increases the susceptibility of the soil to erosion by concentrated flow. Soil susceptibility to erosion immediately after tillage for seedbed preparation is very high, but the soil becomes resistant to erosion over the next few months as the soil experiences wetting and drying and other processes. Soil can also be highly susceptible to erosion by concentrated flow during and immediately after thawing. Untilled soil is often quite resistant to erosion by concentrated flow. Consequently, untilled soil acts as a non-erodible layer, which produces ephemeral gullies that are wide shallow channels. These channels are primarily eroded by erosion of the channel sidewall. In contrast, ephemeral gullies in fields that are not regularly tilled tend to be narrow and incised. Erosion by headcuts moving up concentrated flow areas is the dominant erosion process.

The usual conservation planning objective is to prevent ephemeral gully erosion. Practices are available that control ephemeral gully erosion, but many of these practices have drawbacks that are objectionable to farmers. Conservative tillage and other cover-management practices can greatly reduce ephemeral gully erosion.

Models are needed for conservation planning for the whole field that considers rill-interrill erosion and deposition on the overland flow areas and erosion and deposition in the concentrated flow areas. These models are used to guide land management decisions that protect the landscape from degradation by excessive erosion and that control the sediment that impact downstream water quality and water conveyance and storage structures. These models must consider topographic variability in greater detail than is usually considered and input topographic data must be on a much increased resolution. A major need is topographic data on a significantly finer resolution than the common 30 m grid. Also, these models need to represent the concentrated flow system in farm fields separate from overland flow areas. Without these improvements, typical watershed runoff, erosion, and sediment delivery models based on a grid or similar system will continue to produce erosion and sediment yield estimates for farm fields that are easily in error by a factor of two.

References

Brown, L.C., G.R. Foster, and D.B. Beasley. 1989. Rill erosion as affected by incorporated crop residue and seasonal consolidation. Transactions of American Society of Agricultural Engineers 32:1967-1978, 1979.

Foster, G.R. 2004. User's Reference Guide for Revised Universal Soil Loss Equation, Version 2 (RUSLE2). Unpublished Report. National Sedimentation Laboratory, USDA-Agricultrual Research Service, Oxford, Mississippi.

Foster, G.R. 1982. Modeling the erosion process. Chapter 8. *In:* Hydrologic Modeling of Small Watersheds. C.T. Haan, H.P. Johnson, D.L. Brakensiek, eds. American Society of Agricultural Engineers. St. Joseph, MI. pp. 297-382.

Foster, G.R. 1985. Understanding ephemeral gully erosion (concentrated flow erosion). *In:* Soil Conservation, Assessing the National Resources Inventory. National Academy Press. Washington, D.C. pp. 90-125.

Foster, G.R. L.F. Huggins, and L.D. Meyer. 1984. A Laboratory study of rill hydraulics: II. shear stress relationships. Transactions of the American Society of Agricultural Engineers 37:797-804.

Foster, G.R. and L.J. Lane. 1983. Erosion by concentrated flow in farm fields. *In:* Proceedings of the D.B. Simons Symposium on Erosion and Sedimentation. Colorado State University, Ft. Collins. pp. 9.65-9.82.

Foster, G.R. L.J. Lane, J.D. Nowlin, J.M. Laflen, and R.A. Young. 1980a. A model to estimate sediment yield from field sized areas: Development of model. *In:* CREAMS - a field scale model for Chemicals, Runoff, and Erosion from Agricultural Management Systems. Vol. I: Model Documentation. Conservation Research Report No. 26. USDA-Science and Education Administration. pp. 36-64.

Foster, G.R., L.J. Lane, and J.D. Nowlin. 1980b. A model to estimate sediment yield from field sized areas: Selection of parameter values. *In:* CREAMS - a field scale model for Chemicals, Runoff, and Erosion from Agricultural Management Systems. Vol. II: User Manual. USDA-Conservation Research Report No. 26. USDA-Science and Education Administration. pp. 193-281.

Foster, G.R., L.J. Lane, J.D. Nowlin, J.M. Laflen, and R.A. Young. 1981. Estimating erosion and sediment yield on field sized areas. Transactions of the American Society of Agricultural Engineers 24:1253-1262.

Foster, G.R. and L.D. Meyer. 1975. Mathematical simulation of upland erosion by fundamental erosion mechanics. *In:* Present and Prospective Technology for Predicting Sediment Yields and Sources. ARS-S-40 USDA-Science and Education Administration. pp. 190-204.

Foster, G.R., R.A. Young, and W.H. Neibling. 1985. Sediment composition for nonpoint source pollution analyses. Transactions of the American Society of Agricultural Engineers 28:133-139, 146.

Huang, C. and J.M. Laflen. 1996. Seepage and soil erosion for a clay loam soil. Soil Sci. Soc. Am. J. 60: 408-416.

Meyer, L.D., G.R. Foster, and M.J.M. Römkens. 1975. Source of soil eroded by water from upland slopes. *In:* Present and Prospective Technology for Predicting Sediment Yields and Sources. ARS-S-40. USDA-Science and Education Administration. pp. 177-189.

Renard, K.G., G.R. Foster, G.A. Weesies, D.K. McCool, and D.C. Yoder. 1997. Predicting soil erosion by water: A guide to conservation planning with the Revised Universal Soil Loss Equation (RUSLE). U.S. Dept. of Agriculture, Agricultural Handbook 703, U.S. Govt Printing Office, Washington, D.C. 384 pp.

Skaggs, R.W., A Nassehzadeh-Tabrizi, and G.R. Foster. 1982. Subsurface drainage effects on erosion. Journal of Soil and Water Conservation 37:167-172.

Smerdon, E.T. and R.P. Beasley. 1959. Tractive force theory applied to stability of open channels in cohesive soils. Research Bulletin No. 715. Agricultrual Experiment Station., University of Missouri, Columbia, MO. 36 pp.

Thomas, A.W., R. Welch, and T.R. Jordan. 1986. Quantifying concentrated-flow erosion on cropland with aerial photogrammetry. Journal of Soil and Water Conservation 41: 249-252.

Toy, T.J., G.R. Foster, and K.G. Renard. 2002. Soil Erosion: Processes, Prediction, Measurement, and Control. John Wiley and Son, New York, NY. 338 pp.

Tiwari, A.K., L.M. Risse, and M.A. 2000. Evaluation of WEPP and its comparison with USLE and RUSLE. Transactions of the American Society of Agricultural Engineers 43:1129-11135.

Van Klaveren, R.W. and D.K. McCool. 1998. Erodibility and critical shear stress of a previously frozen soil. Transactions of the American Society of Agricultural Engineers 41: 1315-1321.

Van Liew, M.W., and K.E. Saxton. 1983. Slope steepness and incorporated residue effects on rill erosion. Transactions of the American Society of Agricultural Engineers 26: 1738-1743.

Table 1. Effect on sediment yield of averaging steepness over lower part of a concave profile for an overland flow path.

Complete profile representation				Using average steepness for last 3 segments			
Segment No.	Steep ness (%)	Distance to lower end of segment (m)	Segment length (m)	Segment No.	Steepn ess (%)	Distance to lower end of segment (m)	Segment length (m)
1	1	4.6	4.6	1	1	4.6	4.6
2	3	9.1	4.6	2	3	9.1	4.6
3	6	13.7	4.6	3	6	13.7	4.6
4	9	18.3	4.6	4	9	18.3	4.6
5	10	22.9	4.6	5	10	22.9	4.6
6	8	27.4	4.5	6	8	27.4	4.5
7	5	32.0	4.6	7	5	32.0	4.6
8	3	36.6	4.6	8	2	45.7	13.7
9	2	41.1	4.5				
10	1	45.7	4.6				
Sediment yield = 15.0 Mg/ha				Sediment yield = 26.8 Mg/ha			

List of Figures

Figure 1. Rilling pattern on different parts of a typical landscape. Source: Toy et al., 2002.

Figure 2. Classical gully with headcuts advancing up concentrated flow areas.

Figure 3. Ephemeral gully farmed across in farm field. Source: Toy et al., 2002.

Figure 4. Effect of off-contour tillage on overland flow directions and ephemeral gully erosion.

Figure 5. Figure 5. Effect of on-contour tillage on overland flow directions and ephemeral gully erosion.

Figure 6. Parallel tile outlet terrace system.

Figure 7. Multiple headcuts in a small concentrated flow area about 150 mm wide.

Figure 8. Deeply incised rills not affected by a non-erodible layer.

Figure 9. Equilibrium channel moving downward in soil where a non-erodible layer is not present.

Figure 10. Effect of non-erodible layer on erosion rate for a steady flow rate.

Figure 11. Final channel width for a steady flow rate.

Figure 12. Soil layers left by primary and secondary tillage.

Figure 13. Overland flow and concentrated flow areas on a typical farm field.

Figure 14. Erosion, deposition, and sediment load along concentrated flow on a uniform grade.

Figure 15. Erosion, deposition, and sediment load along concentrated flow on a concave profile.

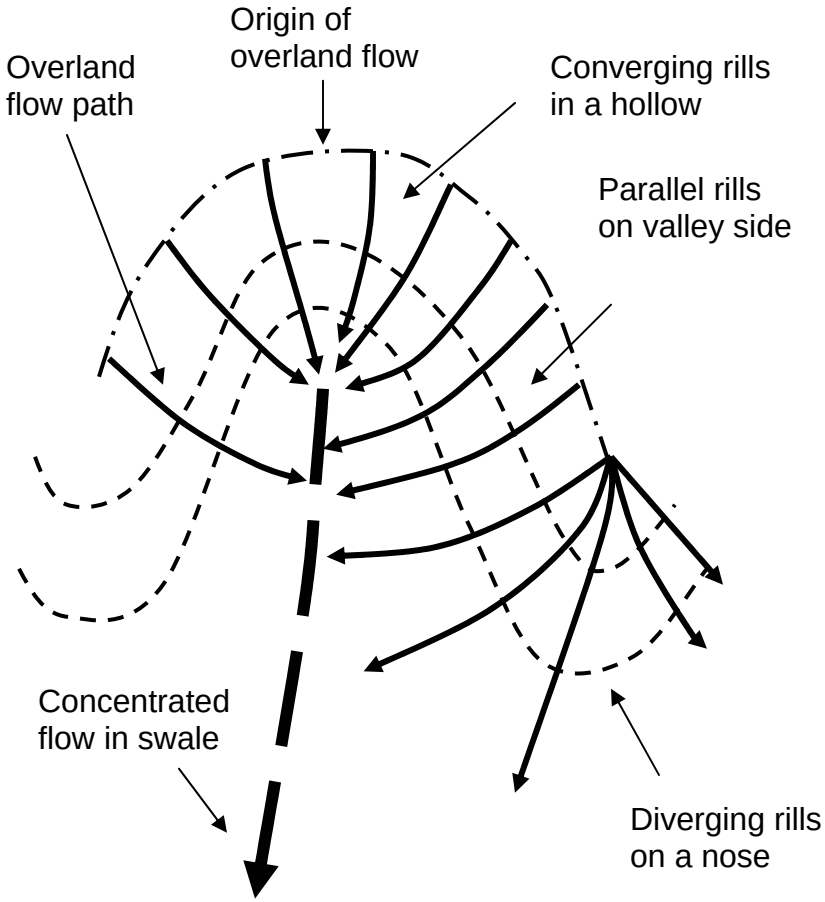

Figure 1. Rilling pattern on different parts of a typical landscape. Source: Toy et al., 2002.

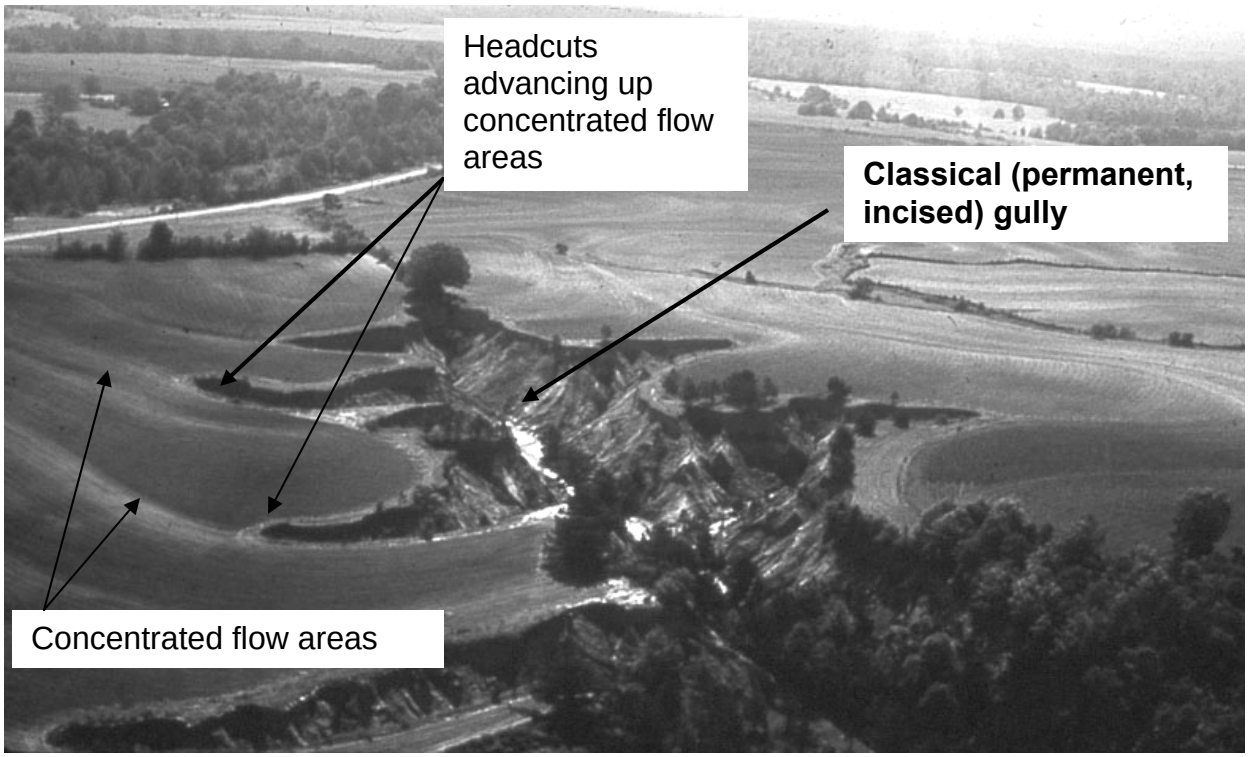

Figure 2. Classical gully with headcuts advancing up concentrated flow areas.

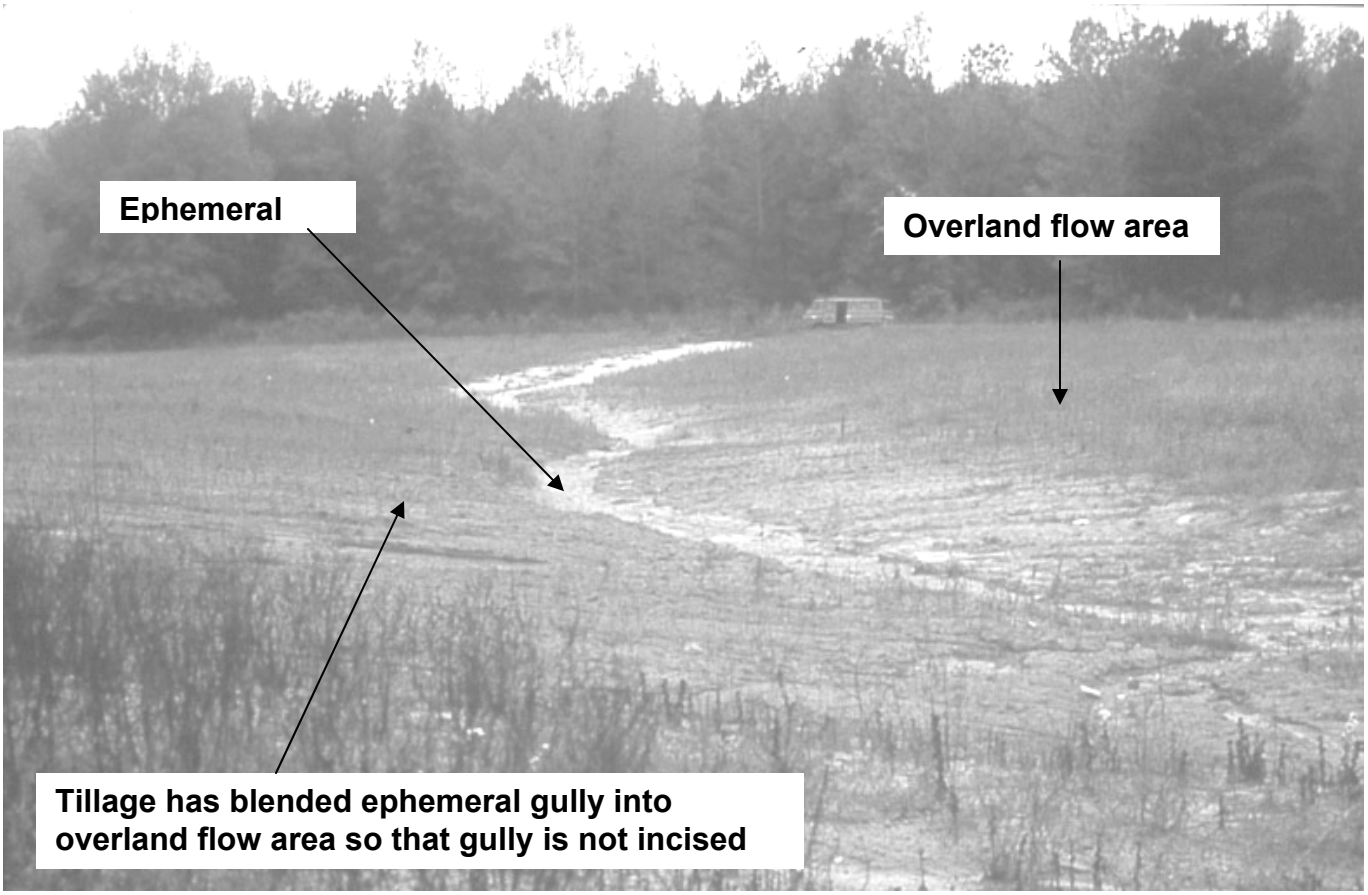

Figure 3. Ephemeral gully that is tilled across in farm field. Source: Toy et al. 2002.

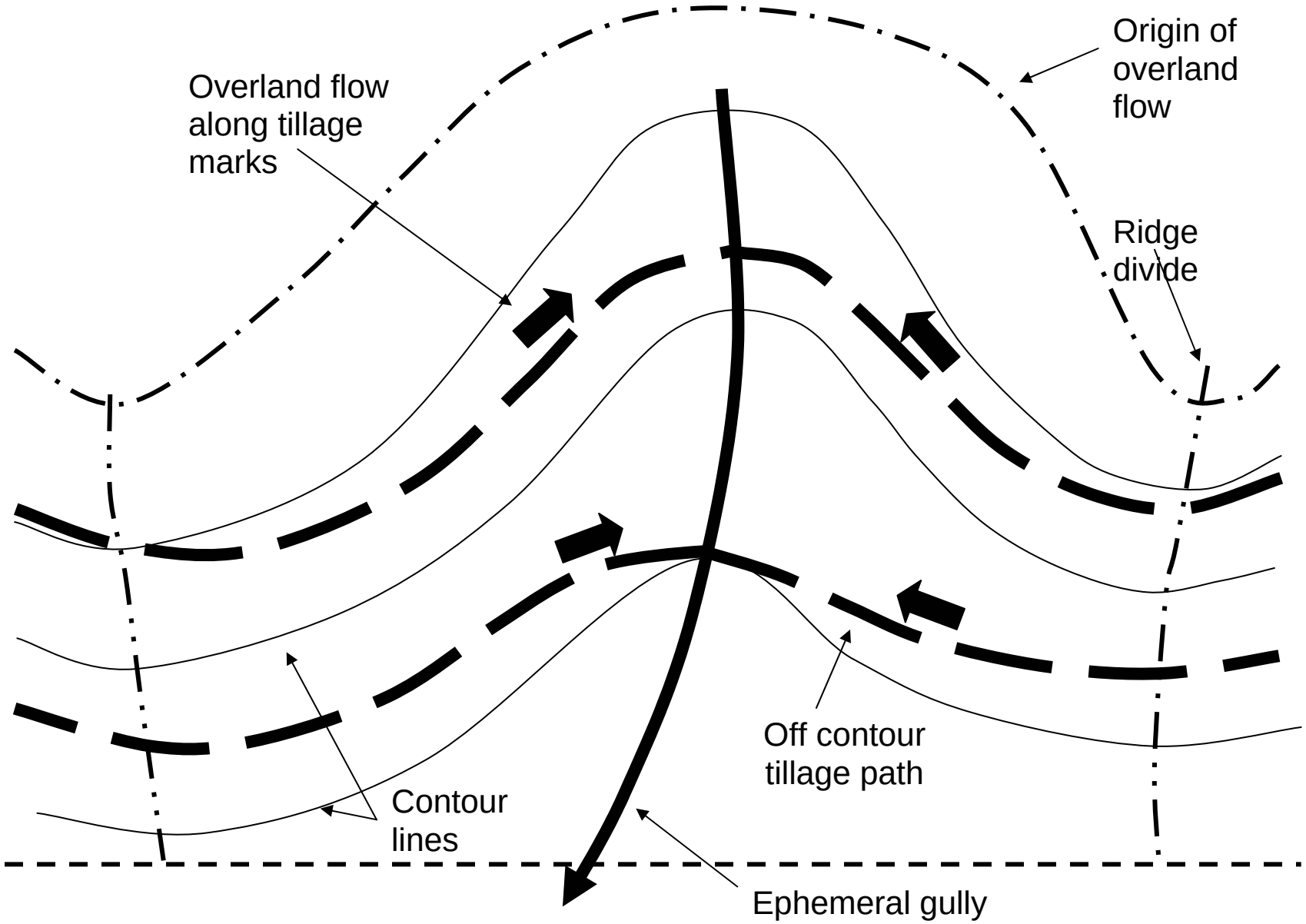

Figure 4. Effect of off-contour tillage on overland flow directions and ephemeral gully erosion.

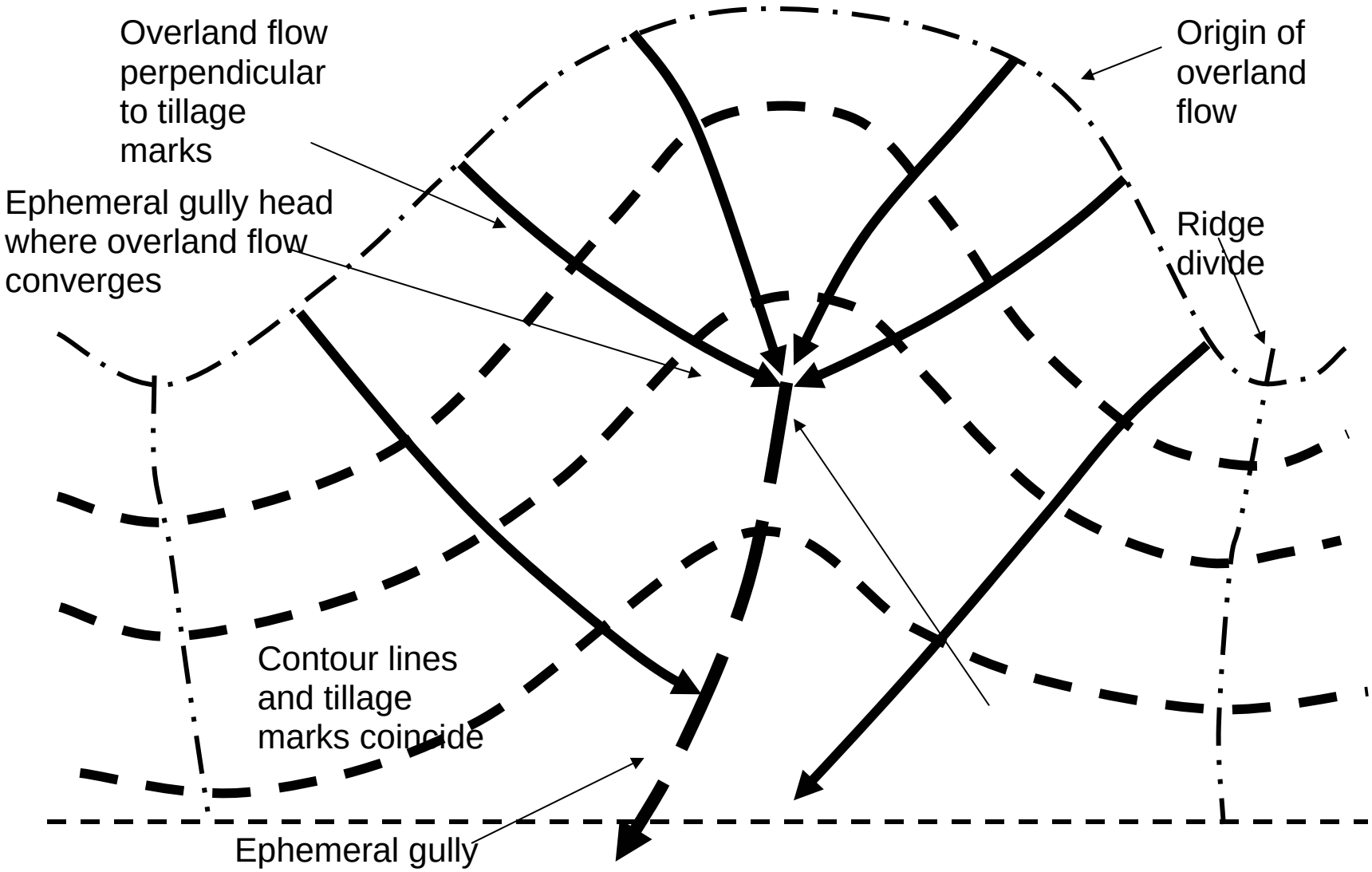

Figure 5. Effect of on-contour tillage on overland flow directions and ephemeral gully erosion.

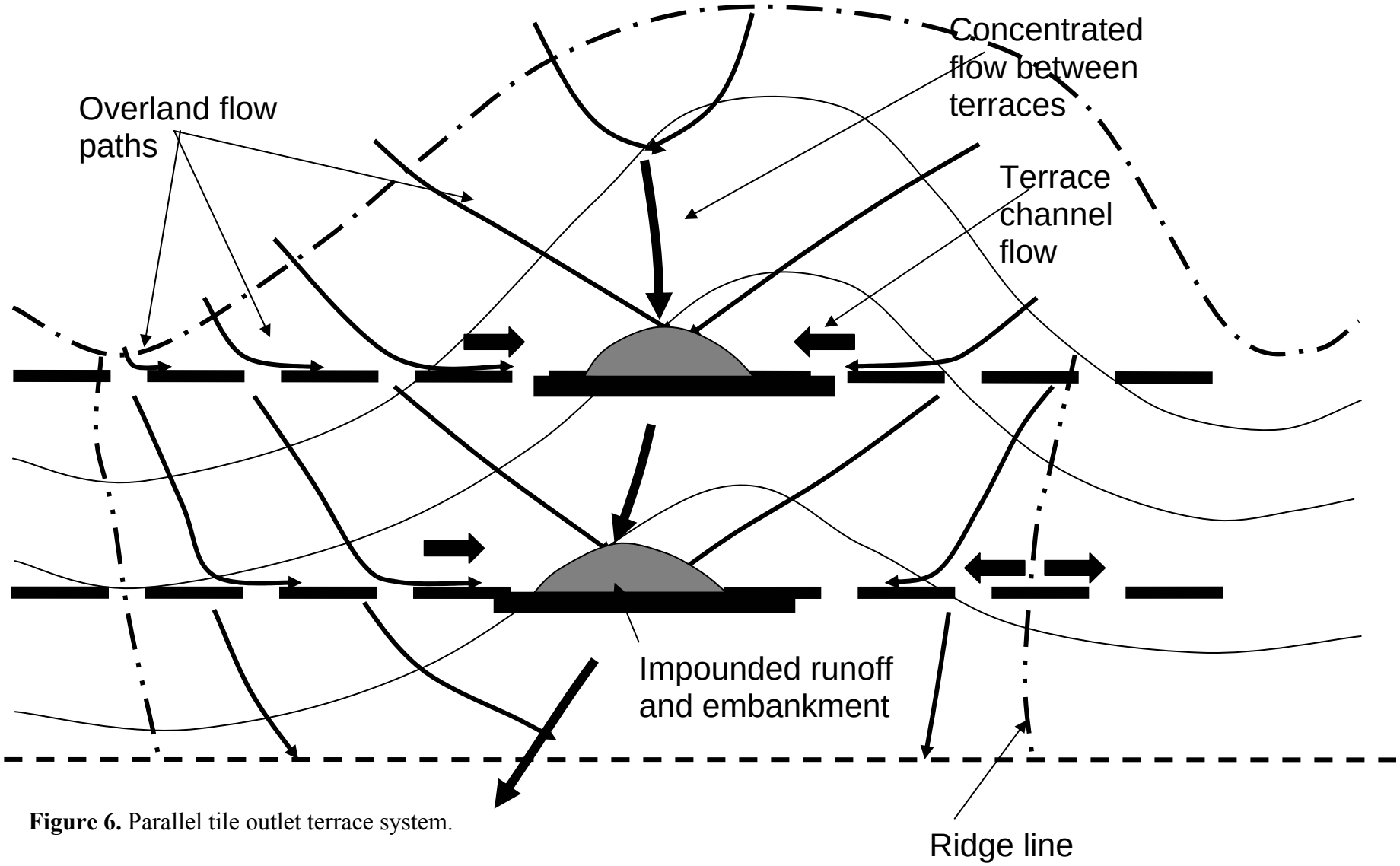

Figure 6. Parallel tile outlet terrace system.

Figure 7. Multiple headcuts in a small concentrated flow area about 150 mm wide.

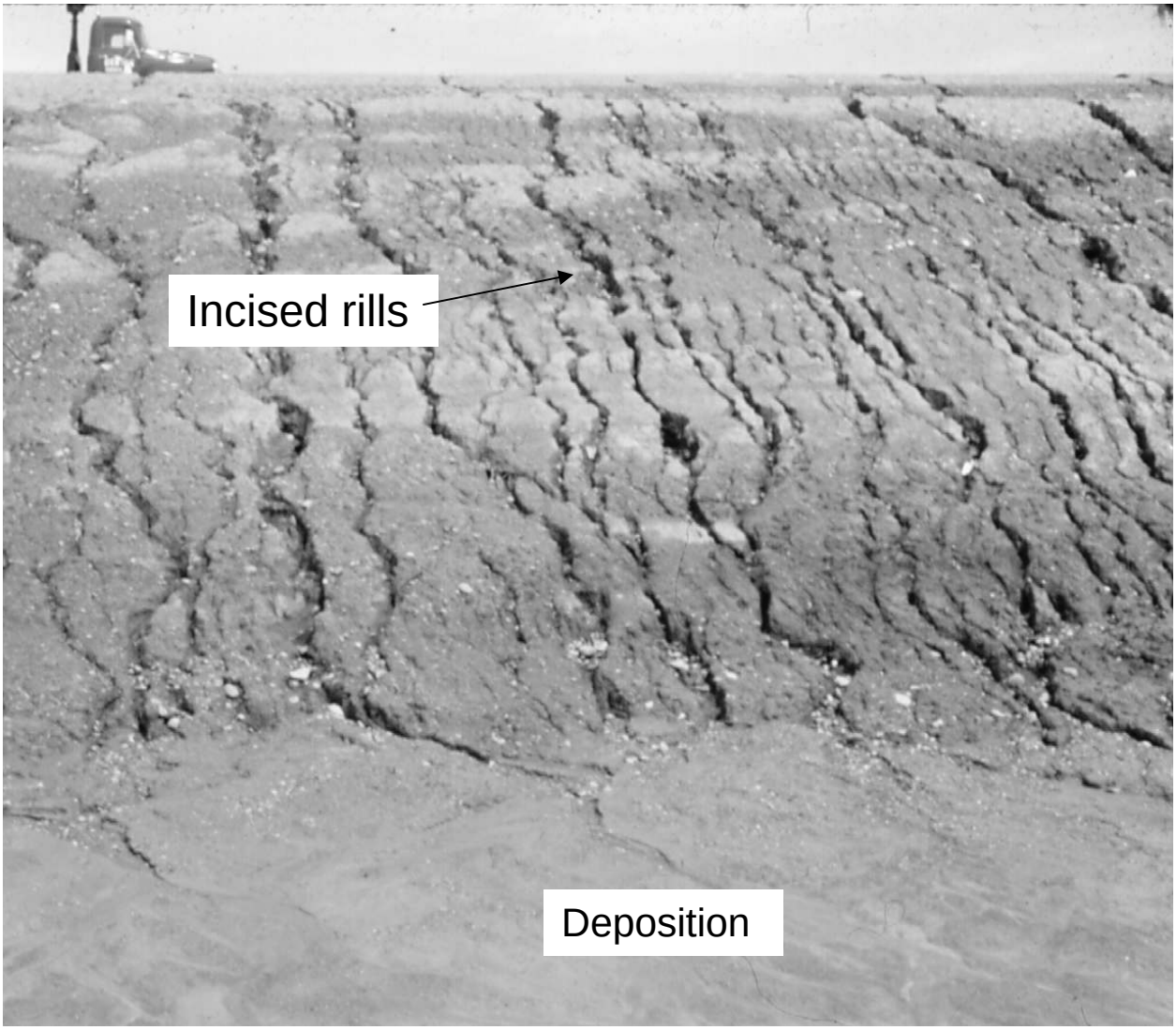

Figure 8. Deeply incised rills not affected by a non-erodible layer.

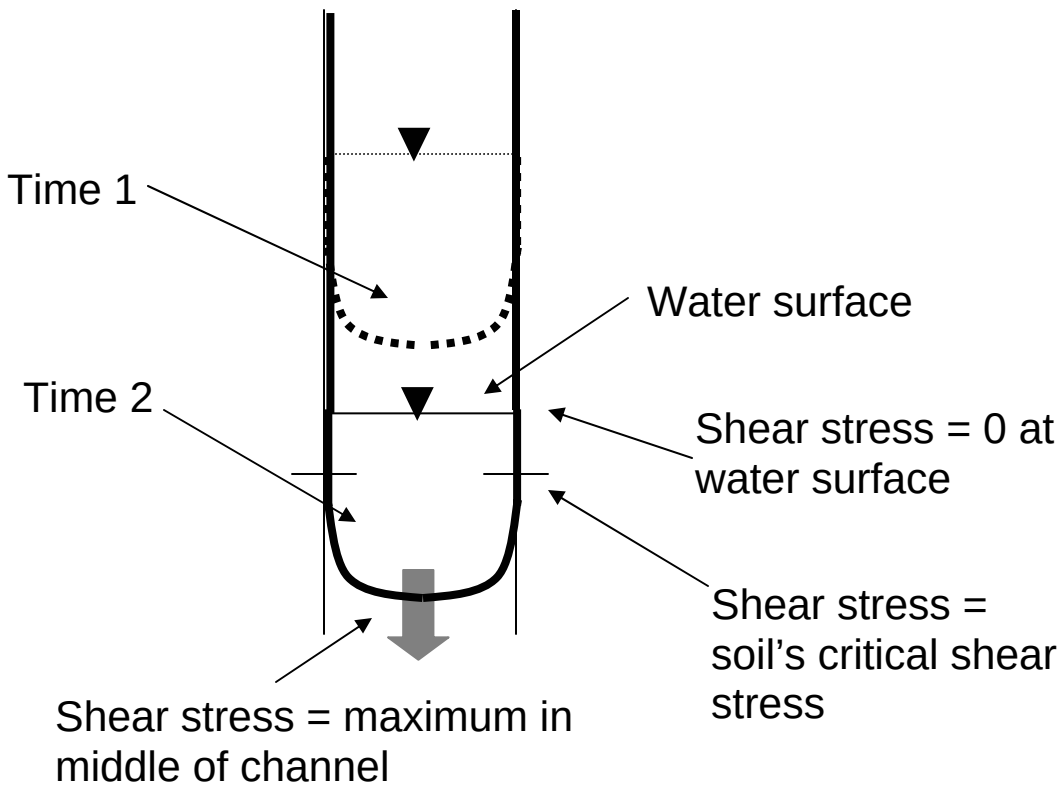

Figure 9. Equilibrium channel moving downward in soil where a non-erodible layer is not present.

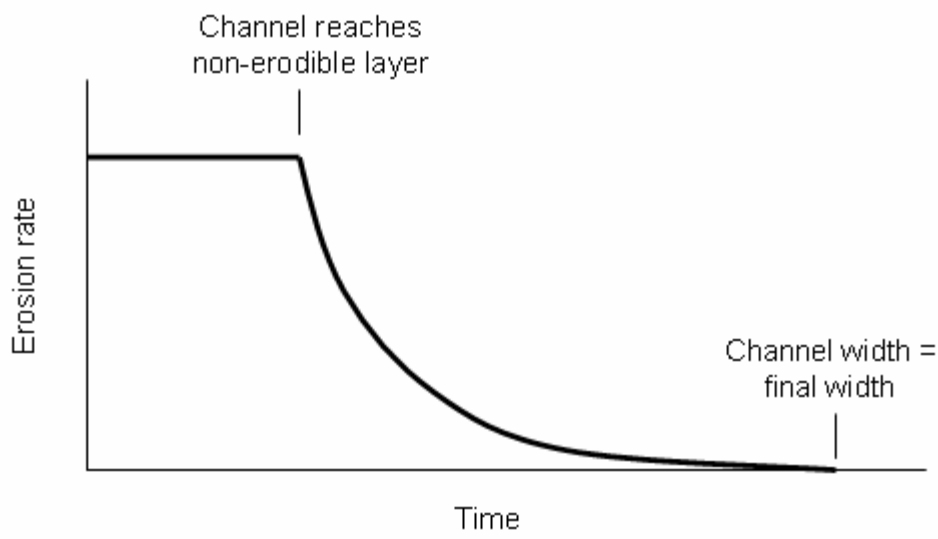

Figure 10. Effect of non-erodible layer on erosion rate for a steady flow rate.

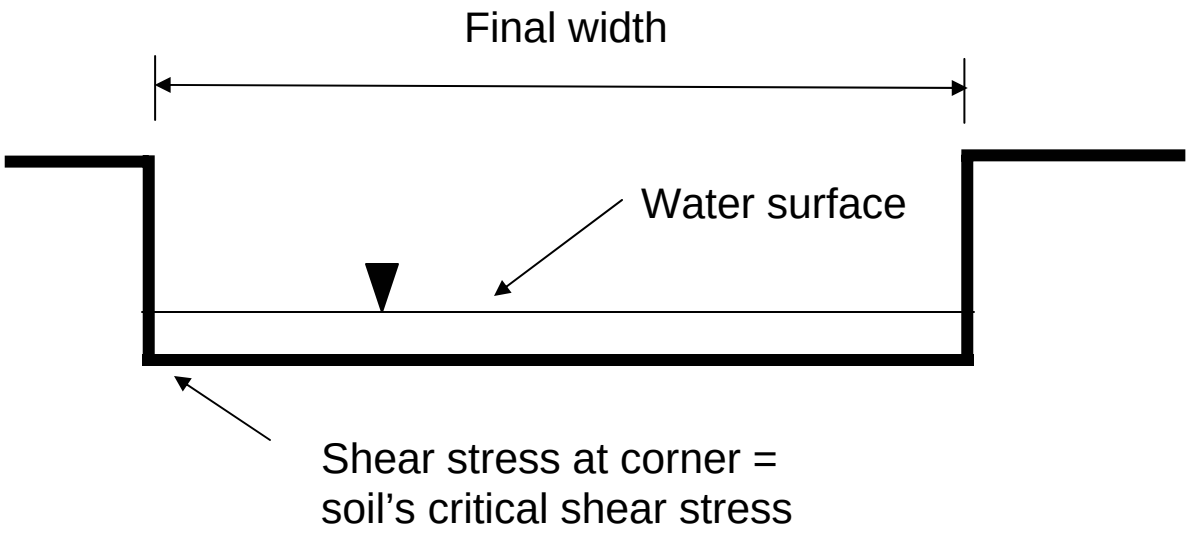

Figure 11. Final channel width for a steady flow rate.

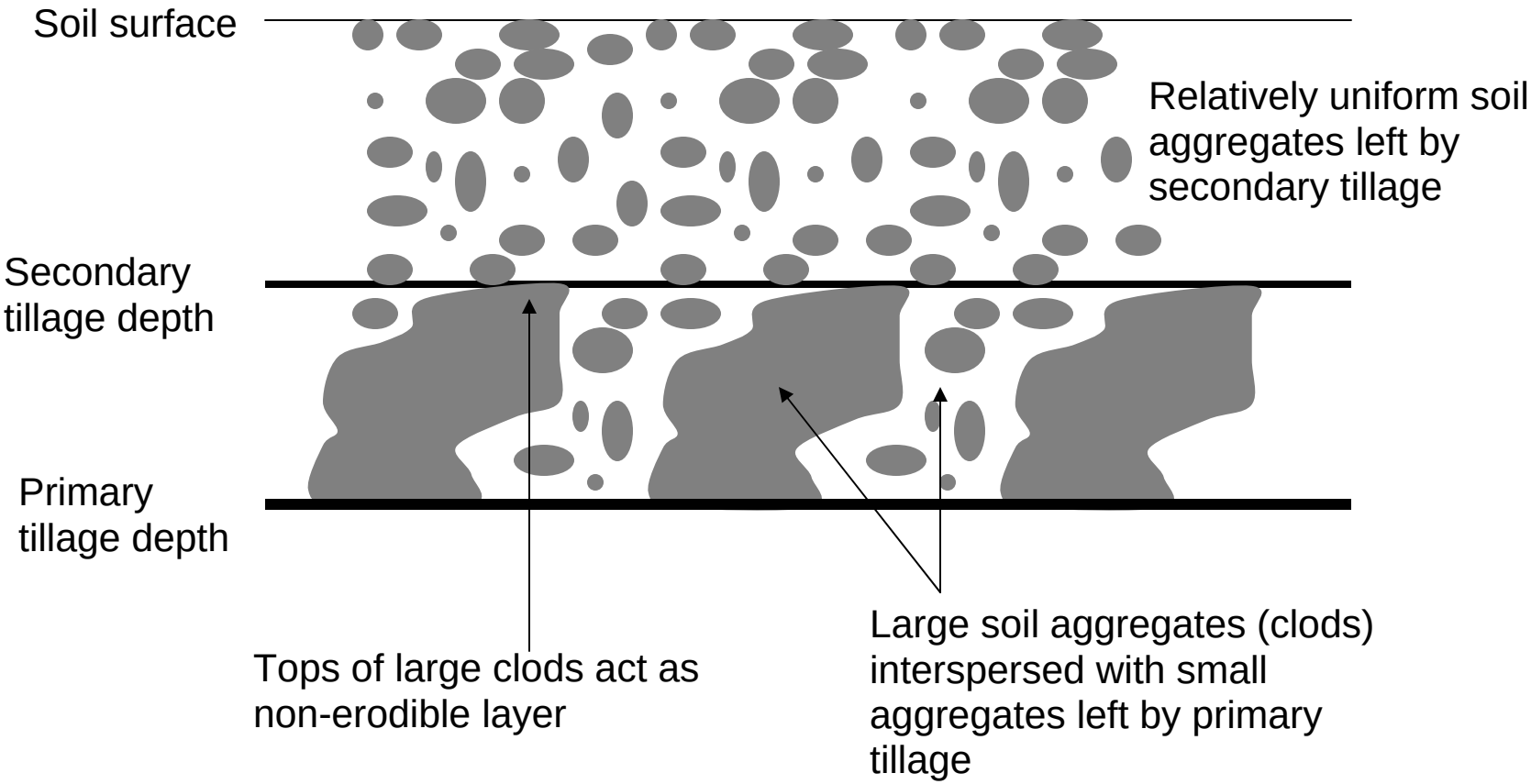

Figure 12. Soil layers left by primary and secondary tillage.

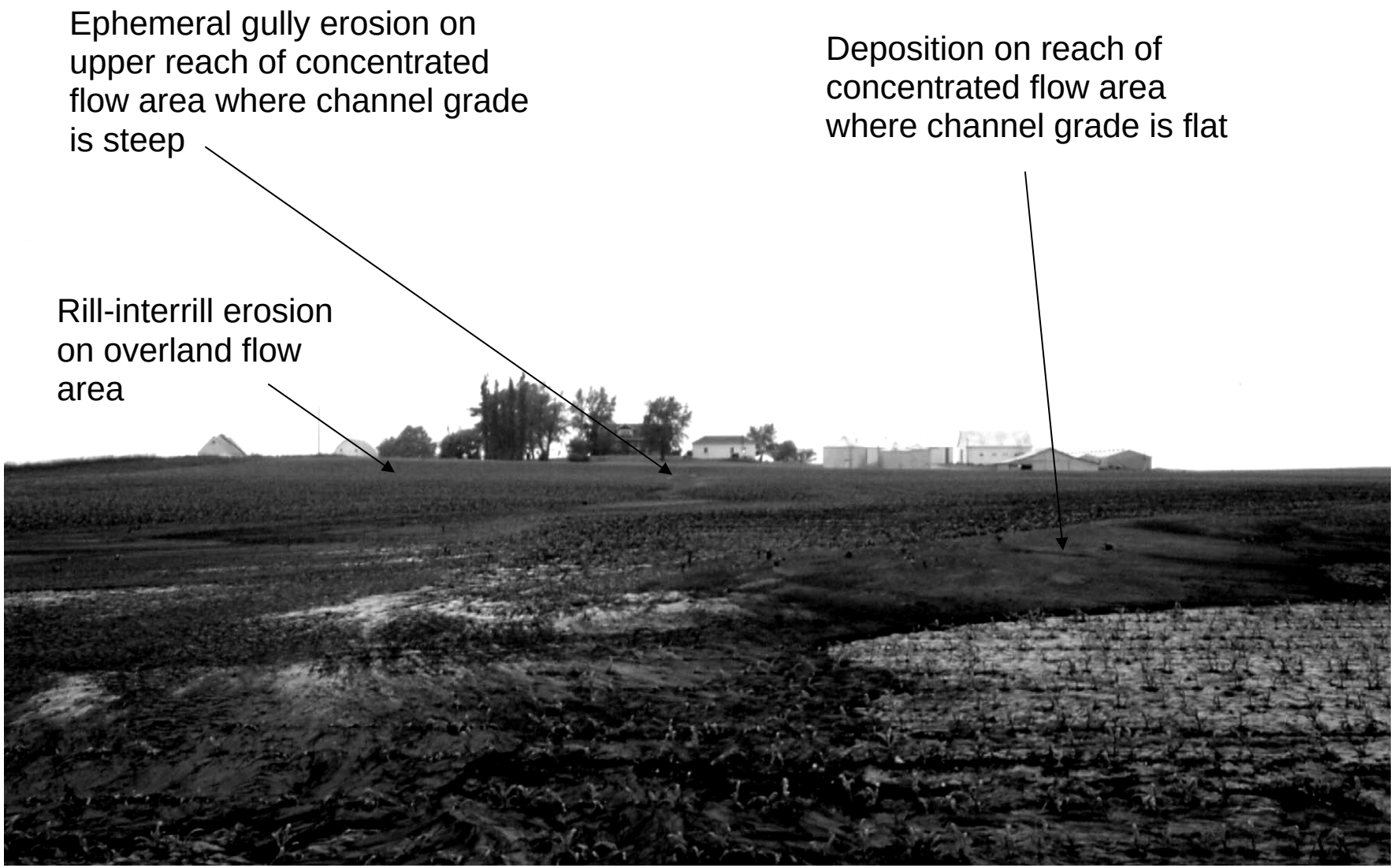

Figure 13. Overland flow and concentrated flow areas on a typical farm field.

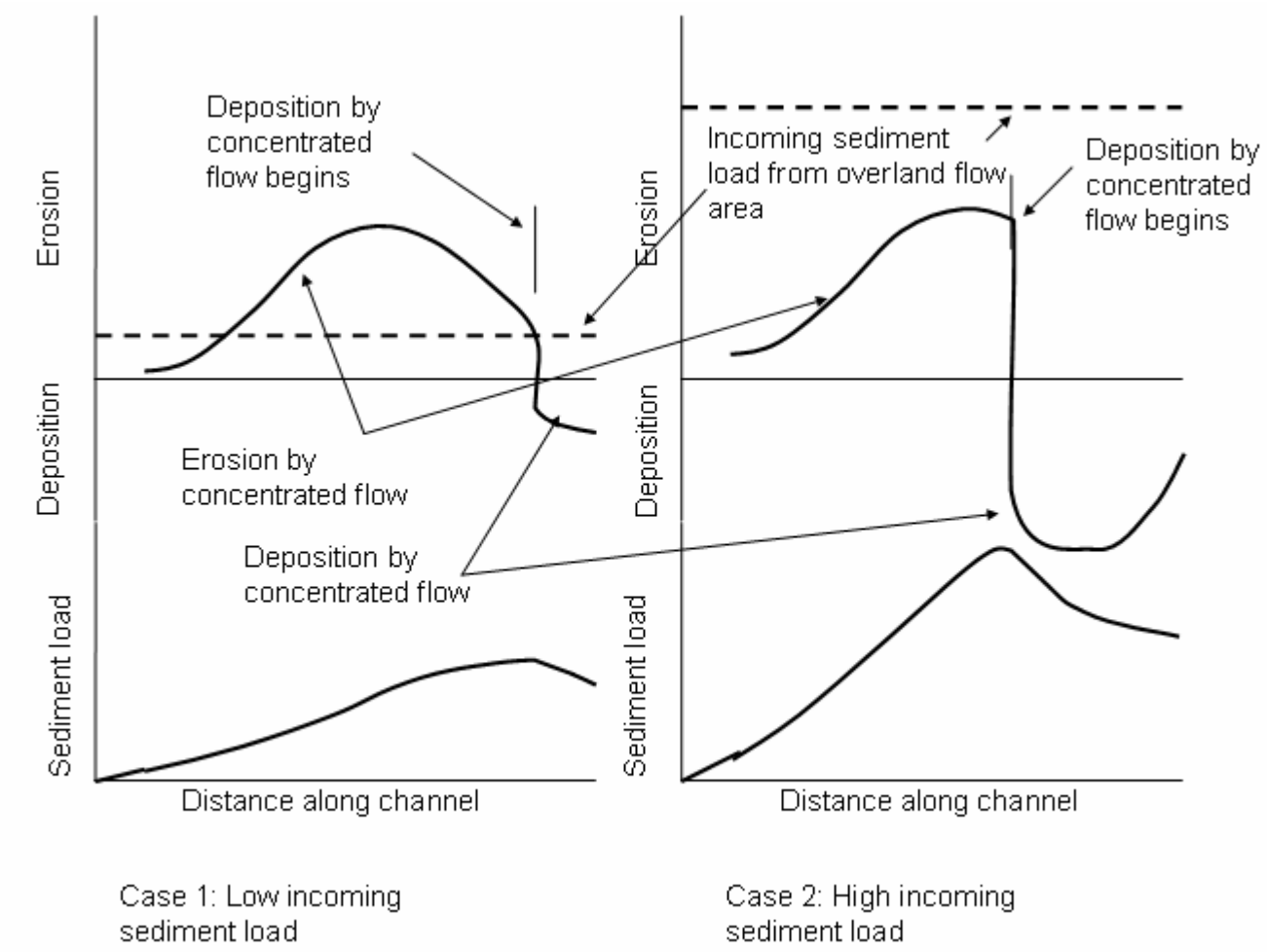

Figure 14. Erosion, deposition, and sediment load along concentrated flow on a uniform grade.

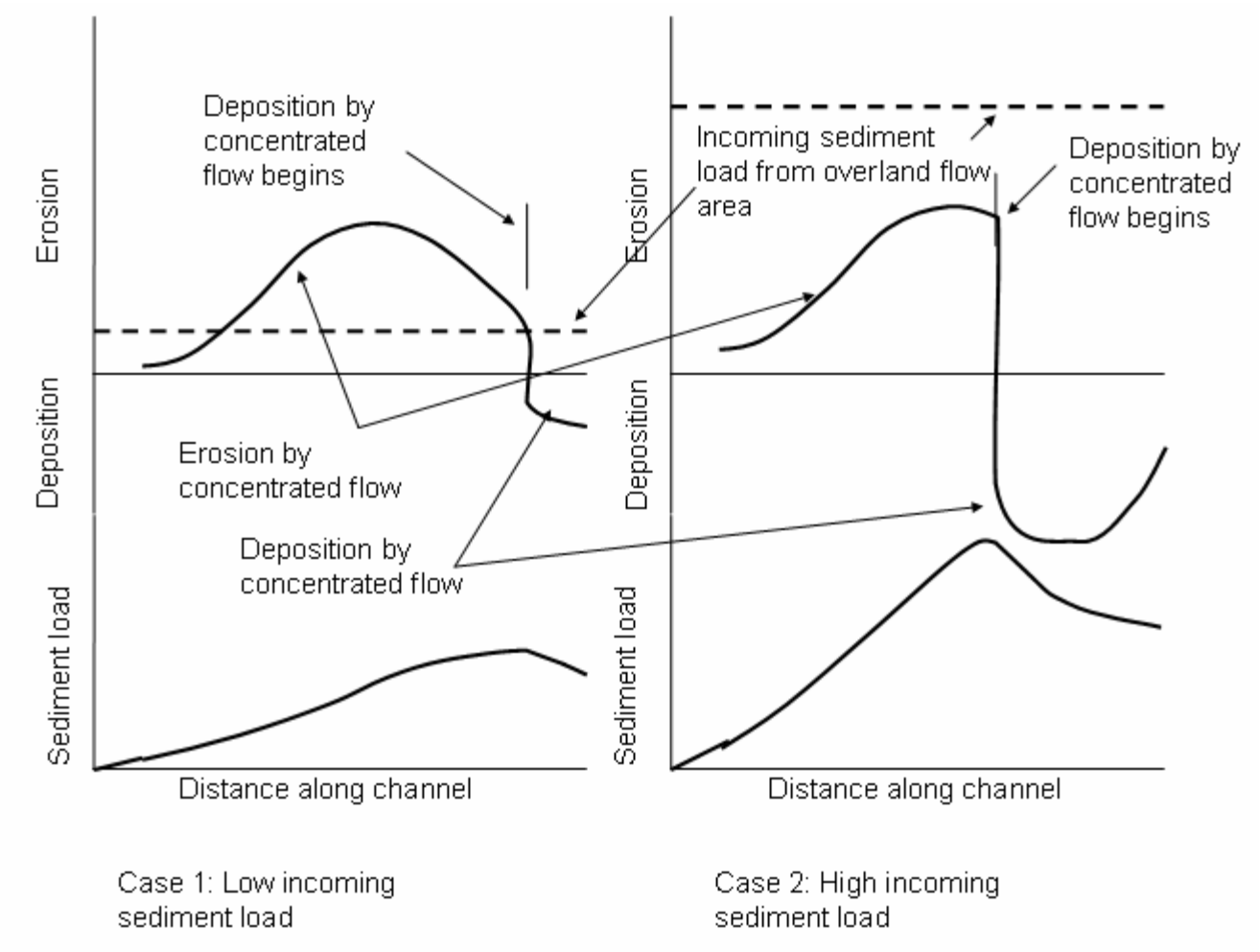

Figure 15. Erosion, deposition, and sediment load along concentrated flow on a concave profile.

The Next Generation of Watershed-scale Erosion Models: Towards a Dynamic, Spatially Adaptive Representation of Rills and Gullies

David Favis-Mortlock*
Queen's University Belfast
School of Geography
Belfast BT7 1NN, Northern Ireland, UK

Paul Van Dijk
Université Louis Pasteur
C.E.R.E.G., 3, rue de l'Argonne
67083 STRASBOURG Cedex, France

Abstract

"The right answer for the wrong reason": this notion has bedevilled results from the present generation of watershed-scale erosion models. For example, the GCTE Soil Erosion Network's evaluation of watershed-scale erosion models (Jetten et al., 1999) found that the models (once calibrated) could do a reasonable job of estimating hydrographs and sedigraphs at the catchment outlet. However, predictions of the source of this eroded material within the catchment were of poor quality.

This limitation of current models notably constrains their usefulness for within-catchment management. Unless sediment source 'hotspots' can be reliably identified, how can they be managed? A future generation of models must do better.

By contrast, recent developments in plot-scale modelling have shown a convincing ability to represent spatial patterns of detachment and deposition, by assuming that within-storm changes of soil-surface microtopography by erosive flows can be modelled as a self-organizing dynamic system (Favis-Mortlock, 2000; in preparation; Favis-Mortlock and De Boer, 2003). But with cell sizes of centimetres or millimetres, computational (and data) constraints mean that this approach cannot be used directly in a watershed-scale model.

An indirect approach may nonetheless be possible. This paper presents a conceptual framework which aims at a spatially inhomogenous representation of rills and gullies. The highest resolution is reserved for the most erosionally active parts of the watershed. This representation also aims to be both dynamic and adaptive, so that the model itself increases spatial resolution during a simulation, but only at those locations where high resolution is necessary to adequately represent erosive flow.

Keywords: erosion model, spatial resolution, self-organization, adaptive mesh

*Correspondence author

Numerical Simulation of Migration of Head-cut with a Two-layered Bed

Yafei Jia* (E-Mail: jia@ncche.olemiss.edu)
The University of Mississippi
National Center for Computational Hydroscience and Engineering
University of Mississippi
University, MS 38677

Tadanori Kitamura (E-mail: tkita@genv.nagoya-u.ac.jp)
Hydraulics & Environmental Engineering
Dept. of Geo- & Environmental Eng
Nagoya University.

Sam S. Y. Wang (E-mail: wang@ncche.olemiss.edu)
The University of Mississippi
National Center for Computational Hydroscience and Engineering

Abstract

Gully erosion is one of the main sources causing top soil loss, land deterioration and deposition downstream. Headcut often occurs in the gully erosion process when erodability of the soil layers varies, and the gully profile cuts through a hard layer at a point. A scouring hole appears downstream of the head cut which migrates upstream due to strong erosion in the scour hole. This paper presents numerical analyses of turbulent flow and sediment transport processes of a head-cut associated with a two-layer soil stratigraphic formation. The flow in the scour hole is three-dimensional induced by the water jet from brink of the top layer; the sediment transport model considers sediment entrainment by the impinging jet, erosion underneath the hard layer and the retreat of the hard layer. The 3D flow simulation in the scour hole and the scouring process is verified with physical model data. The two-layer head cut migration is simulated with different flow and soil parameters, the trends of the simulated results reasonably revealed contributions of these parameters to the scouring and migration process.

Keywords: head-cut migration, impinging jet, numerical simulation, local scour, sediment transport

1. Introduction

The rate of gully erosion is dominated by the upstream migration of existing nick-points called headcut. Due to the shape of the headcut, the flow from upstream channel impinges into the pool of the scour hole and forms complex three-dimensional flow structure. The turbulent flow deepens the scour hole, transports the eroded material downstream, undercuts the headcut wall and creates gravitational slumping of the gully head material. In reality, the occurrence of a head cut is often related to the soil structure: a stable top cohesive soil layer is underplayed by a dispersible non-cohesive subsoil layer. When such two soil layers are present and the headcut is formed, the erosion mechanism on the top and bottom soil layers differs. A scouring hole is

*Corresponding author

formed in the sub-layer in which turbulent fluctuation and flow shear dominate sediment particle entrainment and transport; an overhang of the top-layer will then form at the headcut face when the underlying material is washed away. The subsequent collapses of the overhang into the scour hole advance the headcut migration.

Stein and Julien (1993) investigated the criteria for the above patterns. Robinson (1996) has carried out a series of head-cut experiments in a large-scale flume. Three major categories of experiments were conducted to study the effect of soil property, the effect of a sand layer underlying the soil and the effect of hydraulic condition on the head-cut migration. Soil properties are measured and the soil is compacted in a 29m long flume with fixed bed. No scour hole was formed since the bed of the flume was fixed, and nor the deposition was observed in the lower part of the flume. Bennett (1997) conducted the head-cut experiments with movable bed. The bed near the brink was scoured while the head-cut migrates, and part of the eroded bed material deposited downstream of the scour hole. In these experiments, the shape of the scour hole was approximately unchanged during the migration of the head-cut. This dynamically balanced phenomenon is quit interesting, and it provides important information to understanding of the mechanism of the head-cut.

In this paper, numerical simulations of headcut process using a three dimensional model, CCHE3D, are presented. To ensure the numerical simulation is consistent with the realistic process, two soil layers are considered. The top layer is of cohesive material and the sub-layer is of non-cohesive material. In the computational model, the erosion of sub-layer is resulted from the computed frictional shear and lift of pressure fluctuation due to a flow jet impingement, the erosion of the top cohesive layer is simulated by block slumping due to gravitational force. The jet flow simulation model and the scouring simulation model have been validated using physical model data. The simulation of the headcut process has been performed using a variety of flow and soil parameters. The series of simulation results provide information of parametric sensitivity of the headcut process and illustrate the advantage of using numerical simulation to study erosion processes.

2. Methods and Material

Simulation of Impinging Flow in the Pool of Scour Hole

A finite element based 3D model, CCHE3D, has been applied to simulate the flow in the pool induced by impinging flows and the local scouring process of the plunge pool. This model solves fully three-dimensional, unsteady, Reynolds stress equations and continuity equation. Collocation method has been adopted to make the model efficient as finite difference method. Velocity correction method has been applied to solve the dynamic pressure and enforce the mass conservation.

Figure 1 shows the configuration of the numerical simulation and associated geometric parameters and boundary conditions. The scour hole was formed from an initially flat bed due to an impinging flow and sediment transport. The flow condition, sediment size, and the simulation parameters were set according to the physical model data (Stein and Julien, 1993). The flow simulation capability was validated by using physical model data (Robinson, 1996) of an oblique jet and a fixed flat bed in the plunge pool. The simulated maximum shear stresses on the bed were in agreement with the trend observation (Fig. 2). Figure 3 shows the computed flow field in the plunge pool: the jet was weakened while approaching the bed, and the water flowing along the bed surface in both forward and backward direction of the impinging point, respectively. An eddy appeared between the jet and the end vertical wall behind the jet, and a bigger one in the front.

Sediment Entrainment and Transport Due to Impact of a Plunging Jet

Sediment transport in the scour hole is strongly affected by the impact of the water jet. Particles are entrained near the impingement point and are carried by the flow to a short distance downstream and deposit there. The non-equilibrium sediment transport model of Nakagawa and Tsujimoto (1980) was employed, which considers the mechanism of sediment pick-up, transport and deposition processes. The probability density of step length is given by the following exponential function (Nakagawa and Tsujimoto, 1980):

$$f_S(\xi) = \frac{1}{\Lambda}\exp\left(-\frac{\xi}{\Lambda}\right) \tag{1}$$

where ξ = sediment step length; Λ = mean step length, which is model constant. In a nearly uniform open channel flow, the mean step length is about 100 to 200 times as large as the particle size of bed-material in the case of bed-load. This step length model was developed for quasi-uniform flow, it is only valid partially in the case of the plunge pool. It has to be modified to take the effect of jet impingement into account.

The flow in a scouring hole is highly turbulent with a strong pressure fluctuation due to the impinging jet. The sediment transport functions normally derived for uniform or gradual change flow are no longer valid for this case, because the sediment pick-up mechanism is not dominated only by frictional shear but also by pressure fluctuation (Simons and Stevens, 1971, Liu and Dong, 1998). Sediment pick-up rate formula of Nakagawa and Tsujimoto, (1980) has been modified by adding the lift force due to pressure fluctuation to the frictional shear stress so that both forces contribute to the pick up of sediment particles:

$$p_{\mathrm{Sm}*} = \int_{-\infty}^{\infty} p_{\mathrm{S}*}(\tau_{\mathrm{m}*}, \eta)\psi(\eta)d\eta \tag{2}$$

The mean pick up rate is a function of the pick up rate probability density function and the distribution function of the fluctuating lift force which is assumed to be of normal distribution:

$$\psi(\eta) \equiv \frac{1}{\sqrt{2\pi}}\exp\left(-\frac{\eta^2}{2}\right), \qquad \eta \equiv \frac{L_{\mathrm{p}*}}{\sigma_{\mathrm{Lp}*}} \tag{3}$$

The non-dimensional pick up rate reads:

$$\begin{aligned} p_{\mathrm{S}*}(\tau_{\mathrm{m}*}, L_{P*}) &\equiv \frac{p_{\mathrm{S}}}{\sqrt{(\sigma/\rho - 1)g/d}} \\ &= \begin{cases} F_0(\tau_{\mathrm{m}*} + L_{\mathrm{p}*})\left[1 - \dfrac{k_2\tau_{*\mathrm{c}}}{(\tau_{\mathrm{m}*} + L_{\mathrm{p}*})}\right]^{\mathrm{m}}, & (\tau_{\mathrm{m}*} + L_{\mathrm{p}*} \geq \tau_{*\mathrm{c}}) \\ 0, & (\tau_{\mathrm{m}*} + L_{\mathrm{p}*} < \tau_{*\mathrm{c}}) \end{cases} \end{aligned} \tag{4}$$

where $\tau_{\mathrm{m}*}$ = non-dimensional mean shear stress; $\tau_{*\mathrm{c}}$ = non-dimensional critical shear stress; $L_{\mathrm{p}*}$ = non-dimensional fluctuating lift force due to pressure fluctuation; $\sigma_{\mathrm{Lp}*}$ = standard deviation of

L_{p*}; σ = density of bed-material; ρ = density of water; g = gravitational acceleration; d = diameter of bed-material particles; F_0, k_2, m = empirical constants (F_0=0.03, k_2=0.7, and m=3). Details of this modification can be found Jia et al. (2001) and Kitamura et al. (1999).

Head-Cut Migration Model

A headcut model with a two-layered soil stratigraphic formation is proposed. The top layer of the soil is of cohesive and erosion resistant material lying on the second, non-cohesive, erodable, sandy material. The upper cohesive layer is undermined, whence the non-cohesive layer is exposed and scoured, the overhanging part of the cohesive layer at the brink would collapse periodically into the scour hole. The collapsed blocks of the cohesive material are then being carried to downstream after breaking into small pieces by the jet. This process is similar to the erosion of a composite bank: when the lower loose bank material is eroded by the channel flow, the upper cohesive material collapses (Thorne and Tovey, 1981; Fukuoka, 1994). To estimate the critical overhang length of the cohesive layer, Fukuoka (1994)'s cantilever model is applied in the present study.

The critical balance of weight of the soil and the resistance of the cohesive force (see Figure 4) is found

$$\gamma D_h L_C \frac{L_C}{2} = \frac{1}{6} D_h^2 T_C \tag{5}$$

Therefore,

$$L_C = \left(\frac{T_C D_h}{3\gamma} \right)^{1/2} \tag{6}$$

where L_C = critical overhang length; T_C = tensile strength, D_h = height, and γ = bulk density of cohesive soil layer.

In reality, the overhanging cohesive material collapses periodically, the lasting time period of the overhang and the sizes of fallen blocks vary. The fallen blocks of the material with varying length are then broken into small pieces by the jet and carried away by the flow. It is difficult to model these chaotic events exactly, a time-averaged head-cut advance model, therefore, is proposed. It is assumed that the overhang length of the brink can be maintained at the critical condition during the migration process. The portion of the brink length excessive of the critical value evaluated by (6) falls into the scour hole continuously.

A detailed numerical simulation model is presented in Figure 5. The critical condition of the overhang is shown in Figure 5(a). Sedimentation processes under the overhang brink is assumed to be dominated by the gravity which drives the sediment particles along the bed slope toward the bottom of the scour hole. This approximation is consistent with the experimental observation of Stein et al (1993) in which the scour hole of an impinging jet expanded to beneath the flow flume. The bed slope of the hole under the flume was close to the repose angle. If one starts the computation from a flat bed condition, the cohesive brink layer would not overhang until the scour hole reaches to a critical depth. Further development of the hole in depth and size would undermine the brink since the sandy material would slide into the scour hole. If the scour hole continue to develop, the overhang length of the brink increase accordingly until the critical length is reached. From this time, the cohesive material start collapsing continuously from the tip of the brink and the headcut migrates upstream. Because the jet moves with the brink and so does

the impingement point of the jet, the scour hole will migrate.
The sediments in the part (A) and (B) (Fig. 5b) account for the sediment input to sour hole. As having been mentioned above, the actual process of transport of the collapsed material from the brink is complicated, it is assumed that the collapsed cohesive material is immediately broken into loose particles, the fine, cohesive portion is washed away without deposition; the coarse, non-cohesive portion is deposited on the upstream slope of the scour hole (Fig. 5c). The amount of deposition is expressed as $A + B(1 - p_n)$, with p_n being the non-cohesive material portion in the cohesive layer. The rate of the souring in the scour hole determines the rate of the retreat of its upstream slope and therefore the rate of collapse of the top cohesive layer. The location of the new brink becomes the new boundary of the computation domain. After the new domain is determined, the mesh is shifted upstream to catch the new boundary, all of the quantities of the flow field are interpolated to the new mesh; the flow field and the bed-deformation are then calculated again. These steps are repeated until the termination time of the simulation is reached.

There is no physical experimental data available to validate this head-cut migration model. In fact, this study is interested in exploring the relationship between flow conditions and soil properties of these two earth layers use only numerical simulation, the so called numerical experimentation. The simulation is based on validated erosion of scour hole due to jet impingement and the proposed two layer head-cut model is also physically reasonable. One experiment was selected (Case 22, Stein, 1993), and the head-cut was simulated based upon its flume and hydraulic conditions. The tensile strength, T_C, and the content of non-cohesive material in the cohesive soil layer, p_n, were then adjusted and more simulations were conducted to investigate the effects of these parameters on the head-cut migration. The effects of the specific discharge, q, was also studied. Experimental conditions are summarized in Table 1. The boundary condition of jet velocity, impinging angle and location were calculated assuming the jet is of a free fall. The equivalent bed roughness height is assumed to be equal to the sediment size. The critical shear stress is given by van Rijn's equation (1993). The angle of repose of the bed-material is set to be 30 degree. The mean step length of the sediment is set to be 500 times as large as the sediment diameter in the present study.

3. Computational Results and Discussion

The change of the simulated scour hole with specific discharge is shown in Figure 6. The size of the scour hole increases by several times when the discharge was increased from 0.001 m^3/s to 0.005 m^3/s. Impact of the discharge expanding the scour hole on the downstream side. The trend that higher discharge will result in deeper and larger scour hole is reasonable.

Figure 7 indicates head cut migration rate is lower with more non-cohesive material in the cohesive layer, due to the assumption that the non-cohesive material in the top layer becomes bed material to be transported by the flow while cohesive portion becomes wash load. Higher p_n value means the flow has to move more material out of the scour hole and the migration should be slower.

Figure 7 also shows the migration speed of scour holes will reduce when the tensile strength of the overhang cohesive material increases. This is reasonable since the overhang will collapse tensile value of the top layer, it is natural that when the overhang is longer the scour hole will be deeper.

Figure 9 shows an example of the simulated scour hole shape and location. One can see that the scour hole initially develops in size and depth, the location of the maximum depth moves gradually downstream. When it reaches to a certain depth, the scour triggered collapsing of the

cohesive upper layer and the brink migration process starts; the point of maximum depth starts migrating upstream. When the head-cut migration reaches to an equilibrium state, the shape of the scour hole is almost the same. This is because the sediment input due to the collapse of the upper cohesive soil layer and the sediment output due to scour and transport downstream by the impinging jet are balanced. One observation is that the bottom of the scour hole is flatter in the case of head-cut migration.

Conclusion

The flow associated with head-cut and its migration is highly turbulent and three-dimensional. The flow velocity magnitude and direction change significantly in the scour hole. Sediment transport model has to include mechanism of entraining particles due to pressure fluctuation. In this study, the non-equilibrium sediment transport model of Nakagawa and Tsujimoto (1980), which considers sediment pick-up, transport and deposition processes, was adopted. This model is further modified to accommodate the influence of pressure fluctuation due to the jet impingement.

The head-cut model of a two-layered stratigraphic bed, a loose soil layer covered by a cohesive layer, is proposed. It combines the bed-scour model for simulating the scour process in the non-cohesive soil layer beneath the cohesive soil layer, and a cantilever collapsing model estimating the critical overhang length of the cohesive layer. The time-averaged head-cut advance was assumed to approximate the collapsing process of cantilever brink numerically. The simulated processes of head cut migration, the influence of soil tensile strength, content of non-cohesive material, and flow discharge on migration rate and the size of scour hole, are realistic and reasonable.

Acknowledgement

This work is a result of research supported in part by the USDA Agriculture Research Service under Specific Research Agreement No. 58-6408-7-035 (monitored by the USDA-ARS National Sedimentation Laboratory) and the University of Mississippi. Dr. K. Robinson (Hydraulic Lab/ARS, Stillwater, Oklahoma) has kindly helped the authors with insight of the head-cut problem and provided the data of large-scale flume experiments.

References

Bennett, S. J., Alonso, C. V., Prasad, S. N. and Romkens, M.J.M., 1997. Dynamics of head-cuts in upland concentrated flows. Proceedings of the Conference on Management of Landscapes Disturbed by Channel Incision, Oxford, Mississippi, pp.510-515.

Fukuoka, S., Kogure, Y., Satoh, K. and Daitoh, M., 1994. Annual Journal of Hydraulic Engineering, Vol.37, pp.643-648.

Jia, Y., Kitamura, T., and Wang, S.S.Y., 2001. Simulation scour process in a plunge pool with loose material. Journal of Hydraulic Engineering, ASCE, Vol. 127, No. 3, pp219-229.

Kitamura, T., Jia, Y., Wang, Sam. S. Y. and Tsujimoto, T., 1999. A model for bed-scour induced head-cut. Annual Journal of Hydraulic Engineering, JCSE, Vol.43, pp.611-616 (in Japanese).

Liu, P.Q., and Dong, J.R., 1998. Experimental investigation of fluctuation uplift on rock blocks at the bottom of the scour pool downstream of Three-Gorges spillway. Journal of Hydraulic Research, Vol. 36, No. 1, pp 55-68.

Nakagawa, H. and Tsujimoto, T., 1980. Sand bed instability due to bed load motion. Journal of Hydraulic Engineering, ASCE, Vol.10, No.12, pp.2029-2051.
Robinson, K. M., 1996. Gully erosion and headcut advance. PhD thesis, Oklahoma State University.
Simons, D.B. and Stevens, M.A., 1971. Scour controlled in rock basins at culvert outlets. Chapter 24, in River Mechanics, Vol. II, Shen, H.W. (ed.).
Stein, O. R., Julien, P. Y. and Alonso, C. V., 1993. Mechanics of jet scour downstream of a headcut. Journal of Hydraulic Research, Vol.31, No.6, pp.723-738.
Stein, O. R. and Julien, P. Y., 1993. Criterion delineating the mode of headcut migration, Journal of Hydraulic Engineering, ASCE, Vol.119, No.1, pp.37-49.
Thorne, C. R. and Tovey, N. K., 1981. Stability of composite river banks. Earth Surface Processes & Landforms, pp.469-484.
Van Rijn, 1993. Principles of Sediment Transport in Rivers Estuaries and Coastal Seas. Aqua Publications, The Netherlands.

Table 1. Experimental conditions

RUN	d (m)	q(m^2/s)	D_h (m)	(N/m^3)	T_c (N/m^2)	p_n (-)	c (m/s) x10^{-4}
s22h	0.00015	0.00166	0.02	16000	50.0	0.5	1.17
s22h2	0.00015	0.00166	0.02	16000	250.0	0.5	1.03
s22h3	0.00015	0.00166	0.02	16000	1000.0	0.5	0.973
s22h4	0.00015	0.00166	0.02	16000	250.0	0.0	1.27
s22h5	0.00015	0.00166	0.02	16000	250.0	1.0	0.919
s22h6	0.00015	0.00166	0.02	16000	0.0	0.5	1.48
s22h7	0.00015	0.00166	0.02	16000	0.0	0.0	1.61
s22h8	0.00015	0.00166	0.02	16000	0.0	1.0	1.15
s22h9	0.00015	0.00166	0.02	16000	1000.0	1.0	0.744
s22h10	0.00015	0.00166	0.02	16000	1000.0	0.0	1.17
he1	0.00015	0.005	0.02	16000	250.0	0.5	1.67
he11	0.00015	0.005	0.02	16000	1000.0	0.5	1.24
he12	0.00015	0.005	0.02	16000	0.0	0.5	2.13
he6	0.00015	0.003	0.02	16000	250.0	0.5	1.22
he3	0.00015	0.001	0.02	16000	250.0	0.5	0.917
he31	0.00015	0.001	0.02	16000	1000.0	0.5	0.768
he32	0.00015	0.001	0.02	16000	0.0	0.5	1.3
he4	0.00015	0.00166	0.04	16000	250.0	0.5	1.59
he5	0.00015	0.00166	0.01	16000	250.0	0.5	1.09
he7	0.00015	0.00166	0.06	16000	250.0	0.5	1.47

List of Figures

Figure 1. Sketch of flow pattern in headcut zone: jet impingement into a pool.

Figure 2. Comparison of computed maximum shear stress and measurements.

Figure 3. Simulated flow pattern near the jet impingement with flat bed.

Figure 4. Weight balance of cohesive top layer.

Figure 5. Model of head cut mechanism simulation.

Figure 6. Simulated scour hole with several flow discharges.

Figure 7. Influence of tensile strength and non-cohesive material on migration rate.

Figure 8. Influence of tensile strength of top cohesive layer on scour hole.

Figure 9. Simulated headcut migration.

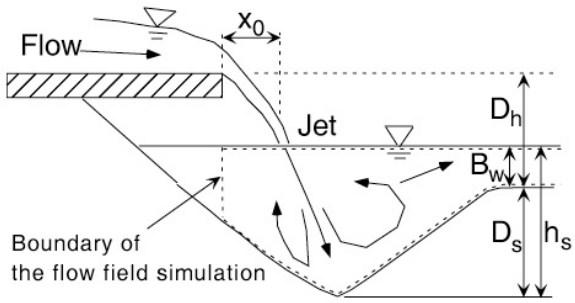

Figure 1. Sketch of flow pattern in headcut zone: jet impingement into a pool.

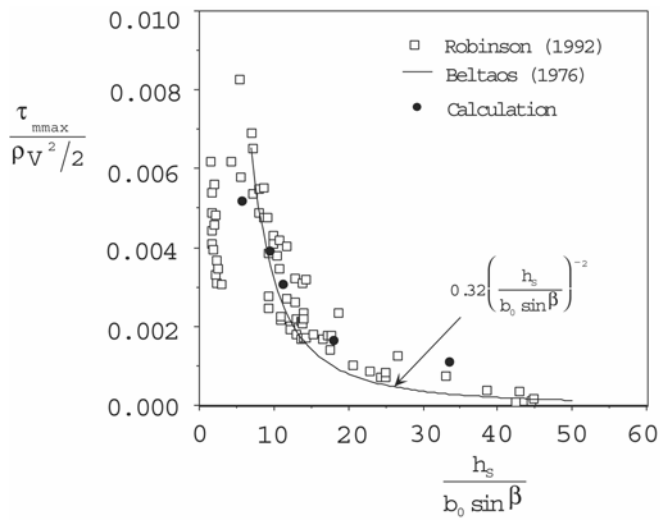

Figure 2. Comparison of computed maximum shear stress and measurements.

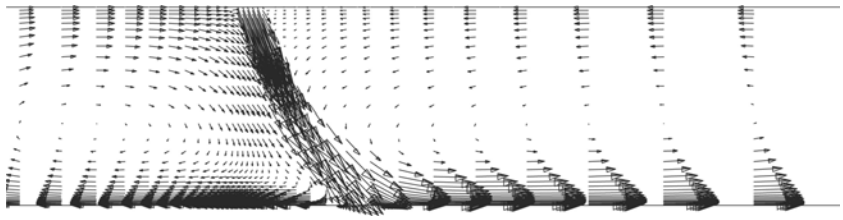

Figure 3. Simulated flow pattern near the jet impingement with flat bed.

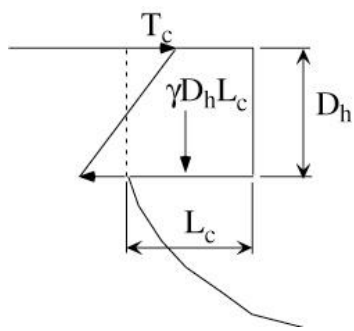

Figure 4. Weight balance of cohesive top layer.

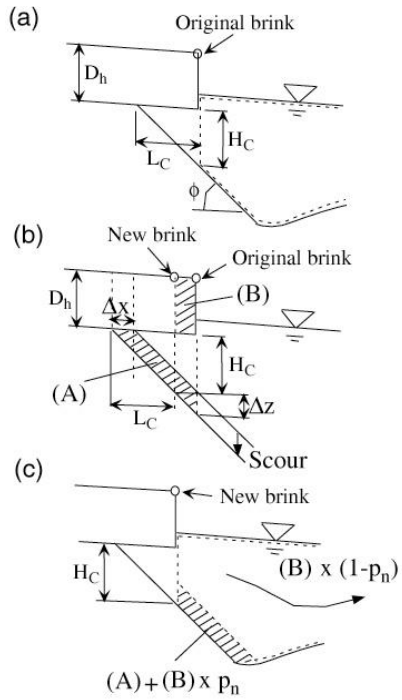

Figure 5. Model of head cut mechanism simulation.

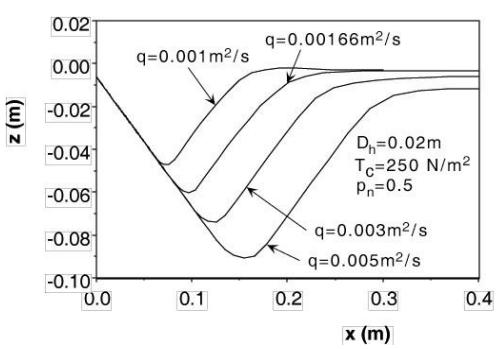

Figure 6. Simulated scour hole with several flow discharges.

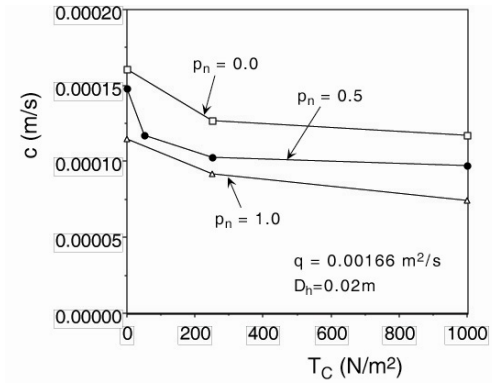

Figure 7. Influence of tensile strength and non-cohesive material on migration rate.

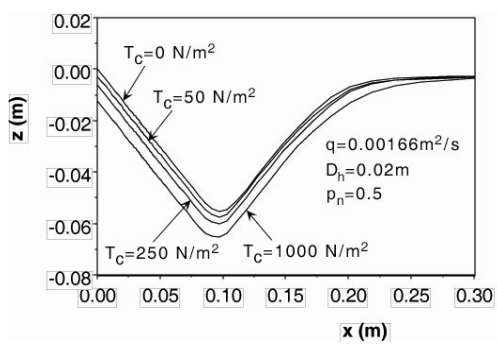

Figure 8. Influence of tensile strength of top cohesive layer on scour hole.

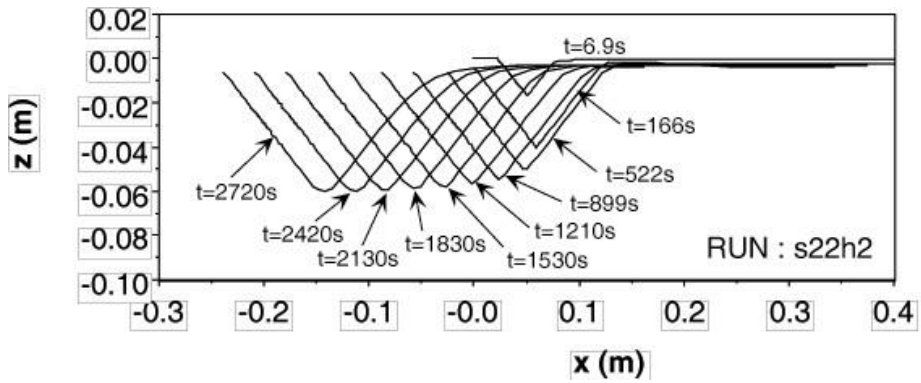

Figure 9. Simulated headcut migration.

Modeling Headcut Development and Migration in Upland Concentrated Flows

Sean J. Bennett∗ (E-mail: seanb@buffalo.edu)
Department of Geography, University at Buffalo, Buffalo, NY 14261-0055
Tel: 716-645-2722 ext. 65, fax: 716-645-2329

Carlos V. Alonso (E-mail: calonso@msa-oxford.ars.usda.gov)
USDA-ARS National Sedimentation Laboratory
P.O. Box 1157, Oxford, MS 38655
Tel: 662-232-2969, Fax: 662-281-5706

Abstract

On hillslopes and agricultural fields, discrete areas of intense, localized soil erosion commonly take place in the form of migrating headcuts. These erosional features significantly increase soil loss and landscape degradation, yet the unsteady, transient, and migratory habits of headcuts complicate their phenomenological and erosional characterization. Here a unique experimental facility was constructed to examine actively migrating headcuts typical of upland concentrated flows. Essential components of the facility include a deep soil cavity with external drainage, rainfall simulator, overland flow, and a video recording technique for data collection. Results from these experiments show that (1) after a short period of adjustment, headcut migration can attain a steady-state condition, where the rate of migration, scour hole geometry, and sediment discharge remain constant with time (headcuts displayed morphologic self-similarity), (2) boundary conditions of higher overland flow rates, steeper bed slopes, and larger initial headcut heights produced systematically larger scour holes with higher rates of soil erosion, (3) during migration, the turbulent flow structure within the scour hole remained unchanged, consisting of an overfall nappe at the brink transitioning into an impinging jet with two wall jets within the plunge pool, and (4) the morphology of the scour holes near the headcut face displayed morphologic similarity. The systematic behavior of headcut development and migration enabled the application of modified jet impingement theory used to predict with good success the characteristics of the impinging jet, the depth and maximum scour, the rate of headcut migration, and the rate of sediment erosion. These data and analytical formulation can be used in conjunction with soil erosion prediction technology to improve the management of agricultural areas impacted by headcut development and ephemeral gully erosion.

Keywords: Soil erosion, headcuts, rills, gullies, jet impingement

1. Introduction

Headcuts and knickpoints are step-changes in bed surface elevation where intense, localized erosion takes place (Brush and Wolman, 1960; Gardner, 1983). The formation of headcuts and knickpoints and their upstream migration have been linked to the concentration of

∗ Corresponding author

overland flow (Mosley, 1974; Merritt, 1984), rill and gully erosion and development (Seginer, 1966; Piest et al., 1975; Bryan and Poesen, 1989; Bryan, 1990; Slattery and Bryan, 1992), erosion of bedrock channels (Miller, 1991; Seidl et al., 1994), and the initiation of drainage systems and landscape evolution (Seginer, 1966; Piest et al., 1975; Parker, 1977; Gardner, 1983; Dietrich and Dunne, 1993).

In upland concentrated flows such as rills, the occurrence and migration of headcuts is commonly associated with significant increases in sediment yield (Mosley, 1974; Meyer et al., 1975; Bryan, 1990). For example, Römkens et al. (1996, 1997) observed the failure of surface seals on soils immediately followed by headcut formation, bed incision, and rill development. Prior to bed incision, sediment yield from the soil surface was essentially zero. Moreover, migrating headcuts can account for up to 60% of the total rill erosion on some soils (Elliot and Laflen, 1993).

At present, little information exists on the processes of headcut migration and soil erosion, variation of scour hole morphology, the mechanics of headcut erosion, and effect of flow discharge, bed slope, and other initial boundary conditions on headcut dynamics (see review in Bennett et al., 2000). This deficiency is primarily due to the logistical difficulties in examining actively migrating headcuts. To address these difficulties, Bennett and his colleagues (Bennett, 1999; Bennett et al., 2000; Bennett and Casalí, 2001) designed a unique experimental facility to examine actively migrating headcuts in soils at a length scale similar to rills and crop furrows and at times scales similar to individual storm events. These unique data greatly facilitated the application of jet impingement theory to the problem of a migrating headcut (Alonso et al., 2002). The objectives of this paper are (1) to describe the experimental facility for physically modeling headcut migration in upland flows, (2) to summarize the main experimental findings for actively migrating headcuts, (3) to present the analytical framework for modeling headcut erosion, and (4) to discuss the implications of this work on soil erosion prediction technology. The papers by Bennett and his colleagues will be collectively referred to as the Bennett dataset.

2. Experimental Facility, Equipment, and Procedure

A non-recirculating, 5.5-m long tilting flume was designed and constructed specially to examine the soil erosion processes associated with migrating headcuts (Figure 1). Flow discharge was controlled by two adjustable intake valves and monitored with a manometer and a pressure transducer connected to an inline Venturi meter. A raised floor, 1 m long and 0.165 m wide, located immediately upstream of a soil cavity 2 m long, 0.165 m wide, and 0.25 m deep, provided excellent hydraulic entry conditions. A subsurface drainage system was installed along the base of the soil cavity and provided escape routes for both air and water during rainfall application.

A multiple-intensity rainfall simulator consisting of two oscillating nozzles spaced 1.64 m apart (Meyer and Harmon, 1979; Figure 1) was suspended approximately 4 m above the flume. Rainfall intensity (mm h^{-1}) was governed by the oscillation frequency of the nozzles, operated by an electronic controller to within ±1.3% and calibrated for the bed area under investigation. With the bed prepared and headcut-forming plate installed (see below), rainfall intensities of 20 to 30 mm h^{-1} were applied for 4 to 6 h to a bed slope of 5%.

A single soil was used in deriving the Bennett dataset, which was a sandy loam to sandy clay loam texture (Ruston Series; fine-loamy, siliceous, thermic, Typic Paleudult; Römkens et al., 1997), commonly found in the southeastern U.S. The material consisted of 20.0% clay, 2.9%

silt, and 77.1% sand. An appreciable amount of iron oxide in the soil greatly enhanced its stability (Rhoton et al., 1998).

All soil was air dried in a greenhouse, mechanically crushed, and passed through a 2 mm sieve, which ensured minimum variation in aggregate size amongst experiments. Soil was packed incrementally in layers of about 0.02 m using a 9-kg block of aluminum mounted to an aluminum frame 0.6 m long and 0.165 m wide, constructing uniformly packed soil beds with bulk densities ranging from 1350 to 1450 kg m^{-3}.

An aluminum frame was placed 1.52 m downstream of the soil cavity's entrance for the purpose of forming a headcut. This frame had a variable vertical face, from 5 to 50 mm, and once in place it had little impact on the applied rainfall. After installation, soil was packed upstream of the frame producing a pre-formed vertical step in the bed profile.

The soil material within the uppermost 0.02 m, which was non-recycled soil, was treated with 0.75 cmol of $Ca(OH)_2$ per 100 g of soil (about 0.74 g per 1 kg of soil) to promote a physio-chemically favorable condition for seal development (Römkens et al., 1995, 1997). Following the application of simulated rain, a well-developed and reproducible surface seal formed, which served two purposes. First, upon the introduction of overland flow the seal negated surface soil detachment both upstream and downstream of the headcut. Thus all sediment erosion was the result of headcut growth and migration. Second, it produced the requisite two-layer stratigraphy common to many stepped headcuts and knickpoints observed in field and flume studies (e.g. Holland and Pickup, 1976; Bryan and Poesen, 1989). This stratigraphy allowed the headcut to maintain a nearly vertical headwall during migration.

The Plexiglas sidewall of the flume had a superimposed grid system allowing for visual observation of many morphologic and hydraulic parameters. A video camera mounted on a tripod during rainfall application and to a movable carriage during the overland flow recorded each experimental run. From these images, the following information could be determined with sufficient accuracy (length scales to within 3%): progression of the wetting front within the soil profile during rainfall application, position and morphology of the headcut, overland flow depth, and angle of the overfall nappe.

Turbulent flow velocities within fixed headcut models were obtained using a two-component, 300-mW Argon-ion Laser Doppler anemometer with dual 14-bit processors. The LDA was used with a 400 mm lens in backscatter mode, and vertical and horizontal velocity data were collected at each point for 60 to 120 s at data rates from 20 to 300 Hz. The probe head was mounted to a high-precision two-component axis system for positioning, and the measurement volume was positioned in the center of the flow. All data were post-processed with user-defined software. Two headcut models were used. The first headcut profile, spatially-averaged from steady-state conditions, was based on Bennett et al. (2000) using a flow discharge of 70.2 l min^{-1} and a bed slope of 1%. The second headcut profile was based on Bennett (1999) using a flow discharge of 51.6 l min^{-1} and a bed slope of 5%, and the profile was obtained toward the end of the experimental run (not steady state).

3. Results

3.1 Experimental Results

In the experiments of Bennett et al. (2000), bed slope and an initial headcut height were held constant at 1% and 25.4 mm, but overland flow rate varied from about 20 to 80 l min^{-1}. As the overland flow passed over the pre-formed step, flow impinged the surface seal just downstream of the step. This impinging overfall caused surface seal failure and soil erosion, and

a scour hole developed and enlarged. During this initial period of bed adjustment, normally from one to three minutes, both the scour depth S_D (the vertical length from the brinkpoint to the maximum scour depth) and sediment production increased (Figure 2). Once the scour hole attained an 'equilibrium' or maximum depth, downstream deposition began, scour hole length S_L (the horizontal length from the brinkpoint to the maximum scour depth) was maintained, and sediment yield decreased.

After this initial period of growth, the headcut brinkpoint migrated upstream in a gradual and linear fashion through time (Figure 2). Headcut migration rate was constant during each run, ranging from 1.2 to 2.0 mm s^{-1}. In rill erosion studies where headcuts were observed, migration rates varied from 0.1 to 1.3 mm s^{-1} depending on headcut height and unit discharge (Bryan and Poesen, 1989; Bryan, 1990; Slattery and Bryan, 1992). For a cohesive soil overlying a layer of sand, Stein and LaTray (2002) observed headcut migration rates of 0.7 to 1.4 mm s^{-1}.

The peak in sediment yield at about 50 s (Figure 2) coincided with initiation of both headcut movement and downstream deposition. Because downstream bed height was fixed in place by the soil retaining wall, sediment erosion was moderated by downstream deposition of thickness d_T. After this initial pulse, steady-state sediment yield was attained when the rate of sediment production due to headcut migration and the rate of sediment deposition downstream of the headcut did not change with time. Steady-state sediment yield occurred after 300 to 400 s (Figure 2). Parker (1977) also observed constant, but short-lived, rates of headcut migration and sediment yield in his experiments on drainage network development.

Within individual experiments, the morphology of the headcut did not vary significantly during migration once steady-state conditions were achieved (Figure 3). Deviations from the mean headcut profile at any given time were due to random spatial and temporal variations in boundary conditions such as bulk density, packing efficiency, soil water content, subsurface pore pressure, soil adhering to the sidewall, and physical, hydraulic, and chemical characteristics of the surface seal. The headcut self-corrected these random boundary conditions to maintain a similar morphology. The ratio S_L/S_D remained relatively unchanged for each run, ranging from 1.04 to 1.73 (Figure 2). From bed profiles of headcuts in a laboratory channel, Bryan and Oostwoud Wijdenes (1992) reported S_L/S_D values of 1.2 and 1.9. With a four-fold increase in flow discharge, dimensions of the steady-state scour hole and its associated sediment yield increased accordingly: both S_D and S_L increased by about 200%, d_T increased by almost 300%, and sediment yield increased by as much as 100% (Bennett et al., 2002).

The flow structure within the equilibrium headcut scour hole was the same for all experiments past the initial headcut development stage. Supercritical flow converges at the headcut brink, and an overfall nappe enters the plunge pool (Figures 5 and 6). The overfall nappe turns into a turbulent diffusing jet, which extends to and impinges the bed well upstream of the maximum scour depth. Two wall jets also are created by this turbulent jet. The upstream wall jet remains fixed against the headcut face during migration, held captive by the impinging jet. The downstream wall jet is larger and extends well downstream. An area of upwelling demarcates the end of the plunge pool circulation pattern. As the steady-state headcut migrates upstream, the turbulent flow structure depicted in Figures 4 and 5 remained unchanged, allowing for the application of jet impingement theory to the scour hole domain (see later).

The conservation of scale over a range of flow can be demonstrated by normalizing the headcut profiles. Because the wall jets extended over the entire scour hole region, the scour hole length scales S_L and S_D can be used to scale all time-averaged headcut profiles (Figure 6). Such normalization has been used in examining dimensional similarity of scour holes formed by plane

turbulent wall and impinging jets (Rajaratnam, 1981). Near the headcut face, the bed shape was wholly dependent on the erosive recirculation within the upstream wall jet, and virtual collapse of all bed profiles is observed, indicating the existence of morphologic similarity in this region. With identical soil materials and soil properties, the increase in flow discharge was accommodated by a systematic and predictable increase in scour hole dimensions. As discussed above, erosive potential of the impinging jet increased as flow discharge increased (see also Rajaratnam, 1981). Moreover, the mode of seal failure at the brinkpoint position was consistently observed in all experiments. Thus the mechanisms of headcut erosion did not change with increased flow rate.

In the experiments of Bennett (1999), the same experimental facility, soil materials, and initial headcut height were used, but bed slope was varied from 1 to 10% and overland flow rate was held constant at 52 l min^{-1}. The rate of headcut migration was constant within each experiment, but higher bed slopes generally resulted in lower migration rates. At bed slopes 2% and smaller, the overfall nappe at the headcut brinkpoint remained submerged, and a steady-state condition was achieved: sediment yield and scour hole geometry remained constant as the headcut migrated upstream. For bed slopes 3% and greater, the overfall nappe became aerated, and as the headcut migrated upstream, the depth of scour increased. Higher bed slopes resulted in deeper scour holes. Soil erosion mechanisms included tension crack formation and seal removal at the headcut brinkpoint, soil washout along the aerated headcut face, and plunge-pool scour. The slope of the sediment deposit d_T downstream of the migrating headcut was 2.2% for all experiments, suggesting that flow discharge and not initial bed slope controlled transport capacity and downstream bed adjustment. However, morphologic similarity of headcut scour holes was again demonstrated over a 10-fold range in bed slope (Figure 6).

In the experiments of Bennett and Casalí (2001), the same experimental facility and soil materials were used, but bed slope and overland flow rate were held constant at 1% and 70 l min^{-1}, and initial headcut height varied from 5 to 50 mm. After an initial period of bed adjustment, similar steady-state conditions were observed. Using specific criteria for determining the time to steady-state soil erosion, it was shown that initially large steps reached steady-state erosion conditions faster (by more than an order of magnitude) and over a shorter distance (by less than an order of magnitude) than do initially small steps. Initially small steps take almost twice the amount of time to reach steady-state conditions for sediment transport parameters as do initially large headcuts. On the other hand, both initially small and large steps reach steady-state conditions after migrating about the same distance upstream. For the smallest initial headcuts of 5 mm, a trend line could not be fitted to the sediment yield time series because these data did not reach true steady-state conditions with regard to sediment transport.

As initial step height increased, Bennett and Casalí (2001) showed that headcut migration rate increased (not statistically significant), maximum scour depth increased (statistically significant), length to maximum scour depth decreased (not statistically significant), and headcut aspect ratio S_L/S_D decreased (statistically significant). The jet entry angle also increased as initial step height increased (statistically significant). As initial step height increased, sediment yield, downstream deposit thickness, and the slope of the sediment deposit increased (each statistically significant). For a given bed slope and overland flow discharge, larger initial steps caused the formation of headcuts with greater rates of sediment production, deposition, and yield and a steepening of the bed slope downstream.

3.2 Analytic Results

Based on the experimental results of the Bennett dataset, Alonso et al. (2002; herein called the Alonso Model) defined predictive equations for the magnitude of headcut scour depth and the rate of headcut migration. Direct numerical simulation of headcut erosion processes is possible but not practical primarily because of an inadequate understanding of the physics of soil erosivity and sediment movement within a headcut scour hole environment. Alonso et al. (2002) adopted an approximate analytical procedure whereby the eroded soil mass can be readily computed. The Alonso Model is applicable to relatively small upland concentrated flows with little or no upstream sediment supply, where the eroded soil depth can be treated as a homogeneous medium, and exfiltration erosion processes are neglected. The model is not suitable for settings impacted by shallow soil horizons and hard pans or where seepage forces and surface weathering can play a dominant role on soil erosion.

The main components of the Alonso Model are (1) the overfall domain where the jet entry angle is determined, (2) the plunge pool domain where both the scour depth and rate of headcut migration is determined, and (3) mass conservation that relates headcut erosion rate, deposition rate, and sediment loss (discharge). In the overfall domain, flow in the neighborhood of the brink is treated as a classical overfall where the nappe is regarded as a free jet where both ventilated and nonventilated conditions are considered. In the former case, one readily obtains the following expressions for the jet angle, θ_e, at the entry point:

$$tan\,\theta_e = \frac{\sqrt{2gH}}{V_b} = T_e \tag{1}$$

where H is the jet plunging height given by:

$$H = h + \frac{d_b}{2} \tag{2}$$

d_b and V_b denote the flow depth and average velocity at the overfall brink point, and h is the vertical distance from the brink to the pool surface. Nonventilated overfalls are treated by examining the conservation of linear momentum within within the nappe and realizing that suction can occur within a nonventilated overfall. Thus, Alonso et al (2002) derived the following expression for the jet entry angle:

$$\theta_e = \tan^{-1}\left[\left(1 + \varepsilon\lambda\frac{h}{d_b}\right)\Phi_H\right]^{1/2} \tag{3}$$

$$\Phi_H = (T_e)^2\sqrt{1+(T_e)^{-2}} + \ln\left[(T_e)\left(1+\sqrt{1+(T_e)^{-2}}\right)\right] \tag{4}$$

where ε is a shape parameter (assumed here to be of order 2) used to regulate the pressure gradient across the nappe, and λ is a calibrating suction-head coefficient. Equation (3) converges to within 10 percent of the angles predicted by Equation (1) as $\lambda \to 0$ and h increases.

As the free jet enters the plunge pool domain, it turns into a turbulent diffusing jet that ends impinging the bed (see Figures 4 and 5). Using an approach based on the conceptual model of equilibrium depth presented by Stein et al (1993), neglecting the *Coanda* effect that results in the impinging jet pulled upstream (Sawyer, 1960; Newman, 1961), and introducing results reported by Albertson et al. (1950), Rajaratnam (1976), and Beltaos (1976), Alonso et al. (2002) derived the following

$$S_D = \sigma V_e q_w^{4/5}\sin\theta_e + h \tag{5}$$

$$\sigma = \frac{c_d^2 \delta_f \, \rho_w \, \nu^{1/5}}{2(\tau_c / \beta)} \tag{6}$$

$$\frac{V(J)}{V_e} = c_d \sqrt{\frac{b_e}{J}} \tag{7}$$

where q_w is unit discharge, c_d is the turbulent diffusion coefficient of a submerged jet (taken here as 5/2), ρ_w and ν are the density and kinematic viscosity of water, τ_c is the critical shear stress of the soil, δ_f and β are calibrating coefficients, $V(J)$ and V_e are the centerline and average jet velocity at the point of entry to the pool, and b_e is the transversal width of the nappe at the entry point.

Alonso et al. (2002) assumed that as the headcut propagates upstream, scouring soil as it does so, energy must be consumed to overcome the resistance presented by the soil and only the impinging jet can supply that energy. By applying the conservation of energy to a plunge-pool control volume and employing an erodibility coefficient k_d for the soil, the following expression for the rate of headcut migration M was derived:

$$M = V_e \sqrt{\frac{\mu \, q_w}{S_D - h}} \tag{8}$$

$$\mu = \frac{1}{2} \rho_w \, k_d \sin^2 \frac{\theta_e}{2} \tag{9}$$

Since the migrating headcut profile remains invariant with time within a moving frame of reference and by invoking the conservation of mass, Alonso et al. (2002) demonstrated that the rates of erosion by headcut migration m_e and deposition m_d are independent of the shape of the headcut, and depend only on the rate of migration and the heights of the eroding and depositing surfaces, i.e.,

$$m_e = \rho_e M S_D \tag{10}$$

$$m_d = \rho_d M d_t \tag{11}$$

and that m_e, m_d, and the rate of sediment loss (discharge) m_y are related by

$$m_e = m_d + m_y \tag{12}$$

A similar result was obtained by Begin et al. (1980) using a less rigorous analysis and an idealized headcut geometry.

Equations for jet entry angle, headcut scour depth, rate of headcut migration, and mass balance were compared to the Bennett dataset (Figure 2). These results show that there is excellent agreement between the Alonso Model predictions and experimental observations. Deviations from perfect agreement between predictions and observations were due to the propagation of uncertainty errors in the predictions, caused by the uncertainties in θ_e, τ_c, and k_d, the latter two parameters were estimated using available literature.

4. Discussion

4.1 Systematic Behavior of Headcut Growth and Migration

The development and migration of headcuts in soils and other geologic materials are important areas of research in a number of disciplines. Research is needed to further understand the erosivity of these phenomena and the relation between headcut migration and soil losses in agricultural areas. Moreover, research is required to develop appropriate models for the

formation, evolution, and migration of headcuts in upland areas in the context of soil erosion prediction technology.

A purpose-built flume was constructed and an experimental procedure designed to study actively migrating headcuts in a controlled, laboratory setting. The experimental results show that (1) headcut erosion displayed systematic and self-similar organization for a variety of flow rates, bed slopes, and initial headcut heights, and that (2) headcut scour hole dimensions and migratory characteristics were related to bulk hydraulic and hydrodynamic parameters. These systematic results point to a common erosion phenomenon: an impinging jet and wall jets that control the morphologic characteristics of an actively migrating headcut scour hole.

An analytical formulation for predicting the jet entry angle, scour depth, migration rate, and sediment discharge associated with an actively migrating headcut developed in soil materials was constructed using modified jet-impingement theory. The model construct took full advantage of the systematic and organized behavior of the headcut scour holes, as observed in the Bennett dataset, and the results show the great utility and potential applicability of this approach.

4.2 Soil Erosion Prediction Technology

Soil erosion is a critical concern for the sustainable management of agricultural soils within the U.S. and worldwide. Soil erosion is the primary cause of soil degradation in the U.S., and off-site impacts of sedimentation can severely affect water quality, ecology, and ecological habitat. According to the U.S. EPA (1998, 2000), sedimentation is the leading cause of water quality degradation in the U.S. On-site and off-site costs of soil erosion in the U.S. have been estimated to be $30 to $44 billion annually (Pimentel et al., 1995; Uri and Lewis, 1999). It is imperative that the United States has a strong scientific basis to understand, assess, and control erosion by water so as to protect our soil resource from its potentially devastating effects.

Current soil erosion prediction technology such as WEPP (Nearing et al., 1989) and RUSLE (Renard et al., 1997) cannot address ephemeral gully erosion because (1) the spatial scales of ephemeral gullies are smaller than those currently employed in the models, and (2) no analytical formulation is available that could predict the dimensions of headcuts and their rates of migration. The formulation presented herein could be modified and combined with topographic indices for ephemeral gully development (e.g., Thorne et al., 1986; Vandaele et al., 1996; Casalí et al. 1999), thereby predicting both the location of gullies as well as the maximum scour depth and scour length. Such combined technology could provide some measure of soil losses and sediment yields from upland areas impacted by headcut migration and gully erosion.

5. Conclusions

On hillslopes and agricultural fields, step-change in bed surface elevation commonly occur, and these headcuts and knickpoints are areas of intense, localized soil erosion. The development and migration of headcuts can significantly increase soil losses and accelerate landscape degradation. A unique experimental facility was constructed to examine actively migrating headcuts typical of upland concentrated flows. The experimental results show that (1) headcut erosion displays systematic and self-similar organization for a variety of flow rates, bed slopes, and initial headcut heights, (2) headcut scour hole dimensions and migratory characteristics were related to bulk hydraulic and hydrodynamic parameters, and (3) the turbulent flow structure within the actively migrating scour holes comprised an overfall nappe, impinging jet, and two wall jets. An analytical formulation for predicting the jet entry angle, scour depth, migration rate, and sediment discharge associated with an actively migrating

headcut developed in soil materials was constructed using modified jet-impingement theory. The model construct took full advantage of the systematic and organized behavior of the headcut scour holes, and the results show the great utility and potential applicability of this approach to the prediction of soil losses in agricultural areas.

Acknowledgements
Financial support for this work was provided by the USDA-ARS.

References
Albertson, M.L., Dai, Y.B., Jensen, R.A., Rouse, H., 1950. Diffusion of submerged jets. Trans. ASCE 115, 639-664.

Alonso, C.V., Bennett, S.J., Stein, O.R., 2002. Predicting headcut erosion and migration in upland flows. Water Resourc. Res. 38(12), doi:10.1029/2001WR001173.

Begin, Z.B., Meyer, D.F., Schumm, S.A., 1980. Knickpoint migration due to baselevel lowering. J. Waterway, Port, Coastal and Ocean Div. ASCE 106, 369-388.

Bennett, S.J., 1999. Effect of slope on the growth and migration of headcuts in rills. Geomorphology 30, 273-290.

Bennett, S.J., Casalí, J., 2001. Effect of initial step height on headcut development in upland concentrated flows. Water Resourc. Res. 37(5), 1475-1484.

Bennett. S.J., Alonso, C.V., Prasad, S.N., Römkens, M.J.M., 2000. An experimental study of headcut growth and migration in upland concentrated flows. Water Resourc. Res. 36(7), 1911-1922.

Brush, L.M., Jr., Wolman, M.G., 1960. Knickpoint behavior in noncohesive material: a laboratory study. Geol. Soc. Am. Bull. 71, 59-74.

Bryan, R.B., 1990. Knickpoint evolution in rillwash. In: Bryan, R.B. (Ed.), Soil Erosion—Experiments and Models. Catena Supplement 17, pp. 111-132.

Bryan, R.B., Oostwoud Wijdenes, D., 1992. Field and laboratory experiments on the evolution of microsteps and scour channels on low-angle slopes. In: Schmidt K.-H., de Ploey J. (Eds.), Functional Geomorphology: Landform analysis and models. Catena Supplement 23, pp. 1-29.

Bryan, R.B., Poesen, J., 1989. Laboratory experiments on the influence of slope length on runoff, percolation, and rill development. Earth Surf. Proc. Landf. 14, 211-231.

Casalí, J., López, J., Giráldez, J.V., 1999. Ephemeral gully erosion in Southern Navarra (Spain): description and measurement. Catena 36, 65-84.

Dietrich, W.E., Dunne, T., 1993. The channel head. In: Beven, K., Kirkby, M.J. (Eds.), Channel Network Hydrology. John Wiley & Sons, Chichester, pp. 175-219.

Elliot, W.J., Laflen, J.M., 1993. A process-based rill erosion model. Trans. ASAE 36, 65-72.

Gardner, T.W., 1983. Experimental study of knickpoint and longitudinal profile evolution in cohesive, homogenous material. Geol. Soc. Am. Bull. 94, 664-672.

Holland, W.N., Pickup, G., 1976. Flume study of knickpoint development in stratified sediment. Geol. Soc. Am. Bull. 87, 76-82.

Merritt, E., 1984. The identification of four stages during micro-rill development. Earth Surf. Proc. Landf. 9, 493-496.

Meyer, L.D., Harmon, W.C., 1979. Multiple-intensity rainfall simulator for erosion research on row sideslopes. Trans. ASAE 22, 100-103.

Meyer, L.D., Foster, G.R., Nikolov, S., 1975. Effect of flow rate and canopy on rill erosion. Trans. ASAE 18, 905-911.

Miller, J.R., 1991. The influence of bedrock geology on knickpoint development and channel-bed degradation along downcutting streams in south-central Indiana. J. Geol. 99, 591-605.

Mosley, M.P., 1974. Experimental study of rill erosion. Trans. ASAE 17, 909-913.

Nearing, M.A., Foster, G.R., Lane, L.J., Finkner, S.C., 1989. A process-based soil erosion model for USDA—water erosion prediction project technology. Trans. ASAE 32, 1587-1593.

Newman, B.G., 1961. The deflection of plane jets by adjacent boundaries – Coanda effect. In: Lachmann, G.V. (Ed.), Boundary Layer and Flow Control 1. Pergamon Press, pp. 232-264.

Parker, R.S., 1977. Experimental study of basin evolution and its hydrologic implications. Ph.D. Thesis, Colo. State Univ., Ft. Collins.

Piest, R.F., Bradford, J.M., Wyatt, G.M., 1975. Soil erosion and sediment transport from gullies. J. Hydraul. Div. ASCE 101, 65-80.

Pimentel, D., Harvey, C., Resosudarmo, P., Sinclair, K., Kurz, D., McNair, M., Crist, S., Shpritz, L., Fitton, L., Saffouri, R., Blair, R., 1995. Environmental and economic costs of soil erosion and conservation benefits. Science 267, 1117-1123.

Rajaratnam, N., 1976. Turbulent Jets, Development in Water Science, No. 5. Elsevier Scientific Publishing Co.

Rajaratnam, N., 1981. Erosion by plane turbulent jets. J. Hydraul. Res. 19, 339-358.

Renard, K.G., Foster, G.R. Weesies, G.A. McCool, D.K., Yoder, D.C., 1997. Predicting Soil Erosion by Water: A Guide to Conservation Planning with the Revised Universal Soil Loss Equation (RUSLE). USDA Agric. Handbk. No. 703.

Rhoton, F.E., Lindbo, D.L., Römkens, M.J.M., 1998. Iron oxides erodibility interactions for soils of the Memphis catena. Soil Sci. Soc. Am. J. 62, 1693-1703.

Robinson, K.M., 1989. Hydraulic stresses on an overfall boundary. Trans. ASAE 35, 1269-1274.

Römkens, M.J.M., Prasad, S.N., Gerits, J.J.P., 1995. Seal breakdown on a surface soil and subsoil by overland flow. In: So, H.B., Smith, G.D., Raine, S.R., Schafer, B.M., Loch, R.J. (Eds.), Sealing, Crusting and Hardsetting Soils: Productivity and Conservation. Australian Soc. Soil Sci., Brisbane, pp. 139-144.

Römkens, M.J.M., Prasad, S.N., Gerits, J.J.P., 1997. Soil erosion modes of sealing soils: a phenomenological study. Soil Tech. 11, 31-41.

Römkens, M.J.M., Prasad, S.N., Helming, K., 1996. Sediment concentration in relation to surface and subsurface hydrologic soil conditions. In: Proc., Sixth Federal Interagency Sedimentation Conf.. Las Vegas, NV, vol. 2, pp. IX-9-16.

Sawyer, R.A., 1960. The flow due to a two-dimensional jet issuing parallel to a flat plate. J. Fluid Mech. 9, 543-560.

Seginer, I., 1966. Gully development and sediment yield. J. Hydrol. 4, 236-253.

Seidl, M.A., Dietrich, W.E., Kirchner, J.W., 1994. Longitudinal profile development into bedrock: An analysis of Hawaiian channels. J. Geol. 102, 457-474.

Slattery, M.C., Bryan, R.B., 1992. Hydraulic conditions for rill incision under simulated rainfall: a laboratory experiment. Earth Surf. Proc. Landf. 17, 127-146.

Stein, O.R., LaTray, D.A., 2002. Experiments and modeling of head cut migration in stratified soils. Water Resourc. Res., v. 38, doi: 10.1029/20001WR001166.

Stein, O.R., Julien, P.Y., Alonso, C.V., 1993. Mechanics of jet scour downstream of a headcut. J. Hydraul. Res. 31, 723-738.

Thorne, C.R., Zevenbergen, L.W., Grissinger, E.H., Murphey, J.B., 1986. Ephemeral gullies as sources of sediments. In: Proc. Fourth Federal Interagency Sedimentation Conference, Las Vegas, NV. Vol 1, pp. 3-152 to 3-161.

U.S. Environmental Protection Agency, 1998. National Water Quality Inventory: 1998 Report to Congress. Report EPA841-R-00-001, Washington, D.C.

U.S. Environmental Protection Agency, 2000. The Quality of Our Nation's Waters, A Summary of the National Water Quality Inventory: 1998 Report to Congress. Report EPA841-S-00-001, Washington, D.C.

Uri, N.D., Lewis, J.A., 1999. Agriculture and the dynamics of soil erosion in the United States. J. Sustain. Agric. 14, 63-82.

Vandaele, K., Poesen, J., Govers G., van Wesemael., B., 1996. Geomorphic threshold conditions for ephemeral gully incision. Geomorphology 16, 161-173.

List of Figures

Figure 1. Schematic diagram of flume facility located at the USDA-ARS National Sedimentation Laboratory, Oxford, MS.

Figure 2. For different overland flow discharges, plots show the time variation of headcut brinkpoint position with constant rates of migration, sediment yield (discharge) with asymptotic trends, and average headcut aspect ratio with conservation of form (circles—all experiments, squares—only eight experiments; triangles—only one experiment; error bars show minimum and maximum values).

Figure 3. Time-averaged bed profiles of a steady-state headcut for two experiments showing morphologic self-similarity during headcut migration (error bars show minimum and maximum values).

Figure 4. Time-averaged vectors and streamlines for turbulent flow within a fixed headcut model. Flow discharge was 70.2 l min^{-1} and bed slope was 1%. Bed and water surface profiles also are shown.

Figure 5. Time-averaged vectors and streamlines for turbulent flow within a fixed headcut model. Flow discharge was 51.6 min^{-1} and bed slope was 5%. Bed and water surface profiles also are shown.

Figure 6. Normalized headcut profiles for experiments with varying discharge (time-averaged) and bed slope (not time averaged) showing collapse of the headcut profiles.

Figure 7. Comparison of measured and predicted values for the jet entry angle for both ventilated and unventilated nappes (data from Robinson (1989) and Bennett dataset). Also shown are the source and relative magnitude of the propagated errors of the estimate.

Figure 8. Comparison of measured and predicted values for the headcut scour depth. Also shown are the source and relative magnitude of the propagated errors of the estimate.

Figure 9. Comparison of measured and predicted values for the headcut rate of migration. Also shown are the source and relative magnitude of the propagated errors of the estimate.

Figure 10. Comparison of measured rates of sediment deposition and discharge and the predicted headcut erosion rate. Cause for the systematic departure is not known, but there may have been errors in determining the bulk soil density.

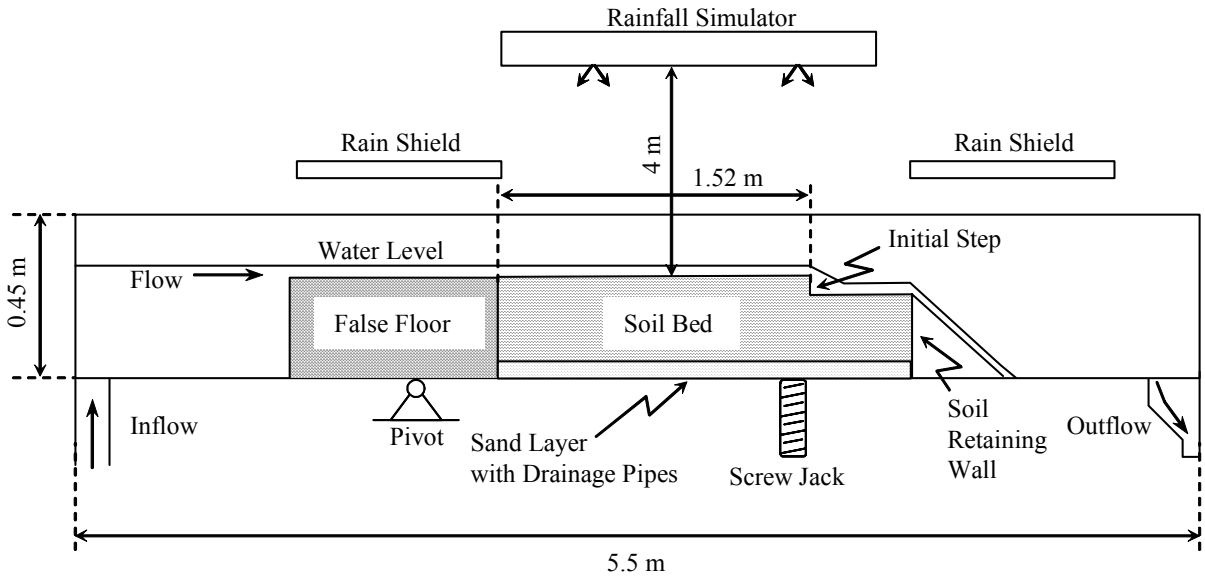

Figure 1. Schematic diagram of flume facility located at the USDA-ARS National Sedimentation Laboratory, Oxford, MS.

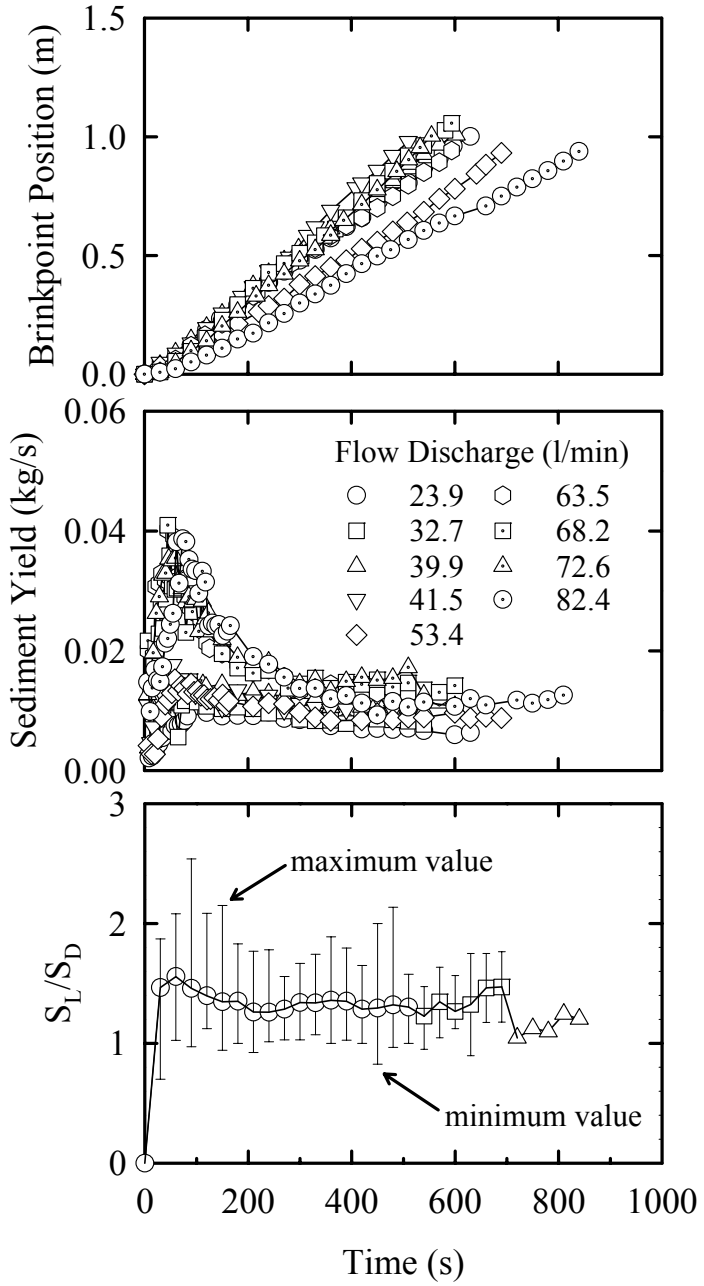

Figure 2. For different overland flow discharges, plots show the time variation of headcut brinkpoint position with constant rates of migration, sediment yield (discharge) with asymptotic trends, and average headcut aspect ratio with conservation of form (circles—all experiments, squares—only eight experiments; triangles—only one experiment; error bars show minimum and maximum values).

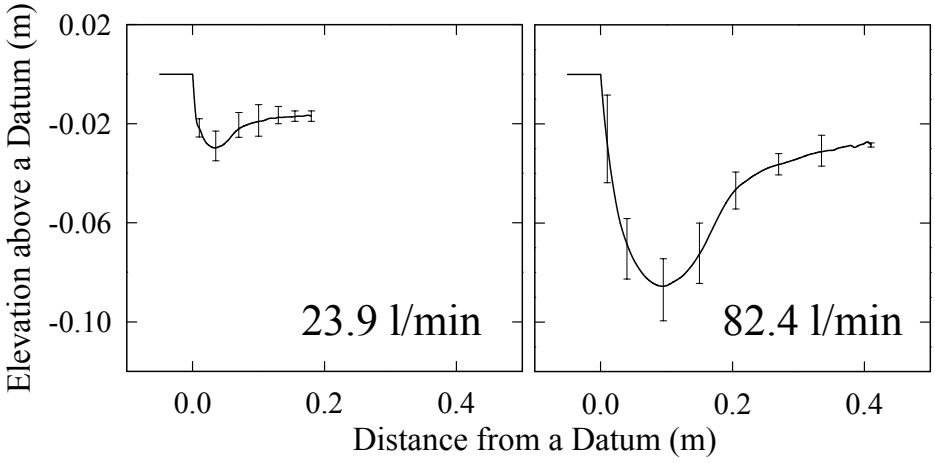

Figure 3. Time-averaged bed profiles of a steady-state headcut for two experiments showing morphologic self-similarity during headcut migration (error bars show minimum and maximum values).

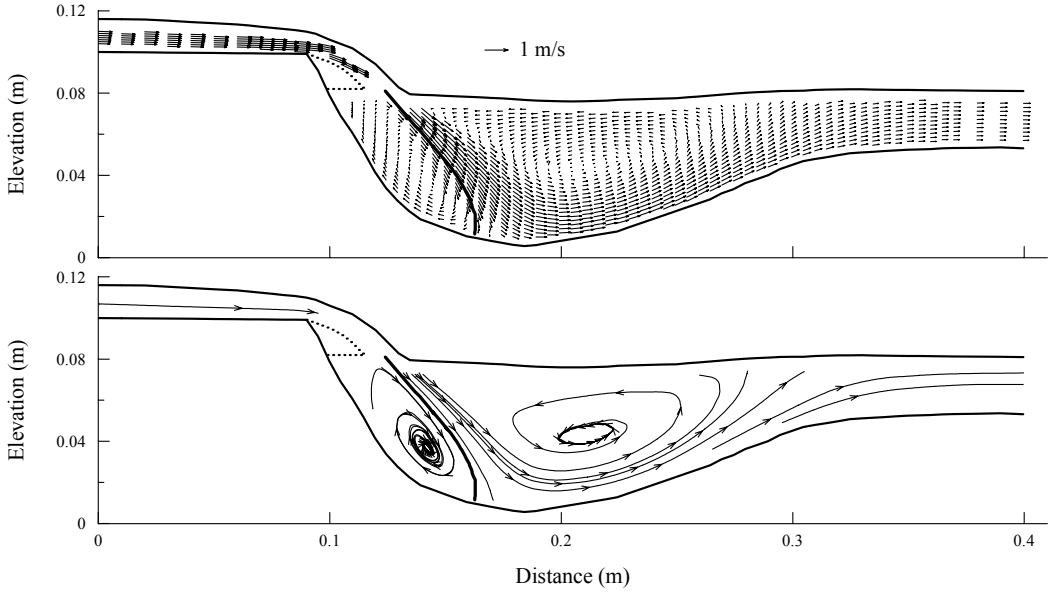

Figure 4. Time-averaged vectors and streamlines for turbulent flow within a fixed headcut model. Flow discharge was 70.2 l min^{-1} and bed slope was 1%. Bed and water surface profiles also are shown.

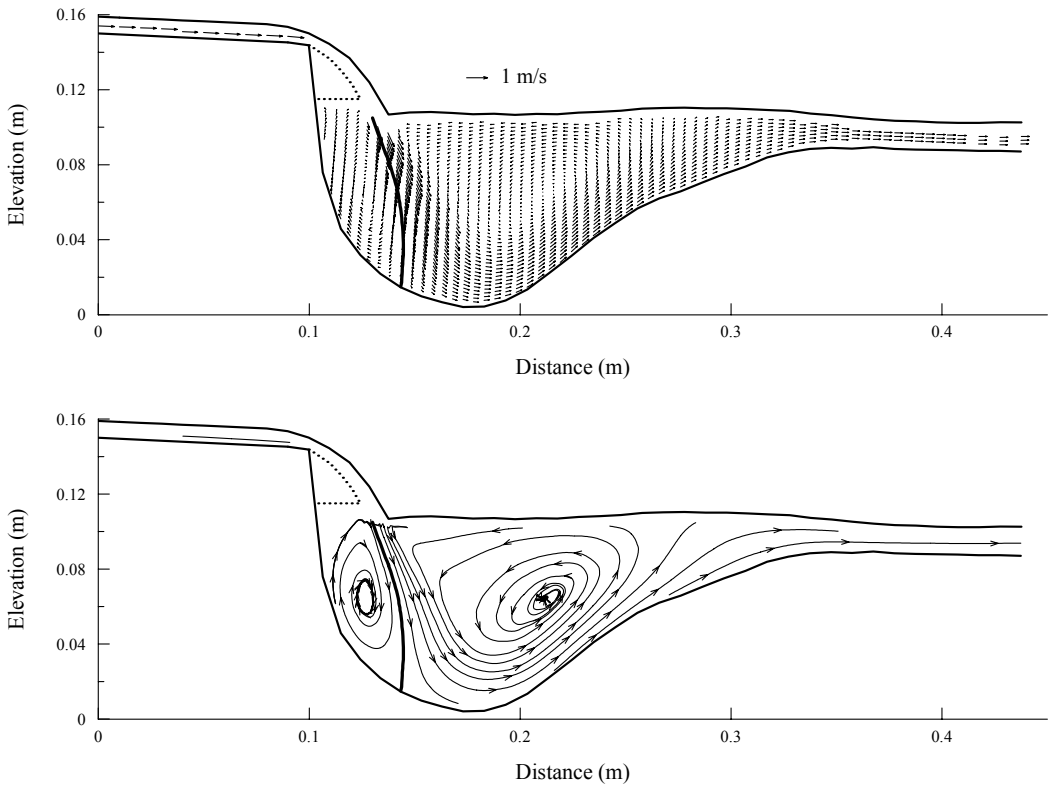

Figure 5. Time-averaged vectors and streamlines for turbulent flow within a fixed headcut model. Flow discharge was 51.6 min^{-1} and bed slope was 5%. Bed and water surface profiles also are shown.

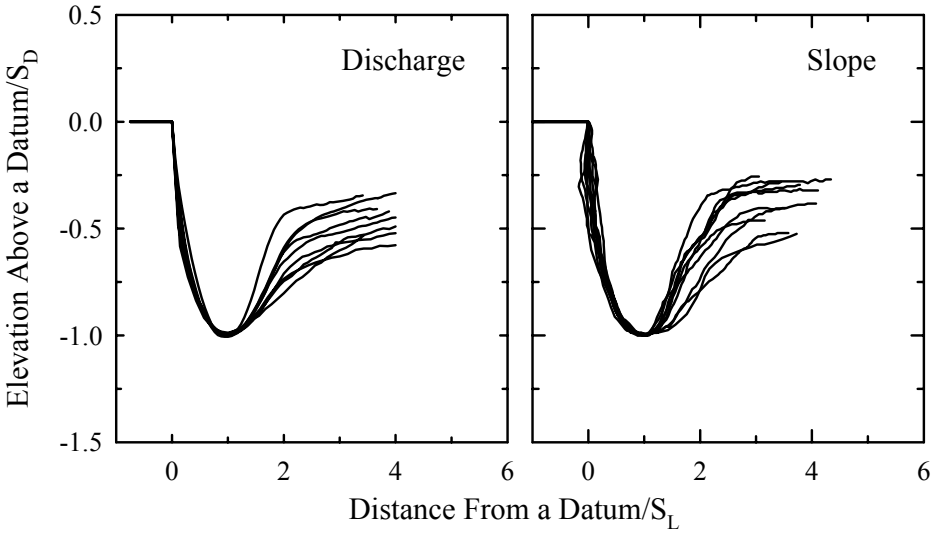

Figure 6. Normalized headcut profiles for experiments with varying discharge (time-averaged) and bed slope (not time averaged) showing collapse of the headcut profiles.

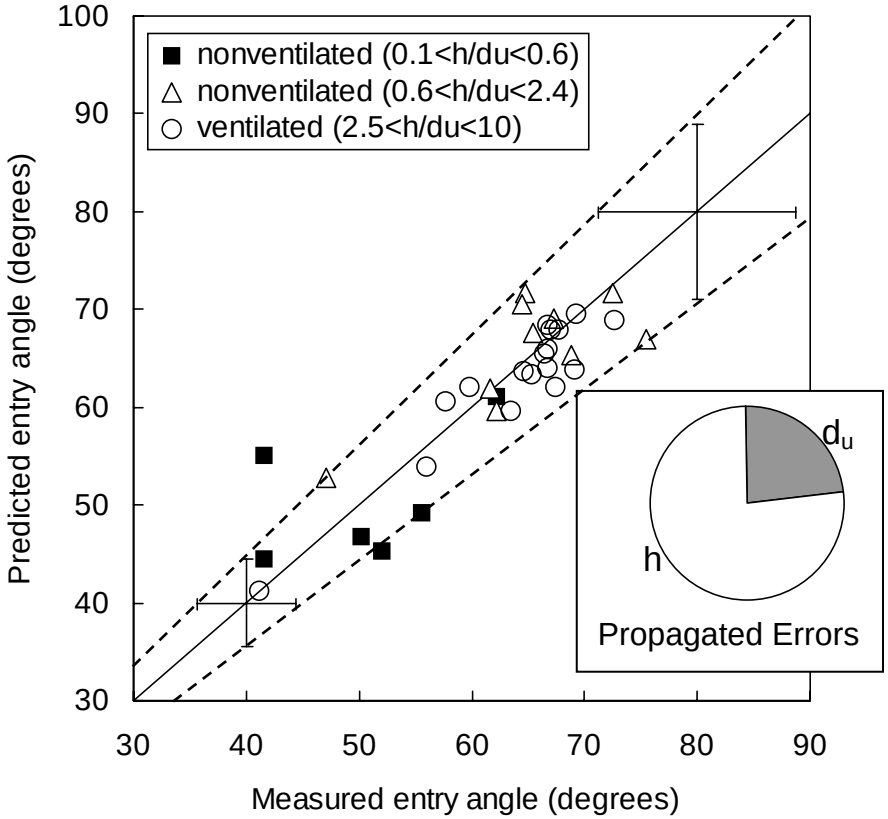

Figure 7. Comparison of measured and predicted values for the jet entry angle for both ventilated and unventilated nappes (data from Robinson (1989) and Bennett dataset). Also shown are the source and relative magnitude of the propagated errors of the estimate.

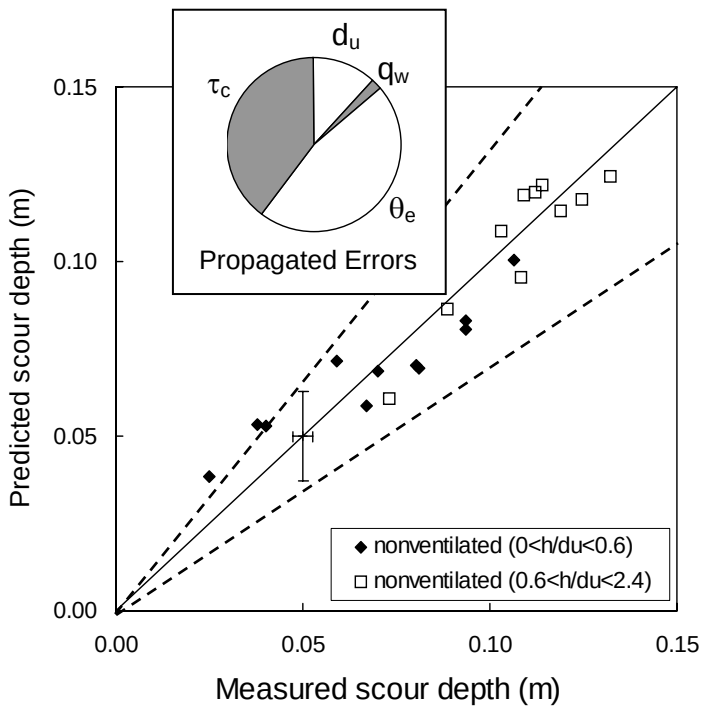

Figure 8. Comparison of measured and predicted values for the headcut scour depth. Also shown are the source and relative magnitude of the propagated errors of the estimate.

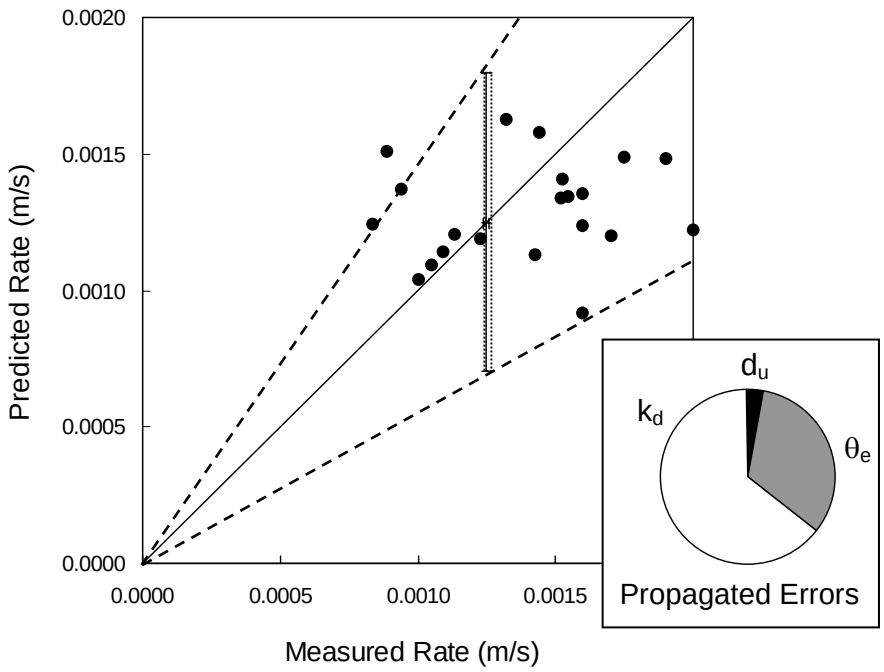

Figure 9. Comparison of measured and predicted values for the headcut rate of migration. Also shown are the source and relative magnitude of the propagated errors of the estimate.

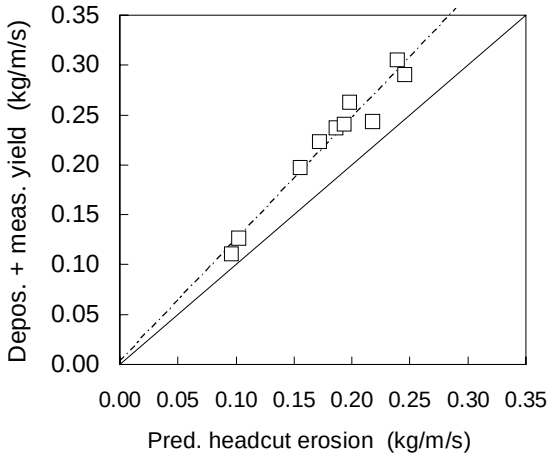

Figure 10. Comparison of measured rates of sediment deposition and discharge and the predicted headcut erosion rate. Cause for the systematic departure is not known, but there may have been errors in determining the bulk soil density.

Empirical-Numerical Analysis of Headcut Migration

W. Wu* (E-mail: wuwm@ncche.olemiss.edu)
S.S.Y. Wang (E-Mail: wang@ncche.olemiss.edu)
The University of Mississippi
National Center for Computational Hydroscience and Engineering
University of Mississippi
University, MS 38677

Abstract

Headcut migration is studied by using empirical and numerical modeling approaches. Empirical formulas for the headcut migration are established using available measurement data, which consider not only the flow strength but also the properties of soil. Numerical models for the headcut migration are proposed. The influences of dynamic pressure gradient,downward flow, bed slope and turbulence intensity on sediment entrainment are considered. The flow and sediment transport models are first tested against the measurement data for the flow and local erosion due to jet impingement below the fixed headcut or overfall, and then extended to simulate the headcut migration that is a moving boundary problem. The local erosion patterns and migration speeds of headcuts with one-layer and two-layer soils are calculated by the numerical models. The simulated results agree reasonably well with the measurements.

Keywords: headcut migration, empitical formula, numerical model

1. Introduction

A headcut is a vertical or near-vertical drop or discontinuity on the channel bed of a stream, rill or gully, at which a free overfall flow often occurs, as shown in Fig. 1. A headcut is usually eroded by the action of hydraulic stress, basal sapping, weathering, or the combination of these processes. Headcut erosion can accelerate the soil loss, increase the sediment yields in streams, damage an earth spillway, and disturb the bank stability. Therefore, the prediction of headcut migration is a very important task for engineers who design earth spillways and embankments, and evaluate soil loss and sediment yields.

A detailed examination of energy loss below a free overfall was conducted by Moore (1943). Rouse (1943) derived a relationship for the ultimate vertical thickness of the nappe, and Bakmeteff and Feodoroff (1943) discussed the difference of the behaviors of aerated and non-aerated nappes. Piest et al. (1975) described the importance of boundary tractive forces, sidewall erosion, mass failure and cleanout of wasted soil in headcut migration processes. Robinson (1992) experimentally studied the flow of water over a headcut. The shear stress and pressure on the vertical wall and basin floor were measured in a straight drop overfall model, and generalized equations were developed to predict the nappe profile, the magnitudes and locations of maximum shear stress and pressure on the boundaries in Robinson's study. Stein and Julien (1993) proposed a headcut stability parameter to determine the model of headcut migration. This stability parameter was defined as the ratio of the time required to erode the headcut surface from above to the time required to undermine the headcut surface from below. If the upstream erosion dominates, then the overfall gradually decreases and approaches an eroding channel bed. If the

*Corresponding author

downstream erosion dominates, then the headcut with a vertical surface migrates upstream with time. Robinson and Hanson (1995; also see Robinson, 1996) performed experiments to test large-scale headcut migration. The influences of varying overfall heights, flow discharges, backwater levels and soil properties on headcut advance were examined. The impact of placing a sand layer in the profile was also examined. Bennett et al. (1997) investigated the small-scale headcut migration in rills in an experimental flume, considering the effect of flow discharge and bed slope on headcut growth and migration.

To predict the headcut migration, Barfield et al. (1991) and Robinson and Hanson (1994) developed deterministic models, which calculate the boundary shear stress and the erosion on the vertical headwall face. The models predict mass failure by analyzing the stability of the headwall. The scour hole development was predicted in the model of Barfield et al. (1991). De Ploey (1989), Temple (1992) and Temple and Moore (1994) developed simple empirical models to describe the time-averaged headcut migration rate. These models relate the time-averaged headcut migration rate with the energy or energy change on the overfall and soil properties. These models can be easily used once the required parameters of hydraulic condition and soil property are known. Hanson, et al. (1997) analyzed the material-dependent coefficients in these three models by using their experimental data, and found that these coefficients are significantly related to the soil void ratio, dry unit weight, moisture content and so on.

Considering the complexity of the problem, we adopt here both empirical analysis and numerical simulation approaches to study the headcut migration. To achieve better predictions in a wider range of flow and soil conditions, the De Ploey's (1989) and Temple's (1992) empirical models are re-analyzed by using Robinson and Hanson's and Bennett et al.'s experimental data, and an empirical model to relate the fluvial erosion rate on the vertical headwall to the maximum shear stress acting on the headwall and the soil properties is also developed and verified. A numerical model is established to simulate the vertical two-dimensional headcut migration in details, which considers the hydraulic erosion on the vertical headwall of the headcut and the geotechnical failure of headcut due to the scour at the toe of headcut.

2. Empirical Analysis of Headcut Migration

2.1. Experimental Data Used in This Study

Two sets of experimental data are used in this study. One set was measured by Robinson and Hanson (1995) in large-scale headcut advance experiments in a 1.8*m* wide and 29*m* long outdoor test flume with 2.4*m* high side-walls. The test flume was filled by placing soil in horizontal loose layers of 0.15 to 0.20*m*. If necessary, water was added to achieve the desired soil moisture. A tiller was used to mix the soil layer and to reduce aggregate size. A 0.86*m* wide vibratory padfoot roller was used to compact each layer, and a hand-held pneumatic compactor was used to compact the soil against the flume walls. Compactive effort was varied by altering the number of compactor passes and using the vibratory head. The surface of the fill was protected by overlapped all-weather carpet strips or a 0.1m thick soil-cement surface layer to minimize the surface erosion and emphasize the headcut advance. There were 52 test cases with different flow discharges, overfall heights, backwater levels and different soil properties in Robinson and Hanson's experiments. A red sandy clay soil (CL) and a silty sand soil (SM) were examined in the experiments. The red sandy clay soil (CL) exhibited a liquid limit of 26, a plasticity index of 15, and a gradation of 25% clay, 40% silt and 35% sand. The silty sand displayed a liquid limit of 16 and a plasticity index of 3. The silty sand soil (SM) had 13% clay, 30% silt and 57% sand. Standard Proctor test on the CL soil exhibited a maximum dry density of

1900 kg/m^3 at optimum moisture of 12%, while the SM soil exhibited a maximum dry density of 1960 kg/m^3 at optimum moisture of 10.5%. The CL soil was used in forty-three test cases, and the SM soil was used in only two cases. In the other seven cases a 0.31*m* thick sand layer was placed at the bottom of CL soil in order to contrast the influence of a presumably more erodible layer on headcut advance, but these seven runs with an underlying sand layer are not analyzed in this study.

The other set of data was measured by Bennett et al. (1997) in the experiments of small-scale headcut advance in rills and crop furrows. The laboratory flume used was 5.5*m* long, and the test part was a soil cavity 2*m* long, 0.165*m* wide and 0.25*m* deep. The bed slope of the flume was 1%. The soil was packed incrementally in layers of 0.02*m* into the cavity. At the downstream end of the cavity a pre-formed headcut was constructed. The soil used was the parent material of the Ruston silt loam after being crushed and air-dried, which consists of 20.0% clay, 2.9% silt and 77.1% sand (all the sand was less than 2*mm* in diameter). Application of simulated rain produced a surface seal layer to negate any detachment of the soil material by the subsequent overland flow. The flow at the headcut overfall developed a scour hole downstream and then produced headcut erosion and upstream migration. The steady-state scour hole morphology and headcut migration were measured.

2.2. Analysis of De Ploey's (1989) and Temple's (1992) Empirical Models

Most of the empirical relationships for headcut migration have focused on energy at the overfall as the driving mechanism (Kohl et al., 1988; De Ploey, 1989; Temple, 1992; Elliot and Laflen, 1993; Temple and Moore, 1994). The De Ploey's (1989) formula relates the headcut migration rate to the kinetic energy at the overfall as

$$\frac{dl}{dt} = E_r q\left(g + \frac{u^2}{2h}\right) \tag{1}$$

where *dl/dt* is the headcut migration rate (*m/s*); E_r is a material-dependent coefficient for the headcut migration rate (s^2/m^2); *q* is the flow discharge per unit channel width (m^2/s); *g* is the gravitational acceleration (m/s^2); *u* is the mean velocity of flow at the overfall brinkpoint (*m/s*); and *h* is the headcut height (*m*).

The relationship proposed by Temple (1992) is

$$\frac{dl}{dt} = Cq^{1/3}H^{1/2} \tag{2}$$

where *C* is a material-dependent coefficient of headcut migration rate ($m^{-1/6}s^{-2/3}$); *H* is the elevation change in energy grade line through the headcut (*m*).

Using Robinson and Hanson's (1995) experimental data, Hanson et al. (1997) found that the parameters E_r and *C* are significantly correlated with the soil properties such as void ratio, dry unit weight, moisture content, etc. Among all the analyzed parameters the void ratio has the most significant effect. However, in Hanson et al.'s analysis the clay content was not considered. In this study, based on the same data, the relationships of the parameters E_r and *C* with the soil saturation degree and the clay content are analyzed. The relationships are shown in Figs. 2 and 3 and are represented by the regression equations

$$\log(E_r) = -4.726 s_t p_c^{0.2} - 2.156 \quad (3)$$

$$\log(C) = -4.516 s_t p_c^{0.2} - 1.179 \quad (4)$$

where p_c is the clay content; s_t is the saturation degree of the soil, defined as the ratio of moisture content and void ratio, $s_t = w_c G_s / e$; G_s is the specific gravity of the soil assumed equal to 2.67; w_c and e are the moisture content and void ratio of the soil.

Because the moisture content and saturation degree of the soil are not available in Bennett et al.'s (1997) experiment, Bennett et al.'s data are not included in Figs. 2 and 3. However, the bulk density and clay content of the soil were measured in both Robinson and Hanson's and Bennett et al.'s experiments. Therefore, the relationships of E_r and C with the bulk density and clay content of the soil are obtained using these two sets of experimental data, as shown in Figs. 4 and 5. Because the soils were compacted in Robinson and Hanson's experiments but not in Bennett et al.'s experiments, the values of E_r and C in Bennett et al.'s cases are much higher than in Robinson and Hanson's cases. The regression relationships in Figs. 4 and 5 read

$$\log(E_r) = -0.00575 \rho'_b \, p_c^{0.1} + 5.187 \quad (5)$$

$$\log(C) = -0.00451 \rho'_b \, p_c^{0.1} + 4.184 \quad (6)$$

where ρ'_b is the bulk density of the soil (kg/m^3).

2.3. Empirical Model for Superficial Erosion on Vertical Headwall of Headcut

The headcut migration can be attributed to the superficial erosion on the vertical headwall, the headcut toe erosion and the mass failure. To establish a dynamic model of headcut migration, all three factors should be considered. Empirical model for the superficial erosion is developed here, while the modeling of toe erosion and mass failure are investigated in the next section.

Because the plunge pool bed was fixed, the headcut migration in Hanson and Robinson's (1995) experiments was mainly due to the turbulent shear of the roller between the vertical headwall and nappe. Therefore, Hanson and Robinson's data can be used to quantify the relationship between the superficial erosion rate and the maximum shear stress on the vertical headwall. Since the shear stress was not directly measured in Hanson and Robinson's headcut migration experiments, the maximum shear stress on the headwall, τ_{vm}, is determined by using Robinson's (1992) empirical formula that was derived from his earlier experimental study of flow near the headcut. Fig. 6 shows the relationship of the headwall erosion rate *dl/dt* with the maximum shear stress on the headwall, the soil saturation degree and clay content. In Fig. 6 there are two points far away from the main trend. These two points were the first two runs in Robinson and Hanson's experiment series, in which the soils were compacted with larger loose lift layers and the uniformity of compaction might be questioned. The other points in Fig. 6 distribute along a curved data stripe, which can be represented by

$$\frac{dl}{dt} = a_1 \frac{\tau_{vm}}{M} + a_2 \left(\frac{\tau_{vm}}{M} \right)^2 + a_3 \left(\frac{\tau_{vm}}{M} \right)^3 \tag{7}$$

where M is a material-dependent parameter, and $M = \left(s_t p_c^{\ 0.2} \right)^2$; $a_1 = 1.783 \times 10^{-6}$, $a_2 = -8.063 \times 10^{-11}$ and $a_3 = 5.830 \times 10^{-12}$. The erosion rate *dl/dt* is in m/s.

The relationship using the bulk density and clay content as the soil properties is also shown in Fig. 7 and expressed as

$$\frac{dl}{dt} = \begin{cases} 0.0000625 \dfrac{\tau_{vm}}{M} & \dfrac{\tau_{vm}}{M} < 8 \\ 0.00977 - 0.00238 \dfrac{\tau_{vm}}{M} + 0.000153 \left(\dfrac{\tau_{vm}}{M} \right)^2 & \dfrac{\tau_{vm}}{M} \geq 8 \end{cases} \tag{8}$$

where $M = \left(1 - \rho'_b / \rho_s \right)^{-2} p_c^{\ 0.4}$; ρ_s is the density of the soil (kg / m^3).

3. Numerical Model of Headcut Migration

3.1. Hydrodynamic Model

The flow is simulated by using the model developed by Wu et al. (2000), which solves the Reynolds-averaged Navier-Stokes equations with the finite volume method on an adaptive, curvilinear, non-staggered grid. The pressure is calculated by the SIMPLE algorithm, with the momentum interpolation procedure of Rhie and Chow (1983) to avoid spurious oscillations usually encountered with the non-staggered grid. The convection terms are discretized by the HLPA scheme and three other schemes (Zhu, 1992). The effect of turbulence is determined with the $k - \varepsilon$ turbulence model. The effect of bed and bank roughness is taken into account with a wall-function approach. The boundary roughness is set as constant for rigid walls or calculated by van Rijn's(1984) method for movable beds. The water surface is calculated by a Poisson equation derived from the depth-averaged 2-D momentum equations for shallow open-channel flow but can be treated as a rigid lid in appropriate cases.

In the calculation of headcut migration, the boundaries vary with time due to the free-surface change, bed deformation and headcut migration. An adaptive-grid technique in the longitudinal direction is implemented to capture the moving boundary due to the headcut migration, combined with the original adaptive-grid technique in the vertical direction to trace the water-surface change and bed deformation. At each time step or iteration step, the computational grid is adapted after the calculations of water level, bed deformation and headcut migration.

3.2. Sediment Transport Model

The suspended-load transport is simulated by solving the general convection-diffusion equation with the finite volume method, the bed-load transport is calculated by a non-equilibrium transport model, and the bed deformation is determined by the mass-balance equation integrated over the water depth (Wu et al., 2000). The bed-load transport capacity and the equilibrium near-bed suspended-load concentration required in the model are calculated by van Rijn's methods (1984). Because the sediment transport process in the plunge pool below a headcut is strongly affected by the three-dimensional characteristics of the rapidly-varying flow, the empirical

functions for sediment transport in the uniform flow may not be applicable. Wu et al. (1999) proposed an approach to modify the van Rijn's (1984) formulas of bed-load transport capacity and near-bed suspended-load concentration for the simulation of local scour below headcut. Here, a different formulation is adopted, in which the modified van Rijn's formulas read

$$q_{b*} = 0.053\left(\frac{\rho_s - \rho}{\rho} g\right)^{0.5} \frac{d^{1.5}}{D_*^{0.3}} \left(\frac{\tau_e}{\tau_c} - 1\right)^{2.1} \tag{9}$$

$$c_{b*} = 0.015 \frac{d}{bD_*^{0.3}} \left(\frac{\tau_e}{\tau_c} - 1\right)^{1.5} \tag{10}$$

where q_{b*} is the equilibrium transport rate of bed load; c_{b*} is the equilibrium concentration of suspended load at the reference level; b is the distance from the reference level to the bed; D_* is the non-dimensional particle size parameter $D_* = d\left[g(\rho_s - \rho)/\rho\nu^2\right]^{1/3}$; ρ_s and ρ are the densities of sediment and water; g is the gravitational acceleration; ν is the kinematic viscosity; τ_c is the critical shear stress for the sediment incipient motion in the rapidly-varying flow, defined as

$$\tau_c = K_p K_d K_s \tau_{c0} \tag{11}$$

where τ_{c0} is the critical shear stress for sediment incipient motion from Shields curve. K_p is the correction factor to take into account the effect of dynamic pressure gradient on the vertical direction. The dynamic pressure gradient on the vertical direction decreases (or increases) the effective weight of sediment particles in water, and hence decreases (or increases) the critical shear stress required to move the sediment particles. K_p is expressed as

$$K_p = 1 + \frac{1}{(\rho_s - \rho)g} \frac{\partial p_d}{\partial z} \tag{12}$$

where p_d is the dynamic pressure, and z is along the vertical direction.

K_d is the correction factor due to the downward flow. The downward flow increases the acting area of tractive force on sediment particles, and then decreases the critical shear stress for sediment incipient motion. $K_d = 1/(1+\sin\beta)$, in which β is the impact angle of flow to the bed, defined as the angle between the near-bed resultant flow and the bed.

K_s is the correction factor to consider the effect of gravity on the incipient motion of sediment on steep bed slope. $K_s = \sin(\phi - \varphi)/\sin\phi$, in which φ is the bed slope angle with the horizontal, with positive values denoting the downslope bed; and ϕ is the repose angle of bed material. It should be mentioned that when the bed slope angle is close to the repose angle, K_s is close to zero, which has to be limited by imposing a small value.

The τ_e in Eqs. (9) and (10) is the effective tractive force including the bed shear stress and the stream-wise component of dynamic-pressure-gradient force, i.e.

$$\tau_e = \tau_b - \frac{a\pi}{6} d \frac{\partial p_d}{\partial s} \tag{13}$$

where τ_b is the bed shear stress due to the grain roughness. Because the method for τ_b used by van Rijn (1984) in the case of uniform flow is not appropriate to the case of the rapidly-varying flow below the headcut, in this study τ_b is directly set to the bed shear stress calculated by the flow model. However, to be consistent with the van Rijn's original formulas, the bed roughness height k_s that is used in the wall-boundary approach in the flow model is set as the grain roughness $3d_{90}$. The second term on the right-hand side of Eq. (12) considers the influence of the stream-wise dynamic pressure gradient; *s* is along the stream-wise direction near the bed, and *a* is a shape factor of particle, assumed as 1.

Compared Wu et al.'s (1999) approach, the present approach considers the effect of the gravity on the sediment transport in sloped channels in a different way. The effect of turbulence intensity is not considered in the present approach. Apparently, the present approach is simpler.

If the slope angle is larger than the submerged repose angle of sediment, a loose bed will collapse due to the gravity. This physical phenomenon has been considered in the calculation by adjusting the steeper bed slope to the submerged repose angle of sediment according to mass conservation.

3.3. Headcut Migration Model

There are three modes of erosion occurring at the headcut. The first mode is the superficial erosion along the vertical headwall due to the hydraulic shear of the flow. The second mode is the toe erosion due to the scour hole development in the plunge pool. After the superficial erosion and toe erosion develop to a certain extent, the headwall will exceed the criterion of stability and a mass failure will occur, which is the third mode of headcut migration. In reality, the mass failure occurs periodically in a very short time. Simulating this discontinuous phenomenon directly by numerical model is difficult because the collapsed block of soil will strongly disturb the flow field in the plunge pool. In this study, a time-averaged model of headcut migration is adopted.

The idealized configuration of a headcut is shown in Fig. 8. Bennett et al.'s (1997) experiments showed that the vertical headwall of the headcut and the curvature of the erosional surface are very similar between different experimental runs. Certainly, the height of the vertical headwall may be dependent on the soil properties and flow conditions, but it is found to be in a narrow range of 0.015-0.02*m* because the soils used in Bennett et al.'s (1997) experiments are nearly the same. The erosion rate on the vertical headwall due to the hydraulic shear of flow is determined with Eq. (8). In each time step Δt, Eq. (8) gives the erosion length Δl_s on the vertical headwall. From the calculation of sediment transport introduced above, the bed change Δz_2 at the center of the first control volume near the toe of vertical headwall in a time step Δt can be obtained, and the retreat length of the headcut due to the toe scour is given as $\Delta l_t = \Delta z_2 / \tan\phi$, as shown in Fig. 8. The real migration length of a headcut in the time step Δt is the maximum of Δl_s and Δl_t.

The above time-averaged headcut migration model simulates the headcut migration caused by the superficial erosion on the vertical headwall and the toe erosion, and gradually distributes the mass failure into the follow-up time steps. Actually, the frictional erosion on the vertical headwall surface and the toe erosion are the main factors of headcut advance because they induce the mass failure and wash out the wasted sediment debris. Therefore, the time-averaged model can grasp the main properties of headcut migration.

3.4. Model Testing against Experimental Data

The experimental run 2 of Bennett et al. (1997) is calculated in this study. Because the soil is cohesive, the submerged repose angle of sediment is set to be 40°. The critical shear stress, τ_{c0}, for the sediment incipient motion is set as $0.15pa$. Fig. 9 shows the calculated flow field in the plunge pool. Two recirculation eddies exist due to the jet impingement. One is near the water surface, and the other one is between the headwall and the nappe. Figs. 10 and 11 shows the comparisons between the measured and calculated scour hole morphologies, and between the measured and calculated brinkpoint migration distances with time. The model provides good predictions for the headcut migration rate and the scour hole profile below the headcut. Fig. 12 shows the calculated headcut migration process. It can be seen that the scour hole maintains a steady profile when the headcut migrates upstream.

4. Conclusions

Empirical models of headcut migration developed by De Ploey (1989) and Temple (1992), which relate the time-averaged headcut migration rate to the energy or energy change on the overfall and the soil properties, are re-analyzed by using Robinson and Hanson's and Bennett et al.'s experimental data. The material-dependent parameters E_r and C are related to the saturation degree, bulk density and clay content of the soil. An empirical relationship of the superficial erosion rate of the vertical headwall with the maximum shear stress on the headwall and the soil properties is developed. This new relationship is verified by using Robinson and Hanson's experimental data.

It is recognized that the sediment transport in the rapidly-varying flow with strong three-dimensional features has different mechanisms from that in uniform flow. In order to simulate the headcut migration, van Rijn's (1984) formulas for the bed-load transport capacity and the equilibrium near-bed suspended-load concentration are modified by considering the influence of the dynamic pressure gradient, downward flow and bed slope. To avoid simulating the discontinuous process of headcut migration, a time-averaged headcut migration model is adopted. The superficial erosion on the vertical headwall is determined with the newly developed empirical formula, and the toe scour is simulated with the sediment transport model implemented with the modified van Rijn's formulas. The real headcut migration rate is set as the maximum of the superficial erosion rate of the vertical headwall and the retreat rate of headcut due to the toe scour. This numerical model is tested in the calculation of the headcut migration experimentally studied by Bennett et al. (1997). The steady-state morphology of the scour hole below the headcut and the headcut migration rate calculated by the numerical model agree well with the experimental measurements.

5. Acknowledgements

This study is a part of the research project sponsored by the USDA Agricultural Research Service Specific Research Agreement No.58-6408-2-0062 (monitored by the USDA-ARS

National Sedimentation Laboratory) and the University of Mississippi. Drs. T. Kitamura, Y. Jia, K.M. Robinson and S. Bennett are acknowledged for their suggestion and comment to this study.

References

Bakmeteff, B.A., Feodoroff, N.V., 1943. Discussion of energy loss at the base of a free overfall written by W.L. Moore. Transactions, ASCE, 108, 1364-1373.

Barfield, B.J., Fogle, A., Froelich, D., Rohlf, R., 1991. Deterministic models of channel headwall erosion: Initiation and propagation. Report, University of Kentucky, Lexington.

Bennett, S.J., Alonso, C.V., Prasad, S.N., Romkens, M.J.M., 1997. Dynamics of headcuts in upland concentration flows. Proceedings of the Conference on Management of Landscapes Disturbed by Channel Incision. Mississippi, USA, pp.510-515.

De Ploey, J., 1989. A model for headcut retreat in rills and gullies. *CATENA*, Supplement 14, pp. 81-86, Cremlingen, Germany.

Elliot, W.J., Laflen, J.M., 1993. A process-based rill erosion model. Transactions of the ASAE, 36(2), 65-72.

Hanson, G.J., Robinson, K.M., Cook, K.R., 1997. Headcut migration analysis of a compacted soil. Transactions of the ASAE, 40(2), 335-361.

Kohl, K.D., Elliot, W.J., Laflen, J.M., 1988. Evaluating rill headcutting in the field. ASAE Paper No. 88-2596, St. Joseph, Mich., ASAE.

Moore, W.L., 1943. Energy loss at the base of a free overfall. Transactions of the ASCE, 108, 1343-1360.

Piest, R.F., Bradford, J.M., Wyatt, G.M., 1975. Soil erosion and sediment transport from gullies. J. Hydr. Div., ASCE, 101, 65-80.

Rhie, T.M., Chow, A., 1983. Numerical study of the turbulent flow past an isolated airfoil with trailing-edge separation. AIAA J., 21, 1525-1532.

Robinson, K.M., 1992. Predicting stress and pressure at an overfall. Transactions of the ASAE, 35(2), 561-569.

Robinson, K.M., 1996. Gully erosion and headcut advance. PhD Thesis, Oklahoma State University.

Robinson, K.M., Hanson, G.J., 1994. A deterministic Head-cut advance model. Transactions of the ASAE, 37(5), 1437-1443.

Robinson, K.M., Hanson, G.J., 1995. Large-scale headcut erosion testing. Transactions of the ASAE, 38(2), 429-434.

Rodi, W., 1993. Turbulence Models and Their Applications in Hydraulics. 3rd Edition, IAHR Monogragh, Balkema, Rotterdam.

Rouse, H., 1943. Discussion of Energy loss at the base of a free overfall written by W.L. Moore. Transactions of the ASCE, 108, 1383-1387.

Stein, O.R. and Julien, P.Y., 1993. Criterion delineating the mode of headcut migration. J. Hydr. Engrg., ASCE, 119(1), 37-50

Temple, D.M., 1992. Estimating flood damage to vegetated deep soil spillways. Applied Engineering in Agriculture, 8(2), 237-242.

Temple, D.M., Moore, J.S., 1994. Headcut advance prediction for earth spillways. ASAE Paper No.94-2540, St. Joseph, Mich., ASAE.

Van Rijn, L.C., 1984. Sediment transport, part I: Bed Load Transport. J. Hydr. Engrg., ASCE, 110(10).

Wu, W., Rodi, W., Wenka, T., 2000. 3D numerical modelling of flow and sediment transport in open channels. J. Hydr. Engrg., ASCE, 126(1), 4-15.

Wu, W., Wang, S. S.Y., Jia, Y., Robinson, K.M., 1999. Numerical simulation of two-dimensional headcut migration. The 1999 International Water Resources Engineering Conference, Seattle, USA. (on CD-ROM)

Zhu, J., 1992. An introduction and guide to the computer program FAST3D. Research Report, Institute for Hydromechanics, Karlsruhe University.

List of Figures

Figure 1. Schematic Diagram of Headcut

Figure 2. Relationship of E_r with Saturation Degree and Clay Content of Soil

Figure 3. Relationship of C with Saturation Degree and Clay Content of Soil

Figure 4. Relationship of E_r with Bulk Density and Clay Content of Soil

Figure 5. Relationship of C with Bulk Density and Clay Content of Soil

Figure 6. Relationship of Headwall Erosion Rate and $\tau_{vm} /(s_t^{\ 2} p_c^{\ 0.4})$

Figure 7. Relationship of Headwall Erosion Rate and $\tau_{vm} \left(1 - \rho'_b / \rho_s\right)^2 \big/ p_c^{\ 0.4}$

Figure 8. Headcut Migration due to Toe Scour

Figure 9. Calculated Steady-State Velocity Vectors and Magnitudes below a Headcut in Bennett et al.'s (1997) Experiments (Run 2)

Figure 10. Steady-State Scour Hole Profile

Figure 11. Brinkpoint Migration with Time

Figure 12. Calculated Headcut Migration Process (Run 2)

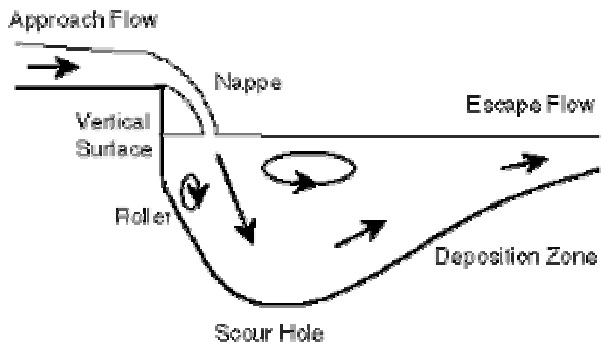

Figure 1. Schematic Diagram of Headcut

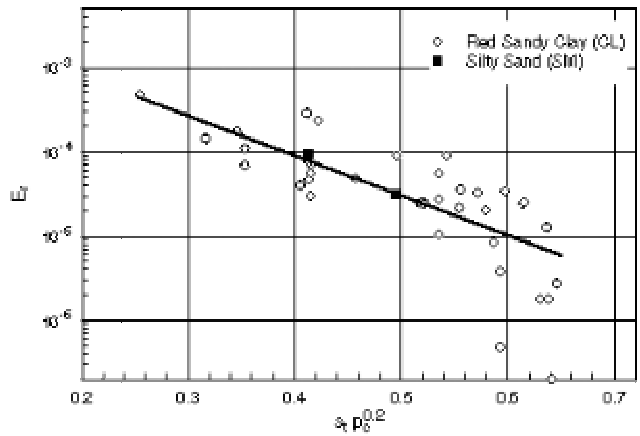

Figure 2. Relationship of E_r with Saturation Degree and Clay Content of Soil

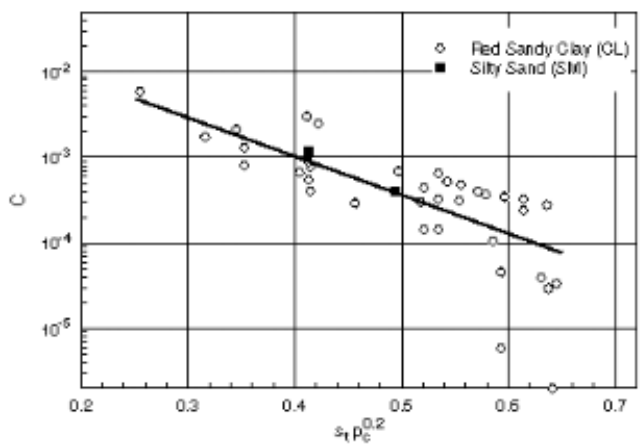

Figure 3. Relationship of *C* with Saturation Degree and Clay Content of Soil

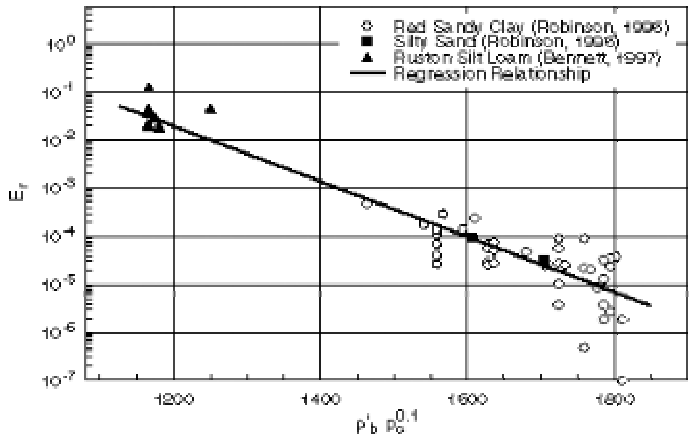

Figure 4. Relationship of E_r with Bulk Density and Clay Content of Soil

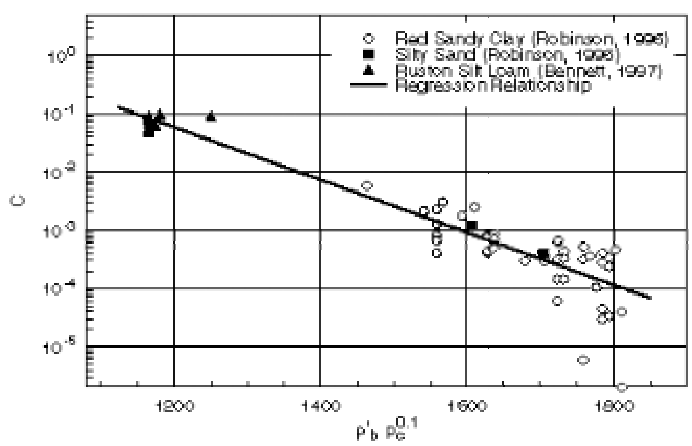

Figure 5. Relationship of *C* with Bulk Density and Clay Content of Soil

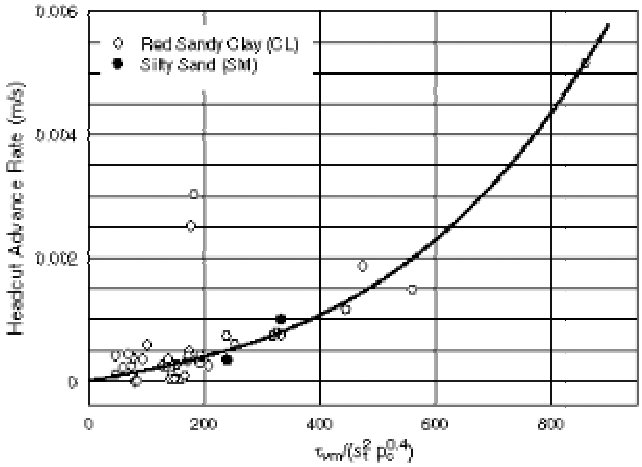

Figure 6. Relationship of Headwall Erosion Rate and $\tau_{vm}/(s_t^{\,2} p_c^{\,0.4})$

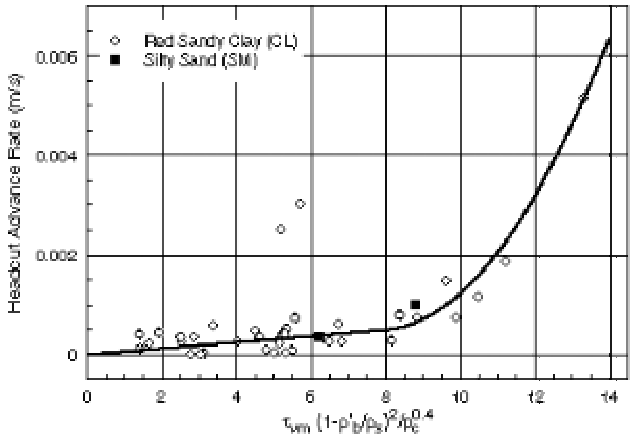

Figure 7. Relationship of Headwall Erosion Rate and $\tau_{vm}\left(1-\rho'_b/\rho_s\right)^2 \big/ p_c^{\,0.4}$

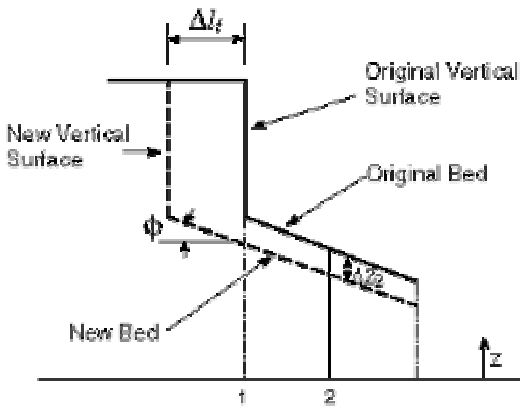

Figure 8. Headcut Migration due to Toe Scour

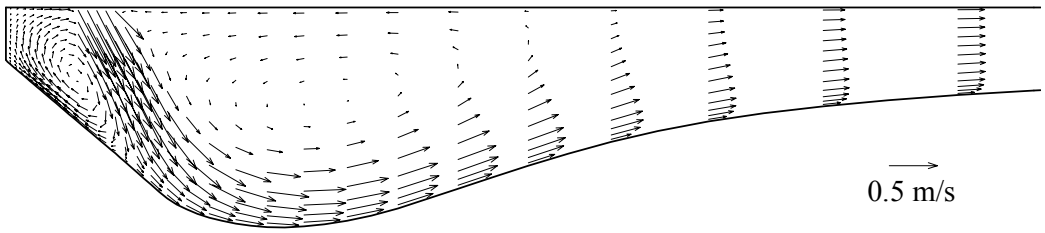

Figure 9. Calculated Steady-State Velocity Vectors and Magnitudes below a Headcut in Bennett et al.'s (1997) Experiments (Run 2)

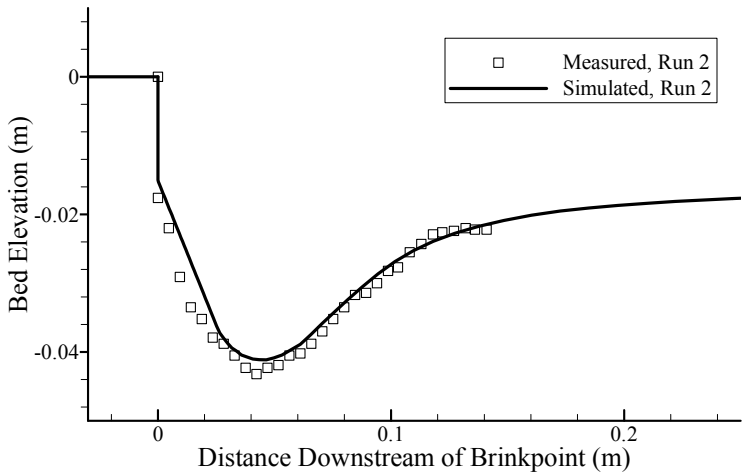

Figure 10. Steady-State Scour Hole Profile

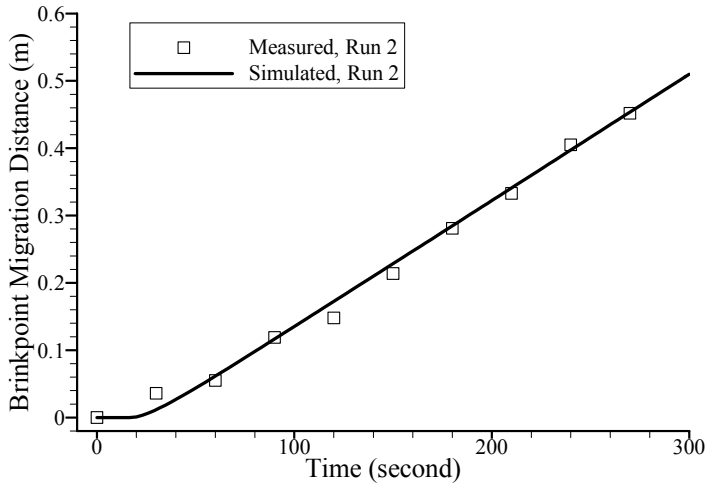

Figure 11. Brinkpoint Migration with Time

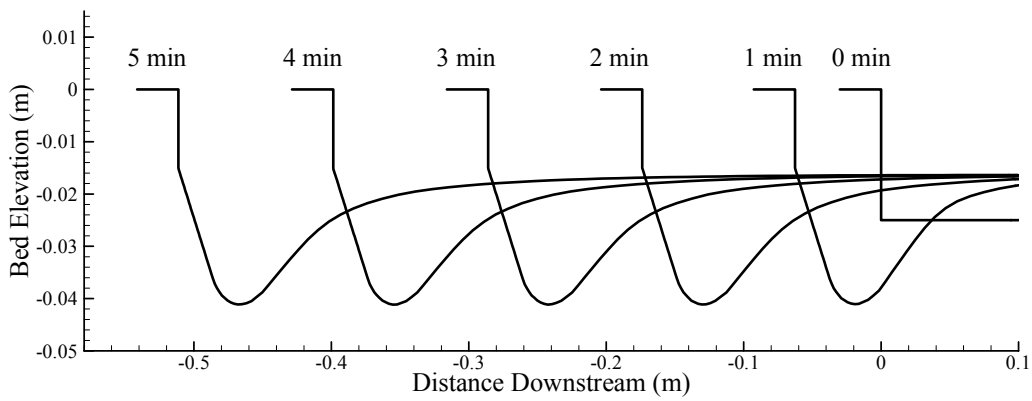

Figure 12. Calculated Headcut Migration Process (Run 2)

Computer Modeling of Erosion and Sediment Delivery

Yong G. Lai*
Bureau of Reclamation
Sedimentation and River Hydraulics Group (D-8540)
Denver, CO 80225, USA

C. Ted Yang
Colorado State University
Fort Collins, CO, USA

Abstract

This presentation summarizes the concept and preliminary progresses of a multi-year project on the development of a computer model, GSTARS4, for erosion on watershed and sediment delivery to river systems. Extensive literature review reveals that existing erosion models are limited by various simplifying assumptions and intended target use. A model that can be used for predicting the Total Maximum Daily Load (TMDL), with reasonable confidence, is still lacking. The objective of this project is to develop a unified computer model incorporating the unified erosion theories and useful to sediment TMDL estimation.

GSTARS4 model is a physically-based, process-oriented, and distributed model. It builds on years of experience in sediment and erosion research and practice at the Bureau of Reclamation. It also incorporates the latest technologies of other leading models. GSTARS4 consists of two major sub-models: the sediment delivery erosion model and the channel/reservoir system model, with a seamless integration of the two. The erosion model adopts a new overland hydrology methodology that uses combined kinematic, diffusive-wave and dynamic routing. Flexible meshing strategy is adopted with the Arbitrarily Shaped Element Method (ASEM) for geometry representation. ASEM unifies existing grid strategies and numerical formulations under one framework and facilitates modeling of widely varying scales. The overland erosion model incorporates the latest sheet, rill and gully erosion research results and is based on the minimum energy dissipation rate theory or its simplified minimum unit stream power theory. Under this theory, sheet, rill and gully erosion, as well as the sediment transport in the channel/reservoir system, are modeled under one unified approach. The channel/reservoir sediment model is based on GSTARS3 with some adaptations and enhancements. The channel/reservoir model allows arbitrary channel cross-sections, quasi-three-dimensional alluvial channel evolution with bank erosion, and extensive reservoir modeling. The same method is also used to model channels such as classical gullies, which is not available in most existing models.

Presentation will focus on the progress which has been made so far. A preliminary case study is presented to show the potential benefits of the proposed GSTARS4 methodology. The watershed hydrological component of the model will be demonstrated with laboratory as well as field cases.

Keywords: computer modeling, erosion and sedimentation delivery, unified erosion theory

*Correspondence author

AnnAGNPS & Ephemeral Gullies

F. D. Theurer* (E-Mail: Fred.Theurer@verizon.net)
USDA, NRCS, NWCC
7413 Cinnabar Terrace
Gaithersburg, MD 20879-4575

R.L. Bingner (E-Mail: rbingner@ars.usda.gov)
USDA National Sedimentation Laboratory
598 McElroy Drive
Oxford, MS 38655

J. Stafford
USDA, NRCS, OH

W. Merkel
USDA, NRCS, NWCC
Gaithersburg, MD

Abstract

Ephemeral gully erosion is a significant source of cropland erosion. With the installation of best management practices (BMPs) for sheet & rill erosion protection, the magnitude of gully erosion becomes very important. AnnAGNPS includes a gully feature that accepts regression coefficients generated from an event-type, ephemeral gully model (EGEM) developed and supported by NRCS. This paper will explain how the gullies are described for input to EGEM, how the regression coefficients are generated, and how AnnAGNPS uses this gully data to calculate gully erosion, yield, and loading. Data from the Upper Auglaize watershed, which is in the Maumee River basin, will be presented to shown the significance of gully versus sheet & rill erosion. The significance of the source of the sediment is important when planning and implementing BMPs to reduce sediment from cropland reaching the Toledo Harbor.

Keywords: ephemeral, gullies, model, erosion, sediment

*Correspondence author

Evaluation of Rill and Ephemeral Gully Erosion in Cultivated Areas of Navarre (Spain)

L.M. De Santisteban* (E-mail: luisa.satinsteban@unavarra.es)
J. Casalí (E-mail: jcs@unavarra.es)
J.J. López (E-mail: jjlr@unavarra.es)
Department of Projects and Rural Engineering, Universidad Pública de Navarra
Campus de Arrosadia s/n, 31006 Pamplona (Navarra), Spain
Fax: 34 948 169148

Abstract

Although there are many evidences of intense soil erosion in cultivated areas of Navarre (Spain), scarce information is currently available regarding soil loss rates and their effects, spatial and temporal distribution of erosion and factors controlling the processes involved. Rills and ephemeral gullies are frequently responsible of a high percentage of total soil erosion, and these erosion types can be considered as a good approximation to the minimum erosion rates. With the main purpose of determining the annual soil loss rates in cultivated areas of Central Navarre, a detailed and continuous assessment of rainfall in a ten minutes basis and of rill and gully erosion was made in 19 small watersheds, representative of wide Navarrese and Spanish areas, located in three different town councils (study areas). After detailed topographic surveys, maps of most watersheds were also obtained. Seventeen of the watersheds were selected randomly among those affected by ephemeral gully erosion at the moment of starting the field surveys, and were cultivated with winter grains or vineyards. The other two watersheds remained uncultivated (abandoned) after around ten years. Watershed surface areas ranged between 0.1 and 1.4 ha, and the average slopes ranged between 2.0 and 9.0 %. Prevalent texture class was silty-loam. The study period ranged from 1995 to 2001. Rill and ephemeral gully cross sections size and shape were determined by using a 1 m wide micro-topographic profile meter, provided with fifty 1 m long pins. The distance between the measured cross sections was determined with a tape, so that the total rill or gully volume could be calculated. In total, 632 cross sections were very precisely described, processing information from 31,600 pins. Erosive events happened every year in all three study areas during the study period. For cereal watersheds, soil losses were caused by only one or two rainfall events each year. This erosive events mainly happened in early winter and in humid summers, when an early tillage well before seeding was possible. High erosion rates were found (0.20-11.50 kg m^{-2} y^{-1}), well exceeding in several cases the maximum local soil loss tolerances, despite that in only one of the studied years rainfall reached the annual average depth. In vineyards, soil losses were caused by many or several rainfall events per year, and they could be found in any season. This is due to the small percentage of surface covered by the crop throughout the year, and to the management practices as well, since they are oriented to keep the soil bare to avoid competition for nutrients and water. Again, high erosion rates were found (0.33 y 16.19 kg m^{-2} y^{-1}). No tillage practices arises as an effective conservation measure, because no erosion was observed in watersheds cultivated in that way during the study period. From this large data set, it can be concluded that rill and ephemeral gully erosion can be very significant in Mediterranean regions, and much more attention should be paid to the problem.

*Corresponding author

Keywords: assessment of erosion; rill erosion; ephemeral gully erosion; abandoned plots; Spain; Navarre

1. Introduction

Soil erosion by water on cultivated areas is considered as a very important environmental problem around the world, in Spain and in Navarre (Walling and Webb, 1996). Nevertheless, and even in developed countries and regions as the case of Spain and Navarre, the real extension of the phenomenon and its consequences remain basically unknown. Despite the quite spread social concern, it is not possible today, in most cases, to answer questions like: which are the erosion rates in a certain location, with a certain soil use and management?; are that rates tolerable?; which are the most important erosion classes in a certain location or region?; which are the economic and environmental consequences of erosion?; which are the most suitable methods of erosion control in a certain context?; which are the effects that recent events like land abandonment and agricultural mechanization have on soil erosion?; how important is soil erosion on irrigated lands? On table 1, main available information on soil erosion in Navarre is shown. From it, it can be stated that: a) there is very few information on erosion rates; b) it is constrained to few locations and collected along short periods of time; c) that information is mainly limited to agricultural lands; d) high erosion rates have been detected. Such lack of information is even more relevant regarding all Spain.

Ephemeral gullies are channels of various size formed by the scouring of concentrated surface runoff flowing on erodible soils during rain events (Foster, 1986; Thorne et al., 1986). In many cases the channels are refilled by the farmers, shortly after the rains, but they reappear in the next rainy season. While the presence of rills is restricted to planar elements of watersheds, ephemeral gullies occur on valley bottoms or within swales. Ephemeral gully systems are common in cultivated soils in many areas around the world (Bennett et al., 2000; Poesen et al., 2003). Rill erosion consists on the development of numerous minute closely spaced channels resulting from the uneven removal of surface soil by running water that is concentrated in streamlets of sufficient discharge and velocity to generate cutting power. It is an intermediate process between sheet erosion and gully erosion (Jackson, 1997).

Ephemeral gully and rill erosion are common types of water erosion in the loamy soils formed on the Miocene Marls of Southern Navarra. A study was conducted by Casalí et al. (1999) to describe the different types of ephemeral gullies and to determine their origin, evolution and importance as sediment sources. Three main ephemeral gully types were identified according with their origin: classic ephemeral gullies formed within the same field where runoff starts, drainage ephemeral gullies collecting the runoff from another upstream area, and discontinuity ephemeral gullies due to some abrupt slope change in the landscape. During two consecutive years of normal precipitation, ephemeral gully erosion caused significant soil losses in the study area. In each year, one short and intense rainfall event was responsible for almost all soil losses from ephemeral gullies. Conventional tillage practices provoked gully occurrence, while the maintenance of stubble or vegetation cover completely prevented their formation. Early winter was the most critical period for gully formation, when the soil is wetter and the surface cover is scarce.

Despite the existence of this previous work, there is the need for much more information regarding other areas and obtained after a much longer period of time.

Consequently, the objectives for the work whose main results are shown in this paper, were: 1) have a better knowledge of the importance of soil erosion in Navarre through the

assessment of annual erosion rates due to rills and ephemeral gullies in a number of different cultivated or abandoned agricultural lands, representative of wide Navarrese regions; 2) identify and describe the main factors that control rill and ephemeral gully erosion. To achieve these objectives, 19 small watersheds located in three different town councils in Central Navarre were selected. Among them, 10 cultivated with winter grains or sunflower; 6 were cultivated with vineyards; 1 with both winter grains and vineyards; the reminding two were abandoned during last years. Within the watersheds, frequent and detailed field assessments of rills and ephemeral gullies were made, as well as detailed measurements of rainfall. The study period covered in this paper ranged from October 1999 to September 2001, although other previous information from 1993 to 2001 is also analyzed with the purpose of providing a wider view of the problem.

2. Description of the Study Areas

The studied watersheds were spread through the town councils of Tafalla, San Martín de Unx and Pitillas (figure 1). On figure 2, the topographic maps of that watersheds where specific surveys were done, are shown. The usual location of ephemeral gullies is also indicated. On tables 2 and 3, additional characteristics of the watersheds and of the study areas are summarized. The watersheds were selected randomly at the beginning of the field work, among typical ones in the different town councils, and after observing active erosion within them following rainfall events. For the case of watersheds located in Pitillas, this paper is an extension of the previous works made by Casalí *et al*. (1999), who selected the watersheds studied there according with the same criterion.

Climate in the study areas (tables 2 y 3) can be classified as Continental Mediterranean, with average annual temperatures around 13.5 ºC and average annual rainfall depths od around 500-600 mm. Rainfall erosivity, here defined by the USLE *R* factor (Wischmeier and Smith, 1978) can be considered as low, if compared with other Spanish regions (ICONA, 1988).

Some properties of the soils that cover the watersheds, all of them corresponding to the Ujué Facies, which extends over around 62,000 ha in Navarre, can be observed on tables 2 y 3. Although there are remarkable differences among these soils, they share some of their characteristics, like the high silt content and the presence of salts, as well as the relatively high erodibility, according with the estimated values of USLE *K* factor (Wischmeier and Smith, 1978). In the study areas, intense erosion processes occurred, as can be seen on figure 3.

Fields cultivated with winter grains are sown at the beginning of October, after preparing the seedbed with a moldboard plow or a chisel pass. A common practice of some farmers of this region is to leave a fallow every other year, although the benefits of this practice in terms of water economy are not granted. Average cereal yields are low, about 3,000-4,000 kg ha^{-1} y^{-1}, with great inter-annual variability.

On vineyards, moldboard plow or a chisel passes are frequent, trying to remove any kind of vegetation to avoid competition for water and nutrients. As a consequence, soil reminds most time poorly protected against rainfall events, and field assessments of rills and gullies must be made very frequently.

3. Results and Discussion

The selected watersheds were visited after every relevant rainfall event since October 1999, describing the evolution of the observed erosion, and assessing several times rill and gully volumes (tables 2, 3 and 4). In total, 632 cross sections were very precisely described, and information from 31,600 pins was processed.

On watersheds cultivated with winter grains, one only annual field measurement was made, in summer, and before the preparation of the seedbed. Such annual field measurement is enough to known the amount of erosion occurred in a growing season, because from seeding to seedbed preparation, the rills and gullies formed are not affect by any tillage operation. Any way, in rainy summers, some tillage was made previous to seeding, obliterating the present rills and gullies. It caused that some information were lost, as it was impossible to measure the rill and gully volumes before tillage in all cases. Not always rill erosion was assessed because at the beginning of the research project, the attention was mainly focused on ephemeral gully erosion (tables 2, 3 and 4).

As explained above, much more frequent measurements were required in watersheds cultivated with vineyards. Nevertheless, it was not always possible to assess erosion volumes after each tilling operation. Consequently, some erosion episodes were not completely assessed. Another additional obstacle in vineyards was the presence of structures like spaliers or trellis, that made the transit through the fields very uncomfortable, increasing greatly the required time for field assessments. As shown on table 2, one only field assessment was made in the abandoned plots.

Gully cross section areas were measured with a profiler (Smith, 1993; Casalí et al., 1999), whereas the distance between cross sections was measured with a tape. The eroded soil volume within channel reaches were estimated by the product of the average cross section of every reach times the distance between the successive cross sections.

For a precise characterization of rainfall, several rain gauges were placed in the study areas.

On figure 4, daily rainfall recorded during the study period, and the accumulated annual hyetograph are shown. These data were collected by our own rainfall gauges up to 1 minute basis (is he case for Pitillas y San Martín de Unx, figure 1), and by the automated rainfall gauge of Tafalla, operated by the Government of Navarre. On that figure, the rainfall events that caused erosion at least in one of the watersheds are indicated by one arrow. For the case of Pitillas, data recorded before October 1999 (Casalí et al., 1999) are also included, in order to consider a wider scenario.

The presence of the three ephemeral gully types previously identified by other authors was confirmed for the three study areas.

During the two complete years considered and within the three study areas, total annual rainfall depths, lower than the historical average values (tables 2 and 3). Exceptional rainfall rates were not recorded, being the maximum daily rainfall of around 40 mm, what corresponds to low return periods.

In the two study areas cultivated with winter grains, the high annual erosion rates (figure 5) were caused by only one or two erosive rainfall events during the year (figure 4). Such erosive events usually happened at the beginning of the winter, with almost bare soil and high soil moisture contents, and in summer, during thunderstorms, if the soils are unprotected. Erosion control measurements, like direct drilling used in Cobaza 1 and Cobaza 2 watersheds, were very effective, preventing almost completely the formation of new rills or gullies. A permanent presence of vegetation or stubble on the cultivated plots, what is not very frequent in the study area, seemed to be enough to almost completely avoid rill and ephemeral gully erosion.

In the areas cultivated with vineyards, erosive events happened more frequently (between 2-5 a year) and in any time during the year (figure 4). Consequently, the erosion rates were higher than in winter grain plots (figure 5). In fact, the erosion rate at Navafría watershed

reached up 16 kg m^{-2} y^{-1}. Besides, this rate seems to be the closest to the real annual rates in the area, because Navafría 1 watershed, exceptionally, was not was not ploughed during one complete year. So, the only field assessment made there corresponds to the annual value (table, 3, figure 5).

On table 4 additional characteristics of rill and gully systems in the cultivated watersheds can be seen. In general, ephemeral gully erosion was responsible of more soil losses than rill erosion (figure 5). During all the time periods considered and within the three study areas, erosive events happened, causing in many cases high erosion rates, well above the tolerances usally accepted, despite that: a) total annual rainfalls depths were close or lower than the historical average values and exceptional rainfall rates were not recorded; b) some intense erosive events, documented from visits of the authors and from pictures, could not be assessed at all, like the one in August 1997, because the plots were ploughed very soon by the farmers, being that statement even more valid for the case of vineyards; c) rill erosion rates were not assessed in some watersheds at the beginning of the study period; d) sheet erosion rates were not assessed either.

On the other hand, soil erosion tolerances are not known either but, there can be no doubt that they are in general quite much lower than the 1.12 kg m^{-2} y^{-1} accepted as a maximum, because soils are quite shallow and most soils in the study area could be considered as nonrenewable (Hall et al., 1985).

According with these results, in many other Spanish and Navarrese areas high erosion rates can be expected. For example, among the thousands hectares cultivated with vineyards and with other species that require a similar management, like almond and olive trees, crops that are very important for the Spanish economy. Besides, such crops are particularly spread on the Spanish regions more prone to desertification.

On table 5, main results of the field assessments for the abandoned plots are shown. Short time after abandonment, a dense network of rills and gullies developed. Average soil losses from rills and gullies were about 12.0 kg m^{-2} y^{-1}. Ephemeral gully erosion rates were again higher than the erosion rates due to rill erosion. Recently, wild vegetation slowly covered the soil surface in La Abejera (A) watershed, greatly decreasing gully and rill growth rate. It did not happen at Pikarana watershed because of the constant sheep grazing. Despite that the surface area covered by this studied abandoned plots is very small, the results suggest that the abandonment of marginal lands without considering any method for erosion control can lead to intolerable erosion rates.

The data set outlined here, which can be seen in full in De Santisteban (2003) and can be considered as unique in the Spanish con, show that soil erosion can be a serious problem in typical Spanish agricultural environments. Thus, much more attention should be paid to the problem. This already available information allows for the deeper study of rill and gully erosion processes and for further evaluation of predictive tools.

4. Conclusions

Despite the many evidences of intense soil erosion in cultivated areas if Spain, scarce information is currently available. Our field assessments show that high erosion rates, often well above the tolerances, occur frequently, over wide areas and for different soil uses. The erosion rates for watersheds cultivated with vineyards were higher than those in watersheds cultivated with winter grains. Thus, much more attention should be paid to the problem. The critical period for gully and rill formation is any time when the soil surface remains bare. A well-designed

surface drainage system is possibly the most reliable, enduring conservation measure, complemented with reduced tillage practices. Results from erosion assessments in abandoned plots suggest that such abandonment of marginal lands without considering any method for erosion control can lead to intolerable erosion rates.

Acknowledgements

This work was possible by the financial support of: a) the Department of Education and Culture of the Government of Navarre, with a graduate and postdoctoral fellowship awarded to the first author; b) by the financial support of the Department of Education and Culture of the Government of Navarre, through the Research Project *Caracterización de la erosión de suelo en áreas cultivadas de Navarra*; c) by the financial support of the Spanish Ministry of Science and Technology, through the Research Project REN2003-03028/HID. This material is based upon work supported by the U. S. Department of Agriculture, under Agreement No. 58-6408-0-F137. Any opinions, findings, conclusion, or recommendations expressed in this publication are those of the authors and do not necessarily reflect the view of the U. S. Department of Agriculture.

References

Asiain, J.M., Valentín, A., 2001. El Sistema de Información Territorial de Navarra: SITNA. Mapping, 67, 2-4.

Bennett, S.J., Casalí, J., Robinson, K.M., Kadavy, K.C., 2000. Characteristics of actively eroding ephemeral gullies in an experimental channel. Transactions of the ASAE 43 (3), 641-649.

Casalí, J., López, J.J., Giráldez, J.V., 1999a. Ephemeral gully erosion in Southern Navarra (Spain). Catena 36, 65-84.

Casalí, J., Laburu, A., López, J.J., García, R., 1999b. Digital terrain modelling of drainage channnel erosion. Journal of Agricultural Engineering Research 74, 421-426.

Casalí, J., López, J.J., Agirre, U., Gastesi, R., Goñi, M., Moreira, I., 2001. Escorrentía y calidad de las aguas generadas en cuencas agrarias: primeros resultados de la red de cuencas experimentales del Gobierno de Navarra. XIX. Congreso Nacional de Riegos, Zaragoza.

De Santisteban, L.M., 2003. Análisis de factores topográficos para predecir la erosión por cárcavas efímeras. Ph.D. Thesis, School of Agricultural Engineers, Department of Projects and Rural Engineering, Public University of Navarre. Pamplona, Spain.

Donézar, M., Illarregui, M., Del Val, J., Del Valle de Lersundi, J., 1990a. Erosión actual en Navarra. Gobierno de Navarra. Ministerio de Comercio y Turismo. Pamplona.

Donézar, M., Illarregui, M., Del Val, J., Del Valle de Lersundi, J., 1990b. Erosión potencial en Navarra. Gobierno de Navarra. Ministerio de Comercio y Turismo. Pamplona.

Donézar, M., Del Valle de Lersundi, J., 2001. Red de Cuencas Experimentales Agrarias de Navarra. XIX Congreso Nacional de Riegos. Zaragoza.

Foster, G.R., 1986. Understanding ephemeral gully erosion. In: Soil Conservation. Assesing the National Resources Inventory, 2. Comittee on Conservation Needs and Opportunities. Board on Agriculture. National Research Council. National Academy Press. Washington, pp. 90-125.

Gobierno de Navarra, Departamento de Agricultura, Ganadería y Montes, Servicio de Estructuras Agrarias, 1992. Erosión hídrica en las áreas no cultivadas de Navarra. Documento sin publicar. Pamplona.

Gobierno de Navarra, Servicio de Estructuras Agrarias, 2001. Estudio agroclimático de Navarra. Gobierno de Navarra. Dpto. de Agricultura, Ganadería y Alimentación. Pamplona.

Hall, G.F., Logan, T.J., Young, K.K., 1985. Criteria for determining tolerable erosion rates. In: Follett, R.F., Stewart, B.A. (Eds.), Soil erosion and crop productivity. American Society of Agronomy, Inc., Crop Science Society of America, Inc., Soil Science Society of America, Inc., Madison, Wisconsin, USA.

ICONA, 1988. Agresividad de la lluvia en España. Valores del factor *R* de la ecuación universal de pérdidas de suelo. Servicio de publicaciones del MAPA. Madrid.

Jackson, J.A., 1997. Glossary of Geology. American Geological Institute. Alexandria, Virginia (USA).

Lorenzo L., 2002. Aplicabilidad de los modelos USLE, RUSLE y MUSLE a Navarra. Trabajo fin de Carrera de Ingeniero Agrónomo. Departamento de Proyectos e Ingeniería Rural. Universidad Pública de Navarra. E.T.S.I.A. Documento sin publicar. Pamplona.

Lorenzo, L., Casalí, J., López, J.J., Del Valle de Lersundi, J., 2002. Long term assessment of soil erosion rates in vineyards, and its application for USLE model evaluation. European Society of Agronomy, Córdoba (Spain).

Poesen, J., Nachtergaele, J., Verstraeten, G., Valentin, C., 2003. Gully erosion and environmental change: importance and research needs. CATENA 50, 91-133.

Sabando, C., 2001. Información Geográfica y Nuevas Tecnologías. Web del Sistema de Información Territorial de Navarra: SITNA. Mapping, 67,5-7.

Smith, L.M., 1993. Investigation of ephemeral gullies in loessial soils in Mississippi. US Army Corps of Engineers. Technical Report GL-93-11.

TRAGSA, 2003. La ingeniería en los procesos de desertificación. Mundi-Prensa. Madrid.

Thorne, C.R., Zevenbergen, L.W., Grissinger, E.H., Murphey, J.B., 1986. Ephemeral gullies as sources of sediment. Proceedings of the Fourth Federal Interagency Sedimentation Conference, 1:3-152, 3-161.

Walling, D.E., Webb, B.W. (Eds.), 1996. Erosion and sediment yield: global and regional perspectives. IAHS Publication nº. 236, Wallinford.

Wischmeier, W.H., Smith, D.D., 1978. Predicting rainfall erosion losses. USDA Agricultural Research Service Handbook 537. Washington D.C.

Table 1. Main available information on soil erosion in Navarre

Reference	Location and study surface area	Soil use and management	Study time period	Assessment-prediction method	Results, comments
Donézar *et al*. (1990a,b); Gobierno de Navarra (1992)	All Navarre, 1,042,716 ha	Varied	-	Photo interpretation	The obtained information is qualitative: 11.9 % of Navarrese surface corresponds to cultivated areas with moderate water erosion 15.6 % of Navarrese surface corresponds to cultivated areas with severe water erosion 12.8 % of Navarrese surface corresponds to non cultivated areas with severe water erosion
TRAGSA (2003)	Aragón river basin at Yesa, 2,190 km^2	41.1 % forest; 37.1 % scrub; 15.2 % cultivated; 6.5 % non-productive	Around 30 y	Bathymetric chart at Yesa reservoir	Specific degradation 0.95 kg m^{-2} y^{-1} Only an small portion of the watershed flows from Navarre
Casalí *et al*. (2001); Donézar and Del Valle de Lersundi (2001); Lorenzo (2002)	Latxaga (205 ha) and La Tejería (159 ha) experimental watersheds	Winter grains	September 1996-August 1998	Daily average sediment concentration from water samples at the watershed outlet	0.08-0.6 kg m^{-2} y^{-1} Estimation with USLE applied to a typical plot yields 1.8-2.5 kg m^{-2} y^{-1}
Casalí *et al*. (1999[a])	Town Council of Pitillas, around 5 ha	Winter grains	October 1995-September 1997	One meter wide with 50 needles mechanical profile meter for measuring gully cross sections	0.15->2.60 kg m^{-2} y^{-1} caused by ephemeral gullies
Lorenzo *et al*. (2002)	Four plots in Central Navarre of 0.125 ha, 0.225 ha, 0.497 and 0.552 ha	Vineyards	25-80 y	Measurement of the vertical distance between the ground level and the enlarged graft in a large number of isolated vineyards	1.9-4.4 kg m^{-2} y^{-1} attributed to sheet and rill erosion Very similar erosion rates calculated with USLE
Casalí *et al*. (1999b)	Town Council of Pitillas, erosion in a 610 m drainage channel draining 48.6 ha	Drainage channel Winter grains in the watershed	10 y	Comparison between the initial size of the drainage channel with its present condition using digital terrain models and a terrain representation system	3.68 m^3 m^{-1}; 0.648 kg m^{-2} y^{-1}

Table 2. Characteristics of the Pitillas study area

Watershed and downstream end UTM coordinates (X, Y)	A (m^2); S	P (mm); R; T (ºC); $P_{24,10}$ (mm)	Clay, silt, sand (%) and soil texture (USDA)	K; SAR; E (dS/m)	Soil use and management	Field assessment dates, and crop/soil condition when erosion occurred	Erosion class assessed
La Matea 1 617,560; 4,699,559	2,900; 9.4	546; 50; 13.5; >90	14.5-20.1; 41.0-43.9; 38.7-43.2; loam-silty loam	0.28-0.49; 9.01-32.5; 9.53-53.90	Sunflower, winter grains; chisel	September 1996$^+$; emergence December 1998; sunflower stubble September 21, 1999; contour tillage	Classical ephemeral gully and rills
La Matea 2 617,560; 4,699,565	5,000; 9.1				Sunflower, winter grains; chisel	September 1996$^+$; emergence August 1997$^+$; emergence December 1998; sunflower stubble September 21, 1999; contour tillage	Classical ephemeral gully and rills
La Matea 3 617,449; 4,699,400	2,700#; 2.9				Winter grains; chisel	September 1996$^+$; emergence August 1997$^+$; emergence September 21 1999; contour tillage September 1, 2000; contour tillage October 24, 2001; contour tillage	Drainage ephemeral gully; and rills
La Matea 4 617,504; 4,699,401	2,500#; 2.5				Winter grains; chiseled, and directly drilled	September 1996$^+$; emergence August 1997$^+$; emergence September 1, 2000; contour tillage	Drainage ephemeral gully
La Matea 5 617,520; 4,699,622	1,300#; 3.0				Winter grains; chisel	August 1997$^+$; emergence September 21 1999; contour tillage September 1, 2000; stubble	Drainage ephemeral gully
La Abejera 0 617,627; 4,699,368	16,000; 7.8		17.9-22.9; 45.0-60.8; 21.3-32.1; loam-silty loam		Winter grains; moldboard	January 13, 1996$^+$; fallow August 1997$^+$; emergence September 21, 1999; steepest slope tillage October 7, 2000; steepest slope tillage October 25, 2001; steepest slope tillage	Classical ephemeral gully and rills
La Abejera 1 617,411; 4,699,372	9,600; 4.4		13.7-20.5; 43.1-55.6; 30.7-39.5; loam-silty loam		Winter grains; chisel	September 1996$^+$; emergence	Classical ephemeral gully
Cobaza 1 617,922; 4,698,997	5,300; 10.0		loam-silty loam		Winter grains; moldboard and directly drilled	September 1996$^+$; emergence September 21, 1999; stubble	Classical ephemeral gully
Cobaza 2 617,812; 4,698,901	1,800#; 5.0				Winter grains; moldboard and directly drilled	September 1996$^+$; emergence September 21, 1999; stubble	Drainage ephemeral gully and rills
Camino 617,451; 4,698,864	3,500#; 1.5		loam-silty loam		Winter grains; chiseled	September 1996$^+$; emergence August 1997$^+$; emergence September 21 1999; contour tillage October 7, 2000; contour tillage October 3, 2001; stubble	Drainage ephemeral gully and rills
La Abejera (A) 617,331; 4,699,391	3,390* (452); 3.6		13.7-20.5; 43.1-55.6; 30.7-39.5; loam-silty loam		Abandoned	August 1997; abandoned	Gullies and rills
Pikarana 619,682; 4,667,660	3,743* (588); 4.0		Not available		Abandoned	August 1997; abandoned	Gullies and rills

A: watershed surface area; S: watershed average slope; P: annual average rainfall (Gobierno de Navarra, 2001); R: USLE rainfall erosivity (hJ cm m^{-2} h^{-1} a^{-1}) (ICONA, 1988); T: annual average temperature (Gobierno de Navarra, 2001); $P_{24,10}$: 24 hr rainfall for a 10 year return period (Gobierno de Navarra, 2001); K: USLE soil erodibility (T m^2 h/ha hJ cm); SAR: sodium absorption ratio (mol$^{1/2}$/m$^{3/2}$); E: electrical conductivity of saturated paste extract; #: portion of the total watershed area located within the plot; *: between brackets, the surface area of the abandoned plot; $^+$: data from Casalí *et al*., 1999.

Table 3. Characteristics of Tafalla and San Martín de Unx study areas

Watershed and municipality; UTM coordinates of the downstream end (*X*, *Y*)	*A* (m^2); *S*	*P* (mm) ; *R* ; *T* (ºC); $P_{24,10}$ (mm)	Clay, silt, sand (%) and soil texture (USDA)	*K*; *SAR*; *E* (dS/m)	Soil use and management	Field assessment dates, and crop/soil condition when erosion occurred	Erosion class assessed
Portillo del Sastre; Tafalla 606,844; 4,711,895	38,000э; 3.0	508; 50; 13.4; 80	19.9-32.8; 32.8-50.3; 14.1-38.5; loam-clay loam	0.36; 0.31; 0.55-0.91	Winter grains; chiseled	July 2000; emergence July 2001; emergence October 23, 2001; contour tillage	Drainage ephemeral gully
					Vineyard; plough	August 2000; ploughed last July October 23, 2001; ploughed last July	Classical ephemeral gully and rills
Beramendi; Tafalla 612,039; 4,708,352	9,000; 7.0		10.9-22.8; 36.8-57.2; 22.9-52.4; silty loam	0.36; 0.15; 1.5	Vineyard; plough	March 21, 2001; contour tillage	Classical ephemeral gully and rills
La Canaliza; S. Martín de Unx 613,981; 4,707,929	1,200; 2.3	508; 50; 13.4; 80	19.8-22.2; 41.6-42.1; 36.1-38.1; loam	0.32; 0.23; 0.44	Vineyard; plough	June 21, 2000; contour tillage October 23, 2001; contour tillage	Classical ephemeral gully and rills
Navafría 1; S. Martín de Unx 614,654; 4,706,947	3,400; 4.5		14.5-17.8; 38.6-43.8; 41.7-44.1; loam	0.32; 0.31; 0.55-0.91	Vineyard; plough	May 2001; contour tillage	Classical ephemeral gully and rills
Navafría 2; S. Martín de Unx 614,643; 4,706,971	1,900#; 4.5			0.32; 0.31; 0.55-0.91	Vineyard; plough	May 2001; contour tillage	Drainage ephemeral gully
Lakar 1; S. Martín de Unx 615,022; 4,706,280	14,000; 2.8		18.3-20.1; 42.9-51.3; 30.4-37.3; loam	0.32; 0.46; 0.88	Vineyard; plough	October 2001; contour tillage	Classical ephemeral gully and rills
Lakar 2; S. Martín de Unx 615,013; 4,706,299	1,800#; 3.0		6.8-17.6; 17.5-38.9; 43.5-75.7; sandy loam	0.32; 0.46; 0.88	Vineyard; plough	October 2001; contour tillage	Drainage ephemeral gully

A: watershed surface area; *S*: watershed average slope; *P*: annual average rainfall (Gobierno de Navarra, 2001); *R*: USLE rainfall erosivity (hJ cm m^{-2} h^{-1} a^{-1}) (ICONA, 1988); *T*: annual average temperature (Gobierno de Navarra, 2001); $P_{24,10}$: 24 hr rainfall for a 10 year return period (Gobierno de Navarra, 2001); *K*: USLE soil erodibility (T m^2 h/ha hJ cm); *SAR*: sodium absorption ratio ($mol^{1/2}/m^{3/2}$); *E*: electrical conductivity of saturated paste extract; #: portion of the total watershed area located within the plot; э: 12,000 ha cultivated with vineyards, and 26,000 with winter grains.

Table 4. Main characteristics of rill and gully systems in the cultivated watersheds

	Gully			Rill		
Watershed and measurement year	A_M (m^2), A_A (m^2), A_{cv}, n	L (m)	WDP$_A$	A_M (m^2), A_A (m^2), A_{cv}, n	L (m)	WDP$_A$
La Matea 1, 1998	0.11; 0.09; 0.18; 6	16.1	3.36	0.06; 0.048; 0.37; 3	7.1	3.54
La Matea 1, 1999	0.13; 0.08; 0.41; 9	24.0	4.20	0.10; 0.090; 0.18; 4	9.0	4.43
La Matea 2, 1998	0.11; 0.14; 1.20; 8	16.6	2.23	0.1 0; 0.048; 0.04; 31	243.1	0.73
La Matea 2, 1999	0.25; 0.14; 0.41; 8	28.0	3.22	0.05; 0.030; 0.67; 3	28.0	2.61
La Matea 3, 1999	0.17; 0.07; 0.57; 19	94.1	12.31	-	-	-
La Matea 3, 2000	0.12; 0.08; 0.75; 6	115.0	13.66	0.10; 0.10; n.a.; n.a.	35	n.a.
La Matea 3, 2001	0.05; 0.05; -; 1	26.0	13.50	-	-	-
La Matea 4, 2000	0.15; 0.08; 0.49; 4	26.6	11.70	-	-	-
La Matea 5, 1999	0.22; 0.09; 0.56; 14	63.0	9.51	-	-	-
La Matea 5, 2000	0.14; 0.11; 0.27; 3	12.0	4.45	-	-	-
La Abejera 0, 1999	0.13; 0.08; 0.28; 21	67.5	8.40	0.12; 0.07; 0.04; 3	91.4	n.a.
La Abejera 0, 2000	0.09; 0.07; 0.29; 10	39.7	16.65	-	-	-
La Abejera 0, 2001	0.10; 0.05; 0.52; 15	226.4	9.76	0.03; 0.03; n.a.; n.a.	46.0	0.75
Cobaza 1, 1999	0.07; 0.04; 0.42; 10	121.6	26.90	-	-	-
Cobaza 2, 1999	0.80; 0.05; 0.42; 8	111.0	22.90	0.08; 0.05; 0.43;4	22.4	5.43
Camino, 1999	0.25; 0.09; 0.64; 12	67.0	13.37	0.13; 0.09;0.31;3	10.0	7.27
Camino, 2000	0.19; 0.10; 0.70; 6	98.9	15.52	0.22; 0.10; 0.72; 6	103.4	4.23
Camino, 2001	0.14; 0.06; 0.73; 15	81.2	2.61	n.a.	6.0	n.a.
Portillo del Sastre (winter grains), 2000	0.08; 0.05; 0.35; 4	211.5	3.25	-	-	-
Portillo del Sastre (winter grains), 2001	0.05; 0.05; -; 2	144.4	5.30	-	-	-
Portillo del Sastre (vineyards), 2000	0.01; 0.01; 0.55; 6	151.3	n.a.	0.05; 0.009; 1.23; 22	672.3	6.6
Portillo del Sastre (vineyards), 2001	0.01; 0.01; -; 1	69.0	12.60	0.05; 0.02; 1.17; 3	975.2	10.99
Beramendi, 2001	0.41; 0.12; 0.74; 66	272.4	n.a.	0.10; 0.04; 0.53; 27	136.8	n.a.
La Canaliza, 2000	0.04; 0.04; n.a.; 3	77.0	n.a.	0.004; 0.004; n.a.; n.a.	208.0	n.a.
La Canaliza, 2001	0.02; 0.02; n.a.; n.a.	110.0	n.a.	-	-	-
Navafría 1, 2001	0.12; 0.05; 0.47; 43	638.1	11.8	0.04; 0.03; 0.4; 4	41.7	2.84
Navafría 2, 2001	0.05; 0.04; 0.27; 6	62.4	6.50	-	-	-
Lakar 1, 2001	0.16; 0.06; 0.55; 22	457.8	6.40	0.12; 0.05; 1.67; 20	275.6	2.95
Lakar 2, 2001	0.08; 0.05; 0.46; 5	141.0	7.20	-	-	-

A_M: Maximum cross section area; A_A: Average cross section area; A_{cv}: cross section area variation coefficient; n: number of cross sections; L: length; WDP_A: average with-depth ratio; n.a.: not available

Table 5. Main characteristics of rill and gully systems in the abandoned watersheds and the corresponding erosion rates

	Gully				Rill			
Watershed, measurement date and years after abandonment	A_M (m^2), A_A (m^2), A_{cv}, n	L (m)	WDP_A	E (kg m^{-2} y^{-1})	A_M (m^2), A_A (m^2), A_{cv}, n	L (m)	WDP_A	E (kg m^{-2} y^{-1})
La Abejera (A), August 1997, 10	0.62; 0.21 0.81; 9	87.6	3.38	8.43	0.19; 0.06; 0.87; 66	260.2	5.50	4.77
Pikarana, August 1997, 7	0.38; 0.19; 0.65; 24	108.9	3.11	9.74	0.14; 0.05; 0.91; 34	174.5	2.18	2.27

A_M: Maximum cross section area; A_A: Average cross section area; A_{cv}: cross section area variation coefficient; n: number of cross sections; L: length; WDP_A: average with-depth ratio; E: average annual erosion rate

List of Figures

Figure 1. Location of the study areas (green circles) and of rain gauges (red circles for automated stations in a ten minute basis, and blue circles for daily basis gauges) within them. The continuous line delimits the three different townships.

Figure 2. Topographic maps of the surveyed watersheds. The usual location of ephemeral gullies is also indicated by circles, whereas the dotted line delimits the watershed divide.

Figure 3. Daily rainfalls during the study period for the three study areas. Arrows indicate the events that caused either ephemeral gully erosion or rill erosion, or both, at least in one of the watersheds of each study area, corresponding the grey arrows to vineyards. For the Pitillas area, data prior to 1999 are also included (Casalí et al., 1999) to cover a wider scope for discussion.

Figure 4. Annual rill and ephemeral gully erosion rates for the study watersheds cultivated with winter grains (a) and with vineyards (b). For Pitillas area, data prior to 1999 are also included (Casalí et al., 1999) to cover a wider scope for discussion. The maximum soil loss tolerance level usually accepted is shown.

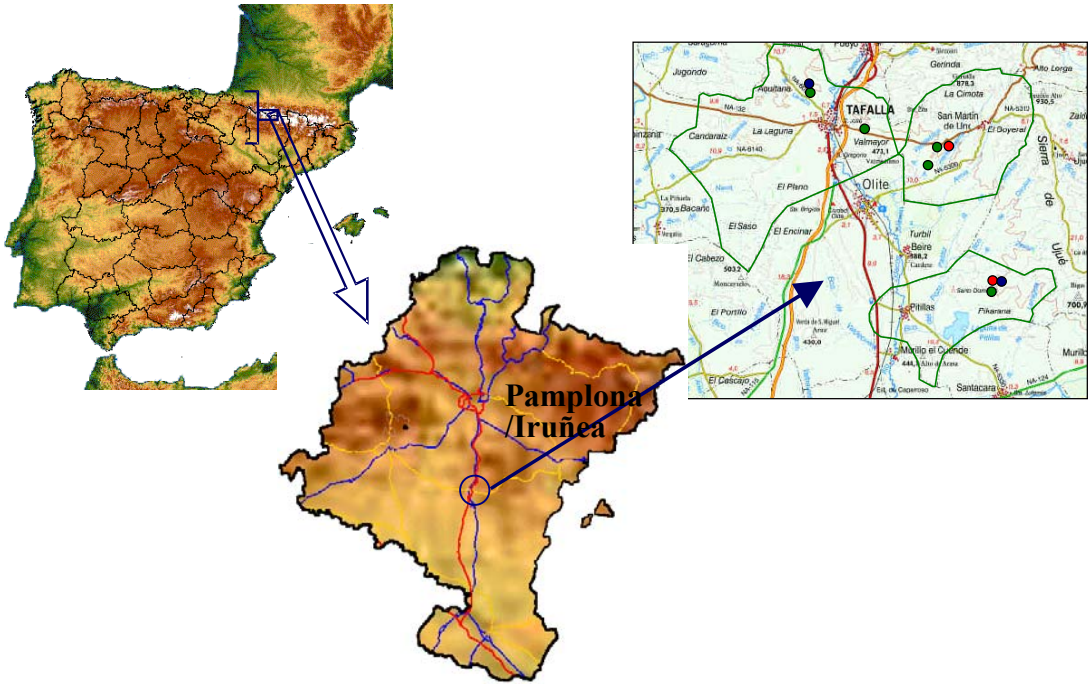

Figure 1. Location of the study areas (green circles) and of rain gauges (red circles for automated stations in a ten minute basis, and blue circles for daily basis gauges) within them. The continuous line delimits the three different townships.

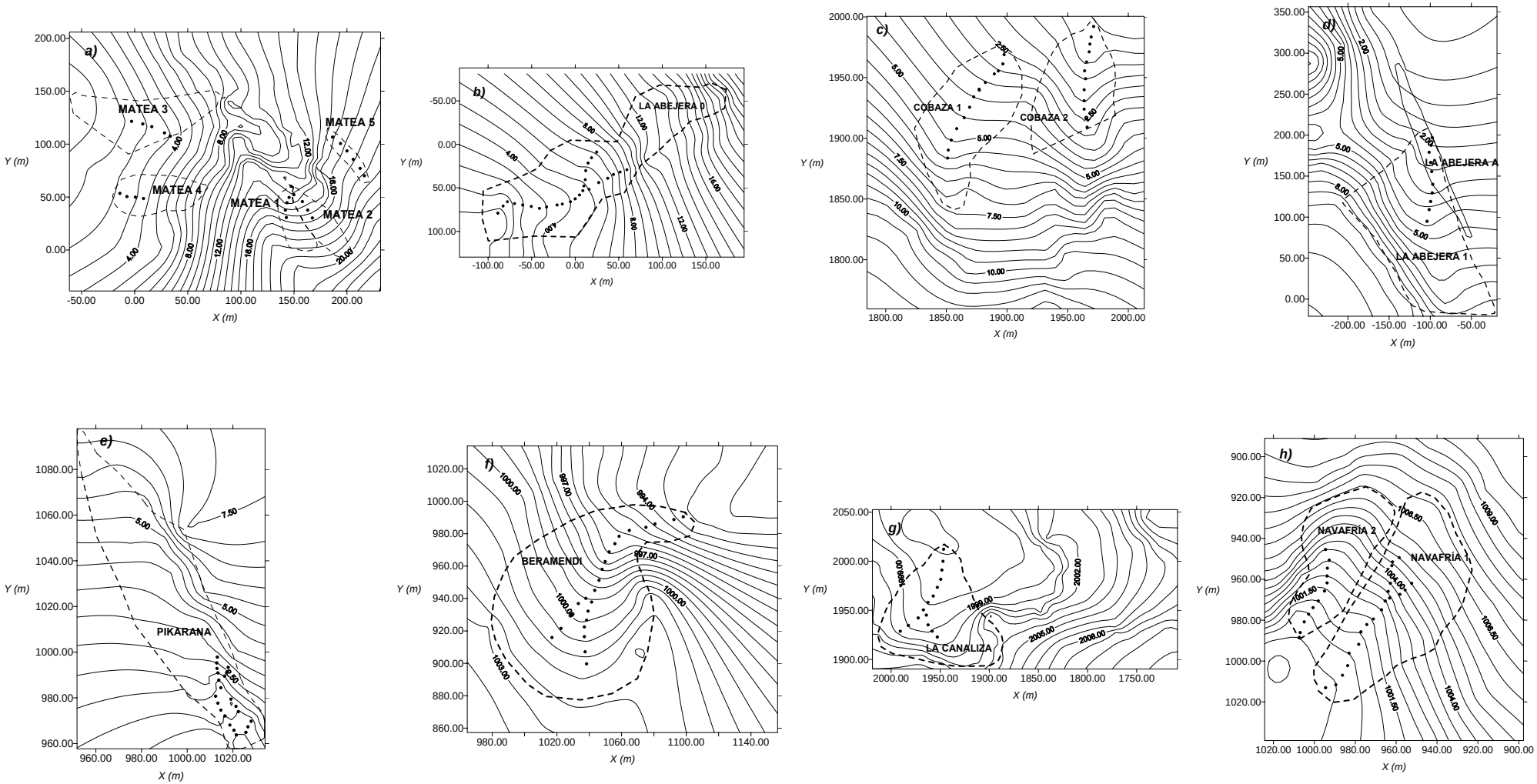

Figure 2. Topographic maps of the surveyed watersheds. The usual location of ephemeral gullies is also indicated by circles, whereas the dotted line delimits the watershed divide.

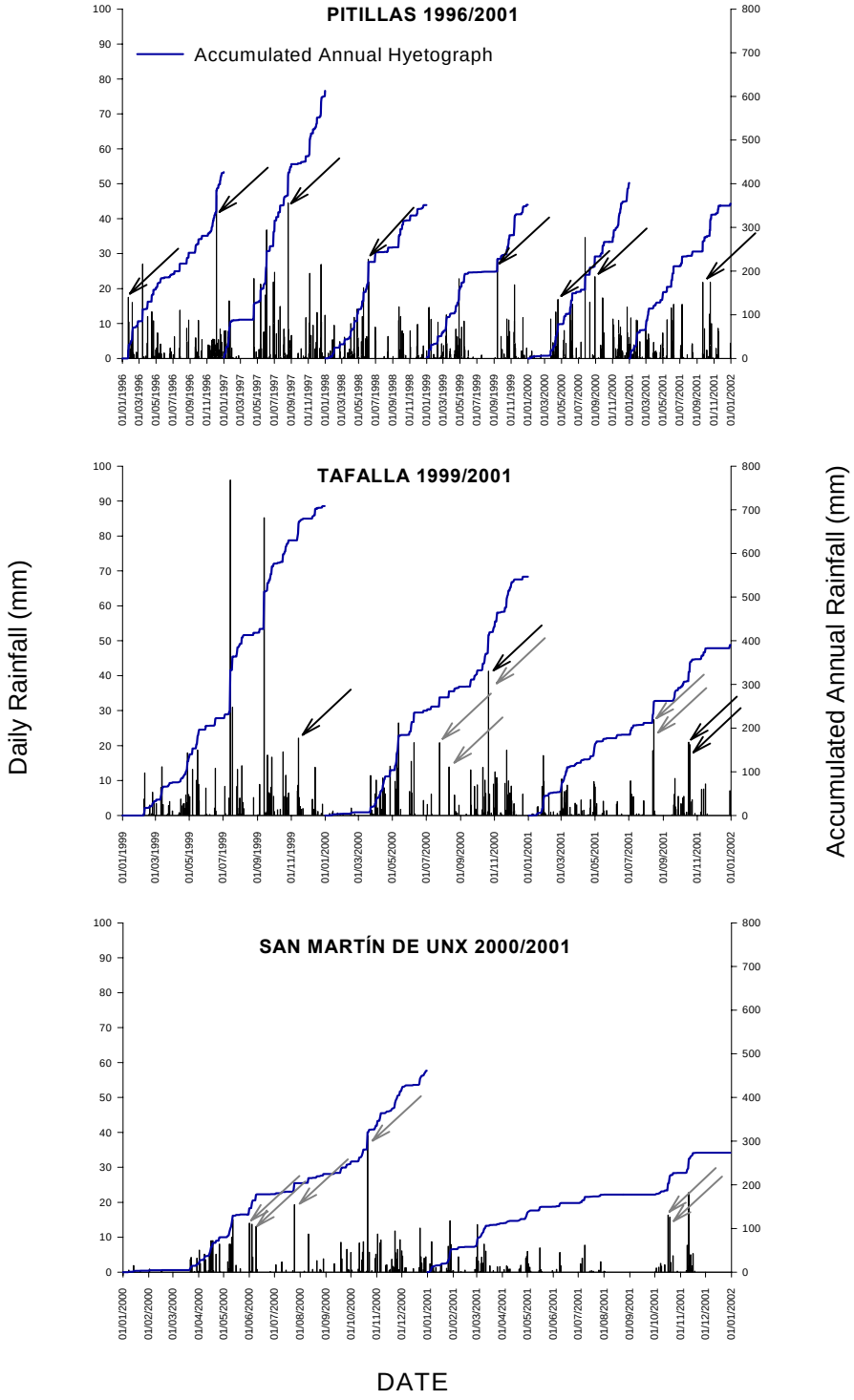

Figure 3. Daily rainfalls during the study period for the three study areas. Arrows indicate the events that caused either ephemeral gully erosion or rill erosion, or both, at least in one of the watersheds of each study area, corresponding the grey arrows to vineyards. For the Pitillas area, data prior to 1999 are also included (Casalí et al., 1999) to cover a wider scope for discussion.

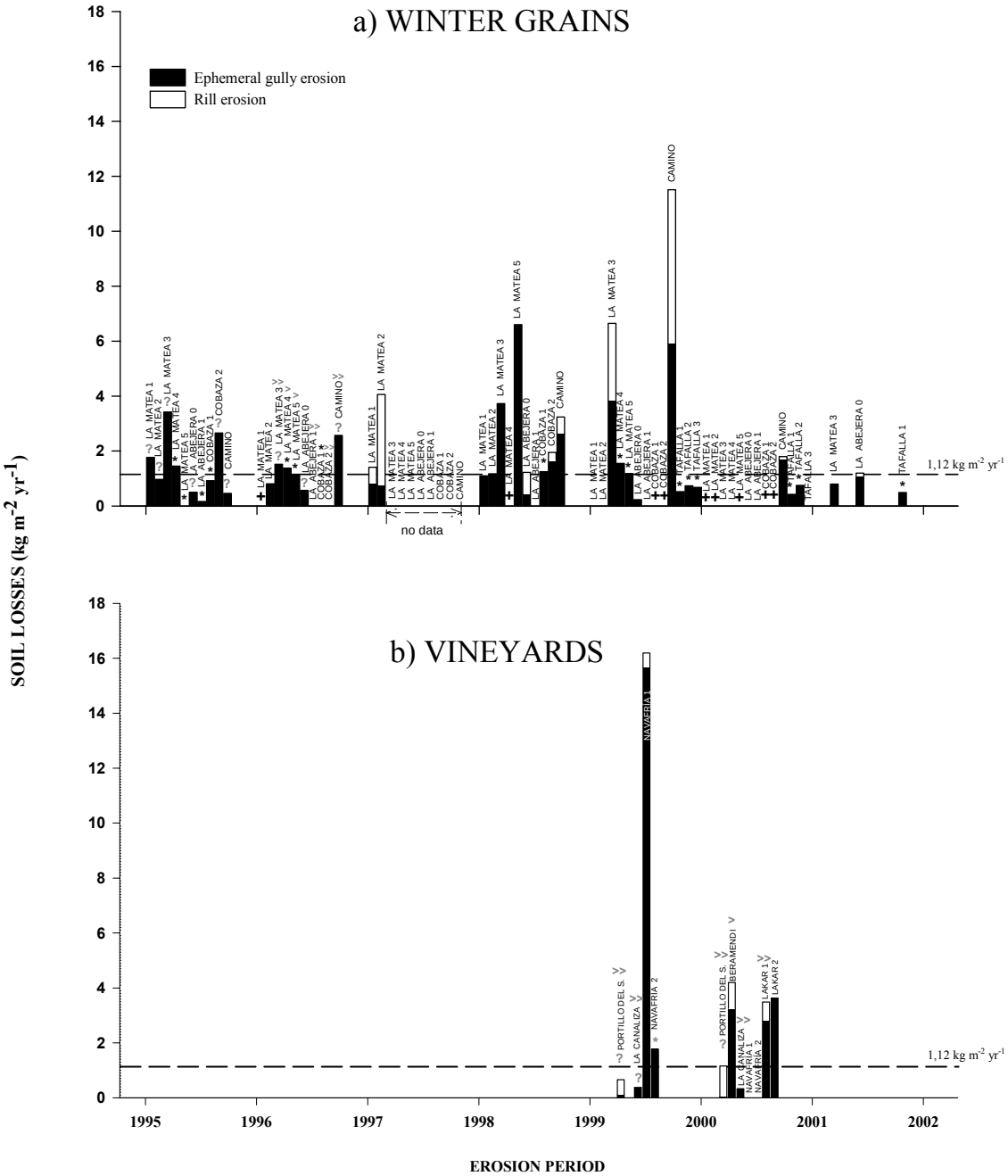

It was not possible to assess or monitore all rill erosion (?) or gully erosion (¿) occured; (*) rill erosion was never observed; soil losses higher (>) or much higher (>>) than the shown rate; no column: no erosion was observed; (+) direct seeding

Lakar 1

Figure 4. Annual rill and ephemeral gully erosion rates for the study watersheds cultivated with winter grains (a) and with vineyards (b). For Pitillas area, data prior to 1999 are also included (Casalí et al., 1999) to cover a wider scope for discussion. The maximum soil loss tolerance level usually accepted is shown.

Experimental Study of Conditions for Rill Bank Collapse

Jovan R. Stefanovic*
Rorke B. Bryan
University of Toronto - Soil Erosion Laboratory
1265 Military Trail
Toronto, Ontario M1C 1A4, Canada

Abstract

Rill bank collapse is an important component in the adjustment of channel morphology to changes in discharge and sediment flux. By delivering abundant, easily erodible sediments, bank collapse causes abrupt changes in flow resistance, flow pattern and downstream sediment concentrations. Generally, bank retreat involves gradual lateral erosion, caused predominantly by flow shear stress, and instantaneous bank collapse, triggered by complex relationships between channel flow and rill bank soil and water conditions. Bank collapse occurs when bank height exceeds the critical height where gravitational forces exceed soil shear strength. This experimental flume study examined conditions for collapse in eroding rill channels. Experiments with and without a deep water table were carried out with meandering rill channels in loamy sand and sandy loam soils in a laboratory flume under simulated rainfall and controlled runon. Different discharges were used to initiate knickpoint incision and produce different rill depths. Soil moisture dynamics were precisely monitored with microstandpipes, tensiometers and TDR probes. Bank collapse occurred with newly developed or rising pre-existing water tables near rill banks, associated with knickpoint migration. The knickpoint caused positive pore pressure in the bank foot, and raised negative pore pressures in the tension saturation zone close to positive. Matric potential in unsaturated parts of the bank can be an important stabilizing factor, while positive pressure at bank foot is the main cause of destabilization Knickpoint incision also produced the critical bank heights necessary for bank collapse. With moisture contents of >37% (sandy loam) and >23% (loamy sand), critical bank heights were 11-12 cm and 6-7 cm, respectively. Undercutting of the outside bank is also an important trigger for bank instability. Bank displacement patterns were quite different in the two soils: on the loamy sand, the failed block slides to channel bed, revealing only the upper half of the failure plane at collapse; on the sandy loam the failure plane was exposed for the complete bank height.

Keywords: soil water dynamics, hydraulic gradients, knickpoint migration, critical bank height

*Correspondence author

Modeling of Erosion Processes and Estimation of Interrill Erodibility Soil Parameters in Forest-Steppe Zone of Ukraine

Nataliya Vasyliv*
Environmental Research Scientist
Environmental Biology Department
Khmelnytskyy Institute of Agroecology and Biotechnology
40/1 Shestakova Street
Khmelnytskyy, 29000 Ukraine

Abstract

Erosion models which are able to describe erosion processes correctly under a number of given parameters in the specified point of space and time are an important apparatus of erosion-resistant agrolandscapes design and creation. The Water Erosion Prediction Project (WEPP) model is used to study erosion processes of soils of Ukraine as water flow physical laws to incline plane are in its basis.

Since 1999 till 2003 it has been conducted the researches of the grey forest and chernozem soils erodibility in forest-steppe zone of Ukraine on the Khmelnytskyy, Vinnitsa and Zhytomyr regions territory. According to WEPP methodic field experiments were fulfilled to define parameters of rill and interrill zones erodibility. The process of water erosion was simulated by water filling method without raindrops energy bringing. Both rill and interrill erosion research experiments were held on the same objects of Letychiv experimental station of Khmelnytskyy Institute of Agroecology and Biotechnology in the Southern Bug basin and also on the territory of three agricultural farms. To conduct these experiments it was used the sprinkling simulator worked out by scheme described in publication of Karlos. It was designed four rain regimes different by intensity. The reiteration of the experiment was double.

As a result of the experiments in contrast to earlier received data it has been determined appearance of the nonlinear dependence of interrill erosion value D_i from I_qSf (where I – rain intensity, S – surface down gradient) under high rain intensity. The received data indicate the necessity in unification to realize field experiments to define coefficient of interrill soil erodibility K_i. In view of WEPP model structure and general requirements to physical modeling (highest possible approximation of modeling conditions to natural one), according to the research experiments, it is necessary to model “typical” downpour for research region. With the above purpose central Ukrainian territories, including Khmelnytskyy region, territory zoning has been conducted by downpour risk based on downpour probabilistic estimation. The research data were received with all four intensions use of its “typical” for region research downpour. The interrill soil erodibility K_i coefficients calculated by means of different models were analyzed. The models estimations, which are characterized by coefficients of correlation between interrill erosion D_i value and flow determinative indexes, were fulfilled. The analysis of the research data showed that interrill erodibility coefficient value strongly vary depending on formula used. According to the above, soil losses calculated by WEPP model based on the generally accepted formula of K_i determination significantly differ from the received data. As a result of the research formula for under consideration soils on Ukrainian territory has been calculated. It has been also

*Corresponding author

determined the conditions when WEPP model methods incorrectly evaluate the interrill erosion value and interrill erodibility coefficient.

It has been also determined coefficient K_i value by a different way – by obtaining regression dependence K_i from soil main parameters based on the experimental data. In view that it is impossible to use dependences received on soils in the USA, according to model WEPP calculations, it have been conducted researches to define interrill erodibility coefficient by experimental methods for maximum quantity of soils various by its genesis in Ukraine. As a result of data processing by method of direct single-step regression it has been constructed regression model of interrill erodibility coefficient estimation that gives possibility to estimate coefficient K_i according to data of granulometric structure and organic carbon contents without active experiment realisation. It has also been estimated correctness of this model on the territory of Ukraine.

Macropore Flow and Mass Wasting of Gullies in the Loess Plateau, China

G.V. Wilson* (E-Mail: gvwilson@ars.usda.gov)
USDA National Sedimentation Laboratory
598 McElroy Drive
Oxford, MS 38655
FAX: 662-232-2915

Xu Mingxiang
Chen Yun Ming
Liu Guobin
Institute of Soil Water Conservation (ISWC)
Chinese Academy of Sciences
26 Xiong Rd
Yangling, Shaanxi China 712100

Abstract

Due to the extensive gullying from historically excessive erosion in the loess plateau of China, much of this region is being removed from cropping and converted to native grass and shrub vegetation. The effects of this conversion on soil physical properties that result in preferential flow have not been established. Tunnel scour and mass wasting are important gully erosion processes resulting from preferential flow through macropores (pores > 1 mm diameter). The objective of this study was to assess the changes with time in macropore flow characteristics of soils on the loess plateau following conversion to grass vegetation and the associated degree of mass wasting of gully faces. Ridge areas that had been revegetated for 1 year, 6 year, and > 15 years, following tilling and for 6 years following contour-ditching and the adjacent gully faces were characterized for their macropore and soil matrix properties on a 50 cm by 50 cm area. The macropore and soil matrix infiltration rates were measured on the ridge areas and soil loss by mass wasting was measured on gully faces. The total number of macropores increased from 11.6 m^{-2} to 39.6 m^{-2} from 1 to 6 years and to 51.6 m^{-2} after 15 years of revegetation following tillage. The macroporosity increased from 0.0008 m^3 m^{-3} to 0.0018 m^3 m^{-3} from 1 to 6 years of revegetation following tillage but the lowest macroporosity (0.0005 m^3 m^{-3}) was 6 years of revegetation following contour-ditching. The contour-ditched area had the lowest infiltration rate (95 m d^{-1}) through the soil matrix (areas without macropores) with the tilled areas having similar infiltration rates regardless of the years revegetated (averaged 146 m d^{-1}). Due to macropore erosion in the 1 year revegetated area enlarging pore diameters by > 200% during the infiltration event, this condition had the highest macropore infiltration rates (7967 m d^{-1}). Macropores in all other areas were stable, no macropore erosion. The 6 year, tilled areas had significantly higher macropore infiltration rates (4665 m d^{-1}) than the 6 years since contour-ditching areas (91 m d^{-1}). The number of macropores on the gully faces was triple (92.8 m^{-2}) and the macroporosity quadruple (0.004 m^3 m^{-3}) that of the ridge surfaces. The upper gully faces exhibited 1.1 slumps m^{-1} for a total soil loss of 48622 kg ha^{-1}.

Keywords: pipe flow, macropores, infiltration, mass wasting, gully erosion

*Corresponding author

1. Introduction

Erosion by subsurface flow occurs by one of two mechanisms: seepage flow or pipe flow. The distinction in the flow process is important to understanding the erosion mechanisms. Seepage flow is common, particularly at footslopes and valley bottoms, where downward percolation is restricted and the resulting lateral flow emerges from the ground surface. Seepage flow can initiate the development and headward migration of gullies by liquification of soil particles that are entrained in the seepage flow. The resulting development of vertical gully faces, also common with streambanks, not only exhibits the seepage flow but exasperates the process as the erosion of entrained materials causes undercutting of the gully face. The undercutting causes mass wasting , also termed slumping or sapping, of gully walls. This process was considered by Parker (1963) to be important with unconsolidated material, whereas, consolidated material was thought to be more affected by pipe-flow erosion.

Geomorphologist have long recognized the role of preferential flow through macropores and pipes on gully erosion and its impact on landscape development (Dunne, 1990). Due to the rapid and often turbulent flow through macropores, defined by Luxmoore et al. (1990) as pores greater than 1 mm in diameter, the periphery of the macropore is eroded when the shear forces exceed the frictional strength binding particles, also termed tunnel scouring. Tunnel scour may also cause gully development when the pipes collapse. Mass wasting has also been attributed to pipe flow (Pierson, 1983) when the internally eroded material blocks or clogs the pipe resulting in an abrupt pressure rise that causes bank failure.

Both of these subsurface erosion processes are common in forested hillslope conditions. Uchida et al. (2002) concluded that pipe flow was the dominant process of streamflow generation in steep hillslopes during large (>70 mm) rainfall events. Under small events (<30 mm), the hydraulic conductivity of the soil matrix, as measured with 100 $cm^{\Delta 3}$ cores, could be used with Darcy's law to quantify the runoff process. The existence of an extensive network of macropores at the surface of forest soils are typically capable of infiltrating all rainfall with no Hortonian flow (Uchida et al. 2002, Wilson et al., 1989). It is also common in forested watersheds to observe exponentially reduced permeability with depth. The existence of water-restricting horizons produce perched water during storm events, which combined with the topographic gradient (Leaney et al., 1993; Wilson et al. 1990), make forested hillslopes particularly susceptible to subsurface preferential flow processes.

Germann et al. (1984) indicated that experimental information on the spatial variability of macropore flow contributions to infiltration were limited. Since then, many studies (Watson and Luxmoore, 1986; Wilson and Luxmoore, 1988; Wilson et al., 1989; Sobieraj et al., 2002) have characterized the spatial variability in macropore flow under forested hillslope conditions. However, the contribution of macropore flow processes under agronomic hillslope conditions is less documented. It is a common practice under cropland conditions to purposefully exclude macropores from the sampling and consider excessively high conductivity values due to macropores as outliers that are omitted from the data base.

The loess plateau region of China has long been deforested to the point of being completely denuded of trees. This region, which covers 0.62 million km^2, has the highest erosion rates in the world with average soil losses of 3720 t km^{-2}. The current landscape morphology exhibits this historical erosion with extensive gullies that are better described as canyons with shear cliffs. It has been estimated that 45% of the region has been affected by erosion with most of these affected areas being almost 100% disturbed by human activity. Subsurface flow is not

considered to be the current governing process of erosion in these areas due to the land-alterations, such as terracing of vast areas, and continual disturbance by farming activities that disrupt biogenic pore formation and instead facilitate surface runoff. As a result, the emphasis has been placed on quantifying infiltration through the soil matrix and sheet erosion processes.

Despite the efforts to reduce the erosion by terracing and other landscape altering practices, erosion continues to be excessive. The Chinese government has, therefore, instituted an aggressive conservation program of allowing these highly erosive areas to naturally revegetate or vegetate by planting of trees, shrubs, and grasses, or a combination of the two. Most of these areas have been revegetated for less than 10 years with the exception of the steepest areas, e.g. the head of gullies, which have been out of agriculture production for decades and undergone natural revegetation.

The importance of macropore flow to infiltration and erosion in these revegetated areas has not been considered to date. It can be hypothesized that as vegetation is reestablished and the land is maintained in a undisturbed condition, biogenic pores will proliferate at the surface resulting in an increased contribution of macropore flow to infiltration. The inherit increase in preferential subsurface flow, i.e. pipe flow, could increase the significance of mass wasting of gully faces. The objectives of this study were to quantify the macropore distribution under different conservation practices and compare the contribution of macropore infiltration to infiltration through the soil matrix. Inferences are made to the significance of macropores to mass wasting of gully faces through characterization of the macropore distribution on gully faces and the extent of soil loss by mass wasting.

2. Area Description and Methods

The Ansai station of the Institute of Soil and Water Conservation is located in the Zhi Fangguo watershed at longitude E109E 19', latitude N36E 51' with an elevation range of 1040 to 1400 m. This watershed has an area of 8.27 km^2 and is situated in the middle part of the loess plateau in the Shaanxi Province of China. The climate is transitional between semi-humid and semi-arid with a mean annual temperature of 8.8E C and an annual precipitation of 500 mm. Precipitation occurs mainly, 60-70%, from June to September, which coincides with the primary period of water erosion. Liu (1999) reported that annual soil loss is approximately 38 times higher in the loess plateau than in the Mississippi River region of the U.S. with annual soil losses as high as 20000 t km^{-2} yr^{-2} and 25% of the area exhibiting annual rates greater than 5000 t km^{-2} yr^{-2}. Most of the soil loss occurs during a few major rainstorms each year with soil losses from these infrequent individual storms ranging from 60-75% of the annual soil loss.

The loess plateau soils were formed in the Quaternary period, 2.5 million years ago, with 50-200 m thick parent material. The Zhi Fangguo watershed has 50-80 m thick parent material (Xu et al., 2002) that has uniform silt loam texture with depth. The soils generally consist of 85% silt and 10% clay, 0.5% organic matter, and bulk densities around 1.3 Mg m^{-3} for cropland. Xu et al. (2002) reported that soil characteristics were strongly affected by landuse with OM, aggregate stability, cohesion, and infiltration rates being higher under woodland, shrubland and grassland than under cropland. As a result of the historically severe erosion, the watershed has dramatic topographic variations typical of this gully region. The research site consisted of two adjacent ridge top areas, Fig. 1, in natural grass revegetation for different periods of time. Four different grass revegetation systems were selected for study: tilled land allowed to naturally revegetate with grasses for periods of 1 year, 6 years, and more than 15 years, and land that was contour-ditched then allowed to revegetate for 6 years. Both ridges were bounded on 2 sides by a deep (>

100 m) gully or canyon with irregular shaped edges of ridge areas extending like fingers out into the gully. The gully typically consisted of a 1.5 to 2 m deep face at the top with a small highly sloped bench below that ended at a large gully face (> 100 m) that extended into an ephemeral stream at the canyon bottom. Some of the ridge fingers were steeply sloped (>40%) and had been established in grasses and not cropped for decades. These gully head areas represented the greater than 15 years of revegetation condition.

The irregular boundary of the ridge had a much larger gully face length than the linear distance of the ridge. The linear distance of gully face per ridge area was determined by manually walking the ridge edges and measuring the distance. This distance was also estimated from a contour map. The rate of mass slumping per length of gully face was estimated on the upper most gully face by directly measuring the volume of freshly displaced soil from a 3 m long by 1.5 m high area (Fig 2). The soil loss by mass slumping was calculated from the product of the volume displaced and the average bulk density for the ridge conditions.

For each gully face and each ridge top revegetation system studied, a representative area was selected for macropore distribution measurement and the location identified by GPS coordinates. A 50 cm by 50 cm frame, Fig. 3, was placed on the soil surface or for the gully it was placed against the face from the surface down to 50 cm. All pores greater than 1 mm diameter inside the 2500 cm^2 area were counted and the diameter of all pores greater than 5 mm diameter were measured.

A typical large macropore (> 5 mm diameter) was selected for macropore infiltration measurement. The pore was isolated using a 50 mm diameter by 50 mm high ring that contained an outflow tube at 30 mm from the bottom, Fig 4. The ring was inserted 10 mm into the soil such that a 20 mm head would be maintained on the inner surface and macropore. Soil was packed tightly around the outside of the ring to prevent leakage. A cloth was placed inside the ring to limit disturbance during establishment of a hydraulic head. A constant head of 20 mm was maintained and the fall in the water reservoir was measured with time and corrected for any water loss through the outflow tube. The ring infiltration rate, I_{ra} (m/d, expressed on total ring area basis), was measured until steady state flow was established or the macropores collapsed due to erosion. Prior to flow measurement, an antecedent soil water content sample was obtained from the soil surface. After terminating flow, the pore diameter was measured and the soil profile sampled in 50 mm depth increments for soil water content from the surface to below the wetting front. In cases in where exfiltration was evident, the runoff rate was measured.

An undisturbed soil core, Fig 5, was obtained at each site for measuring the soil matrix infiltration capacity using the standard method used on the loess plateau (Xu et al., 2002). A 10 cm diameter by 12 cm long steel core with a tapered cutting edge was pressed into the soil to a depth of 10 cm at a location that did not contain a macropore. In core samples in which a macropore was evident after excavation, the core was discarded and another core obtained. The core was excavated from the surface and a metal plate placed on the bottom. The core was placed in a protective bag for transport to the laboratory. Soil cores were saturated from the bottom with tap water for a minimum of 24 hours before processing. After saturation, cores were placed on a drainage rack, a constant 20 mm head was maintained, and outflow measured in 4 minute time increments until steady state matrix infiltration, I_{sm} (m/d), was established. Following steady state, the constant head was removed and the cores were placed into a weighing dish immediately after ponded water on the surface disappeared. The steel core was removed and the wet weight measured before placing cores in an oven at 105E C for a minimum

of 24 h. The oven-dry weight was determined and the total porosity and bulk density calculated from these measurements.

The steady state infiltration rate through the soil matrix was used to correct the ring infiltration measurement for infiltration through the non-macropore area inside the ring. The infiltration rate through the macropore alone, I_{mac} (m/d expressed on area of macropore basis), was:

$$I_{mac} = [I_{ra}*A_r - I_{sm}*(A_r-A_{mac})]/A_{mac} \quad (1)$$

where A_r (m^{-2}) is the area of the ring and A_{mac} (m^{-2}) is the area of the macropore opening. Statistical analysis was performed using SAS (1999) Proc ANOVA procedures to determine significant differences among revegetated conditions (1 year since tillage, 6 years since tillage, 6 years since contour-ditching, and >15 years since tillage) at the 0.05 level.

3. Results and Discussion

3.1. *Physical Properties*

The number of macropores increased as the number of years following revegetation increased, Table 1. This is evident by the >15 years since tillage condition having significantly more macropores (pore diameters > 1 mm) than the areas revegetated for 1 year after tilling and the contour-ditched areas revegetated for 6 years. The majority of the increase (70%) occurred from years 1 to 6 resulting in the increase from the 6 year to > 15 year areas not being significantly different. This pattern of significant increase with time following revegetation held true for the number of large (>5 mm diameter) macropores. However, this was not true for the maximum pore size. The 6 years since tillage area had the largest pores (mean maximum pore diameter=17 mm) which was significantly larger than observed for the 6 years since contour-ditching area and the >15 years since tillage areas. Surprisingly, the 1 year revegetated areas, while having the fewest macropores and fewest large pores, had the second largest pores and was not significantly different from the 6 years since tillage condition.

Each of the revegetated areas had been taken directly out of conventional tillage agriculture. The conventional tillage system consisted of extensive and frequent tilling of the soil surface with hoes. Due to the lack of disturbance and infrequent precipitation of this remote, semi-arid area, the newly established area exhibited very little reconsolidation after 1 year and appeared to be freshly tilled with sparse vegetation. As a result, the total porosity was highest in this 1 year since tillage area and significantly higher than the 6 years since contour-ditching and >15 years since tillage areas. While very few macropores had been established in this newly revegetated areas, the ones that did exist were highly erosive. During the course of the macropore infiltration experiments, these macropores enlarged significantly due to pipe flow. The result was a 221% increase on average in pore diameter during the infiltration event while all pores tested in the other areas remained unchanged. The other areas were stabilized by the formation of a surface crust with an average thickness of 5-7 mm. As a result of the highly erosive nature of the tilled soil, the few macropores that did exist in the newly established areas (1 year since tillage) were large and susceptible to rapid increase in diameter during infiltration events.

Despite the newly revegetated area having the highest total porosity and second largest maximum pore sizes, the macroporosity (volume of pores > 1mm diameter per total volume) was second lowest. The 6 years since tillage area had the highest macroporosity and was significantly

higher than the 6 years since contour-ditching and newly established (1 yr-tilled) areas. This area also had the greatest proportion of its total porosity being macropores with 0.33% as compared to 0.18% for the >15 year area, 0.14% for the 1 year area, and only 0.10% for the 6 years since contour-ditching area. It is not clear why the contour-ditched area was so different than the non-ditched area after 6 years of revegetation. The contour-ditched area was clearly more firm for walking despite the bulk density not being significantly different from the non-ditched area, Table 2. These areas were significantly different in other physical properties. The contour-ditched area had fewer large pores, smaller maximum pore sizes, lower macroporosity, and total porosity.

3.2. *Hydraulic Properties*

As a result of these significant difference in physical properties, the infiltration rate, Table 2, through the soil matrix (soil excluding macropores) was lowest for the 6 years since contour-ditching area among the conditions tested. It was significantly lower than the 1 year and >15 years since tillage areas. While the matrix infiltration rate was numerically smaller (30% lower) for the contour-ditched than the non-ditched area, their differences were not significant. As expected, the newly established area (1 year since tillage) had the highest soil matrix infiltration rate; however, it was surprising to find that the >15 years since tillage area had an essentially identical soil matrix infiltration rate and their values were not significantly different from the 6 years since tillage area. It was anticipated that the development of surface crust, which was prevalent in the older revegetated areas, would limit the matrix infiltration rate. However, this was not the case. This is likely due to the type of crust. The crust observed on this loess plateau region was due to biological growth and not a physical crust formed by clogging of surface pores by displaced particles during infiltration.

The macropore infiltration rate was expected to be lowest for the newly established revegetation areas and increase with time since vegetation establishment. This was clearly not the case. The newly established area had the highest geometric mean macropore infiltration rate, Table 2. This was clearly a result of the macropores in the loose soil eroding during the infiltration test. These pores increased in diameter by 221% on average during a single event, resulting in a related increase in their macropore infiltration rate and decrease in matrix area contributing to the infiltration. In contrasts, the macropores remained completely unchanged in the other areas with stable macropore infiltration rates.

3.3. Mass Wasting

The linear distance of the ridge-gully interface was measured to be 1109.5 m ha^{-1} of ridge area. The macropore distribution was measured on the 1.5 m vertical face along a 3 m length section of the ridge-gully interface. Seventeen sites were characterized for their macropore distribution and soil loss by mass wasting. Due to the prolific growth of algae on the soil and gully face surface that forms a surface crust, recent (this rainy season) slump areas were easily identified, Fig 6.

The overall mean total number of macropores for the ridge surface (all conditions) was 34.8 m^{-2} as compared to 92.8 m^{-2} macropores for the gully face. Not only were there more macropores on the gully face but also more than twice as many large (> 5mm diameter) pores (28.4 m^{-2}) as compared to the revegetated ridge surface (12.9 m^{-2}). In addition, the largest pores averaged 18.4 mm on the gully faces as compared to 12.3 for the ridge surface. The result was four times greater macroporosity on the gully face (0.0040 m^3 m^{-3}) as compared to the ridge surface (0.0010 m^3 m^{-3}).

The correlation of the surface macropores to the gully face macropores was not plausible as this would require tracking of macropore paths to confirm their origins. Deposition of eroded material on the gully face below macropores indicated that some of these macropores were hydrologically active. However, a distinction between hydrologically active and non-active macropores was not made. Recent mass wasted areas did not always exhibit the soil deposition features on the freshly exposed soil face. This suggest that if pipe flow was the controlling process, at least some of the mass wasting occurred after preferential flow through the macropores had ceased. The number of areas on the gully face that exhibited recent mass slumping totaled 54 for the 17 (3 m long) sites measured for an average of 1.06 slumps m^{-1}. Their size averaged 40.0 cm by 32.2 cm by 3.1 cm deep for an average volume wasted of 35375 cm^3. Using the average bulk density (1.17 g cm^{-3}), the average slumped contributed 41.1 kg of soil loss. Given the linear distance of 1109.5 m ha^{-1} of ridge area, this equates to 48622 kg ha^{-1} (4765 t km^{-2}) of soil loss by gully bank failure alone.

4. Conclusions

The conservation measure of removing the highly erosive ridge areas from agronomic production and allowing these areas to naturally revegetate with native grasses clearly resulted in significant changes in their physical and hydraulic properties with time. The total number of macropores (> 1 mm) and number of large (> 5 mm) macropores increased with time. As a result, the macroporosity increased with time. The extent of this increase in number of macropores and macroporosity was affected by the land preparation at the time of conversion as areas that were contour-ditched had fewer macropores and lower macroporosity.

The soil matrix infiltration rate was highest in the newly established (1 year) and the oldest (>15 years) revegetated areas. The newly established area still exhibited characteristics of freshly tilled soil so the high matrix infiltration was expected. However, it was expected that the biological crust on the surface, which was greatest on the > 15 years since tillage areas, would limit the matrix infiltration rate. This did not appear to be the case as the rate did not appear to increase with time in vegetation establishment. It did appear to be effected by the land preparation at the time of revegetation as the contour-ditched area had lower matrix infiltration rates as well as the highest bulk density and significantly lower total porosity than the other areas. These findings suggests that the human traffic required to construct the contour-ditches was a detriment to the surface infiltration. Improvements in controlling runoff by contouring ditches will likely be offset by the increased runoff from this area. The highly erosive nature of the loess soil was evident by the significant enlargement of macropores during the infiltration tests in the newly established revegetated area. This resulted in this area having the highest macropore infiltration rates but it had the fewest macropores. Unexpectedly, the oldest revegetation area had the lowest macropore infiltration rates but it did have the greatest number of macropores.

Soil loss by mass wasting of the upper most gully face was greater than total soil losses reported by others for the region. Not all this material was transported off site as much of this material was deposited on the steeply sloped bench below this upper gully face. How long this deposited material remains on the bench before being washed off the larger gully face and into the ephemeral stream system below is uncertain. However, it should be noted that this deposition would not occur for material slumped off the larger gully face below the bench which also appeared to have substantially more slumping with orders of magnitude larger slumped areas than the small upper gully face.

References

Dunne, T. 1990. Hydrology, mechanics, and geomorphic implications of erosion by subsurface flow. IN Higgins, C.G., and D.R. Coates, eds., Groundwater Geomorphology; The Role of Subsurface Water in Earth-Surface Processes and Landforms. Boulder, CO., Geol. Soc. Am. Special Paper 252.

Germann, P., W.M. Edwards, and L.B. Owens. 1984. Profiles of bromide and increased soil moisture after infiltration into soils with macropores. Soil Sci. Soc. Am. J. 48:237-244.

Leaney, F.W., K.R.J. Smettem, and D.J. Chittleborough. 1993. Estimating the contribution of preferential flow to subsurface runoff from a hillslope using deuterium and chloride. J. Hydrol. 147:83-103.

Liu, Guobin. 1999. Soil conservation and sustainable agriculture on the Loess Plateau: Challenges and prospects. Ambio 28(8): 663-668.

Luxmoore, R.J., P.M. Jardine, G.V. Wilson, J.R. Jones, and L.W. Zelazny. 1990. Physical and chemical controls of preferred path flow through a forested hillslope. Geoderma, 46:139-154.

Parker, G.C., 1963. Piping, a geomorphic agent in landform development of the drylands. : International Association of Hydrology Publication 65, p. 103-113.

Pierson, T.C., 1983. Soil pipes and slope stability. Quarterly Journal of Engineering Geology. 16:1-11.

SAS Institute, Inc. 1999. The SAS system for Windows. PC Release Version 6.08. Cary, N.C.

Sobieraj, J.A., H. Elsenbeer, R. Marques, B. Newton. 2002. Spatial variability of soil hydraulic conductivity along a tropical rainforest catena. Geoderma 108:79-90.

Uchida, T., K. Kosugi, and T. Mizuyama. 2002. Effects of pipe flow and bedrock groundwater on runoff generation in a steep headwater catchment in Ashiu, central japan. Water resources Res. 38(7):24-1 to 24-14.

Watson, K. W., and R.J. Luxmoore. 1986. Estimating macroporosity in a forested watershed by use of a tension infiltrometer. Soil Sci. Soc. Am. J. 50:578-582.

Wilson, G.V., and R.J. Luxmoore. 1988. Infiltration, macroporosity, and mesoporosity distributions on two forested watersheds. Soil Sci. Soc. Am. J., 52:329-335.

Wilson, G.V., J. M. Alfonsi, and P. M. Jardine. 1989. Spatial variability of saturated hydraulic conductivity of the subsoil of two forested watersheds. Soil Sci. Soc. Am. J. 53:679-685.

Wilson, G.V., P.M. Jardine, R.J. Luxmoore, and J.R. Jones. 1990. Hydrology of a forested watershed during storm events. Geoderma 46:119-138.

Xu Mingxiang, Liu Guobin, Bo Chunfeng. 2002. Experimental Study on Soil Infiltration Characteristics Using Disc Permeameter. Transactions of the CSAE, 16(4): 53-57.

Table 1. Physical properties of revegetated areas on Loess Plateau in Ansai, China.

Condition	Total # Macropores (> 1 mm)	# Large Macropores (> 5 mm)	Max. Pore Size	Macro-Porosity	Total-Porosity
	m^{-2}	m^{-2}	mm	$m^3\ m^{-3}$	$m^3\ m^{-3}$
1 yr	11.6c	5.6b	12.3ab	0.00076b	0.565a
6 yr	39.6ab	17.2a	17.0a	0.00180a	0.539ab
6yr, contour-ditched	30.8bc	8.4b	9.3b	0.00051b	0.495c
>15 yr	51.6a	18.4a	10.3b	0.00093ab	0.514bc

Note: Significant differences among conditions within a column at the 0.05 level indicated by different letters.

Table 2. Hydraulic properties of revegetated areas on Loess Plateau in Ansai, China.

Condition	Bulk Density	K_{sat}	Matrix Infiltration Rate	Macro-Infiltration Rate
	$Mg\ m^{-3}$	$m\ d^{-1}$	$m\ d^{-1}$	$m\ d^{-1}$
1 yr	1.148a	1.274a	152.9a	7967a
6 yr	1.163a	1.114ab	133.7ab	4665a
6 yr, contour-ditched	1.209a	0.791b	94.9b	91b
>15 yr	1.142a	1.269a	152.2a	47b

Note: Significant differences among conditions within a column at the 0.05 level indicated by different letters.

List of Figures

Figure 1. Typical ridge-gully interface on the loess plateau representative of the two ridges surrounded by gullies studied at the Ansai Station, China.

Figure 2. Upper gully face where the macropores distribution and mass slumping is characterized on a 1.5 m by 3 m length section.

Figure 3. The 50 cm by 50 cm metal frame placed on the soil surface for measuring the macropore distribution properties.

Figure 4. The 50 mm diameter ring inserted around a macropore to isolate it for macropore infiltration measurements under a 20 mm constant head.

Figure 5. Soil core being removed for quantifying the hydraulic properties of the soil matrix.

Figure 6. Recent mass slumped area evident by fresh soil face surround by crust cover gully face.

Figure 1. Typical ridge-gully interface on the loess plateau representative of the two ridges surrounded by gullies studied at the Ansai Station, China.

Figure 2. Upper gully face where the macropores distribution and mass slumping was characterized on a 1.5 m by 3 m length section.

Figure 3. The 50 cm by 50 cm metal frame placed on the soil surface for measuring the macropore distribution properties.

Figure 4. The 50 mm diameter ring inserted around a macropore to isolate it for macropore infiltration measurements under a 20 mm constant head.

Figure 5. Soil core being removed for quantifying the hydraulic properties of the soil matrix.

Figure 6. Recent mass slumped area evident by fresh soil face surrounded by crust covered gully face.

Hydraulic Characteristics of Knickpoints in Rill Confluence Zones

D.A. Brunton*
R.B. Bryan
Soil Erosion Laboratory; University of Toronto
1265 Military Trail; Scarborough, Ontario M1C1A4
Canada

Absract

Rill initiation is a critical process in soil erosion and hillslope development, usually associated with rapid increase in sediment transport rates. Many research data on critical threshold hydraulic conditions for rill initiation are available, but very little attention has been paid to rill systems, and particularly the effect of rill confluences on network evolution and water and sediment flux. While excellent studies of confluence conditions are available at the river scale, it is not clear if the results can be applied to the very different hydraulic conditions at rill scale. Fixed bed and erodible bed laboratory flume experiments under runoff have been used to address the hydraulic characteristics of knickpoints as they migrate upstream and bifurcate through a confluence zone. High-speed photography of silver tracers was used to determine velocity vectors through confluences with different angles, discharge ratios and knickpoint locations. In addition, cross-sectional water surface and bed elevations were measured at regular intervals throughout the junctions. Velocities decreased in the confluence region and the presence of a knickpoint in this zone generally amplified this effect and also served to disrupt standing wave development.

Keywords: rill, confluence, hydraulics

*Corresponding author

Hydrologically Driven Mechanisms of Head-Cut Development

M.J.M. Römkens*
(E-Mail: mromkens@msa-oxford.ars.usda.gov)
USDA-ARS
National Sedimentation Laboratory
Oxford, MS 38655

S.N. Prasad
Department of Civil Engineering
University of Mississippi
University, MS 38677

Abstract

This study concerns an analytical investigation of the effect of surface seal mechanical properties, overland flow, and subsurface hydrology on head-cut development. It has often been observed that head-cut growth rates on upland areas are quite small (less than one centimeter per minute) and that they occur in increments in which chips break off at points where cracks have developed in surface seals. The substrate soil under the seal collapses and is removed by the flow. This mode of head-cut development is the result of a strong interaction between the surface and the subsurface processes. The surface process is energetically controlled by the mechanical features of the seal whereas the subsurface process is hydrologically controlled. The analysis yields estimates of the temporal scale of head-cut velocities. In cases of infiltration from the vertical gully wall into the substrate, it was found that the flexural wave velocity (seismic sound velocity) inversely affects head-cut velocity.

1. Introduction

Most soil erosion research of the last seventy years has focused on the development of management practices and prediction tools for conserving productive agricultural land on upland areas. Significant research efforts were also expended on stream bed or channel erosion in order to stabilize the stream system, preserve its navigability, or improve its drainage capability. However, the weakest link in soil erosion research has been the area of gully erosion. This type of erosion mainly occurs between uplands and the stream system where drainage and erosion occurs through rills and gullies. On upland areas itself, soil erosion mainly occurs through the developing rill network system, that usually drains through the larger gully incisions. This type of soil erosion has also received comparatively less attention than that caused by raindrop impact. In part this lack of attention in gully and rill erosion research can be attributed to the highly dynamic and complex nature of the processes involved and in part to the logistically difficult and costly nature of the research that needs to be done.

Often, three components are recognized in rill and gully erosion: scouring action, head-cut advance, and sidewall sloughing (Meyer et al., 1975; Stern and Julien, 1993; Elliott and Laflen, 1993). Of those, the first two are usually considered to be the primary modes of erosion. Several attempts have been made to quantify the relative contribution of gully and rill erosion by scour and head-cuts. Zhu et al. (1985) conducted an experimental laboratory study in which soil

* Corresponding author

detachment by bed scour and head-cuts without tail water control in rills were measured for five soils, five discharge rates, and 3 slope steepnesses and found that soil losses by head-cuts were nearly an order of magnitude larger than those by scour. Similar observations have been made by other investigators. The dominant nature of head-cuts in soil erosion by overland flow is therefore the reason of its principal focus in the comparatively few soil erosion studies by overland flow. Stern and Julien (1993), developed a criterion of separating the rotating head-cut mode of erosion from that of a stepped head-cut based on upstream and downstream erosion time scales. These concepts of gully erosion were introduced by Holland and Pickup (1976). In this approach, the criterion developed is a parameter that represents the ratio of time that is required to erode the head-cut face up-stream over the time required to erode the head-cut face downstream. This ratio is a function of flow, sediment, and geometry parameters. The stepped head-cut mode was examined by Jia et al. (2002) through a numerical analysis for a head-cut in a two layered channel bed consisting of a cohesive layer overlaying a non-cohesive layer in which the head-cut migration was caused by mass failure of the cantilever brink that developed by the eroding action of the impinging overfall jet at the head-cut foot of non-cohesive material. DePloey (1989) presented a mathematical model for knickpoint or head-cut retreat based on measurable topographic and hydrodynamic parameters, that include flow kinetic energy and discharge. His model is a fairly simple one and represents an approach based on dissipating energy considerations rather than shear forces.

With few exceptions, most gully studies dealt with the hydrodynamic aspects of gully development and gully advance. With the exception of the Jia et al. (2002) study, these studies always involve one soil type. Very little attention has been given to the role of subsurface flow in gully development. Huang and Laflen (1996) observed rill/gully development due to seepage during the post-storm period on slightly sloping land in eastern Indiana, USA. On upland areas, one often observes during storm events on freshly tilled, sloping land, a sequence of small head-cuts in the concentrated flow paths. These head-cuts reflect differences in the mechanical properties of the thin sealed surface layer relative to the undisturbed bulk substrate. The differences are induced by rain drop impact, during which process the soil surface structure degrades and becomes compacted and cohesive. The seals often appear to retain a higher degree of stability and are more cohesive than the underlying substrate. In this article, we examine in more detail how upslope head-cut migration is affected by the mechanical properties of the seal, the hydrodynamic property of the surface flow, as well as the soil water flow regime in the substrate. Details of the analysis concerning the first two factors are given by Prasad and Römkens (2003). In this article, we add to the analysis on the effect of the substrate water regime on head-cut migration. The case of water intrusion into the subseal area through the head-cut face, was largely discussed by Prasad and Römkens (2004). The effect of water exfiltration or seepage on head-cut retreat is the major focus of this study. In most field situations, outflow or seepage effects, are the dominant mode of head-cut instability in soil erosion.

2. Description Physical Model

The physical model assumes a sloping surface with incident rain as illustrated in Fig. 1. The soil profile has an impervious layer at a finite depth and at the foot slope there is a seepage zone. Streamlines indicate the subsurface flow regimes. Excess rainwater concentrates in flow paths at various locations on the surface. At places where the velocity of concentrated flow is sufficiently high, the flow incises into the soil surface leading to the formations of rills and

gullies. The incisions often include a series of head-cuts or stepwise changes in the concentrated flow path, where most of the sediment is generated. During the early stages of rainfall, the exposed soil usually develops a surface seal due to the destructive effect of impacting raindrops. This surface seal tends to reduce the infiltration rate and offers increased resistance so erosion by overland flow. In places where head-cuts develop, a complex array of processes involving surface and substrate flow, in combination with the soil mechanical properties, control sediment detachment, entrainment, and deposition.

Water flows in concentrated pathways over a sealed/crusted surface and jettisons into small plunge pools, or surface cavities from where it subsequently moves downslope. A schematic representation of this model is shown in Fig. 2. Due to the swirling action of plunge pool water or as a consequence of the impact pressure of the water jet, soil is being detached, entrained into the flow and either deposited, once the carrying capacity of the local hydrologic regime has been reached, or transported further downstream. During this process, subsurface water may either exit in the head-cut region, thus adding to the detachability of the soil material, or surface water may enter into the soil profile. In the latter case, the local soil water potential increases and thereby reducing the cohesion between the soil particles of the substrate.

The seal/crust material has a greater internal strength or cohesion than the substrate. However, the eroding and receding substrate no longer supports the surface seal, which now must carry its own, increasing self-weight as well as the weight of the fluid flow that it supports. There is another force that acts on the suspended seal. This is a force which results from the thrust of the flow itself over the seal. Though different in magnitude, its operational mode can best be understood by comparing the principles of operation with that of a jet engine or with rocket propulsion. That is, the water flow (water jet) over the seal is balanced by a resistance force in the opposite direction. This force is transmitted to the seal, which together with its self weight and weight of the flow, comprise the total forces or load acting on the seal. This load causes stresses within the seal/crust leading to seal bending with the maximum load supported by the substrate near the cavity. From a mechanical standpoint this mechanism may be called a plastic hinge. Also, stresses develop in the substrate adjacent and in the immediate vicinity of the head-cut. At the point where the seal is no longer supported by the substrate, maximum bending occurs. The longer the non-supported part of the seal or "overhang" over the cavity or plunge pool area, the greater the bending moment at the plastic hinge. There is a critical length of this "overhang" where for a given hydraulic flow, the seal is unable to withstand the load and failure occurs.

3. Mathematical Description of Head-cut Growth

3.1. Seal failure dynamics

A detailed description of the analysis of seal failure dynamics has been described by Prasad and Römkens (2003). Briefly, seal failure occurs when the total work done by all external loads on the seal exceeds the allowable strain energy stored in the seal. The total mechanical energy of the load acting on the seal equals the sum due to the seal self-weight, the weight of the flow, W_1 and the hydraulic thrust (W_2).

$$W_1 = \int_0^{\ell} q\, y\, dx \qquad (1)$$

$$W_2 = \int_0^{\ell} F\cos\varphi \, dx - F\delta^* \sin\varphi \qquad (2)$$

where q is the sum of the seal weight per unit length with thickness h and the water column of height H supported by the seal. Here ****** = y(0) is the maximum deflection of the seal at the tip (x=0), **N** is the angle of the water jet with the horizontal and F is the thrust generated by the water jet over the seal and x and y are coordinates with the origin located at the "hinge" point.

The energy stored in the seal area consists of three components: (1) the strain energy in the seal itself given by the expression:

$$U_1 = \frac{1}{2E_yI}\int_0^{\ell} M^2 \, dx \qquad (3)$$

where M is the bending moment of the section x, and E_yI is the flexural rigidity of the seal, in which E_y is Young's modulus of elasticity and I is the moment of inertia; (2) The main energy U_2 stored in the substrate due to compression by the weight of the seal, and (3) the energy U_3 stored in the plastic hinge under a rotation angle **2** at x=R which is given by the expression

$$U_3 = M_u \, \Phi \quad \text{where} \quad M_u = \frac{1}{4}\sigma_y \, h^2 \qquad (4)$$

M_u is the ultimate moment of the seal at the plastic hinge and **M** is the angle between the horizontal and the seal taken at x=R, $\mathbf{F}_y$ is the yield stress of the seal material, while h is the seal thickness. For seal failure to occur, the total energy W acting on the seal must equal the allowable energy V stored in the seal. Thus:

$$V = U_1 + U_2 + U_3 = W = W_1 + W_2 \qquad (5)$$

Of the strain energies operable, the dominant contribution (U_3) is stored in the plastic hinge. The energy balance equation can thus be approximated by:

$$\int_0^{\ell} q\,y\,dx + \int_0^{\ell} F\cos\varphi\,dx - F\delta^*\sin\varphi = M_u\,\Phi \qquad (6)$$

which can be simplified to

$$\frac{q\ell\delta}{2} + F\ell\cos\varphi - F\delta^*\sin\varphi = \frac{1}{4}\sigma_y h^2\Phi \qquad (7)$$

Thus

$$F = \frac{1}{\cos\varphi - \frac{\delta^*}{\ell}\sin\varphi}\left(\frac{\sigma_y h^2}{4\ell}\Phi - \frac{q\delta^*}{2}\right) \qquad (8)$$

The maximum deflection which occurs at the seal tip can be approximated by

$$\delta^* = \Phi \ell = \frac{q \ell^4}{8 E_y I} \tag{9}$$

which yields the following expression for the thrust:

$$F = \frac{1}{\cos\varphi - \Phi \sin\varphi} \left(\frac{\sigma_y h^2}{4} \cdot \frac{q \ell^2}{8 E_y I} - \frac{1}{2} \frac{q^2 \ell^4}{8 E_y I} \right) \tag{10}$$

For seal failure to occur, the critical hydraulic thrust can be obtained by setting $\frac{\partial F}{\partial \ell} = 0$. This yields:

$$\ell_{cr} = \sqrt{\frac{\sigma_y h^2}{4q}} \tag{11}$$

and

$$F_{cr} = \frac{1}{\cos\varphi} \left(\frac{\sigma_y h^2}{4} \right)^2 \frac{1}{16 E_y I} \tag{12}$$

in which the **M** sin **n** term of Eq. (10) is neglected because of its small magnitude. The critical seal length is thus a function of the yield stress, the seal thickness, and the weight per unit length of the seal with over-burden water depth. Equation (11), thus provides a link for establishing the various time scales which are commonly observed in natural systems.

3.2. Soil water movement into substrate

The soil water pressure in the substrate at any point is determined by the combined effect of the wetting front penetration and the retreat of head-cut. The latter is controlled by the degree of surface protection of the growing seal overhang and the hydrodynamics near the head-cut face of the flow in the plunge pool.

The wetting front advance for this case can be approximated by the horizontal infiltration equation in which the wetting front tip is given by the relationship (Kirkham and Feng, 1949; Bruce and Klute, 1956)

$$\delta_w = A \sqrt{t} \tag{13}$$

where $*_w$ is the wetting front advance in the substrate and A is usually referred to as the Boltzmann variable. A solution of the Richard's equation for horizontal infiltration using the Ahuja-Swartzendruber (A-S) diffusivity equation (Ahuja-Swartzendruber, 1972) and a spectral series solution (Römkens and Prasad, 1992) given respectively by the relationships:

$$D(\theta_w) = \theta_{ws}^n \frac{a}{(\theta_w - \theta_{ws})^{n/5}} \tag{14}$$

$$\theta_w = \sum_{n=0}^{m} a_i(t)\,(\delta - x)^{\alpha+m} \tag{15}$$

yields an expression for A in terms of the constants in the A-S diffusivity equation. This expression is:

$$A^2 = \frac{2\alpha a}{\theta_{ws}^{n/5}} \left[\frac{1}{2}(\alpha+1)(\alpha+2)\theta_{ws} \right]^n \tag{16}$$

where θ_{ws} is the saturated water content, $a_i(t)$ are time dependent coefficients, δ is the wetting front depth, and a and n are characteristic constants for a given soil which may be obtained from the diffusivity function. Analytical considerations (Römkens and Prasad, 1992) based on horizontal infiltration with concentration type boundary conditions show, that

$$\alpha = \frac{1}{n} \tag{17}$$

This relationship indicates that there is an important linkage between the diffusivity equation and the spectral series solution for the soil water wetting front. In fact, " or n are parameters that describe the slope of the wetting front. Thus in this interval of time scale between seal failures, the wetting front progresses a finite distance further into the substrate, thereby creates a dynamic situation in which a certain balance is established and leads to an identifiable parameter which in the limit becomes a certain velocity. The details of this analysis follows.

3.3. Head-cut migration rate – the infiltration case

During the short time interval that a seal overhang develops and breaks, the wetting front progresses a finite distance) * into the substrate due to infiltration of water entering the vertical wall of the head-cut, which period is referred to as the short time scale, denoted by)t. It is assumed that infiltration through the seal is negligible. Under steady and constant flow conditions, it may be expected that, on the average, the next seal failure will again take place in a subsequent time interval)t and that the failed "overhang" length R_{cr} will be similar in length to that of the previous failure. Taken over many periods of)t, it is reasonable to deduce that the failed length R_{cr}, which in effect represents the larger time scale, is proportional to)*$_w$. Thus

$$\Delta\delta_w \propto \ell_{cr}$$

or at any moment

$$\delta_w = C_p\, \ell_{cr} \tag{18}$$

where C_p is the proportionality constant.

Substitution of (11) and (13) into (18) yields.

$$A\sqrt{\Delta t} = C_p \sqrt{\frac{\sigma_y h^2}{4q}} \tag{19}$$

or

$$A^2 \Delta t = C_p^2 \sqrt{\frac{\sigma_y h^2}{4q}} \cdot \sqrt{\frac{\sigma_Y h^2}{4q}} \tag{20}$$

The reason for writing in product form the two radical terms on the right hand side of (20) is to let one of them be equal to ℓ_{cr} as defined in (11). This enables us to introduce head-cut velocity as shown below.

The self-weight plus water load on the seal, q, per unit seal width is given by the relationship:

$$q = \gamma h + \gamma_1 H \tag{21}$$

where h is the seal thickness, γ is the seal density, H is the flow depth and γ_1 is the density of water. Substitution of (21) into (11) yields

$$\frac{\sigma_y h^2}{4q} = \frac{\sigma_y}{4} \cdot \frac{h^2}{\gamma h + \gamma_1 H} = \frac{\sigma_y}{4\gamma} \cdot \frac{h}{1 + \frac{\gamma_1}{\gamma}\frac{H}{h}} \tag{22}$$

Using this identity in (20) one obtains

$$A^2 = \frac{C_p^2}{2\Delta t} \cdot \sqrt{\frac{\sigma_y h^2}{4q}} \cdot \sqrt{\frac{\sigma_y}{\gamma} \cdot \left(\frac{h}{1 + \frac{\gamma_1}{\lambda}\frac{H}{h}} \right)} \tag{23}$$

Define:

$$C = \frac{\ell_{cr}}{\Delta t}, \quad C^* = \sqrt{\frac{\sigma_y}{\rho}}, \quad \gamma = \rho g \tag{24}$$

Note that both C, the head-cut velocity and C*, the seismic velocity have the dimensions L/T (velocity), whereas, ρ is the mass density of the seal material and g is the acceleration due to gravity. In terms of the above definitions, we now have

$$C = \frac{2A^2}{C_p^2} \cdot \frac{1}{C^*} \cdot \sqrt{\frac{g}{h}\left(\frac{\gamma_1}{\gamma} + \frac{H}{h}\right)} \tag{25}$$

which may be written as

$$C = \frac{b}{C^*} \tag{26}$$

where

$$b = \frac{2A^2}{C_p^2} \cdot \sqrt{\frac{g}{h}\left(\frac{\gamma}{\gamma_1} + \frac{H}{h}\right)} \tag{27}$$

Thus, the rate of head-cut advance becomes faster as the seal material becomes softer (C^* is smaller). Further, an estimate of the order of the temporal velocity scale may be made by observing that g/h is of the order of 10^4/sec^2 for a 1 mm-thick seal, C^* of the order 10^4 cm/sec and A^2 is of the order 10^{-1} cm^2/sec, so that C is of the order 10^{-3} cm/sec.

3.4. Head-cut velocity in shallow soil – the seepage case

In many situations severe erosion takes place during storm events when a shallow soil layer exists over an impervious bottom. This soil profile condition encourages overland flow and subsurface flow in case of a leaking seal. This case may also cause erosion due to head-cut development. Such a situation is depicted in Fig. 3, in which a hillslope section of a hill of length L in a landscape is shown with streamlines and a seepage zone with a soil layer of thickness H on top of an impervious layer. The seepage flow not only destroys the adherence between the seal and the substrate, but also causes stresses in the soil matrix, due to the friction of the flow with the soil particles. These additional forces may be included in the seal failure analysis as was previously presented but for the sake of simplicity we outline here an approximate result which is based on equation (11) of the previous section. We assume that we have a slowly permeable seal through which the infiltration rate (recharge) into the layer is steady with magnitude i_0 (L/T). There is no flux through the upper boundary at X=O. The subsurface profile (water table) will be approximated to become horizontal as shown. Infiltrated water leaves the system at the downstream boundary x=0 with flux q_o and the top surface where seal failure has taken place with the magnitude of the flux q*. As discussed before let the failure length be R_{cr} given by (11).

The forces acting on a soil volume in the seepage zone consists of: (1) the self weight of the soil material with water, (ii) the frictional force due to cohesion of the soil material, and (iii) the seepage force, which the internal flow exists on the soil medium. Fig. 4 depicts a schematic of the forces acting on a unit soil volume. At equilibrium, the frictional force equals the weight and seepage force as given by the following relationship:

$$\frac{\partial \tau}{\partial y} = (\rho_b - \rho_o) g \cdot \sin\theta + f_x \tag{28a}$$

and $$\frac{\partial \sigma}{\partial y} = \left(\rho_b - \rho_o\right) q \cdot \cos\theta + f_y \tag{28b}$$

where τ and σ are the shear stress (along the x-axis) and the normal stress (along the y-axis), respectively. θ is the slope angle with the normal to be the soil surface, g is the acceleration due to gravity, and $(\rho_b - \rho_o)$ is the net bulk density. When failure occurs Coulomb's law applies, and the relationship used is:

$$\tau = \sigma \tan \phi \tag{29}$$

where φ is the angle of internal friction. Differentiation with respect to y yields:

$$\frac{\partial \tau}{\partial y} = \frac{\partial \sigma}{\partial y} \tan \phi \tag{30}$$

The seepage force components f_x and f_y in relationships (29) can be expressed in terms of the hydraulic gradient according to the expressions:

$$f_x = -\rho_o g \frac{\partial h}{\partial x} \tag{31a}$$

and $$f_y = -\rho_o g \frac{\partial h}{\partial y} \tag{31b}$$

where h is the hydraulic head. The seepage vector makes an angle ψ with the normal to the soil surface. The magnitude and direction of the seepage vector is determined by the geometry of the soil profile, the hydraulic conductivity of the soil, the upstream rain infiltration, and local conditions. The appropriate relationships are given by

$$\frac{\partial h}{\partial x} = -S \sin \psi \tag{32a}$$

$$\frac{\partial h}{\partial y} = S \cos \psi \tag{32b}$$

Combining eqs. (31) and (32) yields:

$$f_x = \rho_o \; g \; S \sin \psi \tag{33a}$$

and $$f_y = -\rho_o \; g \; S \cos \psi \tag{33b}$$

Substitution of eqs (33) into eq (28) and following several algebraic manipulations, the following relationship can be obtained for the magnitude of the seepage vector:

$$S = \frac{\rho_b - \rho_o}{\rho_o} - \frac{\sin(\varphi - \theta)}{\sin(\psi - \varphi)} \tag{34}$$

Relationship (34) indicates that seepage depends on the slope angle of the soil, θ, the coefficient of internal friction of the soil, ψ, and the exit angle of the seepage vector relative to the normal, φ. This is an important finding as it indicates how the seepage force depends on the flow field. For determination of the seepage vector, the flow field must be determined.

The application of the mass balance for water is in the slope area yields the following relationship for the migration rate:

$$V = i_o \frac{L}{H} - q_o - \frac{KS}{H}\sqrt{\frac{\sigma_Y h^2}{4q^*}} \tag{35}$$

where i_o is the rainfall intensity per unit area, L and H are the slope profile parameters (length and depth), q_o is the seepage through the gully vertical wall, k is the soil hydraulic conductivity, h is the seal thickness, σ_y is the yield stress, q* is the seepage through the zone of failure. The first term represents the total amount of infiltrated water per unit time, the second term is the water that exists at the bottom of the slope through the gully wall, and the third term is the water loss through the eroded part of the gully where the

$\sqrt{\frac{\sigma_y h^2}{4q^*}}$ term represents the seal critical length term of failure.

Equation (35), similar to (25), establishes the scale (dynamic) of rapid head-cut migration rate. Note that L/H will be quite large whereas h/H will be quite small. Further q_o may be evaluated from an analysis based on the principle of ground water flow model, whereas q* may be obtained from certain boundary value solution of Laplace equation as applied to the present problem.

Summary

Head-cut migration on sloping land with sealing susceptible soils, was analyzed in terms of material properties of the seal (seal yield stress, seal thickness) and the hydraulic flow characteristics of overland and subsurface flow. Two cases were considered. For the case where infiltration through the seal upstream from the head-cut is very small, the seal properties largely control the migration velocity of the head-cut (infiltration case) and the time scale is in the range of cm/hr. For the case where upstream infiltration is significant, water will exit through the head-cut face and the seal area near the head-cut (seepage). In this case, the runoff component was for simplicity reasons, not included.

References

Ahuja, R.L. and D. Swartzendruber. 1972. An improved form of soil water diffusivity function. Soil Sic. Soc. Amer. Proc. 36 : 9-14.

Bruce, R.R. and A. Klute. 1956. The measurement of soil moisture diffusivity. Soil Sci. Soc. Amer. Proc. 20(4):458-462.

de Ploey, J. 1989. A model for head-cut research in rills and gullies. Catena Supplement 14:81-86.

Elliott, W.J. and J.M. Laflen. 1993. A process based rill erosion model. Trans. ASAE 36:65-72.

Holland, W.W. and G. Pickup. 1976. Flume study of knick point devlopment in stratified sediment. Geol. Soc. Am. Bull. 87(1):76-82.

Huang, C. and J.M. Laflen. 1996. Seepage and soil erosion for a clay loam soil. J. Soil Sci. Soc. Amer. 60(2):408-416.

Jia, Y. T. Kitamura, and S.S.Y. Wang. 2002. Numerical experiment on head-cut of two-layered channel bed. Accepted for publication in Advances in Hydroscience and Engineering. Vol. 5 (CD ROM).

Kirkham, D. and C.L. Feng. 1949. Some tests of the diffusion theory and laws of capillary flow in soils. Soil Sci. 67:29-40.

Kohl, K.D., W. J. Elliott, and J.M. Laflen. 1988. Evaluating rill head-cutting in the field. ASAE -- paper 88-2596.

Meyer, L.D., G.R. Foster, and S. Nikolov. 1975. Effect of discharge rate and canopy or rill erosion. Trans. ASAE 18: 905-911.

Prasad, S.N. and M.J.M Römkens. 2003. Energy formulations of head-cut dynamics. Catena. 50:469-487.

Prasad, S.N. and M.J.M. Römkens. 2004. Mechanical energy and subsurface hydrologic effects in head-cut processes. Proc. Second International Gully Erosion Conference on Global Climate Change, Chengdu, Sichuan, P.R. China, (In Press).

Römkens, M.J.M, and S.N. Prasad. 1992. A spectral series approach to infiltration for crusted and non-crusted soils. In: Soil Crusting-Chemical and Physical Processes. pp 151-178. Eds: M.E. Summer and B.A. Stewart. Adv. in Soil Science. Lewis Publishers, Boca Raton, FL.

Stern, O.R. and P.Y. Julien. 1993. Criterion delineating the mode of head-cut migration. J Hydr. Eng. 119(1).

Zhu, J.C., C.J. Gantzer, R.L. Peyton, E.E. Alberts, and S.H. Anderson. 1985. Simulated small-channel bed scour and head-cut erosion rates compared. Soil Sci. Soc. Am. J. 59: 211-218.

List of Figures

Figure 1. A schematic cross-section through a slope in a landscape.

Figure 2. A schematic representation of head-cut moving through a sealer soil surface. The solid line delineates the surface water body at time $t = t_1$, and the broken line represents the surface water body at $t = t_1 + \Delta_t$. BC and B′C′ represent the wetting front at t_1 and $t_1 + \Delta_t$, respectively. O is the origin of the x-y coordinate system.

Figure 3. A schematic cross-section of a down-slope section of a hill with a seepage zone.

Figure 4. A schematic representation of the gravity and seepage forces acting on an unit soil volume in the seepage zone.

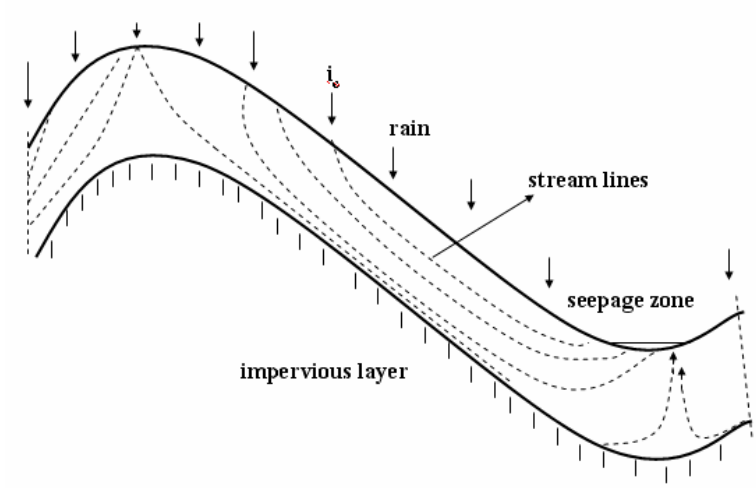

Figure 1. A schematic representation of the gravity and seepage on an unit soil volume in the seepage zone.

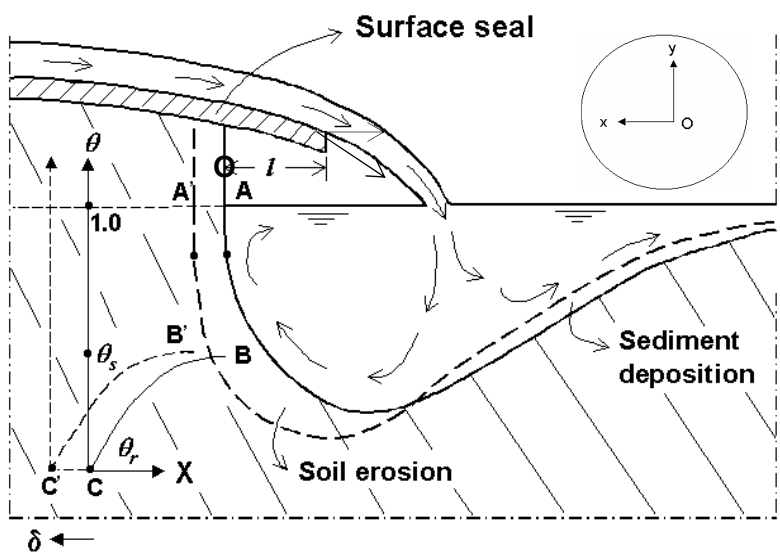

Figure 2. A schematic representation of a head-cut moving through a sealer soil surface. The solid line delineates the surface water body at time $t = t_1$, and the broken line represents the surface water body at $t = t_1 + \Delta_t$. BC and B′C′ represent the wetting front at t_1 and $t_1 + \Delta t$, respectively. O is the origin of the x-y coordinate system.

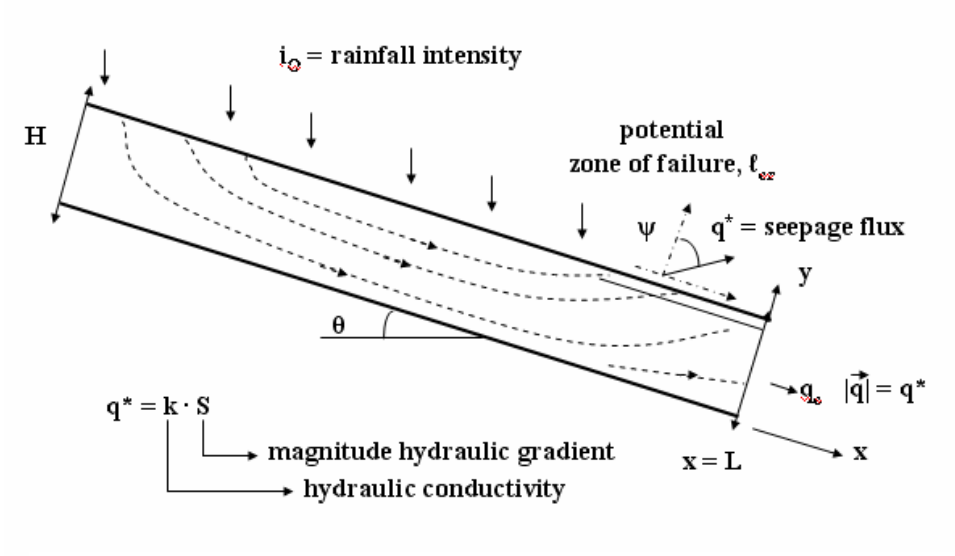

Figure 3. A schematic cross-section of a down-slope section of a hill with a seepage zone.

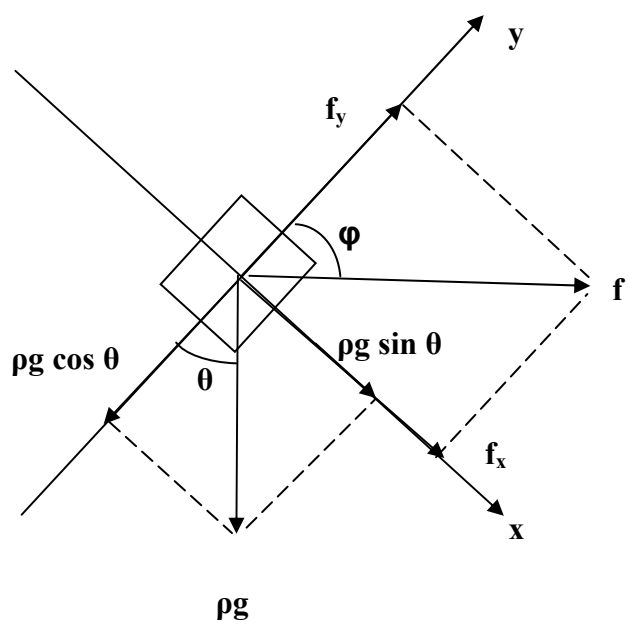

Figure 4. A schematic representation of the gravity and seepage forces acting on an unit soil volume in the seepage

Overview of Dam Gully Erosion Research

G. J. Hanson* (E-Mail: Greg.Hanson@ars.usda.gov)
D. M. Temple (E-Mail: Darrel.Temple@ars.usda.gov)
USDA-ARS Hydraulic Engineering Research Unit
Stillwater, Oklahoma, USA
FAX 405 624 4136

K. M. Robinson (E-Mail: Kerry.Robinson@ftw.nrcs.usda.gov)
USDA-NRCS Watershed Science Institute
Raleigh, North Carolina, USA
FAX 919 828 7366

K. R. Cook
USDA-ARS Hydraulic Engineering Research Unit
Stillwater, Oklahoma, USA
FAX 405 624 4136

Abstract

Traditionally gully erosion has been identified with the dissection of the landscape in agricultural settings but it is also recognized as a prevalent erosion feature in earthen dam auxiliary spillways and embankments. Flows through earthen spillways and over dam embankments, due to large rainfall events, have the potential to erode and breach the dam or spillway and result in catastrophic releases from the reservoir. The gully erosion process in an earthen spillway or on an embankment can be characterized by stages of initiation, development, and migration of a headcut. A headcut is defined as a near vertical drop at the upstream end of a gully. The rate of headcut migration is important in determining the breach potential of an earthen spillway and dam embankment. A research program is being conducted to examine the gully erosion processes of earthen dam auxiliary spillways and embankments. This paper describes: 1) the unique test facilities constructed to examine the dominant factors affecting the erosion of earthen spillways and embankments; 2) the observations of the erosion processes and results to date; and 3) the predictive relationships that have been developed for dam gully erosion research at the ARS Hydraulic Engineering Research Unit laboratory in Stillwater, OK.

1. Introduction

The most common type of dam in operation today is the earthen embankment dam. While the safety record for all types of dams is good, embankment dams in particular are considered remarkably safe based on the number of earthen dams in existence versus the number that have failed (Singh, 1996). Even though dams have an enviable safety record failures do occur. When a dam does fail, large quantities of water may be released, endangering life and damaging property downstream. Middlebrooks (1953), in a description of earth-dam practices in the United States, observed that overtopping, accounted for 30% of all partial or complete failures. Shuibo et al. (1993) reported that 98% of dam failures in China were associated with earth dams, and that overtopping including inadequate spillways accounted for 51.5% of those

*Corresponding author

failures. These statistics are important from the perspective that earth dams account for the vast majority of dams that have been constructed in the United States. Ralston (1987) observed that some 57,000 dams in the United States dam inventory have the potential for overtopping. Earth dams are also of specific interest to the USDA, which has assisted in the design and construction of over 10,000 watershed flood control dams, representing an approximate $14 billion investment (Caldwell, 1999). These structures, as part of their design, typically have an earthen auxiliary spillway and an earthfill embankment. Therefore the process by which earthen auxiliary spillways and embankments erode and sometimes fail during extreme flood events is of national and international concern.

Performance of structures during extreme events has been observed and documented in several cases (Miller and Ralston 1987, Singh and Scarlatos 1988, Temple and Moore 1997, Walder and O'Connor 1997, and Wahl 1998). Singh and Scarlatos (1988) observed that the time of dam failure for 33 historical cases was between 30 minutes and 12 hours and that breach width for 52 historical dam failure cases ranged from 0.8 to 10.9 times the breach depth, with a mean value of 4.2. The USDA conducted field studies on over 80 auxiliary earthen spillway sites that sustained a range of no damage to complete breach of the structure as a result of flood events (Temple and Moore, 1997). Even though observation and analysis of the performance of these structures following extreme events is important, the information collected is often limited. Total time for the erosion event and volume of erosion can usually be determined from field surveys, but the processes and rate of erosion are more difficult to assess due to the fact that most of the information is gathered after the event, and rarely while it is occurring.

The observations that have been made during and after spillway flows or embankment overtopping, in both the field and laboratory, indicate that the erosion that does occur has much in common with the erosion observed in other settings that experience concentrated flows, such as in agricultural fields and natural streams. The primary erosion process observed in nature that is also observed in spillway flows and embankment overtopping is gully erosion (Ralston 1987, Temple 1992). Gully initiation and formation is a concentrated flow process that is clearly an erosion threshold and rate phenomenon (Poesen et al. 2003). The threshold for gully initiation and development is most commonly expressed in terms of the boundary flow shear stress. The rate of erosion in the concentrated flow environments is most commonly expressed in terms of the excess stress equation:

$$\dot{\varepsilon} = k_d(\tau_e - \tau_c)^a \tag{1}$$

where
ε = the rate of erosion,
k_d = the detachment coefficient,
τ_e = the effective boundary flow shear stress,
τ_c = the critical or threshold shear stress, and
a = empirical constant with a value on the order of 1.

Gullies typically form on steep slopes, with the initial formation caused by a perturbation in the vegetation, or changes in surface slope (Thornes 1980). Once initiated, one of the more common and notable features of gully erosion is the upstream formation and migration of the waterfall or headcut (Ireland et al. 1939, Thompson 1964, Deploey 1989, Bocco 1991, Stien and Julien 1993, Alonso et al. 2002, and Poesen et al. 2003). Gully headcuts and walls have been described as moving in a sporadic fashion as the driving forces on the soil mass equal or exceed

the resisting forces (Bradford and Piest 1977). Due to the implications of headcut migration on sediment production and dissection of the landscape, prediction of headcut location and migration rate has been a focus of gully modeling. Early quantitative predictions of headcut migration were empirical equations based on drainage area, slope, rainfall, and clay content and were limited to regional application (Thompson 1964, SCS 1966). More recent prediction equations of headcut movement on the landscape have focused on deterministic modeling methods (Deploey 1989, Stein and LaTray 2002, Alonso et al. 2002, Prasad and Romkens 2003). Headcut migration is a complex process, and the existing deterministic models that have been developed are necessarily simplifications, often focused on a specific set of conditions. These models, relative to the hydraulic parameters driving the headcut migration, tend to fall into two basic categories; energy based (Deploey 1989, Prasad and Romkens 2003), hydraulic stress based (Stein and Latray 2002), or both (Alonso et al. 2002). The models listed here exclude headcut migration due to seepage and weathering even though most of them, due to the nature of their development, could incorporate these factors into their stress or energy components.

Gullies tend also to form in earthen spillways and embankments in situations similar to natural settings, on steep slopes (the exit channel or downstream face) and often in association with a perturbation (i.e. changes in vegetation, materials, slope, structures, paths, or roads) (Ralston 1987, Temple 1992) (Figure 1). Observations of earthen spillway flows in the field and results from laboratory tests have led to the development of a sequential three-phase erosion model (Temple and Hanson 1994, and Temple and Moore 1997) that has been integrated into the USDA-NRCS Sites model (NRCS, 1997). Observations of the erosion of overtopped embankments, both in the field and during large-scale laboratory tests indicate that a similar component sequential description can also be made of the embankment erosion process as was made with the spillway erosion process (Ralston 1987, Hanson et al. 2003) with additional inclusion of widening and a 4th phase of erosion; removal of the upstream face of the embankment after the headcut becomes submerged following entry into the reservoir. The three-phases describing the progress of erosion to the point of breaching the structure are primarily a description of gully initiation, development, and growth: 1) local destruction of the vegetal cover, if any, and development of concentrated flow, 2) concentrated flow erosion leading to the development of a headcut capable of advancing upstream, and 3) upstream advance and deepening of the headcut as it progresses upstream (Figure 2).

The USDA Agricultural Research Service Hydraulic Engineering Research Unit, Stillwater OK has conducted and is conducting laboratory research to help provide needed information to quantify the three phases of erosion that occur during spillway flow events and embankment overtopping. This research program has covered a 25-year period beginning with research initially on earthen spillways and presently on overtopped embankments. The description of testing facilities and results that follow are based on the three-phase erosion model. The predictive relationships that have been and are being developed as a result of this work are stress based and energy based relationships. The objective of this paper is to describe: 1) the unique test facilities that have been constructed to examine the dominant factors involved in the erosion of earthen spillways and embankments; 2) the observations of the erosion processes and results; and 3) the current predictive relationships that have been developed for dam gully erosion to describe the three phases of erosion from vegetal failure to headcut migration.

2. Dam Gully Erosion Testing

2.1. Phase 1

Vegetal stability tests have been conducted in outdoor channels at the laboratory on slopes of 5% to 33% (Temple 1985, Temple 1992, Temple and Alspach 1992, Temple and Hanson 1994, Temple and Hanson 1998, and Hanson and Temple 2002). Tests on these channels, as well as field data, have provided information and confirmation of phase 1 erosion of earthen spillways and overtopped embankments. The initial tests were designed to investigate the effective stresses, roughness, and protective capability of vegetation in spillways. The more recent and ongoing tests have been designed to investigate the protective capability of vegetation on steep slopes and the applicability of the relationships determined for the spillways to embankment overtopping.

The primary data for the stability studies of vegetation in spillways was taken from flow measurements in eight channels in the outdoor laboratory (Figure 3a). Each of the channels was flat bottomed with a width of 0.91 m, a length of 30.5 m, and a slope of 5%. Individual channels were separated by concrete dividers and vertical wooden walls either 0.3 or 0.6 m high were mounted on the concrete dividers immediately prior to testing. Forming the channel in this fashion minimized the wall effect on both vegetation and flow. Additional base line data was taken from flows in a 6.1 m wide flat-bottomed, 9% slope channel (Figure 3b) and a rounded bottom, 8% slope channel. Data collected from these tests included discharge, flow duration, flow velocities, water surface elevations, bed elevations, soil type, vegetal type, vegetal length, vegetal density, and vegetal condition. Various vegetal covers and soils conditions were tested. The impact of vegetal discontinuities on flow conditions and channel stability were also studied.

Physical model tests to extend the research on vegetation in spillways to embankments were carried out on a 3 m high embankment constructed in the outdoor laboratory (Figure 3c). After construction of the embankment, six 0.9 m wide channels were cut into the embankment to allow tests to be conducted on individual sections. The slope of the channels was 33% and the soil classified as CL-ML in the Universal Soil Classification System. Tests were conducted on green bermudagrass, dormant bermudagrass, and green fescue (Temple and Hanson 1998). Effective overtopping depths for the tests ranged from 0.27 to 0.67 m. Duration of testing was up to 75 hr with mean velocities up to 5 m/s.

2.2. Phase 2

The primary focus of phase 2 erosion is the detachment of soil materials experiencing hydraulic stresses once the vegetation has been removed. Outdoor flume tests were conducted to determine rate of erosion of soil materials (Hanson 1989 and 2001, Hanson and Temple 2002) in channels ranging in slope from 0.5% to 33%. An in-situ and laboratory cohesive soil erodibility-testing device has also been developed (Hanson 1991, Hanson 2001). These tests have been designed to investigate the effective stresses, roughness, and resistance of materials placed at densities comparable to soils in earthen spillways and embankments.

The primary data for describing erosion resistance of soil materials was taken from flow measurements in six channels in the outdoor laboratory (Figure 4a). Each of the channels was flat bottomed with a width of 0.91 m, a length of 30.5 m, and slopes of 0.5 to 3%. Soil materials, ranging from a non-plastic SM sandy loam to a plastic CL clay loam, were placed in temporary channels separated by 0.2 m wood dividers, with vertical wooden walls 0.3 m high mounted on the dividers immediately prior to testing. Additional data has been taken from flows in 1.8 m wide flat-bottomed channels, 1 and 3% sloped (Figure 4b) and two 0.9 m wide trapezoidal channels cut into a 3 m high embankment on a 33% slope. Data collected from these tests

included discharge, flow duration, flow velocities, water surface elevations, bed elevations, soil type, density, strength and erodibility.

Although open channel testing is widely recognized as the most reliable method of testing soil erodibility, the cost and physical requirements led to the development of a submerged jet testing apparatus for field and laboratory use (Hanson 1991, Hanson 2001) (Figure 4c). The apparatus consists of a jet submergence tank, a jet tube and orifice with a fixed upstream pressure, a water supply, and a method of measuring maximum scour of the soil surface directly below the soil surface. The apparatus has been used to compare field channel test results and in-situ measurements. It has also been used in the laboratory to investigate the effects of compaction on material erodibility.

2.3. Phase 3

2.3.1. Hydraulic Stresses

The hydraulic stress and pressure forces in the vicinity of the headcut are considered key components in the advance rate of a gully headcut. Due to the lack of information on stress and pressure forces in the vicinity of the headcut, physical model tests were conducted to measure hydraulic shear stress on the channel bed upstream of the headcut brink (Robinson and Cook 1998) and to measure hydraulic shear stress and pressure downstream of the headcut (Robinson 1992) (Figure 5a). The boundary shear stresses in both cases were measured using hot-film anemometry. Hydraulic pressures along the boundary downstream of the overfall were measured using pressure transducers. Upstream of the overfall, stresses were measured in time and space for various Froude numbers and flow rates. Downstream of the overfall, stresses were measured in time and space for various overfall heights, flow rates, and tailwater conditions.

2.3.2. Headcut Erosion Flume Testing

Due to the importance of headcut migration in spillway and embankment performance, a headcut erosion test facility was constructed at the laboratory (Figure 5b). The headcut erosion test facility is composed of three concrete structures connected by earthen dikes. Flow measurement is provided with a 2.4 m wide modified Parshall flume. Immediately downstream of this flume is a 2.7 m wide straight drop spillway with a 3.0 m vertical drop. A 2.4 m long concrete transition section is located at the upstream end of the flume to provide uniform approach flow conditions in the test section of the flume. The flume is a 29m long horizontal test flume 1.8 m wide with 2.4 m tall sidewalls. One of the flume walls has two windows that allow a side view of erosion processes. A rail mounted carriage on top of the walls is used to measure water surface elevations, bed profiles, and velocities. Tailwater elevation is controlled at the outlet with an overflow tailgate.

Typical flume testing was conducted following a routine sequence of events. The test flume fill was prepared by placing soil in loose lifts ranging in thickness from 100 to 150 mm. Water was added to the soil to achieve the desired compaction moisture. A tractor mounted PTO-operated tiller was used to mix the lifts and reduce aggregate size. Each lift was compacted with repeated passes of a 0.9 m wide, self-propelled vibratory sheepsfoot roller. The fill procedure was repeated for each layer until the desired fill depth was obtained. Soil sampling was conducted for each test to determine water content, density, strength, and erodibility. A headcut was then preformed at the downstream end of the soil section using hand shovels. The tailgate was set to the desired position and the flow was introduced into the upstream forebay. Once the forebay was filled and the flow reached the overfall, the headcut position and/or scour depth was monitored with time. Water surface elevations, bed profiles, and discharge were measured periodically during testing.

2.3.3. Breach Formation and Progression Testing

A series of tests on 7 embankment test sections were conducted in the outdoor laboratory to examine the breach formation and progression (Figure 5c). In these tests, non-vegetated homogeneous embankments were tested to breach. Therefore, all phases of the process that occurred between vegetal failure and the complete breach were included in the observation and data acquisition. Three soil materials and two embankment heights were included in the test program. These materials were a very erodible SM, a slightly more resistant SM, and a relatively erosion resistant CL, with embankment test section heights of 1.5 and 2.0 m. Maximum overtopping depths ranged from 0.3 to 0.46 m. The most rapid breach test was completed in approximately 1 hour after beginning of overtopping. The test involving the most erosion resistant soil was terminated after 72 hours without complete development of the breach. Details of these tests and preliminary data analyses are presented by Hanson et al. (2003). Testing to further examine breach widening following full breach development are ongoing.

3. Observations and Results

3.1. Phase 1

Phase 1 of the spillway and embankment erosion processes is defined as the local destruction of the vegetation, if any vegetation, and development of concentrated flow. Research in the laboratory channels combined with field experience led to the development of relationships for the removal of vegetal cover and development of concentrated flow in auxiliary earth spillways. These relationships assume that the vegetation fails as a result of erosion through the vegetal cover or local destruction of the vegetation due to shallow rooting or large stresses (Temple and Hanson 1994). Prediction of the failure of the vegetation as a result of erosion through the vegetal cover is based on the excess stress equation [1] with the effective stress on the soil boundary in vegetation (Temple 1985) given by:

$$\tau_e = \gamma dS(1 - C_f)\left(\frac{n_s}{n}\right)^2 \qquad (2)$$

where
γ = unit weight of water,
d = flow depth,
S = slope of energy grade line,
C_f = vegetal cover factor,
n_s = soil grain roughness in terms of Manning's coefficient, and
n = Manning's n.

Application of these equations to spillways was made by the development of a relationship between plasticity index of soil and an integration of effective stress due to the flow through the spillway up to time of failure, assuming that $\tau_e >> \tau_c$ (Temple 1992). For the purpose of analyzing data from field spillways, failure of the vegetation, the transition from phase 1 to phase 2 was considered to have occurred when eroded areas were greater than 2.5 m and eroded depths were greater than 0.3 m. Local destruction of vegetation may occur prior to erosion of the vegetal cover if the gross stress is great enough to cause sod stripping or "rafting". Based on field experience, sod stripping and rafting can happen as a result of either; (1) the potential rooting depth of the vegetation less than approximately 0.3 m or (2) relatively large hydraulic shear stresses, 600 to 700 Pa (Temple and Hanson 1994).

The vegetal tests on the steep sloped channels (33 %), confirmed that the erosionally effective stress approach used to predict vegetal failure in earth spillways can be applied to provide a reasonable estimate of the time to failure of vegetal cover on the embankment face. The relatively small flow depths and high velocities developed above the grass on these steeper slopes suggest however, that minor discontinuities are more significant for the embankment slopes than for the spillway slopes. In conclusion, field conditions will seldom be sufficiently uniform to gain full benefit from the vegetal cover. Results for these tests were reported by Temple and Hanson (1998) and Hanson and Temple (2002).

3.2. Phase 2

Phase 2 is defined as concentrated flow erosion leading to the development of a headcut capable of advancing upstream. The erosion occurring during phase 2 is assumed to be governed by equation 1 and the effective stress as defined by equation 2 where $C_f = 0$ and, without better information, let $n_s/n = 1$. Once phase 2 is initiated in the spillway or embankment, it is assumed that, because of the high hydraulic stress environment, the detachment coefficient is the controlling parameter in defining the material erodibility. Research results in the laboratory channels, as well as information from channel tests in the literature, led to the development of a prediction equation to estimate the detachment coefficient of cohesive soils (Temple and Hanson 1994):

$$k_d = \frac{10\gamma_w}{\gamma_d} \exp\left(-0.121 c\%^{0.406} \left(\frac{\gamma_d}{\gamma_w} \right)^{3.10} \right) \tag{3}$$

where
k_d = detachment coefficient [cm^3/N-s],
c%= percent clay,
γ_d = dry unit weight [Mg/m^3], and
γ_w = unit weight of water [Mg/m].
Because spillway damage surveys typically report on the basis of volume of material eroded, the detachment coefficient is therefore based on volume rather than weight of material removed.

The in-situ and laboratory jet test apparatus provides an alternative method to determine soil material erodibility. The method of analysis for the jet apparatus is based on submerged jet diffusion characteristics and the resulting maximum stress at the water/soil boundary (Hanson 2001). This method of analysis determines the detachment coefficient and critical stress for use in equation 1. Results from field and laboratory testing using this apparatus indicate that soil erodibility is a function of a number of factors including soil gradation, bulk density, water content, and degree of weathering.

3.3. Phase 3

The transition from phase 2 to phase 3 is defined as the point in time at which the flow plunges and develops a vertical face in the channel. This point is defined as the location at which the erosion depth is greater than or equal to the critical depth of flow (Temple and Hanson, 1994). Once the flow starts to plunge, the stresses developed downstream of the headcut becomes influenced by the interaction of the plunging jet, the overfall height, and the tailwater.

3.3.1. Hydraulic Stresses

Results from stress measurements in the headcut environment have led to the development of dimensionless relationships for stress along the bed upstream of the headcut brink (Robinson and Cook 1998) and for the maximum stress and pressure in the impingement area of the jet and on the vertical face of the headcut (Robinson 1992). The following equations are examples of relationships to express the maximum stress in the impingement region of the plunging jet for low and high backwater environments:

$$\tau_e = 0.011\gamma._a \left(\frac{q^2}{gd_a^3}\right)^{-0.001} \left(\frac{H}{d_a}\right)^{0.582} \left(\frac{B_w}{d_a}\right)^{-0.114} \quad \text{(Low Backwater)} \qquad \textbf{(4)}$$

$$\tau_e = 0.032\gamma d_a \left(\frac{q^2}{gd_a^3}\right)^{0.204} \left(\frac{H}{d_a}\right)^{0.852} \left(\frac{B_w}{d_a}\right)^{-1.796} \quad \text{(High Backwater)} \qquad \textbf{(5)}$$

and the magnitude of the maximum stress on the vertical face of the headcut is given as:

$$\tau_e = 0.025\gamma d_a \left(\frac{q^2}{gd_a^3}\right)^{-1.295} \left(\frac{H}{d_a}\right)^{-0.026} \left(\frac{B_w}{d_a}\right)^{0.22} \left(\frac{X_p}{d_a}\right)^{-1} \qquad \textbf{(6)}$$

where

q = the unit discharge at the overfall,

g = acceleration due to gravity,

d_a=depth of approach,

H=headcut height,

B_w=the depth of backwater, and

X_p= location of maximum pressure on the headcut floor.

Backwater levels were defined by Robinson (1992) as low when the ratio of nappe diffusion length and nappe width is less than 6. Conversely, backwater levels are considered high when the ratio was greater than 6. The measured stresses on the horizontal floor ranged from 0 to 30 Pa and on the vertical headcut face from 0 to 10 Pa. The results and equations have been applied

to the modeling and prediction of headcut scour (Hanson and Temple 2002) and headcut migration (Robinson and Hanson 1994, Hanson et al. 2001).

3.3.2. Headcut Erosion

Headcut migration and scour in the jet impingement area are the two primary aspects of headcut erosion processes studied in the large headcut erosion facilities. Several factors that influence headcut migration and scour have been tested, including overfall height, discharge, tailwater, velocities, stratified soils, degree of weathering, structure, soil strength, compaction effort, compaction bulk density, and compaction moisture (Robinson and Hanson 1995, Hanson et al. 1997, Robinson et al. 2002). As a result of field performance data collected on eroded earthen spillways, and headcut migration studies at the laboratory, three models have been developed to predict headcut migration in earthen spillways and embankments (Temple 1992, Robinson and Hanson 1994, Temple and Moore 1997, and Hanson et al. 2001). The model developed by Temple and Moore (1997) has been used in the USDA-NRCS Sites model (NRCS, 1997) for predicting spillway erosion. All three models have potential for being used in modeling embankment breach.

The models presented in Temple (1992), and Temple and Moore (1997) are similar in that both are energy-based. The model proposed by Temple (1992) simply uses headcut height H and unit discharge q as the basis for hydraulic attack and a material dependent rate coefficient C:

$$\frac{dX}{dt} = Cq^{v}H^{z} \tag{7}$$

where
dX/dt = rate of headcut migration (m/s), and
v and z = exponents.
Temple (1992) recommended values of 0.33 and 0.5 for v and z, respectively. Using these exponents Temple (1992) determined a range of C values for four earthen spillways from 0.55 to 3.6 $s^{1/3}/(m^{1/6}\text{-h})$. Hanson et al. (1997) determined C values from flume experiments conducted on sandy clay and observed values that ranged from 0 to 21.4 $s^{1/3}/(m^{1/6}\text{-h})$. It was observed that the C value was dependent on soil placement conditions (i.e. compaction effort, bulk density, and moisture content). Determining the hydraulic attack is relatively easy but the material resistance parameter C requires calibration and can only be determined by experience, at this time.

The model proposed by Temple and Moore (1997) differs from Temple (1992) in that the exponents on q and H are equal to 1/3, it includes a material dependent threshold term A_o, and the material dependent advance rate coefficient B and threshold term A_o are dependent on an independently determined material parameter, a headcut erodibility index K_h. For this model, the headcut advance rate is given by:

$$\frac{dX}{dt} = B[(q\gamma H)^{1/3} - A_0] \tag{8}$$

where
B = a material dependent advance rate coefficient, $(m\text{-}s^{1/3})/(N^{1/3}\text{-h})$,
γ = unit weight of water, (N/m^3), and

A_o = threshold term indicating the minimum attack required to generate headcut advance, (N/s).
The terms B and A_o depend on K_h as:

$$B = b' \log_e(K_h) + d' \tag{9}$$

where
b' = -0.0369 m-s$^{1/3}$/N$^{1/3}$h,
d' = 0.142 m-s$^{1/3}$/N$^{1/3}$h, and
K_h = headcut erodibility index of earthen material.
The attack treshold is defined as:

$$A_o = \begin{cases} \left[aK_h^{1/2} e^{\left(\frac{b}{\ln(101K_h)}\right)} \right]^{1/3} & K_h \geq 0.01 \\ 0 & K_h < 0.01 \end{cases} \tag{10}$$

where
a = 52,500 N/s, and
b = -3.23
The headcut erodibility index K_h is a function of material strength and structure parameters that enables characterization of earth materials on a continuum from loose soil to hard rock to express resistance to headcut migration in earth spillways (Moore et al. 1994). K_h values for (1) flume experiments on sandy clay soil were determined to range between 2 x10^{-10} to 2 x10^{-1} (Hanson et al. 1997), and (2) studies conducted on materials in earthen spillways ranged from 10^{-2} to 10^{5} (Temple and Moore 1997).

Robinson and Hanson (1994) developed a hydraulic stress based mass wasting model that was later simplified by Hanson et al. (2001) to:

$$\frac{dX}{dt} = \frac{T}{t_f} = Rk_d(\tau_e - \tau_c) \tag{11}$$

where
T = distance of headcut movement, m
t_f = time between each failure, s
R = a dimensionless rate coefficient,
k_d = the erodibility detachment coefficient of the soil material, m^3/N-s
τ_e = effective stress at the headcut face, N/m^2 and
τ_c = critical stress of the soil material, N/m^2.
The model suggests that the time averaged headcut migration rate is linear for uniform conditions, occurring by mass failures of length T over discrete time steps t_f. The dimensionless coefficient R was defined by Hanson et al. (2001) as R= [H/(2E_v)]. E_v is the erosion on the

vertical face of the headcut required to cause the headcut to move a distance of H/2 at failure. E_v is determined based on a force balance that assumes failure occurs by a tension crack forming at H/2 upstream of the headcut brink.

4. Summary

Gully erosion, a recognized erosion feature in nature, is also an important erosion feature for earthen spillway flows and embankment overtopping that occurs during extreme events. The need for determining the performance and potential risk of failure of these structures during extreme flood events has resulted in the development of computational erosion breach prediction models. Field experience with earthen spillways and laboratory testing led to the development of a three-phase erosion model that has been used to predict earthen auxiliary spillway erosion. This three-phase model describes the initiation, development, and upstream growth of gully erosion. Research on earth embankment overtopping confirms these same processes are also important in prediction of embankment overtopping erosion. This paper reports an overview of the completed and ongoing research at the USDA-ARS Hydraulic Engineering Research Unit Laboratory. It also summarizes fundamental relationships and their underlying assumptions developed for application to spillway and embankment erosion. The embankment erosion process includes the additional phase of embankment widening following breach and although important, is not included in this discussion of dam gully erosion.

References

Alonso, C. V., Bennett, S. J., and Stein, O. R. 2002. Predicting Headcut Erosion and Migration in Concentrated Flows Typical of Upland Areas. Water Resources Research 38(10):39-1 to 39-15..

Caldwell, L.W. 1999. Rehabilitating our Nation's Aging Small Watershed Projects. Proceedings of the Annual Conference of the Association of Dam Safety Officials, St. Louis, MO, CD-ROM.

Bocco, G. 1991. Gully Erosion: Processes and Models. Progress in Physical Geography 15(4):392-406.

Bradford, J. M., and Piest, R. F. 1977. Gully Wall Stability in Loess-derived Alluvium. Soil Science Society of America Journal 41(1):115-122.

Deploey, J. 1989. A Model for Headcut Retreat in Rills and Gullies. CATENA Supplement 14, 81-86. Cremlingen, West Germany.

Hanson, G. J. 1989. Channel Erosion Study of Two Compacted Soils. Transactions of the ASAE 32(2):485-490.

Hanson, G. J. 1991. Development of a Jet Index to Characterize Erosion Resistance of Soils in Earthen Spillways. Transactions of the ASAE 34(5):2015-2020.

Hanson, G. J. 2001. Field and Laboratory Jet Testing Method for Determining Cohesive Material Erodibility. Proceedings of the Seventh Federal Interagency Sedimentation Conference. CD-ROM V:1-8.

Hanson, G. J., Cook, K. R., Hahn, W., and Britton, S. L. 2003. Observed Erosion Processes During Embankment Overtopping Tests. ASAE meeting Paper No: 032066. pp. 15.

Hanson, G. J., Robinson, K. M., and Cook, K. R. 1997. Headcut Migration Analysis of a Compacted Soil. Transactions of the ASAE 40(2):335-361.

Hanson, G. J., Robinson, K. M., and Cook, K. R. 2001. Predictions of Headcut Migration Using a Deterministic Approach. Transactions of the ASAE 44(3):525-531.

Hanson, G. J., and Temple, D. M. 2002. Performance of Bare-Earth and Vegetated Steep Channels Under Long-Duration Flows. Transactions of the ASAE 45(3):695-701.

Ireland, H. A., Sharpe, C. F. S., Eargle, D. H. 1939. Principles of Gully Erosion in the Piedmont of South Carolina. USDA Technological Bulletin 633. pp. 143.

Middlebrooks, T. A. 1953. Earth-Dam Practice in the United States. Transactions of the ASCE 118:697-722

Miller, S. P., and Ralston, D. C. 1987. Embankment Overtopping – Case Histories. Proc. of the 1987. National Conf. on Hydraulic Engineering, Hydraulics Division of ASCE. pp. 739-744.

Moore, J. S. 1997. Field Procedures Guide for the Headcut Erodibility Index. Transactions of the ASAE 40(2):325-336.

Natural Resources Conservation Service (NRCS). 1997. Earth Spillway Erosion Model. Chapter 51 *National Engineering Handbook Part 628 Dams*.

Poesen, J., Nachtergaele, J., Verstraeten, G., and Valentin, C. 2003. Gully Erosion and Environmental Change: Importance and Research Needs. CATENA Vol. 50:91-33.

Prasad, S. N., and Romkens, M. J. M. 2003. Energy Formulations of Headcut Dynamics. CATENA Vol. 50(2-4):469-487.

Ralston, D. C. 1987. Mechanics of Embankment Erosion During Overflow. Proc. of the 1987. National Conf. on Hydraulic Engineering, Hydraulics Division of ASAE. pp. 733-738.

Robinson, K. M. 1992. Predicting Stress and Pressure at an Overfall. Transactions of the ASAE 35(2):561-569.

Robinson, K. M., and Cook, K. R. 1998. Stress Measurement Upstream of an Overfall. Transactions of the ASAE 41(4):1019-1024.

Robinson, K. M. and Hanson, G. J. 1994. A deterministic Headcut Advance Model. Transactions of the ASAE 37(5):1437-1443.

Robinson, K. M., and Hanson, G. J. 1995. Large-Scale Headcut Erosion Testing. Transactions of the ASAE 38(2):429-434.

Robinson, K. M., Hanson, G. J., and Cook, K. R. 2002. Scour Below and Overfall: Part I. Investigation. Transactions of the ASAE 45(4):949-956.

Shuibo, P., Mingsen, Q., Lianxiang, W., Guoyi, X., Yongqiang, S., Longda X., Cuiyu, M., Loukola, E. Pyyny, J. Reiter, P., Rytkonen, T. and Alanko, M. 1993. Chinese-Finnish Cooperative Work on Dam Break Hydrodynamics. Report by National Board of Waters and the Environment Series A 167 Finland. pp. 3-39.

Singh V. P. 1996. *Dam Breach Modeling Technology*. Water Science and Technology Library Volume 17. Kluwer Academic Publishers. Boston. pp. 242.

Singh, V. P. and Scarlatos, P. D. 1988. Analysis of Gradual earth Dam Failure. Journal of Hydraulic Engineer ASCE 114(1):21-42.

Soil Conservation Service (SCS, Now NRCS). 1966. Procedure for Determining Rate of Land Damage, Land Depreciation, and Volume of Sediment Produced by Gully Erosion. Technical Release 32. In: FAO(Eds.), Guidelines for Watershed Management. FAO Conservation Guide 1, Rome, pp. 125-141.

Stein, O. R., and Julien, P. Y. 1993. Criterion Delineating the Mode of Headcut Migration. Journal of Hydraulic Engineering ASCE 119(1):37-50.

Stein, O. R., and LaTray, D. A. 2002. Experiments and Modeling of Headcut Migration in Stratified Soils. Water Resources Research 31:723-738.

Temple, D. M. 1985. Stability of Grass-lined Channels Following Mowing. Transactions of the ASAE 28(3):750-754.
Temple, D. M. 1992. Estimating Flood Damage to Vegetated Deep Soil Spillways. Applied Engineering in Agriculture 8(2)237-242.
Temple, D. M. and Alspach, S. D. 1992. Failure and Recovery of a Grass Channel Lining. Transactions of the ASAE 35(1):171-173.
Temple, D. M., and Hanson, G. J. 1994. Headcut Development in Vegetated Earth Spillways. Applied Engineering in Agriculture 10(5):677-682.
Temple, D. M. and Hanson, G. J. 1998. Overtopping of Grassed Embankments. Proceedings of the 1998 Annual Conf. of the Association of State Dam Safety Officials. pp. 10.
Temple, D. M., and Moore, J. S. 1997. Headcut Advance Prediction for Earth Spillways. Transactions of the ASAE 40(3):557-562.
Thompson, J. R. 1964. Quantitative Effect of Watershed Variables on Rate of Gull-head Advancement. Transactions of the ASAE 7:54-55.
Thornes, J. B. 1980. Gully Growth and Bifurcation. Erosion Control: Man and Nature, International Erosion Control Association. pp. 131-140.
Walder, J. S., and O'Connor, J. E. 1997. Methods for Predicting Peak Discharge and Floods Caused by Failure of Natural and Constructed Earth Dams. Water Resources Research, Vol. 33(10).
Wahl, T. L. 1998. Prediciton of Embankment Dam Breach Parameters – A Literature Review and Needs Assessment. U.S. Bureau of Reclamation Dam Safety Report DSO-98-004.

List of Figures

Figure 1. Formation of gullies in earthen spillways is associated with; (a) steep slopes, (b) roads, (c) vegetation (i.e. trees in spillway contribute to gully formation during flow event.).

Figure 2. Three phase erosion process; (a) local destruction of the vegetal cover, (b) concentrated flow erosion leading to the development of a headcut, and (c) upstream migration and deepening of the headcut at progresses upstream.

Figure 3. Facilities used in phase 1 erosion; (a) vegetated channels 0.91 m wide and 30.5 m long, 5% slope, (b) wide flat-bottomed channel, 9% slope, and (c) steep trapezoidal channels, 33% slope.

Figure 4. Facilities used in phase 2 erosion; (a) bare soil channels 0.91 m wide and 30.5 m long, 0.5, 1.5, and 3% slope, (b) large flume 1.8 m wide, 1 and 3% slopes, and (c) submerged jet apparatus for testing material erosion resistance.

Figure 5. Facilities used in phase 3 erosion; (a) smooth boundary hydraulic stress and pressure measurement facilities, (b) large outdoor headcut migration testing facilities; and (c) large scale embankment breach testing facilities.

(a) (b) (c)

Figure 1. Formation of gullies in earthen spillways is associated with; (a) steep slopes, (b) roads, (c) vegetation (i.e. trees in spillway contribute to gully formation during flow event.).

(a) (b) (c)

Figure 2. Three phase erosion process; (a) local destruction of the vegetal cover, (b) concentrated flow erosion leading to the development of a headcut, and (c) upstream migration and deepening of the headcut at progresses upstream.

(a) (b) (c)

Figure 3. Facilities used in phase 1 erosion; (a) vegetated channels 0.91 m wide and 30.5 m long, 5% slope, (b) wide flat-bottomed channel, 9% slope, and (c) steep trapezoidal channels, 33% slope.

(a) (b) (c)

Figure 4. Facilities used in phase 2 erosion; (a) bare soil channels 0.91 m wide and 30.5 m long, 0.5, 1.5, and 3% slope, (b) large flume 1.8 m wide, 1 and 3% slopes, and (c) submerged jet apparatus for testing material erosion resistance.

(a) (b) (c)

Figure 5. Facilities used in phase 3 erosion; (a) smooth boundary hydraulic stress and pressure measurement facilities, (b) large outdoor headcut migration testing facilities; and (c) large scale embankment breach testing facilities.

Freeze/Thaw Effects on Rill and Gully Erosion in the Northwestern Wheat and Range Region

D. K. McCool* (E-mail: dkmccool@wsu.edu.)
Supervisory Agricultural Engineer
Land Management and Water Conservation Research
USDA-ARS, Pullman, Washington
Fax (509) 335-7786

J. D. Williams (E-mail: johnd.williams@oregonstate.edu.)
Hydrologist
Columbia Plateau Conservation Research Center
USDA-ARS
Pendleton, Oregon,
FAX (541) 278-4372

Abstract

Hydrology of the Northwestern Wheat and Range Region (NWRR) of the Pacific Northwest USA is dominated by winter events. Fifty-five to sixty-five percent of the precipitation occurs from November through March, and formation of impermeable frost, intensified by excessive tillage and tillage pans, has long been a major factor in rill and gully formation in the region. Saturated zones can form above tillage pans, freeze solid, and significantly reduce infiltration. Frost heaved surface soils thaw and weaken with warming temperatures or rain. Under these conditions, runoff with rain or snowmelt or a combination of the two is inevitable, concentrating in rills and channels, and carrying with it the loosened soil. Slopes are frequently quite steep and there may be little deposition above the toe slope.

Classical over-fall head-cut gullies are uncommon. Concentrated flow channels form because of collection of water from impervious areas such as conventionally tilled fall seeded small grains and bare grass seed fields. Gullies are also created by seepage from saturated layers above permanent restrictive layers in the soil. Gullies can also result from terrace failures due to rodent burrows and low compaction at the time of construction. In naturally unconsolidated soil, rodent activity can lead to piping failures that remove large quantities of subsurface soil; unchecked, they become gullies.

Rill measurements on conventionally tilled fields in Oregon, Washington, and Idaho were used to determine coefficients for relationships between slope length and steepness and size of rills. This paper describes these studies and the results as well as other research opportunities that have not yet been addressed.

Keywords: erosion, slope length, slope steepness, topography, Pacific Northwest

Introduction

The Northwestern Wheat and Range Region includes approximately 4 million ha of non-irrigated cropland in eastern Washington and Oregon, and northern and southern

*Corresponding Author

Idaho (figure 1). Non-irrigated crops are grown in a 2-year winter wheat /summer fallow rotation with as little as 230 mm of annual precipitation, in a 3-year rotation including one year of fallow in the zone from 305 mm to 405 mm of precipitation, and in an annual crop rotation in areas with greater than 430 mm of precipitation. Winter storms, particularly freeze-thaw events, drive this region's hydrologic and erosion processes. Soil freezes and thaws and snow accumulates and melts multiple times throughout the winter. Only on cropland in higher elevation or foothill areas subject to colder temperatures does snow accumulate and experience a spring melt period. In the most productive cropped areas, soils are silt loams, have low organic matter content, and are intensely managed with mechanical tillage. As a result, these soils are weakly aggregated, and susceptible to slaking and plating due to wetting, especially during freeze/thaw events. Rill erosion, the predominant erosion process in the region, develops quickly from low-intensity rain or snow-melt as the soil thaws from the surface.

Data collected by an annual sampling of selected small grain fields in Whitman, County Washington during a 43-year period from 1939/40 through 1980/82, indicates the importance of rain and snowmelt on thawing soil (figure 2). A major precipitation or snowmelt event on previously frozen soil was responsible for most of the erosion during each of the 11 years in which approximately 45 percent of the total erosion occurred during the 43-year period. Aggressive tillage combined with high volume runoff can produce severe erosion (figure 3). Water from large contributing areas collected in drill furrows and wheel tracks to create these large rills and concentrated flow channels. Concentrated flow and rill erosion will physically remove plants, create visible gaps in the crop, and reduce crop yield (figure 4).

When the precipitation occurs at a low intensity as the soil thaws over an impermeable frozen layer, deposition higher on toe slopes is observed (figure 5). This deposition is not seen this far up the slope when the soil is not thawing at the time of the event. This increased deposition indicates the ease of detachment of the thawing soil. This observational data indicates that on the steep slopes of the region, erosion is limited by detachment rather than by transport, even under weakened soil conditions.

Management and rotation have a major effect on runoff and soil erosion. The field in the foreground is seeded to winter wheat after a spring crop (figure 6). Tillage was minimal and a good residue cover was retained. In the immediate background is the field shown in the previous figure, in winter wheat after summer fallow, with excessive tillage and almost no residue cover. In addition to tillage and residue effects, soil water content was greater in the wheat after fallow field, leading to lower infiltration at a reduced rate as compared to the annually cropped field in the foreground.

The role of summer storms varies across the region. In eastern Washington and Oregon and northern Idaho, summer storms are less frequent than in southern Idaho. Still, erosion damages from summer storms can be severe in eastern Washington, as shown in the photo from 1931 (figure 7). A photo taken in 1978 indicates continuation of the summer fallow practice and resulting exposure to spring and summer erosion damage (figure 8). The summer fallow practice is much less prevalent in the higher precipitation area in 2004, but is still in use in the intermediate and lower rainfall areas. Damages from late spring storms are greatest on newly seeded spring legumes under conventional tillage, and damages from summer storms occur mainly on tilled summer fallowed fields,

due to the fact that these fields are left rough-tilled or undisturbed until late spring or early summer.

Winter erosion on this seeded winter wheat field includes rill and concentrated flow or gully erosion (figure 9). There are no head cuts visible in either the rills or concentrated flow channel. Note depositional areas at the base of the steep slope. A summer storm on an unseeded field in summer fallow caused this rill and concentrated flow erosion (figure 10). The flow cut through the weak tillage pan created by a rod-weeder.

In both naturally unconsolidated soil and in terrace ridges with low compaction at the time of construction, rodent activity can lead to piping failures that remove large quantities of subsurface soil; unchecked, they become gullies. Sometimes the initial source of the runoff can be as small as a mouse run (figure 11).

Deep soil slips are not a freeze/thaw phenomenon. They generally occur when large snow drifts melt, and the melt water infiltrates and reaches a less permeable soil layer. The soil liquefies above the layer, sometimes in a very narrow band, and the unsupported drier soil will slide down the slope on this fluid layer (figure 12). Sometimes when a soil slip occurs the bulk of the soil above the impervious layer is all at high water content, and it liquefies and flows down the slope and continues down into the concentrated flow channel or waterway (figure 13).

Classical head-cut gullies as are frequently seen in the Midwest are less common in the NWRR. Photos from 1933 and 1932, respectively, show in one scene a classic gully and in the other a new side gully caused by inappropriate tillage methods and filling of the old gully with grass and sediment (figure 14). A more recent side gully in Tom Beall Creek Watershed in northern Idaho was caused by a high volume and rate of winter runoff that exceeded the capacity of the existing channel plugged with grass, brush and sediment (figure 15).

Some soils have restrictive layers that lead to seepage pressure and return flow on lower slope areas (figure 16). Concentrated flow channels can produce large amounts of sediment, damage harvest equipment, and eventually divide fields into unmanageable units. Grassed waterways are designed to convey runoff from fields and small watersheds. High flows before the vegetation is established and lack of maintenance can result in failures. This gully in bottomland was due to a failed grass waterway (figure 17).

An aerial photo of a field seeded to winter wheat shows a pattern of rills and concentrated flow channels where the rills have collected (figure 18). The evenly spaced lines that have collected and channeled rills are tracks left by the tires on the double disk drill. Rills on this site are very short before the flow collects in the drill tracks.

Problem

Applying empirical hydrology and erosion models developed from eastern US data has generally been problematic in the NWRR. Unlike the eastern US, winter is the primary erosion period, rainfall is generally of low intensity, and the soil can freeze and thaw several times each winter. During thaw, soil strength can be quite low and erodibility increased. Under conventional tillage and seeding of winter crops, rilling is highly visible and the primary form of soil loss. When the USLE was developed,

attempts were made to apply it to the NWRR. Numerous problems were apparent, not the least of which was the topographic effect or length-steepness factors, LS.

The quadratic slope steepness relationship that appeared in AH 282 (Wischmeier and Smith, 1965) was developed from runoff plots with steepness no more than about 20% slope (figure 19). When extrapolated to slopes of 50% steepness, not uncommon in the NWRR, the slope steepness factor, a direct multiplier for erosion in the USLE or RUSLE1, is about 16 times the value at a slope steepness of 10%. When applied in the NWRR, the relative effect of slope steepness appeared to be much larger than observed. This relative over-prediction on steep slopes was observed in humid regions of the United States as well, but was largely ignored because such slopes were rarely cultivated. Because of the steepness of the slopes commonly cultivated in the NWRR, this over-prediction could not be ignored. This problem led to a study to collect rill erosion data from naturally occurring rills in the field and to develop a new relationship for the effect of topography on rill erosion (McCool et al., 1993).

Theory

The approach to collect and use field data to determine slope length and steepness effects was developed starting with the basic form of the USLE:

$$A = RKLSCP \tag{1}$$

where

A = soil loss per unit area
R = rainfall and runoff erosivity factor
K = soil erodibility factor
L = slope length factor
S = slope steepness factor
C = cover and management factor
P = supporting conservation practice factor.

Based on previous research results (Zingg, 1940; Musgrave, 1947; Smith and Whitt, 1947; Wischmeier and Smith, 1965), we assumed an equation for LS of the form

$$LS = (\lambda/22.13)^m (\sin \theta/\sin 5.143°)^n \tag{2}$$

where

LS = slope length and steepness factor relative to a 22.13 m slope length of uniform 9% (5.143°) slope
λ = horizontal slope length in meters
θ = slope angle in degrees
m, n = regression coefficients

Equation 1 can be rearranged and equation 2 substituted for LS:

$$A/KCP = R(\lambda/22.13)^m (\sin \theta/\sin 5.143^o)^n \tag{3}$$

Taking the natural logarithm yields a linear equation

$$\ln (A/KCP) = \ln (R) + m \ln (\lambda/22.13) + n \ln (\sin \theta/\sin 5.143°) \quad (4)$$

Erosion A in mass per area was calculated from rill meter readings and bulk density data collected in the field, K was obtained from soil survey data and the erodibility nomograph, and C and P were estimated from field observations of surface cover, canopy cover, random roughness, and knowledge of prior crop. P was estimated from furrow grade and ridge height. R was assumed a fitted parameter that did not affect values of m and n.

Data Collection

Data on rill cross sections was collected from natural rill patterns with a profile or rill meter (figure 20). The rill meter was 1.83-m wide with lightweight aluminum pins on 12.7-mm centers. The pin tops were recorded photographically against a grid background (figure 21). The data was originally digitized and the voided rill area digitized manually, but more automated systems are now available to use a digital camera and read the data more easily and quickly. This field is typical of those from which data was collected (figure 22).

The data was collected for 10 years along an 80-km transect across eastern Washington and northern Idaho. The study area was along a line nearly perpendicular to lines of equal elevation and precipitation in Whitman County, Washington and Latah County, Idaho. Mean precipitation ranges from 350 mm at the west to 650 mm at the east end of the area. Measurement sites were selected at the end of each winter erosion season; no attempt was made to return to the same field or farm in subsequent years, although the same field or farm was frequently visited more than one year because of crop management or topographic uniformity. Because of severe drought in the fall and winter of 1976/77, erosion was quite low and no data was collected. Segment slope length ranged from 1.5 to 56% steepness, and total slope lengths ranged from 19 to 201 m. Mean slope steepness was 28.4%, and 95% of the data points were collected from slopes between approximately 9 and 48% steepness. The mean total slope length was 51 m.

Data Reduction and Analysis

The data were reduced to erosion rates by various manual, photographic, and digitizer techniques and were developed into sets of slope segment values. These data sets included site number, latitude, longitude, azimuth, location on strip, soil bulk density, slope steepness, segment length, segment average width, and segment average soil loss in mass per unit area. Separate data sets of K, C, and P values were developed. Data were reduced into a form suitable for analysis with a standard package (SAS version 6.07) on a main frame computer using an extension of the nonuniform slope method of Foster and Wischmeier (1974). Data fits were attempted by various means, but the one selected was based on equation 4 with R considered a regression coefficient. Data from 2179 slope segments was available for analysis.

Discussion and Conclusions

Values of m and n varied from year to year as can be seen in table 1. Analysis of the composite data set yielded the relationship

$$LS = (\lambda/22.13)^{0.5} (\sin \theta/\sin 5.143°)^{0.6} \quad (5)$$

Equation 5 is shown graphically in figure 23. This new relationship provides a much different S factor from the original USLE quadratic relationship when comparing a 50% steepness slope with a 10% steepness slope. The S ratio is now approximately 2.5 instead of 16.

Rill and interrill erosion in the NWRR can generally be addressed by management practices such as eliminating summer fallow and using annual cropping rotations in higher precipitation areas, reducing summer fallow in the intermediate precipitation zone, and using conservation tillage or direct seeding wherever possible. Concentrated flow erosion can still be a problem, as can be seen on this bluegrass seed field (figure 24). Solutions offered to address concentrated flow erosion have included terrace systems, grassed waterways, and impoundments with tile outlets to carry runoff to main channels at the base of the slope. Concentrated flow erosion is not yet addressed by the Revised Universal Soil Loss Equation, although runoff is estimated by the Runoff Curve Number Method in order to determine the effect of conservation support practices such as contouring, strip cropping, and buffer strips. Consideration of concentrated flow erosion would add to the utility of this planning model. The consideration in more sophisticated watershed models of subsurface lateral flow above restrictive layers, and seepage pressure on the lower slopes of these areas, is a needed improvement in predicting channel and gully erosion.

References

Foster, G. R., and W. H. Wischmeier. 1974. Evaluating irregular slopes for soil loss prediction. Transactions of the ASAE. 17(2):305-309.

McCool, D. K., G. O. George, M. Freckleton, C. L. Douglas, Jr., and R. I. Papendick. Topographic effect on erosion from cropland in the Northwestern Wheat Region. Trans. of the ASAE 36(4):1067-1071. 1993.

Musgrave, G. W. 1947. The quantitative evaluation of factors in water erosion—a first approximation. J. Soil and Water Conservation. 2(3): 133-138, 170.

Smith, D. D., and D. M. Whitt. 1947. Estimating soil losses from field areas of claypan soil. Soil Science Society Proceedings. 12: 485-490.

Wischmeier, W. H., and D. D. Smith. 1965. Predicting rainfall erosion losses from cropland east of the Rocky Mountains. USDA-ARS. Agriculture Handbook No. 282. Washington, DC: GPO.

Zingg, A. W. 1940. Degree and length of land slope as it affects soil loss in runoff. Agricultural Engineering 21(2): 59-64.

Table 1. Slope length (m) and steepness (n) exponents.

Year	Number of Segments	m	n	Coefficient of Determination
1973	199	0.44	0.60	0.71
1974	466	0.47	0.64	0.46
1975	183	0.45	0.67	0.48
1976	219	0.48	0.87	0.32
1978	223	0.51	0.58	0.44
1979	166	0.67	0.62	0.64
1980	167	0.47	0.38	0.40
1981	212	0.58	0.38	0.69
1982	159	0.55	0.77	0.51
1983	185	0.64	0.21	0.56
10-year Composite	2179	0.50	0.59	0.45

List of Figures

Figure 1. Nonirrigated grain producing areas of the Northwestern Wheat and Range Region.

Figure 2. Over-winter soil loss from small grain fields in Whitman, County, Washington from 1939/40 through 1980/82.

Figure 3. Severe rill and concentrated flow erosion on seeded winter wheat.

Figure 4. Visible erosion pattern on a mature winter wheat crop.

Figure 5. Erosion from rain or snowmelt on thawing soil on a conventionally tilled winter wheat after summer fallow field.

Figure 6. Management and rotation affect runoff and erosion. Winter wheat after spring crop in foreground; field in figure 5 in background.

Figure 7. Erosion damage on summer fallow from a summer storm in eastern Washington in 1931.

Figure 8. Erosion damage on summer fallow from a summer storm in eastern Washington in 1978.

Figure 9. Winter erosion on this seeded winter wheat field includes rill and concentrated flow or gully erosion.

Figure 10. Rill and concentrated flow erosion caused by a summer storm on an unseeded field in summer fallow.

Figure 11. In unconsolidated soil, rodent activity can lead to piping failures that remove large quantities of subsurface soil.

Figure 12. Deep soil slips can occur when snow drift melt water infiltrates and creates a weak fluid layer over an impermeable soil layer.

Figure 13. When all soil above the impermeable layer is at high water content, the entire soil slip liquefies and flows down the slope.

Figure 14. Classical gully (left) and creation of secondary channel (right).

Figure 15. New secondary channel from storm event in Tom Beall Watershed in northern Idaho.

Figure 16. Large concentrated flow channel .

Figure 17. Gully caused by a failed grass waterway.

Figure 18. A winter wheat field shows a pattern of rills and concentrated flow channels caused by seeding pattern and drill wheels.

Figure 19. Slope steepness relationship from USLE.

Figure 20. Schematic of rill pattern for topographic study.

Figure 21. Rill meter in field.

Figure 22. Typical rilling pattern of study fields.

Figure 23. LS factors for nonirrigated cropland of the Northwestern Wheat and Range Region.

Figure 24. Improved accounting for concentrated flow erosion would add to the utility of many planning models

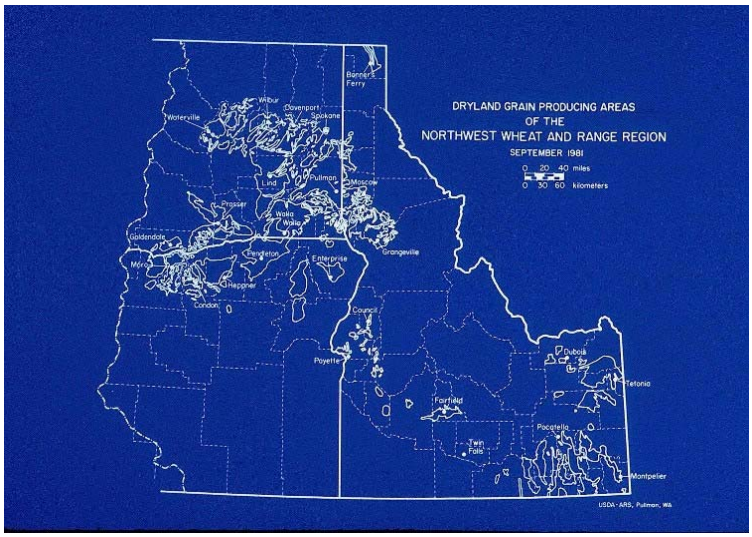

Figure 1. Nonirrigated grain producing areas of the Northwestern Wheat and Range Region.

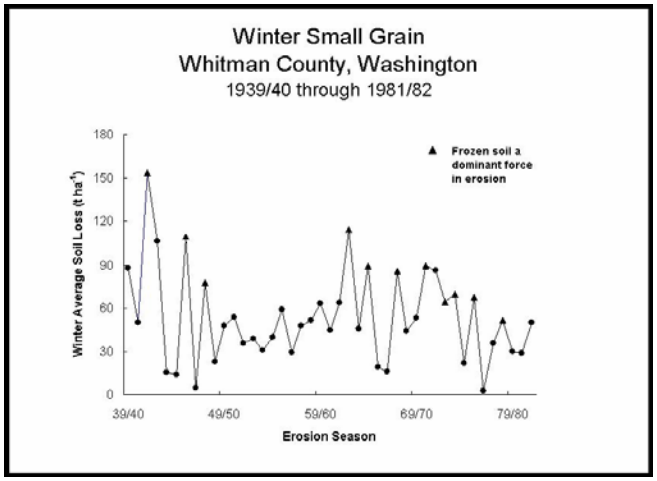

Figure 2. Over-winter soil loss from small grain fields in Whitman, County, Washington from 1939/40 through 1980/82.

Figure 3. Severe rill and concentrated flow erosion on seeded winter wheat.

Figure 4. Visible erosion pattern on a mature winter wheat crop.

Figure 5. Erosion from rain or snowmelt on thawing soil on a conventionally tilled winter wheat after summer fallow field.

Figure 6. Management and rotation affect runoff and erosion. Winter wheat after spring crop in foreground; field in figure 5 in background.

Figure 7. Erosion damage on summer fallow from a summer storm in eastern Washington in 1931.

Figure 8. Erosion damage on summer fallow from a summer storm in eastern Washington in 1978.

Figure 9. Winter erosion on this seeded winter wheat field includes rill and concentrated flow or gully erosion.

Figure 10. Rill and concentrated flow erosion caused by a summer storm on an unseeded field in summer fallow.

Figure 11. In unconsolidated soil, rodent activity can lead to piping failures that remove large quantities of subsurface soil.

Figure 12. Deep soil slips can occur when snow drift melt water infiltrates and creates a weak fluid layer over an impermeable soil layer.

Figure 13. When all soil above the impermeable layer is at high water content, the entire soil slip liquefies and flows down the slope.

Figure 14. Classical gully (left) and creation of secondary channel (right).

Figure 15. New secondary channel from storm event in Tom Beall Watershed in northern Idaho.

Figure 16. Large concentrated flow channel .

Figure 17. Gully caused by a failed grass waterway.

Figure 18. A winter wheat field shows a pattern of rills and concentrated flow channels caused by seeding pattern and drill wheels.

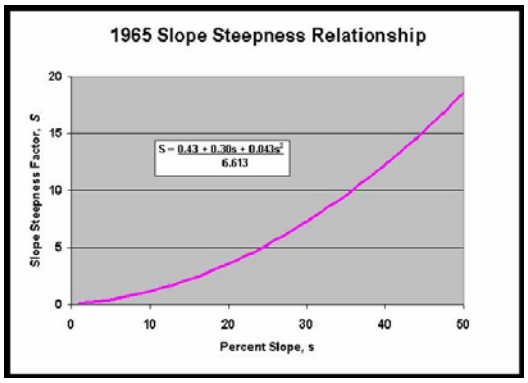

Figure 19. Slope steepness relationship from USLE.

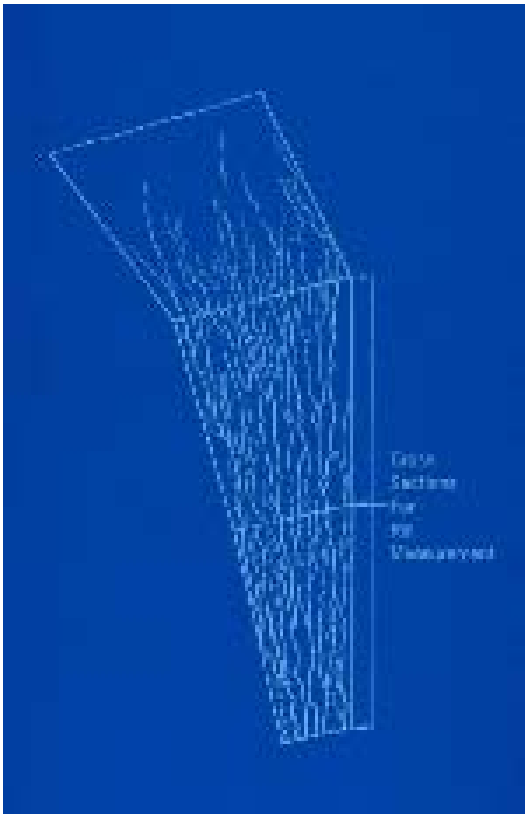

Figure 20. Schematic of rill pattern for topographic study.

Figure 21. Rill meter in field.

Figure 22. Typical rilling pattern of study fields.

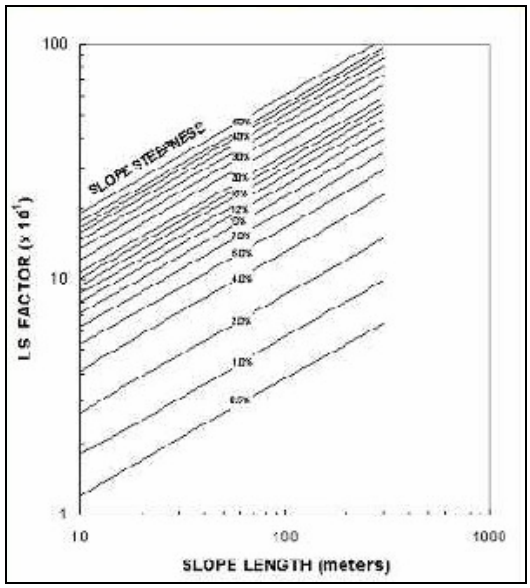

Figure 23. LS factors for nonirrigated cropland of the Northwestern Wheat and Range Region.

Figure 24. Improved accounting for concentrated flow erosion would add to the utility of many planning models.

Resistance of Topsoils to Concentrated Flow Erosion: a Review of the Available Experimental Data

Anke Knapen* (E-Mail: anke.knapen@geo.kuleuven.ac.be)
J. Poesen
Catholic University of Leuven
Laboratory for Experimental Geomorphology
K.U.Leuven
Redingenstraat 16
B-3000 Leuven, Vlaams Brabant
Belgium

Abstract

Although concentrated flow erosion is restricted to small areas on arable land, it represents an important sediment source in a range of agricultural environments (Poesen et al., 2003). In addition, the creation of erosion channels leads to an increased connectivity between the upper and lower parts of the landscape, aggravating off-site effects as flooding and silting up of reservoirs (Nachtergaele, 2002). Thanks to the limited spatial extent of the process, minor erosion control efforts can lead to a distinct decrease in water erosion problems. This justifies the current increasing number of water erosion studies focusing on concentrated flow erosion.

Since the earliest days of erosion research, the importance of topsoil resistance has been recognized. Originally, topsoil resistance was considered to be a constant soil characteristic that was equal for all water erosion processes (Bryan, 2000). Recognition of spatial and temporal variability of topsoil resistance later proved this concept to be too simplistic. Erosion resistance should be regarded as a complex concept, influenced by spatially and temporally varying soil characteristics and by macro-environmental variables. Moreover, topsoil resistance was shown to differ depending on the water erosion process studied. Whereas topsoil resistance to rill and interrill erosion has been intensively studied the last decades, information on resistance against concentrated flow erosion is rather limited. Therefore, the objective of this study is to review all existing experimental data on topsoil resistance to concentrated flow erosion and to summarize all parameters controlling it.

Since concentrated flow erosion is a threshold phenomenon, hydraulic thresholds can be defined to quantify the erosion resistance of a soil against this process. Soil erodibility (Kd) and critical shear stress (tc) are two parameters that are often used in erosion resistance research. They originate from the 'excess stress equation' expressing detachment due to concentrated flow, Dr = Kd (t - tc), with Dr, the detachment rate (cm h-1), Kd the erodibility (cm h-1 Pa-1) and t and tc respectively the actual and critical flow shear stress (Pa). Most experimental data for Kd and tc are obtained by measuring Dr for varying t-values in a hydraulic flume.

*Correspondence author

Existing data on Kd and tc for concentrated flow erosion (rilling and gully erosion) will be summarized and a relation between these two parameters will be investigated. Soil properties (e.g. texture, organic matter content), experimental conditions (e.g. soil moisture content, bulk density density) and cultivation practices (e.g. tillage, no tillage, double drilling) have a great influence on topsoil resistance and its spatial and temporal variability. An overview of all parameters that control the erosion resistance of topsoils provides an insight into the spatial and temporal variability of topsoil resistance as a function of the variability of these parameters and helps selecting appropriate erosion control measures.

Keywords: topsoil resistance, concentrated flow erosion, hydraulic threshold

Grass Hedge Effects on Gully Hydraulics and Erosion

S.M. Dabney* (E-Mail: sdabney@msa-oxford.ars.usda.gov)
FAX: 662-232-2988
F.D. Shields, Jr. (E-Mail: dshields@msa-oxford.ars.usda.gov)
E.J. Langendoen (E-Mail: elangendoen@msa-oxford.ars.usda.gov)
FAX: 662-281-5706
USDA-ARS National Sedimentation Laboratory, Oxford, Mississippi

D.M. Temple (E-Mail: dtemple@pswcrl.ars.usda.gov)
USDA-ARS Hydraulic Engineering Research Unit
Stillwater, Oklahoma
FAX 405-624-4136

Abstract

Concentrated flow can cause gully formation on sloping lands and in riparian zones adjacent to incising stream channels. Current practice for riparian gully control involves blocking the gully with a structure comprised of an earthen embankment and a metal or plastic pipe. Measures involving native vegetation would be more attractive for habitat recovery and economic reasons. To test the hypothesis that switchgrass (*Panicum virgatum* L.) hedges planted at 0.5-m vertical intervals within a gully would control erosion, we established a series of hedges in four concentrated flow channels. Two of the channels were previously eroded trapezoidal channels cut into compacted fill in an outdoor laboratory. The other two channels were natural gullies located at the margin of floodplain fields adjacent to an incised stream. While vegetation was dormant, we created artificial runoff events in the two laboratory gullies and one of the natural gullies using synthetic trapezoidal-shaped hydrographs with peak discharge rates of approximately 0.03, 0.07, and 0.16 $m^3 s^{-1}$. During these tests we monitored flow depth, velocity, turbidity, and soil pore water pressures. The fourth gully was subjected to a series of natural runoff events over a five-month period with peaks up to 0.09 $m^3 s^{-1}$. Flow depths in all tests were generally < 0.3 m, and flow velocities varied spatially and exceeded 2.0 m s^{-1} at the steepest points of the gullies. Erosion rates were negligible for controlled flow experiments, but natural flows in the fourth gully resulted in 1 m of thalweg degradation, destroying the central portions of the grass hedges, most likely due to the highly erodible nature of the soils at this site. Geotechnical modeling of soil steps reinforced with switchgrass roots showed that factors of safety > 1 for step heights < 0.5 m, but instability was indicated for step heights >1 m, consistent with our observations.

Keywords: erosion, vegetative barriers, grass hedges, buffers, runoff, soil conservation

1. Introduction

In tropical areas, planting vetiver grass (*Vetivaria zizainoides* L.) hedges has been used as a soil and water conservation practice for over 50 years (Vélez, 1952). However, it was not until 2001 that the United States Department of Agriculture - Natural Resources Conservation Service

*Corresponding author

(NRCS) officially added the use of grass hedges to their National Handbook of Conservation Practices, with the title "Vegetative Barriers, Code 601." In this paper we will use the more descriptive term “grass hedge” interchangeably with the more general “vegetative barrier.” The vegetative barrier practice is designed for controlling runoff and thereby reducing soil erosion by water in cropland and for stabilizing steep slopes. However, control of gullies in non-cropped areas is not included in this standard.

Where floodplains are farmed adjacent to deeply incised stream channels, streambank failure frequently occurs by mass failure, and gullies form where overbank runoff concentrates. In the United States, such edge-of-field gullies are normally controlled with "drop-pipe" structures comprised of earthen dams drained with a pipe culvert (Shields et al., 2002; Trest, 1997). Drop-pipes have proven quite effective, but require capital investment and eventually deteriorate due to corrosion (metal pipes) or by burning in wild fires (plastic pipes).

Throughout most of the United States where winter temperatures drop below -15°C, switchgrass (*Panicum virgatum* L.) forms more robust barriers than vetiver grass. Switchgrass is a tall, coarse species with the longest root system of all grasses comprising the native American prairie (Weaver, 1968). Some switchgrass accessions form aerenchymous roots that help the plants survive waterlogged conditions. Switchgrass roots also form rhizomes. These are very short in most strains so that the grass is generally characterized as a bunch grass, but when planted in a single row, most accessions can form a functional hedge.

Flume studies have shown that switchgrass hedges can remain erect in flows great enough to produce head losses exceeding 0.4 to 0.5 m across the barrier (Temple and Dabney, 2001). We concluded from these flume studies that intact single-row grass hedges could keep upstream flow velocities below critical limits for specific discharges less than 0.2 $m^2 s^{-1}$, and we hypothesized that grass hedges placed at 0.5-m vertical intervals would protect the gully bed by creating a series of low-velocity backwater areas (Dabney et al. 2002). If successful, gully control with grass hedges would be less capital-intensive than the structures described above and would replace the eroding gully with habitats associated with a stand of native grass. Grass barriers also offer a promising alternative to long-recognized methods of gully control such as rock and brush check dams (e.g., Heede, 1976). Grass hedges have the advantages of root systems and the ability to re-grow when partially buried by sediment.

The success of grass hedges for gully control, however, is uncertain during the period of plant establishment. For example, erosive flow velocities might develop just downslope of each grass hedge whenever backwater effects do not fully cover regions between hedges (Fig. 1). If the hedges are not destroyed or flanked by erosion, trapped sediment will raise the bed level upslope of each hedge, while erosion lowers it downslope, producing a series of “steps” stabilized by the grass. Slopes between hedges will be reduced so that hydraulic conditions will be non-erosive for all flows. During this “mature” phase, the grass roots will likely play an important role in preventing mass failure of the “steps” and in attenuating the scour effects of the reverse roller developed below the overfall.

The objectives of this study were to evaluate the effectiveness of a series of vegetative hedges in controlling gullies formed in a range of soil types. The test plantings were subjected to a range of surface and subsurface stresses associated with varying slopes, flows, soil moisture regimes, and vertical spacing of hedges.

2. Materials and Methods

The grass hedge concept was tested in three experiments with increasing levels of environmental stress:

1. Established hedges growing in two nearly identical artificial gullies (S5 and S6) cut into compacted, cohesive fill were subjected to a series of controlled, nearly sediment-free flows.
2. Established hedges growing in a natural gully (L3) formed in highly erosive soils were subjected to a similar series of controlled, sediment-free flows.
3. Established hedges growing in fill placed in a natural gully (R4) were subjected to a season of natural runoff events from cultivated fields.

For Experiment 1, we established a series of six grass hedges in each of two outdoor test channels (sites S5 and S6) at the USDA – Agricultural Research Service (ARS) Hydraulic Engineering Research Laboratory at Stillwater, OK, USA (Fig. 2). These "gullies" were initially constructed as trapezoidal channels with 0.91-m-wide bases and 1H:1V side slopes cut into compacted fill borrowed from the 0.2 to 1.5 m depth of a nearby Pulaski fine sandy loam soil (Coarse-loamy, mixed, superactive, nonacid, thermic Udic Ustifluvents). The channels were built with an average 3H:1V slope. Channels were lined with bermudagrass (*Conodon dactylon* (L) Pers.), and used for simulating erosion of embankment dams subjected to overtopping (Temple and Hanson, 1998). Each channel was tested in 1997 with a flow rate of 1.1 $m^3 s^{-1}$ for 64 to 75 hours, resulting in the formation of a gully with an approximately 1-m deep headcut near each toe (Fig. 2). These headcuts were left to weather in the eroded condition creating regions along the middle portion of the slope as steep as 2H:1V. Switchgrass hedges were transplanted in spring 2000, and protected from flow for two years while the switchgrass became established and shaded out remnant bermudagrass. Runoff was excluded from both Stillwater test gullies during switchgrass establishment, and supplemental irrigation was applied to ensure adequate grass growth. A pool of water was maintained in a depression near the crest of each channel to create a phreatic surface within the underlying soil.

Gullies tested during Experiments 2 (site L3, Fig. 3) and 3 (site R4, Fig. 4) were natural gullies draining from fields into a sinuous reach of Little Topashaw Creek (33.7457 N, -89.1750 W) in Chickasaw County, MS, USA. At the study location, the stream channel was incised about 6 m from its flood plain, had a top bank width of about 35 m, had a bed slope was about 0.002, and drained a watershed of about 37 km^2. Adjacent to the study reach, five fields comprising 75 ha were cropped to cotton (*Gossypium hirsutum* L.) and corn (*Zea Mays* L.). The dominant soil type was Arkabutla silt loam (Fine-silty, mixed, active, acid, thermic Fluvaquentic Endoaquepts). Gullies were "shaped" to smooth contours with a track hoe prior to planting hedges of transplanted switchgrass, producing slopes of about 2.5H:1V or more gradual. Shaping of the gully for Experiment 3 (R4) included placing uncompacted fill. This gully was protected during the period of grass establishment by diverting all runoff away from the upstream end of the gully for two growing seasons.

Preliminary studies (Dabney et al. 2002 and 2004) were used to determine the hydrograph characteristics to be used in our controlled flow tests (Experiments 1 and 2). Controlled flows applied during Experiments 1 and 2 were trapezoidal-shaped "hydrographs" with peak discharges of 0.03, 0.07, and 0.16 $m^3 s^{-1}$ and durations ranging from 0.5 to 3 hours. Flows during Experiment 3 were entirely natural runoff. A total of 19 events were gaged over a period of 3 months, with peak flows ranging from 0.001 to 0.091 $m^3 s^{-1}$ and durations ranging from 0.3 to 4 hours.

During each of the simulated hydrographs in Experiments 1 and 2, we monitored depth and depth-averaged velocity at one-minute intervals at four locations using acoustic Doppler instruments (ADV), turbidity at two points using two optical backscatter instruments, and positive and negative soil water potentials at depths of 0.15, 0.3, 0.45, 1.0, and 1.5 m using tensiometers. Turbidity readings were calibrated to suspended sediment concentration as described by Dabney et al. (2004) and used in conjunction with total station thalweg surveys to compute the quantity of sediment eroded between the instruments. High water marks were flagged during each peak discharge to establish water surface profiles. Additionally, during Experiment 1, static manometers were placed upstream of each barrier. Following each test, we used a total station to survey high water marks and thalwegs. Depth and velocity were not monitored during the natural events of Experiment 3, but flow rates were measured using a 0.45-m metal H-flume, and precipitation records were obtained using a recording tipping-bucket gage. Flow rates were converted to unit discharges by assuming a flow depth and measuring a flow width from topographic surveys of the gully.

Soil particle size distributions and bulk densities were determined at each site using standard techniques. Soil cohesion and friction angle were determined from consolidated/drained triaxial tests and unconfined compression tests (US Navy, 1986) at Stillwater (Experiment 1) and bore-hole shear tests (Luttenegger and Hallberg, 1981) at Topashaw (Experiments 2 and 3). We determined soil conductivity by the shallow-well pump-in method (Amoozegar and Wilson, 1999).

Hedge vegetative characteristics were determined prior to testing by counting all stems within 0.5 m sections of each hedge; measuring the width of each hedge (in the direction of water flow) at both ends of this counted section at elevations of 0.05 and 0.3 m above the soil surface; determining the internode diameter of three representative stems at heights of 0.05, 0.3, 0.6, and 1.0 m in each hedge; and determining the largest gap in each hedge by inspection. During Experiment 1, a screen was set up in the drainage channel downstream from S5 in order to trap stems washed from the hedges.

In order to study the effect of switchgrass hedges on the stability of steps or headcuts within the gullies, we utilized the ARS Bank Stability Model v.3.4 (Simon et al., 2000; http://msa.ars.usda.gov/ms/oxford/nsl/cwp_unit/bank.html, accessed September, 2003) that calculates a slope factor of safety (Fs) as the ratio of resisting strength to shearing force for a planar failure surface. Unfortunately, the model does not simulate the influence of seepage or sapping on slope stability, the importance of which likely varies with soil types. We separately and jointly compared the offsetting influences of increased cohesion due to root reinforcement and the destabilizing force of the extra weight of ponded water. Because we were interested in the stability of step heights less than 1 m high, we modified the model to permit the effect of switchgrass root reinforcement on apparent soil cohesion to be distributed through three shallow soil layers using data presented by Simon and Collison (2002): 30 kPa for 0 to 0.2 m, 10 kPa for 0.2 to 0.5 m, and 1.1 kPa for 0.5 to 1.0 m. We further modified the model to account for the additional horizontal hydrostatic force on the grass hedge and the vertical force on the soil failure block due to the weight of 20 cm of ponded water. We ran (1) a sensitivity analysis of Fs for a headcut in a silty soil as a function of step height, and (2) a stability analysis using the measured field conditions of our study sites.

3. Results and Analyses

Soil Characteristics

Characteristics of the soils at the study sites are summarized in Table 1. The biggest difference in soils was the greater bulk density (ρ_b) and lower saturated conductivity (K_{sat}) of the constructed embankment at Stillwater compared to the natural alluvial deposits at Topashaw. Since the Stillwater channels (Experiment 1, sites S5 and S6) were constructed in engineered fill, only a single (0 to 1.2 m) depth increment was sampled for soil properties. Topashaw soils (Experiments 2 and 3, sites L3 and R4) were siltier near the surface, and became much sandier with depth. Neither the Stillwater channels nor L3 had appreciable cohesion (c') when saturated, and both sites had a soil friction angles (ϕ') between 22 and 40 degrees. Based on the available data, R4 soils likely had values of cohesion and friction angle similar to L3 (Table 1).

Vegetation Characteristics

Properties of vegetation hedges prior to testing at each site are characterized in Table 2. Barriers were wider at Topashaw site L3, but denser in the other channels, where flow was excluded during plant establishment. The ability of the hedges to resist concentrated runoff is indicated by the MEI product (Kouwen, 1988) of stem density, modulus of elasticity, and moment of inertia of individual stems. Measured values at all sites except R4 were nearly equal to or less than the value of 50 N known to withstand unit discharges of 0.2 $m^2 s^{-1}$ (Dunn and Dabney 1996). The lower MEI values were the result of lower stem densities due to competition between hedges planted close together on steep slopes, compact and/or infertile soil conditions, and washouts during the establishment period.

Flow Characteristics

Key characteristics of test flow events are summarized in Table 3. The highest total discharges for the controlled flow events (Experiments 1 and 2) exceeded total runoff gaged during the largest natural events (Experiment 3), but the sum of the discharges for all of the gaged natural events was 1570 m^3. Peak flow rates for controlled flows were quite similar, as planned, but unit discharges (flow discharge divided by flow width) varied by a factor of two among the largest events because the steeper Stillwater channels were narrower. Although the graded ("shaped") contours of both L3 and R4 produced flow widths on the order of 1.5 to 5 m at flow depths of 0.5 m (Fig. 1), progressive failure at R4 undercut the center of several hedges and created a (~0.3-0.4-m wide) "notch" down the thalweg of the gully, concentrating flows and eventually scouring the gully bed as much as 1 m (Fig. 5). Unit discharges of flows confined to the narrow channel reached 0.09 $m^2 s^{-1}$ (Table 3), roughly twice as high as those observed in controlled flow testing, but still less than the maximum loading (0.2 $m^2 s^{-1}$, Temple and Dabney 2001) that could have been withstood by intact hedges.

The depth, velocity, and depth-velocity product (VD) presented for Experiments 1 and 2 are the range of time-averaged values recorded by four ADV loggers in each gully (Fig. 2 and Fig. 3) during the "peak" discharge. In a given flow event, the temporal variation in flow conditions recorded by a given ADV (CV = 11% for depth; CV = 29% for velocity; CV=31% for VD) was less extreme than variation between sampling points. This reflects the different conditions immediately above and below individual grass hedges. However, even the variation between the four ADV loggers (Table 3) does not fully reflect the total variation in flow depth recorded with surveys and static manometers (Fig. 5). Flow was characterized by a series of hydraulic jumps. Usually, jumps began upslope of a vegetative hedge but did not reach their sequent depths until they passed the hedge. Some flow passed through the hedges, but most passed over the top in the jump that cascaded down slope either as free-fall or adhering to bent

over grass stems until plunging into the soil surface or a backwater pool created by the next downslope barrier. Water depth was least, and velocity and VD greatest, in the overfall nappe downslope of hedges on steep slope segments.

The range of measured VD (Table 3) exceeded the range of specific discharges previously tested in flumes (Temple and Dabney, 2001). The higher observed VD is evidence of flow concentration at the ADV locations (gully centerlines). Earlier tests featured hedges that were similar to those tested here (Table 2) but were denser (approximately 300 stems m^{-1}) because they grew widely spaced in well-watered channels and thus were not subjected to competition or washouts (Temple and Dabney, 2001). Peak velocities during Experiment 1 (events 2 through 4 in S5 and S6, Table 3) exceeded the critical value for bare soil of 0.6 m s^{-1} by 200 to 400%. These locally high velocities were associated with bending and overtopping of the hedges, causing non-uniformity in flow conditions across the gully. High local velocity and VD values were associated with increased soil erosion inferred from turbidity data (Table 3).

Maximum measured velocities at specific points during Experiment 2 exceeded the critical value for bare soil by 10 to 45%, and maximum recommended slopes were locally exceeded at the upper end of the gully (Fig. 5). Since the soil was somewhat vegetated between switchgrass hedges at this site, it is not surprising that the observed erosion was small (Table 3), and did not increase with flow rate. In contrast, major erosion occurred during the natural events of Experiment 3, even though the associated peak flow rates were less, and hedge densities were greater than those in Experiments 1 and 2.

The total numbers of stems recovered from below S5 were 4, 22, 11, and 127 after events 1, 2, 3 and 4, respectively. Thus, overtopping bent over many segments of the hedges, and broke off but removed less than 10% of the stems originally present in the dormant hedges. Stem removal would presumably be smaller if the hedges are green and growing rather than in the dormant condition tested.

Mass Failure

The dominant erosion feature observed during Experiment 2 was the mass failure of soil blocks, one of which contained part of the most downslope vegetative hedge during the recession period of event 4 (Fig. 5). This block failure followed deepening and widening of the plunge pool below the overfall, which initially was between 1 and 2 m high. Pre- and post-test surveying indicated a volume of 53 m^3 was eroded during the tests. Most of the removal came from creek sediments previously deposited in and around to a large woody debris structure and from older creek bank materials. Much of the erosion was associated with widening of the gully downslope of the lowest hedge and is therefore not fully reflected in thalweg profile (Fig. 5). Based on the volume of erosion and estimates of sediment and bank bulk density (Table 2), the mass of soil lost through migration of the gully headcut was 65 to 75 Mg, roughly 200 times that lost due to erosion between the turbidity sensors (Table 3). No similar block failure occurred at Stillwater where step heights between barriers did not exceed 0.5 m.

Figure 6 schematically illustrates how we employed the bank stability model to conduct an analysis of the influence of vegetative hedges on the likelihood of mass failure as a function of step height. In each test, we assumed a 57.5 degree (recommended for the given soil friction angle and cohesion) shear plane emerged at a 0.2 m undercut of a vertical bank made up of uniform silty material (friction angle = 30 degrees; cohesion = 5 kPa; saturated unit weight = 18 kN m^{-3}). We calculated the factor of safety, Fs, for step heights of 0.25 to 2.0 m under three test cases: (1) saturated step with no grass roots, (2) saturated step with added cohesion due to switchgrass roots (Simon and Collison, 2002), c_r, in layers 2, 3, and 4 (Fig. 6), and (3) a 20 cm

deep water surcharge (layer 1) on top of a bank reinforced with switchgrass roots. Water surcharge was modeled as a soil layer with a density 1000 kg m^{-3} and zero strength (Fig. 6).

Modeled results indicate that the saturated step would be unstable for heights exceeding 0.7 m, while a saturated step reinforced with switchgrass roots would be stable up to a height of 1.7 m. Even with the extra weight of ponded water, the vegetated step was predicted to be stable to a height of about 1.5 m. However, this level of stability would be achieved only if the roots intersect the shear plane in layers 2, 3, and 4 (Figure 6). As step height increases, the shear plane moves away from the step edge and from the root zone of a narrow strip of vegetation located at the edge. The shear plane from a 1.5 m step height would emerge 1.2 m from the bank edge and could bypass much of the root-reinforced area of a narrow grass hedge. For root reinforcement to have the modeled effect, the width of the vegetation would have to increase as step height increased. For step heights up to 0.5 m, used as a design value in the current study, the shear plane would be completely contained within the root-reinforced zone of even a narrow hedge. For this design step height, Fs = 3.6 even with a 20 cm water surcharge, so no mass failure would be expected. In fact, even when soil cohesion was set to zero other than that provided by switchgrass roots, the model predicts Fs > 1 for step heights up to 1 meter. A note of caution, this analysis does not apply to cracking soils where roots might be severed by desiccation cracks.

When we applied the bank stability model to the pre-test L3 thalweg profile (Fig. 5), without any undercutting or root reinforcement, using geotechnical data from Table 1 and assuming a saturated profile, the estimated Fs = 0.97. Thus, the initial profile approximates an equilibrium bank shape for the site without vegetation or water surcharge. At the time that mass failure was observed at L3, measured pore water pressures included a saturated surface horizon, an unsaturated zone with pore water pressure = -5 kPa between 0.5 and 1.0 m depth, another deeper saturated zone with artesian pressure of 4 kPa below 1.0 m. The scour hole had created a 30 cm undercut at the toe of the plunge pool where the shear plane emerged at a depth of 1.6 m below the hedge (about 89 m above MSL, Fig. 5). When we modeled these conditions, Fs = 0.78 without root reinforcement and Fs = 1.72 with root reinforcement. We believe that in this case, the shear plane partially bypassed much of the switchgrass root zone so that root reinforcement was incomplete, resulting in mass failure. In addition, the model (Simon and Collison 2002) may overestimate the contribution of roots to soil strength because it assumes that all roots break simultaneously as soil shears. When applied to the gullies tested in Experiments 1 and 3, Fs was above 10 for the duration of the tests.

Root Reinforcement

After Experiment 1, inspection showed that there had been some local scour of soil between hedges 3 and 4 (counted from the top, Fig. 2) in S5 and between 4 and 5 in S6. Both locations were on lower portions of the steepest regions of the gully (~ 2:1, or 27 degrees, Fig. 2). In S5, we counted 3700 roots/m^2 protruding from exposed surfaces located about 30 cm below the plant crown, and the mean root diameter was 0.38 mm, median diameter was 0.1 mm, and root area ratio (ratio of the total root cross sectional area to planer soil surface sampled) was 0.0015. In S6, we counted 2900 roots/m^2 protruding, the mean root diameter was 0.69 mm, median diameter was 0.4 mm, and root area ratio was 0.0022. This curtain of exposed roots undoubtedly disrupted the impinging wall jet (Alonso et al., 2002) and reduced local scour during the period of our tests but may not have provided sufficient protection during prolonged flows. This local scour could have been more severe for a less compact, more erodible soil.

After Experiment 2 was completed, we counted roots protruding from the 60 cm deep failed block at the lower end of L3. Root density (2200 roots/m^2) was lower than for S5 and S6,

but root size and root area ratio were larger. The mean root diameter was 1.0 mm, median diameter was 0.6 mm, and root area ratio was 0.0028, similar to that reported for switchgrass at 20 cm depth by Simon and Collison (2002). This suggests that our application of their data for c_r in the mass failure analysis was appropriate. However, prior to the L3 block failure, and in addition to the deepening and widening of the plunge pool at the base of the overfall (Alonso et al., 2002), we observed progressive oozing and sloughing of soil away from roots as a result of seepage flow (Crosta and di Prisco, 1999) and adhesive flow (Oliveria, 2001). Thus, prior to shearing failure, some of the roots on the overfall side and below the root ball of the vegetative hedge were hanging in the air as a curtain.

4. Discussion and Conclusions

The reasons that grass hedges were successful in stabilizing gullies in Experiments 1 and 2 but not Experiment 3 are not entirely clear, although a comparison of some of the key conditions for each experiment is revealing (Table 4). In all three experiments, the hedges had been in place for two growing seasons. Since root depth and development increase the durability of hedges to resist undercutting and mass failure, hedge reliability should increase with age over the first few years, depending on site conditions. In some ways, Experiments 1 and 2 were more rigorous tests of the grass hedges, since flows were clear and hedges were dormant throughout the period of testing. However, soils underlying the Experiment 3 gully (R4) were more erodible, and when subjected to a sequence of natural events, this site responded by a deep, narrow central notch that served as positive feedback to erosion processes. Experiment 1 erosion rates might have been considerably higher if the Stillwater soil had not been compacted to a bulk density of 1.78 Mg m^{-3}, since erodibility of this material can decrease by two orders of magnitude if bulk density is increased from 1.70 and 1.85 Mg m^{-3} (Hanson and Temple, 2002).

Concentrated flow soil erosion rates increase dramatically when knickpoints form and migrate headward. A series of grass hedges encourages the development of steps and knickpoints in the bed of a gully (Fig. 1). On the other hand, the tall, thick grass stems greatly increase the roughness of the channel, slowing flow, and the dense root systems add to the cohesion of the soil. The question becomes, can the vegetative hedges that encourage the development of steps prevent knickpoint migration?

Conceptually, flow control by grass hedges can be divided into three regimes. During <u>low flow</u>, backwater depth insufficient to protect the entire upstream reach between hedges and erosion below the hedge, deposition above the hedge is the dominant process (Fig. 1, top). Through an <u>intermediate flow</u> range, the hedges remain upright, tailwater protects the areas immediately downstream of the hedges, and the erosion/deposition processes are substantially damped (Fig. 1, bottom). For <u>higher flows</u>, the hedges are locally overtopped, flow is concentrated, and the protective capability of the hedges results from a combination of the "prone" stems reducing velocity near the bed, the ponding effect reducing mean velocity, and the energy loss associated with the resulting high turbulence in some areas, where boundary adjustment rates depend on soil erodibility.

Observations at Stillwater (Experiment 1) suggest that gully slopes treated with grass hedges must be $\leq$ 3H:1V even when vertical intervals are < 0.5 m because of: (1) retardation of hedge development due to plant crowding and (2) the dimensions of hydraulic jumps. Switchgrass is a plant that thrives in full sunlight. When planted at a vertical spacing of 0.5 m, horizontal spacing would be only 1.0 m apart on a 2H:1V slope. This crowding would cause competition that would limit hedge growth and development (hedge width, stem density, stem

diameter). The situation would be aggravated in northern-facing or deeply incised gullies. A second constraint on gully slope is provided by hydraulic jump behavior. Increasing bed slope generally increases the Froude number, increases the height and length of a hydraulic jump, and moves the jump initiation point downslope. When the sequent depth of the jump exceeds the flow depth at a hedge, the maximum flow depth is not reached until the flow is past the hedge, and the jump takes the form of a "standing swell," which well describes Experiment 1 observations. On the steepest portions (~2H:1V) of S5 and S6, the overfall nappe leaving the swell bypassed the next hedge and plunged into the backwater created by the second downslope hedge (Fig. 5). This greater fall allowed acceleration of the overfall nappe (Alonso et al., 2002) and enhanced the local scour that exposed roots. Empirical relationships for hydraulic jump dimensions (Chow 1959) support the conclusion that a 0.5-m hedge spacing on a 3H:1V slope would allow each hedge to create its own jump without being bypassed.

The results of this study indicate that stabilizing gullies with a series of grass hedges has potential, but more research is needed to improve reliability. Established switchgrass hedges with a 0.5-m vertical interval on slopes $\leq$ 3H:1V were effective in preventing measurable erosion during 8 hr of testing with specific discharges up to 0.09 $m^2 s^{-1}$. Energy was effectively dissipated in a series of cascading hydraulic jumps. Erosion by mass failure was not observed when step heights between hedges $\leq$ 0.5 m. However, mass failure was the dominant mechanism where conditions at the gully mouth produced a hedge with a 1- to 2-m overfall. Specific discharges of about 0.09 $m^2 s^{-1}$ did produce significant thalweg erosion and undercutting of grass hedges in a gully formed in sandy soils with low (~1.3 Mg m^{-3}) bulk densities. Protection of such highly erodible soils exposed between hedges using turf reinforcement mattresses or similar products might render this type of gully treatment more robust.

Acknowledgments

John Massey, Calvin Vick, Brian Dahl, Brian Bell, Kem Kadavay, Kevin Cook, and Bobby Sappington provided assistance with data collection. Don Gray, Natasha Pollen, and Garey Fox read an earlier version of this paper and made many helpful suggestions.

References

Alonso, C.V., S.J. Bennett, and O.R. Stein. 2002. Predicting head cut erosion and migration in concentrated flows typical of upland areas. Water Res Res, 38(10):39-1 to 39-15.

Amoozegar, A. and G. V. Wilson. 1999. Methods for measuring hydraulic conductivity and drainable porosity. In Agricultural Drainage, 1149-1205. R. W. Skaggs and J. Van Schhilfgaarde, eds. Agronomy Monograph No. 38. Am. Soc. Agron., Madison, Wisconsin.

Chow, V.T. 1959. Open-Channel Hydraulics. McGraw-Hill, New York, 680 pp.

Crosta G. and C. di Prisco. 1999. On slope instability induced by seepage erosion. Can. J. Geotech., 36:1056-1073.

Dabney, S. M., L. D. Meyer, G. H. Dunn, G. R. Foster, C. V. Alonso. 1996. "Stiff-grass Hedges, a Vegetative Alternative for Sediment Control." Proceedings of the Sixth Federal Interagency Sedimentation Conference, Vol. 2 (X):62-69.

Dabney, S., F. D. Shields, Jr., D. Temple, A. Collison, and A. Simon. 2002. Layout and Establishment of Grass Hedges for Gully Control. Proceedings of the 12th Conference of the International Soil Conservation Organization. 26-31 May, Beijing, China. Volume III, p. 464-470.

Dunn, G. H. and S. M. Dabney. 1996. Modulus of elasticity and moment of inertia of grass hedge Stems. Trans. Am. Soc. Agric. Engr., 39(3):947-952.

Hanson, G. J. and D. M. Temple. 2002. Performance of bare-earth and vegetated steep channels under long-duration flows. Trans. Am. Soc. Agric. Engr., 45(3):695-701.

Heede, Burchard H. 1976. Gully Development and Control: The Status of Our Knowledge. Research Paper(RM-169),USDA-Forest Service, Fort Collins, Colo.

Kouwen, N. 1988. Field estimation of the biomechanical properties of grass. J. of Hyd. Res., 26(5):559-568.

Luttenegger J.A., and B. R. Hallberg. 1981 Borehole shear test in geotechnical investigations. American Society of Testing Materials, Special Publication 740:566-578.

Mamo, M., and G.D. Bubenzer. 2001. Detachment rate, soil erodibility and soil strength as influenced by living plant roots Part I: laboratory study. Trans. Am. Soc. Agric. Engr., 44(5):1167-1174.

Meyer L.D., G.R. Foster, and S. Nikolov. 1975. Effect of flow rate and canopy on rill erosion. Trans.. Am. Soc. Agric. Engr., 18(5):905-911.

Nearing, M.A., L.J. Lane, E.E. Alberts, and J.M. Laflen. 1990. Prediction technology for soil erosion by water: status and research needs. Soil Sci. Soc. Am. J., 54:1702-1711.

Oliveira, M.A.T. 2001. Adhesion flow and regressive gully-head expansion in southern Brazil: field experiment results. In Soil Erosion Research for the 21st Century, 603-606. J.C. Ascough II and D.C. Flanagan, eds. Am. Soc. Agric. Engr., St. Joseph, Michigan.

Shields, F. D., Jr., Morin, N., and Kuhnle, R. A. 2001. "Effects of Large Woody Debris Structures on Stream Hydraulics." Proceedings, Wetlands Engineering and River Restoration Conference, ASCE, Reston, VA, CD-ROM.

Shields, F. D., Jr., Smiley, P. C., Jr. and Cooper, C. M. 2002. Design and Management of Edge-of-Field Water Control Structures for Ecological Benefits. J. Soil and Wat Consv. 57(3):151-157.

Simon, A. and A. J. C. Collison. 2002. Quantifying the mechanical and hydrologic effects of riparian vegetation on streambank stability. Earth Surf. Proc. Landf., 27:527-546.

Simon, A., Curini, A., Darby, S.E., and Langendoen, E.J. 2000. Bank and near-bank processes in an incised channel. Geomorph. 35:193-217.

Temple, D. M., S. M. Dabney. 2001. Hydraulic performance testing of stiff grass hedges. Proceedings of the Seventh Interagency Sedimentation Conference, Vol. 2 (XI):118-124.

Temple, D. M., G. J. Hanson. 1998. Overtopping of grassed embankments. Proceedings of the 1998 annual conference of state dam safety officials, Las Vegas, NV, U.S.A. (CD-ROM).

Trest, J. W. 1997. Design of structures for the Yazoo Basin Demonstration Erosion Control Project. In: Wang, S. Y., E. Langendoen, and F. D. Shields Jr. (eds). Management of landscapes disturbed by channel incision: stabilization, rehabilitation, and restoration, Center for Computational Hydroscience and Engineering, University of Mississippi, 1017-1022.

USDA-NRCS. 1989. Estimating Runoff and Peak Discharges. Chapter 2 in National Engineering Handbook, Part 650, Engineering Field Handbook, Washington, D.C., 91 pp.

U.S. Navy. 1986. Soil mechanics. NAVFAC Design Manual DM-7. Washington, D.C.

Vélez, I. Soil conservation practices in the Caribbean archipelago. The Scientific Monthly 1952. 74 (3), 183-185.

Weaver, J. E. 1968. Prairie plants and their environment. University of Nebraska Press, Lincoln.

Table 1. Soil characteristics of the tested gullies

Experiment	Location (site), Sample depth m	Organic Matter %	Sand %	Silt %	Clay %	ρ_b Mg m^{-3}	K_{sat} mm h^{-1}	ϕ' degrees	c' kPa
1	Stillwater (S5 and S6)								
	0 to 1.2	0.27	57	30	13	1.78	4.8	40	0
2	Topashaw (L3)								
	0 to 0.15	1.80	34	55	11	1.28			
	0.15 to 0.3	0.53	66	25	8	1.42	34.8		
	0.3 to 0.6	0.35	76	18	6	1.53	34.9	28	3.3
	0.6 to 0.9	0.50	60	31	9			24	2.3
	0.9 to 1.5	0.35	73	20	7			22	1.3
3	Topashaw (R4)								
	0 to 0.5	1.63	9	71	20	1.34			
	0.5 to 1	1.29	18	65	17	1.41			
	1 to 1.6	1.32	11	70	19	1.40			
	1.6 to 2.1	0.54	40	47	13	1.53			
	2.1 to 2.6	0.26	56	34	11	1.63			

Table 2. Average characteristics of switchgrass hedges in each gully prior to testing.

Experiment	Location (site)	Width1 Hedge @ 0.05 m height m	Width Hedge @ 0.30 m height m	Stems per meter of Hedge m^{-1}	Stem Internode Diameter mm	Average Maximum Gap in Hedge m	MEI2 @ 0.15 m N
1	Stillwater (S5)	0.25	0.54	178	5.1	0.12	51
1	Stillwater (S6)	0.23	0.52	199	4.4	0.08	32
2	Topashaw (L3)	0.45	0.65	107	4.6	0.18	25
3	Topashaw (R4)	0.33	0.80	331	5.0	0.11	71

[1] The word "width" when applied to a grass hedge refers to the dimension parallel and not perpendicular to flow.

[2] Product of stems per m^2, modulus of elasticity assumed to be 3.5 GPa, and moment of inertia calculated from average stem diameter (Dunn and Dabney, 1996).

Table 3. Total discharge during each run, flow characteristics during the quasi-steady peak of each run, and total erosion or deposition between the two turbidity sensors.

Location/Event	Total Discharge m^3	Peak Flow Characteristics					Erosion (+) or Deposition1 kg
		Flow $m^3 s^{-1}$	Unit Discharge $m^2 s^{-1}$	Velocity $m s^{-1}$	Depth m	VD $m^2 s^{-1}$	
Experiment 1 (Stillwater S5)							
1	48	0.035	0.02	0.14 to 0.18	0.08 to 0.22	0.03 to 0.04	16
2	198	0.079	0.02	0.16 to 2.46	0.10 to 0.29	0.04 to 0.37	40
3	296	0.067	0.04	0.09 to 1.67	0.07 to 0.21	0.02 to 0.24	42
4	1085	0.166	0.09	0.71 to 2.08	0.09 to 0.22	0.16 to 0.36	272
Experiment 1 (Stillwater S6)							
1	32	0.020	0.01	0.06	0.12 to 0.14	0.01	45
2	201	0.082	0.04	0.03 to 1.51	0.10 to 0.25	0.01 to 0.17	87
3	308	0.069	0.04	0.15 to 1.36	0.09 to 0.19	0.03 to 0.13	200
4	1116	0.169	0.09	0.08 to 1.71	0.09 to 0.20	0.01 to 0.21	296
Experiment 2 (Topashaw L3)							
1	84	0.043	0.02	0.15 to 0.66	0.12 to 0.18	0.02 to 0.06	-112
2	203	0.069	0.04	0.39 to 0.87	0.09 to 0.23	0.06 to 0.09	160
3	353	0.064	0.03	0.35 to 0.85	0.10 to 0.22	0.06 to 0.11	133
4	676	0.138	0.05	0.46 to 0.66	0.14 to 0.27	0.09 to 0.18	57
Experiment 3 (Topashaw R4)2							
1	53	0.007	0.01				6,000
2	94	0.020	0.02				
3	209	0.079	0.08				
4	224	0.055	0.06				
5	234	0.091	0.09				
6	562	0.091	0.09				

[1] Between turbidity sensors in tests 1 and 2. Erosion at L3 excludes about 70,000 kg eroded by mass failure of soil blocks at large headcut at gully mouth (Fig. 5).

[2] Only the events with the six largest peaks are shown, sorted in ascending magnitude. Erosion was observed over an entire high flow season, which involved at least 19 events.

Table 4. Summary of experiments.

Experiment	Location (site)	Mean (Max) gully slope	Hedge establishment	Hedge width m	Average maximum gap in hedge m	Soil conditions	Mean bulk density of soils Mg m^{-3}	Total discharge m^{-3}	Total discharge duration hr	Peak unit discharge $m^2 s^{-1}$	Outcome
1	Stillwater (S5 & S6)	3H:1V (2H:1V)	Protected for two growing seasons	0.54	0.12	Compacted fill	1.78	1640, clear water from reservoir	8	0.09	Negligible erosion
2	Topashaw (L3)	5H:1V (2.4H:1V)	Natural (but small) flows during two growing seasons	0.65	0.18	Natural gully, graded to smooth shape	1.3-1.5	1320, clear water from stream	7	0.05	Negligible erosion in protected region of gully, but major mass failure at downstream headcut
3	Topashaw (R4)	2.6H:1V	Protected for two growing seasons	0.80	0.11	Uncompacted fill to shape natural gully	1.3-1.5	1570, sediment-laden runoff from fields1	29	0.09	~ 1 m of thalweg degradation

[1] Flow-weighted composite runoff samples from 10 storm events at this site and an adjacent gully had suspended sediment concentrations ranging from 159-8,963 mg/L, mean = 2,430 $\pm$ 2,612 mg/L.

List of Figures

Figure 1. Schematic of concept for stabilizing gully with a series of grass hedges placed at vertical intervals of 0.5 m

Figure 2. Shaded relief contour map (0.2 m contour interval) of pre-test conditions of test gullies for Experiment 1, showing the extent of grass hedges, locations of turbidity sensors (OBS), acoustic Doppler depth and velocity transducers (ADV), tensiometer nests (Tens), and pre-existing headcuts at the toe of each gully.

Figure 3. Shaded relief contour map (0.5-m contour interval) of pre-test conditions for Experiment 2 indicating locations of grass hedges, turbidity sensors (OBS), acoustic Doppler depth and velocity transducers (ADV), and tensiometer nests. Flow was introduced only into the northern arm of the gully. The location of a large woody debris structure that trapped creek sediments at the toe (LWD) is also indicated.

Figure 4. Shaded relief contour map (0.5 m contour interval) of pre-test condition of test gully for Experiment 3, showing the extent of grass hedges and location of H-flume.

Figure 5. Gully thalweg, high water profiles, and grass hedge locations during the first and last event at each location. Thalweg changes during Experiment 1 were not measurable. High water profiles for Experiment 3 were not measured.

Figure 6. Use of bank-stability model to determine the effect of switchgrass hedges on the likelihood of mass failure of steps in a silty soil as a function of step height.

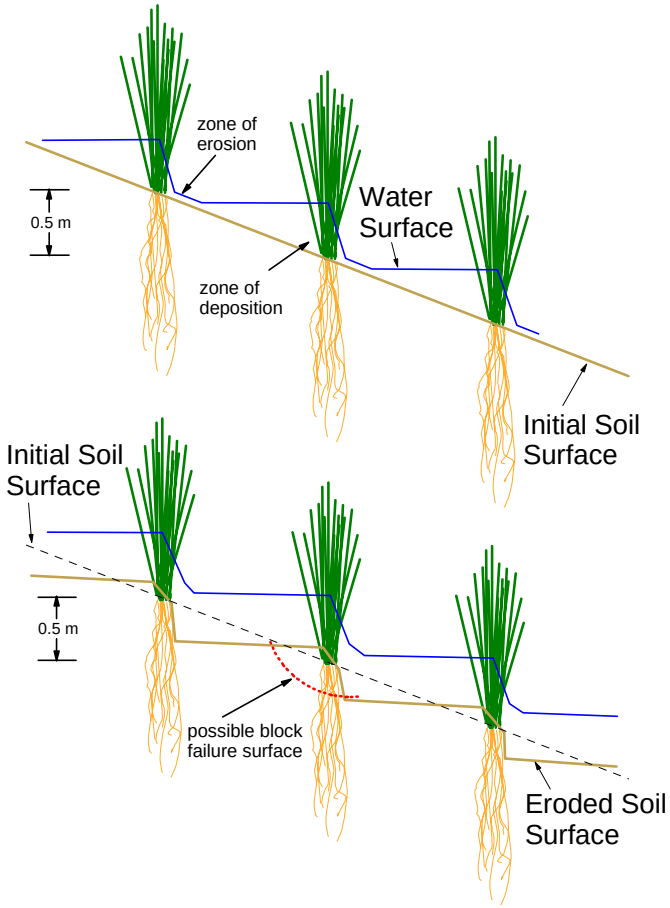

Figure 1. Schematic of concept for stabilizing gully with a series of grass hedges placed at vertical intervals of 0.5 m

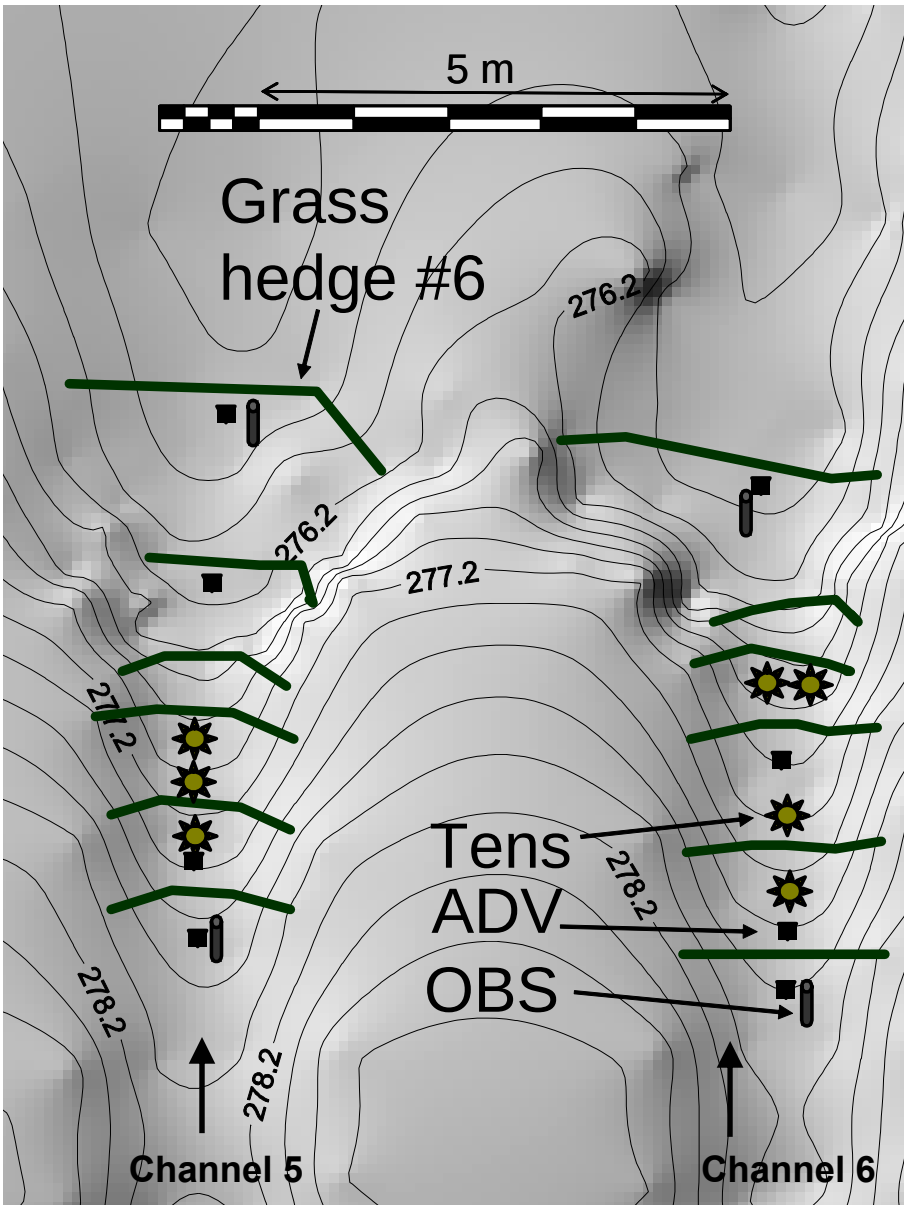

Figure 2. Shaded relief contour map (0.2 m contour interval) of pre-test conditions of test gullies for Experiment 1, showing the extent of grass hedges, locations of turbidity sensors (OBS), acoustic Doppler depth and velocity transducers (ADV), tensiometer nests (Tens), and pre-existing headcuts at the toe of each gully.

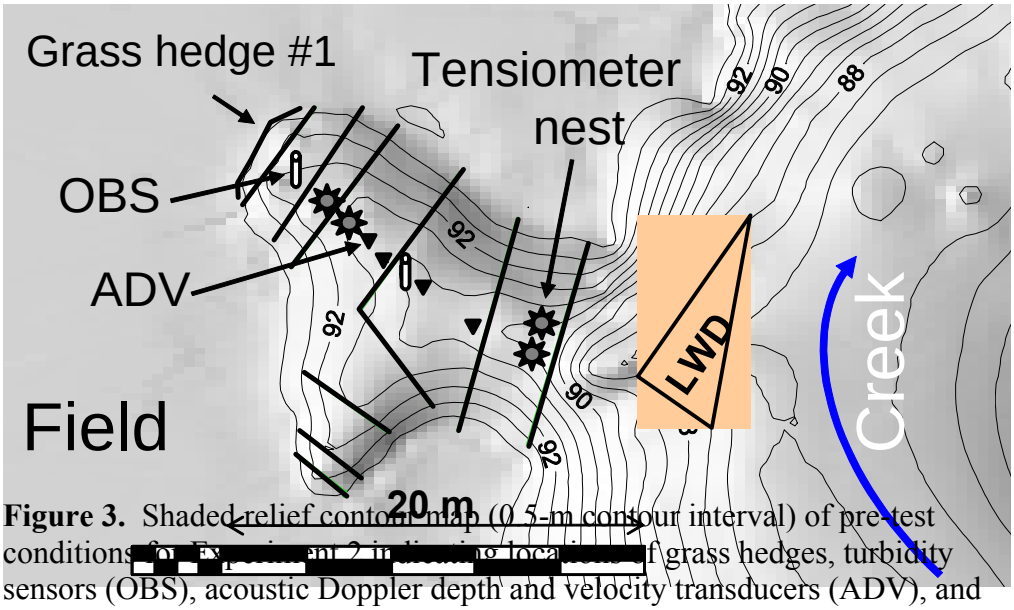

Figure 3. Shaded relief contour map (0.5-m contour interval) of pre-test conditions for Experiment 2 indicating locations of grass hedges, turbidity sensors (OBS), acoustic Doppler depth and velocity transducers (ADV), and tensiometer nests. Flow was introduced only into the northern arm of the gully. The location of a large woody debris structure that trapped creek sediments at the toe (LWD) is also indicated.

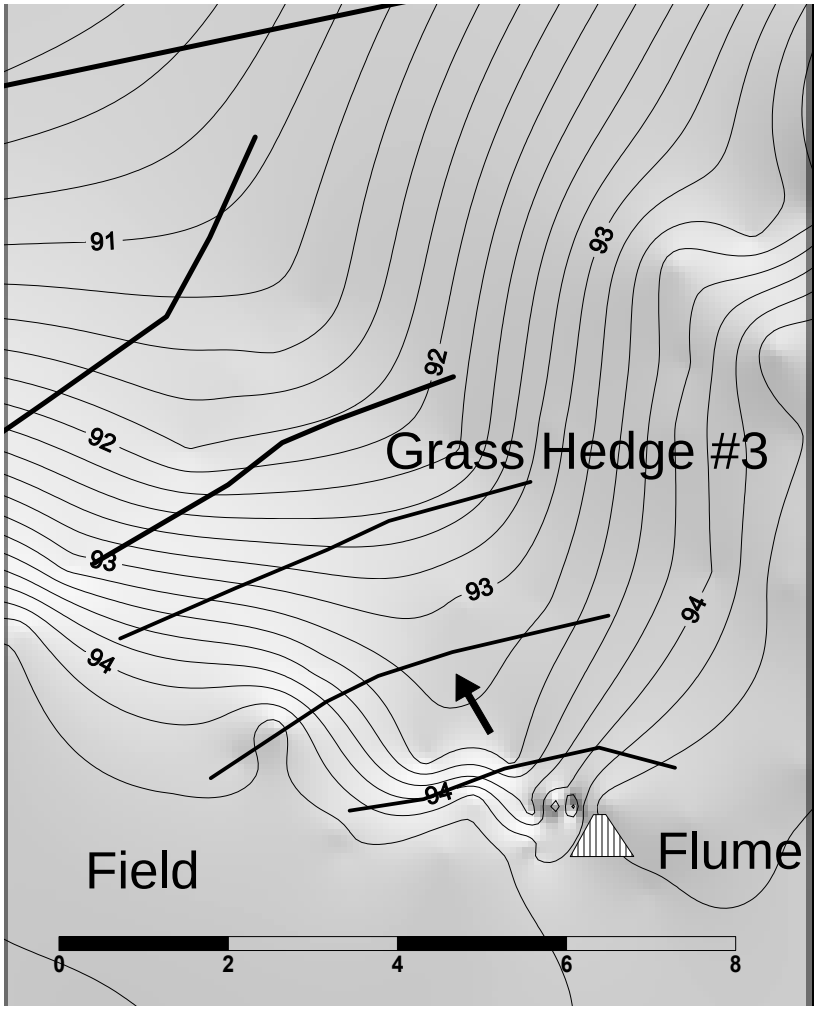

Figure 4. Shaded relief contour map (0.5 m contour interval) of pre-test condition of test gully for Experiment 3, showing the extent of grass hedges and location of H-flume.

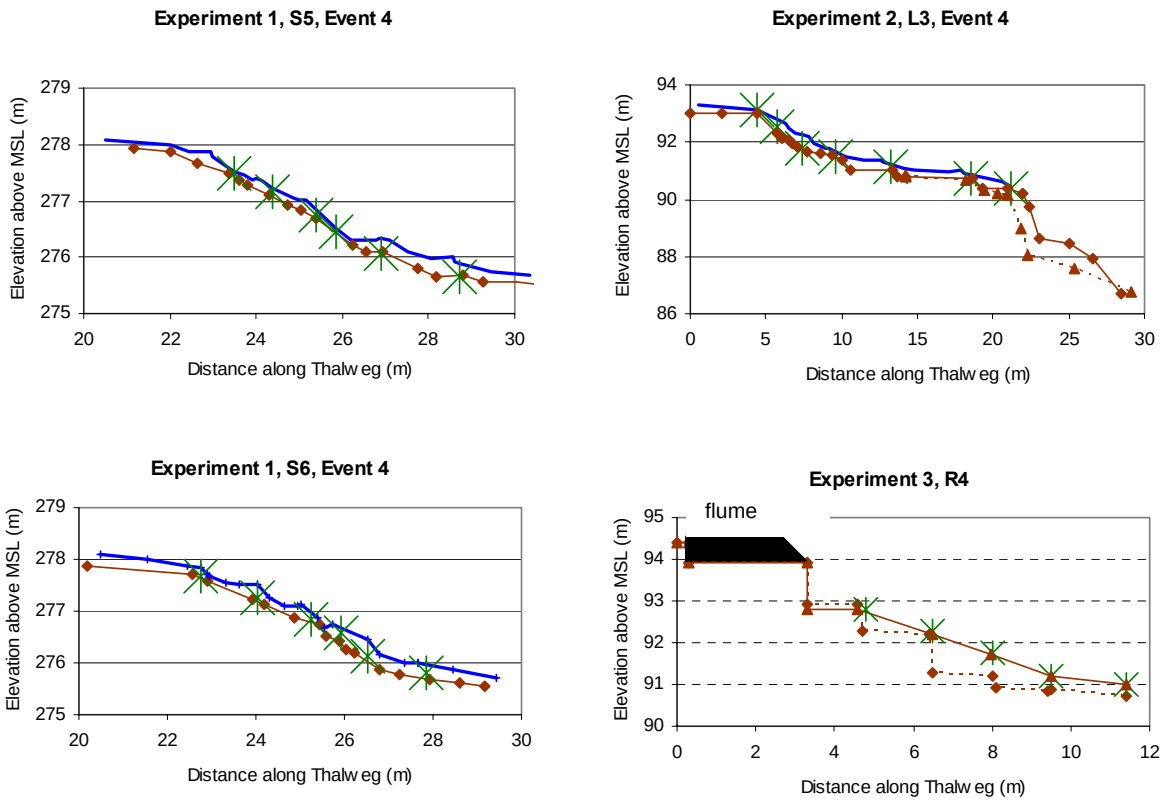

Figure 5. Gully thalweg, high water profiles, and grass hedge locations during the first and last event at each location. Thalweg changes during Experiment 1 were not measurable. High water profiles for Experiment 3 were not measured.

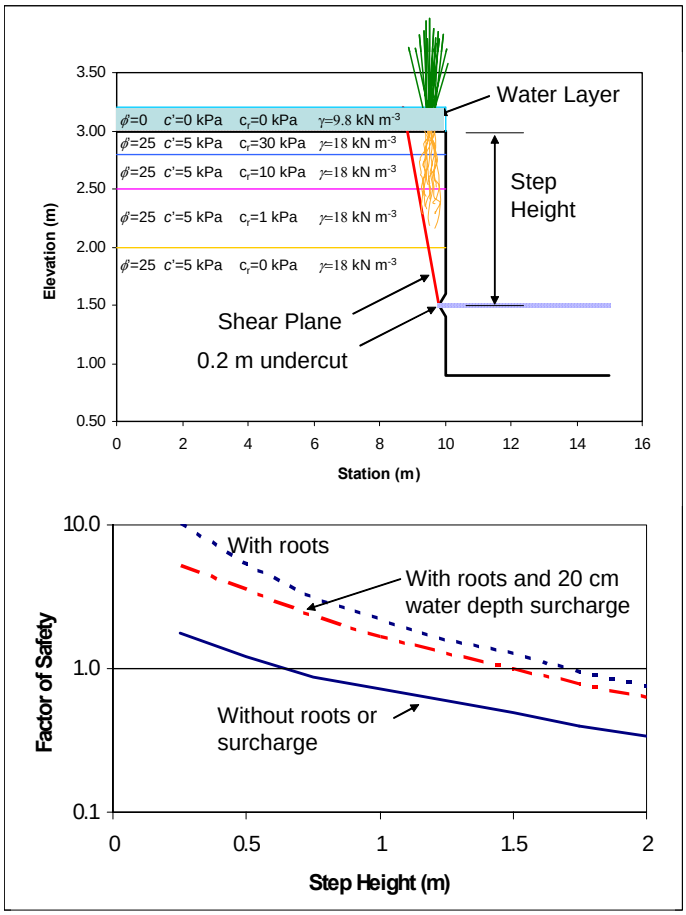

Figure 6. Use of bank-stability model to determine the effect of switchgrass hedges on the likelihood of mass failure of steps in a silty soil as a function of step height.

To Table of Contents

Gully Erosion Land Use and Reclamation

Regional Ecosystem Rehabilitation on the Loess Plateau (Abstract only)
Rui, Li, Oinke Yang, Guobin Liu (Keynote)

Soil Structural State and Erosion by Concentrated Flow: in Situ Experiments on Three Different Cropping Systems (Abstract only)
Léonard, J., H. Boizard, J. Duval, and G. Richard

Sediment from a Small Ephemeral Gully in South Carolina
Hansen, William F. and Dennis L. Law

Native Plants and Fertilization Help to Improve Sites and Stabilize Gullies on the Sumter National Forest
Law, Dennis L. and William F. Hansen

Response of Gully Development to Land Use Change in West China (Abstract only)
Li, Yong, Lingyu Bai, Xingchang Zhang, Fuhong He, and Dignhui Liu

Agroecological Estimation of Grey Forest-steppe Soil of South Bug's Basin and its Erosion Reduction Methods (Abstract only)
Yerychuk, Saveta

Gully Erosion Prediction and Warning in Black Soil Region of Northeastern China (Abstract only)
Wu, Yongqiu, Gang Hu, and Baoyuan Liu

Gullies in China: Form, Process and Control: a Comprehensive Literature Review (Abstract only)
Li, Y.Q.

Comprehensive Gully Reclamation in the Loess Plateau, Northwest China: from Warping Dams to Gully Gardens (Abstract only)
Liu, Rengkui and Y.Q. Li

Keynote

Regional Ecosystem Rehabilitation on the Loess Plateau

Li Rui*
Oinke Yang
Guobin Liu
Institute of Soil and Water Conservation
Chinese Academy of Sciences and Ministry of Water Resources
NWSUAF, Yangling, Shaanxi 712100, PRC

Abstract

The Loess Plateau is well known for its deep loess deposits and serious soil erosion. The region covers five provinces and 0.62 million km^2; 45% of the area is eroded and there is an average soil loss of 3720 tonnes/km^2/year. Since 1985, the comprehensive reclamation of the Loess Plateau has been listed as a key science and technology project in China. Eleven small catchments have been selected as experimental and demonstration areas for ecosystem rehabilitation in different regions of the plateau. After 15 years, each of the 11 catchments has formed a good model for local areas. A set of technologies to control land degradation has been developed. The average yield of farmland has increased by 100--300%, the area under crops has decreased by 30--70%, vegetation cover has increased by 70--150% and soil erosion has decreased by 60--80%. The economic structure of the region has undergone major changes, with income from grain down from 80% to 30%. Farmers' incomes are 5--10 times greater than previous levels.

The key task in the region is to improve land use. In the loess hill region, cultivated land occupies more than 40% of the total area, most of which is on steep slopes (more than 15) and about 20--30% of which is on slopes of more than 25 . Only 12% of the region is forested, and only 6.5% by forest that can effectively control soil erosion. Only 30.5% is grassland, of which almost 69% has deteriorated from overgrazing. Land use should consist of flat area cropping for subsistence; forestry in gullies to protect the local ecology; and fruit growing and animal husbandry on sloping land for income.

Results from the 11 trial areas indicate that small catchments can be ecologically rehabilitated, but that they must pass through three stages --- restoration, stabilisation and sustainable development --- taking 15--20 years. The prospects for the Loess Plateau are bright, but there is a long way to go.

Keywords: ecology rehabilitation, soil erosion, loess plateau

*Correspondence author

Soil Structural State and Erosion by Concentrated Flow: in Situ Experiments on Three Different Cropping Systems

J. Léonard*
INRA rue Fernand Christ
Laon, 02007, France

H. Boizard
J. Duval
G. Richard
INRA, Unité d'Agronomie Laon-Reims-Mons

Abstract

Soil structure exerts a strong influence on erosion by concentrated flow. It controls flow rates through infiltration and the production of excess water, the hydraulics of flow through roughness and micro relief, the size of soil elements and the bonds between them. The present study concentrates on detachment and transport of soil elements by concentrated flow in relation to the structural state of the soil. A runoff simulator has been developed which allow to simulate a concentrated flow in situ, with a controlled and stable flow discharge, and to estimate locally the water depth, the water surface slope and shear stress. This device has been used to simulate runoff on three contrasted situations: (i) maize crop with conventional tillage (plow); (ii) maize crop with reduced tillage (no plow) and numerous compacted zones in the soil profile; (iii) pea crop with reduced tillage and few compacted zones in the soil profile. Both micro (50-250 µm) and macro (>250 µm) aggregates have been sampled at the outlet of the plot. Observation have been made on where and how sediments are detached, what is the nature of these sediments, how they are transported by runoff, under what conditions. Results should help us to better understand the processes of erosion by concentrated flow on agricultural soils, to evaluate what are the most appropriate variable characterizing soil structure with regard to detachment and transport by runoff, to evaluate the relationships between detachment-transport and soil structure.

Keywords: detachment-transport processes, soil structure, cropping systems

*Correspondence author

Sediment from a Small Ephemeral Gully in South Carolina

William F. Hansen[*] (E-mail: wfhansen@fs.fed.us)
Dennis L. Law (E-Mail: dllaw@fs.fed.us.)
USDA Forest Service
4931 Broad River Road
Columbia, SC 29212,
FAX 803-561-4004,

Abstract

Since the Sumter National Forest (SNF) was acquired in the 1930s, emphasis on land stabilization and restoration of eroded landscapes included many gully treatments. Public concern over the intensity of ground disturbing activities associated with many gully treatments suggested the need to verify when gullies were still actively contributing sediments. In 1992, a land parcel was purchased containing several ephemeral gullies within Chester County, South Carolina. Although barren and eroding, generous leaf covered the downstream channel. Treatment to control sediment delivery to streams did not appear justified at that time. Normally in this circumstance, efforts to reduce erosion would concentrate on revegetation and fertilization within the gullies. However, questions remained on their activity level. How can an area be actively eroding, and not contribute sediment? This paper discusses the findings over nearly a decade from the sediment measured from a small gully approximately 0.10 hectares (0.25 acres) in size.

Measurement began in July 1994 with the installation of a filter fabric dam supported by a wire fence to capture the sediment. In August 1994, Hurricane Jerry delivered 4.5 tonnes (5 tons) of sediment. Over 4.5 years, 40 tonnes (44 tons) of sediment accumulated behind the sediment fences indicating an average sediment delivery rate of 89 tonne/ha/year (39 tons/acre/year). The delivery of sediment was relatively dormant during nearly 5 years of below normal rainfall and drought conditions during much of 1997 to 2002. However, higher than normal rainfall during the spring and summer of 2003 reactivated the delivery of sediments. Remeasurement in March 2004 indicated another 8 tonnes of sediment had deposited since the 1999 measurement. After 9.5 years, the fabric dams accumulated 48 tonnes (53 tons) of sediment, resulting in an average annual sediment delivery rate of 51 tonnes/hectare (22 tons/acre).

Based on intermittent observations over nearly a decade, soil erosion regularly occurred during intense rainfall events and freeze-thaw cycles. Only severe storms produced enough flow to deliver sediment. Indicators of erosion included soil pedestals, rills, exposed fine root networks, sandy textures and layers of buried leaves within the profile. Within the gully channel, headcuts (nickpoints), cavitation, soil piping, tree root exposure and light reddish soil deposits were indicators of ongoing erosion activity for this site. During inactive periods, autumn leaf-fall effectively hid most of the downstream sediment transport path, giving an appearance of stability and low sediment activity that was maintained until the next major event.

Discussion includes information on fabric dam construction, maintenance, measurement of the sediments and gully boundaries. Properly reinforced, the filter fabric dams were effective at storing sediments, which could be measured at any time. They

[*]Corresponding author

produced both a measurable and a visible record of the sedimentation that others can relate to.

The results suggest that small ephemeral gullies should not necessarily be neglected when indicators suggest episodes of activity and sediment delivery. Attention to detail may help in recognizing and assessing their activity. The Criterion survey laser was an effective tool in characterizing the pinnacle-like sections of the gully boundaries.

Keywords: ephemeral gully, sediment filter fence, survey laser, erosion

1. Introduction

The Sumter National Forest (SNF) was primarily acquired in the 1930s within the authority granted in the Weeks Law of 1911 to obtain and improve denuded and eroding lands within navigable watersheds to help produce sustained water and timber resources. Since then, SNF emphasis has included land stabilization and restoration of eroded landscapes and addressing sources of active erosion and sediment, including gullies. Primary work began with the Civilian Conservation Corps in efforts to reforest denuded lands and stabilize expanding gully networks. Ongoing efforts to address severely eroding lands and the effects from past erosion continue. As a result, thousands of acres of land and eroding terrain have been improved through reforestation and treatment of actively eroding sites (Hansen, 1991, Hansen and Law, 1996).

This study began as an effort to help address issues of gully activity and need for treatment. Many others have studied or discussed various aspects of gullies (Hoover, 1949, Heede, 1976, 1982, Singer et al, 1978, Yoho, 1980, Schumm et al, 1984, Hansen, 1995). The study area is within a land parcel purchased in 1992 in Chester County, South Carolina, east of the town of Union. It is contained within the upper reaches of Little Turkey Creek, a minor tributary within the Broad River basin (figure 1). Several small, but actively eroding gullies were many decades old and easily identifiable on aerial photos taken during in 1974 (figure 2). Another aerial photo taken in 1990 suggested that there were no major changes in the gully shape during that period (figure 3). In addition, due to the small size of the gullies and limited contributing drainage area, there was uncertainty in whether the ongoing surface erosion could produce concentrated flows and sediment delivery sufficient to justify treatments. Internally, the gully was active, but the downstream channels appeared stable and well covered in leaves suggesting limited or no sediment delivery.

This paper summarizes the sediment captured from a 0.1 hectare (0.25 acre) ephemeral gully during almost a decade. Many observations were also made during this time as the site was occasionally visited after major storm or ice events, and during field tours.

2. Area Description, Methods and Material Studied

Portions of the study area were probably farmed about a century ago. Severe erosion and gullies developed and extended into the hillslopes (figure 4). Eventually much of the farmed area became depleted and probably naturally converted or was planted to loblolly pine (*Pinus taeda*) forest land. However, the severely eroded soils within the gully have been unable to support vegetation for many decades. Many of the bottomland trees adjacent to the area are mature timber probably over 50 years old. Many of the sparse trees within the gully exhibit characteristics of low site conditions

such as fusiform disease, chloritic needles, rank branching, rough bark, exposed roots and poor form. Other indicators associated with the low site conditions for this area include the presence of Eastern redcedar (*Juniperus virginiana*) and lichens on the soil surface (figure 5).

Rainfall averages about 114 cm (45 inches) per year in this area of the piedmont, and is typically well dispersed through the year with average monthly rainfall between 7 and 13 cm (3 and 5) inches. Water yield averages about 43 cm (17 inches) per year on the gauged larger streams.

Filter fabric dams were constructed with steel T posts, wire fencing, filter fabric, and wire C clamps and post ties in July, 1994 to capture sediment (Dissmeyer, 1982) (figure 6). From past experience in working with silt fences on slopes and small ephemeral channels, we did not expect much to occur. Steel fence posts (1.5 m or 5 feet) were initially installed at 0.9-1.5 m (3-5) foot spacing, but more were later added to handle the weight of the sediment and water. The 1.2 meter (4 feet) wire fence and filter fabric were buried into the soil surface about 0.15 m (6 inches) to assure that the sediment would be retained and the water filtered through the fabric. The filter fabric was attached to the wire fence with C clamps using hognose pliers. In installation, care was taken that the lowest point in the fabric remained in the center of the channel, and the edges were higher to allow for overflow to occur if needed without damaging the integrity of the structure.

Measurements were made infrequently as time permitted. Sediment deposits behind the dams were taken by measuring the elevation changes as sediment accumulated in 1994, 1999 and 2004 at 0.3-0.6 m (1 to 2 foot) spacing intervals for cross sections every 0.9 m (3 feet) up the channel. Elevation differences were measured with a Nikon Laser Level with rod sensor, and cross sections were marked with rebar pins. Measurements were located with an expandable 7.6 m (25-foot) survey rod adjusted to fit between the rebar pins at either end. Soil samples were taken to determine bulk densities at each sampling time to be sure that any settling was taken into account for each measurement.

The fine detail of the drainage boundary was surveyed using a Criterion 400 Survey Laser (Griswold, 1993) (figure 7). Traverse (PC) software was used to map station locations by distance, angle and slope from base locations. The survey laser rapidly located key points to set reference locations as trees, boundary markers and was used in triangulating the angles, distances and slopes along the boundary and also across a narrow, pinnacle-like portion of the gully that could not be walked. In March 2004, a total station survey instrument was used to survey the area.

3. Results and Analysis

In August 1994, about 15 cm (6 inches) of rain from Hurricane Jerry delivered over 4.5 tonnes (5 tons) of sediment. The amount sediment captured from one storm event within such a small drainage area was a surprise (Figure 8). The filter fence was partially filled with sediment and the steel fence posts were partially bending from the weight of the sediment and water. Some of the sediment was lost from that storm due to overflow, but we were able to save the structure by adding more steel posts, bending back those that bent over and using lumber braces to help support the weight. Therefore, the amount measured and reported is conservative because of the lost sediment. Two other filter dams were located below the first filter dam. This was done to help insure no added losses would occur. Over the next 4.5 years, a total of 40 tonnes (44 tons) of sediment

accumulated behind the sediment fences indicating an average sediment delivery rate of 89 tonne/ha/year (39 tons/acre/year) (figure 9). Very little of the sediment reached the third filter fabric fence, suggesting that the fabric was effective in removing most of the fine sediments. The delivery of sediment was relatively dormant during 1997 to 2002 when rainfall was below normal and extended drought conditions for many areas of South Carolina were present during much of this time. During the spring and summer of 2003, much higher than normal rainfall had reactivated the delivery of sediment within the gully. Remeasurement in March 2004 indicated another 8 tonnes (9 tons) of sediment had deposited since the 1999 measurement. So after 9.5 years, total sediment accumulated was 48 tonnes (53 tons), resulting in an average annual sediment delivery rate of 51 tonnes/hectare (22 tons per acre). This amount is probably conservative due the amount lost at the beginning overflow, and the extended drought with below normal rainfall.

From the 0.1 hectare (quarter-acre) gully drainage, the equivalent of 45 tonnes/ha (20 tons/acre) of sediment was delivered in the August 1994 event. The second measurement at the site was made in February 1999. Organic layers in the sediment deposits suggested that two other major events were responsible for the majority of the sediment delivered between 8/94 and 2/99. The total sediment captured over the 4.5 years from the small gully was about 40 tonnes (44 tons), which is equivalent to a total of 400 tonne/ha (180 tons/acre). Remeasuring in March 2004 produced another 8 tonnes (9 tons) captured in the sediment fences, for a total amount of 48 tonnes (53 tons), which is equivalent to 480 tonne/ha (210 tons/acre) in 9.5 years from 1994 to 2004.

The five-year drought from 1997-2002 produced an extended period of below average streamflow for South Carolina. Erosion within the gully was less active, but still active enough to keep most of the gully barren. Some soil erosion probably accumulated in the channel, but very little was delivered as sediment to the filter fences during this time. Besides rainstorms, freezing rain and freeze-thaw events also dislodged soil particles so they could be moved by gravity or water to the channel for storage. February to September 2003 brought in above normal rainfall with storms producing one of the wettest spring and summer seasons on record. Added fresh sediments at the gully were observed on several occasions, but were not remeasured until March 2004.

During the March 2004 sampling of the sediments to determine bulk densities of the materials, specific layers of the materials varied from 1.38 to 2.3 g/cc. When comparing the densities with the location within the accumulated sediment, it became apparent that the sediment from the August 1994 event (derived from Hurricane Jerry) continued to be substantially lower in bulk density. The August 1994 event initially had bulk densities averaging about 1.08 g/cc and over time, these materials settled to densities varying between the 1.38 to 1.9 g/cc. More recent sediments deposited from August 1994 to February 1999 had bulk densities ranging from 1.5 to 2.0. The sediments sampled since 1999 have accumulated primarily at the upper end of the first fabric dam and the lower portion of the second dam with bulk densities ranging from 2.0 to 2.3.

Besides the sediments accumulated in the filter fabric fence, on-site erosion processes were evident on much of the exposed gully area. The soil erosion aspects of gully activity were most easily seen following intense rainfall events and freeze-thaw cycles. Freeze events expanded ice crystals within the montmorillonite clays, heaving soil and small plants above the soil surface. Many of the fine surface roots were undermined with erosion and then left exposed on the bare surface (figure 10). Only severe rainfall events would transport the detained or accumulated sediments

downstream. During inactive periods, the seasonal leaf-fall and wind-blown leaves would hide much of the sediment accumulation within the channels, giving an appearance of low activity, with no sediment being delivered (figure 11).

Observations of stain lines at the base of trees in the channel were noticed on several occasions and appear to be a more reliable indicator of activity (figure 12). The stain lines were caused from sediment laden rainfall splash on fresh deposits of red clay materials. The sediment track and stained trees were followed to a perennial stream, several hundred feet away. Stain depth was sometimes higher and brighter on the portion of the tree facing the channel flow. Soil cores into recent alluvial deposits revealed brighter soil colors which will eventually darken with weathering and organic incorporation. In the sediment path on an alluvial terrace, the trunks of mature trees showed no enlargement at their base, another indicator that the sediment buried their trunks. In addition, a nearby perennial tributary also exhibited signs of red clay along the channel margins, which could be traced back to the area.

Within the gully area, surface soil erosion evidence included soil pedestals (i.e., leaving soil pinnacles under pebbles), exposed surface root systems, barren surface, rill erosion, headcuts (nickpoints), cavitation and soil deposits in channels and within surface depressions. Indicators that helped to interpret the gully activity levels included exposed, entrenched channels, increase in bright soil materials with sediment accumulations in the main channel and deposits of fine bright sediments on channel margins downstream, windfall trees, and tree root exposure (Figure 13).

4. Discussion and Conclusions

Public or resource issues can question gully activity and their priority for treatment. Professionals dedicated to erosion and sediment control seldom have all the answers or can back up their observations or judgment with appropriate data. Although this study was intended to only characterize sedimentation associated with a specific gully, it adds knowledge of how ephemeral gullies function. Gullies have many characteristics that make them difficult to read. This study focused on an actively eroding gully that appeared to be not delivering sediments. Following the gully activity for nearly 10 years demonstrated that ephemeral gullies may have their own timing and activity level, and effects are not always obvious. The information on the low density sediments delivered in the August 1994 storm, with increasing densities of materials with time suggests that there are perhaps different erosion and sorting processes going on in extreme events as compared to more normal events that occur every year or two such as bankfull. Although not specifically determined, it seems that the coarser materials are accumulating in the channel as evidenced by the increases in sediments in the channel affected by the upper reaches of the filter fabric fence. The accumulation of the coarse materials may be filtering the finer and or less dense particles before they are delivered as sediment. The gradient change in the channel caused by the filling of the initial filter fabric dam may be enough to get larger particles to settle in the upper reaches before they can be delivered downstream. In addition, the sediments contained within the dam may be retaining, absorbing and/or filtering some of the finer materials and sediments in the surface flows before they can reach the second fabric dam. Although interesting, the study was not set up to determine or verify the specific processes that may be associated with the apparent differences in sediment densities with storm intensities and time.

This study of a gully has provided an example that can be used to help describe and communicate some of the indicators, processes and timing of ephemeral gullies to

managers and interested public. This information and the accumulated sediments in the filter fabric fences are powerful tools that nearly all audience levels can relate to.

There are some major differences between silt fences and filter fabric fences. Under normal circumstances and construction methods, silt fences and concentrated surface waters such as found in channel systems are incompatible. Typical silt fences are often misused on construction sites, with frequent failure due to poor location, installation or materials. However, with proper technique, they can capture and retain sediments if not overwhelmed.

The difference with the effectiveness of a filter fabric fence is in the construction materials and in the installation across the slope contour, making sure the edges are stable and the channel is the low point for overflow. The filter fabric is a heavy-duty, woven cloth that will last for over a decade. The wire fence helps to support the fabric, making sure that the amount of stress is spread out when filled with water and/or sediment. The frequent steel posts and supporting lumber braces add stability so the fence can capture and filter sediment laden water without folding. Installing the top of the fence on the contour requires either a good eye or help from a construction level, a brick layers string level or other type of leveling device. The relatively new construction levels with laser pointers or lines would also helpful during installation to avoid low ends or non-horizontal installation. This was not the first time the filter fabric fences were installed in small ephemeral channels. They have proven to be an effective tool to install following nearly severe wildfire and dozer fireline construction activities in steep terrain to determine effects. Typically with attention to proper drainage dips and erosion control methods, the only sediment captured is indicated with a low turbid watermark left on the fabric. With careful installation, modifications, maintenance and attention to detail, filter fabric dams appear to be an effective tool to capture, filter and retain sediments, even in relatively small, ephemeral gully channels. And when they are installed and do not capture sediment, that is also important to know.

If installing these in a channel, locating them in areas with low gradient that offer reduced stream velocity and more channel storage would be important. Designing for overflow at the channel and overflow plunge with splash protection to the channel below should be factored in. Allowing overflow plunge in unconsolidated materials without splash protection could cause excessive channel erosion, plunge pool development and possibly structure failure. To be effective, a sediment retention dam must be constructed to withstand a variety of forces and pressures. Under the circumstances of this study, the longevity of the filter fabric dams is at least a decade. Some signs of green algae growth in the fabric have not produced any obvious areas of weakness or failure.

In less actively eroding terrain with quality vegetative cover and less rainfall intensity and duration, the filter fabric fences designed for sediment retention may work on substantially larger drainage areas. Other considerations such as the severely eroded character of the soil, minimal soil cover and rooting structure with moderate to steep slopes within the gully make help determine the drainage size where the structure could be used. Within this study, the Universal Soil Loss Equation average annual rainfall index was relatively high at 275 (units in 100 foot tons/acre)(inches/hour) (Wischmeier and Smith, 1978).

As described, the filter fabric fence can be effective in storing sediment. For individuals with limited time, they can be measured on any schedule to produce various levels of detail. No matter the conditions, the sediment dam can provide a visual indicator of the accumulated sediment captured. Though great as a monitoring tool,

fabric dams should not be considered permanent structures. Sooner or later, failure would probably occur. Unless stabilized, the deposits should be removed to a stable location and vegetated.

The study does highlight that even a small 0.1 hectare acre gully can produce enough internal erosion and periodic runoff to transport a significant sediment load downstream in response to infrequent events. Unless gullies are visited after severe events, their activity can be hidden by leaves. In assessing the activity level, what can be immediately seen is not always enough. Ephemeral gullies may exhibit many dormant characteristics, but still be active enough to affect water quality and aquatic habitats. Careful field review includes looking at a variety of onsite and downstream features for signs of erosion, sediment accumulation, color changes, buried leaves or needles, sediment marks, and other indicators.

For those in no hurry, assessment of gully activity and downstream areas after major disturbance events would be ideal, but the frequency of these events can make them poor indicators to rely upon unless you just had one. And if you put in a filter fabric fence and it fails in an ephemeral channel, there is good reason to believe that periodically, the channel has ample flow and forces to move the sediments.

Acknowledgements

Thanks to Alvin R. Feltman, James N. Shannon, Jr., Jay Swafford, Luis Mundo, Charles H. Drew, Wade Hopkins, James Hodges, Todd Bennett, and Peter Green of the Sumter National Forest for assistance during the study. The USDA Forest Service provided the funding for this study.

References

Dissmeyer, G.E. 1982. How to Use Fabric Dams to Compare Erosion from Forestry Practices. USDA Forest Service, SE Area, Forestry Rep. SA-FR 13, Atlanta, GA. 10 pp.

Griswold, G.W. 1993. Field Application and Review of Hand-Held Laser Survey Instrument. Unpublished report, USDA Forest Service, Region 2, Grand Mesa, Uncompahgre and Gunnison National Forests, Gunnison Engineering Zone, pages 7-15.

Hansen, W.F., 1991. Land Rehabilitation on the Sumter National Forest, In Proceedings of the Fifth Federal Interagency Sedimentation Conference, Drs. S. Fan and Y. Kuo (Editors), Las Vegas, Nevada. Volume 1, pp. 3-110 to 3-117.

Hansen, W.F., 1995. Gully Treatments. In Proceedings of Watershed Assessment and Restoration Workshop, National Advanced Resource Technology Center, USDA Forest Service, Marana, Arizona. 17pp.

Hansen, W.F. and D.L. Law, 1996. Watershed Restoration After Calamity. In Proceedings on Watershed Restoration Management. J.J. McDonnell, J.B. Stribling, L.R.Neville and D.J.Leopold (Editors). AWRA Symposium, Syracuse, New York pp. 187-198.

Heede, B.H.,1976. Gully Development and Control - The Status of Our Knowledge. USDA Forest Service Research Paper RM-169. Rocky Mountain Forest and Range Experiment Station, Fort Collins, Colorado. 42 pp.

Heede, B.H., 1982. Gully Control: Determining Treatment Priorities for Gullies in a Network. Environmental Management, Volume 6, Number 5. Published by Springer-Vertag New York Inc. pp. 441-451.

Hoover, M.D., 1949. Hydrological Characteristics of South Carolina Piedmont Forest Soils. Proceedings of the Soil Science Society. pp 353-358.

Schumm, S.A., M.D. Harvey and C.C. Watson, 1984. Incised Channels, Morphology, Dynamics and Control, Water Resource Publications, Littleton, Colorado, U.S. Library of Congress number 83-050243, 200 pp.

Singer, M.J., J. Blankard, E. Gillogley and K. Arulanandan, 1978. Engineering and Pedological Properties of Soils as They Affect Soil Erodibility. California Water Resource Center, Techical Report No. 166, ISSN 0575-4941. 32 pp.

Yoho, N.S, 1980. Forest Management and Sediment Production in the South - A Review. Southern Journal of Applied Forestry, Volume 4, Number 1. pp. 27-35.

List of Figures

Figure 1. Gully vicinity taken from 1968 LEEDS, S.C. Quadrangle - USGS Topographic Contour Map, Lat 34° 44' N, Long 81° 25' W. For approximate map scale, the distance from the gully southeast to the sharp bend in the road by the marked elevation 582 feet (177 m) is about 0.57 km (0.36 miles). Contour interval on map is 10 feet (3 m).

Figure 2. Aerial photo was taken in April 1974. Gully measured is the long narrow gully in the upper left portion of the photo. Note the 6-meter width of the gravel road at the bottom of the picture.

Figure 3. Aerial photo was taken in February 1990, just prior to tract being purchased as public land. No major changes in gully size were noted in comparison to 1974 photo.

Figure 4. General view of gullied area within tract. Sharp pinnacle-like boundaries separated the individual gully channels.

Figure 5. Lichens on the soil surface were an indicator of poor site and low nutrient conditions.

Figure 6. The fabric dam was installed in July 1994 below the 0.1 hectare ephemeral gully. The filter fabric was supported with steel posts, wire fencing and C clamps.

Figure 7. Criterion 400 survey laser provided quality measurements. Laser has filter that can detect prism through vegetative cover, or can shoot directly to any solid surface, measuring distance, azimuth, slope and elevation change.

Figure 8. About 5 tons of sediment were deposited from the Hurricane Jerry storm in August 1994. Sediment surface elevations and bulk density measurements were taken to estimate sediment amount.

Figure 9. Additional dams were added to capture sediment. In 1999 after 4.5 years, a total of 40 tonnes of sediment were captured for an average sediment yield of 89 tonne/ha/year (36 tons/acre/year). Most of the sediment was delivered during three major storm events.

Figure 10. Soil erosion was evident on low to moderate sloping areas with exposure of fine roots and pedestaling of soils are indicators of the raindrop energy and poor infiltration on these barren soils.

Figure 11. Following autumn leaf fall, indicators of gully activity with respect to sediment delivery disregarding the filter fabric fence are masked to the casual observer.

Figure 12. Sediment marks within the flow path are especially evident from the reddish clay soils onto the base of trees.

Figure 13. Surface erosion along the upper edges of the gully was enough to remove almost all the soil supporting this pine tree during its lifetime.

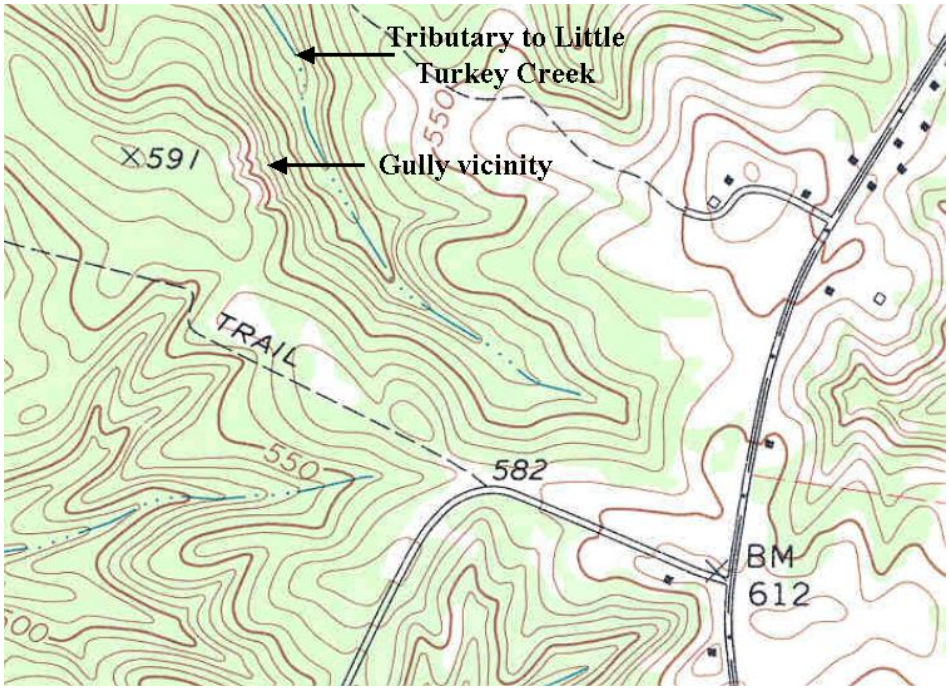

Figure 1. Gully vicinity taken from 1968 LEEDS, S.C. Quadrangle - USGS Topographic Contour Map, Lat 34° 44' N, Long 81° 25' W. For approximate map scale, the distance from the gully southeast to the sharp bend in the road by the marked elevation 582 feet (177 m) is about 0.57 km (0.36 miles). Contour interval on map is 10 feet (3 m).

Figure 2. Aerial photo was taken in April 1974. Gully measured is the long narrow gully in the upper left portion of the photo. Note the 6-meter width of the gravel road at the bottom of the picture.

Figure 3. Aerial photo was taken in February 1990, just prior to tract being purchased as public land. No major changes in gully size were noted in comparison to 1974 photo.

Figure 4. General view of gullied area within tract. Sharp pinnacle-like boundaries separated the individual gully channels.

Figure 5. Lichens on the soil surface were an indicator of poor site and low nutrient conditions.

Figure 6. The fabric dam was installed in July 1994 below the 0.1 hectare ephemeral gully. The filter fabric was supported with steel posts, wire fencing and C clamps.

Figure 7. Criterion 400 survey laser provided quality measurements. Laser has filter that can detect prism through vegetative cover, or can shoot directly to any solid surface, measuring distance, azimuth, slope and elevation change.

Figure 8. About 5 tons of sediment were deposited from the Hurricane Jerry storm in August 1994. Sediment surface elevations and bulk density measurements were taken to estimate sediment amount.

Figure 9. Additional dams were added to capture sediment. In 1999 after 4.5 years, a total of 40 tonnes of sediment were captured for an average sediment yield of 89 tonne/ha/year (36 tons/acre/year). Most of the sediment was delivered during three major storm events.

Figure 10. Soil erosion was evident on low to moderate sloping areas with exposure of fine roots and pedestaling of soils are indicators of the raindrop energy and poor infiltration on these barren soils.

Figure 11. Following autumn leaf fall, indicators of gully activity with respect to sediment delivery disregarding the filter fabric fence are masked to the casual observer.

Figure 12. Sediment marks within the flow path are especially evident from the reddish clay soils onto the base of trees.

Figure 13. Surface erosion along the upper edges of the gully was enough to remove almost all the soil supporting this pine tree during its lifetime.

Native Plants and Fertilization Help to Improve Sites and Stabilize Gullies on the Sumter National Forest

Dennis L. Law* (E-Mail: dllaw@fs.fed.us)
William F. Hansen (E-Mail: wfhansen@fs.fed.us)
USDA Forest Service
4931 Broad River Road
Columbia, SC 29212
FAX 803-561-4004

Abstract

The Sumter National Forest (SNF) lands were acquired in the early 1930s under the Weeks Law of 1911 to provide sustained timber and water resources. Most areas were depleted of nutrients and surface soils from long-term erosion due to farming practices. Soil productivity was drastically lower across most of the landscape, and approximately twenty thousand hectares (fifty thousand acres) of actively eroding gullies and galled barrens dissected the area.

Reforestation and active stabilization measures have been used to help restore the landscape. However, some gullies and galled barren areas continue to produce sediment at excessive rates. Trees and other vegetation present on severely eroded lands are often sparse and in poor health. Surface erosion and productivity problems have been reduced or eliminated on most of the treated areas with measures to improve soil cover, infiltration and nutrients. A variety of techniques have been used to treat gullies. This paper will mention other treatments used, but will focus on activities involved with using native plants and fertilization. Soil ripping, disking, fertilizing, seeding and mulching are used to assist in site recovery to native plant species. In the past, seed was selected primarily on its ease of growth and ability to control erosion. Some of the species selected were persistent and had some invasive characteristics that are not desired.

Recent emphasis has been placed on the development of native seed sources, testing, planting and harvesting native plants. A multi-agency agreement with the SC Native Plant Society, USDA Natural Resources Conservation Service, Clemson University, SC Department of Natural Resources, Tall Timbers Research Station and Abbeville Soil and Water Conservation District was developed in 1998 to assist in providing cost and technical sharing of native plant information. The desired result was to convert the barren and eroded land to a permanent soil cover to control erosion and be resistant to disturbance such as drought, poor nutrients and fire. Converting dense pine forests to low density pine stands with native grass understories should improve root density and rates of organic buildup in the soil surface. Added benefits to soil infiltration and other properties are also expected.

The presentation will highlight pictures of soil recovery efforts using physical, chemical and biological means. Efforts have included increased cooperation among agencies with over 1,000 person days of volunteer time for cooperative native plant work. The information will show how native plants are collected within the ecotypes and grown in both nursery and field conditions for use on gullies and other disturbed or barren areas.

*Corresponding author

Examples of the activities involved with preparing the sites for treatment and results will be provided.

Keywords: gully, fertilization, native plants, cooperative agreements

1. Introduction

This paper briefly presents the history, methods and present status of the soil and water restoration effort including gully treatments on the Sumter National Forest (SNF) in the piedmont of South Carolina (Hansen, 1991; Hansen and Law, 1996). The program is probably the largest ongoing program in the USDA Forest Service of over 150 National Forests. Public and agency concern about relying more on native species has expanded to help support this work. Some recent treatments have included the use of native plants for erosion control and site recovery work due in part to their ability to withstand poor site and natural disturbances. Information transfer continues to be a critical consideration in resource decisions to prevent and mitigate erosion and sedimentation problems.

The national concern for land stewardship and conservation in the Weeks Law of 1911 resulted in the acquisition of lands to sustain timber and water resources. These federal holdings eventually led to their designation as the SNF by Congress in the 1930s. Portions were worn out and abused lands of the cotton farming days with a barren wasteland character. The repeated tillage of soil, burning of surface vegetation and failing to use or maintain adequate surface water control structures contributed to the extent and severity of the erosion problems. On average, over 0.3 m (1 foot) of soil was lost from the soil surface for much of the piedmont. Extensive gullies and galls became a testimony to the long-term effects of untreated erosion. Gullies are entrenched, ephemeral channels extending into areas with previously undefined or weakly defined channel conditions (Hansen, 1995). Active gullies are recognized by headcuts (primary nickpoints) where there is an abrupt elevation drop and channel enlargement (Schumm et. al., 1984. Cycles of storm runoff and saturated soils contribute to the headcut cavitation and plunge enlargement with eventual slope failure. Winter frost heaving and slope raveling also cause soil loss and sediment delivery from exposed soil surfaces. Decline in soil productivity is common from the long-term effects of gully erosion. Reported annual erosion rates in Mississippi for gullies are up to 1,800 tonnes/ha (800 tons/acre) (Yoho, 1980). Actual rates of continuing erosion vary with the circumstances. Downstream of headwater gully networks, secondary nickpoints may indicate a response to downstream gradient change or differences or they may be due to localized response to areas of sediment accumulation that have exceeded the threshold stability factor and are initiating nickpoint migration upstream into the deposited materials (Schumm et al, 1984).

The Civilian Conservation Corps (CCC) assisted in the SNF recovery of some gullies and other barren areas with the large scale planting of trees on about 16,000 hectares (40,000 acres) in the 1930s. Gully stabilization and rehabilitation efforts had both successes and failures. Funding and programs were sporadic and little consistency was provided in checking and maintaining past accomplishments which contributed to some failures. Poor planting stock, little attention to fertilization needs and lack of overflow protection for structural work were just a few of the problems that contributed to delayed recovery of many areas. Some improvements took decades to develop stable conditions.

Repeated soil disturbing activities, lack of attention to conservation practices and the resultant severe erosion led to gully formation. The surface soil properties including infiltration were gradually lost (Hoover, 1957). On average, the soil A horizon was removed including a portion of the B horizon. The B horizon was more resistant to erosion due to its greater percentage of clay and other minerals that bind soil particles. However, properties in the C horizon are characterized as having a severe to extreme erosion hazard. Subsoils contained saprolite, a highly weathered parent material derived from a variety of materials including mica-schist, granitics, slate and gneiss. When erosion exposed the saprolite to surface flow, gully enlargement and expansion occurred.

The results of the erosion and drainage flow patterns have left the SNF soils across the piedmont in various stages of erosion. The severity of the erosion is included in SNF soil classification and mapping criteria. Four stages of erosion identify and map each soil series, ranging from non-eroded to severely eroded. The soil data were digitized into a Geographic Information System (GIS) with associated interpretations based on soil productivity and any management limitations.

Concern for the recovery of the soil conditions has led activities away from relying just on dense pine dominated forest stands. A more natural revegetation approach would use both pine and hardwood trees at low to moderate densities with native grass understories to be maintained when needed with disturbance from prescribed fire. The abundant grass cover adds substantially to root and organic development, especially near the soil surface. The dense layer of pine needles that accumulate on pine dominated lands are an effective erosion deterrent, but the dense pine stands and needles also limit understory development and surface soil building rates. Native grass species are believed to be more effective at improving organic content and rebuilding the soil. Much of the native grass presence has been lost across much of the eroded piedmont landscape. A substantial project was started in 1998, with multi-agency involvement to collect, test, plant, grow and harvest native plant species for inclusion in erosion control mixtures.

2. Area Descriptions, Methods and Material Studied

Farming practices of nearly a century ago produced severe erosion of varying intensities to the piedmont of South Carolina. Eroding areas were naturally or intentionally converted primarily to loblolly pine *(Pinus taeda).* The heavily eroded soils are nutrient poor in nitrogen, phosphorus and sometimes other elements. Loss of organics reduced the retention and storage of water, causing droughty conditions. Some of the early planting stock was either poor or responded to the low site with fusiform disease, chloritic needles, rank branching, rough bark and other indicators. Many of the poor stands have eventually outgrown their unhealthy state, but even many decades later, litter layers are dominated by pine needles resting on the B or C soil horizons, with limited duff or humus accumulation.

Rainfall averages about 114 cm (45 inches) per year and is typically well dispersed through the year with average monthly rainfall between 7 and 13 cm (3 and 5) inches. Water yield averages about 43 cm (17 inches) per year on the gauged larger streams. The piedmont is underlain by several complex sequences of crystalline, mixed acid, micaceous rocks and Carolina slates. Soils surfaces are generally thin with sandy clay loam surfaces. Carolina slate surfaces consist of silt loams and subsurfaces consist of silty clay loams. Area vegetation is primarily loblolly pine, with some shortleaf pine *(Pinus echinata).* Secondary vegetation includes red oak *(Quercus falcate),* white oak (*Quercus alba*), hickory *(Carya spp.),* sweetgum (*Liquidambar styraciflua*), yellow polar

(*Liriodendron tulipifera*), water oak (*Quercus nigra*), willow oak (*Quercus phellos*), river birch (*Betula nigra*), sycamore *(Platanus accidentalis),* cottonwood *(Populus deltoides),* elm *(Ulmus spp.),* green ash (*Fraxinus pennsylvanica*), and red maple (*Acer rubrum*).

A variety of methods have been used over the years to stabilize, rehabilitate or restore forest ecosystems from the effects of gully, gall and road erosion (Norcross, 1936; Heede, 1982). Specific terms help to describe the intensity of the improvements. The term stabilization refers to minimum practices that halt erosion, limit gully expansion and sedimentation. Rehabilitation indicates reduction to many of the erosion and water quality impacts, but also try to enhance other resources. Restoration goes farther than either stabilization or rehabilitation in accelerating the recovery of the functions and conditions as well as improving affected resources. Restoration typically involves land reshaping and recontouring to a stable landform with complete treatment to establish vegetation. With so much soil surface lost from past erosion, restoration to a historic condition is not viable. Soil recovery rates are slow. Many of the affected slopes, streams and landforms have been altered. Along with the long term results from extensive farming and severe erosion on the presence of many of the native grass species, limited use of prescribed fire may have also reduced their abundance.

Reforestation

The Civilian Conservation Corps (CCC) planted pine by hand on about 50,000 acres of worn out farmlands of the SNF resulting in improved ground cover and watershed conditions. Since the little leaf disease was linked with the native short leaf pine (*Pinus echinata*) on nutrient poor, eroded sites, there was little desire to return to that species at that time. In the future, desired conditions of the forest include returning suitable areas to short leaf pine. Poor site conditions and tree growth also attract other types of undesired insects and disease that can be a concern. At one time autumn olive and a few other non-native tree species were used to help improve wildlife habitat, but more effort is being made to avoid non-native persistent species and there is a general ban on those that tend to move off site and invade other areaas.

Gully Plugs

Gully plugs consist of a soil dam constructed at some point along the ephemeral gully. A dozer is used to push and compact fill material into the barren gully channel. To provide for adequate overflow, spillway or drop inlet structure should be installed.

Debris Dams

Debris dams were used on some of the CCC and other early efforts to help stabilize gullied areas. Structures included small cedar trees that were hand piled between posts in the gully or accumulations left within the channel. Sometimes, chicken wire was stapled to the posts to help support the debris.

Rock Check Dams

Rock check dams can also help stabilize eroding channels or waterways and provide permanent channel protection, water dispersal and allow for high water overflow. Rock was usually placed with a wheel tractor with a gravel “Super Scoup” connected to the rear power takeoff. Care is taken to keep the overflow within the channel, armor spill apron and insure structure dimensions will not permit channel diversion. Low rise gradient control structures used a filter fabric lined backhoe trench across the active channel to the terrace or hillslope that would contain floodflows, and the trench was filled to the surface with surgestone or other suitable rock.

Gravel Treatments

Gravel (surgestone - ungraded aggregate about 4 inch minus) has been placed in numerous active gully heads or at secondary channel nickpoints to provide armoring of the surface while maintaining the present surface water movement pattern. The porous gravel allows flow and adds channel roughness. For best results, filter fabric is often used under the aggregate material to reduce the direct contact of soil with flowing water. Gravel is occasionally used to stabilize or maintain waterways, terraces or diversion ditches where excessive erosion occurs prior to vegetative cover. In most instances, gravel is placed by dump truck, wheel tractor with scoup or heavy equipment with bucket.

Water Diversion

Analysis of flow sources is a critical element in assessing and stabilizing gully problems. Roads, old agricultural terraces and other surface changes may capture and concentrate flow into gully systems. Diverting excessive sources of water from active gullies is typically done with a dozer. The diversion extends to an area where the water can be released into the forest without causing damage.

Land Reshaping

Land reshaping was a common method used to restore gully erosion on the Sumter National Forest, that is still used when needed to treat complex active gully problems. Some public concern has been expressed over the intensity of these ground disturbing treatments. Practices associated with land reshaping may include building diversion ditches, waterways, terraces, contour trenches, ripping the soil (depth 0.5-0.6 m or 18-24 inches), disking, liming, fertilizing, mulching, seeding, and planting trees. Primary costs are for a dozer and/or pan earthmover to reshape and smooth the area to a stable landform. In most instances, some adjacent stable forested areas are also affected in these treatments. Waterways and terraces are designed to handle concentrated flows that can occur within the gully during the early recovery period without resulting in excessive erosion. A balanced fertilizer of 0.8 tonnes/ha (0.35 tons/acre) of 17-17-17 and 3.4 tonnes/ha (1.5 tons/acre) of lime is initially spread on the gully or other treatments involving major ground disturbance or nutrient deficiencies. A wheel tractor is often used in spreading the lime, fertilizer and seed. A mulch blower is used to apply about 4-7 tonnes/ha (2-3 tons/acre) of straw when needed to help maintain moisture and keep seed in place.

Fertilization

Fertilization has proven to be an excellent tool to help eroded and depleted lands of the piedmont recover from the past (McKee and Law, 1985; McKee, et. al., 1995). Sites are sampled with soil and leaf/needle tests for nutrient deficiencies. On-site indicators of nutrient deficiencies besides the lack of organic accumulation include the presence of lichens and cedar in the understory, chlorotic pine needles and/or little leaf disease in the forest stands. Pine trees under nutrient stress also have a greater presence of fusiform and other diseases that affect their form and growth. Fertilization with slow release formulation can help to achieve maximum absorption of the chemicals in the vegetation during rainfall and growth cycles. Fertilization is accomplished during the early spring period when rapid growth on plants is most beneficial. Failure to apply fertilizer during a suitable period can lead to volatilization during hot weather, excessive runoff during intense rainfall periods or leaching during the wet winter dormant season. Loss in investment can occur if there is not good connection between soil nutrient deficiency, application, weather and active plant growth. Slow release fertilizer helps to reduce some of these potential losses as the nutrient releases over a longer period of time

so that plants can assimilate the nutrients over time. Multiple treatments with fertilizer are often needed on many of these severely eroded gullies and other poor sites. Problem sites should be checked at about a 5-year frequency to determine if added treatments are needed. On established stands over 5 years and older, 0.4 tonnes/ha (0.2 tons/acre) of 35-17-0 slow release fertilizer is applied by helicopter with a cost of approximately $250 per hectare ($100 per acre) for large areas.

Revegetation

Some vegetative treatments are best to avoid. Kudzu (*Pueraria lobata*) was an introduced plant for possible forage and other uses in the United States. Some of the early users of kudzu liked its invasive character and that it provided rapid gully cover from rainfall impact. Unfortunately surface erosion may continue underneath the dense network of leaves and vines. Without cattle grazing to keep this species in check, it can aggressively overcome adjacent areas including forests, farm buildings and stationary equipment. Kudzu is invasive, persistent, and difficult to control.

Revegetation with grasses has been a regular part of treating gullies and barren lands. Until recently, the less expensive and effective non-native species were commonly used. Unfortunately some of these species have an invasive and/or persistent character which can prevent native species from establishing. For many years, *Sericea lespedeza* was one of the best legumes for erosion control and nutrient infusion through nitrogen fixation. Unfortunately, deserved or not, it has obtained a reputation for being not only persistent, but invasive. Many pine forests produced substantial increases in tree growth, producing 10-15 year commercial pole timber stands on former gully sites with heavy *S. lespedeza* understories. About a decade ago, some areas were treated with *Kobe lespedeza* because it is a better source of food for wildlife. *Kobe lespedeza* is still used as it is also less invasive and persistent. Other past commonly used grasses for erosion control include fescue, bahia, rye, orchard and burmuda grasses. Some of these are either invasive or very persistent, and not currently used for grass covers. Clover (red and crimson), brown top millet, oats, wheat, and many other annual plant species have been used to provide quick cover for more difficult perennial species and are desired in the seed mixture for wildlife purposes. Fescue can dominate sites and prevent establishment of loblolly pine trees.

Because some of the grasses used in the past have been non-native species and considered somewhat invasive or persistent, ongoing efforts since 1998 on the SNF include the development of native plant species for erosion control purposes. Because of the complexity of native plant issues, a partnership with USDA Natural Resources Conservation Service, South Carolina Native Plant Society, South Carolina Department of Natural Resources, Clemson University and others have helped provide needed resources for seed collection, testing and planting fields for future harvests. Primary native species being grown for piedmont uses include little blue stem (*Andropogon scoparius*), big blue stem *(Andropagon gerardi*), splitbeard bluestem (*Andropogon ternaries*), bushy beard blue stem (*Andropogon glomeratus*), broom-sedge *(Andropogon virginicus),* purpletop (*Tridens flavus*), Indiangrass (*Sorghastrum spp.*), switchgrass (*Panicum virgatum)* and partridge pea (*Chamaerista fasciculate*). These and other native species have been collected from sources within the piedmont ecotype primarily in SC and grown in plugs under nursery conditions for outplanting, broadcast sown as seed or seed containing mulch, or planted seed with specialized seeding equipment

Nursery supplies for grass and tree propagation included various size trays containing multiple plugs up to 1 gallon pots (Figure 6). Potting materials included

portions of soil types collected from within the treatment areas, *Baccto* brand potting soil mix, perlite, vermiculite, peat moss, and time release fertilizer. Rooting hormone was used for tree cuttings. A variety of vary basic to complex watering systems were used. Seeds collected were stored and stratified in coolers.

Over the last 5 years, about 180,000 plugs of native grass plants were planted at about 0.6 m (2 foot) spacing in cultivated rows, with another 40,000 plugs nearly ready for use in 2004. Herbicides was sometimes needed to reduce competition in cultivated native plant fields. Some of this planting was accomplished within the severe drought periods during 1999-2002 with high summer temperatures. Temporary watering was done once or twice from fire trucks during a few very hot days chosen to plant to insure the presence of some soil moisture so the plants could stabilize to field conditions. Under normal temperature and soil moisture conditions, this would not have been done. Other road and open field disked areas were treated with broadcast seeding. After establishment, treatments with prescribed fire will regularly be used as needed to curtail other species and maintain the health and productivity of the native plant production fields. Other treated areas such as gullies with limited access are not used for production fields, and these may be burned on a 3-10 year frequency with adjacent forest areas.

3. Results and Analyses

Reforestation

Reforestation alone has probably one of the most cost effective tools at improving the character of severely eroding and gullied terrain. Loblolly pine (*Pinus taeda*) grew slowly on poor sites due to low nutrients, limited water and/or poor planting stock. Eventually the pine needles cast from trees helped to improve soil cover and water absorption, resulting in reduced surface erosion and runoff. The healing process was not immediate by just planting trees, but once established, they provide deep roots, improve soil conditions and utilize a substantial amount of water. Areas with better soils respond best to this limited treatment. Substantial growth and development occurred on relatively poor sites when fertilization was used. Eventual natural entry of other tree species such as sweetgum (*Liquidambar styraciflua*), red maple (*Acer rubrum*), persimmon (*Diospyros virginiana*), and oak (*Quercus spp.*) occur within planted pine stands. In addition, some success was obtained in increasing diversity and habitat from planting sawtooth oak (*Quercus sp*. – non-native), water oak (*Quercus nigra*), Southern red oak (*Quercus falcata*) and chestnut oak (*Quercus prinus*).

Gully plugs

Early failure of this method was often associated with debris left in the fill materials, improper or uncompacted fill material, or failure to provide for excess flow with an adequate overflow, spillway or drop inlet structure. Gully plugs were most successful when applied to small gullied catchments of only a few acres. When used on larger drainages, success depends on providing for excess flow. Fill materials should be free of debris, compacted sufficiently, and contain an adequate clay component. This was not always done with early work in the CCC era, and contributed to failure. There were instances of CCC persistence of rebuilding gully plugs until they held. Probably the reforestation of the gullied contributed to the eventual success.

Gully plugs properly designed and installed are effective at capturing sediment and providing base level control, but the cost of the drop inlet structures and difficulty in getting suitable fill materials to the location are concerns. These structures need to be compacted and designed if their intent is to hold water for extended periods of time for

wildlife and other uses. Conservation efforts such as revegetation and rebuilding the soil organic layer and surface within the gully should eventually reduce surface runoff and sedimentation so the gully plug may have little or no use at that point.

Debris dams

Debris dam structures provided some short-term stability by adding channel roughness, slowing water movement and catching sediment. The debris dams decompose after a few years and lose their effectiveness. Damage to structures occurred if concentrated flow went around structures and/or eroded the downstream side due to overflow. Excessive erosion from flow diversion or plunge led to failure or contributed to either limited benefits in some instances to more damage than normally expected in others. Straw bales with rebar support have also been used with varied temporary results. When carefully installed level and dug partway into a channel, resistant trees such as cedar and straw bales may capture sediment and improve stability. Costs are usually reasonable where they can be used, but maintenance is often needed. They are probably more effective when used on hillslopes to accumulate some sediments and in small channels for primarily a gradient control or to add roughness, rather than as a tool to accumulate sediments into a dam-like structure that will eventually fail under most circumstances.

Rock Check dams

Rock check dams are useful structures for small channels. The costs, proper sizing of materials, installation specifics and frequency of structures are most critical considerations. Where materials are readily available and channel access is not a problem, costs can be reasonable. Low rise check dams and rock filled channel trenches lined with filter cloth have been effectively used to provide grade control and spread flow in ephemeral waterways constructed in highly erodible fill materials. Higher dams located in channel systems often create a hydrologically unstable structure that will eventually fail if not properly designed, installed and maintained. The goal should be more to install a low maintenance structure that will provide gradient control rather than a structure designed to catch and retain sediments. If catching sediments in check dams is a goal, they should be regularly cleaned out to maintain capacity and function.

Gravel treatments

Gravel treatments have been effective in stabilizing ephemeral gully and rill erosion. Gravel placement provides immediate benefits but costs can be a concern if the materials are not readily available or there is limited access. Heavy equipment as well as manual labor are necessary to move, place and shape the gravel on the areas needing treatment.

Water diversion

Water diversions are effective at reducing or removing flow from active gullies when there is a suitable location to absorb the water on an adjacent area. Forested filter areas in stable terrain are the best areas to absorb flow from water diversions. Treatment costs are generally low when access with equipment is available. However, in severely gullied or steep terrain, the ability to divert concentrated water to other locations may be limited.

Land reshaping

Smoothing the surface to a stable slope has been an effective way to restore function to complex and steep landforms associated with severe gully networks so that they can develop ground cover, return to forest, absorb water, and limit runoff. Initial costs and maintenance of reshaping are relatively high and may exceed $12,000 per

hectare ($5,000 per acre). Experience and an active maintenance program are critical components to maintain investment.

Fertilization

On severely affected gullied terrain, fertilization occasionally with slow release fertilizer has produce some benefits to any existing plants and allowed some pioneering plant cover to develop. Generally the first areas to show signs of recovery are within the lower colluvial margins of the eroding slopes and the channels. This can be a slow process, especially if there is limited cover present to utilize the nutrients. On treated areas, identifying and treating nutrient deficiencies with fertilizers is one of the critical elements to have success and improve the rate of recovery.

Revegetation

Revegetation with most native plant species has been achieved with generally good to excellent results, especially when areas were cultivated and planted with nursery grown plugs. Seed germination was mostly high about 80-95 percent for most species under the nursery conditions in plugs. Big blue stem was the only native grass species with low results, and was abandoned for the present as a species to formally grow for erosion control seed mixtures. Portions of gully treatment areas have been revegetated with little blue stem, partridge pea and other native species in the seed mixtures and have produced some good to exceptional results, even in response to drought conditions. Seed mixtures with native plants typically include some relatively fast growing non-native annual species to insure a rapid cover in case the native grasses have delayed germination. Planting native grass plugs in the early spring produced seed the same year and the sparse density fills in rapidly to cover the area over the next year or two. Problems with residual fescue, bahia or other grass species are treated with herbicides or cultivation during establishment to help control weedy species entry into native grass stands until they are fully established. Much of the success of this program has been derived from the multi-agency experience gained from technical staff and voluntary efforts provided.

Maintenance

Maintenance is a regular activity involving use of many similar types of equipment mentioned above to respond to conditions when treatments are not working. The need for maintenance often depends on conditions that occur following treatments. Ground disturbing and channel treatments need periodic checks until stabilization is assured. These checks can save major losses to structures when addressed properly.

Checks and maintenance are critical for the first several years until the treatment areas are revegetated and structural measures to control stormwater are functioning properly. Within 2-5 years time, revegetation generally improves soil conditions sufficiently that most stormwater will be absorbed and retained in the soil, rather than delivered as sheet and/or concentrated flow. Localized problem areas were identified occasionally on past treatments. The problem areas generally are a combination of exceptionally poor soil conditions (such as exposed saprolite), several years of drought and/or extreme storm events. In response to several years of drought in 2000, none of nearly 150 gully and galled barren treatment areas were at risk for loss in the investment. However there were interspersed areas of up to a quarter acre that needed some scarification, fertilizer, seed and mulch to improve cover and reduce surface erosion. Many of the 15-20 year old treatment areas needed some commercial thinning of pine stands to increase tree health and to release hardwoods and native grasses in the understory. One area had loblolly pine trees large enough (30-40 cm or 12 to 15 inches

diameter at breast height (DBH)) to commercially thin in only 11 years after the gully restoration treatment.

4. Discussion and Conclusions

Efforts to stabilize, rehabilitate and restore severe erosion from gully, road and other barren areas within the Sumter National Forest have been very successful. Several methods and approaches have been utilized with varying degrees of cost and rates of improvement. As discussed, a variety of treatment tools and equipment needs are important elements that need to be available for this work. At first glance, some of the ground disturbing work can appear severe, but it has been proven to be effective when needed at stabilizing and restoring functions to complex gullied terrain. On other occasions, other relatively minor changes in surface drainage can also produce desired change to gully erosion. Each circumstance must be evaluated separately. Monitoring and maintaining the treatments are critical until they are fully stabilized. Recent effects from a series of drought years, floods and other disturbances created some localized maintenance needs on the poorest site conditions within the past treatments.

With public awareness increasing, they are bringing in concerns and ideas that need to be considered in our evaluations of how to treat and manage these areas. Fresh ideas and interest have provided some needed adjustments and change that improves our purpose and the program. The work that has been accomplished in using native plants to help with erosion control has been laborious and costly at times. However, the benefits and information obtained are critical to the increased reliance on native plants for erosion control and watershed restoration needs. Watershed improvements continue to change with the times but are still needed to provide sustainable forest resources with soil building, water quality and healthy timber growth that are responsive to normal disturbances as fire, floods, insects and disease. Public interest, partnerships and cooperation among many agencies and resource areas has been instrumental in making this shift to operational use of native plants for erosion control.

Experiences have been positive from thinning and prescribed burning of former gully treatment to remove a portion of the understory of thick pine needles. As long as most of the soil cover is retained and water control structures are intact, the thinned forest stand will have improved understory diversity with other species including native grasses. This may also be a good time to refertilize in response to nutrient deficiencies that limit the development of the understory and residual trees.

Because of the public interest in the National Forests, ecosystem restoration, and use of native plants, more information will be available in the near future to display the better part of many decades of work at improving soil and water conditions. Plans to provide access to available information include using the SNF website. Information provided will include the location (Global Position, Latitude, Longitude); location maps; past, ongoing and current pictures of the areas; plans and other written information that should prove useful to those interested in taking an office, self or guided tour of gully and land restoration activities on the SNF.

Acknowledgements

Many SNF personnel have contributed to the gully treatment program over many decades. Support at National, Regional and Forest leadership and technical levels has been significant over this period. We especially want to recognize and thank Jerome

Thomas, Forest Supervisor; Oscar Stewart, Resource Staff Officer; Dick Rosemeier, Enoree District Ranger; Alvin Feltman, Enoree District Program Manager; and Jay Swafford, Enoree Hydrological Technician for their current support and interest. We appreciate Mr. James Irwin (interested public) for his interest and involvement. With the native grass aspects of this activity, we especially want to thank Don Surrency, USDA Natural Resource Conservation Service (NRCS), William Stringer and Rick Huffman, SC Native Plant Society (NPS), Clemson, SC, and Steve Dix, USDA Forest Service, Francis Marion Seed Orchard, Witherbee, SC. The USDA Forest Service provided funding for the work. Substantial contributions from NRCS and over 1,000 days of volunteer time from NPS were invaluable to the native plant work and results.

References

Hansen, W.F., 1991. Land Rehabilitation on the Sumter National Forest, In Proceedings of the Fifth Federal Interagency Sedimentation Conference, Drs. S. Fan and Y. Kuo (Editors), Las Vegas, Nevada. Volume 1, pp. 3-110 to 3-117.

Hansen, W.F., 1995. Gully Treatments. In Proceedings of Watershed Assessment and Restoration Workshop, National Advanced Resource Technology Center, USDA Forest Service, Marana, Arizona. 17pp.

Hansen, W.F. and D.L. Law, 1996. Watershed Restoration After Calamity. In Proceedings on Watershed Restoration Management. J.J. McDonnell, J.B. Stribling, L.R.Neville and D.J.Leopold (Editors). AWRA Symposium, Syracuse, New York pp. 187-198.

Heede, B.H.,1976. Gully Development and Control - The Status of Our Knowledge. USDA Forest Service Research Paper RM-169. Rocky Mountain Forest and Range Experiment Station, Fort Collins, Colorado. 42 pp.

Heede, B.H., 1982. Gully Control: Determining Treatment Priorities for Gullies in a Network. Environmental Management, Volume 6, Number 5. Published by Springer-Vertag New York Inc. pp. 441-451.

Hoover, M.D., 1949. Hydrological Characteristics of South Carolina Piedmont Forest Soils. Proceedings of the Soil Science Society. pp 353-358.

McKee, W.H. and D.L.Law, 1985. Response to Fertilization on the Francis Marion and Sumter National Forests. Progress and Final Report No. FS-SE-1103-157(2). Southern Experiment Station, Charleston, SC. 16 pp.

McKee, W.H., D.L. Gartner and D.L. Law, 1995. Pilot Scale Fertilization of Pole-Sized Stands of Loblolly Pine on the Sumter National Forest. Final Report No. FS-SE-4102-188(2). Center for Forested Wetlands Research, Southern Research Station, Charleston, South Carolina. 13 pp.

Norcross, T.W., 1936. Handbook of Erosion Control Engineering on the National Forests. US Government Printing Office, Washington, DC. 90 pp.

Schumm, S.A., M.D. Harvey and C.C. Watson, 1984. Incised Channels, Morphology, Dynamics and Control, Water Resource Publications, Littleton, Colorado, U.S. Library of Congress number 83-050243, 200 pp.

Singer, M.J., J. Blankard, E. Gillogley and K. Arulanandan, 1978. Engineering and Pedological Properties of Soils as They Affect Soil Erodibility. California Water Resource Center, Techical Report No. 166, ISSN 0575-4941. 32 pp.

Yoho, N.S, 1980. Forest Management and Sediment Production in the South - A Review. Southern Journal of Applied Forestry, Volume 4, Number 1. pp. 27-35.

List of Figures

Figure 1. Eventually the warn-out, eroded landscapes had lost its capability to support families and produce benefits. Historic photo of unknown origin.

Figure 2. Active gully headcut enlarging by cavitation, soil piping, bank failure and surface erosion extend into hillslopes as they contribute to gully enlargement.

Figure 3. Reforested gully was harvested about 15 years ago. Hardwood trees within gully were left. Gully remained stable as the area was planted and returned to pine forest.

Figure 4. Erosion of the piedmont soils through somewhat resistant B-horizon into the C-horizon (saprolite) caused increased and sometimes rapid gully expansion in the incompetent materials.

Figure 5. Loblolly pine stands developed little understory with the dense pine needle litter layer. Soils also developed slowly as the acidic needles decompose slowly and may contribute to nutrient losses.

Figure 6. Native grasses were collected and grown to test their use for erosion control and site recovery purposes. Over 220,000 plugs have been grown from 1998 to 2004 and planted to production fields, gullies and other exposed sites. Volunteer efforts have contributed heavily to all phases of the native plant work.

Figure 7. Gully plug located within reshaped small ephemeral gully channel. Proper design included using suitable soil fill, compaction and providing overflow protection such as the drop inlet structure of sufficient size to handle storm runoff and release flow at the lower channel level. The gully plugs commonly fill with sediment to the top of the culvert unless perforated.

Figure 8. Debris check dams were used in early gully treatments. Small woody debris was applied to small ephemeral channels.

Figure 9. Debris pile at the base of a reshaped gully provides some needed sediment containment and grade control in an ephemeral channel from a severe storm that occurred within weeks after treatment.

Figure 10. Grade control structures are installed to waterway level to help spread concentrated flows, promote infiltration and limit channel entrenchment and migration. Because they are not dams, they are hydrologically stable.

Figure 11. Loose rock check dams were used in series on a gully section reshaped that included a waterway with about 16 hectares (40 acres) drainage area. The rock dams provided excellent gradient control, increased channel roughness and spread flow to help limit channel degradation. Substantial armoring would be needed if the rock dams were any higher. Low rise rock dams are the most stable in these circumstances. The woody

debris on the upper dam deposited during a major storm event, with some minor channel erosion noted downstream of the structure.

Figure 12. Gravel treatments with surgestone were added to some actively eroding gully heads. In this instance, surface flow from a failed agricultural terrace was still contributing concentrated flow to an active headcut with some expansion up the terrace channel. The surgestone is roughly shaped to contain the flow within its path and deliver it to the non-active gully channel downstream.

Figure 13. Land reshaping of gullies typically uses dozers or other earthmoving equipment to return the land to a stable contour of no more than 25% slope. Followup treatments with water diversions or waterways, soil ripping, terraces, liming, fertilization, seed, mulch and tree planting are used as needed to achieve restoration. The depth of this gully can be estimated by comparing the pine trees near the dozer and the pine tree within the gully channel. Debris is not buried within the treatment area to help limit soil settling.

Figure 14. The green area within this gully treatment was little blue stem native grasses during a drought period. Fescue and other grasses that we have commonly used were brown, dormant and in decline after several years of drought.

Figure 15. Splitbeard bluestem (left) and little bluestem (right) results 5 months after planting them from plug starts on the Enoree Ranger District, Sumter National Forest.

Figure 16. Effects of gully reshaping and associated measures including loblolly pine planting about 5 years after treatment. In this instance, *Sericea lespedeza* was used in the understory. Besides erosion control it also fixes nitrogen. After 10 years, pine trees are typically 15-25 feet tall. Commercial thinning of these areas can typically be done in 15-20 years after treatment. Areas that do not have a nitrogen fixing plant in the understory, sometimes need to be refertilized to maintain tree health and growth.

Figure 17. Until the vegetation and soils have recovered sufficiently to be self sustaining, treatment areas may need maintenance, especially during extended drought periods of after severe storm events. This area had exposed saprolite soils within the treatment area. The chloritic needles and signs of concentrated flow with no needle accumulation all suggest that refertilization is the minimum treatment needed. Added mulch and seed with some scarification of the soil surface with at least hand tools are needed. The bare saprolite soils in themselves will seldom recover without treatment and maintenance until the site is recovered. Stockpiling any surface and B-horizon soils during reshaping treatment and using that to cover the surface will improve recovery efforts.

Figure 18. This stand was treated in about 1960 and the picture was taken about 1985. Older treatments often used poor tree stock and lacked maintenance to promote the most rapid recovery. Today, with improved trees and methods, pine stands grow much faster and need to be commercially thinned in 15 years.

Figure 1. Eventually the warn-out, eroded landscapes had lost its capability to support families and produce benefits. Historic photo of unknown origin.

Figure 2. Active gully headcut enlarging by cavitation, soil piping, bank failure and surface erosion extend into hillslopes as they contribute to gully enlargement.

Figure 3. Reforested gully was harvested about 15 years ago. Hardwood trees within gully were left. Gully remained stable as the area was planted and returned to pine forest.

Figure 4. Erosion of the piedmont soils through somewhat resistant B-horizon into the C-horizon (saprolite) caused increased and sometimes rapid gully expansion in the incompetent materials.

Figure 5. Loblolly pine stands developed little understory with the dense pine needle litter layer. Soils also developed slowly as the acidic needles decompose slowly and may contribute to nutrient losses.

Figure 6. Native grasses were collected and grown to test their use for erosion control and site recovery purposes. Over 220,000 plugs have been grown from 1998 to 2004 and planted to production fields, gullies and other exposed sites. Volunteer efforts have contributed heavily to all phases of the native plant work.

Figure 7. Gully plug located within reshaped small ephemeral gully channel. Proper design included using suitable soil fill, compaction and providing overflow protection such as the drop inlet structure of sufficient size to handle storm runoff and release flow at the lower channel level. The gully plugs commonly fill with sediment to the top of the culvert unless perforated.

Figure 8. Debris check dams were used in early gully treatments. Small woody debris was applied to small ephemeral channels.

Figure 9. Debris pile at the base of a reshaped gully provides some needed sediment containment and grade control in an ephemeral channel from a severe storm that occurred within weeks after treatment.

Figure 10. Grade control structures are installed to waterway level to help spread concentrated flows, promote infiltration and limit channel entrenchment and migration. Because they are not dams, they are hydrologically stable.

Figure 11. Loose rock check dams were used in series on a gully section reshaped that included a waterway with about 16 hectares (40 acres) drainage area. The rock dams provided excellent gradient control, increased channel roughness and spread flow to help limit channel degradation. Substantial armoring would be needed if the rock dams were any higher. Low rise rock dams are the most stable in these circumstances. The woody debris on the upper dam deposited during a major storm event, with some minor channel erosion noted downstream of the structure.

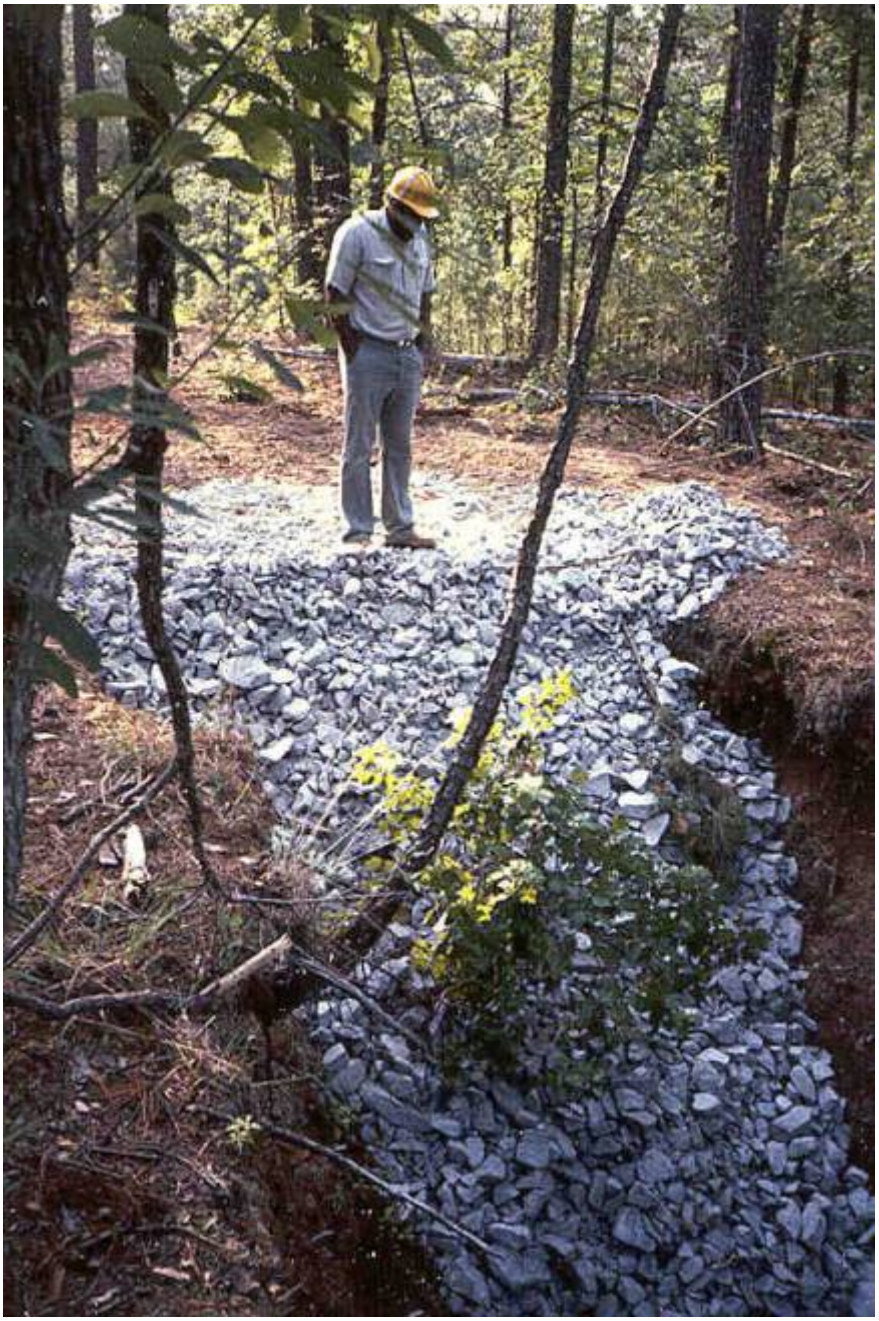

Figure 12. Gravel treatments with surgestone were added to some actively eroding gully heads. In this instance, surface flow from a failed agricultural terrace was still contributing concentrated flow to an active headcut with some expansion up the terrace channel. The surgestone is roughly shaped to contain the flow within its path and deliver it to the non-active gully channel downstream.

Figure 13. Land reshaping of gullies typically uses dozers or other earthmoving equipment to return the land to a stable contour of no more than 25% slope. Followup treatments with water diversions or waterways, soil ripping, terraces, liming, fertilization, seed, mulch and tree planting are used as needed to achieve restoration. The depth of this gully can be estimated by comparing the pine trees near the dozer and the pine tree within the gully channel. Debris is not buried within the treatment area to help limit soil settling.

Figure 14. The green area within this gully treatment was little blue stem native grasses during a drought period. Fescue and other grasses that we have commonly used were brown, dormant and in decline after several years of drought.

Figure 15. Splitbeard bluestem (left) and little bluestem (right) results 5 months after planting them from plug starts on the Enoree Ranger District, Sumter National Forest.

Figure 16. Effects of gully reshaping and associated measures including loblolly pine planting about 5 years after treatment. In this instance, *Sericea lespedeza* was used in the understory. Besides erosion control it also fixes nitrogen. After 10 years, pine trees are typically 15-25 feet tall. Commercial thinning of these areas can typically be done in 15-20 years after treatment. Areas that do not have a nitrogen fixing plant in the understory, sometimes need to be refertilized to maintain tree health and growth.

Figure 17. Until the vegetation and soils have recovered sufficiently to be self sustaining, treatment areas may need maintenance, especially during extended drought periods of after severe storm events. This area had exposed saprolite soils within the treatment area. The chloritic needles and signs of concentrated flow with no needle accumulation all suggest that refertilization is the minimum treatment needed. Added mulch and seed with some scarification of the soil surface with at least hand tools are needed. The bare saprolite soils in themselves will seldom recover without treatment and maintenance until the site is recovered. Stockpiling any surface and B-horizon soils during reshaping treatment and using that to cover the surface will improve recovery efforts.

Figure 18. This stand was treated in about 1960 and the picture was taken about 1985. Older treatments often used poor tree stock and lacked maintenance to promote the most rapid recovery. Today, with improved trees and methods, pine stands grow much faster and need to be commercially thinned in 15 years.

Response of Gully Development to Land Use Change in West China

Yong Li* (E-Mail: yongli@ami.ac.cn)
Lingyu Bai
Xingchang Zhang
Fuhong He
Dignhui Liu
Institute of Agricultural Environment Sustainable Development
Chinese Academy of Agricultural Sciences
Beijing, 100081
P.R. China

Abstract

Gully erosion is the major contributor to the overall sediment delivered to both the Yellow and Yangtze Rivers in the west China. Few studies have been conducted on the long-term impacts of the land use change on gully initiation and gully development. The target areas of our research are the dry-valleys located in the upper Yangtze River Basin, SW-China. Our objectives are: a) to obtain the environmental information on gully patterns and their development at different spatial and temporal scale in the upper Yangtze River Basin, b) to reconstruct the historical record of gully development and land use change over the past 2000 years, and c) to quantify the processes and the effectiveness of land use structures on spatial patterns of gullies. The first investigations were carried out in the Anning Warm-Dry Valley of southern Sichuan in the territory of Xichang. Three gully systems were investigated in details. The size (length, average depth and width) and the volume of the gully system were measured in the field with RTK-GPS. Cs-137 and unsupported Pb-210 dating were used to distinguish the chronology of sediment profiles within the gully systems. Local culture and history records were analyzed, senior experts and farmers were interviewed for a detailed reconstruction of land use history. The temporal patterns of gully development processes at study gully catchments could be subdivided into five time periods. Gullies initiation occurred during 1920-1930, and maximum increase of gully development in the period from 1950 to 1970. Rapid decrease of gully development closely corresponded to increase in vegetation cover and reduction of intensive grazing intensity in the study area.

Keywords: gully development; land use change; Cs-137 and unsupported Pb-210 dating; semi-arid soils; west China.

*Correspondence author

Agroecological Estimation of Grey Forest-Steppe Soil of South Bug's Basin and its Erosion Reduction Methods

Saveta Yerychuk*
Agricultural Chemistry Research Scientist
Department of Soil Science and Agricultural Chemistry
Khmelnytskyy Institute of Agroecology and Biotechnology, UKRAINE

Abstract

The Southern Bug is a river on southwest of Ukraine that flows into the Dnieper estuary of the Black Sea. The basin of Southern Bug includes southern part of Volyno-Podol Hills and also southern slope of Pre-Dniper higher region. The square of its basin is 63 700 km^2. According to geostructural regard the river's basin territory is located on southwestern and southern slope of Ukrainian shield. In view that the Southern Bug flows on Ukrainian crystalline shield, it left an imprint on erosion and denudational processes feature and also on a character of river valley formation. The basin territory is located within erosively-denudational valley with thick valley-gully net. The erosive partition thickness varies from 0.5 – 1.0 km/km^2 in northwestern part of basin up to 0.75 – 1.2 km/km^2 in southeastern one. The high level of plowing (70-85%) and low forest-covering (12-15%) cause useful increase of erosive processes in Southern Bug's basin.

The agroecological estimation of grey forest and forest-steppe soils by Karmanov's methodology to allow define potential of agricultural soil fund in basin of Southern Bug was revealed in the above research. The calculations of soil-ecological indexes were conducted. These calculations are based on complex calculations of soil activities and other factors resulting in erosion and limiting soil fertility. Display of causes of grey forest-steppe soils intensive erosion of the basin Southern Bug was based on its land use structure study. Speed of flowing water stream and rain precipitation under different streamflow formation conditions were defined by means of calculations. It was researched that dark grey forest-steppe soils most often located on relief regions with slope up to 10° (to 66%) where farming is impeded. It was also revealed that part of grey forest-steppe soils increases on slopes with 1-5° (54%) and 10-15° (87%) steepness. The research of the basin of Southern Bug grey forest-steppe soils conditions by its erodibility showed that square in different extents washed off light-grey forest-steppe soils is 32,8% from its total square under tillage condition, 38,9% of dark-grey, and 44,9% of grey ones. It was also established that gully intense formation is observed on slopes lands of 350-1250 m. and 3.15 - 8.9° steepness. It is inhere to zone of grey forest-steppe prevalence of basin soils Southern Bug. It explains by erosion basis increase to 40-60 m. and consequently flowing water's kinetic energy growth. The calculations show reduction of distance along slope with land gradient growth in which speed of flowing waters do not reach a value of abrasive waters.

*Correspondence author

Gully Erosion Prediction and Warning in Black Soil Region of Northeastern China

Yongqiu Wu*
Gang Hu
Baoyuan Liu
Key Laboratory of Environmental Change
and Natural Disaster of the Education Ministry of China
Beijing Normal University, Beijing 100875, P. R. of China

Abstract

There used to be waste and grass land in the black soil region of Northeastern China 50 years ago. Now, most of the lands have been changed into cropland, and accelerated soil erosion occurred during this period. Gullies have also been appearing in this region since then. This study investigated the types of channel and measured its density on the cropland. There are three types of channel on the cropland. The first is a sort of wide and shallow channel on the slope. It can concentrate water on the slope but no soil would be wash away normally. The second is ephemeral gully which distribute downstream of the first one. Soil erosion occurs obviously during the rainfall season but it allow ordinary farm tillage. The third channel, which locate downstream of the second one, is gully. The length and density of the channels were investigated in an area of 4 km2. The densities of the three channels are 273, 408 and 493 m/km2, respectively. The second type of channel (ephemeral gully) will change into the third one (gully) by headcut of the gully in the study area. In the place of the second type of channels gullies will appear.

Keywords: black soil, gully erosion, warning

*Correspondence author

Gullies in China: Form, Process and Control: a Comprehensive Literature Review

Y.Q. Li*
25 Yuetan Street N.
Beijing 100000, China

Abstract

Gullies are a widespread erosional phenomenon in China, which spans several physical geographical zones from the sub-tropics to the cool temperature zone. Invariably, gullies in China are extremely variable in terms of size, cause of formation, morphology, process, course of evolution and ways of control. In South China where rainfall is abundant, *Benggang* (literally collapsing hill) is the most conspicuous form of gullies, while *Gouhe* (literally deep-cut ditch) in the Loess Plateau is the most representative of gullies in North China. While both can be as long as tens of kilometers and as deep as up to several hundred meters, they are represent two ends on the causality spectrum and measures to control them are also different. In particular, initiation of gullies in the Loess Plateau is caused a variety of factors and often in an episodic manner. Classic geomorphic concepts like complex response, threshold and episodic erosion can all find evidence with gully erosion there, but equilibrium and the Davisian cycle of erosion may need revision or reinterpretation. Gully processes are much storm event-based and heavy rainfall remains the most important driving force for gully extension: both headward and sideward. Gully control in China varies with local conditions, with natural rehabilitation and human intervention both at play. Warping dams in the Loess Plateau represent one most innovative, productivity-oriented way of gully reclamation in China.

This paper sets out to offer a comprehensive literature review of the exiting knowledge about gullies in China. It will also highlight those areas of deficiency in contemporary gully research in the country. It will particularly show that while process geomorphology has been the mainstream of international geomorphological inquiry, China has yet to initiate similar research. Nevertheless it is hoped that its rich gullies can provide a good testing ground for some of the core concepts of contemporary process geomorphology.

Keywords: gully, gully evolution, gully form, gully process, gully control

*Corresponding author

Comprehensive Gully Reclamation in the Loess Plateau, Northwest China: from Warping Dams to Gully Gardens

Rengkui Liu
GIS Laboratory
Northern Jiaotong University
Beijing 100044, China

Y.Q. Li* (E-Mail: jimmyli2008@yahoo.com)
25 Yuetan Street N.
Xicheng District, Beijing 100000, China

Abstract

The vast Loess Plateau in Northwest China is dissected by deep gullies of varying sizes, causing enormous soil erosion, land degradation and reduced agricultural productivity. Yet, in the fight against severe gully erosion over hundreds of years, local farmers have developed some very effective and innovative ways to harvest water and sediment from upland slopes through a series of dams built along the gully bottom and use the accumulated gully bed land to practise intensive farming and improve their livelihood in this predominantly semiarid landscape. Compared with upland slopes, the gully bottom land boasts of better moisture regime, rich soil fertility and much enhanced agricultural productivity, often referred to by farmers as their "survival land" in dry years. Enjoying enormous popularity with farmers, this traditional gully reclamation practice has been significantly improved through modern engineering following the successful use of hydraulic filling technique in the 1970s. Now viewed as a viable approach to remaking the Loess Plateau and taming the mighty Yellow River, warping dams have been designated by the Chinese Ministry of Water Resources as a "Flashing Engineering Project" for water conservancy work in China for 2003.

Central to this indigenous way of gully reclamation are warping dams, which are often built in a downstream cascade series along the gully bottom. Depending on the gully watershed size, such warping dams may have different functionalities: some store water to provide a source for irrigation purposes, some silt up sediment and build up new land for cultivation uses while some key dams serve as the backbone for flood control. Intricately arranged in space to form what is theoretically called an equilibrium dam system, the gully land thus created will grow in size and eventually reach a stage when further sediment and water contributed from the upstream are thinly spread over the gully land and cause no threat to crop harvest. When this ideal stage is reached, the gully land becomes a gully garden, where a variety of agricultural and cash crops are grown and farmers can have a much ensured livelihood.

Correspondence author

This paper reviews the development of warping dams and gully gardens in the Loess Plateau and explains some of the mechanisms behind this unique way of comprehensive gully reclamation. Implications are also drawn as how to rehabilitate severely eroding gullies in various physical landscapes.

Keywords: loess plateau, gully, warping dam, gully garden, comprehensive gully reclamation

To Table of Contents

3rd International Symposium on Gully Erosion Panel Discussions

Panel Discussion on the main findings of the Gully Symposium, related to:

State-of-the-art gully erosion research needs
Gully erosion prediction technology
Gully erosion control methods

PANELISTS

Chair, **Jerry M. Bernard**, National Geologist, United States Department of Agriculture-Natural Resources Conservation Service, Washington, DC
Dr. Rorke Bryan, Dean and Professor, Faulty of Forestry, University of Toronto, Ontario, Canada
Prof. Dr. Jean Poesen, Laboratorium Voor Experimentele Geomorfologie, Katholieke Universiteit, Leuven, Belgium
Dr. Li Rui, Director, Institute of Soil and Water Conservation (ISWC), CAS & MWR; Vice President, World Association of Soil and Water Conservation (WASWC); Yangling, Shaanxi, China
Dr. Fred D. Theurer, Hydraulic Engineer and AnnAGNPS Co-Manager, United States Department of Agriculture-Natural Resources Conservation Service, Beltsville, Maryland

APPROACH:

Focus was on the three topics above, with emphasis on key elements or needs. Each panelist made a short presentation and addressed questions and remarks from the audience.

INTRODUCTION: JERRY M. BERNARD, PANEL CHAIR

Jerry Bernard made some introductory remarks, including the following observations about the conference:

1. Gully erosion problems are international.
2. Terminology must be uniform, so that research and application of best management practices can be communicated effectively. Some gully erosion terms that were used this week include the following: “concentrated flow erosion,” “classic gully,” “ephemeral gully,” “Type I and Type II gullies,” “permanent gullies,” “bank gullies,” “valley trenches,” and others.
3. Sediment production from ephemeral gullies is significant. As much as 70% of total erosion that occurs in some areas is attributed to ephemeral gully erosion processes. As an aside, sheet and rill (rill and interill) erosion has been largely controlled in the

US where no till farming is practiced, but sediment continues to be the #1 pollutant of US waters (EPA).

4. Connectivity or process continuum affects our ability to estimate all types of erosion occurring in a field, in a landscape, or in a watershed. The relationship between the various erosion processes requires more research in order to develop tools to estimate erosion and sediment production. The research that is needed includes field and laboratory, model development, and numerical analysis. Rainfall-driven and runoff-driven erosion processes must be integrated in order to estimate the full extent of erosion damage, sediment production, sediment deposition, and sediment transport off the field. This process continuum begins with raindrop impact (or snowmelt), with the following erosion and sediment transport processes in order, and interrelated: sheet and rill (rill and interill) → sediment deposition → intensified rills → ephemeral gully → episodic deposition and →sediment transport offsite
5. The operative questions that recurred throughout the conference include the following:
   a. WHAT is gully erosion?
   b. WHERE does gully erosion occur?
   c. WHEN does gully erosion occur?
   d. HOW does gully erosion happen (processes)?
   e. How do we predict it?
   f. How do we treat it?
   g. WHY care? If gully erosion is so serious, then why don't Congress, the public, and landowners become upset? Will the equivalent of a "Dust Bowl" for gully erosion be needed to focus attention?
   h. WHO cares? Landowners, Congress, public, etc., care because erosion damages soil, crop, and land use values; produces sediment that damages water quality and the environment; and the costs of government programs to treat erosion problems are substantial and need to be applied efficiently to fix the erosion problems.

REMARKS: **DR. RORKE BRYAN**

1. Understanding the processes that affect complex, large gully systems is a challenge. Data are not available, and sometimes not possible to obtain (physically as well as economically).
2. Modeling the evolution of network systems is a practical problem.
3. Where should efforts be concentrated in a large system? Where are the active processes or points of most concern?
4. Predicting tributary development in gully systems is a particular challenge. Field observations can provide useful information to make predictions.

5. Some gully erosion occurs through piping or tunnel erosion, and not simply from the combination of sheer stress and collapse by gravity. Methodologies need to be developed for these kinds of gully erosion processes.
6. Gullies can occur on extremely steep slopes (30 to 50% slopes). The interrelationship between the sheer stresses of flowing water and associated landsliding processes are not well understood.
7. Methodologies are needed for identifying the stages in the life-cycle of a gully. Are there simple methodologies for identifying where to concentrate stabilization efforts?

REMARKS: **DR. JEAN POESEN**

1. The gully erosion studies presented at this conference were very complimentary: i.e., gully erosion in a wide range of environments, gully erosion occurring over different time and spatial scales (headcut development over minutes to gully evolution over centuries).
2. Although this conference addressed various aspects of gully erosion and increased our insight in rates and factors controlling gullies, there still remain a series of important issues which deserve more attention, including:
   a. Clear cut definitions of gully types are needed.
   b. Need for definitions of boundaries for application of erosion prediction technology and modeling. The transition from rill erosion to ephemeral gully erosion to classical gully erosion and to river channel erosion represents a continuum, and any classification of hydraulically related erosion forms into separate classes, such as microrills, rills, megarills, ephemeral gullies, permanent gullies is, to some extent, subjective. However, we do need to have clear boundaries between these erosion phenomena for users of soil erosion models or soil erosion control techniques in order to avoid misuse or failures.
   c. We are still lacking appropriate and standardized techniques for measuring gully erosion itself. We know little about the accuracy of the various measuring techniques. At this conference we learned about the potential for airborne scanning laser technology and submerged jet erosion devices for measuring critical shear and channel erodibility coefficients.
   d. Gully erosion processes about headcut retreat and nickpoint migration were focused on in papers, very well. Unresolved issues, however, include how to apply these research results to real-world gullying processes. How do we go from detailed process understanding of small headcuts and knickpoints to large (e.g. 10 m high) bank gully headcuts where processes such as tension cracking and piping play a crucial role in controlling headcut retreat rates?
   e. Water erosion models do not adequately handle gully erosion processes, despite the fact that gully erosion can account for a significant part of sediment production within the watershed. Prediction of the location of different gully types (e.g. ephemeral gullies, bank gullies) in different landscapes needs methods

and tools. Hence, there is also a need for detailed monitoring and experimental work as a basis to increase our capacity to predict impacts of land use change or of gully erosion control measures.

f. Innovation in gully erosion control techniques is rather limited compared to innovation in gully erosion process understanding. We need more innovation in gully erosion control techniques. Also, we need to evaluate past gully erosion control programmes in order to learn lessons about failures and successes.

REMARKS: **DR. LI RUI**

1. Dr. Li Rui expressed appreciation for the symposium, meeting old friends, making new friends.
2. More soil and water conservation (SWC) research is needed on the Regional Scale.
   a. Regional planning, development, and implementation need more SWC research.
   b. Research results from small plots may not provide information suitable for large scale application.
3. What should we do?
   a. Regional soil erosion process is different from one on a single slope.
   b. Regional scale will require the use of different factors.
   c. Remote sensing data and GIS are very useful for regional soil erosion research.
4. Regional considerations are important also for SWC and environmental impacts, including global climate change as well as soil erosion.

REMARKS: **DR. FRED THEURER**

1. End-user focus is needed. Tools, models, and treatments should be tailored to the needs of the people who will use them.
2. We need to identify and quantify all erosion processes that affect producing lands.
   a. Sheet and rill
   b. Ephemeral
   c. Edge of field
   d. Valley trenching
   e. Landsliding
3. NRCS needs to quantify all types of erosion and identify them to recommend solutions.
   a. Solutions need conservation plans. One action may fix one type of erosion but not have any affect on the others.

DISCUSSION

Comment: Total Maximum Daily Load (TMDL) issue of daily load, not annual load. Any model used must not be a "black box," must be adjustable, and must not be too complex for end user. A problem persists in that it is still difficult to distinguish between "rill" and "gully" erosion (definition problems). Where does a gully end, and a 1st order stream begin? We need an integrated approach. There's hope in getting people together, as this symposium has accomplished, to address the issue. C. Ted Yang

Comment: Greg Wilson noted that Soil Science of America is revamping its definitions.

Question: How do you analyze gully pipe systems? Smoke tracing can work in gully pipe systems, with crossing across watersheds in the subsurface. Seismic probes and ground-penetrating radar (GPR) could also be used. Flooding is also a possibility, when combined with tracers and dyes. Infrared (IR) photography may also help.

Comment: Dr. Sam S. Y. Wang, University of Mississippi, noted that numerical modeling needs additional development before it can be utilized to simulate gully erosion with a high level of accuracy. The National Center for Computational Hydroscience and Engineering (NCCHE) has developed a series of models capable of simulating a number of soil erosion and sediment transport and water quality problems closely related to gully erosion. These include headcut migration, channel bank erosion, water and sediment routing in channel networks, evaluation of channel stabilization measures, as well as watershed management plans, etc. His center is willing to collaborate with government agencies to study these and related problems. And, due to a broad interest in numerical modeling as expressed at this symposium, it may be a topic to emphasize at the next Gully Erosion Symposium.

Comment: Dr. Greg Hansen noted that tunneling and piping processes are also important in embankment failures. He also remarked that tools must also provide the end-user with guidance for the appropriate solution (the right thing to do).

Comment: Dr. Jim Dungan Smith noted that we are not making full use of tools (reference Moore's law related to exponential increases in computer processing capabilities, for example). We need diverse tools to address gully erosion problems, as well as field work to characterize the processes and problems. Some things cannot be accurately measured in the field and must be researched in the laboratory. Numerical modeling must also be used where theoretical techniques are needed to further research. He recommended strongly that researchers fully consider form drag, as appropriate, as part of shear stress analysis. Solutions may be found in fundamental physics.

Comment: Dr. Feng-li noted that the definition of gully types is critical. Also, we need to understand when gullies are active, when they are headcutting, etc. This information is needed in order to develop treatment systems that are cost-effective.

Comment: Dr. C. Ted Yang (Borland Professor of Water Resources and Director of Hydroscience and Training Center; Colorado State University) made some detailed comments about the conference and the subject of gully erosion. He also provided these in writing after the conference, and they are included here:

> I am pleased to note that you and many others agree with some of the ideas in my Keynote Presentation "A Unified Approach in Erosion and Sedimentation Studies". At the closing panel discussion, I pointed out the following:
>
> EPA has identified that sediment is the number one pollutant in the United States. EPA will develop and enforce TMDL (Total Maximum Daily Load) of sediment criterion to all Federal and state agencies. A useful model which can be applied for the estimation of TMDL of sediment should meet the following requirements:
>
> 1. It is a process based model. It starts with rainfall, runoff, surface, rill, and gully erosion followed by sediment transport, scour, and deposition in rivers, lakes, and reservoirs. This model should not be a "black box" model. The model must be based on sound theories.
>
> 2. The parameters used in the model must be easily obtained or computed using field data generally available.
>
> 3. There is no clear theoretical and meaningful differences among surface, rill, gully, channel, and river sedimentation and erosion processes. A unified approach applicable to all the above processes should be used to develop the next generation of models.
>
> 4. We should be open-minded, be rational, put agency historical approach aside, and work together. EPA TMDL Rules apply to all agencies in the future regardless what an agency has done or accepted in the past.